

**Can Ethylene Tetra Fluoro Ethylene cushions double skin
façade applications improve buildings envelope performance,
reduce energy consumption and enhance visual and thermal
comfort in UAE buildings?**

هل باستطاعة تطبيقات وسائد الإيثيلين تيترا فلورو إيثيلين بالواجهات المزدوجة
الطبقات تحسين أداء غلاف المباني و تقليل استهلاك الطاقة و دعم الراحة البصرية
و الحرارية في مباني دولة الامارات العربية المتحدة؟

by

AHMED ABDELAZIZ YOUSSEF MANSY

**Dissertation submitted in fulfilment
of the requirements for the degree of
MSc SUSTAINABLE DESIGN OF BUILT ENVIRONMENT
at**

The British University in Dubai

March 2019

DECLARATION

I warrant that the content of this research is the direct result of my own work and that any use made in it of published or unpublished copyright material falls within the limits permitted by international copyright conventions.

I understand that a copy of my research will be deposited in the University Library for permanent retention.

I hereby agree that the material mentioned above for which I am author and copyright holder may be copied and distributed by The British University in Dubai for the purposes of research, private study or education and that The British University in Dubai may recover from purchasers the costs incurred in such copying and distribution, where appropriate.

I understand that The British University in Dubai may make a digital copy available in the institutional repository.

I understand that I may apply to the University to retain the right to withhold or to restrict access to my thesis for a period which shall not normally exceed four calendar years from the congregation at which the degree is conferred, the length of the period to be specified in the application, together with the precise reasons for making that application.

Signature of the student

COPYRIGHT AND INFORMATION TO USERS

The author whose copyright is declared on the title page of the work has granted to the British University in Dubai the right to lend his/her research work to users of its library and to make partial or single copies for educational and research use.

The author has also granted permission to the University to keep or make a digital copy for similar use and for the purpose of preservation of the work digitally.

Multiple copying of this work for scholarly purposes may be granted by either the author, the Registrar or the Dean only.

Copying for financial gain shall only be allowed with the author's express permission.

Any use of this work in whole or in part shall respect the moral rights of the author to be acknowledged and to reflect in good faith and without detriment the meaning of the content, and the original authorship.

Abstract

Innovative façade design technique as a response to the ambient weather conditions has been investigated continuously by building specialists as they have a direct impact on internal conditions and energy consumption in any building. However, the subject of the light weight double skin façade, as a strategic solution to enhance the envelope performance for new and existing buildings, have not been covered sufficiently in our region under the middle east weather conditions. Also, the performance of the ETFE double skin facade is still questionable due to the lack of the experience, recorded data especially in the UAE.

The research focused on analysing the impacts of installing ten light weight ETFE double skin façade options on an office building in Abu Dhabi, UAE in order to evaluate these design options as strategic sustainable solutions that can reduced energy consumption and enhance visual and thermal comfort within new or existing buildings. After testing different simulation programs, IES-VE was selected for the study. The software was validated by comparing the basic-model simulation results with the electrical loads calculation that were approved by Abu Dhabi Distribution Company. The ten design scenarios included different passive and active applications and covered changes in the ETFE cushions parameters and the addition of different ceramic frit pattern, two different types of building integrated thin film photovoltaic panels (BIPVs) and ETFE single foil dynamic shades to the system. The final scenario was the optimal option which included all combined design strategies.

The analysis of these different options in IES-VE aimed to assess their impact on energy consumption, comfort index, room temperature, people dissatisfaction level, daylighting levels, daylight factor levels, daylight glare index (DGI), Guth visual comfort probability (GVCP) and daylighting harvesting potential. Also, the study included computer fluid dynamics (CFD) to understand changes in temperature and air velocity within the DSF cavity. The results of each scenario were compared with base model/existing building results to evaluate the increment and reduction in each of the studied parameters.

The CFD analysis of all scenarios proved that there was a vertical air flow with different rates within the cavity of the corridor DSF which helped to discharge the hot air from the top outlet. The addition of the double layer ETFE cushions as a second envelope layer improved most of the factors with a minor reduction in both daylight factor and daylight illumination levels and managed to reduce energy consumption by 11.594~11.603%. The addition of ETFE layer reduced the total energy consumption by additional 0.85% while maintaining similar thermal comfort analysis results, doubling the reduction of daylighting quality while improving visual comfort. The addition of 30%~60% frit pattern reduced the total annual electricity consumption by additional 0.15% ~ 0.25% with remarkable reduction in people dissatisfied index and DGI. However, it massively reduced the daylighting levels. When the different BIPV types were added, energy consumption was reduced by additional 2% and 4.4% while improving thermal and visual comfort and reducing daylighting quality. The addition of dynamic shades reduced energy consumption by additional 2.2% while having similar impacts on the other factors. The final optimal scenario achieved a total electricity consumption reduction of 19.1% comparing to the basic model with a major improvement in thermal and visual comfort factors. However, these improvements were associated with noticeable reduction in daylighting levels.

الملخص

دراسة تقنيات تصميم واجهات المباني المتطورة كنتيجة لظروف البيئة المحيطة هو عمل متواصل يقوم به خبراء تصميم المباني بسبب تأثيرها المباشر علي الظروف الداخليه و استهلاك الطاقة داخل المباني. ومع ذلك لم يتم تغطية موضوع الواجهة المزدوجة الخفيفة الوزن كحل استراتيجي لتعزيز أداء الواجهات المغلفة للمباني الجديدة أو القائمة بما فيه الكفاية في منطقتنا تحت ظروف الطقس في الشرق الأوسط. بالإضافة الي ذلك لا يزال أداء الواجهات المزدوجة التي تشتمل علي وسادات الايثيلين نيترا فلورو ايثيلين الخفيفة تحت التساؤل نظرا لعدم توفر الخبرة و المعلومات الخاصة بها خاصة في دولة الامارات العربية المتحدة.

ركز البحث علي تطبيق عشر خيارات واجهات مزدوجة مشتملة علي وسادات الايثيلين نيترا فلورو ايثيلين علي مبني مكتبي خدمي في مدينة ابوظبي بدولة الامارات من اجل تقييم هذه الخيارات كحلول استراتيجية مستدامة يمكن ان تقلل من استهلاك الطاقة و تعزز الراحة البصرية و الحرارية في المباني القائمة. بعد اختبار برامج المحاكاة المختلفة تم اختيار برنامج اي اس في اي للدراسة . تم التأكد من صحة البرنامج من خلال مقارنة نتائج محاكاة المبني الاساسي بحسابات الاحمال الكهربائية التي قامت شركة ابوظبي للتوزيع بالموافقة عليها. تضمنت سيناريوهات التصميم العشرة تطبيقات مختلفة كاختلافات تصميمية في الواجهات الخفيفة و اضافة انماط تزجيج خزفي مختلفة و نوعين مختلفين من الخلايا الشمسية الرقيقة و وحدات تظليل متحركة خفيفة مصنوع من نفس مادة الواجهات.

يهدف تحليل هذه الخيارات المختلفة في برنامج المحاكاة الي تقييم تأثيرها علي استهلاك الطاقة و مؤشر الراحة و درجة حرارة الغرفة و مستوي عدم رضا الناس و مستويات نور النهار و مستويات عامل ضوء النهار و مؤشر وهج نور النهار و احتمالات الراحة البصرية لجوئ و قابلية حصاد نور النهار. كما اشتملت الدراسة علي قياس حرارة و سرعة حركة الهواء الرأسية داخل فراغ الواجهات المزدوجة. و تم مقارنة النتائج بنموذج المبني الاساسي القائم لتقييم الزيادة و النقصان في كل من العوامل المدروسة. أثبت التحليل الديناميكي لجميع السيناريوهات بوجود تدفق هواء رأسي بمعدلات متغيرة و الذي ساعد علي تفرغ الهواء الساخن من اعلي. إضافة الواجهات كواجهة مزدوجة ساعد علي تقليل استهلاك الطاقة بنسبة 11.594 ل 11.6% مع تحسين اعلي العوامل و تقليل الاضاءة النهارية بصوره بسيطة. بعد اضافة طبقة اخري خفيف للواجهات تم زيادة تخفيض الطاقة ب 0.85% مع الحفاظ علي معدلات راحة حرارية مماثلة و زيادة الراحة البصرية مع تقليل كمية الاضاءة النهارية. أدت اضافة 30% الي 60% من التزجيج الخزفي الي زيادة تخفيض الطاقة ب 0.15% و 0.25% مع تخفيض معدل عدم رضا الاشخاص و الوهج النهاري بصورة كبيرة و تقليل اضافي للنور النهاري. أنواع الخلايا الشمسية المختلفه زادت من تخفيض الطاقة بنسبة 2.2% و 4% و تحسين الراحة الحرارية والبصرية والحد من جودة ضوء النهار . أدت إضافة وحدات التظليل امتحركة إلى خفض استهلاك الطاقة بنسبة إضافية قدرها 2.2% مع وجود تأثيرات مشابهة على العوامل الأخرى. حقق السيناريو الأمثل النهائي خفضًا كبيرًا في استهلاك الكهرباء بنسبة 19.1% مقارنة بالنموذج الأساسي مع تحسن كبير في عوامل الراحة الحرارية والبصرية. ومع ذلك ، ارتبطت هذه التحسينات مع انخفاض ملحوظ في مستويات ضوء النهار.

Acknowledgement

First of all, I would like to express my sincere thanks to Dr. Hanan Taleb, Associate Professor in the Faculty of Engineering in BUID. Her door was always open whenever I needed help or support in my thesis. I would like to thank her for continues encouragement and guidance through all the dissertation stages. I really value the honour of being her student.

Furthermore, this research would have never been achieved without my beloved wife Heba's encouragement, full support, love and patience.

Finally, I must express my full gratitude to my parents and sister who supported me in my entire life and my brother Bassem who motivated me to take the MSc step and helped me in several ways in various situations to achieve my dreams.

Table of Contents

| | | |
|-------|---------------------------------------------------------------------------|----|
| 1 | INTRODUCTION AND BACKGROUND | 1 |
| 1.1 | URBANIZATION AND ENVIRONMENT THROUGH HISTORY | 1 |
| 1.2 | BUILDINGS IMPACTS ON THE ENVIRONMENT ON A GLOBAL SCALE | 2 |
| 1.3 | SUSTAINABLE BUILDING DESIGN AS A SOLUTION..... | 2 |
| 1.4 | BUILDINGS AND ENERGY IN THE UAE..... | 3 |
| 1.5 | SUSTAINABLE PASSIVE AND ACTIVE DESIGN TECHNIQUES | 5 |
| 1.6 | STATEMENT OF THE PROBLEM AND RESEARCH INTEREST | 7 |
| 1.7 | AIMS AND OBJECTIVES | 8 |
| 1.8 | RESEARCH LIMITATIONS..... | 10 |
| 1.9 | RESEARCH OUTLINE | 11 |
| 2 | LITERATURE REVIEW..... | 13 |
| 2.1 | BUILDING'S FAÇADE AND SKIN..... | 13 |
| 2.1.1 | DIFFERENCE BETWEEN BUILDING'S FAÇADE AND SKIN | 13 |
| 2.1.2 | DOUBLE SKIN FACADE..... | 15 |
| 2.2 | ETHYLENE TETRAFLUORO ETHYLENE (ETFE) APPLICATIONS IN A DSF..... | 19 |
| 2.2.1 | DEFINITION AND BACKGROUND OF ETFE | 19 |
| 2.2.2 | BUILDING INTEGRATED PHOTOVOLTAICS | 29 |
| 2.2.3 | DYNAMIC SCREENS AND SHADING DEVICES..... | 35 |
| 2.3 | THERMAL COMFORT IN BUILDINGS | 44 |
| 2.3.1 | THERMAL COMFORT AND STATIC MODELS | 44 |
| 2.3.2 | THERMAL COMFORT AND ADAPTIVE MODELS | 50 |
| 2.4 | DAYLIGHTING IN BUILDINGS | 51 |
| 2.4.1 | DAYLIGHTING AND ARTIFICIAL LIGHTING | 51 |
| 2.4.2 | VISUAL COMFORT | 53 |
| 2.4.3 | DAYLIGHT CONTROL SYSTEMS | 54 |
| 2.5 | ETFE IN THE UAE | 57 |
| 2.6 | BIPVS IN THE UAE..... | 58 |
| 2.7 | DYNAMIC FACADES IN THE UAE..... | 61 |
| 2.8 | PREVIOUS GENERAL STUDIES ON ETFE APPLICATIONS..... | 65 |
| 2.9 | PREVIOUS STUDIES ON ETFE AND BIPV APPLICATIONS | 73 |
| 2.10 | PREVIOUS STUDIES ON ETFE AND DYNAMIC SHADE APPLICATIONS | 79 |
| 2.11 | PREVIOUS STUDIES ON DSF | 82 |
| 2.12 | SUMMARIZED LITERATURE REVIEW | 89 |
| 3 | METHODOLOGY AND RESEARCH STRUCTURE..... | 99 |
| 3.1 | INTRODUCTION..... | 99 |
| 3.2 | APPLICABLE METHODOLOGY TYPES | 99 |
| 3.3 | EXAMPLES OF RELATED STUDIES THAT USED LITERATURE REVIEW METHODOLOGY | 99 |

| | | |
|-------|------------------------------------------------------------------------------------------------------------------------------------------------|-----|
| 3.4 | ADVANTAGES AND DISADVANTAGES OF LITERATURE REVIEW METHODOLOGY | 100 |
| 3.5 | EXAMPLES OF RELATED STUDIES THAT USED NUMERICAL METHODOLOGY | 100 |
| 3.6 | ADVANTAGES AND DISADVANTAGES OF NUMERICAL METHODOLOGY | 101 |
| 3.7 | EXAMPLES OF RELATED STUDIES THAT USED FIELD MEASUREMENT/ EXPERIMENT METHODOLOGY | 101 |
| 3.8 | ADVANTAGES AND DISADVANTAGES OF FIELD MEASUREMENT/ EXPERIMENT METHODOLOGY | 102 |
| 3.9 | SELECTED METHODOLOGY FOR THE STUDY | 103 |
| 3.10 | ENERGY MODELLING SOFTWARE | 106 |
| 3.11 | BUILDING SELECTION | 106 |
| 3.12 | STUDIED BUILDING DESCRIPTION | 107 |
| 3.13 | SIMULATION SOFTWARE VALIDATION | 110 |
| 3.14 | METHODOLOGICAL MAP AND RESEARCH STRUCTURE | 112 |
| 4 | STUDIED BUILDING AND MODELS' SETUP | 116 |
| 4.1 | BASIC MODEL | 116 |
| 4.1.1 | BASIC SPACES MODELLING | 116 |
| 4.1.2 | PROJECT LOCATION AND WEATHER DATA | 117 |
| 4.1.3 | MATERIAL SET-UP | 121 |
| 4.1.4 | PROFILES DATABASE | 124 |
| 4.1.5 | THERMAL PROFILE | 125 |
| 4.1.6 | APACHE SIM APPLICATION - DYNAMIC SIMULATION | 128 |
| 4.2 | BUFFER DSF/CORRIDOR FACADE- SCENARIOS-01,02 AND 03: DOUBLE LAYERS ETFE CUSHION MODELLING IN IES VE | 129 |
| 4.3 | BUFFER DSF/ CORRIDOR FACADE -SCENARIO 04: TRIPLE LAYERS ETFE CUSHION MODELLING IN IES VE. | 133 |
| 4.4 | BUFFER DSF/ CORRIDOR FACADE -SCENARIOS 05 AND 06: TRIPLE LAYER ETFE CUSHION WITH TWO DIFFERENT FRIT PATTERN TYPES MODELLING IN IES VE | 134 |
| 4.5 | BUFFER DSF/ CORRIDOR FACADE -SCENARIOS 07 AND 08: BIPVS ON THE FRONT LAYER OF THE CUSHION | 137 |
| 4.6 | BUFFER DSF/ CORRIDOR FACADE -SCENARIO 09: DYNAMIC OPAQUE ETFE FOIL SHADE | 139 |
| 4.7 | BUFFER DSF/CORRIDOR FAÇADE- SCENARIO 10: DYNAMIC OPAQUE ETFE FOIL SHADE WITH BIPVS | 141 |
| 5 | RESULTS AND FINDINGS | 143 |
| 5.1 | BASIC MODEL | 143 |
| 5.1.1 | BASIC MODEL THERMAL COMFORT RESULTS | 143 |
| 5.1.2 | BASIC MODEL DAY LIGHT ANALYSIS | 144 |
| 5.1.3 | BASIC MODEL GLARE ANALYSIS | 150 |
| 5.1.4 | BASIC MODEL DAYLIGHT HARVESTING POTENTIAL ANALYSIS | 157 |
| 5.2 | BUFFER DSF/CORRIDOR FACADE- SCENARIOS-01,02 AND 03: DOUBLE LAYERS CUSHION WITH THREE DIFFERENT GAP DEPTHS | 159 |
| 5.2.1 | SCENARIOS 01,02 AND 03 CFD SIMULATION AND ANALYSIS | 159 |
| 5.2.2 | SCENARIOS 01,02 AND 03 ANNUAL ELECTRICAL CONSUMPTION RESULTS | 161 |
| 5.2.3 | SCENARIOS 01,02 AND 03 THERMAL COMFORT RESULTS | 163 |
| 5.2.4 | SCENARIOS 01,02 AND 03 DAYLIGHT ANALYSIS | 167 |
| 5.2.5 | SCENARIOS 01,02 AND 03 GLARE ANALYSIS | 175 |
| 5.2.6 | SCENARIOS 01,02 AND 03 DAYLIGHT HARVESTING POTENTIAL ANALYSIS | 185 |
| 5.3 | BUFFER DSF/ CORRIDOR FACADE -SCENARIO 04: TRIPLE LAYERS CUSHIONS | 186 |
| 5.3.1 | SCENARIOS 04 CFD SIMULATION AND ANALYSIS | 186 |

| | | |
|-------|------------------------------------------------------------------|-----|
| 5.3.2 | SCENARIOS 04 ANNUAL ELECTRICAL CONSUMPTION RESULTS | 188 |
| 5.3.3 | SCENARIOS 04 THERMAL COMFORT RESULTS..... | 189 |
| 5.3.4 | SCENARIO 04 DAYLIGHT ANALYSIS | 192 |
| 5.3.5 | SCENARIO 04 GLARE ANALYSIS | 201 |
| 5.3.6 | SCENARIO 04 DAYLIGHT HARVESTING POTENTIAL ANALYSIS | 211 |
| 5.4 | BUFFER DSF/ CORRIDOR FACADE -SCENARIOS 05 AND 06 ANALYSIS | 212 |
| 5.4.1 | SCENARIO 05 CFD SIMULATION AND ANALYSIS..... | 212 |
| 5.4.2 | SCENARIO 06 CFD SIMULATION AND ANALYSIS..... | 214 |
| 5.4.3 | SCENARIOS 05 AND 06 ELECTRICAL CONSUMPTION..... | 217 |
| 5.4.4 | SCENARIOS 05 AND 06 THERMAL COMFORT RESULTS | 219 |
| 5.4.5 | SCENARIOS 05 DAYLIGHT ANALYSIS | 223 |
| 5.4.6 | SCENARIOS 06 DAYLIGHT ANALYSIS | 230 |
| 5.4.7 | SCENARIO 05 GLARE ANALYSIS | 239 |
| 5.4.8 | SCENARIO 06 GLARE ANALYSIS | 249 |
| 5.4.9 | SCENARIOS 05 AND 06 DAYLIGHT HARVESTING POTENTIAL ANALYSIS | 259 |
| 5.5 | BUFFER DSF/ CORRIDOR FACADE -SCENARIOS 07 AND 08 ANALYSIS | 260 |
| 5.5.1 | SCENARIOS 07 AND 08 CFD SIMULATION AND ANALYSIS | 260 |
| 5.5.2 | SCENARIOS 07 AND 08 ELECTRICAL/ENERGY CONSUMPTION..... | 262 |
| 5.5.3 | SCENARIOS 07 AND 08 THERMAL COMFORT RESULTS | 265 |
| 5.5.4 | SCENARIOS 07 AND 08 DAYLIGHT ANALYSIS | 269 |
| 5.5.5 | SCENARIOS 07 AND 08 GLARE ANALYSIS..... | 277 |
| 5.5.6 | SCENARIOS 07 AND 08 DAYLIGHT HARVESTING POTENTIAL ANALYSIS | 287 |
| 5.6 | BUFFER DSF/ CORRIDOR FACADE -SCENARIO 09 ANALYSIS..... | 288 |
| 5.6.1 | SCENARIO 09 CFD SIMULATION AND ANALYSIS..... | 288 |
| 5.6.2 | SCENARIO 09 ELECTRICAL/ENERGY CONSUMPTION | 290 |
| 5.6.3 | SCENARIO 09 THERMAL COMFORT RESULTS..... | 293 |
| 5.6.4 | SCENARIOS 09 DAYLIGHT ANALYSIS | 297 |
| 5.6.5 | SCENARIO 09 GLARE ANALYSIS | 306 |
| 5.6.6 | SCENARIO 09 DAYLIGHT HARVESTING POTENTIAL ANALYSIS | 316 |
| 5.7 | BUFFER DSF/ CORRIDOR FACADE -SCENARIO 10 ANALYSIS..... | 317 |
| 5.7.1 | SCENARIO 10 CFD SIMULATION AND ANALYSIS..... | 317 |
| 5.7.2 | SCENARIO 10 ELECTRICAL/ENERGY CONSUMPTION | 319 |
| 5.7.3 | SCENARIO 10 THERMAL COMFORT RESULTS..... | 322 |
| 5.7.4 | SCENARIO 10 DAYLIGHT ANALYSIS | 326 |
| 5.7.5 | SCENARIO 10 GLARE ANALYSIS | 335 |
| 5.7.6 | SCENARIO 10 DAYLIGHT HARVESTING POTENTIAL ANALYSIS | 345 |
| 6 | CONCLUSION | 347 |
| 6.1 | CONCLUDING REMARKS | 347 |
| 6.2 | LINKING RESEARCH RESULTS TO PREVIOUS STUDIES..... | 351 |
| 6.3 | RECOMMENDATIONS FOR FUTURE STUDY | 352 |
| 7 | REFERENCES..... | 354 |

Table of Figures

| | |
|-----------------------------------------------------------------------------------------------------------------------------------------------------------------------------------------------------------------------------------------|----|
| FIGURE 1.1. TOTAL ELECTRICITY CONSUMPTION CHART IN 2013 (UAE MINISTRY OF ENERGY 2015). | 4 |
| FIGURE 2.1. ENVIRONMENTAL PRESSURE ON BUILDING ENVELOPE (MWASHA 2018)..... | 14 |
| FIGURE 2.2. AN EXAMPLE OF A BOX WINDOW SKIN ELEMENT WHICH CONTAINS MULTIPURPOSE MULTI LAYERS ELEMENTS INCLUDING DOUBLE-GLAZED UNIT, SINGLE-GLAZED UNIT, INTERNAL SHADING DEVICES AND EXTERNAL LOUVERS (KNAACK ET AL. 2007). | 14 |
| FIGURE 2.3. HEAT TRANSFER AND HEAT FLOW WITHIN A DSF THAT IS NATURALLY VENTILATED (CHAN AND CHOW 2014). | 15 |
| FIGURE 2.4. DSF CLASSIFICATION BASED ON VENTILATION STRATEGY (MOHAMMED AND ALIBABA 2015). | 17 |
| FIGURE 2.5. DSF CLASSIFICATION BASED ON DESIGN (MOHAMMED AND ALIBABA 2015)..... | 18 |
| FIGURE 2.6. ETFE CUSHIONS SCHEMATIC (LAMNATOU ET AL.2017). | 22 |
| FIGURE 2.7. ETFE CLAMPING ALUMINIUM FRAME (NOVUM STRUCTURE 2018)..... | 23 |
| FIGURE 2.8. WESTRAVEN BUILDING ETFE DETAIL (GAO 2012). | 24 |
| FIGURE 2.9. ALLIANZ ARENA STADIUM IN MUNICH WITH THE ETFE ENVELOPE (SCHITTICH 2012). | 25 |
| FIGURE 2.10. ALLIANZ ARENA STADIUM IN MUNICH WITH THE ETFE ENVELOPE (SCHITTICH 2012). | 25 |
| FIGURE 2.11. ALLIANZ ARENA ENVELOPE DETAIL (SCHITTICH 2012)..... | 26 |
| FIGURE 2.12. ALLIANZ ARENA STADIUM IN MUNICH WITH THE ETFE ENVELOPE (SCHITTICH 2012). | 27 |
| FIGURE 2.13. EDEN PROJECT LAYOUT AND AERIAL SHOT (SCHITTICH 2012). | 28 |
| FIGURE 2.14. EDEN PROJECT ENVELOPE DETAIL (SCHITTICH 2012). | 28 |
| FIGURE 2.15. BASIC PV CELL DIAGRAM (DAS 2014). | 30 |
| FIGURE 2.16. DOUBLE JUNCTION A-SI SOLAR CELL SECTION (AGRAWAL & TIWARI 2011)..... | 31 |
| FIGURE 2.17. REGION MAP OF ANNUAL SOLAR IRRADIATION LEVELS (DUBEY, SARVAIYA & SESHADRI 2013).... | 32 |
| FIGURE 2.18. REGION MAP OF PREDICTED ANNUAL PV GENERATED POWER BASED ON HIGHLY EFFICIENT PVS (C-SI) (DUBEY, SARVAIYA & SESHADRI 2013)..... | 33 |
| FIGURE 2.19. PV PANEL COOLING SYSTEM DIAGRAM (PENG, HERFATMANESH & LIU 2017)..... | 34 |
| FIGURE 2.20. COMPARISON BETWEEN THE OVERALL OUTPUT OF THE THREE EXPERIMENT CONDITIONS (PENG, HERFATMANESH & LIU 2017). | 35 |
| FIGURE 2.21. PROJECT KIEFER TECHNIC SHOWROOM (ARCHITONIC 2018). | 37 |
| FIGURE 2.22. PROJECT KIEFER TECHNIC SHOWROOM (ARCHITONIC 2018). | 37 |
| FIGURE 2.23. PROJECT KIEFER TECHNIC SHOWROOM (ARCHITONIC 2018). | 38 |
| FIGURE 2.24. DEBIS HEADQUARTERS PROJECT (COUNCIL ON TALL BUILDINGS AND URBAN HABITAT 2018)..... | 38 |
| FIGURE 2.25. DEBIS HEADQUARTERS PROJECT (COUNCIL ON TALL BUILDINGS AND URBAN HABITAT 2018)..... | 39 |
| FIGURE 2.26. DEBIS HEADQUARTERS PROJECT FAÇADE DETAIL (LAWRENCE BERKELEY NATIONAL LABORATORY 2006). | 39 |
| FIGURE 2.27. THE FLARE KINETIC FAÇADE SYSTEM (WHITE VOID 2008)..... | 40 |
| FIGURE 2.28. MODULAR DYNAMIC FAÇADE WHICH ALLOWS DIFFERENT POSITIONING FOR THE SHADES/SCREEN FOR VARIOUS PURPOSES (NAGY ET AL. 2016). | 42 |
| FIGURE 2.28.1. MODULAR DYNAMIC FAÇADE WHICH ALLOWS DIFFERENT POSITIONING FOR THE SHADES/SCREEN FOR VARIOUS PURPOSES (NAGY ET AL. 2016). | 43 |
| FIGURE 2.29. PNEUMATIC POSITIONING ACTUATOR (NAGY ET AL. 2016)..... | 43 |
| FIGURE 2.30. PSYCHROMETRIC CHART (LECHNER 2015). | 46 |

| | |
|--------------------------------------------------------------------------------------------------------------------------------------------------|----|
| FIGURE 2.31. PSYCHROMETRIC CHART (LECHNER 2015)..... | 47 |
| FIGURE 2.32. COMFORT ZONE IN THE PSYCHROMETRIC CHART (LECHNER 2015)..... | 48 |
| FIGURE 2.33. COMFORT ZONE IN THE PSYCHROMETRIC CHART CAN BE SHIFTED DEPENDING ON THE SEASON ACCORDING TO ASHRAE STANDARDS (LECHNER 2014)..... | 49 |
| FIGURE 2.34. VISIBLE LIGHT IN ELECTROMAGNETIC SPECTRUM (KITTLER, KOCIFAJ & DARULA 2012)..... | 51 |
| FIGURE 2.35. SUN PATH IN ABU DHABI AS SHOWN IN THE IES VE SOFTWARE WEATHER DATA (AUTHOR 2019).. | 52 |
| FIGURE 2.36. DAYLIGHT CONTROL SYSTEM (ROSSI ET AL. 2015)..... | 55 |
| FIGURE 2.37. DAYLIGHT CONTROL DIAGRAM WHERE EM IS THE REQUIRED ILLUMINANCE LEVEL AND EA,DL IS TOTAL ILLUMINANCE LEVEL(ROSSI ET AL. 2015)..... | 56 |
| FIGURE 2.38. YAS MALL ABU DHABI(YAS MALL 2019)..... | 57 |
| FIGURE 2.39. YAS MALL ABU DHABI(YAS MALL 2019)..... | 57 |
| FIGURE 2.40. DIRECT NORMAL SOLAR IRRADIATION IN THE UAE (RECREMA 2013)..... | 58 |
| FIGURE 2.41. MADAR CITY AERIAL VIEW (CONSTRUCTION WEEK ONLINE 2010). | 59 |
| FIGURE 2.42. ECO-VILLA IN MASDAR CITY (NAGRAJ 2015)..... | 60 |
| FIGURE 2.43. THE SUSTAINABLE CITY (THE SUSTAINABLE CITY 2019)..... | 60 |
| FIGURE 2.44. AL BAHR TOWER SCREEN DIFFERENT POSITIONS (REID 2013)..... | 62 |
| FIGURE 2.45. AL BAHR TOWER (COUNCIL ON TALL BUILDINGS AND URBAN HABITAT 2018)..... | 62 |
| FIGURE 2.26. THE APPLE STORE TERRACE WITH THE SOLAR WINGS (YOUNG 2017). | 63 |
| FIGURE 2.27. THE APPLE STORE TERRACE WITH THE SOLAR WINGS (YOUNG 2017). | 64 |
| FIGURE 2.28. DYNAMIC FAÇADE CONCEPT (HAMMAD & ABU-HIJLEH..... 2018)..... | 64 |
| FIGURE 2.29. 3D MODEL OF THE STUDIED DYNAMIC SHADE CONFIGURATIONS (HAMMAD & ABU-HIJLEH 2018)..... | 65 |
| FIGURE 2.30. NEW FOIL TYPES (CREMERS AND MARX2017)..... | 67 |
| FIGURE 2.31. LUMINANCE MAP FROM THE STUDY (MASIH, LAU AND CHILTON 2015)..... | 69 |
| FIGURE 2.32. MEMBRANE TEST SAMPLES (LIU ET AL. 2016)..... | 70 |
| FIGURE 2.33. EXPERIMENTAL MOCK-UP (ZHAO ET AL. 2015)..... | 74 |
| FIGURE 2.34. SYSTEM STRUCTURE (HU ET AL. 2016). | 76 |
| FIGURE 2.35. TEMPERATURE DISTRIBUTION (HU ET AL. 2015)..... | 77 |
| FIGURE 2.36. DOUBLE LAYER ETFE WITH PVS ON BOTTOM LAYER (HU ET AL. 2017). | 78 |
| FIGURE 2.37. DOUBLE LAYER ETFE WITH PVS ON TOP LAYER (HU ET AL. 2017)..... | 79 |
| FIGURE 2.38. TRIPLE LAYER ETFE WITH PVS ON MIDDLE LAYER (HU ET AL. 2017) | 79 |
| FIGURE 2.39. STUDIED PATTERN WITH DIFFERENT TRANSPARENCY PERCENTAGE (MICHAEL, GREGORIOU AND KALOGIROU 2017)..... | 80 |
| FIGURE 2.40. DIFFERENT CUSHIONS ANGELS (MICHAEL, GREGORIOU AND KALOGIROU 2017)..... | 80 |
| FIGURE 2.41. ROTATION OPTIONS (MICHAEL, GREGORIOU AND KALOGIROU 2017)..... | 81 |
| FIGURE 2.42. SCHEMATIC DIAGRAM OF THE SYSTEM (PENG ET AL. 2016). | 82 |
| FIGURE 2.43. SCHEMATIC DIAGRAM OF THE HEAT TRANSFER AND AIR FLOW MECHANISM IN THE BASIC MODEL (BARBOSA, IP &SOUTHALL 2015)..... | 83 |
| FIGURE 2.44. DSF OPENING CONDITIONS (KIM ET.AL 2018). | 84 |
| FIGURE 2.45. SIMULATED MODELS IN ENERGY PLUS (KIM ET.AL 2018)..... | 84 |
| FIGURE 2.46. SCHEMATIC DIAGRAM OF THE BIPV-DSF OPTION (LUO ET.AL 2018)..... | 85 |
| FIGURE 2.47. SCHEMATIC DIAGRAM OF THE STUDIED ROOM (YANG ET.AL 2016)..... | 87 |

| | |
|-----------------------------------------------------------------------------------------------------------------|-----|
| FIGURE 2.48. STUDIED DSF DETAILS (JOE ET.AL 2014). | 87 |
| FIGURE 3.1. RESULTS COMPARISON BETWEEN THE DIFFERENT PROGRAMS (REEVES, OLBINA & ISSA 2012). | 105 |
| FIGURE 3.2. RECEPTION BUILDING PLAN (AUTHOR 2019). | 108 |
| FIGURE 3.3. RECEPTION BUILDING 3D PLAN FROM THE REVIT MODEL (AUTHOR 2019). | 108 |
| FIGURE 3.4. RECEPTION BUILDING SECTION (AUTHOR 2019). | 109 |
| FIGURE 3.5. BUILDING WALL SECTION (AUTHOR 2019). | 109 |
| FIGURE 3.6. COMPARISON BETWEEN SIMULATED AND ACTUAL ELECTRICAL LOADS (AUTHOR 2019). | 111 |
| FIGURE 3.7. TOTAL ANNUAL ELECTRICITY CONSUMPTION RESULTS IN IES VE (BY THE AUTHOR). | 111 |
| FIGURE 3.8. METHODOLOGICAL MAP (AUTHOR 2019). | 112 |
| FIGURE 3.9. SCENARIOS RESEARCH STRUCTURE (AUTHOR 2019). | 113 |
| FIGURE 4.1. RECEPTION-BUILDING MODEL IN IES VE SOFTWARE (AUTHOR 2019). | 116 |
| FIGURE 4.2. RECEPTION-BUILDING MODEL IN IES VE SOFTWARE (AUTHOR 2019). | 116 |
| FIGURE 4.3. RECEPTION-BUILDING MODEL COMPONENTS IN IES VE SOFTWARE (AUTHOR 2019). | 117 |
| FIGURE 4.4. BASIC LOCATION DATA AS SHOWN IN THE IES VE SOFTWARE (AUTHOR 2019). | 117 |
| FIGURE 4.5. PROJECT LOCATION IN YAS ISLAND NEAR THE CITY OF ABU DHABI (GOOGLE MAP 2018). | 118 |
| FIGURE 4.6. PROJECT LOCATION IN YAS ISLAND AND THE WEATHER STATION LOCATION (GOOGLE MAP 2018). | 118 |
| | 118 |
| FIGURE 4.7. BASIC DESIGN DATA AS SHOWN IN THE IES VE SOFTWARE (AUTHOR 2019). | 119 |
| FIGURE 4.8. SUN PATH AS SHOWN IN THE IES VE SOFTWARE (AUTHOR 2019). | 119 |
| FIGURE 4.9. SUN PATH WITH RELATION TO THE BUILDING ORIENTATION IN IES-VE (AUTHOR 2019). | 120 |
| FIGURE 4.10. BASIC DESIGN DATA AS SHOWN IN THE IES VE SOFTWARE (AUTHOR 2019). | 120 |
| FIGURE 4.11. INSERTED EXTERNAL WALL LAYERS IN THE ADJUSTED CONSTRUCTION TEMPLATE IN IES-VE (AUTHOR 2019). | 121 |
| FIGURE 4.12. EXTERNAL WALL INSULATION (CELLULAR GLASS) PROPERTIES IN THE TECHNICAL SPECS (DUNN ET AL. 2017). | 122 |
| FIGURE 4.13. AUTOCLAVED AERATED CONCRETE BLOCKS (AAC) PROPERTIES IN THE TECHNICAL SPECS (DUNN ET AL. 2017). | 122 |
| FIGURE 4.14. INSERTED ROOF LAYERS IN THE ADJUSTED CONSTRUCTION TEMPLATE IN IES-VE (AUTHOR 2019). | 122 |
| | 122 |
| FIGURE 4.15. ROOF INSULATION PROPERTIES IN THE TECHNICAL SPECS (DUNN ET AL. 2017). | 123 |
| FIGURE 4.16. INSERTED DOUBLE GLAZED UNIT WINDOWS IN THE ADJUSTED CONSTRUCTION TEMPLATE IN IES-VE (AUTHOR 2019). | 123 |
| FIGURE 4.17. GLAZING PROPERTIES IN THE TECHNICAL SPECS (DUNN ET AL. 2017). | 123 |
| FIGURE 4.18. INSERTED APPRO DAILY PROFILE IN IES-VE (AUTHOR 2019). | 124 |
| FIGURE 4.19. INSERTED APPRO WEEKLY PROFILE IN IES-VE (AUTHOR 2019). | 124 |
| FIGURE 4.20. INSERTED SPACE CONDITIONS PROPERTIES IN IES-VE (AUTHOR 2019). | 125 |
| FIGURE 4.21. INSERTED COMPUTER (MISCELLANEOUS EQUIPMENT) INTERNAL GAIN DATA IN IES-VE (AUTHOR 2019). | 126 |
| FIGURE 4.22. INSERTED LIGHTING INTERNAL GAIN DATA IN IES-VE (AUTHOR 2019). | 126 |
| FIGURE 4.23. INSERTED PEOPLE INTERNAL GAIN DATA IN IES-VE (AUTHOR 2019). | 127 |
| FIGURE 4.24. INSERTED AIR EXCHANGE PROPERTIES IN IES-VE (AUTHOR 2019). | 127 |
| FIGURE 4.25. INSERTED OA PARAMETERS IN IES-VE (AUTHOR 2019). | 127 |
| FIGURE 4.26. INSERTED APACHE SIM PARAMETERS IN IES-VE (AUTHOR 2019). | 128 |

| | |
|----------------------------------------------------------------------------------------------------------------------------------------------------------------------------------------------------------------------------------------------------|-----|
| FIGURE 4.27. ETFE DOUBLE LAYERS CUSHION LAYERS PARAMETERS AS INSERTED IN THE CONSTRUCTION TEMPLATE (3 SCENARIOS) IN IES-VE (AUTHOR 2019)..... | 130 |
| FIGURE 4.28. ETFE CUSHIONS IN IES-VE (AUTHOR 2019)..... | 131 |
| FIGURE 4.29. ETFE CUSHIONS IN IES-VE (AUTHOR 2019)..... | 131 |
| FIGURE 4.30. BUILDING WALL SECTION WHICH SHOWS THE CUSHION AND DSF POSITIONING (AUTHOR 2019)..... | 132 |
| FIGURE 4.31. BUILDING WALL SECTION WHICH SHOWS THE CUSHION POSITIONING (AUTHOR 2019)..... | 133 |
| FIGURE 4.32. ETFE TRIPLE LAYERS CUSHION AS INSERTED IN THE CONSTRUCTION TEMPLATE IN IES-VE (AUTHOR 2019)..... | 134 |
| FIGURE 4.33. VARIOUS FRIT PATTERNS WITH THEIR COVERAGE RATIO (O'DONNELL 2015)..... | 135 |
| FIGURE 4.34. ETFE TRIPLE LAYERS CUSHION AS INSERTED IN THE CONSTRUCTION TEMPLATE. SCENARIO05 ON THE TOP AND SCENARIO 06 ON THE BOTTOM (AUTHOR 2019)..... | 136 |
| FIGURE 4.35. BUILDING WALL SECTION WHICH SHOWS THE CUSHION POSITIONING (BY THE AUTHOR)..... | 136 |
| FIGURE 4.36. SCENARIO 07 PV PANEL TYPE IN IES-VE (AUTHOR 2019)..... | 137 |
| FIGURE 4.37. SCENARIO 08 PV PANEL TYPE IN IES-VE (AUTHOR 2019)..... | 137 |
| FIGURE 4.38. BUILDING WALL SECTION WHICH SHOWS THE CUSHION POSITIONING (AUTHOR 2019)..... | 138 |
| FIGURE 4.39. BIPVS AS MODELLED ON THE EASTERN FAÇADE CUSHIONS IN IES-VE (BY THE AUTHOR)..... | 138 |
| FIGURE 4.40. BIPVS AS MODELLED ON THE WESTERN FAÇADE CUSHIONS IN IES-VE (AUTHOR 2019)..... | 138 |
| FIGURE 4.41. EASTERN SHADE OPERATION PROFILE IN IES-VE (AUTHOR 2019)..... | 139 |
| FIGURE 4.42. WESTERN SHADE OPERATION PROFILE IN IES-VE (AUTHOR 2019)..... | 140 |
| FIGURE 4.43. BUILDING WALL SECTION WHICH SHOWS THE CUSHION POSITIONING (AUTHOR 2019)..... | 140 |
| FIGURE 4.44. BUILDING WALL SECTION WHICH SHOWS THE CUSHION POSITIONING (AUTHOR 2019)..... | 141 |
| FIGURE 5.1. DAYLIGHT FACTOR SIMULATION RESULTS ON THE 21ST OF MARCH (AUTHOR 2019)..... | 145 |
| FIGURE 5.2. DAYLIGHT FACTOR SIMULATION RESULTS ON THE 21ST OF JUNE (AUTHOR 2019)..... | 146 |
| FIGURE 5.3. DAYLIGHT FACTOR SIMULATION RESULTS ON THE 23RD OF SEPTEMBER (AUTHOR 2019)..... | 147 |
| FIGURE 5.4. DAYLIGHT FACTOR SIMULATION RESULTS ON THE 21ST OF DECEMBER (AUTHOR 2019)..... | 148 |
| FIGURE 5.5. SUMMARY OF THE BASIC MODEL DAYLIGHTING ILLUMINANCE (LUX) RESULTS (AUTHOR 2019)..... | 149 |
| FIGURE 5.6. SUMMARY OF THE BASIC MODEL DF RESULTS (AUTHOR 2019)..... | 149 |
| FIGURE 5.7. EYE/CAMERA LOCATION IN BOTH ROOMS. IES VE CONSIDER NEGATIVE ANGLES ON THE RIGHT OF NADIR AND POSITIVE ANGLES ON LEFT OF IT (AUTHOR 2019)..... | 150 |
| FIGURE 5.8. WAITING ROOM LUMINANCE MAP IN ALL CASES INCLUDING 21ST OF MARCH CASE ON THE TOP LEFT, 21ST OF JUNE CASE ON THE TOP RIGHT, 23RD OF SEPTEMBER CASE ON THE BOTTOM LEFT AND 21ST OF DECEMBER CASE ON THE BOTTOM RIGHT (AUTHOR 2019)..... | 151 |
| FIGURE 5.9. RECEPTION ROOM LUMINANCE MAP IN ALL CASES INCLUDING 21ST OF MARCH CASE ON THE TOP LEFT, 21ST OF JUNE CASE ON THE TOP RIGHT, 23RD OF SEPTEMBER CASE ON THE BOTTOM LEFT AND 21ST OF DECEMBER CASE ON THE BOTTOM RIGHT (AUTHOR 2019)..... | 154 |
| FIGURE 5.10. RECOMMENDED DIMMING PROFILE WHICH IS ASSOCIATED WITH DAYLIGHT SENSORS (IES 2018)..... | 157 |
| FIGURE 5.11. FORMULA DAILY PROFILE AS INSERTED IN IES VE (AUTHOR 2019)..... | 158 |
| FIGURE 5.12. CFD ANALYSIS OF NORTHER, EASTERN AND WESTERN CUSHIONS IN MICROFLO (AUTHOR 2019)..... | 159 |
| FIGURE 5.13. CFD ANALYSIS OF THE EASTERN CUSHIONS IN IES VE (AUTHOR 2019)..... | 160 |
| FIGURE 5.14. COMBINED DIAGRAM OF THE BASIC MODEL RESULTS AND THE THREE SCENARIOS RESULTS (AUTHOR 2019)..... | 162 |
| FIGURE 5.15. COMBINED DIAGRAM OF THE BASIC MODEL RESULTS AND THE THREE SCENARIOS RESULTS (AUTHOR 2019)..... | 165 |

| | |
|--------------------------------------------------------------------------------------------------------------------------------------------------------------------------------------------------------------------------------------------------------------------|-----|
| FIGURE 5.16. COMBINED DIAGRAM OF THE BASIC MODEL RESULTS AND THE THREE SCENARIOS RESULTS (AUTHOR 2019)..... | 166 |
| FIGURE 5.17. SCENARIOS 01,02 AND 03 DAYLIGHT FACTOR SIMULATION RESULTS ON THE 21ST OF MARCH (AUTHOR 2019)..... | 167 |
| FIGURE 5.18. SCENARIOS 01,02 AND 03 DAYLIGHT FACTOR SIMULATION RESULTS ON THE 21ST OF JUNE (AUTHOR 2019)..... | 168 |
| FIGURE 5.19. SCENARIOS 01,02 AND 03 DAYLIGHT FACTOR SIMULATION RESULTS ON THE 23 RD OF SEPTEMBER (AUTHOR 2019)..... | 169 |
| FIGURE 5.20 SCENARIOS 01,02 AND 03 DAYLIGHT FACTOR SIMULATION RESULTS ON THE 21ST OF DECEMBER (AUTHOR 2019)..... | 170 |
| FIGURE 5.21. COMBINED DIAGRAM OF THE BASIC MODEL DI RESULTS AND THE THREE SCENARIOS DI RESULTS IN WAITING ROOM (AUTHOR 2019). | 171 |
| FIGURE 5.22. COMBINED DIAGRAM OF THE BASIC MODEL DI RESULTS AND THE THREE SCENARIOS DI RESULTS IN RECEPTION ROOM (AUTHOR 2019). | 172 |
| FIGURE 5.23. COMBINED DIAGRAM OF THE BASIC MODEL DF RESULTS AND THE THREE SCENARIOS DF RESULTS IN THE WAITING ROOM (AUTHOR 2019)..... | 172 |
| FIGURE 5.24. COMBINED DIAGRAM OF THE BASIC MODEL DF RESULTS AND THE THREE SCENARIOS DF RESULTS IN RECEPTION ROOM (AUTHOR 2019)..... | 173 |
| FIGURE 5.25. WAITING ROOM LUMINANCE MAPS ON THE 21ST OF MARCH (TOP IMAGES) AND 21ST OF JUNE (BOTTOM IMAGES). THE IMAGES ON THE LEFT SHOW SCENARIOS01,02 AND 03 RESULTS AND THE IMAGES ON THE RIGHT SHOW THE BASIC MODEL RESULTS (AUTHOR 2019). | 175 |
| FIGURE 5.26. WAITING ROOM LUMINANCE MAPS ON THE 23RD OF SEPTEMBER (TOP IMAGES) AND 21ST OF DECEMBER (BOTTOM IMAGES). THE IMAGES ON THE LEFT SHOW SCENARIOS01,02 AND 03 RESULTS AND THE IMAGES ON THE RIGHT SHOW THE BASIC MODEL RESULTS (AUTHOR 2019)..... | 176 |
| FIGURE 5.27. RECEPTION ROOM LUMINANCE MAPS ON THE 21ST OF MARCH (TOP IMAGES) AND 21ST OF JUNE (BOTTOM IMAGES). THE IMAGES ON THE LEFT SHOW SCENARIOS01,02 AND 03 RESULTS AND THE IMAGES ON THE RIGHT SHOW THE BASIC MODEL RESULTS (AUTHOR 2019). | 180 |
| FIGURE 5.28. RECEPTION ROOM LUMINANCE MAPS ON THE 23RD OF SEPTEMBER (TOP IMAGES) AND 21ST OF DECEMBER (BOTTOM IMAGES). THE IMAGES ON THE LEFT SHOW SCENARIOS01,02 AND 03 RESULTS AND THE IMAGES ON THE RIGHT SHOW THE BASIC MODEL RESULTS (AUTHOR 2019)..... | 181 |
| FIGURE 5.29. CFD ANALYSIS OF NORTHER, EASTERN AND WESTERN CUSHIONS IN MICROFLO (AUTHOR 2019). 186 | |
| FIGURE 5.30. CFD ANALYSIS OF THE EASTERN CUSHIONS IN IES VE (AUTHOR 2019). | 187 |
| FIGURE 5.31. COMBINED DIAGRAM OF THE BASIC MODEL RESULTS AND THE FIRST FOUR SCENARIOS RESULTS (AUTHOR 2019)..... | 188 |
| FIGURE 5.32. COMBINED DIAGRAM OF THE BASIC MODEL RESULTS AND THE FIRST FOUR SCENARIOS RESULTS (AUTHOR 2019)..... | 190 |
| FIGURE 5.33. COMBINED DIAGRAM OF THE BASIC MODEL RESULTS AND THE FIRST FOUR SCENARIOS RESULTS (AUTHOR 2019)..... | 191 |
| FIGURE 5.34. SCENARIO 04 DAYLIGHT FACTOR SIMULATION RESULTS ON THE 21ST OF MARCH (AUTHOR 2019). | 192 |
| FIGURE 5.35. SCENARIO 04 DAYLIGHT FACTOR SIMULATION RESULTS ON THE 21ST OF JUNE (AUTHOR 2019). . | 194 |
| FIGURE 5.36. SCENARIO 04 DAYLIGHT FACTOR SIMULATION RESULTS ON THE 23RD OF SEPTEMBER (AUTHOR 2019). | 195 |

| | |
|-----------------------------------------------------------------------------------------------------------------------------------------------------------------------------------------------------------------------------------------------------------|-----|
| FIGURE 5.37. SCENARIOS-04 DAYLIGHT FACTOR SIMULATION RESULTS ON THE 21ST OF DECEMBER (AUTHOR 2019). | 196 |
| FIGURE 5.38. COMBINED DIAGRAM OF THE BASIC MODEL DI RESULTS AND THE FOUR SCENARIOS DI RESULTS IN WAITING ROOM (AUTHOR 2019) | 197 |
| FIGURE 5.39. COMBINED DIAGRAM OF THE BASIC MODEL DI RESULTS AND THE FOUR SCENARIOS DI RESULTS IN RECEPTION ROOM (AUTHOR 2019) | 198 |
| FIGURE 5.40. COMBINED DIAGRAM OF THE BASIC MODEL DF RESULTS AND THE FOUR SCENARIOS DF RESULTS IN RECEPTION ROOM (AUTHOR 2019) | 198 |
| FIGURE 5.41. COMBINED DIAGRAM OF THE BASIC MODEL DF RESULTS AND THE FOUR SCENARIOS DF RESULTS IN THE WAITING ROOM (AUTHOR 2019) | 199 |
| FIGURE 5.42. WAITING ROOM LUMINANCE MAPS ON THE 21ST OF MARCH (TOP IMAGES) AND 21ST OF JUNE (BOTTOM IMAGES). THE IMAGES ON THE LEFT SHOW SCENARIO 04 RESULTS AND THE IMAGES ON THE RIGHT SHOW THE BASIC MODEL RESULTS (AUTHOR 2019) | 201 |
| FIGURE 5.43. WAITING ROOM LUMINANCE MAPS ON THE 23RD OF SEPTEMBER (TOP IMAGES) AND 21ST OF DECEMBER (BOTTOM IMAGES). THE IMAGES ON THE LEFT SHOW SCENARIO 04 RESULTS AND THE IMAGES ON THE RIGHT SHOW THE BASIC MODEL RESULTS (AUTHOR 2019) | 202 |
| FIGURE 5.44. RECEPTION ROOM LUMINANCE MAPS ON THE 21ST OF MARCH (TOP IMAGES) AND 21ST OF JUNE (BOTTOM IMAGES). THE IMAGES ON THE LEFT SHOW SCENARIOS 01, 02 AND 03 RESULTS AND THE IMAGES ON THE RIGHT SHOW THE BASIC MODEL RESULTS (AUTHOR 2019) | 206 |
| FIGURE 5.45. RECEPTION ROOM LUMINANCE MAPS ON THE 23RD OF SEPTEMBER (TOP IMAGES) AND 21ST OF DECEMBER (BOTTOM IMAGES). THE IMAGES ON THE LEFT SHOW SCENARIOS 01, 02 AND 03 RESULTS AND THE IMAGES ON THE RIGHT SHOW THE BASIC MODEL RESULTS (AUTHOR 2019) | 207 |
| FIGURE 5.46. CFD ANALYSIS OF NORTHER, EASTERN AND WESTERN CUSHIONS IN MICROFLO (AUTHOR 2019) | 212 |
| FIGURE 5.47. CFD ANALYSIS OF THE EASTERN CUSHIONS IN IES VE (AUTHOR 2019) | 213 |
| FIGURE 5.48. CFD ANALYSIS OF NORTHER, EASTERN AND WESTERN CUSHIONS IN MICROFLO (AUTHOR 2019) | 215 |
| FIGURE 5.49. CFD ANALYSIS OF THE EASTERN CUSHIONS IN IES VE (AUTHOR 2019) | 215 |
| FIGURE 5.50. COMBINED DIAGRAM OF THE BASIC MODEL RESULTS AND THE FIRST SIX SCENARIOS RESULTS (AUTHOR 2019) | 217 |
| FIGURE 5.51. COMBINED DIAGRAM OF THE BASIC MODEL RESULTS AND THE FIRST SIX SCENARIOS RESULTS (AUTHOR 2019) | 220 |
| FIGURE 5.52. COMBINED DIAGRAM OF THE BASIC MODEL RESULTS AND THE FIRST SIX SCENARIOS RESULTS (AUTHOR 2019) | 222 |
| FIGURE 5.53. SCENARIO 05 DAYLIGHT FACTOR SIMULATION RESULTS ON THE 21ST OF MARCH (AUTHOR 2019). | 223 |
| FIGURE 5.54. SCENARIO 05 DAYLIGHT FACTOR SIMULATION RESULTS ON THE 21ST OF JUNE (AUTHOR 2019) | 224 |
| FIGURE 5.55. SCENARIO 05 DAYLIGHT FACTOR SIMULATION RESULTS ON THE 23RD OF SEPTEMBER (AUTHOR 2019) | 225 |
| FIGURE 5.56. SCENARIOS-05 DAYLIGHT FACTOR SIMULATION RESULTS ON THE 21ST OF DECEMBER (AUTHOR 2019) | 226 |
| FIGURE 5.57. COMBINED DIAGRAM OF THE BASIC MODEL DI RESULTS AND THE SIX SCENARIOS DI RESULTS IN WAITING ROOM (AUTHOR 2019) | 227 |
| FIGURE 5.58. COMBINED DIAGRAM OF THE BASIC MODEL DI RESULTS AND THE SIX SCENARIOS DI RESULTS IN RECEPTION ROOM (AUTHOR 2019) | 227 |

| | |
|-----------------------------------------------------------------------------------------------------------------------------------------------------------------------------------------------------------------------------------------------------------|-----|
| FIGURE 5.59. COMBINED DIAGRAM OF THE BASIC MODEL DF RESULTS AND THE SIX SCENARIOS DF RESULTS IN THE WAITING ROOM (AUTHOR 2019). | 228 |
| FIGURE 5.60. COMBINED DIAGRAM OF THE BASIC MODEL DF RESULTS AND THE SIX SCENARIOS DF RESULTS IN RECEPTION ROOM (AUTHOR 2019). | 228 |
| FIGURE 5.61. SCENARIO 06 DAYLIGHT FACTOR SIMULATION RESULTS ON THE 21ST OF MARCH (AUTHOR 2019). | 230 |
| FIGURE 5.62. SCENARIO 06 DAYLIGHT FACTOR SIMULATION RESULTS ON THE 21ST OF JUNE (AUTHOR 2019). | 232 |
| FIGURE 5.63. SCENARIO 06 DAYLIGHT FACTOR SIMULATION RESULTS ON THE 23RD OF SEPTEMBER (AUTHOR 2019). | 233 |
| FIGURE 5.64. SCENARIOS 06 DAYLIGHT FACTOR SIMULATION RESULTS ON THE 21ST OF DECEMBER (AUTHOR 2019). | 234 |
| FIGURE 5.65. COMBINED DIAGRAM OF THE BASIC MODEL DI RESULTS AND THE SIX SCENARIOS DI RESULTS IN WAITING ROOM (AUTHOR 2019). | 235 |
| FIGURE 5.66. COMBINED DIAGRAM OF THE BASIC MODEL DI RESULTS AND THE SIX SCENARIOS DI RESULTS IN RECEPTION ROOM (AUTHOR 2019). | 236 |
| FIGURE 5.67. COMBINED DIAGRAM OF THE BASIC MODEL DF RESULTS AND THE SIX SCENARIOS DF RESULTS IN THE WAITING ROOM (AUTHOR 2019). | 236 |
| FIGURE 5.68. COMBINED DIAGRAM OF THE BASIC MODEL DF RESULTS AND THE SIX SCENARIOS DF RESULTS IN RECEPTION ROOM (AUTHOR 2019). | 237 |
| FIGURE 5.69. WAITING ROOM LUMINANCE MAPS ON THE 21ST OF MARCH (TOP IMAGES) AND 21ST OF JUNE (BOTTOM IMAGES). THE IMAGES ON THE LEFT SHOW SCENARIO 04 RESULTS AND THE IMAGES ON THE RIGHT SHOW THE BASIC MODEL RESULTS (AUTHOR 2019). | 239 |
| FIGURE 5.70. WAITING ROOM LUMINANCE MAPS ON THE 23RD OF SEPTEMBER (TOP IMAGES) AND 21ST OF DECEMBER (BOTTOM IMAGES). THE IMAGES ON THE LEFT SHOW SCENARIO 04 RESULTS AND THE IMAGES ON THE RIGHT SHOW THE BASIC MODEL RESULTS (AUTHOR 2019). | 240 |
| FIGURE 5.71. RECEPTION ROOM LUMINANCE MAPS ON THE 21ST OF MARCH (TOP IMAGES) AND 21ST OF JUNE (BOTTOM IMAGES). THE IMAGES ON THE LEFT SHOW SCENARIOS 01,02 AND 03 RESULTS AND THE IMAGES ON THE RIGHT SHOW THE BASIC MODEL RESULTS (AUTHOR 2019). | 244 |
| FIGURE 5.72. RECEPTION ROOM LUMINANCE MAPS ON THE 23RD OF SEPTEMBER (TOP IMAGES) AND 21ST OF DECEMBER (BOTTOM IMAGES). THE IMAGES ON THE LEFT SHOW SCENARIOS 01,02 AND 03 RESULTS AND THE IMAGES ON THE RIGHT SHOW THE BASIC MODEL RESULTS (AUTHOR 2019). | 245 |
| FIGURE 5.73. WAITING ROOM LUMINANCE MAPS ON THE 21ST OF MARCH (TOP IMAGES) AND 21ST OF JUNE (BOTTOM IMAGES). THE IMAGES ON THE LEFT SHOW SCENARIO 04 RESULTS AND THE IMAGES ON THE RIGHT SHOW THE BASIC MODEL RESULTS (AUTHOR 2019). | 249 |
| FIGURE 5.74. WAITING ROOM LUMINANCE MAPS ON THE 23RD OF SEPTEMBER (TOP IMAGES) AND 21ST OF DECEMBER (BOTTOM IMAGES). THE IMAGES ON THE LEFT SHOW SCENARIO 04 RESULTS AND THE IMAGES ON THE RIGHT SHOW THE BASIC MODEL RESULTS (AUTHOR 2019). | 250 |
| FIGURE 5.75. RECEPTION ROOM LUMINANCE MAPS ON THE 21ST OF MARCH (TOP IMAGES) AND 21ST OF JUNE (BOTTOM IMAGES). THE IMAGES ON THE LEFT SHOW SCENARIOS 01,02 AND 03 RESULTS AND THE IMAGES ON THE RIGHT SHOW THE BASIC MODEL RESULTS (AUTHOR 2019). | 254 |
| FIGURE 5.76. RECEPTION ROOM LUMINANCE MAPS ON THE 23RD OF SEPTEMBER (TOP IMAGES) AND 21ST OF DECEMBER (BOTTOM IMAGES). THE IMAGES ON THE LEFT SHOW SCENARIOS 01,02 AND 03 RESULTS AND THE IMAGES ON THE RIGHT SHOW THE BASIC MODEL RESULTS (AUTHOR 2019). | 255 |
| FIGURE 5.77. CFD ANALYSIS OF NORTHER, EASTERN AND WESTERN CUSHIONS IN MICROFLO (AUTHOR 2019). | 260 |

| | |
|-----------------------------------------------------------------------------------------------------------------------------------------------------------------------------------------------------------------------------------------------------------|-----|
| FIGURE 5.78. CFD ANALYSIS OF THE EASTERN CUSHIONS IN IES VE (SUTHOR 2019). | 261 |
| FIGURE 5.79. COMBINED DIAGRAM OF THE BASIC MODEL RESULTS AND THE FIRST EIGHT SCENARIOS RESULTS (AUTHOR 2019). | 263 |
| FIGURE 5.80. COMBINED DIAGRAM OF THE BASIC MODEL RESULTS AND THE FIRST EIGHT SCENARIOS RESULTS (AUTHOR 2019). | 266 |
| FIGURE 5.81. COMBINED DIAGRAM OF THE BASIC MODEL RESULTS AND THE FIRST EIGHT SCENARIOS RESULTS (AUTHOR 2019). | 268 |
| FIGURE 5.82. SCENARIOS 07 AND 08 DAYLIGHT FACTOR SIMULATION RESULTS ON THE 21ST OF MARCH (AUTHOR 2019). | 269 |
| FIGURE 5.83. SCENARIOS 07 AND 08 DAYLIGHT FACTOR SIMULATION RESULTS ON THE 21ST OF JUNE (AUTHOR 2019). | 270 |
| FIGURE 5.84. SCENARIOS 07 AND 08 DAYLIGHT FACTOR SIMULATION RESULTS ON THE 23RD OF SEPTEMBER (AUTHOR 2019). | 271 |
| FIGURE 5.85. SCENARIOS 07 AND 08 DAYLIGHT FACTOR SIMULATION RESULTS ON THE 21ST OF DECEMBER (AUTHOR 2019). | 272 |
| FIGURE 5.86. COMBINED DIAGRAM OF THE BASIC MODEL DI RESULTS AND THE EIGHT SCENARIOS DI RESULTS IN WAITING ROOM (AUTHOR 2019). | 273 |
| FIGURE 5.87. COMBINED DIAGRAM OF THE BASIC MODEL DI RESULTS AND THE EIGHT SCENARIOS DI RESULTS IN RECEPTION ROOM (AUTHOR 2019). | 274 |
| FIGURE 5.88. COMBINED DIAGRAM OF THE BASIC MODEL DF RESULTS AND THE EIGHT SCENARIOS DF RESULTS IN RECEPTION ROOM (AUTHOR 2019). | 274 |
| FIGURE 5.89. COMBINED DIAGRAM OF THE BASIC MODEL DF RESULTS AND THE EIGHT SCENARIOS DF RESULTS IN THE WAITING ROOM (AUTHOR 2019). | 275 |
| FIGURE 5.90. WAITING ROOM LUMINANCE MAPS ON THE 21ST OF MARCH (TOP IMAGES) AND 21ST OF JUNE (BOTTOM IMAGES). THE IMAGES ON THE LEFT SHOW SCENARIO 04 RESULTS AND THE IMAGES ON THE RIGHT SHOW THE BASIC MODEL RESULTS (AUTHOR 2019). | 277 |
| FIGURE 5.91. WAITING ROOM LUMINANCE MAPS ON THE 23RD OF SEPTEMBER (TOP IMAGES) AND 21ST OF DECEMBER (BOTTOM IMAGES). THE IMAGES ON THE LEFT SHOW SCENARIO 04 RESULTS AND THE IMAGES ON THE RIGHT SHOW THE BASIC MODEL RESULTS (AUTHOR 2019). | 278 |
| FIGURE 5.92. RECEPTION ROOM LUMINANCE MAPS ON THE 21ST OF MARCH (TOP IMAGES) AND 21ST OF JUNE (BOTTOM IMAGES). THE IMAGES ON THE LEFT SHOW SCENARIOS 01,02 AND 03 RESULTS AND THE IMAGES ON THE RIGHT SHOW THE BASIC MODEL RESULTS (AUTHOR 2019). | 282 |
| FIGURE 5.93. RECEPTION ROOM LUMINANCE MAPS ON THE 23RD OF SEPTEMBER (TOP IMAGES) AND 21ST OF DECEMBER (BOTTOM IMAGES). THE IMAGES ON THE LEFT SHOW SCENARIOS 01,02 AND 03 RESULTS AND THE IMAGES ON THE RIGHT SHOW THE BASIC MODEL RESULTS (AUTHOR 2019). | 283 |
| FIGURE 5.93. CFD ANALYSIS OF NORTHER, EASTERN AND WESTERN CUSHIONS IN MICROFLO (AUTHOR 2019). | 288 |
| FIGURE 5.94. CFD ANALYSIS OF THE EASTERN CUSHIONS IN IES VE (AUTHOR 2019). | 289 |
| FIGURE 5.95. COMBINED DIAGRAM OF THE BASIC MODEL RESULTS AND THE FIRST NINE SCENARIOS RESULTS (AUTHOR 2019). | 291 |
| FIGURE 5.96. COMBINED DIAGRAM OF THE BASIC MODEL RESULTS AND THE FIRST NINE SCENARIOS RESULTS (AUTHOR 2019). | 294 |
| FIGURE 5.97. COMBINED DIAGRAM OF THE BASIC MODEL RESULTS AND THE FIRST NINE SCENARIOS RESULTS (AUTHOR 2019). | 296 |

| | |
|-----------------------------------------------------------------------------------------------------------------------------------------------------------------------------------------------------------------------------------------------------------|-----|
| FIGURE 5.98. SCENARIO 09 DAYLIGHT FACTOR SIMULATION RESULTS ON THE 21ST OF MARCH (AUTHOR 2019). | 297 |
| FIGURE 5.99. SCENARIO 09 DAYLIGHT FACTOR SIMULATION RESULTS ON THE 21ST OF JUNE (AUTHOR 2019). | 298 |
| TABLE 5.110. SCENARIO 09 21ST OF JUNE RESULTS SUMMERY (AUTHOR 2019). | 299 |
| FIGURE 5.100. SCENARIO 06 DAYLIGHT FACTOR SIMULATION RESULTS ON THE 23RD OF SEPTEMBER (AUTHOR 2019). | 299 |
| FIGURE 5.101. SCENARIOS 06 DAYLIGHT FACTOR SIMULATION RESULTS ON THE 21ST OF DECEMBER (AUTHOR 2019). | 301 |
| FIGURE 5.102. COMBINED DIAGRAM OF THE BASIC MODEL DI RESULTS AND THE NINE SCENARIOS DI RESULTS IN WAITING ROOM (AUTHOR 2019). | 302 |
| FIGURE 5.103. COMBINED DIAGRAM OF THE BASIC MODEL DI RESULTS AND THE NINE SCENARIOS DI RESULTS IN RECEPTION ROOM (AUTHOR 2019). | 303 |
| FIGURE 5.104. COMBINED DIAGRAM OF THE BASIC MODEL DF RESULTS AND THE NINE SCENARIOS DF RESULTS IN RECEPTION ROOM (AUTHOR 2019). | 303 |
| FIGURE 5.105. COMBINED DIAGRAM OF THE BASIC MODEL DF RESULTS AND THE NINE SCENARIOS DF RESULTS IN THE WAITING ROOM (AUTHOR 2019). | 304 |
| FIGURE 5.106. WAITING ROOM LUMINANCE MAPS ON THE 21ST OF MARCH (TOP IMAGES) AND 21ST OF JUNE (BOTTOM IMAGES). THE IMAGES ON THE LEFT SHOW SCENARIO 04 RESULTS AND THE IMAGES ON THE RIGHT SHOW THE BASIC MODEL RESULTS (AUTHOR 2019). | 306 |
| FIGURE 5.107. WAITING ROOM LUMINANCE MAPS ON THE 23RD OF SEPTEMBER (TOP IMAGES) AND 21ST OF DECEMBER (BOTTOM IMAGES). THE IMAGES ON THE LEFT SHOW SCENARIO 04RESULTS AND THE IMAGES ON THE RIGHT SHOW THE BASIC MODEL RESULTS (AUTHOR 2019). | 307 |
| FIGURE 5.108. RECEPTION ROOM LUMINANCE MAPS ON THE 21ST OF MARCH (TOP IMAGES) AND 21ST OF JUNE (BOTTOM IMAGES). THE IMAGES ON THE LEFT SHOW SCENARIOS01,02 AND 03 RESULTS AND THE IMAGES ON THE RIGHT SHOW THE BASIC MODEL RESULTS (AUTHOR 2019). | 311 |
| FIGURE 5.109. RECEPTION ROOM LUMINANCE MAPS ON THE 23RD OF SEPTEMBER (TOP IMAGES) AND 21ST OF DECEMBER (BOTTOM IMAGES). THE IMAGES ON THE LEFT SHOW SCENARIOS01,02 AND 03 RESULTS AND THE IMAGES ON THE RIGHT SHOW THE BASIC MODEL RESULTS (AUTHOR 2019). | 312 |
| FIGURE 5.110. CFD ANALYSIS OF NORTHER, EASTERN AND WESTERN CUSHIONS IN MICROFLO (AUTHOR 2019). | 317 |
| FIGURE 5.111. CFD ANALYSIS OF THE EASTERN CUSHIONS IN IES VE (AUTHOR 2019). | 318 |
| FIGURE 5.112. COMBINED DIAGRAM OF ALL SCENARIOS RESULTS (AUTHOR 2019). | 320 |
| FIGURE 5.113. COMBINED DIAGRAM OF THE BASIC MODEL RESULTS AND ALL SCENARIOS RESULTS (AUTHOR 2019). | 323 |
| FIGURE 5.114. COMBINED DIAGRAM OF THE BASIC MODEL RESULTS AND ALL SCENARIOS RESULTS (AUTHOR 2019). | 325 |
| FIGURE 5.115. SCENARIO 10 DAYLIGHT FACTOR SIMULATION RESULTS ON THE 21ST OF MARCH (AUTHOR 2019). | 326 |
| FIGURE 5.116. SCENARIO 10 DAYLIGHT FACTOR SIMULATION RESULTS ON THE 21ST OF JUNE (AUTHOR 2019). | 327 |
| FIGURE 5.117. SCENARIO 10 DAYLIGHT FACTOR SIMULATION RESULTS ON THE 23RD OF SEPTEMBER (AUTHOR 2019). | 329 |
| FIGURE 5.118. SCENARIO 10 DAYLIGHT FACTOR SIMULATION RESULTS ON THE 21ST OF DECEMBER (AUTHOR 2019). | 330 |

| | |
|---------------------------------------------------------------------------------------------------------------------------------------------------------------------------------------------------------------------------------------------------------------|-----|
| FIGURE 5.119. COMBINED DIAGRAM OF THE BASIC MODEL DI RESULTS AND ALL SCENARIOS DI RESULTS IN THE WAITING ROOM (AUTHOR 2019)..... | 331 |
| FIGURE 5.120. COMBINED DIAGRAM OF THE BASIC MODEL DI RESULTS AND ALL SCENARIOS DI RESULTS IN RECEPTION ROOM (AUTHOR 2019)..... | 332 |
| FIGURE 5.121. COMBINED DIAGRAM OF THE BASIC MODEL DF RESULTS AND ALL SCENARIOS DF RESULTS IN RECEPTION ROOM (AUTHOR 2019)..... | 332 |
| FIGURE 5.122. COMBINED DIAGRAM OF THE BASIC MODEL DF RESULTS AND ALL SCENARIOS DF RESULTS IN THE WAITING ROOM (AUTHOR 2019)..... | 333 |
| FIGURE 5.123. WAITING ROOM LUMINANCE MAPS ON THE 21ST OF MARCH (TOP IMAGES) AND 21ST OF JUNE (BOTTOM IMAGES). THE IMAGES ON THE LEFT SHOW SCENARIO 04 RESULTS AND THE IMAGES ON THE RIGHT SHOW THE BASIC MODEL RESULTS (AUTHOR 2019)..... | 335 |
| FIGURE 5.124. WAITING ROOM LUMINANCE MAPS ON THE 23RD OF SEPTEMBER (TOP IMAGES) AND 21ST OF DECEMBER (BOTTOM IMAGES). THE IMAGES ON THE LEFT SHOW SCENARIO 04RESULTS AND THE IMAGES ON THE RIGHT SHOW THE BASIC MODEL RESULTS (AUTHOR 2019). | 336 |
| FIGURE 5.125. RECEPTION ROOM LUMINANCE MAPS ON THE 21ST OF MARCH (TOP IMAGES) AND 21ST OF JUNE (BOTTOM IMAGES). THE IMAGES ON THE LEFT SHOW SCENARIOS01,02 AND 03 RESULTS AND THE IMAGES ON THE RIGHT SHOW THE BASIC MODEL RESULTS (AUTHOR 2019). | 340 |
| FIGURE 5.126. RECEPTION ROOM LUMINANCE MAPS ON THE 23RD OF SEPTEMBER (TOP IMAGES) AND 21ST OF DECEMBER (BOTTOM IMAGES). THE IMAGES ON THE LEFT SHOW SCENARIOS01,02 AND 03 RESULTS AND THE IMAGES ON THE RIGHT SHOW THE BASIC MODEL RESULTS (AUTHOR 2019)..... | 341 |

Table of Figures

| | |
|-------------------------------------------------------------------------------------------------------------------|-----|
| TABLE 1.1. PERCENTAGE OF ENERGY CONSUMPTION IN THE UAE BY SECTOR (ABU DHABI STATISTICS CENTRE 2015). | 5 |
| TABLE 2.1. 12 DIFFERENT POSITIONS (JOHNSENA & WINTHERB 2015). | 41 |
| TABLE 2.2. ASHRAE 55 ZONE OF THERMAL COMFORT CLASSIFICATION AND HEAT STRESS INDEX (TALEGHANI ET. AL 2013). | 45 |
| TABLE 2.3. RECOMMENDED FACTORS FOR ACTIVITIES BASED ON ISO 7730 STANDARDS (TALEGHANI ET. AL 2013). | 45 |
| TABLE 2.4. RECOMMENDED FACTORS FOR ACTIVITIES BASED ON ASHRAE 55 STANDARDS (TALEGHANI ET. AL 2013). | 46 |
| TABLE 2.5. RELATION BETWEEN DGI AND GLARE RATING (MCNEIL & BURRELL 2016). | 54 |
| TABLE 2.6. MEMBRANE TEST SAMPLES (LIU ET AL. 2016). | 71 |
| TABLE 4.7. SUMMARIZED LITERATURE REVIEW TABLE 01 (BY THE AUTHOR 2019). | 89 |
| TABLE 4.8. SUMMARIZED LITERATURE REVIEW TABLE 02 (BY THE AUTHOR 2019). | 90 |
| TABLE 4.9. SUMMARIZED LITERATURE REVIEW TABLE 03 (BY THE AUTHOR 2019). | 91 |
| TABLE 4.10. SUMMARIZED LITERATURE REVIEW TABLE 04 (BY THE AUTHOR 2019). | 92 |
| TABLE 4.11. SUMMARIZED LITERATURE REVIEW TABLE 05 (BY THE AUTHOR 2019). | 93 |
| TABLE 4.12. SUMMARIZED LITERATURE REVIEW TABLE 06 (BY THE AUTHOR 2019). | 94 |
| TABLE 4.13. SUMMARIZED LITERATURE REVIEW TABLE 07 (BY THE AUTHOR 2019). | 95 |
| TABLE 4.14. SUMMARIZED LITERATURE REVIEW TABLE 08 (BY THE AUTHOR 2019). | 96 |
| TABLE 4.15. SUMMARIZED LITERATURE REVIEW TABLE 09 (BY THE AUTHOR 2019). | 97 |
| TABLE 3.1. COMPARISON BETWEEN THE SIMULATED TOTAL ENERGY CONSUMPTION IN THE THREE PROGRAMS (AUTHOR 2019). | 106 |
| TABLE 4.1. INVESTIGATED SCENARIOS (AUTHOR 2019). | 130 |
| TABLE 4.2. INVESTIGATED SCENARIO (AUTHOR 2019). | 134 |
| TABLE 4.3. FRIT PATTERN PARAMETERS (WILSON & ELSTNER 2018). | 135 |
| TABLE 4.4. INVESTIGATED SCENARIO (AUTHOR 2019). | 135 |
| TABLE 5.1. COMFORT INDEX RESULTS (AUTHOR 2019). | 143 |
| TABLE 5.2. MEAN ROOM TEMPERATURE (AUTHOR 2019). | 143 |
| TABLE 5.3. PEOPLE DISSATISFIED INDEX RESULTS (AUTHOR 2019). | 144 |
| TABLE 5.4. 21ST OF MARCH RESULTS SUMMERY (AUTHOR 2019). | 145 |
| TABLE 5.5 21ST OF JUNE RESULTS SUMMERY (AUTHOR 2019). | 146 |
| TABLE 5.6. 23RD OF SEPTEMBER RESULTS SUMMERY (AUTHOR 2019). | 147 |
| TABLE 5.7. 21ST OF DECEMBER RESULTS SUMMERY (AUTHOR 2019). | 148 |
| TABLE 5.8. DGI LEVELS FROM DIFFERENT ANGLES FROM NADIR FOR THE FOUR DAYS AT 9:00,12:00 AND 15:00 (AUTHOR 2019). | 152 |
| TABLE 5.9. GVCP LEVELS FROM DIFFERENT ANGLES FROM NADIR FOR THE FOUR DAYS AT 9:00,12:00 AND 15:00 (AUTHOR 2019). | 153 |
| TABLE 5.10. DGI LEVELS FROM DIFFERENT ANGLES FROM NADIR FOR THE FOUR DAYS AT 9:00,12:00 AND 15:00 (AUTHOR 2019). | 155 |
| TABLE 5.11. GVCP LEVELS FROM DIFFERENT ANGLES FROM NADIR FOR THE FOUR DAYS AT 9:00,12:00 AND 15:00 (AUTHOR 2019). | 156 |

| | |
|--------------------------------------------------------------------------------------------------------------------------------------------------------------------------------------------------------------|-----|
| TABLE 5.12. TOTAL ANNUAL ELECTRICITY CONSUMPTION RESULTS SUMMERY (AUTHOR 2019). | 158 |
| TABLE 5.13. AIR TEMPERATURE WITHIN THE DSF CAVITY FROM MICROFLO RESULTS (AUTHOR 2019). | 159 |
| TABLE 5.14. AIR VELOCITY WITHIN THE DSF CAVITY FROM MICROFLO RESULTS (AUTHOR 2019). | 160 |
| TABLE 5.15. TOTAL ANNUAL ELECTRICITY CONSUMPTION OF THE BASIC MODEL AND THE THREE SCENARIOS (AUTHOR 2019)..... | 161 |
| TABLE 5.16. RESULTS SUMMERY AND COMPARISON WITH THE BASIC MODEL (BY THE AUTHOR). | 163 |
| TABLE 5.17. COMFORT INDEX RESULTS COMPARISON BETWEEN THREE SCENARIOS AND THE BASIC MODEL (AUTHOR 2019)..... | 163 |
| TABLE 5.18. MEAN ROOM TEMPERATURE (AUTHOR 2019)..... | 164 |
| TABLE 5.19. PEOPLE DISSATISFIED INDEX RESULTS COMPARISON BETWEEN THE THREE SCENARIOS AND THE BASIC MODEL (AUTHOR 2019)..... | 166 |
| TABLE 5.20. SCENARIOS 01,02 AND 03 21ST OF MARCH RESULTS SUMMERY (AUTHOR 2019). | 168 |
| TABLE 5.21. SCENARIOS 01,02 AND 03 21ST OF JUNE RESULTS SUMMERY (AUTHOR 2019). | 169 |
| TABLE 5.22. SCENARIOS 01,02 AND 03 23RD OF SEPTEMBER RESULTS SUMMERY (AUTHOR 2019). | 170 |
| TABLE 5.23. SCENARIOS 01,02 AND 03 21ST OF DECEMBER RESULTS SUMMERY (AUTHOR 2019). | 171 |
| TABLE 5.24. FINAL COMPARISON BETWEEN SCENARIOS 01,02 AND 03 AND BASIC MODEL (AUTHOR 2019). | 174 |
| TABLE 5.25. DGI LEVELS FROM DIFFERENT ANGLES FROM NADIR FOR THE FOUR DAYS AT 9:00,12:00 AND 15:00 (AUTHOR 2019)..... | 177 |
| TABLE 5.26. GVCP LEVELS FROM DIFFERENT ANGLES FROM NADIR FOR THE FOUR DAYS AT 9:00,12:00 AND 15:00 (AUTHOR 2019)..... | 178 |
| TABLE 5.27. FINAL COMPARISON OF THE WAITING ROOM RESULTS BETWEEN SCENARIOS 01,02 AND 03 AND BASIC MODEL (AUTHOR 2019)..... | 179 |
| TABLE 5.28. DGI LEVELS FROM DIFFERENT ANGLES FROM NADIR FOR THE FOUR DAYS AT 9:00,12:00 AND 15:00 (AUTHOR 2019)..... | 182 |
| TABLE 5.29. GVCP LEVELS FROM DIFFERENT ANGLES FROM NADIR FOR THE FOUR DAYS AT 9:00,12:00 AND 15:00 (AUTHOR 2019)..... | 183 |
| TABLE 5.30. FINAL COMPARISON BETWEEN SCENARIOS 01,02 AND 03 AND BASIC MODEL (AUTHOR 2019). | 184 |
| TABLE 5.31. TOTAL ANNUAL ELECTRICITY CONSUMPTION RESULTS SUMMERY. ON THE LEFT THE THREE SCENARIOS ANNUAL ELECTRICITY CONSUMPTION AND ON THE RIGHT THE DAY LIGHT HARVESTING SCENARIO (AUTHOR 2019)..... | 185 |
| TABLE 5.32. FINAL COMPARISON (BY THE AUTHOR 2019). | 185 |
| TABLE 5.31. AIR TEMPERATURE WITHIN THE DSF CAVITY FROM MICROFLO RESULTS (AUTHOR 2019). | 186 |
| TABLE 5.32. AIR VELOCITY WITHIN THE DSF CAVITY FROM MICROFLO RESULTS (AUTHOR 2019). | 187 |
| TABLE 5.33. TOTAL ANNUAL ELECTRICITY CONSUMPTION FOR SCENARIOS-04 AND THE BASIC MODEL (AUTHOR 2019). | 188 |
| TABLE 5.34. FINAL COMPARISON BETWEEN THE FIRST FOUR SCENARIOS (AUTHOR 2019)..... | 189 |
| TABLE 5.35. COMFORT INDEX RESULTS COMPARISON BETWEEN SCENARIO 04 AND THE BASIC MODEL (AUTHOR 2019). | 189 |
| TABLE 5.36. MEAN ROOM TEMPERATURE RESULTS OF BASIC-MODEL AND SCENARIO 04 (AUTHOR 2019). | 190 |
| TABLE 5.36. PEOPLE DISSATISFIED INDEX RESULTS OF SCENARIO 04 AND THE BASIC MODEL (AUTHOR 2019). | 191 |
| TABLE 5.37. SCENARIO 04 21ST OF MARCH RESULTS SUMMERY (AUTHOR 2019)..... | 193 |
| TABLE 5.38. SCENARIO 04 21ST OF JUNE RESULTS SUMMERY (AUTHOR 2019)..... | 194 |
| TABLE 5. 39. SCENARIO 04 23RD OF SEPTEMBER RESULTS SUMMERY (AUTHOR 2019)..... | 195 |
| TABLE 5.40. SCENARIOS 04 21ST OF DECEMBER RESULTS SUMMERY (AUTHOR 2019)..... | 197 |

| | |
|----------------------------------------------------------------------------------------------------------------------------------------------------------------------------------------------------|-----|
| TABLE 5.41. FINAL COMPARISON BETWEEN SCENARIO 04 RESULTS AND BASIC MODEL RESULTS (AUTHOR 2019). | 200 |
| TABLE 5.42. DGI LEVELS FROM DIFFERENT ANGLES FROM NADIR FOR THE FOUR DAYS AT 9:00,12:00 AND 15:00 (AUTHOR 2019). | 203 |
| TABLE 5.43. GVCP LEVELS FROM DIFFERENT ANGLES FROM NADIR FOR THE FOUR DAYS AT 9:00,12:00 AND 15:00 (AUTHOR 2019). | 204 |
| TABLE 5.44. FINAL COMPARISON BETWEEN THE FIRST FOUR SCENARIOS RESULTS AND THE BASIC MODEL RESULTS IN THE WAITING ROOM (AUTHOR 2019). | 205 |
| TABLE 5.45. DGI LEVELS FROM DIFFERENT ANGLES FROM NADIR FOR THE FOUR DAYS AT 9:00,12:00 AND 15:00 (AUTHOR 2019). | 208 |
| TABLE 5.46. GVCP LEVELS FROM DIFFERENT ANGLES FROM NADIR FOR THE FOUR DAYS AT 9:00,12:00 AND 15:00 (AUTHOR 2019). | 209 |
| TABLE 5.47. FINAL COMPARISON BETWEEN THE FIRST FOUR SCENARIOS RESULTS AND THE BASIC MODEL RESULTS IN THE WAITING ROOM (AUTHOR 2019). | 210 |
| TABLE 5.48. TOTAL ANNUAL ELECTRICITY CONSUMPTION RESULTS SUMMERY. ON THE LEFT THE FOURTH SCENARIO ANNUAL ELECTRICITY CONSUMPTION AND ON THE RIGHT THE DAY LIGHT HARVESTING SCENARIO (AUTHOR 2019). | 211 |
| TABLE 5.49. FINAL COMPARISON BETWEEN THE FIRST FOUR SCENARIOS (AUTHOR 2019). | 211 |
| TABLE 5.50. AIR TEMPERATURE WITHIN THE DSF CAVITY FROM MICROFLO RESULTS (AUTHOR 2019). | 212 |
| TABLE 5.51. AIR VELOCITY WITHIN THE DSF CAVITY FROM MICROFLO RESULTS (AUTHOR 2019). | 213 |
| TABLE 5.52. AIR TEMPERATURE WITHIN THE DSF CAVITY FROM MICROFLO RESULTS (AUTHOR 2019). | 214 |
| TABLE 5.53. AIR VELOCITY WITHIN THE DSF CAVITY FROM MICROFLO RESULTS (AUTHOR 2019). | 216 |
| TABLE 5.54. TOTAL ANNUAL ELECTRICITY CONSUMPTION FOR SCENARIO-02 COMPARING TO THE BASIC MODEL (AUTHOR 2019). | 217 |
| TABLE 5.55. FINAL COMPARISON BETWEEN THE FIRST FIVE SCENARIOS (AUTHOR 2019). | 218 |
| TABLE 5.56. COMFORT INDEX RESULTS COMPARISON BETWEEN TWO SCENARIOS AND THE BASIC MODEL (AUTHOR 2019). | 219 |
| TABLE 5.57. MEAN ROOM TEMPERATURE COMPARISON BETWEEN TWO SCENARIOS AND THE BASIC MODEL (AUTHOR 2019). | 220 |
| TABLE 5.58. PEOPLE DISSATISFIED INDEX RESULTS COMPARISON BETWEEN THE TWO SCENARIOS AND THE BASIC MODEL (AUTHOR 2019). | 221 |
| TABLE 5.59. SCENARIO 05 21ST OF MARCH RESULTS SUMMERY (AUTHOR 2019). | 223 |
| TABLE 5.60. SCENARIO 05 21ST OF JUNE RESULTS SUMMERY (AUTHOR 2019). | 224 |
| TABLE 5.61. SCENARIO 05 23RD OF SEPTEMBER RESULTS SUMMERY (AUTHOR 2019). | 225 |
| TABLE 5.62. SCENARIOS 05 21ST OF DECEMBER RESULTS SUMMERY (AUTHOR 2019). | 226 |
| TABLE 5.63. FINAL COMPARISON BETWEEN SCENARIO 05 AND BASIC MODEL (AUTHOR 2019). | 229 |
| TABLE 5.64. SCENARIO 06 21ST OF MARCH RESULTS SUMMERY (AUTHOR 2019). | 231 |
| TABLE 5.65. SCENARIO 06 21ST OF JUNE RESULTS SUMMERY (AUTHOR 2019). | 232 |
| TABLE 5.66. SCENARIO 06 23RD OF SEPTEMBER RESULTS SUMMERY (AUTHOR 2019). | 234 |
| TABLE 5.67. SCENARIOS 06 21ST OF DECEMBER RESULTS SUMMERY (AUTHOR 2019). | 235 |
| TABLE 5.68. FINAL COMPARISON BETWEEN SCENARIO 06 AND BASIC MODEL (AUTHOR 2019). | 238 |
| TABLE 5.69. DGI LEVELS FROM DIFFERENT ANGLES FROM NADIR FOR THE FOUR DAYS AT 9:00,12:00 AND 15:00 (AUTHOR 2019). | 241 |

| | |
|-------------------------------------------------------------------------------------------------------------------------------------|-----|
| TABLE 5.70. GVCP LEVELS FROM DIFFERENT ANGLES FROM NADIR FOR THE FOUR DAYS AT 9:00,12:00 AND 15:00 (AUTHOR 2019)..... | 242 |
| TABLE 5.71. FINAL COMPARISON BETWEEN SCENARIOS 04,05 AND BASIC MODEL (AUTHOR 2019). | 243 |
| TABLE 5.72. DGI LEVELS FROM DIFFERENT ANGLES FROM NADIR FOR THE FOUR DAYS AT 9:00,12:00 AND 15:00 (AUTHOR 2019)..... | 246 |
| TABLE 5.73. GVCP LEVELS FROM DIFFERENT ANGLES FROM NADIR FOR THE FOUR DAYS AT 9:00,12:00 AND 15:00 (AUTHOR 2019)..... | 247 |
| TABLE 5.74. FINAL COMPARISON BETWEEN SCENARIO 05 AND BASIC MODEL (AUTHOR 2019). | 248 |
| TABLE 5.75. DGI LEVELS FROM DIFFERENT ANGLES FROM NADIR FOR THE FOUR DAYS AT 9:00,12:00 AND 15:00 (AUTHOR 2019)..... | 251 |
| TABLE 5.76. GVCP LEVELS FROM DIFFERENT ANGLES FROM NADIR FOR THE FOUR DAYS AT 9:00,12:00 AND 15:00 (AUTHOR 2019)..... | 252 |
| TABLE 5.77. FINAL COMPARISON BETWEEN SCENARIO 04,06 AND BASIC MODEL (AUTHOR 2019)..... | 253 |
| TABLE 5.78. DGI LEVELS FROM DIFFERENT ANGLES FROM NADIR FOR THE FOUR DAYS AT 9:00,12:00 AND 15:00 (AUTHOR 2019)..... | 256 |
| TABLE 5.79. GVCP LEVELS FROM DIFFERENT ANGLES FROM NADIR FOR THE FOUR DAYS AT 9:00,12:00 AND 15:00 (AUTHOR 2019)..... | 257 |
| TABLE 5.80. FINAL COMPARISON BETWEEN SCENARIO 04,06 AND BASIC MODEL (AUTHOR 2019)..... | 258 |
| TABLE 5.81. TOTAL ANNUAL ELECTRICITY CONSUMPTION RESULTS SUMMERY (AUTHOR 2019). | 259 |
| TABLE 5.82. FINAL COMPARISON (AUTHOR 2019). | 259 |
| TABLE 5.82. AIR TEMPERATURE WITHIN THE DSF CAVITY FROM MICROFLO RESULTS (AUTHOR 2019). | 260 |
| TABLE 5.83. AIR VELOCITY WITHIN THE DSF CAVITY FROM MICROFLO RESULTS (SUTHOR 2019). | 261 |
| TABLE 5.84. TOTAL ANNUAL ELECTRICITY/ENERGY CONSUMPTION FOR SCENARIOS 07 AND 08 COMPARING TO THE BASIC MODEL (AUTHOR 2019). | 262 |
| TABLE 5.84. TOTAL ANNUAL ELECTRICITY GENERATION IN SCENARIOS 07 AND 08 (AUTHOR 2019). | 264 |
| TABLE 5.85. FINAL COMPARISON BETWEEN THE FIRST EIGHT SCENARIOS (AUTHOR 2019). | 264 |
| TABLE 5.86. COMFORT INDEX RESULTS COMPARISON BETWEEN TWO SCENARIOS AND THE BASIC MODEL (AUTHOR 2019)..... | 265 |
| TABLE 5.87. MEAN ROOM TEMPERATURE RESULTS COMPARISON BETWEEN TWO SCENARIOS AND THE BASIC MODEL (AUTHOR 2019)..... | 266 |
| TABLE 5.88. PEOPLE DISSATISFIED INDEX RESULTS COMPARISON BETWEEN THE TWO SCENARIOS AND THE BASIC MODEL (AUTHOR 2019). | 267 |
| TABLE 5.89. SCENARIOS 07 AND 08 21ST OF MARCH RESULTS SUMMERY (AUTHOR 2019). | 269 |
| TABLE 5.90. SCENARIOS 07 AND 08 21ST OF JUNE RESULTS SUMMERY (AUTHOR 2019). | 271 |
| TABLE 5.91. SCENARIOS 07 AND 08 23RD OF SEPTEMBER RESULTS SUMMERY (AUTHOR 2019). | 272 |
| TABLE 5.92. SCENARIOS 07 AND 08 21ST OF DECEMBER RESULTS SUMMERY (AUTHOR 2019). | 273 |
| TABLE 5.93. FINAL COMPARISON BETWEEN SCENARIOS 07,08 AND BASIC MODEL (AUTHOR 2019). | 276 |
| TABLE 5.94. DGI LEVELS FROM DIFFERENT ANGLES FROM NADIR FOR THE FOUR DAYS AT 9:00,12:00 AND 15:00 (AUTHOR 2019)..... | 279 |
| TABLE 5.95. GVCP LEVELS FROM DIFFERENT ANGLES FROM NADIR FOR THE FOUR DAYS AT 9:00,12:00 AND 15:00 (AUTHOR 2019)..... | 280 |
| TABLE 5.96. FINAL COMPARISON BETWEEN SCENARIOS 07 AND 08 AND BASIC MODEL IN THE WAITING ROOM (AUTHOR 2019)..... | 281 |

| | |
|-----------------------------------------------------------------------------------------------------------------------------------------------|-----|
| TABLE 5.97. DGI LEVELS FROM DIFFERENT ANGLES FROM NADIR FOR THE FOUR DAYS AT 9:00,12:00 AND 15:00 (AUTHOR 2019)..... | 284 |
| TABLE 5.98. GVCP LEVELS FROM DIFFERENT ANGLES FROM NADIR FOR THE FOUR DAYS AT 9:00,12:00 AND 15:00 (AUTHOR 2019)..... | 285 |
| TABLE 5.99. FINAL COMPARISON BETWEEN SCENARIOS 06, 07,08 AND BASIC MODEL IN THE RECEPTION ROOM (AUTHOR 2019)..... | 286 |
| TABLE 5.100. TOTAL ANNUAL ELECTRICITY CONSUMPTION RESULTS SUMMERY (AUTHOR 2019). | 287 |
| TABLE 5.101. FINAL COMPARISON (AUTHOR 2019). | 287 |
| TABLE 5.102. AIR TEMPERATURE WITHIN THE DSF CAVITY FROM MICROFLO RESULTS (AUTHOR 2019). | 288 |
| TABLE 5.103. AIR VELOCITY WITHIN THE DSF CAVITY FROM MICROFLO RESULTS (AUTHOR 2019). | 289 |
| TABLE 5.104. TOTAL ANNUAL ELECTRICITY/ENERGY CONSUMPTION FOR SCENARIOS 07 AND 08 COMPARING TO THE BASIC MODEL (AUTHOR 2019). | 290 |
| TABLE 5.105. FINAL COMPARISON BETWEEN THE FIRST NINE SCENARIOS (AUTHOR 2019)..... | 292 |
| TABLE 5.106. COMFORT INDEX RESULTS COMPARISON BETWEEN SCENARIO 09 AND THE BASIC MODEL (AUTHOR 2019)..... | 293 |
| TABLE 5.107. MEAN ROOM TEMPERATURE RESULTS COMPARISON BETWEEN SCENARIO 09 AND THE BASIC MODEL (AUTHOR 2019)..... | 294 |
| TABLE 5.108. PEOPLE DISSATISFIED INDEX RESULTS COMPARISON BETWEEN SCENARIO 09 AND THE BASIC MODEL (AUTHOR 2019)..... | 295 |
| TABLE 5.109. SCENARIO 09 21ST OF MARCH RESULTS SUMMERY (AUTHOR 2019). | 297 |
| TABLE 5.111. SCENARIO 06 23RD OF SEPTEMBER RESULTS SUMMERY (AUTHOR 2019)..... | 300 |
| TABLE 5.112. SCENARIOS 06 21ST OF DECEMBER RESULTS SUMMERY (AUTHOR 2019)..... | 301 |
| TABLE 5.113. FINAL COMPARISON BETWEEN SCENARIO 09 AND BASIC MODEL (AUTHOR 2019)..... | 305 |
| TABLE 5.114. DGI LEVELS FROM DIFFERENT ANGLES FROM NADIR FOR THE FOUR DAYS AT 9:00,12:00 AND 15:00 IN WAITING ROOM (AUTHOR 2019). | 308 |
| TABLE 5.115. GVCP LEVELS FROM DIFFERENT ANGLES FROM NADIR FOR THE FOUR DAYS AT 9:00,12:00 AND 15:00 IN THE WAITING ROOM (AUTHOR 2019)..... | 309 |
| TABLE 5.116. FINAL COMPARISON BETWEEN SCENARIOS 06, 09 AND BASIC MODEL (AUTHOR 2019). | 310 |
| TABLE 5.117. DGI LEVELS FROM DIFFERENT ANGLES FROM NADIR FOR THE FOUR DAYS AT 9:00,12:00 AND 15:00 (AUTHOR 2019)..... | 313 |
| TABLE 5.118. GVCP LEVELS FROM DIFFERENT ANGLES FROM NADIR FOR THE FOUR DAYS AT 9:00,12:00 AND 15:00 (AUTHOR 2019)..... | 314 |
| TABLE 5.119. FINAL COMPARISON BETWEEN SCENARIOS 06, 09 AND BASIC MODEL IN THE RECEPTION ROOM (AUTHOR 2019)..... | 315 |
| TABLE 5.120. TOTAL ANNUAL ELECTRICITY CONSUMPTION RESULTS SUMMERY (AUTHOR 2019). | 316 |
| TABLE 5.121. FINAL COMPARISON (AUTHOR 2019). | 316 |
| TABLE 5.122. AIR TEMPERATURE WITHIN THE DSF CAVITY FROM MICROFLO RESULTS (AUTHOR 2019). | 317 |
| TABLE 5.123. AIR VELOCITY WITHIN THE DSF CAVITY FROM MICROFLO RESULTS (AUTHOR 2019). | 318 |
| TABLE 5.124. TOTAL ANNUAL ELECTRICITY/ENERGY CONSUMPTION FOR SCENARIO 10 COMPARING TO THE BASIC MODEL (AUTHOR 2019)..... | 319 |
| TABLE 5.125. FINAL COMPARISON BETWEEN ALL SCENARIOS (AUTHOR 2019)..... | 321 |
| TABLE 5.126. COMFORT INDEX RESULTS COMPARISON BETWEEN SCENARIO 10 AND THE BASIC MODEL (AUTHOR 2019)..... | 322 |

| | |
|------------------------------------------------------------------------------------------------------------------------|-----|
| TABLE 5.127. MEAN ROOM TEMPERATURE RESULTS COMPARISON BETWEEN SCENARIO 10 AND THE BASIC MODEL (AUTHOR 2019)..... | 323 |
| TABLE 5.128. PEOPLE DISSATISFIED INDEX RESULTS COMPARISON BETWEEN SCENARIO 10 AND THE BASIC MODEL (AUTHOR 2019)..... | 324 |
| TABLE 5.129. SCENARIO 10 AND 08 21ST OF MARCH RESULTS SUMMERY (AUTHOR 2019)..... | 326 |
| TABLE 5.130. SCENARIO 10 21ST OF JUNE RESULTS SUMMERY (AUTHOR 2019)..... | 328 |
| TABLE 5.131. SCENARIO 10 23RD OF SEPTEMBER RESULTS SUMMERY (AUTHOR 2019)..... | 329 |
| TABLE 5.132. SCENARIO 10 AND 08 21ST OF DECEMBER RESULTS SUMMERY (AUTHOR 2019)..... | 331 |
| TABLE 5.134. FINAL COMPARISON BETWEEN SCENARIO 10 AND BASIC MODEL (AUTHOR 2019)..... | 334 |
| TABLE 5.135. DGI LEVELS FROM DIFFERENT ANGLES FROM NADIR FOR THE FOUR DAYS AT 9:00,12:00 AND 15:00 (AUTHOR 2019)..... | 337 |
| TABLE 5.136. GVCP LEVELS FROM DIFFERENT ANGLES FROM NADIR FOR THE FOUR DAYS AT 9:00,12:00 AND 15:00 (AUTHOR 2019)..... | 338 |
| TABLE 5.137. FINAL COMPARISON BETWEEN SCENARIOS 06, 10 AND BASIC MODEL (AUTHOR 2019). | 339 |
| TABLE 5.138. DGI LEVELS FROM DIFFERENT ANGLES FROM NADIR FOR THE FOUR DAYS AT 9:00,12:00 AND 15:00 (AUTHOR 2019)..... | 342 |
| TABLE 5.139. GVCP LEVELS FROM DIFFERENT ANGLES FROM NADIR FOR THE FOUR DAYS AT 9:00,12:00 AND 15:00 (AUTHOR 2019)..... | 343 |
| TABLE 5.140. FINAL COMPARISON BETWEEN SCENARIOS 06, 10 AND BASIC MODEL IN THE RECEPTION ROOM (AUTHOR 2019)..... | 344 |
| TABLE 5.141. TOTAL ANNUAL ELECTRICITY CONSUMPTION RESULTS SUMMERY (AUTHOR 2019). | 345 |
| TABLE 5.142. FINAL COMPARISON (AUTHOR 2019). | 345 |

List of abbreviation

| Word | Definition |
|--------|---------------------------------------------------------------------|
| ETFE | Ethylene tetrafluoroethylene |
| BTU | The British thermal unit |
| EPA | United States Environmental Protection Agency |
| LEED | Leadership in Energy and Environmental Design |
| BREEAM | Building Research Establishment Environmental Assessment Method |
| GBI | The Green Building Institute |
| EGBC | Emirati Green Building Council |
| SHGC | Solar heat gain coefficient |
| VLT | Visible light transmittance |
| BIPV | Building integrated photovoltaics |
| ADUPC | Abu Dhabi Urban Planning Council |
| DSF | Double skin façade |
| ASHRAE | The American Society of Heating, Refrigerating and Air-Conditioning |
| ET | Effective temperature |
| PMV | Predicted Mean Vote |
| PPD | Predicted Percentage of Dissatisfied |
| RH | Relative humidity |
| DPT | Dew point temperature |
| MRT | Mean radiant temperature |
| ACM | Adaptive comfort model |
| AMV | Actual predicted mean vote |
| DF | Daylight factor |
| BRE | Building Research Establishment |
| DGI | Daylight glare index |
| GVCP | Guth visual comfort probability |
| DGR | Discomfort Glare Rating |
| LED | Light emitting diode |
| BAS | Building Automation System |
| FLS | Fire and life safety |
| DLCS | Daylight control systems |
| DA | Daylight Autonomy |
| UDI | Useful Daylight Illuminance |
| LA | lighting adequate |
| GHG | Greenhouse gases |
| PTFE | polytetrafluoroethylene |

CHAPTER 01
INTRODUCTION

1 Introduction and Background

1.1 Urbanization and environment through history

The relation between population growth, and the associated urbanization, and changes in the natural environment is old and possibly had started in 10000 BC in the Neolithic period when population growth and lack of resources forced humans to change their lifestyle and shift from fruit gathering and hunting to agriculture and settle in small villages. Historians call this event the Neolithic transition or the first agricultural revolution (Pinhasi & Taubadel 2012). This advancement led humans to new activities such as manufacturing and trade. The new human needs forced them to invent new technologies, use new power sources, new tools and adjust the surrounding environment accordingly. After thousands of years, a similar advancement led to the industrial revolution in the seventeenth and the eighteenth centuries because of the population growth pressure which was associated with the second agricultural revolution in Europe. These major historical changes encouraged humans to shift from agriculture, which became less labor-intensive, to industry and use alternative energy sources such as steam power and coal. Subsequently, the unprecedented urbanization growth along with the technological developments increased the levels of chemical and smoke pollution in the ecosystem. Historically, that was the first major man-made devastating impact on the environment. The massive urbanization happened because of rapid migration from rural areas to large cities. These series of events led to colonial expansion and development of global trading. As the global economy grew quickly, population growth and urbanization increased quickly. For instance, in England the people living in urban areas increased 300% from 1550 to 1820 (Healy 2015).

1.2 Buildings impacts on the environment on a global scale

Nowadays almost 55% of the world's population are city dwellers and the UN predict that this number will reach 68% after two decades. It is predicted also that in 2050 the overall world's population will become 10 billion which adds almost 2.5 billion humans to urban areas. Currently, cities host around 4.2 billion people (UN 2018). As the built environment is expanding rapidly, energy demand in buildings is increasing with the same rate. This is a direct result of technology advancement, population growth, changes in people's lifestyle which make them spend more time indoors. All these factors increase the demand of buildings equipment and services to enhance the indoor environment quality. For instance, in 2017, the residential and commercial buildings in the U.S. consumed almost 40 % of the total country energy consumption. That is equal to 40 quintillion (10^{18}) Joules or 38 quadrillion (10^{15}) BTU (EIA 2018). It is expected that energy demand for cooling in buildings will increase by almost 150% in the next 30 years globally and by almost 450% in developing countries Without crucial decisions, the rising fossil energy consumption will double the CO₂ emissions after 30 years from now and substantially reduce the global reserves (IEA 2014). Other than buildings impact on air quality which increases greenhouse gases (GHG) in the atmosphere, buildings consume 13.6% of potable water globally. Even most of the materials used in construction have high embedded carbon levels which represent the amount of GHG produced by the manufacturing process. In 2018 in the US, buildings consumed almost 39% of energy, 12% of potable water, 68% of electrical power and produced 38% of CO₂ emissions (EPA 2019).

1.3 Sustainable building design as a solution

As the built environment has negative effects on natural environment, economy, human well-being and health, sustainable design strategies can maximize both environmental and economic performance of buildings. These green strategies can be applied to buildings at any phase starting from design and construction and up to demolishing, recycling or renovation. In general, sustainable design stand on three pillars which are social, economic and environmental. Social benefits of sustainability

include enhancing human health and comfort, improving aesthetic aspects, reducing pressure on local infrastructure network and enhance the quality of life. Economic benefits of green design are expanding green products market, reduce operation cost, improved users' productivity and enhance performance of buildings from an economic life cycle perspective. At last, environmental benefits include protection of the ecosystem and biodiversity, reduce waste and landfill, restore and conserve existing resources and improving quality of water and ambient air (EPA 2019).

Energy efficiency in buildings, utilization of green building materials and renewable power stand among the most effective sustainable strategies that can become decisive solutions to buildings impacts on global warming and greenhouse gases accumulation. Thus, the need of sustainable building design is no longer a matter of personal choice which encouraged many countries to develop codes, rating systems and standards to mandate green building design strategies such as ESTIDAMA and Al Sa'fat in the UAE, LEED internationally, GBI in Australia and BREEAM in the UK. Therefore, sustainability has become greatly popular in the construction industry and architects, engineers and other building professional have been cooperating to create efficient green buildings. All green buildings standards focus on improving building design aspects specifically building sites, water usage efficiency, energy efficiency in buildings, sustainable materials, internal environmental quality, regional needs and design innovation.

1.4 Buildings and energy in the UAE

Currently, due to the economic and population growth in the UAE, the increment in domestic energy consumption rates is a longstanding unsustainable challenge. Subsequently, reduction of the energy demand in buildings is a significant issue on the agenda of the Emirati federal government which launched several initiations in order to address this issue using a tailored integrated strategy that cover all related elements. The case of the UAE was selected for this research as the country is encouraging the implementation of energy saving practices. The UAE depends mainly on fossil fuels namely, natural gas a petroleum for generating electricity. As we are

talking about an oil-rich country, the cheap electricity motivated the consumption rates to rise rapidly. Thence, a large portion of the energy consumption in the UAE goes to the residential sector (figure 1.1 and table 1.1), mainly, for air conditioning purpose (Al-Saleh & Taleb 2014). According to the ministry of Energy report (2015) each resident in the country consumes about 30 kilo-watt per hour (kWh) of electrical power each day and 12500 kWh per year which place the country among the highest consumer per capita globally. In 2013, The residential and commercial sectors share was almost 60 % out of the total electricity consumption in the country. Because of the hot and humid weather, the electricity demand is seasonal which is affected by the ambient temperature. In the city capital of Abu Dhabi, the cooling loads account of 47% of the total energy consumption in building at the beginning of spring then it reached 60% in the middle of the summer. Moreover, 20% of this usage is wasted because of inefficient utilization such as air conditioning empty rooms.

In 2016, these numbers changed as 80% of energy in the UAE was consumed by buildings according to the Emirati Green Building Council (EGBC). For example, annual consumption in some existing buildings in the UAE reached 220-360 kWh/m² while efficient green buildings annual consumption falls between 110-160 kWh/m². The opportunity of changing existing buildings in the UAE to be more efficient is very large as 20% of energy can be saved using low cost design techniques (Clarke 2016).

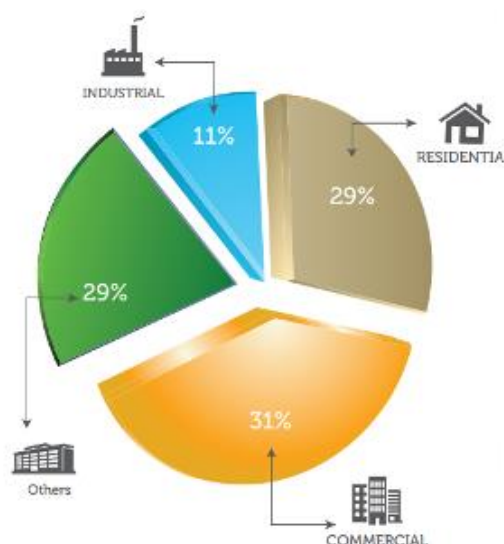


Figure 1.1. Total electricity consumption chart in 2013 (UAE Ministry of Energy 2015).

Table 1.1. Percentage of energy consumption in the UAE by sector (Abu Dhabi Statistics Centre 2015).

| Sector | 2007 | 2012 | 2013 | 2014 | 2015 |
|---------------|------------|------------|------------|------------|------------|
| Total | 100 | 100 | 100 | 100 | 100 |
| Domestic | 45.3 | 30.5 | 29.9 | 29.4 | 26.9 |
| Commercial | 29.2 | 29.8 | 30.0 | 30.2 | 48.2 |
| Government | 17.4 | 23.9 | 24.1 | 24.7 | 9.3 |
| Agriculture | 7.1 | 6.1 | 5.6 | 5.4 | 5.7 |
| Industry | 0.2 | 9.3 | 9.7 | 10.0 | 9.7 |
| Other Sectors | 0.8 | 0.3 | 0.7 | 0.4 | 0.3 |

1.5 Sustainable passive and active design techniques

An essential way to improve energy savings in buildings is to implement passive and active design techniques. It goes without saying that passive architectural strategies are the fixed design elements that either reduce, increase or utilize the effects of any natural phenomenon such as heat, wind and sunlight depending on the building location and the surrounding environment. These elements are beneficial as they don't have any operational cost, they are simple and don't consume any energy. On the other hand, active systems consume power and require regular maintenance and replacement. Passive design can include passive cooling, sophisticated building envelope design such as double skin facade, reflective external finishes, external shades, low emissivity film for glazing, etc. This strategy can affect all envelope components such as windows, doors, glazing and roof. As the main barrier between the indoor environment and the external conditions, building envelope plays a significant role in controlling energy demand by improving internal thermal comfort. There are several approaches that can improve the envelope performance, for instance, reducing the U-Value (thermal transmittance) of the envelope which can cause a substantial energy saving. The overall envelope U-Value is related also to window-to-wall ratio, window type and specifications. The fenestration parameters, such as solar heat gain coefficient (SHGC) and visible transmittance (VT), should be selected carefully as it affects also the visual comfort in the building, efficient usage of daylighting and utilization of artificial lighting. It is required to achieve the right balance between thermal comfort, visual

comfort and energy consumption. Beside the potential energy savings, lighting control strategies and increasing the proper utilization of daylight can improve occupants' productivity and satisfaction. Passive strategies are usually investigated in three levels: entire building, internal zones and fenestration area (Rodriguez-Ubinas et al. 2014).

The concept of BIPVs is based on the photoelectric phenomena. They can convert fallen solar radiation into electrical power with efficiency that varies from 10% to 23%. In this technology, most of the solar power is converted into thermal energy which increases the solar cells temperature and subsequently reduces conversion efficiency. As a solution, the advanced hybrid PV thermal systems can utilize thermal power while generating electricity which increases the overall efficiency which can be used in the building for different applications (Cao, Dai & Liu 2016). BIPV system is integrated within the envelope materials such as ETFE cushions that can be done on roof as skylight or within walls as in windows and cladding systems. Dynamic shading is the technology which controls external or internal shading devices. It can be manually controlled or a part of the building management system. By analyzing input from sensors or following weather data and surrounding conditions, the system can adjust the shading device to prevent or allow sunlight to go through the building envelop.

To sum up, it is required to investigate the potential of reducing buildings negative impacts on the environment using these strategies. An efficient building design can lower energy demand substantially and reduce the overall carbon footprint of the structure while enhancing the users' thermal and visual comfort. Therefore, the proposed research will focus on various active and passive ETFE applications that can achieve this purpose by controlling thermal transmittance into the building, harnessing solar power (renewable power generation) and enhancing the usage of natural lights in occupied spaces.

1.6 Statement of the problem and research interest

Buildings are major consumers of energy in Abu Dhabi. As explained in previous sections, UAE residents stand among the highest consumer per capita globally. That is why the government has a strong national agenda which focuses on energy efficiency and using sustainable power sources to mitigate this issue. Abu Dhabi has been moving towards mandating energy efficiency in new buildings as part of "Plan Abu Dhabi 2030" that was launched by the Abu Dhabi Urban Planning Council (AD UPC) and focused on sustainability as a key direction in the development of the city (AD UPC 2014). That is why ESTIDAMA green building rating system as a sustainable policy was added to the building permit process in the emirate. It is now mandatory for new buildings in the Emirate to achieve minimum requirements following this system. However, existing inefficient buildings which were built before mandating the standard are still a huge challenge in front of the government efforts to reduce the over-all energy consumption in buildings. Mr. Al Abbar, chairman of the EGBC, stated that the government is trying to retrofit existing buildings to meet the standards and become more efficient with the help of reprogramming HVAC systems and adjusting their facades (Clarke 2016).

With regards to office buildings, as the units are leased out to tenants who pay the electricity bills, the owners of the buildings and the facility management do not care much about the over-all operation cost. Besides that, the tenants as they do not own the units, they focus only on the interior design of the space and they do not invest in any strategy that can improve the building performance. If the energy bills are too high, they either scale down the business or move out to a cheaper place to reduce the overall cost. Hence, all those parties do not contribute to solving the problem.

Thus, the dissertation tried to find an effective solution that can be applied to existing building facades. The studied strategy is a light weight treatment of the façade that respects structural limitation and can reduce heat gain and energy consumption in buildings. As changes in building envelope have a major impact on other aspects also such as thermal comfort, visual comfort and daylighting, they were all covered by the study. In general, if the proposed building retrofit options are proven to achieve a

significant energy saving and improve comfort of occupants, it can help owners and FM to market their buildings to new tenants or even receive government incentives.

The research evaluates Ethylene Tetra Fluoro Ethylene (ETFE) double skin façade (DSF) applications as retrofit options for existing buildings. Will they improve building envelope performance, reduce energy consumption and enhance visual and thermal comfort in UAE buildings?

1.7 Aims and Objectives

The aim of the research was to study if Ethylene Tetra Fluoro Ethylene cushions double skin façade applications can improve buildings envelope performance, reduce energy consumption and enhance visual and thermal comfort in UAE buildings.

The objectives were:

- 1- To review the literature to understand the status and background of the investigated applications and systems.
- 2- To select an office building in the UAE to act as a suitable case study.
- 3- To analyse the case study IES-VE software in terms of energy consumption, thermal comfort, daylighting quality, visual comfort and daylight harvesting potential.
- 4- To propose a set of scenarios in order to study the effect of changing ETFE parameters and adding different applications.
- 5- To compare the various scenarios results against the basic model case.
- 6- To evaluate all these design options in order to present the best scenario that can enhance building envelope performance.

To further explain the process, the research investigated various light weight façade options that can be applied to an existing office building to reduce energy consumption and decrease heat gain in summer. Due to Abu Dhabi extreme weather conditions, it was chosen for this study. ETFE was selected as the full average system weight is approximately 0.45 kg/m² that is considered structurally negligible, hence it can be added easily to facades even in existing building with minimum structural

consideration. ETFE weight is almost 1~2% of a typical double-glazed unit. ETFE as a material reflects the soul of modern architecture which is based on innovative technologies in construction. This material has been used successfully in many fascinating projects around the world. However, its usage is limited in the UAE. The research is trying to represent this design option to the society of architects and building specialists in the country while evaluating not only aesthetically, but also from technical and environmental perspectives. In addition, ETFE can resist heat and is dust repellent which suits the local weather conditions. Also, as it is fire-proof, it follows the Abu Dhabi civil defence requirements.

The studied ETFE DSF can improve the envelope performance based on provided ventilation and shading. In naturally ventilated DSFs, vertical buoyancy flow or stack effect, which happens between lower air inlet and upper outlet, can reduce heat gain through external walls.

Total of ten ETFE DSF scenarios were proposed and arranged in an ascending order based on time/cost of installation. The first scenarios represent the most passive and economic options and the last scenarios were the most active and expensive options. The results of each scenario were studied separately in order to adjust parameters for following simulations. The scenarios were built up in a progressive and accumulative way. Those scenarios were compared to a base line case that represents an existing building with conventional façade materials.

The research did not only evaluate the possible reduction in energy consumption but also how to make the interior spaces more efficient for the occupants. The research investigated also the effects of different scenarios on thermal comfort, visual comfort, daylighting parameters and daylighting harvesting potential.

All studied parameters were simulated using a computer software to determine which scenario performed the best in terms of energy saving, thermal and visual comfort. Also, effects on daylighting were studied in parallel with these simulations. As the building is still under construction, the software was validated against the actual

design loads that were approved by Abu Dhabi Distribution Company. Three software were tested and IES VE was proved to be more accurate comparing to the other programs.

Future recommendations for further studies was proposed based on the dissertation limitations and the results. As some of the studied options showed promising results, further investigations can enhance the study and cover any gaps in the dissertation. That will offer various solutions that can contribute to the success of “Plan Abu Dhabi 2030”

1.8 Research Limitations

The first limitation was the lack of information when it comes to ETFE in the UAE as the material is still not popular in the country. Thus, the literature review included various investigations and case-studies that provided a solid foundation to the research. The second limitation was that the researcher had only full access to the design details of new buildings and not old ones. It would have been better if the study was conducted on an old building with major energy inefficiency. However, lack of information could have affected the accuracy of simulation. Thus, a new building was selected for the study to enhance the investigation creditability and quality.

The other limitations were related to the simulation software. The first issue was that the curvature of the cushion could not be modelled in the software. According to previous studies, changes in the curvature has only minimal impact on the results and it can be neglected. Also, the actual ETFE foil thickness is between 50 and 250 μm (0.05 and 0.25 mm), and the minimum layer thickness that can be modelled in the software is 0.3 mm (300 μm). According to the previous investigations, thickness did not have a significant impact on the results.

Last limitation was the software verification. As the building is still under construction and do not have any recent electricity bills. It was agreed with the dissertation supervisor that the results can be compared to the design electrical loads,

which was reviewed and approved by the authorities, in order to validate the software results.

1.9 Research outline

In general, the dissertation investigated several design options that can enhance façade skin performance and the occupants' experience inside the building via the usage of ETEF DSF. It has been divided into six chapters. The first part addressed the background of the problem between the built environment and the natural environment. It also covered the concept of green buildings, buildings environmental issues in the UAE, reasons behind selection of the studied building and aims of the investigation.

The second chapter was in-depth literature review. It covered the foundation of the research in depth such as building skin, basics of DSF design, ETFE background, possible ETFE applications and impact of the building skin on user comfort. The second part of the chapter focused on previous studies related to the research topic which were referred in the study and compared. These studies included many significant aspects such as simulation parameters, design options, material selection, etc. The third chapter covered the methodology to analyse the design options. This includes software selection, each parameter that was studied and simulation days. Base model description and justification of selection was included also along with explanation of the model set-up and hypotheses. All related drawings and images were included in this chapter.

The fourth chapter focus on the models' set-up with the associated parameters while the fifth chapter covered the basic model simulation along with the other 10 scenarios simulations. Also, it included the results and findings which were combined and shown in tabular and graphical forms. Once the eleven batch simulations were done the results were investigated and compared. Due to the accumulative structure of the research, it was assumed then proved that the final option gave the most promising results. The sixth chapter included the conclusions from all simulations in a summarized form. The results between the eleven simulations were cross-analysed and recommendations for future related researches were given. After this part, the list of references was included.

CHAPTER 02
LITERATURE REVIEW

2 Literature review

2.1 Building's Façade and skin

2.1.1 Difference between building's façade and skin

Building façade, in simple words, is the interface between internal and external spaces which shows its structure and value. Its main functions are to show the architectural character of the building, control and provide views, protect occupants from external conditions, allowing daylighting while protecting the users from the sun, resist rain water and controlling humidity in the building and finally to provide insulation against noise, cold and heat and provide energy generation options. They are not only affecting internal space, but also have a major impact on the surrounding environment (Przybylek 2018).

Skin is a modern term that describes a multipurpose and/or multilayers envelope which shifts from tight to loose, from thin to thick and acts like an environmental filter around the building (figures 2.1 and 2.2). In modern architecture, treat the buildings as living creatures which has separated bones and skin. They tried to separate between the envelope, as it should react as a living responsive skin, and the structure as a static element. To achieve that they used conventional materials in conjunction with other materials such as lightweight fabrics, intelligent elements, photovoltaic technologies, active shading systems to form the skin. Recently, the skin can account for 15~40% of the total construction budget of a typical building and it affects up to 40% of the operation cost (Mahmod 2011).

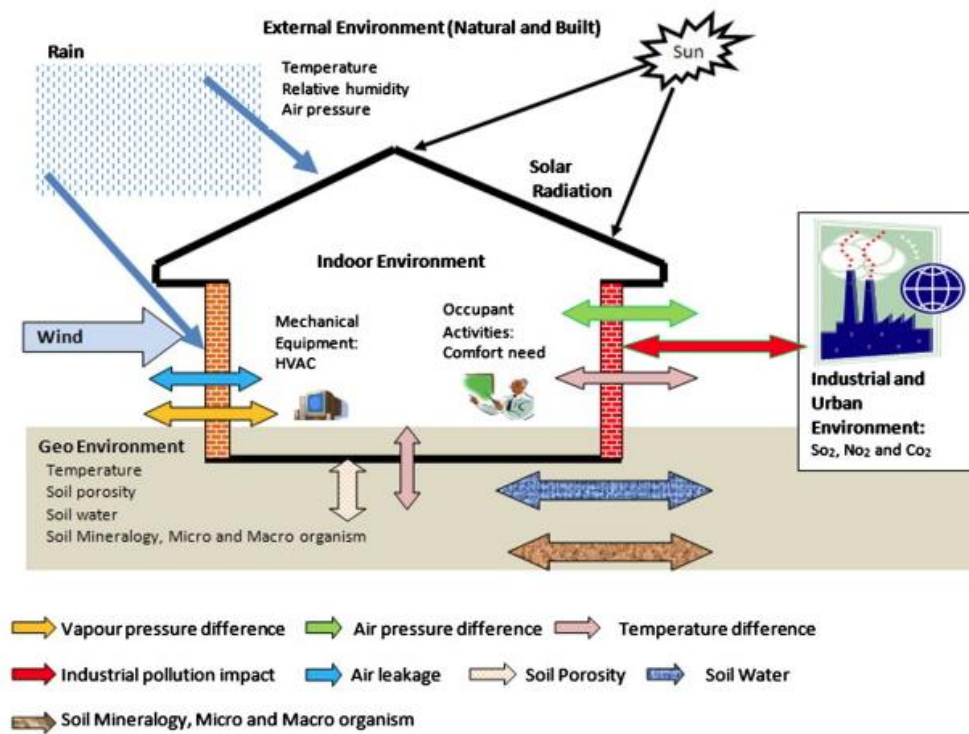


Figure 2.1. Environmental pressure on building envelope (Mwasha 2018).

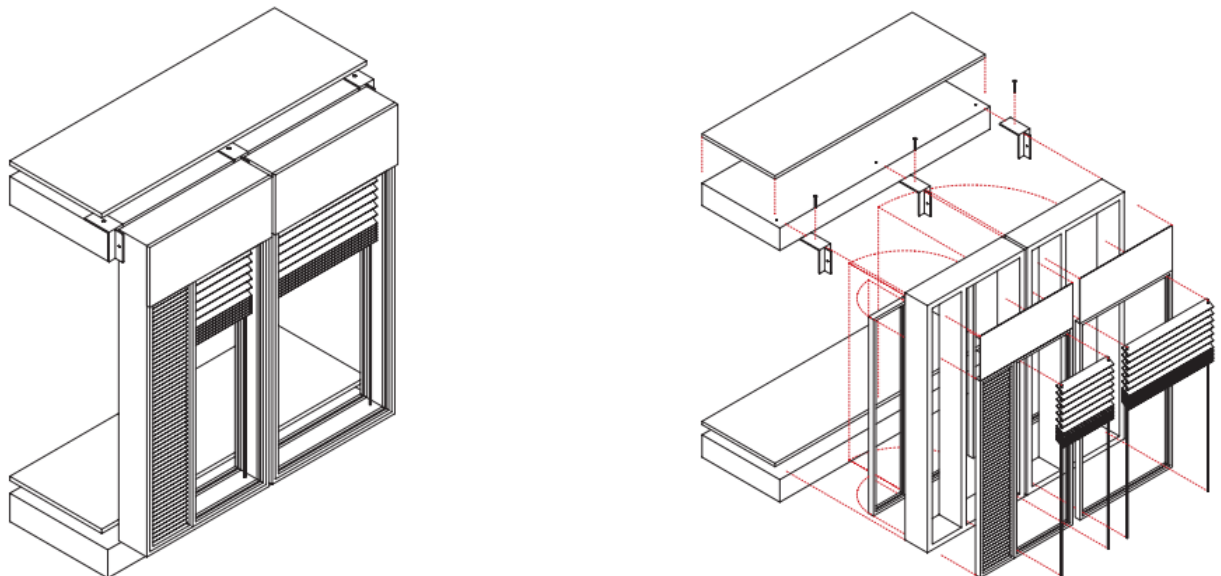


Figure 2.2. An example of a box window skin element which contains multipurpose multi layers elements including double-glazed unit, single-glazed unit, internal shading devices and external louvers (Knaack et al. 2007).

2.1.2 Double skin facade

Double skin (DSF) and multiple skin façade systems has been used in new structures and renovated ones in order to enhance the performance of the building envelopes, reduce energy consumption and increase thermal comfort. The Belgian Building Research Institute (Mahmod 2011) describes both systems as multiple layers glazed or transparent skins which can be air tight or ventilated. The cavity can be either naturally or mechanically ventilated. The systems can include integrated devices that can use active or passive techniques to improve the performance of the envelope. Active systems can be managed using control systems. The DSF consists of three main parts which are the main envelope structure, the air gap or airflow cavity and the transparent boundary layer. The behaviour of DFS depends mainly on ventilation and shading (figure 2.3). Under hot climate conditions, ventilation should be increased as much as possible in order to avoid having a heat sink in the air gap. Solar shading is essential, but its configuration and positioning must be considered so it does not obstruct the air flow. Vertical buoyancy flow or stack effect happens between lower air inlet and upper outlet as natural ventilation movement (Sakellaris 2007).

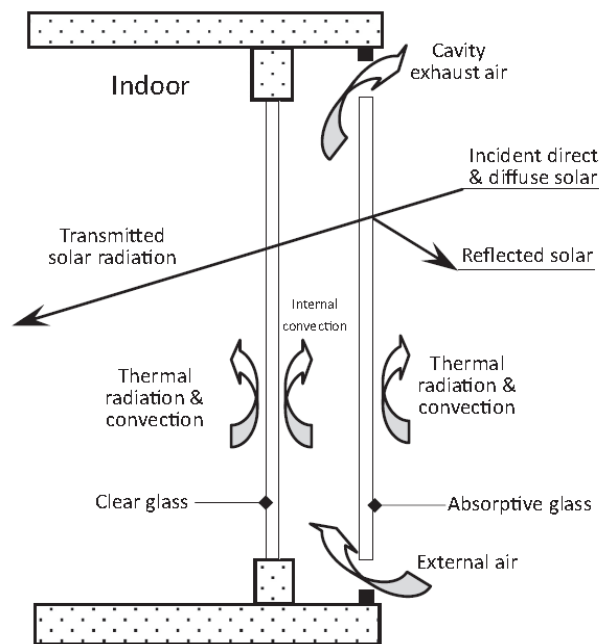


Figure 2.3. Heat transfer and heat flow within a DSF that is naturally ventilated (Chan and Chow 2014).

The classification of DSF is based on either design or ventilation strategy. Based on design, there are four types of DSF which are box window, shaft box façade, corridor façade and multi storey façade (figure 2.5). Shaft box façade is similar to box window but it covers multiple floors, acts as a continuous shaft in front of the façade to provide stack effect and has front openings to increase air flow. Corridor façade is like shaft box façade but has horizontal dividers which provide fire protecting or acoustic separation if required. Multiple storey façade follows the same principle of shaft box façade but without the front openings. Based on ventilation strategy, there are four types of DSF which are buffer DSF where the air gap acts as insulation while the heat gain is removed through stack effect, extract air DSF where the cavity serves as an extract shaft for the HVAC system, twin face DSF where both internal and external layers are openable to allow natural ventilation and hybrid DSF which combines different DSF types in one system (figure 2.4). There are many benefits of DSF systems that are reduction of solar gain, energy consumption and heating demand, improvement of thermal insulation, sound pollution and architectural look of the building. On the other hand, these systems increase construction, operational and maintenance cost, reduce daylight transmission, complicate the control systems and increase the overall area (Mohammed and Alibaba 2015).

When it comes to DSF, several aspects must be covered to evaluate the efficiency of the system. Firstly, as natural light can affect building occupants psychologically and biologically and has a huge impact on the experience of the space, it is one of the main aspects that should be considered in any DSF research. Secondly, investigation of the advantages of using integrated photovoltaics within the DSF as it may improve the over-all effectiveness and performance of the system. Thirdly, DSF material has a major impact on the performance, aesthetics of the system plus structural design. Fourthly, size of cavity depends on type and size of shading device, requirement for maintenance and cleaning, required flow rate and architectural design intent. Fifthly, wind pressure specially in high-rise buildings as the system consists of several layers that will be affected by loads and pressure differences due to the airflow. Sixthly, the system affects also other important factors such as glare, cost, durability and

architectural flexibility. Several studies are arguing that the high cost can be justified by benefits of DSF such as energy saving and appealing architectural look. In general, many experts agree that this system is more cost-effective comparing to a single layer façade as it durable and long lasting while saving energy (Shameri et.al 2011).

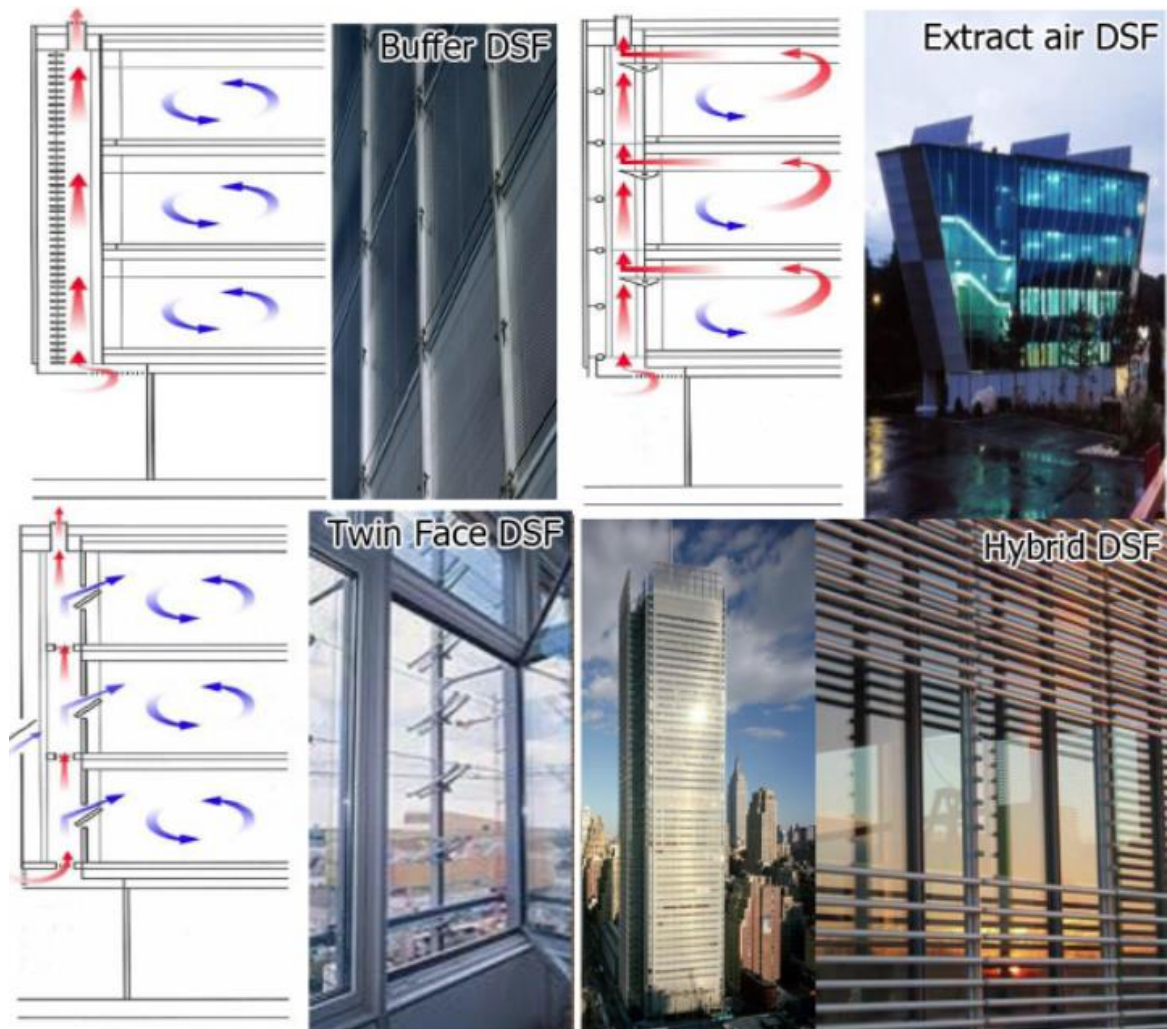


Figure 2.4. DSF classification based on ventilation strategy (Mohammed and Alibaba 2015).



Figure 2.5. DSF classification based on design (Mohammed and Alibaba 2015).

2.2 Ethylene Tetrafluoro Ethylene (ETFE) Applications in a DSF

2.2.1 Definition and background of ETFE

In any structure, the building envelope, which is called also building enclosure, shell or fabric, is the most important architectural elements that can affect the energy consumption throughout the life span of the building. In sustainable architecture, designing an efficient envelope has a key role in controlling the levels of occupant's comfort. It is obvious that glass has been always a very popular component of any building's facade in the UAE as it reflects the common contemporary style in the country. The Majority of the buildings in the country are either fully or partially glazed and as they are facing high solar radiation, the indoor spaced becomes overheated which increases the cooling demand in them. This happens as the typical u-value of a double-glazed unit is almost 1.8 W/m² K, with consideration to window frames, while the u-value of a typical insulated masonry wall is 0.35 W/m² K, thus glass can increase heat gain five times, if compared to a typical solid wall without considering the greenhouse effect. Of course, these are approximate values from personal experience and observation that can vary when the glass or wall parameters change. For example, this change can be a low emitting coating added to the glass unit or adjustment in the wall insulation thickness and density.

There are different light weight structure technologies that can substitute large glazed areas. This lightweight structures include many types such air supported or air inflated elements, domes and free domes, pneumatic systems, tensegrity and cable net and tensile fabric structures (LSA 2015). In the 20th century, new innovative materials and technologies were introduced into the architectural field, but most of them flourished for a while then their popularity started to decline. For example, concrete shells and fabric structure flourished for almost 30 years then they faced a decline. On the other hand, ETFE foil technology market continue to grow as it has a significant impact on design and performance of buildings due to its durability, light weight and other characteristics. An English engineer called Frederick Lanchester was the first one to propose a pneumatic structure design for a small military hospital in 1917. His idea was to support a big tent by low air pressure. The same engineer with his architect

brother proposed a similar design for 1000 feet in diameter exhibition centre which is supported by a steel net and air pressure. But these proposals were never built, so it was only contribution to the concept without physical application. Richard Fuller is considered the real father of light weight architecture. He always had an ecological philosophy that drove his designs for the lightweight transportable buildings that he created for the army. After the second world war he developed his design ideas for civilian applications. He was the first architect to develop lightweight geodesic domes by using a pneumatic sandwich that consisted of double layers membranes. His most famous projects are the gardens of Eden and the Montreal EXPO American pavilion. Frei Otto, the German architect who founded the Stuttgart light weight structure institute, developed the principals of lightweight structures and investigated the potential of air as a part of the structural support of the building envelope. Most of Otto's theories were based on the bubbles, not only for their environmental implication and structural principal but also as he considered the philosophy of using minimum material to achieve maximum efficiency to be a real measure of architectural development (LeCuyer & Böhme 2013) .

Few years later, Expo 1970 in Japan, was the largest event the included pneumatic structures that were air-supported. With inspiration from Otto's ideas, Murata and Kaeaguchi designed the floating theatre which was supported by floating inflated cushions that had an automatic system that can adjust them following the movement and number of audience. In addition, Kenzo Tange designed the festival plaza roof as steel structure frames with embedded multiple layers air inflated translucent cushions that were able to stand weather conditions, dead loads and heat. But the most significant building was U.S. pavilion that was designed by a large team of American and Japanese architects and engineers that included Ohbayashi-Gumi, Brody,Chermayeff, De Harak , David Geiger and others. The project included 140 meters by 83.5 meters light weight pneumatic roof that was supported by steel cables net. The building with a great structural achievement as the diagonal net design reduced the weight of the cables be 33% comparing to the regular rectangular grid, that's why most of the lightweight buildings now follow the same design. The importance of this building came from the fact that its weight was 1% of Fullers smaller geodesic dome

,77 meters in diameter, weight and its cost reached only 50% of the dome cost which reflects the massive development that happened for pneumatic structures in only three years. Following this success event, several architects such as Frei Otto, Ted Happold and Kenzo Tange used the same concepts to propose air-supported light weight structures for scientist projects in Canada and the region around the north pole. Among these proposals, Buro Happold set up a scheme that used ETFE inflated cushions. The new material started a new stage in the evolution of pneumatic structure as the previous similar projects included vinyl coated glass fiber fabric , Teflon-coated fiberglass and multiple polyester film cushions (LeCuyer 2008).

ETFE is a synthetic polymer material made mainly from fluorite, hydrogen sulphate and trichloromethane. These substances when decomposed by high temperature produce tetrafluorethylene transparent gas. When this gas is combined with ethylene, the output becomes the ETFE copolymer resin. As the material basic form is powder, it needs compression in order to have the final pellets (LeCuyer & Böhme 2013).

Ethylene Tetrafluoro Ethylene (ETFE) is part of tensile pneumatic façade systems types. These systems use membrane or foil layers which uses the difference between inner and external pressure to achieve structural stability and to have the required stiffness to support external loads (figure 2.6). The current common systems are the positive pressure types which are either inflated (multiple layers) and air supported (single layer). The multiple layers system has a closed structure with a pressurized non-accessible interior. ETFE is a processed melted fluoropolymer that falls under thermoplastic category. It is a low cost and lightweight alternative to cladding materials and glazing which has free forms with large spans. ETFE is a plastic material that is being used in several building applications due to its durability, sustainable benefits and the flexibility it gives to building structural concepts as it can be used to achieve various unusual geometric forms. The system consists of two to five membranes layers that are welded around the edges and needs air pump to provide constant internal air pressure that falls between 250-700 to acquire the thermal resistance and structural stability. Moreover, its advantages include resistance to ultra

violet rays (UV), low maintenance requirements and low danger possibility in the case of fire (Liu et al. 2016) The unit U-value depends mainly on the number of layers/foils as the molecular difference between the solid membrane and air creates resistance against the transmitted thermal energy. According to Dimitriadou (2015) the average U-value of a 2 layers cushion is 2.9 W/m²K, average U-value of a 3 layers cushion is 2.0 W/m²K, average U-value of a 4 layers cushion is 1.5 W/m²K and average U-value of a 5 layers cushion is 1.2 W/m²K. A single layer ETFE membrane can transmit up to 97% of visible light while a double layer ETFE cushion can transmit up to 76% of visible light which means that number of layers and transparency are inversely proportional.

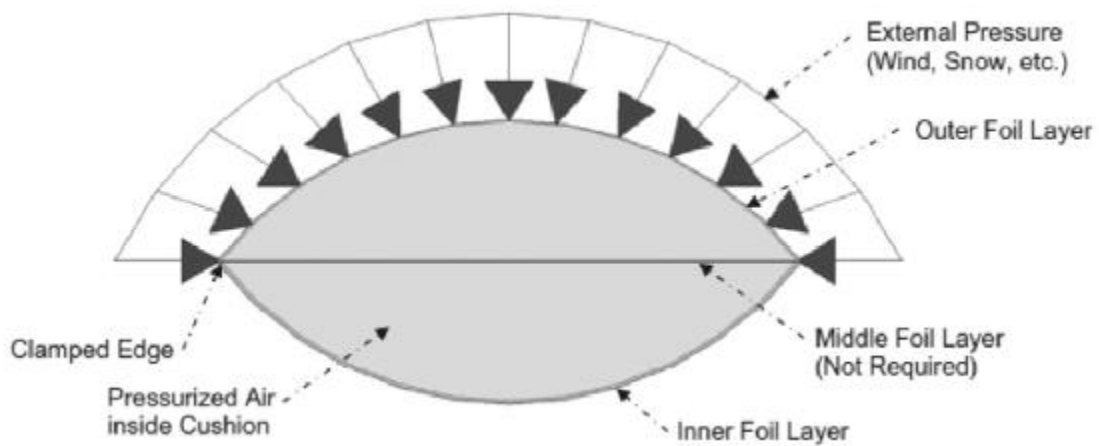


Figure 2.6. ETFE cushions schematic (Lamnatou et al.2017).

The system consists of the cushion which includes extruded ETFE membranes, frame clamping (figure 2.7), most likely aluminium, and air supply system that includes translucent pipes and fans (operating unit and back-up unit) (Novum Structure 2018). Similar to any glass unit, the aluminium frame can have internal thermal insulation layer to resist thermal bridge. The feeding pipes connect to the cushion through air valve which, with the support of the air supply system, keeps internal constant pressure of 250~700 Pa. The purpose of the non-return valve is stopping the cushion from losing air in case of system failure which can keep the pressure in the cushion for approximately 6 hours Usually, a 1000 m² system requires only two fans with 100 Wh of hourly energy consumption. As one the operating fans is only for back-up, the total energy consumption is 438kwh annually. Hence, the average power consumption is

0.44kWh per a square meter of an ETFE pillow area. If required, the system include also a dehumidifier to avoid humidity accumulation in the cushion. For a 1000 square meters interior damp space, a 18L capacity humidifier is needed. The overall energy demand of a typical 20 L capacity dehumidifier is 2321 kWh annually (Dimitriadou 2015). From my experience in the UAE, the dehumidifier is usually a part of the AC system itself and it is only used for humid areas such as enclosed swimming pools. Thus, it is not required as a part of the ETFE cushion system. The Cushion surface can be treated using chemicals or electrical discharge or focused radiation in order to print patterns or what is called in structure as fritting. The printed pattern has the ability to provide shade and reduce heat gain depending on level of transparency and can be used for an aesthetic or visual purpose (Michael, Gregoriou and Kalogirou 2017). Most manufacturers use fluoropolymer inks in this process (Dimitriadou 2015).

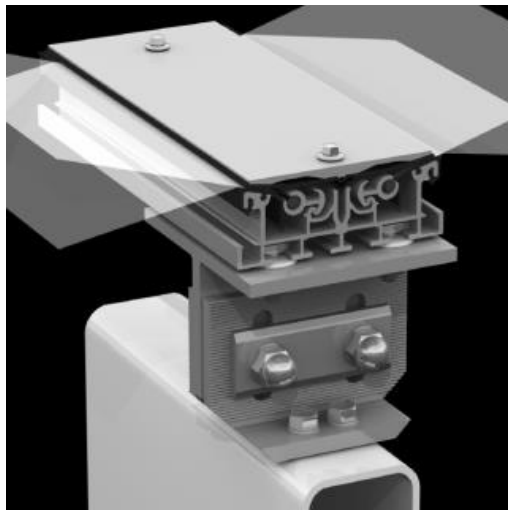


Figure 2.7. ETFE clamping aluminium frame (Novum Structure 2018).

In recent years, this material is being used vastly in prestigious projects such as Allianz Arena which was open in 2005 in Munich, Germany, Eden project which was open in 2001 in Cornwall, England and the Water cube which was open in 2008 in Beijing, China (Dimitriadou 2015).

ETFE was used in the façade of the Westraven building which was fully constructed in 2007 in Utrecht, Netherlands (figure 2.8). The project is a combination of new buildings and existing government buildings. The high entrance of the building

and the sheltered inner garden are fully covered (walls and roof) with double layer ETFE. The designers used also ETFE as a second skin façade in front of glass in order to provide protection against wind and allow opening the main glass windows (Gao 2012).

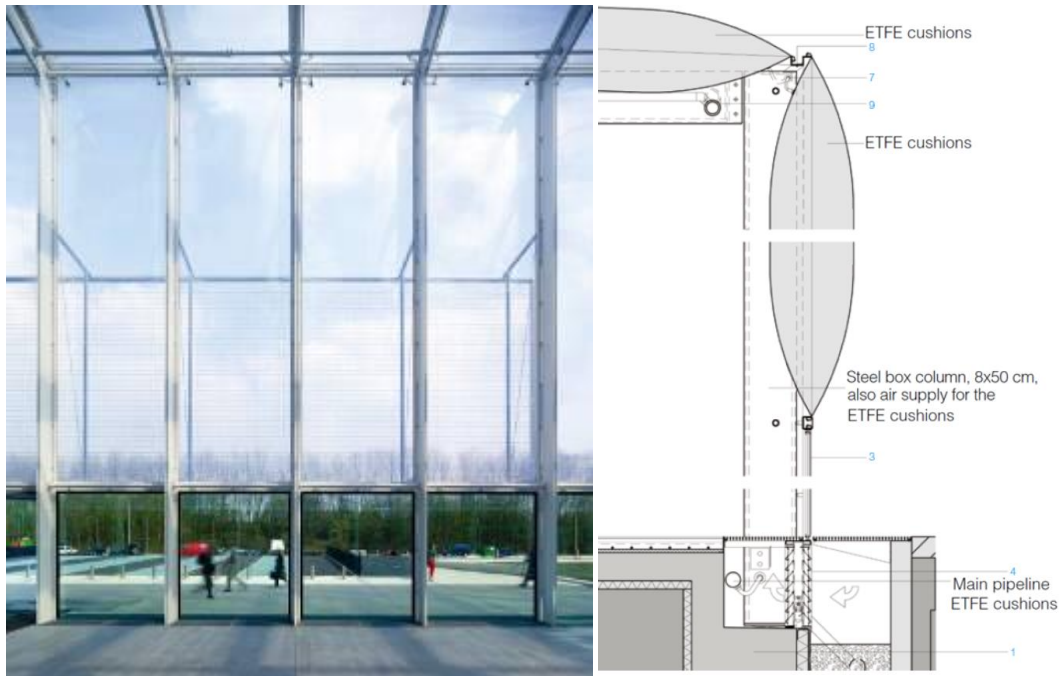


Figure 2.8. Westraven building ETFE detail (Gao 2012).

The most fascinating part in Allianz Arena (Munich's football stadium) is the remarkable envelope which looks like an astonishing sculpture (figure 2.9, 2.10 and 2.12). The ETFE cushions have embedded fluorescent lights that change from white to blue or red depending on which local team is playing. The envelope is divided into 2874 rhomboid-shaped double-layer ETFE cushions supported on steel lattice frames (figure 2.11). The identical cushions are fixed on an aluminium frame. The building has 12 air-pumps that support the constant internal pressure as 300 Pa in the roof cushions and 400 Pa in the façade cushions. The 0.2 mm thick foil is fritted with a gradient pattern. The system weight is less than 1.0 kg/m² and has a high fire-resistant degree rating (B1) (Schittich 2012).



Figure 2.9. Allianz Arena stadium in Munich with the ETFE envelope (Schittich 2012).



Figure 2.10. Allianz Arena stadium in Munich with the ETFE envelope (Schittich 2012).

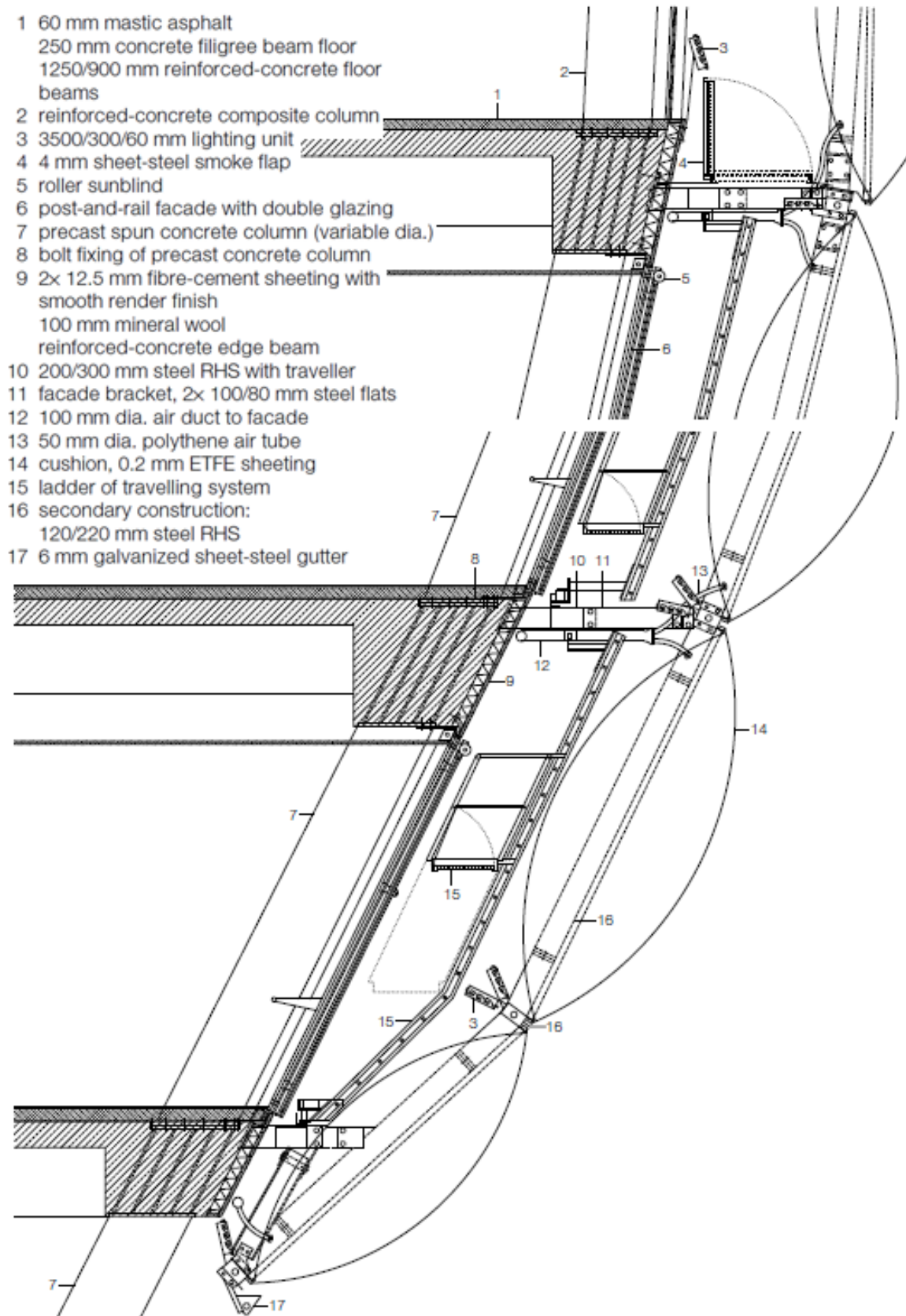


Figure 2.11. Allianz Arena envelope detail (Schittich 2012).



Figure 2.12. Allianz Arena stadium in Munich with the ETFE envelope (Schittich 2012).

Eden project, which is one of the largest botanical gardens in the world, consists mainly from large span (124 m) intersecting domes (figure 2.13). These geodesic domes represent a second sky and supports a light weight ETFE cushions envelope that stands between two structural layers (figure 2.14). The outer layer is a hexagonal steel frame and the internal layer is hexagonal and triangular steel frame. The intersecting parts are supported on triangular steel trusses. The cushions internal pressure is kept constant using compressors (Schittich 2012).

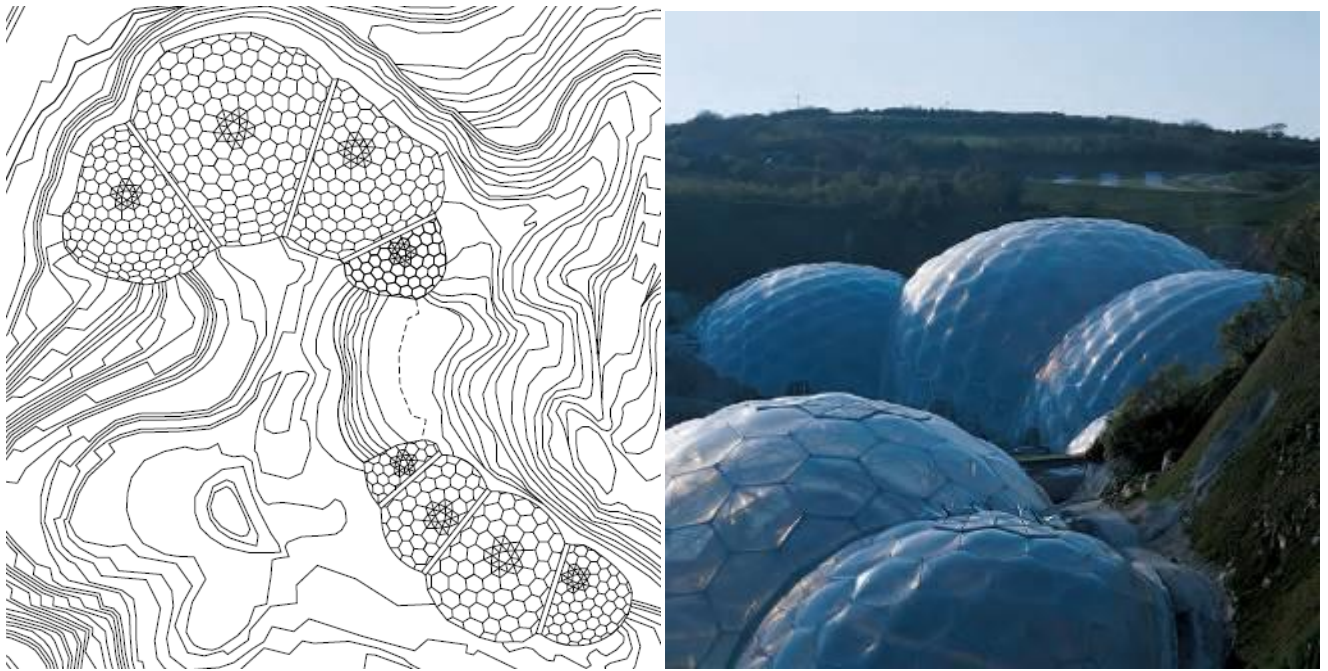


Figure 2.13. Eden project layout and aerial shot (Schittich 2012).

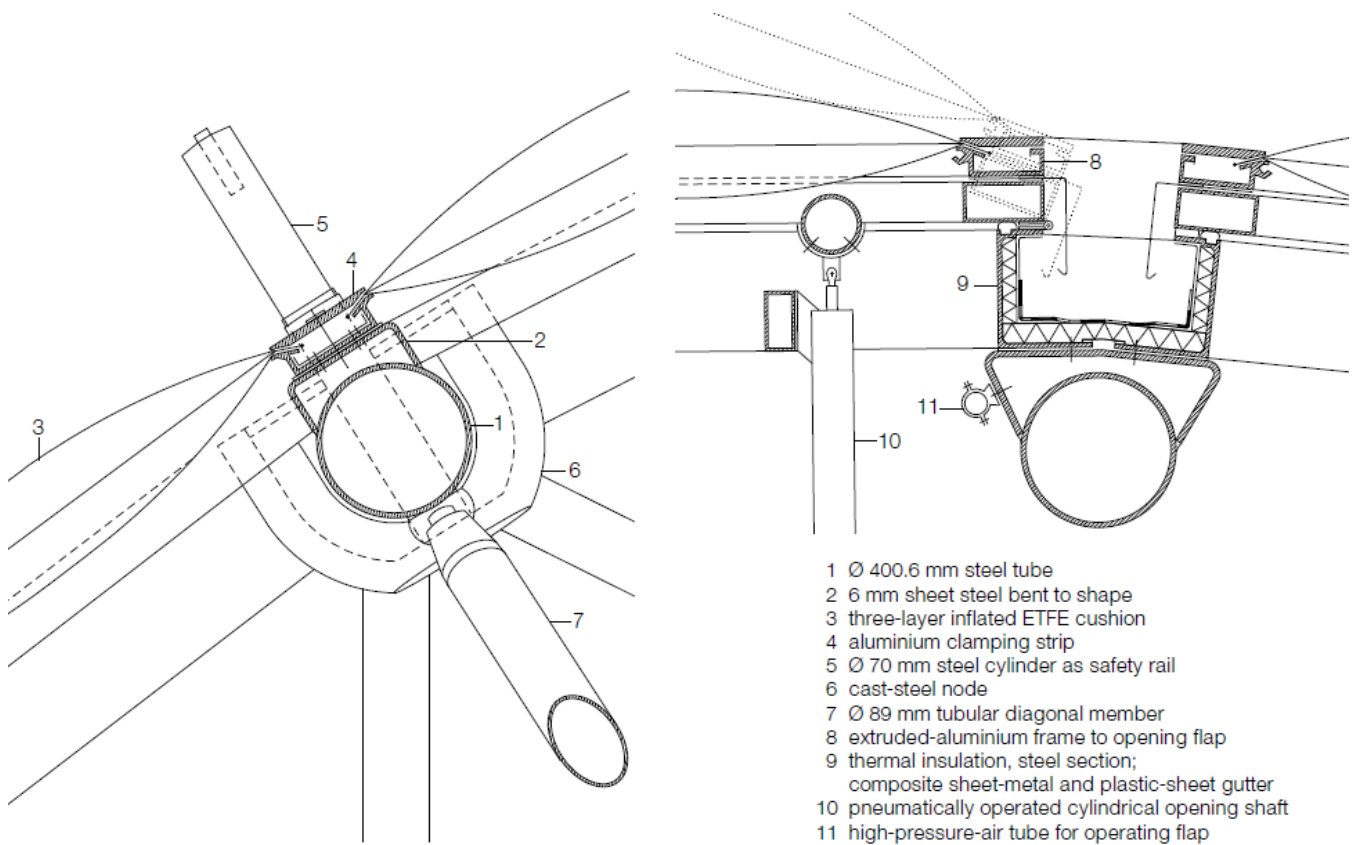


Figure 2.14. Eden project envelope detail (Schittich 2012).

In the literature review section, several studies which investigated ETFE from various points of view, were presented. For instance, some studies focused on mechanical behaviour, other studies examined insulation and light transmittance, some authors investigated the life cycle analysis of the material while others study the integration of PVs into the ETFE cushions. Some authors provided general critical review about ETFE which covered the high-performance material general characteristics, configuration, acoustic behaviour, shading issues, different applications and case studies. It can be seen that this material introduces interesting characteristics and sustainable building application.

2.2.2 Building integrated photovoltaics

As mentioned earlier, the world is facing two major challenges which are the depletion of fossil fuels reserves and the increasing amount of greenhouse gases, mainly due to fossil fuel combustion, in the atmosphere. Therefore, it is a very significant matter to evaluate the benefits of using alternative power sources in buildings, namely, solar power. Photovoltaic cells system is a favourable option of generating electricity due to its advantages such as, it doesn't produce greenhouse gases, it needs minimum maintenance with low operating cost and it is a flexible system. Flexibility comes from the fact that it can be integrated within the envelope material such as ETFE cushions. Solar cells are made mainly from silicon crystal. The reason is that at zero temperature, silicon acts as an insulator but once the temperature is raised the atom bonds breaks and electrons move freely (figure 2.15). It is known that silicon is the second most plentiful material in earth's surface ,25% of its crust, mainly as silicates and silicon oxide (Agrawal &Tiwari 2011).

According to Das (2014), the casted solar irradiation on a square meter of earth can generate, on average, seventeen hundred kilo watts per hour yearly. Also, the total solar radiation on earth can covers the global power demand thousand times over. Thus, sun is a massive source of non-polluting power that is usually wasted. In a photovoltaic cell, solar energy is converted due to the photovoltaic effect which happens when the solar light falls on a semi-conductor material. The basic design of a PV cell consists of four layers which are the front contact grid, n-type top layer, p-type

bottom layer and the back contact. The photons, as energetic particles, when hits the PV cell, they are either reflected, absorbed or penetrate the cell. When they are absorbed, the photon energy shift to the electrons of the p-type layer which frees them from the atoms and pushes them to the n-layer. The lack of electrons in the lower layer makes it positively charged and the additional electrons make the upper layer positively charged. When the two layers are connected with a wire, the electrons flow through it an create an electrical current (Cardona, Chica & Barragán 2018).

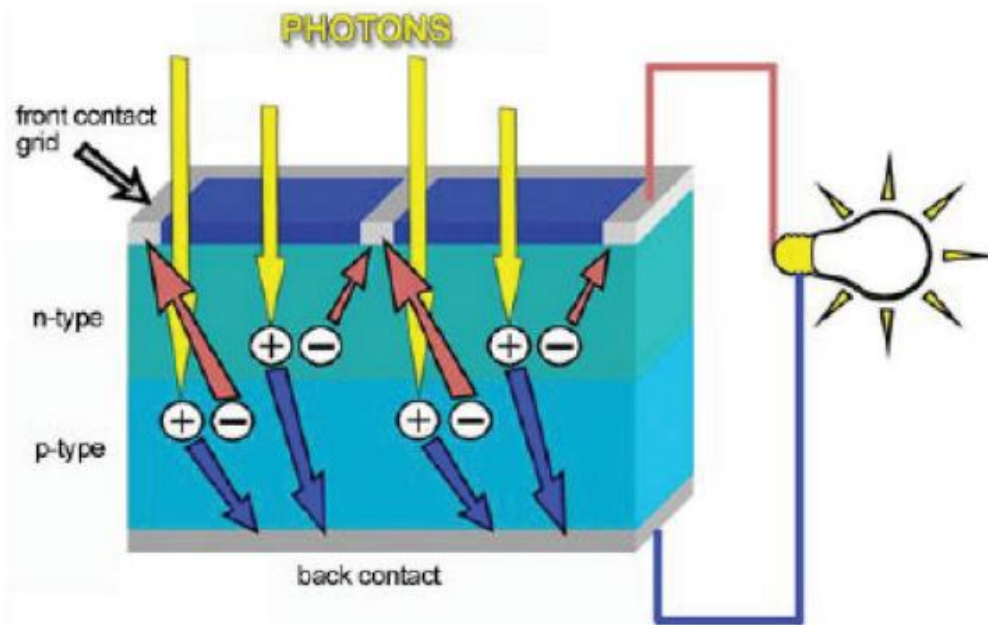


Figure 2.15. Basic PV cell diagram (Das 2014).

The generated power comes in a form of direct electrical current (DC) which can be transformed into alternating current (AC) using an inverter. The most common inverter type used for BIPVs is the self-switching separated type with nominal power that ranges from 1 to 50kVA. However, there is a new embedded type which is attached to the PV module directly that can save cost and installation time. In spite of that, this type makes a challenge for the control system as it handles several invertors at the same time. The system includes also general distribution board, charge controller, battery and monitoring device (Cardona, Chica & Barragán 2018).

The most common PV types are thin-film panels, polycrystalline and monocrystalline. However, organic solar cells and multijunction solar panels are gaining more popularity in the industry. Monocrystalline type, which is called also (c-Si), is made of a single silicon crystal, thus it is expensive but more efficient. On the other hand, Polycrystalline type, which is called also (mc-Si), is made from several silicon crystals, hence is more economic but with less efficiency. Thin-film panels (a-Si) are made of non-crystalline silicon, copper indium gallium selenide or cadmium telluride. The advantages of this type are that the panels are flexible and can be placed on irregular shapes, they can produce electricity from indirect light and cheaper, but they are less efficient. Multijunction types (figure 2.16) contains different layers of various materials and can achieve 40% efficiency. Due to their high price, they are not usually used in residential applications. The cheapest type is the organic cell which is made of organic components and has an efficiency of 7% that is very low comparing to the other types (Das 2014).

Amorphous Silicon Solar Cells (a-Si), part of the thin film solar cells family, is a popular type used for exterior architectural application due to its thickness and visual look. There are two kinds of this type which are transparent and opaque. (Agrawal & Tiwari 2011). a-Si module average efficiency is 6% which is half of the average efficiency of c-Si module (12%) (Dubey, Sarvaiya & Seshadri 2013).

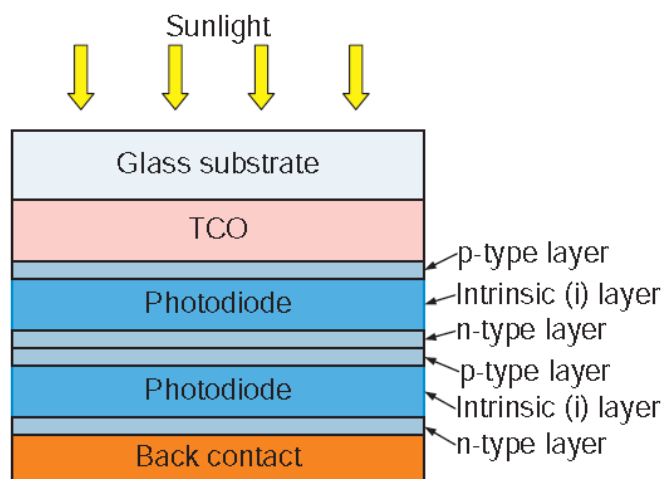


Figure 2.16. Double junction a-Si solar cell section (Agrawal & Tiwari 2011).

It goes without saying that PV efficiency drops when temperature increases as the produced current exponentially due to changes in carrier concentration which reduces the output voltage. Depending on PV type, material and ambient conditions, the efficiency varies from 6% to 20% as most of the received radiation is converted into thermal power (Dubey, Sarvaiya & Seshadri 2013). According to Hu et al. (2015) When the a-Si PVs surface temperature increases by 1°C, the generation efficiency drops by 0.2% considering that the PVs base temperature, or common testing conditions temperature, is 25°C. a-Si can be developed to become photovoltaic thermal unit or PVT which extract the heat by flowing air or water beneath the unit by a thermal collector. It is proved by experiment that PVT liquid collector is better than PVT air collector. PVT improves efficiency by an average of 3%. Another study which tested different types of PVTs (a-Si), which are unglazed type, glazed type and conventional type, proved that the annual efficiency increased to be 7.6%,6.6% and 7.2%. Other factors that can affect efficiency are dust accumulation, wind, solar irradiation (figures 2.17 and 2.18) and solar exposure hours (Dubey, Sarvaiya & Seshadri 2013).

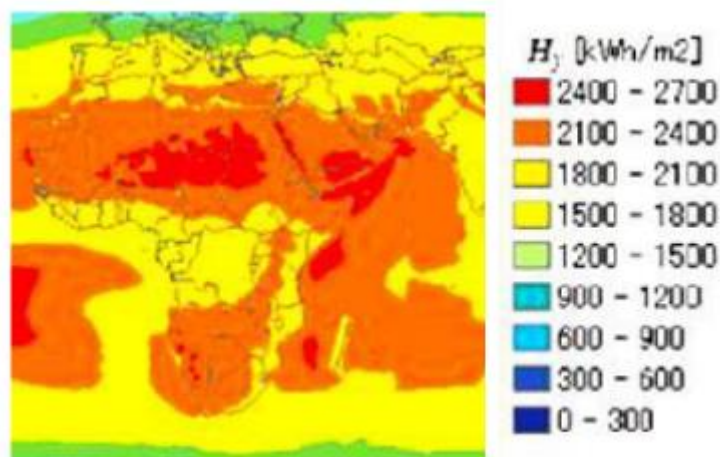


Figure 2.17. Region map of annual solar irradiation levels (Dubey, Sarvaiya & Seshadri 2013).

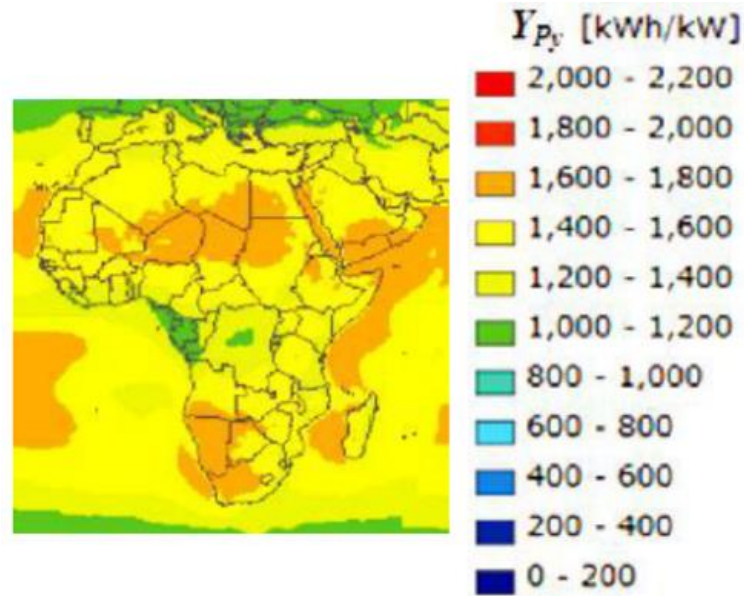


Figure 2.18. Region map of predicted annual PV generated power based on highly efficient PVs (c-Si) (Dubey, Sarvaiya & Seshadri 2013).

Hamoua, Zinea and Abdellaha (2014) conducted an experiment on monocrystalline module (mono-Si) under the ambient conditions in south of Algeria. The purpose was to study the effect of air mass, temperature and solar irradiance on the efficiency of the module in the morning, from sunrise until before sunset by measuring all variables and following W. Durisch empirical model calculations. The increment of solar radiation from morning to noon increased efficiency 8.68% to 9.09%. The increment could have been more but due to the increasing air mass, volume of air with relation to temperature and percentage water vapor, and temperature, the limit of efficiency increment was only 0.41%. With a basic temperature of 25°C, air mass of 1.5 and irradiance of 800w/m², the module reached its maximum efficiency.

Peng, Herfatmanesh and Liu (2017) investigated the relation between PV panels cooling and efficiency improvement. The experiment was made with polycrystalline-Si solar module type with irradiance power of 160W, 300 W and 400W and the output was current and voltage were measured by metering system. Similar to other studies they reported in reduction in output voltage with the increment of surface temperature. The cooling system included a water pump for cooled water, cooling tower unit and water

tank to store the warm water (figure 2.19). When the cool water tube touched the back of the solar panel it absorbed heat, through natural convection. then part of the produced hot water went to the cooling tower in order to become colder and go back to the circulation process while the other part went for the tank which store hot water for domestic use. The cooling tower managed to reduce the water temperature by 10°C in summer. Comparing to a conventional PV system operation, the cooling system managed to improve total output form 1805.76 kWh to 2430.05 kWh (34.6% increment) (figure 2.20). When the calculated power output from using the hot water was included, that added 1311.95 kW to the power saving annually. Subsequently, the total power output improvement was 107%. Comparing to a conventional PV system which had a 15 years of payback period, the cooled system had 12.1 years of payback period considering the additional equipment cost.

The last factor which can affect PV overall efficiency is dust. According to Zaihidee et.al (2016) this factor can cause physical damage and degradation to the PV panel, reduce the received amount of solar irradiation and increase surface temperature. An accumulation of 20grams per square meters can reduce efficiency by 15 to 35%. This factor can be neglected in the research as the PVs will be embedded insides the ETFE cushion, thus there will not be direct contact with airborne particles.

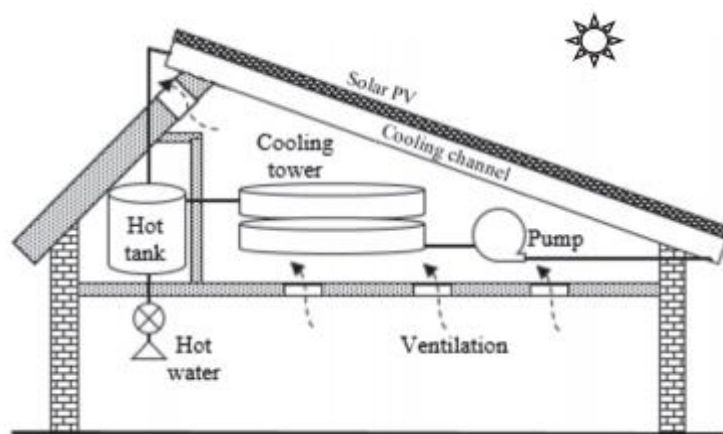


Figure 2.19. PV panel cooling system diagram (Peng, Herfatmanesh & Liu 2017).

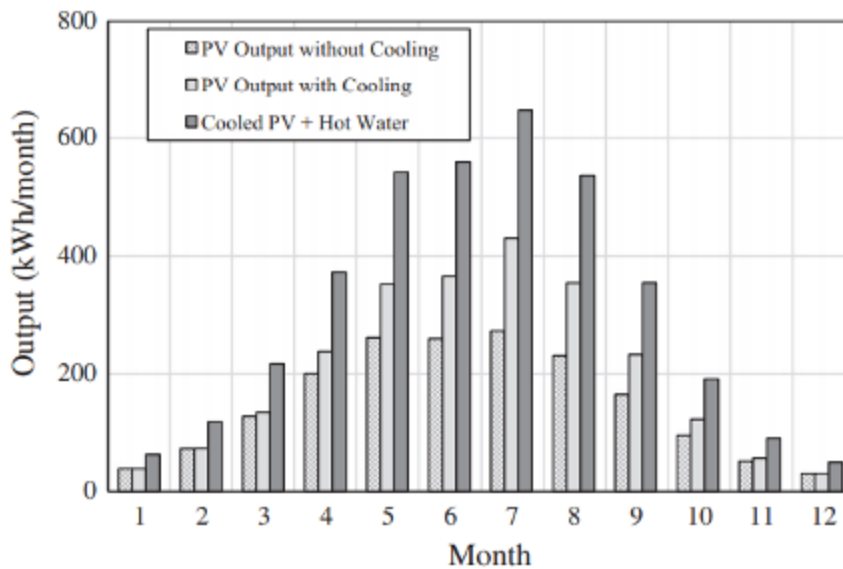


Figure 2.20. Comparison between the overall output of the three experiment conditions (Peng, Herfatmanesh & Liu 2017).

2.2.3 Dynamic Screens and shading devices

Transparent materials such as glass and ETFE is popular among architects in the UAE as they create aesthetic elegance, add pleasant lightness feeling for the building and add more interaction between the internal environment and the external one. As mentioned earlier, transparent façade, especially in a hot and humid country, has a negative impact on the internal thermal comfort and the cooling demand. Besides the basic option of replacing glass with different material to enhance the overall envelope performance, there is another option that should be considered in the research which is the dynamic solar shades. ETFE can be used in this application as the full system weight is approximately 0.45 kg/m² that is considered structurally negligible, hence it can be added easily to facades even in existing building with minimum structural consideration. Generally, if the additional load on the façade is less than 0.5 KN/m² (50 kg/m²), the safety factor (margin) can cover it in the structural calculations (Dehliah ,A.2018,pers. Comm.,24 July).

Dynamic solar shades or dynamic façade is part of kinetic architecture where parts of the building are allowed to move, using mechanical and electronic equipment, in order to respond to the external conditions, enhance the envelope performance, improve thermal and visual comfort and for aesthetic purpose. The system can control heat transmission into the building, solar radiation into the space, daylight utilization, glare protection, external views and privacy. Dynamic façade is more feasible comparing to static one as it can respond reasonably to changes in the exterior environment while the performance of the static façade depends on the exterior conditions only such as season, sun location and external shadows and not on the changing needs of the occupants.

In the second half of the twentieth century, the development of mechanical, electronical systems encouraged evolution of dynamic and kinetic façade systems. One of the first architectural movements that was influenced by this direction was Metabolism and Arshigram movement that emerged in Japan after the second world war. The architects of this movement believed that buildings should be able to grow and change like a living creature and shouldn't last for centuries like traditional buildings. Pioneer architects like Frei Otto, Richard Fuller, Chuck Hoberman and Santiago Calatrava developed many designs that helped to develop the dynamic facade concept. The birth of the concept came with Fuller's early work when he designed the movable pre-cast elements of the deployable house then it grew with the researches of suspended light structures and tensile architecture that were done by Frei Otto. Otto also developed computer programs to assist in light weight structure design which included active parts such as folding roofs. Calatrava, who was always inspired by nature and obsessed by advanced technology, had a key role in the development of kinetic architecture. Furthermore, Chuck Hoberman made huge steps in this fields as he developed structural and mechanical systems which is based on hinged light weight elements to create the dynamic façade. The current trend in dynamic facades is artificial intelligence which controls the active elements via the building management system with minimum human interference (Ramzy & Fayed 2011).

Project Kiefer technic showroom, which was constructed in 2007 in Steiermark, Germany and designed by Ernst Giselsbrecht & Partner, is a great example of dynamic façade and utilization of active shades (figures 2.21,2.22,2.23 and 2.24). The shades adapt automatically to the changing needs and surrounding conditions even without human control. The changes happen almost every hour to create a new façade shape which makes the building an outstanding changing sculpture. The perforated screen movement happens when the screen elements are folded separately to create various forms (Mahmod 2011).



Figure 2.21. Project Kiefer technic showroom (Architonic 2018).



Figure 2.22. Project Kiefer technic showroom (Architonic 2018).



Figure 2.23. Project Kiefer technic showroom (Architonic 2018).

Another example is Debis headquarters project which was built in Berlin and designed by Renzo Piano and Christoph Kohlbecker. The building has a double skin corridor façade with an operable exterior laminated glass screen which rotates around single axis from 0 degree (closed position) to 90 degrees (fully open position) using mechanical motor (figures 2.24,2.25 and 2.26). In summer. In summer, the screen opens to allow natural ventilation to flow inside the double skin to remove heat and in winter the screen closes to trap heat within the façade. (Mahmod 2011).



Figure 2.24. Debis headquarters project (Council on Tall Buildings and Urban Habitat 2018).



Figure 2.25. Debis headquarters project (Council on Tall Buildings and Urban Habitat 2018).

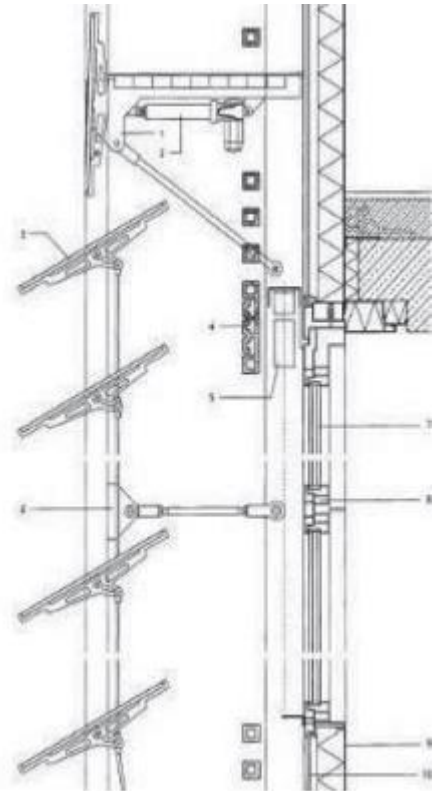


Figure 2.26. Debis headquarters project façade detail (Lawrence Berkeley National Laboratory 2006).

The final example is the Kinetic Ambient reflection membrane building which was constructed in Berlin, Germany in 2008. The project dynamic façade consists of metal screen/pixels that can be tilted individually using pneumatic actuator (figure 2.27). These elements are called the flare system where façade acts like a living component that can change its form to respond and interact with the outer environment. The flare units pattern is so flexible that it can be mounted on any building shape. The main purpose of the system is aesthetic but also it can adjust itself to sun position and thus reflect solar irradiance efficiently (Mahmod 2011).

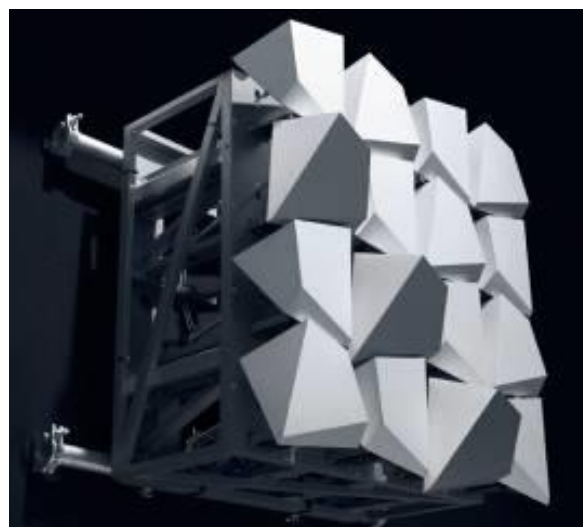


Figure 2.27. The flare kinetic façade system (White Void 2008).

Johnsena and Wintherb (2015) studied the effect of using dynamic shades on the over-all U-value of a high-performance glazed façade comparing to the effects of changing the glazing type. The U-value of the basic glazing unit that consisted of double low-energy glazed unit (6-15-4 mm) was 1.1 W/m²K with a light transmittance (LT) of 0.79. When the researchers used a triple low-energy glazed unit (6-12-4-10-4mm) the U-value dropped to 0.8 W/m²K and LT became 0.7, then they used triple solar protective glazed unit (6-12-4-12-4mm) which achieved a U-value of 0.7 W/m²K and LT of 0.59. When the researchers applied the movable/active screen to the basic glazing unit the U-value varied from 0.5 to 1.1 W/m²K (fully closed shade position to fully open shade position) and LT varied from 0.02 to 0.79 (fully closed shade position to fully open shade position) (table 2.1). They concluded that the dynamic shades provided better performance (54%) comparing to changing the basic glazing unit to an expensive high performance units (27% and 36%) and it gave occupants the ability to control light transmittance into the space which enhance the internal visual comfort when daylight is utilized. Furthermore, the controlled usage of daylight reduced the lighting energy consumption annually by 8 kWh/m². Moreover, they recommended to convert the studies dynamic system to an intelligent type (connected to a building management system) so it can respond automatically depending on the weather forecast and occupant needs. The intelligent system can include 12 basic controlled positions of the shade that changes following season (summer, winter and spring/autumn) , solar intensity (sun and overcast) and occupancy (comfort mode with more day light and off-hours with less daylight).

Table 2.1. 12 different positions (Johnsena & Wintherb 2015).

| Season | Occupants and control 'mode' | Weather |
|---------------|------------------------------|----------|
| Summer | Present: Comfort mode | sun |
| | | overcast |
| | Off -hours: Energy mode | sun |
| | | overcast |
| Winter | Present: Comfort mode | sun |
| | | overcast |
| | Off- hours: Energy mode | sun |
| | | overcast |
| Spring/autumn | Present: Comfort mode | sun |
| | | overcast |
| | Off- hours: Energy mode | sun |
| | | overcast |

Dynamic solar shades can also be modular with separate shades that can be controlled separately for architectural aesthetic purpose to have different artistic pattern all over the façade. The individuality of the modules can also serve different goals in the same type such as allowing view to the outside at human eye level and provide shade at higher level depending on sun location and external conditions (Nagy et al. 2016). Modular dynamic façade can include also BIPVs and trace the sun location like the sun flower which is called adaptive solar façade which is beyond the scope of this research. Nagy et al. (2016) used an elastic pneumatic actuator, from silicon rubber, which uses 3 inflatable chambers to orient the separate modules on two perpendicular axes (figures 2.28,2.28.1 and 2.29). The control system applies air pressure that bends the actuator to the required direction. The researchers used a plugin in rhino software to predict the sun position and added a motion tracking device to the system to calculate altitude and azimuth angles.



Figure 2.28. Modular dynamic façade which allows different positioning for the shades/screen for various purposes (Nagy et al. 2016).

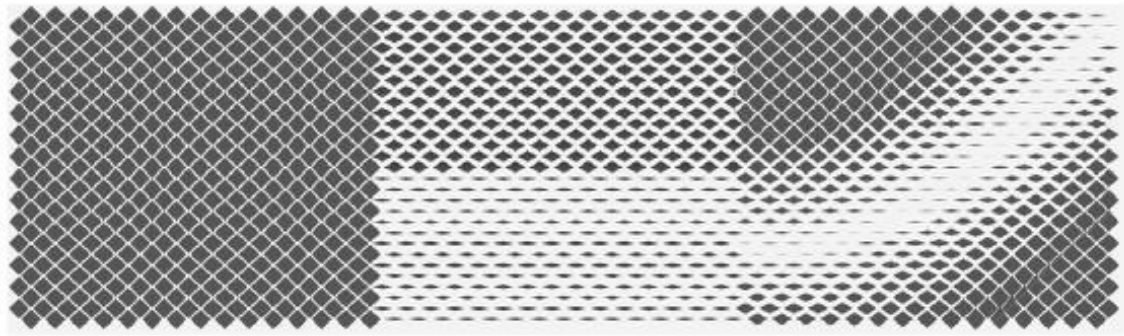


Figure 2.28.1. Modular dynamic façade which allows different positioning for the shades/screen for various purposes (Nagy et al. 2016).

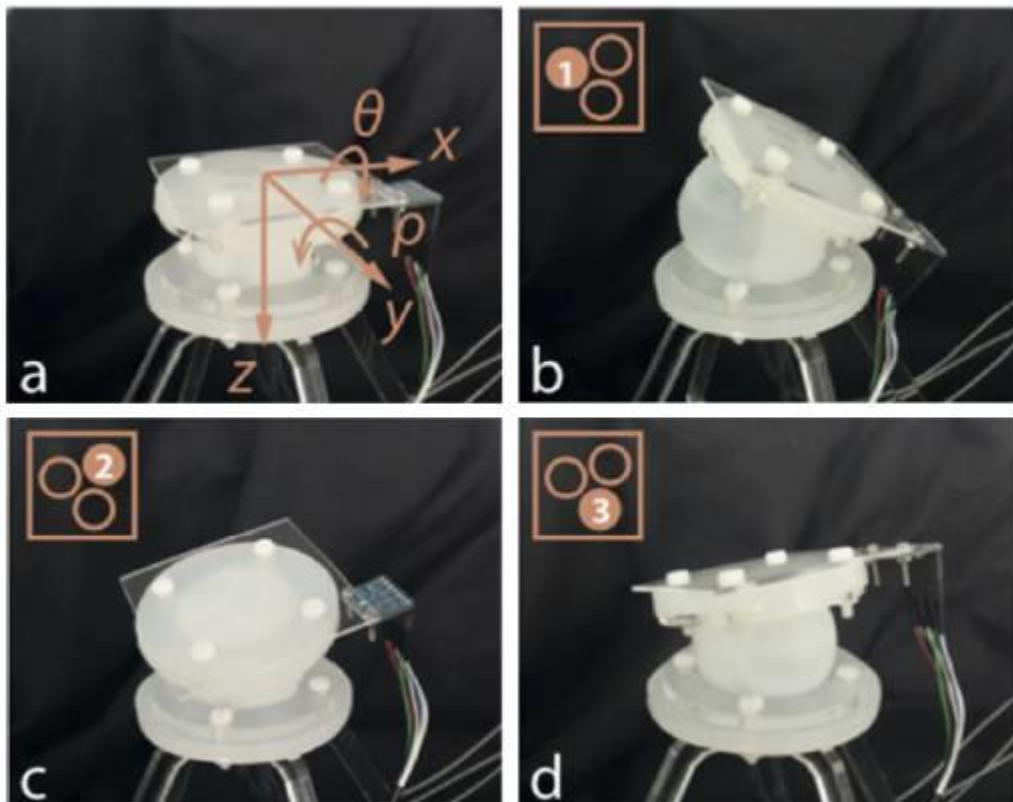


Figure 2.29. Pneumatic positioning actuator (Nagy et al. 2016).

2.3 Thermal Comfort in Buildings

2.3.1 Thermal comfort and static models

Thermal comfort is the criteria which engineers and building physicists follow to estimate building cooling and heating load. In general, thermal comfort is the situation where occupants are satisfied with the thermal condition in a space. Based on field studies and climate chamber testing on different interior conditions and human body heat exchange processes, building specialists created thermo-physiological standards such as European EN15251 standards, ASHRAE standards and Dutch ATG codes. Nowadays, these standards are widely used all over the world to determine thermal comfort in buildings. In general, thermal comfort studies provides satisfactory conditions for occupants, control energy consumption in buildings, control internal environmental conditions, affect building user's productivity and efficiency and reduce sick building syndrome.

Sir Barnard was the first engineer to introduce body heat transfer in 1914 by developing a special thermometer that can calculate air and radiant temperature plus the velocity of air. After 15 years, Dufton developed the definition of equivalent temperature to evaluate thermal comfort, but he did not consider environmental variables in his equations. From 1919 to 1976, ASHRAE based its criteria on effective temperature (ET) which was based on calculating temperature of objects from their radiation. After 4 years, Gagge developed ET_n which considers evaporation, convection and simultaneous radiation. Thus, it was more accurate factor. At the same time, Fanger produced equations and theories related to human body exchange of heat. He based his theory on the idea that the body pursue thermal balance. He proposed his famous formula to summarize his theory which was heat storage (S) is equal to metabolism (M) +external work (W) +heat exchange by radiation (R)+ heat exchange by convection (C)+ heat exchange by conduction (K)- Heat loss be evaporation (E)-heat exchange by respiration from both sensible and latent heat (RES). In his system thermal comfort is measured by comfort vote as shown in ASHRAE zone of thermal comfort classification and heat stress index table (table 2.2). The main six parameters that Fanger considered in his calculations were metabolism which indicates the chemical reactions in human body that happens as a result of various activities (tables 2.3 and 2.4) and measured by

watt, clothing resistance which ranges from 0 to 4 clo where 1 clo is equal to 0.155 1C/W, ideal relative humidity that ranges from 30% to 70%, air velocity which increases convection heat loss, ambient temperature around the body measured in Fahrenheit or Celsius and eventually mean radiant temperature which indicates heat loss and gain between the body and the surrounding environment. Fanger’s theory and equations are the basis of ASHRAE and ISO standards. The following standard tables were driven from his work. Later, several factors were considered in thermal comfort studies such as skin wettedness, natural ventilation and apparent temperature which considers air speed, relative humidity and air temperature (Taleghani et. al 2013).

Table 2.2. ASHRAE 55 zone of thermal comfort classification and heat stress index (Taleghani et. al 2013).

| Vote | ASHRAE | Bedford | HSI | Zone of thermal effect |
|------|--------------------|------------------|-------|------------------------|
| 9 | | | 80 | Incompensable heat |
| 8 | Hot (+3) | Much too hot | 40–60 | |
| 7 | Warm (+2) | Too hot | 20 | Sweat evaporation |
| 6 | Slightly warm (+1) | Comfortably warm | | Compensable |
| 5 | Neutral (0) | Comfortable | 0 | Vasomotor compensable |
| 4 | Slightly cool (-1) | Comfortably cool | | Shivering compensable |
| 3 | Cool (-2) | Too cool | | |
| 2 | Cold (-3) | Much too cool | | |
| 1 | | | | Incompensable cold |

Table 2.3. Recommended factors for activities based on ISO 7730 standards (Taleghani et. al 2013).

| Season | Clothing insulation (clo) | Activity level (met) | Optimum operative temp. (°C) | Operative temp. range (°C) |
|--------|---------------------------|----------------------|------------------------------|----------------------------|
| Winter | 1.0 | 1.2 | 22 | 20–24 |
| Summer | 0.5 | 1.2 | 24.5 | 23–26 |

Table 2.4. Recommended factors for activities based on ASHRAE 55 standards (Taleghani et. al 2013).

| Season | Typical clothing | Clothing insulation (clo) | Activity level (met) | Optimum operative temp. (°C) | Operative temp. range (°C) |
|--------|---------------------------------------------|---------------------------|----------------------|------------------------------|----------------------------|
| Winter | Heavy slacks, long sleeve shirt and sweater | 0.9 | 1.2 | 22 | 20–23.5 |
| Summer | Light slacks, short sleeve shirt | 0.5 | 1.2 | 24.5 | 23–26 |

When it comes to thermal comfort, ANSI/ASHRAE standard 55-2010 is based mainly on static (PMV/PPD) model that was developed by Fanger to calculate Predicted Mean Vote (PMV) where thermal comfort is measured on a seven-point system from (+3) hot to (-3) cold. In this model zero is the ideal case which represents thermal neutrality. He developed also equations of Predicted Percentage of Dissatisfied (PPD) based on PMV equations. ANSI/ASHRAE standard 55-2010 requires that minimum 80% of building users to be satisfied. Based on ASHRAE 55 , psychrometric chart is used to determine PMV ,PDD ,sensation and standard effective temperature (SET) which indicates human response to surrounding thermal conditions (figures 2.30 and 2.31) . The tool allows building specialists to test if the space complies with the standards based on the metabolic rate, clothing level, humidity, radiant temperature (Taleghani et. al 2013)

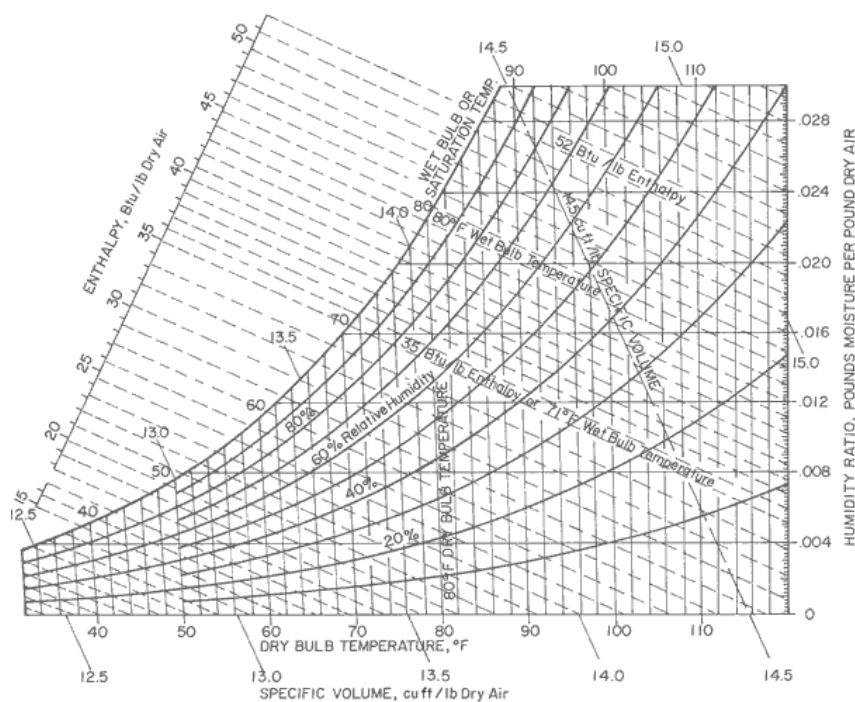


Figure 2.30. Psychrometric chart (Lechner 2015).

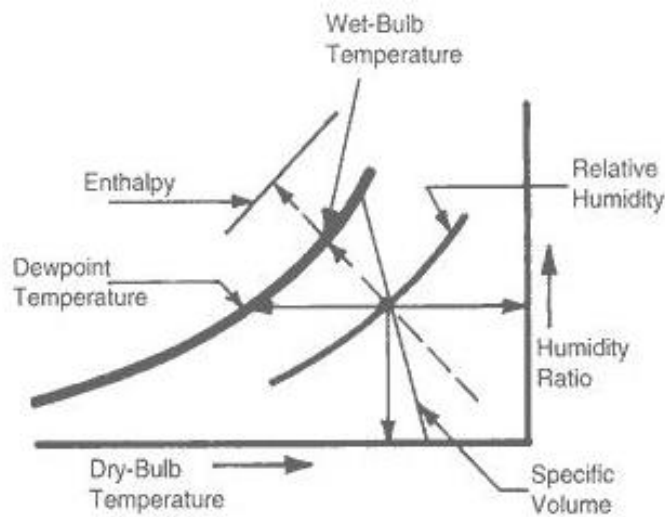


Figure 2.31. Psychrometric chart (Lechner 2015).

The horizontal part indicates the dry pulp temperature of air, the vertical axis indicates the amount of water vapor in air which is called specific humidity or humidity ratio, the curved lines indicates the amount of relative humidity (RH) and the upper curved line indicates the wet pulp temperature (figures 2.30 and 2.31). The chart contains also the enthalpy or total heat content and specific volume which is the ratio between volume and mass. All parameters of the charts are connected, and they affect each other. The lower edge shows that the air is fully dry, or 0% RH and the upper edge shows that the air is fully saturated or 100% RH. The chart upper limit is curved to show that if the air is warmer, it can contain more vapor and if it is colder it contains less water vapor. Thus, the existing vapor level in cold air is usually larger than what air can hold which increases RH. When the air is fully saturated (100% RH), it reaches the dew point temperature (DPT) where it cannot hold any more moisture. Additional cooling beyond DPT causes condensation. Hence, DPT and we-pulp temperature can describe the amount of water vapour in the air. Enthalpy indicates the heat content in air which includes both sensible and latent heat which increases when we go upward on the chart which means that increment in moisture content will increase latent heat while moving to the right increases both temperature and sensible heat. When the air is heated and humidified, we increase both latent and sensible heat and so increase enthalpy. When the air is cooled by evaporation, RH increases and the temperature decreases. Thus, the gain in latent heat is equal to the loss in sensible heat which is called adiabatic phenomenon where the air changes do not change the overall heat content.

The human body reaches the thermal comfort level when certain combination of psychrometric chart parameters plus mean radiant temperature (MRT) and air velocity happens. When this is defined on the chart it indicates what is called the comfort zone (figure 2.32) (Lechner 2015).

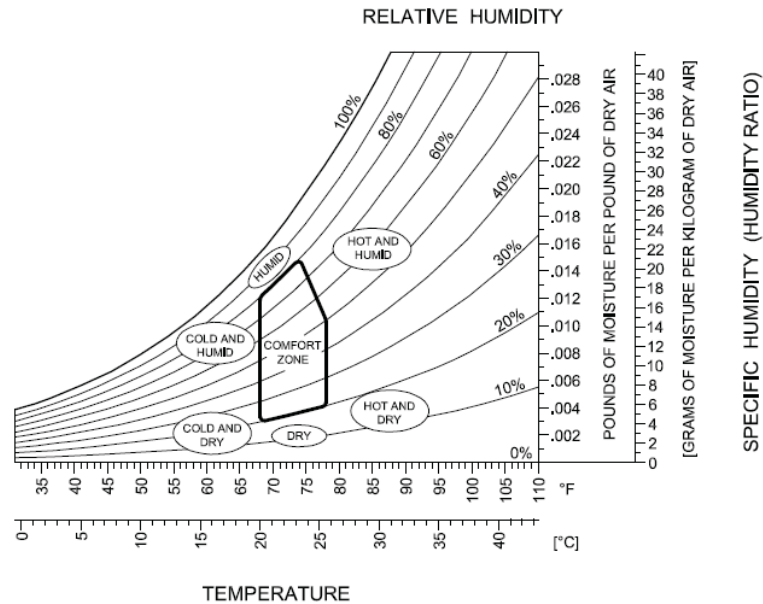


Figure 2.32. Comfort zone in the psychrometric chart (Lechner 2015).

As the chart is related only to humidity and temperature, the other parameters such as MRT and air motion is assumed to be fixed in basic HVAC calculations. The MRT is usually assumed to be controlled to be near the room air temperature. MRT variation can have a great effect of human's body heat gain and loss even when the room air temperature is within the thermal comfort levels. Also, air motion is assumed to be controlled and modest. The thermal zone can be affected by season, health, obesity, culture, clothes and type of physical activity (figure 2.33). However, the comfort zone can be the goal of optimal design as it sets the appropriate thermal conditions of at least 80% of the building occupants. But of course, it is essential to provide control devices that allow them to adjust the indoor thermal conditions. The chart was developed mainly for static conditions that are created by HVAC systems. However, these guidelines are not valid for naturally ventilated buildings where people can have adaptive comfort based on psychological, physiological and behavioural conditions. This is called adaptive comfort (Lechner 2015).

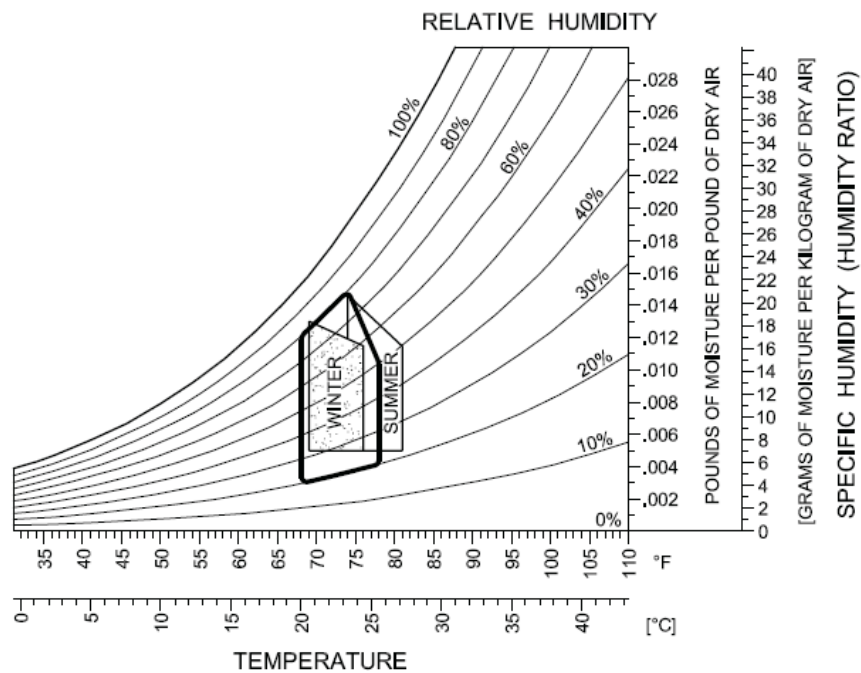


Figure 2.33. Comfort zone in the psychrometric chart can be shifted depending on the season according to ASHRAE standards (Lechner 2014).

According to ANSI/ASHRAE standards 55 of thermal environmental conditions for human occupancy (2013) thermal discomfort can happen to only a part of the human body. The standard sets limits for more factors such as radiant temperature asymmetry as it gives the maximum allowed temperature difference between adjacent surfaces. For example, the ceiling is not allowed to be $>5^{\circ}\text{C}$ warmer than other surfaces. In some situations, the air movement can be unpleasant due to air temperature, speed and type of activity and clothing. This is called a draft. The standard recommends also that the vertical air temperature difference between the head level and the feet level not to be more than 4°C for a standing user and 3°C for a seated user. It also recommends that the floor temperature should be within $19\text{--}29^{\circ}\text{C}$ where occupants have lightweight footwear. ANSI/ASHRAE 55 also accepts the standard effective temperature model (SET) or the Pierce Two-Node model. It is similar to PMV as it is based on a heat balance equation that considers personal factors such as metabolic rate, skin temperature, skin wettedness and clothing level. The standard defines this method as an imaginary condition where RH is 50%, air speed is $<0.1\text{ m/s}$ and MRT is equal to space temperature in which the imaginary user has clothing level of 0.6 clo and activity

level of 0.1met is the same as that from a user under actual conditions (Thermal environmental conditions for human occupancy 2013).

2.3.2 Thermal comfort and adaptive models

Adaptive comfort model (ACM) was first developed in 1970s when researchers included physiological, psychological and behavioural aspects in the thermal comfort model. Recent experiments proved that ACM is more accurate in predicting the level of thermal comfort comparing to static models such as PMV/PDD. ACM for naturally ventilated buildings is now well developed and recognized in many international standards such as ANSI/ASHRAE 55 and EN 15251. On the other hand, there are only few studies that focused on the application of ACM in mechanically air-conditioned buildings. Although PMV is widely used to assess thermal comfort in air-conditioned internal spaces, recent investigations show that there are some variation between PMV and actual predicted mean vote (AMV) of buildings' users. There are two ACMs that can be applied on air-conditioned buildings which are adaptive predicted mean vote (aPMV) which was developed by Yao et al. based on the black box theory. The aPMV considers other parameters such as behavioural, social and psychological adaptations, climate and culture. Black box theory was developed to study the relationship between PMV and the AMV. The other method is new PMV (nPMV) which was proposed by Humphreys and Nicol to consider the difference between users' observation and PMV based on the adaptive comfort theory. They introduced a new term which is DPMV-ASHRAE that is the variation between PMV and AMV. The term includes operative temperature, internal humidity, insulation of clothing, external mean air temperature and metabolic rate. According to the study PMV overestimates the heat resulting from warmer conditions as it ignores other factors. Thus, adaptive models can help providing more accurate simulations and help reduce energy consumption in buildings. However, the studies proved that PMV models were reliable when the internal conditions were within the comfort zone (Kim et. al 2015).

2.4 Daylighting in Buildings

2.4.1 Daylighting and artificial lighting

Light is electromagnetic radiation that falls in a specific location the electromagnetic spectrum and refers to visible portion of light to the human eyes (figure 2.34). In the spectrum, visible light has wavelengths within the range of 400~700 nanometres and comes between long-wavelength radiation or infra-red and short-wavelength radiation or ultraviolet. In photometry, total quantity of visible light is measured by lumens, the intensity of lumens of light which moves within a unit area is called luminance while the total lumens or luminous flux that falls on a surface is called illuminance (Kittler, Kocifaj & Darula 2012). Sun is the largest source of energy and light on earth. The amount and quality of daylighting in building is based on the ratio between direct sun light and diffuse sun light which is the result of the scattering of solar rays in the Earth's atmosphere. In the UAE, as the country is in the Northern Hemisphere near the Tropic of cancer, direct daylighting does not fall on North-facing walls (figure 2.35). In architectural design, daylighting is the act of placing skylights, windows, light shelves and any other transparent surface at the in the building envelope in order to enhance visual comfort, improve occupants' productivity and health, reduce usage of artificial lighting and decrease energy consumption. Daylight levels in any interior space varies depending on location, latitude, time, season, cloud coverage, building orientation, surrounding built environment and local weather conditions.

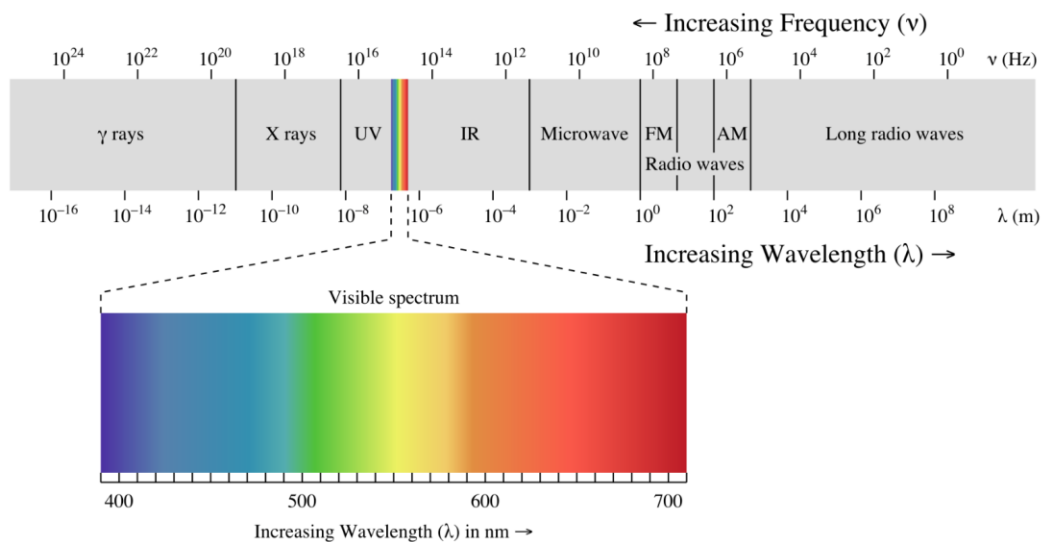


Figure 2.34. Visible light in electromagnetic spectrum (Kittler, Kocifaj & Darula 2012).

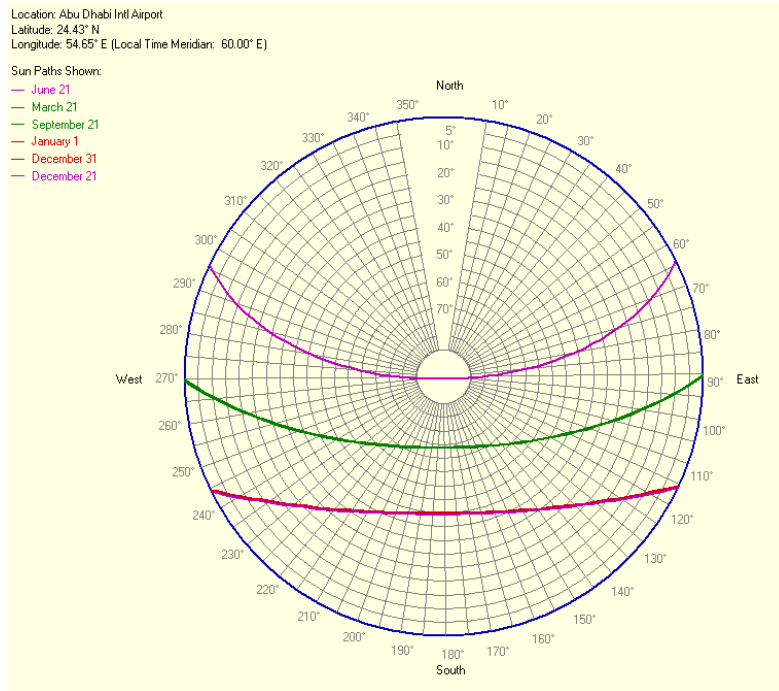


Figure 2.35. Sun path in Abu Dhabi as shown in the IES VE software weather data (author 2019).

Artificial light is used either for practical reason when daylighting level is low or for aesthetic reason. In the US, in 2015, almost 404 million MWh were consumed by artificial lighting in commercial and residential buildings which is equal to 15% of the total consumed energy in these sectors. In the same year in Canada, artificial light consumed 11% of the of total energy consumption in commercial and institutional sectors. Hence, from sustainable point of view, it is necessary to adopt design strategies which can reduce lighting systems energy consumption in buildings such as improving lighting efficiency, using advanced control measures or using the alternative of daylighting (Maltais & Gosselin 2017). In general, natural light has many positive physiological and physical effects on humans. On the other hand, excessive daylight can cause thermal discomfort, overheating and glare. Hence, thermal comfort must be considered carefully when it comes to daylight utilization in buildings, specially, under hot climatic conditions. Using natural lighting in internal spaces can efficiently save energy when the building has a control strategy such as daylight sensors. These sensors can dim or turn off artificial light when enough daylight is available in the monitored spaces. Having control over daylight can reduce lighting energy consumption by almost 40% in many cases (Maltais & Gosselin 2017).

There are common methods that are used to indicate daylight illuminance of interior spaces. In early 1980s, Building Research Establishment (BRE) developed a simplified method to measure lighting performance in daylit spaces. The amount of daylight in a room can be evaluated by comparing it to the available external daylight. The term used for this value is daylight factor (DF) which can be calculated in a specific point (point DF) or as an average over a specific area (DF_{ave}). It is calculated by dividing indoor illuminance over outdoor horizontal unobstructed illuminance then multiplied by 100%. The DF depends on window design, nature of building, frame design, orientation, glazing type, glazing cleanliness, glazing transmission and internal finishes reflectance. It can be measured using field measurement or computer simulation. It is usually calculated under over-cast sky condition to represent the worst-case scenario. Nowadays, DF is still the most common parameter that is used to evaluate quality of daylight in spaces. UK Standards such as DETR guide 245 and CIBSE recommend that the minimum value of DF_{ave} to be 2% in areas where artificial light dominates daylight and 5% in areas that is fully day lit with minimum artificial light usage (Wong 2017). For instance, for achieving BREEAM visual comfort credit it is required to have average DF of 4% for 80% of the office's spaces in single story buildings (BREEAM 2018).

2.4.2 Visual comfort

In general, fine visibility is related to the appropriate amount of light which allows the users to accomplish their tasks. Low levels of light and high levels of light can cause discomfort to the occupants. The quantity of light which reaches a specific location is illuminance. Uniformity of light indicates how evenly the light is distributed in the spaces specially for a task area. Good distribution of light reduces stress as eyes are affected by frequent adaptation between under-lit and over-lit spaces. Hence, uniformity increases visual comfort in the space. It is the ratio between the minimum illuminance level and the mean illuminance level (Carlucci et al. 2015). Thus, the higher the uniformity the better the visual comfort in the place.

In the research two visual comfort factors were considered which were daylight glare index (DGI) and Guth visual comfort probability (GVSP). DGI was developed by Hopkinson in early seventies to calculate glare from large architectural sources such as glazed walls (table 2.5). It is considered a sum of all the glare produced by bright objects as a result of daylight. DGI is different from other calculation methods which are used to measure glare from artificial lights such as CIE unified glare rating system and CIE glare index (McNeil & Burrell 2016). GVSP indicates the percentage of persons who, when looking from a particular location to a specific view, will be satisfied due to the lack of discomfort glare. This factor is associated with Discomfort Glare Rating (DGR) (IES 2018). In general, glare causes visibility difficulty or discomfort to users due to excessive luminance levels in the surrounding environment or the visual field. When the light is too bright it causes physiological glare or disability glare which makes occupants suffer from inability to see or immediate reduction in visibility. There is another form of glare which is called psychological of discomfort glare which happens as a result of high contrast between lit and dark parts of the visual fields. It usually causes discomfort, tiring of the eye and headaches (McNeil & Burrell 2016).

Table 2.5. Relation between DGI and glare rating (McNeil & Burrell 2016) .

| SUBJECTIVE RATING | DGI RANGE |
|--------------------------|------------------|
| Imperceptible Glare | < 18 |
| Perceptible Glare | 18 – 24 |
| Disturbing Glare | 24 – 31 |
| Intolerable Glare | > 31 |

2.4.3 Daylight control systems

Recently, Artificial lighting control is an attractive option for lighting designers as it provides a great energy saving potential, specially, in a sunny country such as the UAE. The main two types used in the country are occupancy sensors and daylight sensors. the spreading usage of light emitting diode (LEDs) lights has facilitated light

control as it is easy to accurately dim each luminaire depending on its position and the lux level in its zone (figure 2.36). This is an important option as light uniformity can change dimming requirement in different locations in one space. Also, different users may require different levels of illumination. In the responsive daylight sensors system, the photosensors, after detecting indecent daylight, send signals to a central controller which changes the dimming levels or the flux emissions for each luminaire (Rossi et al. 2015).

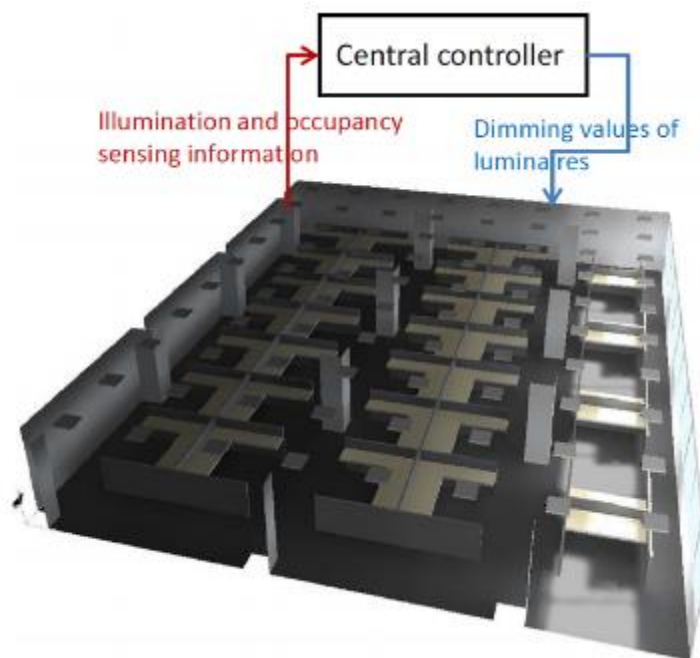


Figure 2.36. Daylight control system (Rossi et al. 2015).

Over that past few years, building specialists and engineers made huge steps in the development of Building Automation System (BAS). BASs, in an integrated network, form the building management system which acts as an artificial brain which controls and monitors all building services such as HVAC, fire and life safety (FLS) and of course lighting control systems. BMS main benefit is to assure building's occupants comfort which sometimes is affected by conflicts between different systems. One of these systems is daylight control systems (DLCSs). In the last decade, several studies focused on design strategies that can maximize daylight use. This includes optimization of façade design, to find a balance between opaque surfaces, glazing and shading devices, and DLCs. Two fundamental parameters are can indicate indoor

daylight availability which are Daylight Autonomy (DA) and Useful Daylight Illuminance (UDI). DA is the percentage of occupied hours per year when the required illuminance levels are achieved using daylight only. UDI is the percentage of occupied hours per year when daylight illuminance is within the useful range between 100 lux and 2000 lux and the light levels are not too bright or too dark to cause visual discomfort. Obviously, these factors affect DLCs output, but in order to increase the system efficiency two more factors must be considered which are the correlation between the photosensor signal and the task space illuminance and lighting adequate (LA) which is the percentage of occupied hours along with total illuminance surpassing the required design illuminance (figure 2.37). Total illuminance is the sum of both daylight illuminance and artificial light illuminance. The previous parameters control the photosensors location and classification. In any space, if the required illuminance is E_m , the DLC should control luminaires to produce a luminous flux which integrated daylight. In a realistic scenario, DLC does not provides light quantity that is higher or lower than required depending on different factors like technical errors or lack of commissioning. So, it is essential to consider how many hours the sum of daylight and artificial light exceeds the required illuminance levels, and this is the main goal of LA that indicates if there is an error with the system (Bellia & Fragliasso 2018).

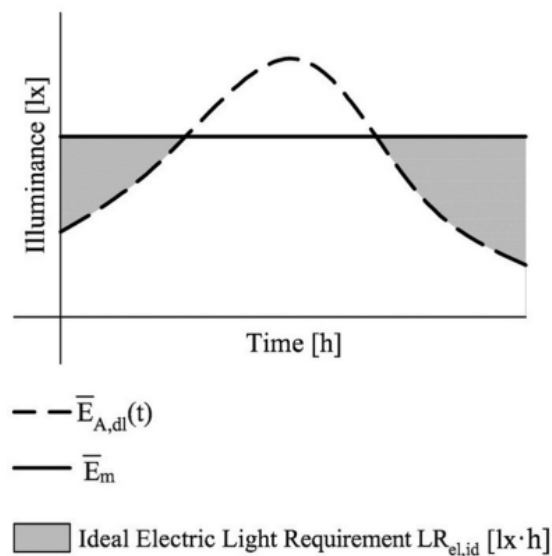


Figure 2.37. Daylight control diagram where E_m is the required illuminance level and $E_{A,dl}$ is total illuminance level(Rossi et al. 2015).

2.5 ETFE in the UAE

Usage of ETFE in the UAE it is still limited, and minimum amount of information related to this material were found. Even suppliers' brochures include only projects and case studies from other countries. It was noted that only one project in the city included this material partially which was Yas Mall in Abu Dhabi. ETFE cushions were used as the entrance roof to adjacent Ferrari World (figures 2.38 and 2.39).



Figure 2.38. Yas Mall Abu Dhabi(Yas Mall 2019).



Figure 2.39. Yas Mall Abu Dhabi(Yas Mall 2019).

2.6 BIPVs in the UAE

Despite of the fact that the UAE receives one of the highest sunshine hours annually (almost 3300 hours) (Al-Saleh & Taleb 2014), the usage of building integrated photovoltaics (BIPV) is still very limited in the country. Direct Solar Irradiance, which describes the amount of solar radiation per unit of area, varies between 120 to 240 kWh/m² which indicates the strong potential of generating power form solar energy in the UAE (figure 2.40) (ReCREMA 2013). In the last decade, the government made several initiations to promote the utilization of renewable power in the country such as the sustainable building construction policies. For instance, in ESTIDAMA system credit SM-2, the building achieves 1 point if 10% of the building envelope, including roof, is covered by BIPVs to reduce the amount of unsustainable materials in buildings (ADUPC 2010). In addition, the UAE national vision of 2021 aims to make the country on of the top market for sustainable development to reduce dependent on fossil fuel and increase energy efficiency. Beside the sustainable regulations, the government is supporting innovation, development and research in the renewable power sector with focus on solar power (Bekhet, Matar & Yasmin 2017).

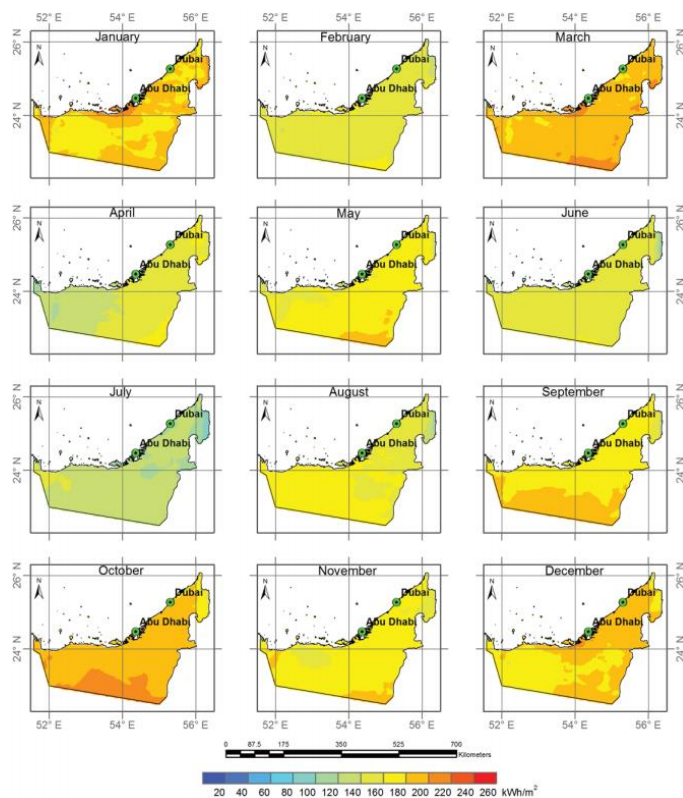


Figure 2.40. Direct normal solar irradiation in the UAE (ReCREMA 2013).

As part of this vision, the Emirati government supported the development of pioneer green projects to set an example for the building industry in the country. For instance, Masdar city and Sustainable city projects promote sustainable development and increase the balance between social, environmental and economic development. Masdar city (figure 2.41) is multibillion development located in Abu Dhabi and powered by several renewable energy sources. The purpose to set an example city in the GCC that can face climate change, develop and enhance renewable energy and reduce energy consumption and GHG emissions. The city area is 600 hectares and has 40000 resident who live in a mixed-use community. The adjacent land of the city hosts the main concentrated solar power plant which provides 10 MW of energy to residents. Most of the buildings' roofs in the city are covered by BIPVs which provides 75% of the energy demand. Eco-Villa prototype in Masdar city is the first building to gain a 4 pearl ESTIDAMA evaluation (figure 2.42). The villa has 87 roof BIPV panels which supplies 40000 kWh to the grid. The construction cost of the villa was equal to the construction cost of a conventional villa with the same GFA (Masdar 2019).



Figure 2.41. Madar city aerial view (Construction week online 2010).



Figure 2.42. Eco-Villa in Masdar city (Nagraj 2015).

The Sustainable City is a net zero energy development which started in 2013 which provides housing for 160000 residents and located on a 46 hectares land. The design of the city and its buildings follows passive and active strategies which can reduce per capita footprint for its residents (figure 2.43). One of the energy efficient strategies was to install 60,000 in the development and over buildings to produce 200 MW of electrical power. The parking shade PVs and the top roofs PVs were multi-crystalline type with 15.8% efficiency. For aesthetic purpose, the BIPVs tilt angle was 5 degrees instead of the recommended 22 degrees which affected the overall output of the PVs (Seenexus 2017).



Figure 2.43. The Sustainable City (The Sustainable City 2019).

BIPVs need to be evaluated not only in the light of cost aspect, but also environmental and social parameters. A trade-off between the cost of this technology and environmental and social benefits should be considered as from monetary point of view the technology is not viable comparing to the conventional power sources. Except in few areas in the country, BIPVs are not subsidized and the users do not receive incentives. However, with the growing awareness in the society, BIPVs market is booming in the country .With the government continuing support, people are more aware that this promising technology can limit the impact of global warming and reduce the production of GHG .To enhance the government's efforts in supporting the usage of BIPVs , this technology must become more cost-effective via subsidies and implementation of tax-cuts for investors, manufactures and suppliers (Radhi 2012).

2.7 Dynamic facades in the UAE

In general, architecture in the UAE is very advanced as the country has the tallest building in the world and several fascinating buildings and skyscraper which encouraged designers and building specialist to adopt the most innovative, complex and promising construction techniques.

The 150 m tall towers of ADIC (Al Bahr Towers) which was designed by Aedas is another example from Abu Dhabi (figures 2.45 and 2.46). The mashrabeya (screen) system was utilized as a traditional Arabic item in architecture, but the main purpose of the designer was to open the screen to cover the façade in case of direct sun radiation and close it to allow indirect daylight and views when the sun is away (figure 2.44). The architect used a simple origami mechanism as a concept and even used folded paper to present the concept before constructing it. Each building has 1000 screens with slight shap and size variation which can be controlled separately using the BMS. The screen has an electrical linear actuator which closes and opens it and it is made of polytetrafluoroethylene (PTFE) that is a light weight material which is easily cleaned. With the help of several sub-consultants, Aedas architects made a 3d solar model to predict solar exposure and various incidence angels to program the controlling software (Reid 2013).



Figure 2.44. Al Bahr Tower screen different positions (Reid 2013).

Sharaidin & Salim (2012) investigated the dynamic façade design early stages. The study found that DSF in Al Bahar towers added a great value to the building from environmental and economic point of views. The designers used computer simulation and proved that the façade design could reduce the cooling loads in the building by controlling thermal gain from the solar rays and enhance usage of daylighting which could reduce energy consumption by artificial light and increase productivity. Later after building completion, the simulation results were proven to be accurate. According to Alotaibi (2015) the design managed to reduce energy consumption in the building by 50% which decreased CO₂ emissions by 1750 ton/year.



Figure 2.45. Al Bahr Tower (Council on Tall Buildings and Urban Habitat 2018).

The second example is the apple store in Dubai mall which spans over two floors along the iconic Burj Khalifa (figures 2.26 and 2.27). The store has a front 56.6-meter-long terrace which faces the dancing fountains. The design of the store focuses on creating special ambience using daylighting. The terrace has 5.5-meter-high dynamic shade which was called “Solar Wings”. The Solar Wings reinterpreted the Arabic traditional shading element or the Mashrabiya which are automatically closed in morning then opened in evening. The shades consist of lightweight fibres with a unique pattern which follows study of solar rays’ angels. The pattern has dense areas which follows the higher concentration of solar radiation in summer. The Solar Wings allow for a clear view to the outside while allowing daylighting with faded shadows in the interior (Young 2017).



Figure 2.26. The apple store terrace with the Solar Wings (Young 2017).



Figure 2.27. The apple store terrace with the Solar Wings (Young 2017).

Hammad and Abu-Hijleh in 2010, investigated the potential energy saving of using external louvers in an office building in the UAE (figures 2.28 and 2.29). They used IES-VE to investigate the impact of dynamic shading on an office building under UAE local weather conditions. The proposed design achieved an energy saving of 30.31%, 28.57% and 34.02% for the west, east and south orientations.

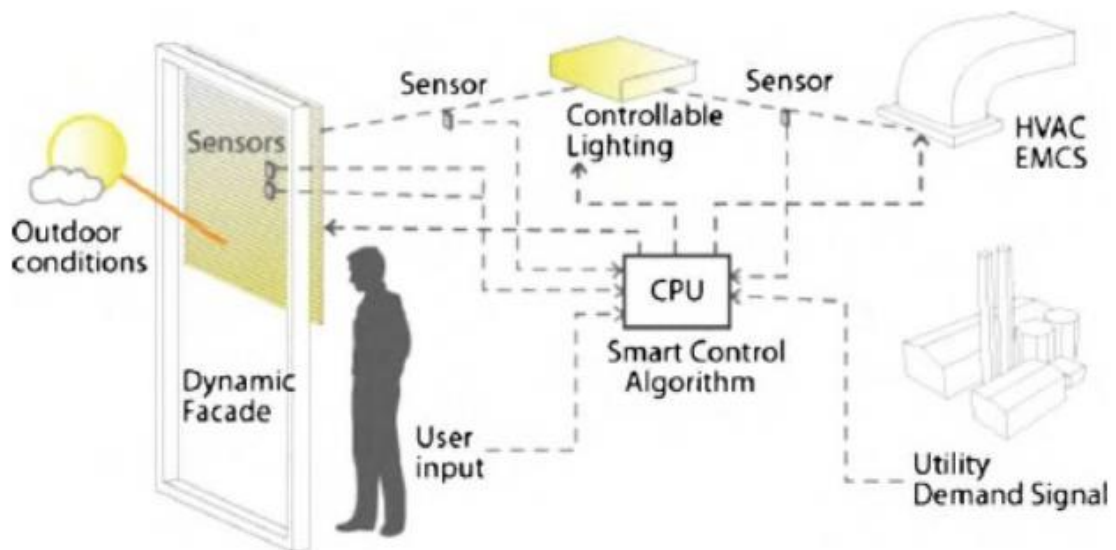


Figure 2.28. Dynamic façade concept (Hammad & Abu-Hijleh 2018).

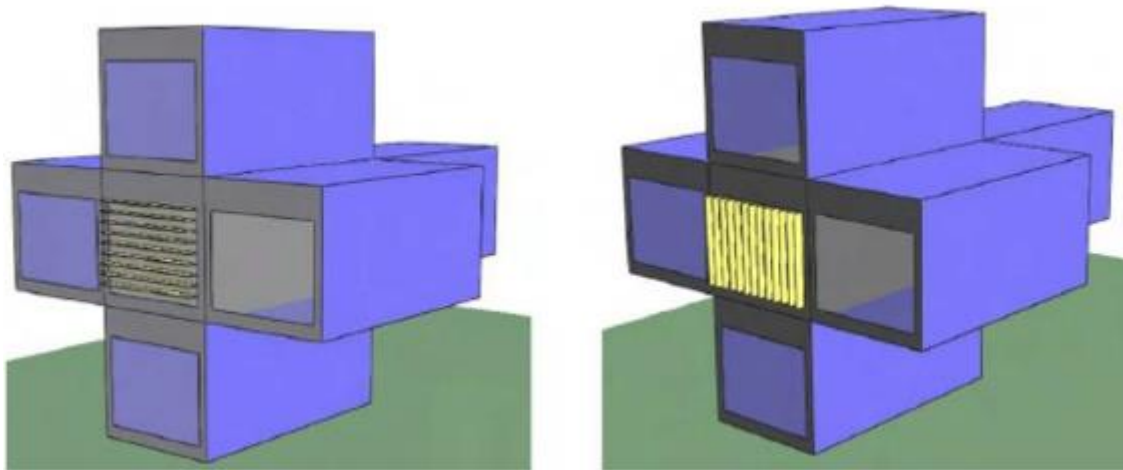


Figure 2.29. 3D model of the studied dynamic shade configurations (Hammad & Abu-Hijleh 2018).

2.8 Previous General Studies on ETFE Applications

Lamnatou et al. (2017) conducted a critical review about ETFE applications on buildings. Their methodology was literature review. Firstly, the researchers discussed the general factors that affect ETFE performance such as structural loads, acoustic requirements, ambient atmosphere, transparency and colour, application type whether it is a skylight or wall cladding, building size and cost, structural limitations, the required arrangement, façade adaptation, usage of active façade system, ventilation consideration, usage of solar control system and comparison with other cladding materials. The researchers explained the difference between façade membrane elements such as woven textiles membrane and thin extrusions (foils) with thickness less than 0.01 cm and presented the main advantages of foils namely ETFE are fire resistance, weather resistance, durability, low maintenance cost, recyclability and low weight. They introduced ECTFE as a new material used in façade application, which is similar to ETFE and gives higher solar transmission. They also mentioned several tests that were conducted to evaluate the mechanical properties of the material, namely stresses test and creep phase/recovery tests. They studied also light transmission properties and concluded that triple layer ETFE have lower U-value comparing to triple glazing and that ETFE can perform better when more layers are added. The cushions U-value

reached $1.95 \text{ W/m}^2 \text{ K}$ and managed to transmit 94~97% of visible light and 83~88% of UV range. They showed another strategy that included a water spray inside the air gap between a double layered ETFE which reduced heat gain by 10% and the film surface temperature by 10°C . The life span studies showed an average lifespan of 30 years. The researchers presented an option of providing a combination of printed (pattern) layers and a translucent layer which can be controlled by inflation of the cushions or movement to provide adaptive shading depending on the ambient conditions of the building to control solar gain. Another option is to provide an infra-red absorbing coating such as Nowoflon ET 6235 Z-IR. An experiment in Germany proved that using such coating can increase thermal comfort by 10% and reduce cooling loads by 5~8% comparing to a conventional ETFE. The researchers investigated also the LCA of the material and pointed out that embodied energy of ETFE is 26.5 GJ/t while the embodied energy of glass is 20 GJ/t . But due to the material light weight, the embodied energy by area is 27.0 MJ/m^2 and 300 MJ/m^2 for glass. They discussed the option of including integrated amorphous PVs inside the triply layers ETFE and pointed out that following the results of previous studies and experiments, this active system was feasible, economic and easy to install and fabricate.

Hu et al. (2017) investigated ETFE physical properties, performance and behaviour. Their methodology was literature review. They pointed out that transparency of the ETFE façade applications is 83~97% and that it needs to have printed opaque graphics in order to control heat gain. The optical properties can last for 25 years without any distinguished reduction. As the foil include fluorine in its structure and has low oxygen component, it is fire resistant. They stated that the U-Value of triple layer ETFE is $1.9 \text{ W/m}^2\text{K}$ but it can reach $1.4 \pm 0.15 \text{ W/m}^2\text{K}$ for new environmental products. The U-Value of double layers ETFE is $2.94 \text{ W/m}^2\text{K}$ and the U-Value of quintuple (five) layers ETFE is $1.18 \text{ W/m}^2\text{K}$. They pointed out that the overall performance is related to the area-to-edge ratio. They clarified that ETFE can improve sustainability in buildings mainly by reducing the structural loads and thus reducing the used construction material and the associated embodied energy. A typical cushion weighs 100~250 times less than equivalent transparent material. In addition, they are easy to install and do not need heavy construction equipment, hence can

reduce the overall energy consumption during the construction process. The researchers concluded that as light transmission of the foil can reach 90%, which can improve the performance of the integrated PVs. However, they pointed out that changes in cushions shape due to pressure difference and internal temperature increment can reduce PVs performance. They recommended having the PVs on the top or the bottom layer and vent out the internal air, which can reach 30°C higher than ambient temperature. They proposed using the extracted air in heating purposes.

Cremers and Marx (2017) investigated solutions to ETFE high solar transmissions in order to increase thermal comfort and reduce cooling loads. They proposed a geometric special (3D) modification (hemispherical, pyramid and saw tooth shapes) in the foil layer (figure 2.30), which can be combined with a printed pattern. The researchers used computer simulations (Trnsys software) to evaluate thermal comfort and calculate cooling loads when a conventional ETFE is installed as sky light on a mall in Germany and when the other option is installed (different shapes). They concluded that comparing to a conventional ETFE, the spatial modified foil reduced cooling loads in summer by 87%. From economic point of view, and they considered the hemispherical shapes to be the best solution.

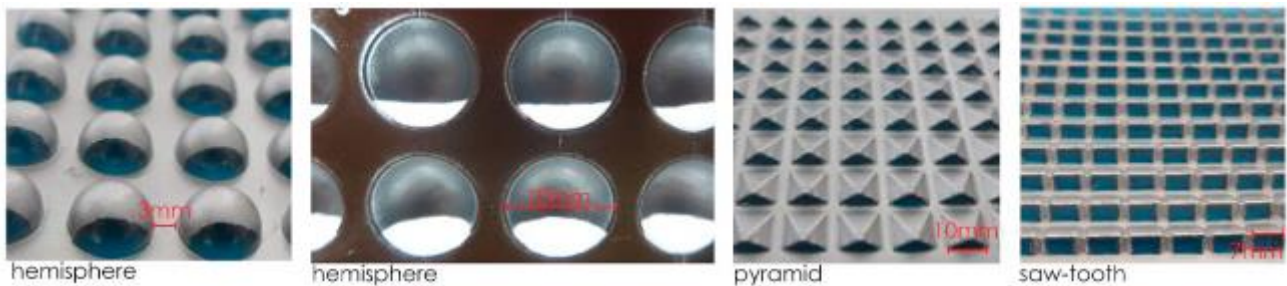


Figure 2.30. New foil types (Cremers and Marx2017).

Dimitriadou (2013) used computer simulation via IES-VE to study performance difference between glass and ETFE with regards to building energy consumption, especially for heating. The research provided information for creating ETFE profile in the software. To support the research, he conducted also an experiment where he installed double layered ETFE cushion and a double glazed unit respectively in different testing chambers. He measured the actual shortwave and longwave radiation

on site and used the loal recording for creating the weather file. The ETFE material properties were provided by a German manufacturer named Vector Foiltec. He mentioned that ETFE membrane was essentially treated by IES as a double glazed unit with different properties. This is the modelling technique as confirmed by the software developers. He pointed out that the software simplified the curved ETFE surface into a flat plane, which had minor impact as cushions had limited curvature. He measured of the relation between the mean value of one variable between the experiment and the IES simulation and found out that correlation coefficients was 0.99 for radiant and air temperatures and 0.98 for other results, thus he suggested that the software provided an accurate model. He confirmed, according to his analysis, that ETFE comparing to glass provided good energy saving potential.

Cremers and Marx (2016) did a comprehensive investigation of IR absorbing membranes that could improve thermal comfort and shading for the ETFE structures as the infra-red rays contains 50% of the energy in the light. They used TRNSYS software for computer simulation and depended on material properties which were provided by a German manufacturer called Nowofol. They simulated three different scenarios with upper absorbing IR membrane that are single layer, double layer with one-meter gap and triple layers with half-meter gaps under Stuttgart weather conditions. Due to software limitations, they did not consider ETFE curvature. Also because of the same reason they considered a minimum foil thickness of 0.2 mm and pointed out that thickness did not have a significant impact on the results as they depends mainly on the air gaps. The results showed that Nowoflon ET 6235 ZIR reduced cooling demand by 1% for the first scenario, 5% for the second scenario and 8% for the third scenario. However, they confirmed that the material is not fully transparent and gives bluish grey colour.

Masih, Lau and Chilton (2015) explored the daylighting performance of the ETFE cushions. The conducted a comparison study between the ESLC centre in the university of Nottingham that has an atrium sky light made of triple layer ETFE with fritted (pattern) top layer and a detached garden house that is fully covered with encapsulated ETFE panels (double layers) in Grantham. The researchers used on-site monitoring method using illuminance meters. They measured day light level 1 m above

the finish floor level to calculate daylight factors and used a camera and a computer software to create luminance maps. In the first case, average internal illuminance was 2736 lux, highest value inside the space was 4000 lux, the minimum value was 854 lux, the daylight factor was 60.8% and Uniformity Ratio was 0.3. In the second case, maximum illuminance value was 1171 Lux, minimum value was 478.7 Lux, the average illuminance was 919.5 Lux, the average DF was 56.4% and uniformity Ratio was 0.7. They concluded that as these lighting conditions will affect the general activities in the building and the occupant's performance, thus transparency and opacity in the ETFE structures should be studied carefully to ensure that an appropriate luminous environment is provided.

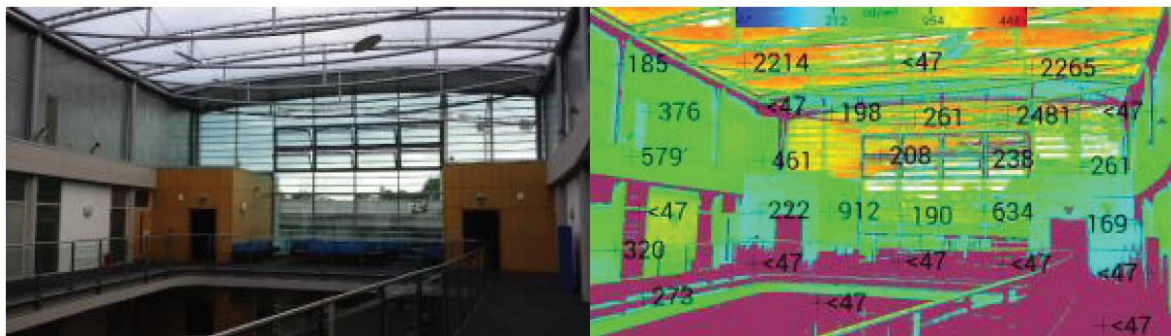


Figure 2.31. Luminance map from the study (Masih, Lau and Chilton 2015).

Afrin, Chilton and Lau (2017) made a comparison study between the thermal behaviour of fritted double and triple layer ETFE cushions atrium skylight. Their methodology was field measurements where they used sensing devices to record ambient temperature, internal temperature, cushions temperature and solar radiation. They collected weather data from two weather stations on top of the two studied buildings in the UK. They found out that the temperature immediately below the ETFE layers was typically 9°C higher than the external temperature when the double layer ETFE is used and 7°C higher when the triple layer ETFE is used. Solar radiation affected the cushions internal temperature with reached 45°C maximum. Thus, the additional layers increased the insulation effect of the cushions but were not enough to reduce the heat gain within the atrium.

Monticelli and Zanelli (2013) conducted a life cycle analysis for lightweight polymer-based membrane structures including ETFE in order to understand their eco-efficiency. The final output included a comparison matrix that summarize environmental data on different membrane types from early stages up to end of life stage. The results showed that for a 5-layer cushion, embodied energy was 315 MJ/m² and global warming potential was 137 CO₂eq/m² and for 3-layer cushion, embodied energy was 326.2 MJ/m² and global warming potential was 170 CO₂eq/kg. Durability of material can reach 50 years and and life span of the total construction system can reach 20~30 years. These results considered the energy which consumed by air pumps to maintain air pressure in the cushions and maintenance requirements. They pointed out that the ETFE gave positive environmental results when it came to end of life phase analysis, as it is a dry assembled homogeneous material easy to be disassembled, separated and then recycled.

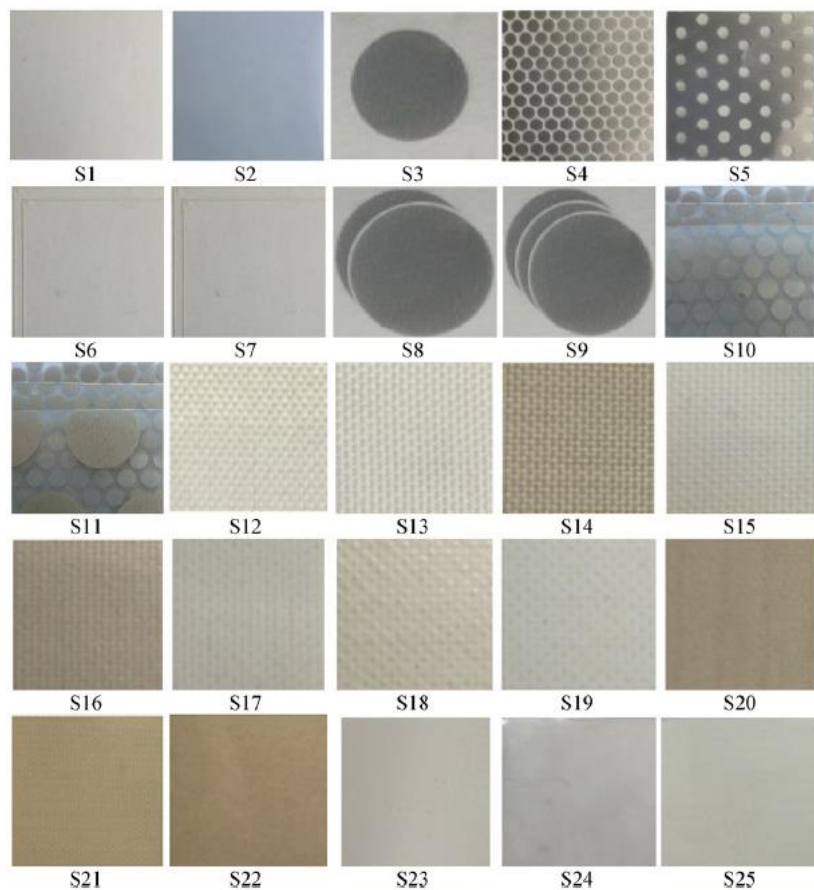


Figure 2.32. Membrane test samples (Liu et al. 2016).

| Specimen number | Membrane type | t/mm | Color | ρ_s | τ_s | α_s |
|-----------------|-------------------------------|------|-----------|----------|----------|------------|
| S1 | ETFE Colorless ETFE | 0.25 | Colorless | 0.08 | 0.80 | 0.12 |
| S2 | Wathet ETFE | 0.25 | Wathet | 0.09 | 0.70 | 0.21 |
| S3 | ETFE printing dots | 0.25 | Silver | 0.61 | 0.05 | 0.34 |
| S4 | ETFE with 63% printing dots | 0.25 | Colorless | 0.37 | 0.32 | 0.30 |
| S5 | ETFE with 80% printing dots | 0.25 | Colorless | 0.52 | 0.16 | 0.32 |
| S6 | Double-layer colorless ETFE | 0.5 | Colorless | 0.15 | 0.69 | 0.16 |
| S7 | Triple-layer colorless ETFE | 0.75 | Colorless | 0.20 | 0.57 | 0.23 |
| S8 | Double-layer printing dots | 0.5 | Colorless | 0.61 | 0.02 | 0.37 |
| S9 | Triple-layer printing dots | 0.75 | Colorless | 0.62 | 0.01 | 0.37 |
| S10 | Triple-layer ETFE (63%63%0%) | 0.75 | Colorless | 0.50 | 0.10 | 0.40 |
| S11 | Triple-layer ETFE (63%63%46%) | 0.75 | Colorless | 0.52 | 0.07 | 0.41 |
| S12 | PTFE FGT-250D-2 | 0.25 | White | 0.62 | 0.24 | 0.14 |
| S13 | FGT-250 | 0.35 | White | 0.72 | 0.14 | 0.14 |
| S14 | FGT-600 | 0.6 | Brown | 0.65 | 0.10 | 0.25 |
| S15 | | | White | 0.73 | 0.10 | 0.17 |
| S16 | FGT-800 | 0.8 | Brown | 0.65 | 0.04 | 0.32 |
| S17 | | | White | 0.77 | 0.05 | 0.18 |
| S18 | FGT-1000 | 1.0 | Brown | 0.73 | 0.02 | 0.25 |
| S19 | | | White | 0.79 | 0.03 | 0.18 |
| S20 | H302 | 0.6 | Brown | 0.64 | 0.02 | 0.34 |
| S21 | B18039 | 0.5 | Brown | 0.56 | 0.04 | 0.40 |
| S22 | B18089 | 0.7 | Brown | 0.60 | 0.02 | 0.38 |
| S23 | TPO TPO | 1.2 | White | 0.81 | 0.00 | 0.19 |
| S24 | PVDF PVC-PVDF | 1.0 | White | 0.87 | 0.03 | 0.10 |
| S25 | PE PE membrane | 0.08 | | 0.08 | 0.74 | 0.18 |

Table 2.6. Membrane test samples (Liu et al. 2016).

Liu et al. (2016) investigated the solar radiation properties of common membrane structures including ETFE, polyvinyl chloride PVC, polyvinylidene fluoride (PVDF), thermoplastic olefin (TOP), polyethylene (PE) and polytetrafluoroethylene (PTFE) (figure 2.32 and table 2.6). In their investigation, they used field experiments, mathematical modelling and computer simulation to study solar radiation coefficient, solar radiation transmittance, reflectance, steel sub-frame temperature changes and internal plate temperature (CFD). The research included eight different specimens of ETFE. They concluded that the worst results was for the colourless single layer ETFE where solar radiation transmittance through the cushion reached 0.8, solar absorbance was 0.12, solar reflectance was 0.08 and the steel sub-frame temperature reached 61.7 °C in summer that was 27.7 °C higher than external temperature. These results were improved significantly by printing reflective patterns on the membrane surface and increasing numbers of layers. The best results came from using the triple layer ETFE with (46%~63%) printed surface where solar radiation transmittance through the

cushion was maximum 0.07, solar absorbance was 0.41, solar reflectance was 0.52 and the steel sub-frame temperature reached 33.9 °C in summer that was lower than external temperature.

Suo, Angelotti and Zanelli (2015) explored the thermal behaviour and energy performance when ETFE cushions envelope is used. The analysed building is a 36m*36m sport hall in Milano with has two different ETFE types installed. Their first step was site measurement and survey to obtain data for the simulation. They installed several temperature sensors different heights to measure the thermal gradient. For the simulation process, they used ESP-r software. Due to the software limitations, the curved geometry of the ETFE membrane was converted to proper arranged plane elements and the main sport hall had to be divided into 8 different thermal zones. Despite of these changes, the model gave accurate results as the membrane area and indoor volume only differed by 0.7% and 1.1% from the real situation. They used Fanger's approach based on percentage of dissatisfied persons (PDD) and predicted mean vote (PMV) to evaluate the comfort conditions. Following this approach, the researcher calculated discomfort index. The analysis was divided into the study of physical thermal behaviour, energy performance and thermal comfort. The double layer membranes and triple layers membranes with a continuously ventilated air gap provided 11% and 18% energy savings respectively comparing to the single layer membrane. They pointed out that the energy demand is mainly affected by air circulation in the air gaps and recommended using exhaust air for the circulation (recovery technique) which can reduce the energy demand by 3% more.

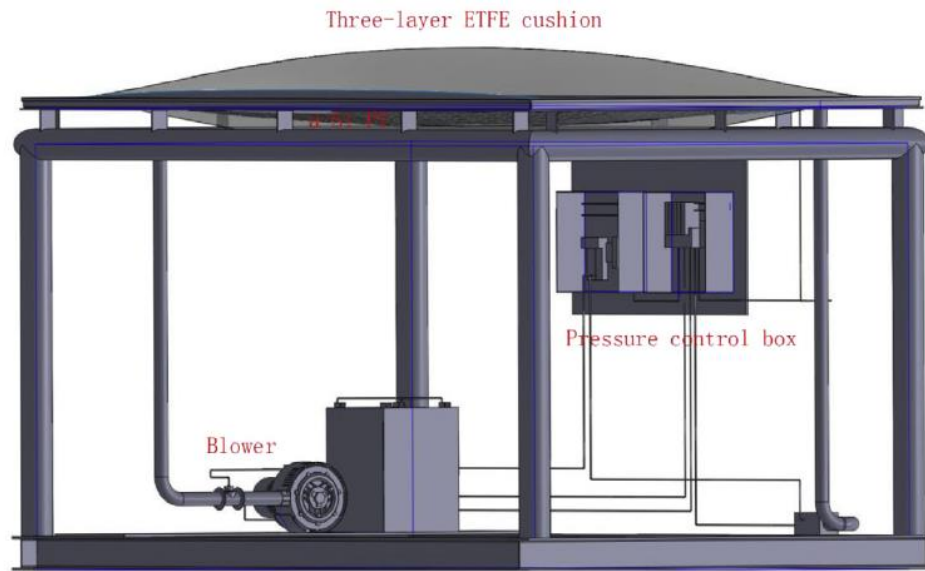
Lau et al. (2017) presented an approach to study the visual environment in building with ETFE (single and double-layer) structure envelope. They conducted two field studies using light mapping and spot measurement in two building in Nottingham and Singapore. They measured illuminance distribution pattern of day light under different weather conditions. They concluded that in the first building, the used ETFE, which had no variation in transparency, provided homogenous luminous environment, which is more suitable for activities that require uniform daylight distribution; such as painting or reading. In addition, ETFE managed to transmit 93% of the external illuminance into the space and the distribution patter was flat with poor gradient effect.

They concluded that in the second building, the used ETFE, which included double layer type at the middle- and single-layer type at the edges, provided better gradient effect and luminance contrast which is more suitable for activities that need visual interest or dynamic lighting. They recommended that ETFE design should go through daylight simulation and testing in order to enhance the visual comfort in the space depending on the desired activities.

2.9 Previous Studies on ETFE and BIPV Applications

Ibrahim et al. (2016) studied the thin film integrated PVs within the ETFE as a membrane structure as the free morphologies of the ETFE structure allows for wide varieties of geometries and shapes. The researchers summarized the design considerations into orientation, solar radiation incidence, shading possibilities, curvature, geometric shape and connection method and arrangement. In order to evaluate this system, they recommended to conduct three tests which are allowable deflection test, orientation test and surface shadow test using computer simulation (Grasshopper and Form TL software).

Zhao et al. (2015) explored thermal properties of integrated amorphous silicon PVs that are imbedded in triple layer ETFE cushion roof under four weather conditions in Milano using Runge–Kutta numerical method and field measurement experiment (figure 2.33). The base of the study was the energy balance equation, which is expressed as converted energy and energy loss is equal to absorbed energy. The study focused mainly on measuring the maximum temperature, which affects the PVs performance, absorbed energy and energy loss. They concluded that the maximum PV temperature within the triple layer ETFE was 362.3 K in summer which was higher than other PV integration application.



(a) Schematic diagram of the experimental mock-up

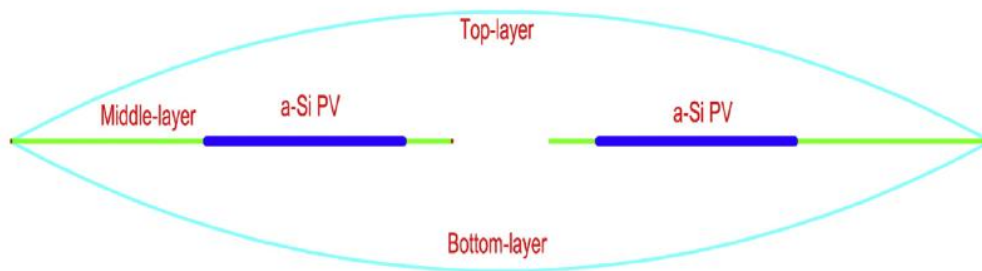


Figure 2.33. Experimental mock-up (Zhao et al. 2015).

Debbarma, Sudhakar and Baredar (2017) conducted an introduction study about building integrated photovoltaics (BIPVs) which can be integrated into the ETFE cushions as one of its various applications. Their method was literature review. BIPVs can provide 20~70% of the building's electricity requirements depending on façade area, location and orientation. They stated that the main factors that should be taken into account while designing the system are the module temperature, shading, orientation, installation angle and solar irradiance. Other advantages can be solar shading, thermal insulation and acoustic insulation. They pointed out that BIPV electrical efficiency reached 4.52% in Turkey, 10% in Lisbon and 9.39% in Hog Kong.

Abdolzadeh, Sadeqkhani and Ahmadi (2017) investigated the efficiency of BIPV in ETFE cushions structure. They made a numerical model and studied the electrical and thermal performance of the system under two scenarios which are cushions with steady mass flow and cushions with regulator (airflow) system. The modelled case with triple layer ETFE with Amorphous Silicon PVs on the middle layer. They stated that comparing to Crystalline Silicon under same conditions; this type has 0.25% less power decrease due to surface temperature increment, better integration on curved surfaces and lower cost. They compared the results of the simulation with results of a similar field experiment that was conducted in China. They concluded that air and PV temperature in the first scenario was lower by 25°C. Although the first case has 0.33%, higher efficiency and higher average power (i.e. 7 W), it consumed most of the power and provided lower net output power.

Hu et al. (2016) investigated PIBV which are integrated in ETFE cushions under hot and cold conditions. The studied system was Amorphous Silicon PVs, as they can perform better than Crystalline Silicon, which were integrated in the middle layer of a triple layer ETFE cushion. The researchers used a cushion system, solar energy control sub system (SECS) and pressure control system (PCS) to establish their experiment (figure 2.34). The SECS provided the required energy for the PCS which inflated the ETFE to form the required shape. They measured photovoltaic electricity, temperatures (inside and outside the cushions), temperature differences and overall system efficiency. They concluded that the utilization of solar energy was evaluated by temperature that represented thermal performance and electricity that represented photovoltaic. The average total net electricity that was produced by the PIBV was 42.9~54.5 Wh. The internal temperature was 16.8~31.0°C higher than external ambient temperature which indicated the potential of collecting thermal energy from inside the cushions. Due to the high performance of Amorphous Silicon PVs, the system efficiency reached 25.5%. The system was proven to be independent on external energy source.

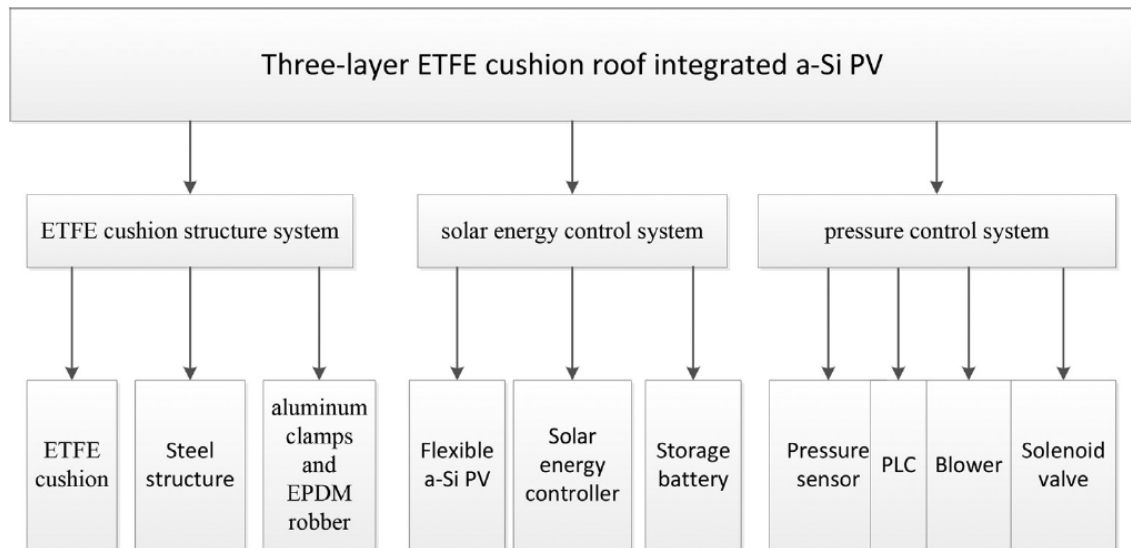


Figure 2.34. System structure (Hu et al. 2016).

Hu et al. (2014) investigated the feasibility of using integrated thermal PVs in the ETFE structure system. They developed a series of six experiments under summer sunny and cloudy conditions with 325~595 W/m² solar irradiance on a mock-up which has a triple layer 2m*4m ETFE cushion structure with silicon photovoltaics panels. The solar energy control system consisted of solar controller and two 0.394 m PVs with batteries. The pressure control system, which was used to maintain the pressure of 240~360 Pa in the cushions two chambers, included programmable logic controller, blower and two valves. The results showed that the average stored energy was 61W per hour , the average ratio between consumption and output energy was higher under sunny conditions comparing to cloudy conditions and the average temperature difference between inside and outside of the cushions was 18 9°C. External load resistance and pressure performance were within the acceptable range, thus the system was structurally feasible. Generally, the system operated steadily, and its electrical feasibility was verified.

Hu et al. (2015) investigated the thermal performance of ETFE structure integrated a-Si PVs with regards to temperature distribution and heat transfer coefficient. The conducted another experience on a triple layer ETFE with integrated a-Si PVs on the middle layer. When the a-Si PVs surface temperature increases by 1 °C, the generation efficiency drops by 0.2%. The pressure control system kept the pressure in the range of 240-300 Pa. The main measured and studied parameters were top layer temperature, middle layer temperature, bottom layer temperature, internal cushion air and solar irradiance. Also, they investigated the temperature field and temperature differentiate due to gravity and buoyancy forces in order to understand the heat transfer mechanism then performed a numerical model as part of the analysis. The hottest layer was the middle, where the PVs are located, then the top and the bottom. The PVs temperature reached 353.8 K due to solar irradiance. The PVs affected the temperature distribution within the cushion (figure 2.35). The maximum internal air temperature was at the minimum distance between the top layer and the centre of the PV where it reached 339.8 K. They managed to calculate the heat transfer coefficient, which proved that the thermal performance of the studied ETFE cushions had better thermal performance comparing to conventional ETFE cushions.

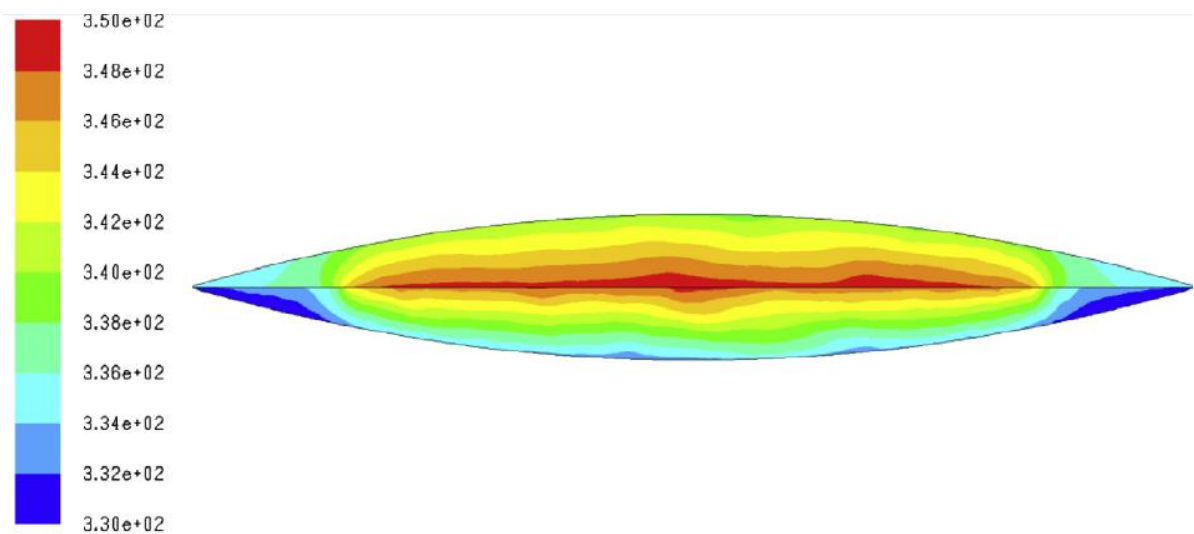


Figure 2.35. Temperature distribution (Hu et al. 2015).

Hu et al. (2017) conducted an experimental study to assess the thermal performance of integrated flexible PVs when they were installed in different locations inside a double layer ETFE cushion (figures 2.36 ,2.37 and 2.38). They focused on studying temperature characteristics and distribution. Flexible PVs are different from silicon PVs as they include transparent top contact layer, green cell, blue cell, red cell as one flexible substrate. Its configuration gives its high efficiency as it can be used on curved surfaces and accommodate full light spectrum. They used infrared thermography to convert the irradiation infrared into temperature distribution colour visual image. Then they developed theoretical thermal model based on energy balance equation. They calculated absorbed energy, converted energy, total energy loss and heat transfer coefficient. The results showed that the temperature distribution resulted from surface curvature, incident angle and solar irradiance. The average heat transfer coefficient for the PVs was 4.9 w/m²K and for the double layer ETFE was 2.39 w/m²K.



Figure 2.36. Double layer ETFE with PVs on bottom layer (Hu et al. 2017).

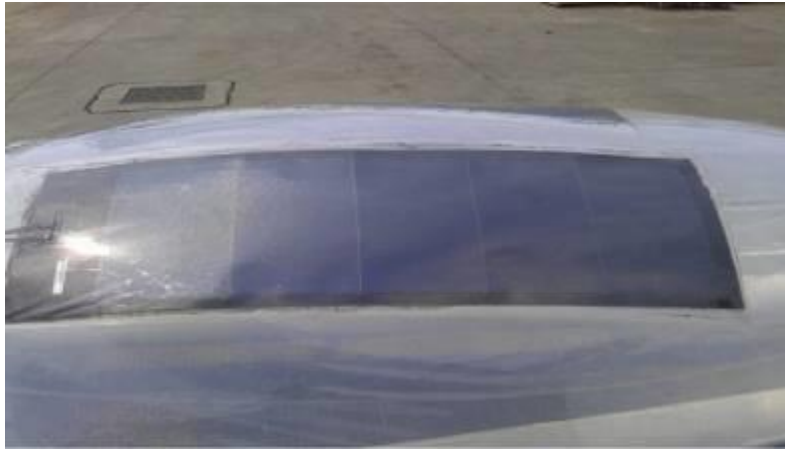


Figure 2.37. Double layer ETFE with PVs on top layer (Hu et al. 2017).

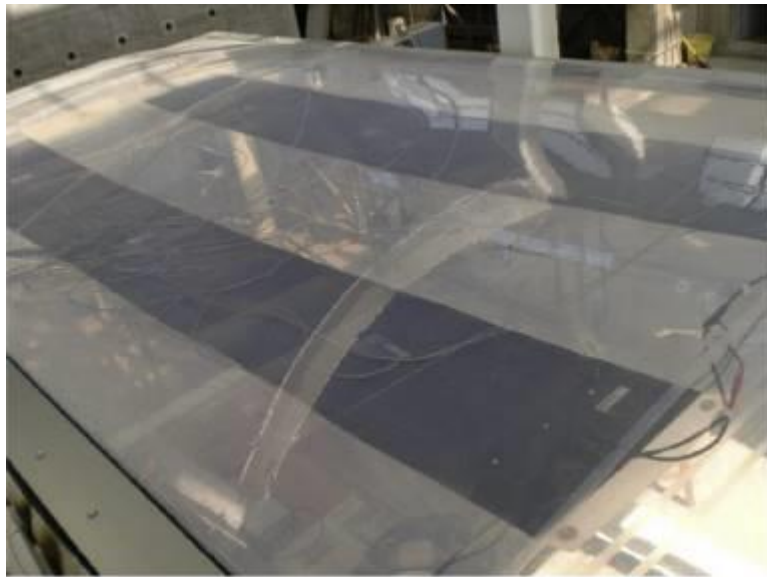


Figure 2.38. Triple layer ETFE with PVs on middle layer (Hu et al. 2017)

2.10 Previous Studies on ETFE and Dynamic Shade Applications

Michael, Gregoriou and Kalogirou (2017) used Desktop Radiance v1.02 and Ecotect v5.2 simulation softwares to conduct an environmental assessment of the adaptive/movable ETFE system with regards to indoor visual comfort. The study was a part of innovative renovation strategies assessments of existing building in Nicosia. The researchers focused on ETFE is this material is 100% recyclable, lightweight structure and could reduce construction time and cost comparing to conventional renovation

techniques. They studied different pattern options (0~70% covered) as passive technique and different screen angles (0~165°) as active technique under various climatic conditions (figures 2.39 and 2.40). In the model, the ETFE cushions were installed in front of existing windows and were controlled by linear drive actuators (figure 2.41). The visual comfort criteria were based on different factors which are required lux levels, daylight factor and the uniformity of daylight factor depending on BS 2008 and CIBSE guidelines. They concluded that the system managed to reduce glare levels while maintaining appropriate illuminance, daylight levels and light uniformity in all indoor spaces. They recommended including integrated PVs as a shading option in any future similar studies in order to provide the required energy for the control system so the full system could be power independent. The proposed system ensures high DF levels which exceeded 2% while uniformity exceeds the threshold of 0.40 with high daylighting levels exceeding 500 lux in 3/4 of the area. The system eliminated the high lux levels (more than 3000 lux) so it minimized glare.

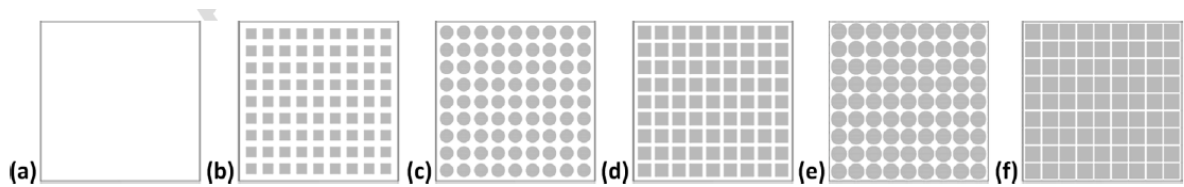


Figure 2.39. Studied pattern with different transparency percentage (Michael, Gregoriou and Kalogirou 2017).

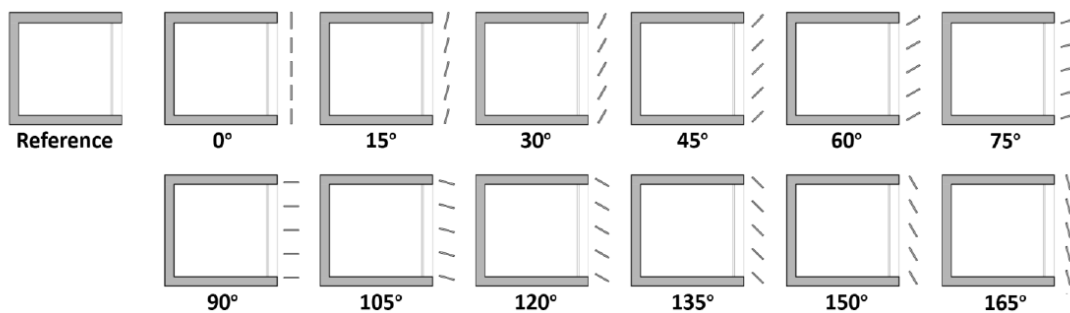


Figure 2.40. Different cushions angles (Michael, Gregoriou and Kalogirou 2017).

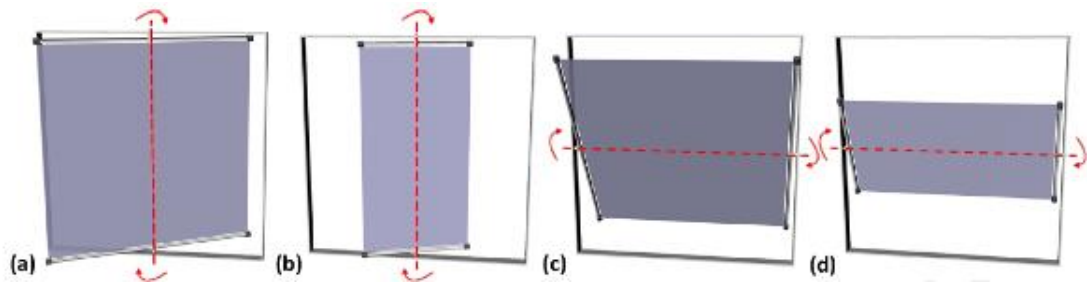


Figure 2.41. Rotation options (Michael, Gregoriou and Kalogirou 2017).

As highlighted in previous section, Hammad and Abu-Hijleh (2010) investigated to the potential energy saving of using external louvers in an office building in the UAE. The proposed design achieved an energy saving of 30.31%, 28.57% and 34.02% for the west, east and south orientations. Sharaidin & Salim (2012) investigated the dynamic façade design early stages and used computer simulation to prove that the façade design could reduce the cooling loads in the building by controlling thermal gain from the solar rays and enhance usage of daylighting. Later after comparing the results to actual electricity bills, they were proven to be accurate. According to Alotaibi (2015) the design managed to reduce energy consumption in the building by 50% which decreased CO₂ emissions by 1750 ton/year.

Mahmoud and Alghazi (2016) investigated the performance of dynamic shade under Cairo weather conditions. The study was conducted on a south oriented façade with high solar gain. The researchers used field measurement and simulation software. In summer and spring, the proposed dynamic shade devices improved daylighting by 50%. They recommended using simulation programs in design early stage to prove the advantages and applicability of the system. They pointed out that although the system gave a better energy-performing façade, it was expensive and hard to maintain.

Johnson and Winther (2015) conducted research on a dynamic shade installed on an office building in Denmark. They concluded that the proposed system provided better performance (54%) comparing to changing the basic glazing unit to an expensive high-performance unit (27% and 36%). Furthermore, the controlled usage of daylight reduced the lighting energy consumption annually by 8 kWh/m². They recommended to convert the studies dynamic system to an intelligent responsive type connected to BMS so it could act automatically depending on the weather forecast and occupant needs.

2.11 Previous Studies on DSF

Peng et al. (2016) conducted a study about PV-DSF which consisted from an external layer of semi-transparent a-Si BIPVs with 7% transmittance, 400 mm cavity and an internal layer of an openable window (figure 2.42). The external layer had an upper and lower louvers to enhance airflow for heat exchange in the cavity and allow natural light to partially pass. Air flow helps to reduced cooling load by almost 15% and increase the PV output by 3%. The researchers used numerical model and Energy Plus software to investigate airflow, daylighting, heat transfer and PV output to evaluate the overall performance of the system. The unit area managed to generate 65 kWh yearly. When cadmium telluride semi-transparent BIPV module was used, the annual output reached almost 130 kWh. The system blocked solar radiation while maintaining adequate daylighting illumination in the space. Under the weather conditions of Berkeley, the system reduced net electricity consumption be 50% comparing to other common single layer façade glazing systems which were double bronze, double low solar low-e clear and double clear with shading always on. They concluded that the semi-transparent BIPVs effectively increased the energy saving potential of the system an made this option more sustainable,

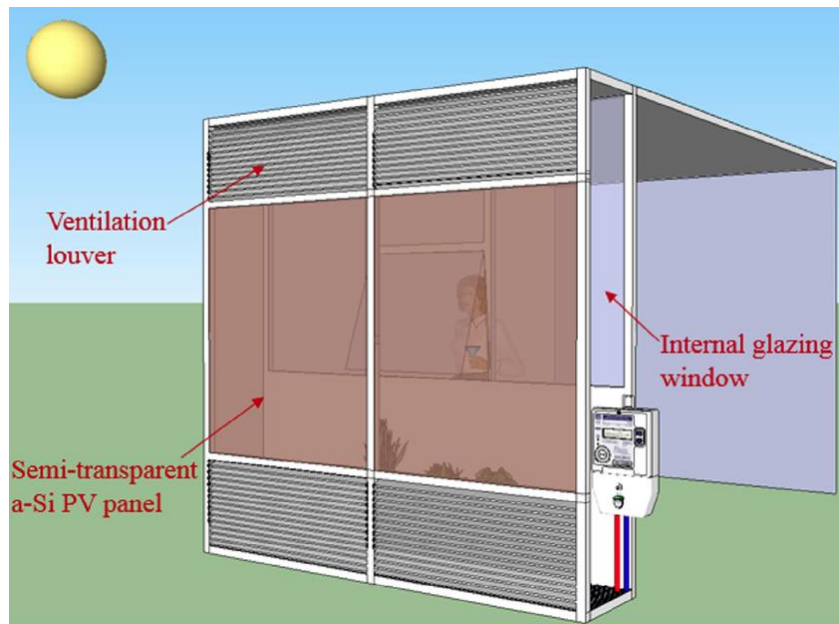


Figure 2.42. Schematic diagram of the system (Peng et al. 2016).

Barbosa, Ip and Southall (2015) studied the thermal comfort in naturally ventilated office building with a DSF under hot humid climate conditions (figure 2.43). They simulated the basic case as the benchmark reference plus 16 alternative cases using IES VE. The variables between the studied scenarios were opening size, structure, outer skin glazing parameters, shading devices, cavity depth, number of covered floor or cavity height, wall to window ratio and internal skin material. The researchers assessed each individual option then choose an optimized design scenario that could maximize thermal comfort in the space. The most influential design option was shading devices followed by cavity depth and inclined external layer. Changes in window positions and configuration improved comfort in specific floors. Extension of the cavity as high chimney above the building improved thermal comfort in higher levels and resolved the reverse air flow issue. The ultimate optimized DSF option achieved the required thermal comfort level in 70% of the occupied hours.

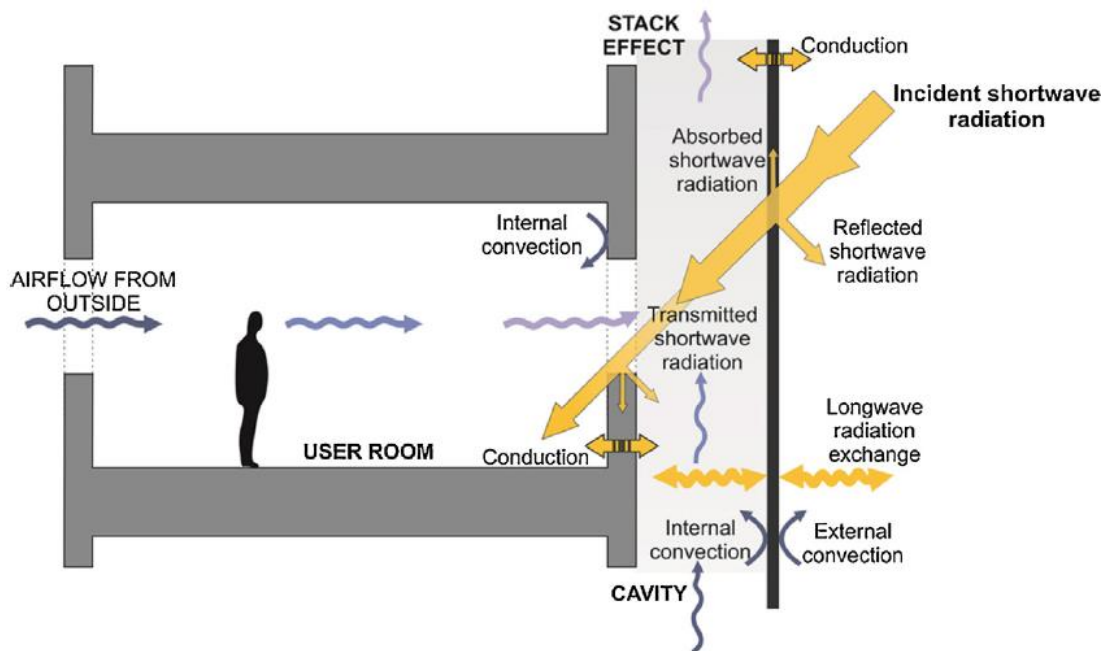


Figure 2.43. Schematic diagram of the heat transfer and air flow mechanism in the basic model (Barbosa, Ip & Southall 2015).

Kim et.al (2018) explored daylight and thermal effects of DSF with exterior and interior shading devices. The researchers used Energy Plus and Daysim computer programs to simulate the basic case (figures 2.44 and 2.45) and the DSF with slat blinds and calibrated the model against measured data from a DSF experimental model that was made in Daejeong, South Korea. The results indicated that the DSF for the studied building can save 5% of total heating and cooling loads. When DSF was combined with the shading devices which had daylight dimming control based on indoor lux levels, the simulated model managed to reduce the thermal loads by 27% and lighting energy consumption by 52%.

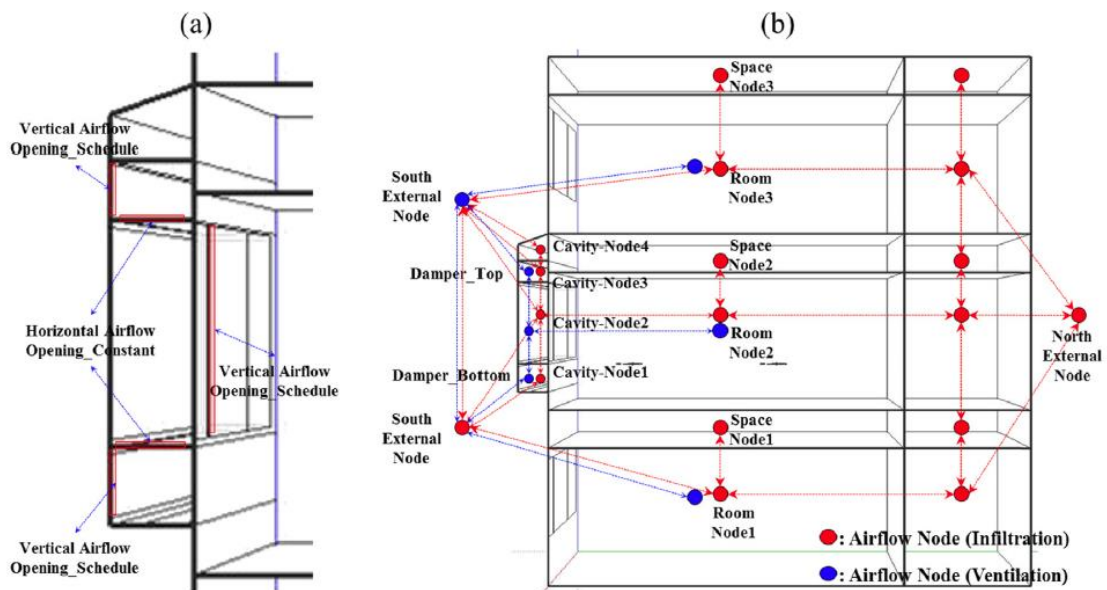


Figure 2.44. DSF opening conditions (Kim et.al 2018).

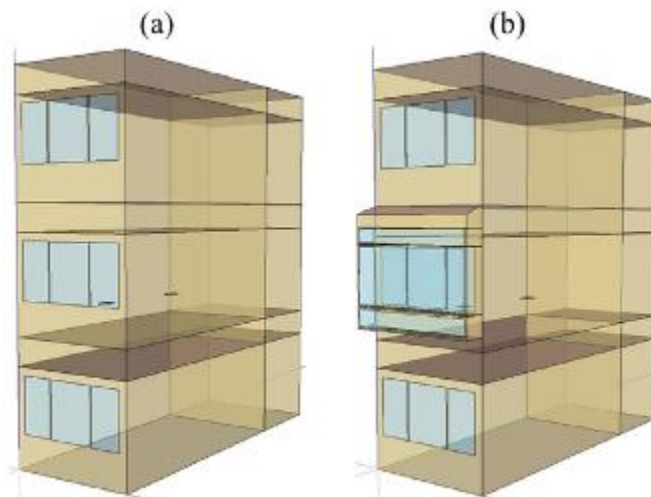


Figure 2.45. Simulated models in Energy Plus (Kim et.al 2018).

Luo et.al (2017) investigated the potential of installing photovoltaics blinds as shading devices installed in the cavity of a DSF system installed on a south facing wall under the climate conditions of Changsha, China. The BIPVs were a-Si cells in the shape of long and narrow shading slats (figure 2.46). They conducted an experimental and numerical models to study the thermal performance of the system under summer conditions comparing to a conventional DSF system. They used thermocouples sensors to measure the ambient temperature of the system and the internal space and the surface temperature of glazing and walls. Also, they used solar pyranometers to measure global and diffuse solar irradiance. The studied DSF had lower and upper louvers for natural ventilation of the system and also included mechanical ventilation as another option. The study included two phases which were the study of the impact of changing BIPVs angle and spaces and comparison between the thermal performance of the two options. The BIPV-DSF option can save 12.16%~25.57% of building energy in summer comparing to the conventional DSF. Both the natural ventilation and the BIPVs spacing affected the system performance. BIPV-DSF lowered the heat transfer coefficient of the system to be 2.247 W/m²K. When forced mechanical ventilation was used, the k-value improved comparing to natural ventilation. However, due to the electric power consumption of the forced ventilation, the study concluded that natural ventilation made better energy saving.

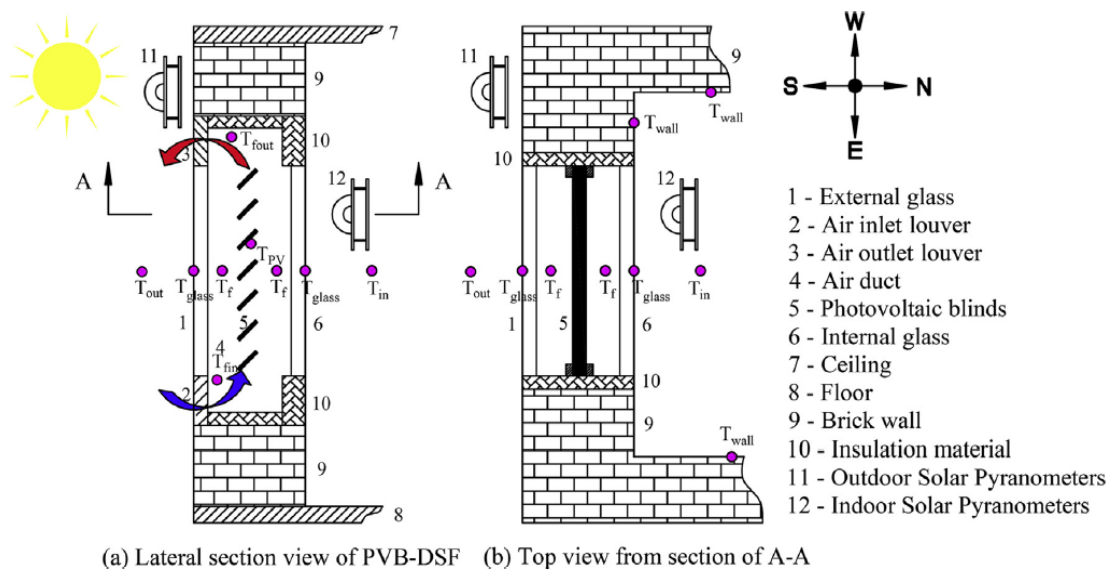


Figure 2.46. Schematic diagram of the BIPV-DSF option (Luo et.al 2018).

Khalifa et.al (2017) assessed the effect of DSF internal layer composition on the energy performance of an air-conditioned office building in Tunisia under the Mediterranean weather conditions. In the study, the DSF was box window with 300 mm cavity and includes an automated solar shading that is lowered when solar radiation exceeds 150 W/m². The system covered three floors of the building facing south and it was naturally ventilated in all season except summer where it was mechanically air conditioned. They used TRNSYS simulation software for the study. In the investigation, the researchers studied the impact of changes in glazing type and window to wall ratio. They concluded that changing glazing type to highly insulated type reduced the cooling loads by 10% in summer.

Yang et.al (2016) investigated the impact of middle shading devices on DSF thermal insulation and air flow inside the cavity in order to propose an optimal design of the shading blades (figure 2.47). They found out that when the blades were fixed the air flow in the gap increased with the inclination of the blades comparing to a similar DSF without internal shading devices. Changes in the incline angle from 0 ° to 90 ° reduced the maximum ventilation rate from 1.32 kg/s to 1.69kg/s while when the blades were removed the maximum flow rate was 1.76 kg/s. Changes in the distance between blades from 0.1m to 0.4m reduced the maximum ventilation rate from 1.61 kg/s to 1.34 kg/s. Thus, when the distance between shading devices increase, the air flow was reduced. However, the incline angle change has minimal impact on the internal room temperature while the changes in blades distance affected it. In general, the addition of the shading devices reduced internal air temperature by 1 °C under the study conditions.

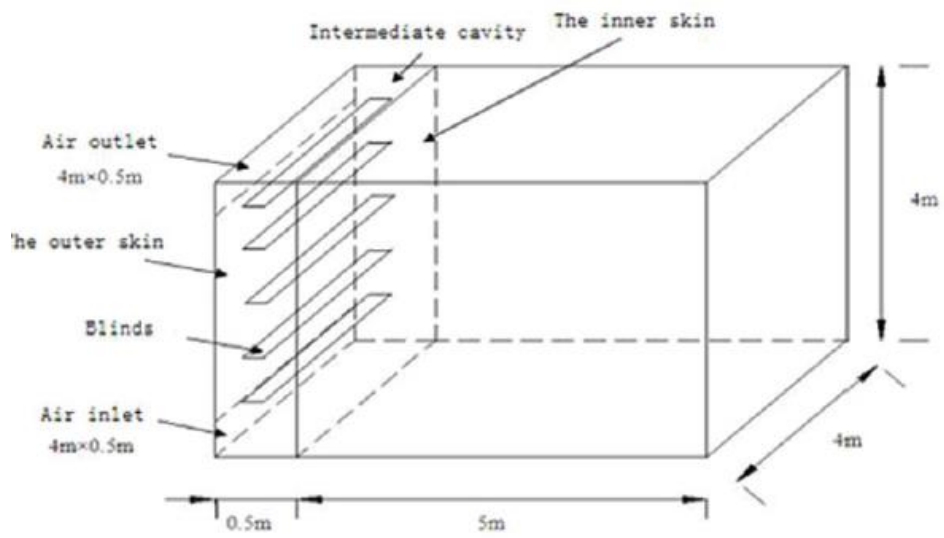


Figure 2.47. Schematic diagram of the studied room (Yang et.al 2016).

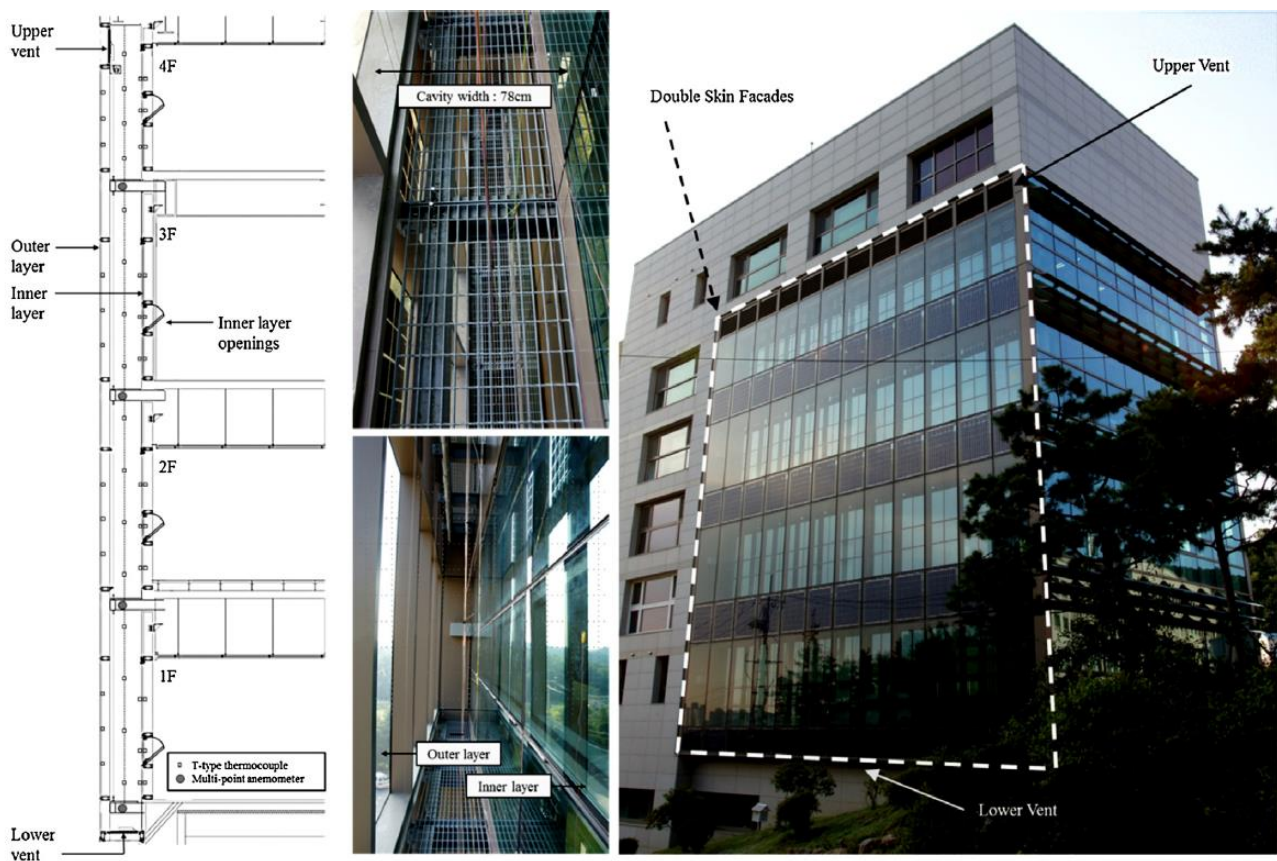


Figure 2.48. Studied DSF details (Joe et.al 2014).

Joe et.al (2014) studied the changes in thermal characteristics of DSF cavity following the glazing and cavity depth changes as these characteristics influence cooling and heating loads in adjacent internal spaces. The researchers used both computer simulation and field measurement methods in the study of four floors high DSF installed on a building in Seoul, Korea (figure 2.48). The study included study on 34 glazing types and various cavity depths from 8 cm to 148 cm. The conclusion was that changes in the external glazing type had larger impact on the energy consumption comparing to changes in the internal layer. There was a proportional relation between cavity depth reduction and energy consumption reduction. The optimal option which included the most efficient design strategies managed to reduce energy consumption by 5.62%.

Wen et.al (2017) investigated the effect of changing inlet and outlet opening sizes on the DSF performance in Wuhan, China under summer conditions. They used field measurement, numerical modelling and ANSYS simulation software to conduct the analysis. Results from all methods matched each other with minimal variation. The results demonstrated that when the height of the inlet and outlet was between 300 mm and 450 mm, the air velocity reached 4m/s and the air temperature in the cavity decreased as the heat gain was discharged effectively. The upper temperature of the cavity was higher than the lower temperature and temperature near the external layer reached 40°C while the temperature near the internal layer was 35°C. They concluded that this was the best design for a DSF under Wuhan weather conditions as when the height was increased to 600 mm the air velocity dropped and temperature increased.

One of the most important factors in DSF performance is the stack effect within the cavity. As the cold dry air replaces hot and warm air, continuous vertical air movement happens between the external and internal components of the DSF. This causes outwards pressure at the top of DSF and negative inward pressure at bottom of DSF. The researchers use neutral plane term to describe the intangible line between the two pressure zones (Etheridge 2012)

2.12 Summarized Literature Review

Table 4.7. Summarized literature review table 01 (by the author 2019).

| Authors | Year | Methodology | Material | Case Study | Highlighted results |
|------------------|------|-------------------|--------------------------------|---------------|---------------------------------------------------------------------------------------------------------------------------------------------------------------------------------------------------------------------------------------------------------------------------------------------------------------------------------------------------------------------------------------------------------------------------------------------------------------------------------------------------------------------------------------------------------------------------------------------------------------------------------------------------------------------------------------------------------------------------------------------------------------------------------------------------------|
| Lamnathou et al. | 2017 | Literature Review | ETFE cushions general study | Various cases | <ul style="list-style-type: none"> • triple layer ETFE have lower U-value comparing to a triple glazed-unit. • The triple layers cushions U-value was 1.95 W/m² K and managed to transmit 94~97% of visible light and 83~88% of UV range. • A water spray inside the air gap between a double layered ETFE reduced heat gain by 10% and the film surface temperature by 10°C • Infra-red absorbing coating Nowoflon ET 6235 Z-IR can increase thermal comfort by 10% and reduce cooling loads by 5~8% comparing to a conventional ETFE. • The embodied energy by area of ETFE is 27.0 MJ/m² and 300 MJ/m² for glass. |
| Hu et al. | 2017 | Literature Review | ETFE cushions general study | Various cases | <ul style="list-style-type: none"> • Transparency of the ETFE façade applications was 83~97%. • As the foil include fluorine in its structure and has low oxygen component, it is fire resistant. • U-Value of triple layer ETFE is 1.9 W/m²K but it can reach 1.4 ± 0.15 W/m²K for new environmental products. • The U-Value of double layers ETFE is 2.94 W/m²K and the U-Value of quintuple (five) layers ETFE is 1.18 W/m²K. • A typical cushion weighs 100~250 times less than equivalent transparent material. • light transmission of the foil can reach 90% • They recommended having the PVs on the top layer as internal gap temperature is higher than external temperature |

Table 4.8. Summarized literature review table 02 (by the author 2019).

| Authors | Year | Methodology | Material | Case Study | Highlighted results |
|------------------------|------|------------------------------------------------------------|-----------------------------------------------------------------------|--------------------------------------------------------------------------------------------------------|----------------------------------------------------------------------------------------------------------------------------------------------------------------------------------------------------------------------------------------------------------------------------------------------------------------------------------------------------------------------------------------------------------------------------------------------------------------------------------------------------|
| Cremers and Marx | 2017 | Computer simulation (Trnsys software) | ETFE cushions with geometric shapes | A mall in Germany | <ul style="list-style-type: none"> comparing to a conventional ETFE, the spatial modified foil reduced cooling loads in summer by 87%. |
| Dimitriadou | 2013 | Computer simulation (IES-VE software) and field experiment | Performance difference between glass and ETFE | Local testing chambers | <ul style="list-style-type: none"> the software simplified the curved ETFE surface into a flat plane, which had minor impact as cushions had limited curvature. He measured of the relation between the mean value of one variable between the experiment and the IES simulation and found out that correlation coefficients were 0.99 for radiant and air temperatures and 0.98 for other results ETFE comparing to glass provided good energy saving potential. |
| Cremers and Marx | 2016 | Computer simulation (Trnsys software) | IR absorbing membranes within the ETFE structures | three different scenarios with upper absorbing IR membrane (single, double and triple layers cushions) | <ul style="list-style-type: none"> The results showed that Nowoflon ET 6235 ZIR reduced cooling demand by 1% for the first scenario, 5% for the second scenario and 8% for the third scenario. The material is not fully transparent and gives bluish grey colour |
| Masih, Lau and Chilton | 2015 | Field experiment (measurement) | triple layer ETFE with fritted (pattern) and double layers clear ETFE | ESLC center in the university of and a detached garden house in Grantham | <ul style="list-style-type: none"> In the first case, average internal illuminance was 2736 lux, highest value inside the space was 4000 lux, the minimum value was 854 lux, the daylight factor was 60.8% and Uniformity Ratio was 0.3. In the second case, maximum illuminance value was 1171 Lux, minimum value was 478.7 Lux., the average illuminance was 919.5 Lux, the average DF was 56.4% and uniformity Ratio was 0.7. |

Table 4.9. Summarized literature review table 03 (by the author 2019).

| Authors | Year | Methodology | Material | Case Study | Highlighted results |
|----------------------------|------|-------------------------------------------------------------------------|---------------------------------------------------------------------------------------------|------------------------------------|--------------------------------------------------------------------------------------------------------------------------------------------------------------------------------------------------------------------------------------------------------------------------------------------------------------------------------------------------------------------------------------------------------------------------------------------------------------------------------------------------------------------------------------------------------------------------------------|
| Afrin, Chilton and Lau | 2017 | Field experiment (measurement) | Fritted double and triple layer ETFE | two studied building in the UK | <ul style="list-style-type: none"> the temperature immediately below the ETFE layers was typically 9°C higher than the external temperature when the double layer ETFE is used and 7°C higher when the triple layer ETFE is used. The additional layers increased the insulation effect of the cushions |
| Monticelli and Zanelli | 2013 | Literature Review | LCA of ETFE and other light weight materials | Various cases | <ul style="list-style-type: none"> for a 5-layer cushion, embodied energy was 315 MJ/m² and global warming potential was 137 CO₂eq/m² and for 3-layer cushion, embodied energy was 326.2 MJ/m² and global warming potential was 170 CO₂eq/kg. Durability of material can reach 50 years and life span of the total construction system can reach 20~30 years. |
| Liu et al. | 2016 | Field experiment (measurement) and mathematical modelling | Solar radiation properties of ETFE and other light weight materials | Eight different specimens of ETFE. | <ul style="list-style-type: none"> the worst results were associated with the clear single layer ETFE where solar radiation transmittance through the cushion reached 0.8, solar absorbance was 0.12, solar reflectance was 0.08 and the steel sub-frame temperature reached 61.7 °C in summer. The best results were associated with the triple layer ETFE with (46%~63%) printed surface where solar radiation transmittance was maximum 0.07, solar absorbance was 0.41, solar reflectance was 0.52 and the steel sub-frame temperature reached 33.9 °C in summer. |
| Suo, Angelotti and Zanelli | 2015 | Field experiment (measurement) and computer simulation (ESP-r software) | Thermal behaviour and energy performance of double and triple layers ETFE cushions envelope | sport hall in Milano | <ul style="list-style-type: none"> The double layer membranes and triple layers membranes with a continuously ventilated air gap provided 11% and 18% energy savings respectively comparing to the single layer membrane. circulation in the air gaps and can reduce the energy demand by 3% more. |

Table 4.10. Summarized literature review table 04 (by the author 2019).

| Authors | Year | Methodology | Material | Case Study | Highlighted results |
|-----------------------------------|------|-----------------------------------------------------------------------|-------------------------------------------------------------------------------------------|-----------------------------------------------------|-------------------------------------------------------------------------------------------------------------------------------------------------------------------------------------------------------------------------------------------------------------------------------------------------------------------------------------------------------------------------------------------------------------------------------------------------------------------------|
| Ibrahim et al. | 2016 | Computer simulation and mathematical modelling | BIPVs in ETFE cushions general discussion about simulation techniques | Various cases | <ul style="list-style-type: none"> The researchers summarized the design considerations into orientation, solar radiation incidence, shading possibilities, curvature, geometric shape and connection method and arrangement. |
| Zhao et al. | 2015 | Field experiment (measurement) and Runge–Kutta mathematical modelling | Thermal properties of integrated amorphous silicon PVs in triple layer ETFE cushion | Various cases | <ul style="list-style-type: none"> The study focused mainly on measuring the maximum temperature, which affects the PVs performance when it is installed on the middle-layer the maximum PV temperature within the triple layer ETFE was 362.3 K in summer which was higher than other PV integration application. Thus, it is recommended to add BIPVs on the top layer |
| Debbarma, Sudhakar and Baredar | 2017 | Field experiment (measurement) and literature review | Amorphous silicon PVs in double layer ETFE cushion | Three case studies in Turkey, Lisbon and Hong Kong. | <ul style="list-style-type: none"> BIPVs can provide 20~70% of the building's electricity requirements depending on façade area, location and orientation. the maximum PV temperature within the triple layer ETFE was 362.3 K in summer which was higher than other PV integration application. Thus, it is recommended to add BIPVs on the top layer BIPV electrical efficiency reached 4.52% in Turkey, 10% in Lisbon and 9.39% in Hog Kong. |
| Abdolzadeh, Sadeqkhani and Ahmadi | 2017 | Mathematical/numerical modelling and field measurement. | Two ETFE with a-si PVs on the middle layer scenarios (steady mass flow regulator airflow) | Local case in China | <ul style="list-style-type: none"> air and PV temperature in the first scenario was lower by 25°C. Although the first case has 0.33%, higher efficiency and higher average power (i.e. 7 W), it consumed most of the power and provided lower net output power. |

Table 4.11. Summarized literature review table 05 (by the author 2019).

| Authors | Year | Methodology | Material | Case Study | Highlighted results |
|-----------|------|---------------------------------------------------------------------|-------------------------------------------------------------------------------------------------------------------|------------------------|-----------------------------------------------------------------------------------------------------------------------------------------------------------------------------------------------------------------------------------------------------------------------------------------------------------------------------------------------------------------------------------------------------------------------------------------------------------------------------------------|
| Hu et al. | 2016 | Field experiment (measurement) and mathematical/numerical modelling | Amorphous Silicon BIPVs which are integrated in ETFE cushions under hot and cold conditions | Local mock-up in China | <ul style="list-style-type: none"> The average total net electricity that was produced by the PIBV was 42.9~54.5 Wh. The internal temperature was 16.8~31.0°C higher than external ambient temperature which indicated the potential of collecting thermal energy from inside the cushions. The system efficiency reached 25.5%. |
| Hu et al. | 2014 | Field experiment (measurement) and mathematical/numerical modelling | Six experiments under summer sunny and cloudy conditions integrated a-si PVs in the ETFE structure system. | Local mock-up in China | <ul style="list-style-type: none"> The results showed that the average produced energy was 61W per hour, the average ratio between consumption and output energy was higher under sunny conditions comparing to cloudy conditions and the average temperature difference between inside and outside of the cushions was 18 9°C. External load resistance and pressure performance were within the acceptable range; thus, the system was structurally feasible. |
| Hu et al. | 2015 | Field experiment (measurement) and mathematical/numerical modelling | Triple layer ETFE with integrated a-Si PVs on the middle layer. | Local mock-up in China | <ul style="list-style-type: none"> When the a-Si PVs surface temperature increase by 1 °C, the generation efficiency drops by 0.2%. The hottest layer was the middle, where the PVs are located, then the top and the bottom. thermal performance of the studied ETFE cushions had better thermal performance comparing to conventional ETFE cushions. |
| Hu et al. | 2017 | Mathematical/numerical modelling and field measurement. | Thermal performance of integrated flexible PVs inside a double layer ETFE cushion. | Local mock-up in China | <ul style="list-style-type: none"> A-si PVs configuration gives it high efficiency as it can be used on curved surfaces and accommodate full light spectrum. The average heat transfer coefficient for the PVs was 4.9 w/m²K and for the double layer ETFE was 2.39 w/m²K. |

Table 4.12. Summarized literature review table 06 (by the author 2019).

| Authors | Year | Methodology | Material | Case Study | Highlighted results |
|----------------------------------|------|----------------------------------------------------------------|----------------------------------------------------------------------------------------------------|------------------------------|-------------------------------------------------------------------------------------------------------------------------------------------------------------------------------------------------------------------------------------------------------------------------------------------------------------------------------------------------------------------------------------------------------------------------------------------------------------------------------------------------------------------------------------------|
| Michael, Gregoriou and Kalogirou | 2017 | Computer simulation (Desktop Radiance v1.02 and Ecotect v5.2) | Adaptive dynamic ETFE shade system | Existing building in Nicosia | <ul style="list-style-type: none"> The system, which covered 0~70% of the windows with changing angels, managed to reduce glare levels while maintaining appropriate illuminance, daylight levels and light uniformity in all indoor spaces. The proposed system ensures high DF levels which exceeded 2% while uniformity exceeds the threshold of 0.40 with high daylighting levels exceeding 500 lux in 3/4 of the area. The system eliminated the high lux levels (more than 3000 lux) so it minimized glare. |
| Hammad and Abu-Hijleh | 2010 | Computer simulation (IES-VE) | Potential energy saving of using external dynamic louvers in buildings | Office building in the UAE | <ul style="list-style-type: none"> The proposed design achieved an energy saving of 30.31%,28.57% and 34.02% for the west, east and south orientations. |
| Alotaibi | 2015 | Literature review, computer simulation and field measurement | Potential energy saving of using external dynamic louvers in buildings | Al Bahar Towers in Abu Dhabi | <ul style="list-style-type: none"> the design managed to reduce energy consumption in the building by 50% which decreased CO2 emissions by 1750 ton/year. |
| Peng et al. | 2016 | Numerical model and computer simulation (Energy Plus software) | PV-DSF which consisted from an external layer of semi-transparent a-Si BIPVs with 7% transmittance | Building in Berkeley | <ul style="list-style-type: none"> Air flow helped to reduce cooling load by almost 15% and increase the PV output by 3%. The a-si unit area managed to generate 65 kWh yearly. The cadmium telluride unit area managed to generate 130 kWh yearly. the system reduced net electricity consumption be 50% comparing to other common single layer façade glazing systems. |

Table 4.13. Summarized literature review table 07 (by the author 2019).

| Authors | Year | Methodology | Material | Case Study | Highlighted results |
|--------------------------|------|-------------------------------------------------------|--------------------------------------------------------------------------------------------------------|-------------------------------------------------------------|-----------------------------------------------------------------------------------------------------------------------------------------------------------------------------------------------------------------------------------------------------------------------------------------------------------------------------------------------------------------------------------------------------------------------------------------------------------------------------------------------------------|
| Barbosa, Ip and Southall | 2015 | Computer simulation (IES-VE) | Thermal comfort in naturally ventilated office building with a DSF under hot humid climate conditions. | 16 alternative cases. | <ul style="list-style-type: none"> • The most influential design option was shading devices followed by cavity depth and inclined external layer. • Extension of the cavity as high chimney above the building improved thermal comfort in higher levels. • The ultimate optimized DSF option achieved the required thermal comfort level in 70% of the occupied hours. |
| Kim et.al | 2018 | Computer simulation (Energy Plus and Daysim computer) | daylight and thermal effects of DSF with exterior and interior shading devices. | Model that was made in Daejong, South Korea. | <ul style="list-style-type: none"> • The results indicated that the DSF for the studied building can save 5% of total heating and cooling loads. • When DSF was combined with the shading devices which had daylight dimming control based on indoor lux levels, the simulated model managed to reduce the thermal loads by 27% and lighting energy consumption by 52%. |
| Luo et.al | 2017 | Experimental and numerical models | potential of installing A-Si photovoltaics blinds in the cavity of a DSF | A building under the climate conditions of Changsha, China. | <ul style="list-style-type: none"> • The BIPV-DSF option can save 12.16%~25.57% of building energy in summer comparing to the conventional DSF. BIPV-DSF lowered the heat transfer coefficient of the system to be 2.247. • When forced mechanical ventilation was used, the k-value improved comparing to natural ventilation. However, due to the electric power consumption of the forced ventilation, the study concluded that natural ventilation made better energy saving. |

Table 4.14. Summarized literature review table 08 (by the author 2019).

| Authors | Year | Methodology | Material | Case Study | Highlighted results |
|---------------------|------|-------------------------------------------------------------------------|---------------------------------------------------------------------------|----------------------------------------------------------|------------------------------------------------------------------------------------------------------------------------------------------------------------------------------------------------------------------------------------------------------------------------------------------------------------------------------------------------------------------------------------------------------------------------------------------|
| Khalifa et.al | 2017 | Computer simulation (TRNSYS) | Effect of DSF internal layer composition | Air-conditioned office building in Tunisia | <ul style="list-style-type: none"> They concluded that changing glazing type to highly insulated units reduced the cooling loads by 10% in summer. |
| Yang et.al | 2016 | Computer simulation and field measurement. | Impact of middle shading devices on DSF thermal insulation and air flow | Office building in Tianjin | <ul style="list-style-type: none"> In general, the addition of the shading devices reduced internal air temperature by 1 °C under the study conditions. |
| Joe et.al | 2014 | Computer simulation and field measurement. | Impact of middle shading devices on DSF thermal insulation and air flow | Office building in Seoul, Korea. | <ul style="list-style-type: none"> The optimal option with a high-performance glazing type on the external side and minimum cavity depth managed to reduce energy consumption by 5.26%. |
| Wen et.al | 2017 | Computer simulation (ANSYS), numerical modelling and field measurement. | Impact of inlet and outlet height on DSF thermal performance and air flow | Office building in Wuhan, China under summer conditions. | <ul style="list-style-type: none"> The best option was when the height of the inlet and outlet was between 300 mm and 450 mm. The air velocity reached 4m/s and the air temperature in the cavity decreased Temperature near the external layer reached 40°C while the temperature neat the internal layer was 35°C. The upper temperature of the cavity was higher than the lower temperature |
| Mahmoud and Alghazi | 2016 | Computer simulation and field measurement. | Impact of dynamic shade on daylighting | Cairo, Egypt. | <ul style="list-style-type: none"> Daylighting quality was improved by 50% in summer and spring |

Table 4.15. Summarized literature review table 09 (by the author 2019).

| Authors | Year | Methodology | Material | Case Study | Highlighted results |
|---------------------|------|-------------------|---------------------------------------------|-----------------------------|---------------------------------------------------------------------------------------------------------------------------------------------------------------------------------------------------------------------------------------------------------------------------------------------------------------------------------------------------------------------------------------------------------------------------------------------------|
| Johnsen and Winther | 2015 | Field measurement | Dynamic shade effects on energy consumption | Office building in Denmark. | <ul style="list-style-type: none"> • The U-value of the basic glazing unit was 1.1 W/m²K with a light transmittance (LT) of 0.79. • When movable/active screen was applied to the basic glazing unit the U-value varied from 0.5 to 1.1 W/m²K and LT varied from 0.02 to 0.79. • The controlled usage of daylight reduced the lighting energy consumption annually by 8 kWh/m². |

CHAPTER 03
METHODOLOGY

3 Methodology and research structure

3.1 Introduction

This Chapter covered analysis of the investigation processes which were followed in the research. The method and techniques were identified and justified to ensure that the study was valid. The literature review showed that similar investigations used several methodologies due to the complexity of studied parameters and depending different goals and objectives. However, the selected scientific method that was used was based on related researches that were conducted in a similar subject. All the studied factors have connections and affected each other. Thus, complex simulation software was required for evaluating all these variables.

3.2 Applicable methodology types

The previous studies used various methodologies such as experimental and field measurement and studies, literature review, numerical modelling and investigation and computer simulations. The advantages and disadvantages of each methodology would justify the selection of the appropriate methodology that could achieve the objectives of the dissertation.

3.3 Examples of related studies that used Literature review methodology

Lamnatou et al. (2017) used literature review methodology to conduct a critical review about ETFE applications. Firstly, the researchers discussed the general factors that affect ETFE performance and presented the main advantages of the material. They concluded that triple layer ETFE have lower U-value comparing to triple glazing and that ETFE can perform better when more layers are added. Also, they studied the option of including water spray inside the air gap which reduced heat gain by 10% and the film surface temperature by 10°C. Also, they studied LCA proved that embodied energy of ETFE is 26.5 GJ/t.

Hu et al. (2017) used the same methodology to investigate ETFE performance. They concluded that due to transparency of the material and that light transmission of the foil can reach 90%, it needs to have printed frit pattern to control heat gain and that the durability of its optical properties is 25 years. With regards to PV integration, they recommended having the PVs on the top or the bottom layer.

Monticelli and Zanelli used previous studies to create a LCA of various lightweight membrane structures including ETFE. They concluded that for a 5-layer cushion, embodied energy was 315 MJ/m² and global warming potential was 137 CO₂eq/m² and for 3-layer cushion, embodied energy was 326.2 MJ/m² and global warming potential was 170 CO₂eq/kg. Durability of material can reach 50 years and and life span of the total construction system can reach 20~30 years.

3.4 Advantages and disadvantages of literature review methodology

It goes without saying that this method can cover a wide range of related studies which covers various parameters, information and previous test results which can be used to support and validate the research. However, comparing to previous studies, the research subject, studied building and site conditions have their unique variables and parameters. Thus, depending solely in this methodology would not give accurate results. It should be combined with other supporting methodologies which can enhance the research creditability.

3.5 Examples of related studies that used numerical methodology

Zhao et al. (2015) studied thermal properties of BIPVs that are imbedded in triple layer ETFE cushion roof under four weather conditions in Milano using Runge–Kutta numerical method and field measurement experiment. The base of the study was the energy balance equation, which as expressed as converted energy and energy loss is equal to absorbed energy. They concluded that the maximum PV temperature within

the triple layer ETFE was 362.3 K in summer which was higher than other PV integration application.

Abdolzadeh, Sadeqkhani and Ahmadi (2017) investigated the efficiency of BIPV on the middle layer of ETFE cushions structure. They made a numerical model and studied the electrical and thermal performance of the system under two scenarios which are cushions with steady mass flow and cushions with regulator (airflow) system. They concluded that comparing to Crystalline Silicon under same conditions; this type has 0.25% less power decrease due to surface temperature increment, better integration on curved surfaces and lower cost. They concluded that air and PV temperature in the first scenario was lower by 25°C. Although the first case has 0.33%, higher efficiency and higher average power (i.e. 7 W), it consumed most of the power and provided lower net output power.

3.6 Advantages and disadvantages of numerical methodology

In this method, researchers use dynamic mathematical equations to study the relationship between the investigated parameters and factors based on various approximations and assumptions. This can affect the accuracy of results and also make the research more complicated. Thus, in the previous examples, the researchers used other methodology which was field experiment and measurement to validate the results. So, it would not be applicable for the study.

3.7 Examples of related studies that used field measurement/ experiment methodology

Masih, Lau and Chilton (2015) studied the daylighting performance of the ETFE cushions. The researchers used on-site monitoring method using illuminance meters. They measured day light level 1 m above the finish floor level to calculate daylight factors and used a camera and a computer software to create luminance maps. They concluded that as these lighting conditions will affect the general activities in the

building and the occupant's performance, thus transparency and opacity in the ETFE structures should be studied carefully to ensure that a appropriate luminous environment is provided

Hu et al. (2016) investigated PIBV which are integrated in ETFE cushions under hot and cold conditions. The researchers used a cushion system, solar energy control sub system (SECS) and pressure control system (PCS) to establish their experiment. They measured photovoltaic electricity, temperatures (inside and outside the cushions), temperature differences and overall system efficiency. They concluded that the average total net electricity that was produced by the PIBV was 42.9~54.5 Wh. The internal temperature was 16.8~31.0°C higher than external ambient temperature with 25.5% system efficiency.

Afrin, Chilton and Lau (2017) made a comparison study between the thermal behaviour of fritted double and triple layer ETFE cushions atrium skylight. Their methodology was field measurements where they used sensing devices to record ambient temperature, internal temperature, cushions temperature and solar radiation. They concluded that the temperature immediately below the ETFE layers was typically 9°C higher than the external temperature when the double layer ETFE is used and 7°C higher when the triple layer ETFE is used while the cushions internal temperature reached 45°C maximum. Thus, the additional layers increased the insulation effect of the cushions but were not enough to reduce the heat gain within the atrium.

3.8 Advantages and disadvantages of field measurement/ experiment methodology

In This methodology, the researchers test an actual model or a mock-up using measuring equipment and sensors under real conditions to reach the required results and conclusion. That can be done in a field experiment or in a lab. In this type of studies, the results tend to be more accurate as the data and the results are collected under real conditions. However, in order to build a real mock-up that simulate and actual building condition, special permits must be obtained. Also, if the study is

conducted on an actual building, there would be several limitations if the building is already occupied or if it has security requirements. The second obstacle is time as the experiment can last for a long time which does not suit specific research subjects. Thirdly, with regards to the dissertation subject, building an actual mock-up can be very expensive and would need supporting man power for the control and monitoring. Finally, in some cases, if the measuring equipment are not well calibrated, the results can have some errors. Thus, more technical support would be required which means more time and cost.

3.9 Selected methodology for the study

The research covers several parameters such as annual energy consumption, thermal comfort, visual comfort and daylighting over ten different scenarios. These different variable, strategies and scenarios increases the research complexity. Thus, due to cost and time limitations, building scale and research complexity, computer simulation was selected to be the methodology of this research. The software developers keep enhancing the capabilities of the simulation programs using the help of building specialists, engineers and physicians. This methodology is usually used in early design stages of any new project, based on literature review, to support decision making then it can be supported by field measurement in final stages.

As highlighted in the previous section, the research aimed to study the proposed enhancement options of existing buildings envelopes using different passive and active techniques under the local weather conditions. There were other advanced parameters that were involved and associated with the study such as lighting and mechanical equipment operation profile, lighting sensors, dimming options, dynamic parts,etc. An advanced simulation software can compute all these parameters and give reliable results. Various programs are available in the market and three of them were considered for the study and only one was chosen after validating the results between them.

As highlighted in the literature review, this methodology is very common in all related new researches. Cremers and Marx (2017) found out solutions to ETFE high solar transmissions using geometric special (3D) modification (hemispherical, pyramid and saw tooth shapes) in the foil layer with the help of computer simulations (Trnsys software) which evaluated thermal comfort and calculate cooling loads. Dimitriadou (2013) used computer simulation via IES-VE to study performance difference between glass and ETFE with regards to building energy consumption, especially for heating then he did a field experiment to validate the software and associated results. He measured of the relation between the mean value of one variable between the experiment and the IES simulation and found out that correlation coefficients were 0.99 for radiant and air temperatures and 0.98 for other results, thus he suggested that the software provided an accurate model. Cremers and Marx (2016) prove that Nowofol, which an infra-red absorbing material, as an enhancement to ETFE can reduce cooling by 8% .The study was done using TRNSYS software. Michael, Gregoriou and Kalogirou (2017) used Desktop Radiance v1.02 and Ecotect v5.2 simulation programs to evaluate dynamic ETFE shade and concluded that the system managed to reduce glare levels while maintaining appropriate illuminance, daylight levels and light uniformity in all indoor spaces. In the UAE,Hammad and Abu-Hijleh (2010) investigated the energy savings potential of using dynamic shade in an office building using IES-VE simulation program.

In the highlighted researches, this methodology was used in various countries to investigate different sustainability concerns which proves that simulation programs are remarkable tools that can contribute towards addressing diverse research questions under various conditions. The increment in computer power and the evolution of these technologies will definitely motivate researchers to identify more problems, find their answers and explore more uncertain areas for the benefit of our community.

Furthermore, Reeves, Olbina and Issa (2012) compared three building energy modelling (BEM) programs which were Ecotect, Green Building Studio and IES-VE. The researchers compared the results from each software with the electricity bills to measure accuracy in their results (figure 3.1). They pointed out that IES-VE was more precise in three of the studied cases which were overall energy consumption, cooling loads and heating loads which was within the acceptable range for their study which was 0-15%.

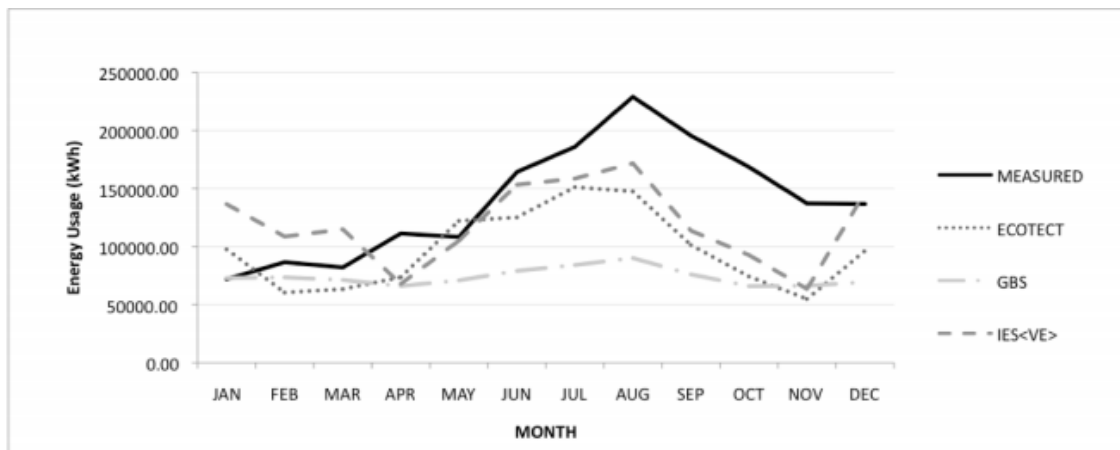


Figure 3.1. Results comparison between the different programs (Reeves, Olbina & Issa 2012).

Attia et al. (2012) conducted a survey among almost 850 engineers and architects to rank the available building performance simulation (BPS) computer programs based on a criterion which included building performance simulation (BPS), usability and information management (UIM), integration of intelligent design knowledge-base (IIKB), usability and information management (UIM), integration of intelligent design knowledge-base (IIKB), accuracy and ability to simulate detailed and complex building components (AADCC) and interoperability of building modelling (IBM). Among architects, IES-VE had the highest rank. Their main reasons were that its friendly interface which provided simple information management and its adaptability during different design phases. Among both groups IES-VE and DB received the highest percentage of comfort and agreement.

3.10 Energy Modelling Software

Three energy modelling programs were tested for the study which were IES VE, Autodesk Green Building Studio and Autodesk insight. After basic evaluation, IES VE gave the most accurate results when energy consumption of the building was simulated with -0.7% bias while the other programs had huge results bias comparing to the actual building consumption (table 3.1). Also, IES VE was the only software among the three that managed to calculate the appropriate factors for the study such as thermal comfort, day light analysis and daylight harvesting potential factors. Thus, IES VE was chosen for the study. According to the literature review ,0~15 results bias between actual loads and simulation results is acceptable for the research.

Table 3.1. Comparison between the simulated total energy consumption in the three programs (author 2019).

| Reference | Total electricity consumption (MWh) | Results bias |
|-----------------------------------------------------------------------|-------------------------------------|--------------|
| Actual electrical loads which are approved by AADC (actual situation) | 43.770 | - |
| IES-VE | 44.5490 | +1.80% |
| Autodesk Green Building Studio | 52.344 | +19.6% |
| Autodesk Insight | 58.325 | +33.3% |

3.11 Building selection

At first, in order to simulate the conditions of a building, its classification and type needs to be selected and considered before the study. The simulation can be accurate when all related studied parameters such as heat gain and illuminance levels are calculated within its operation hours or what is called project time profile. Under local weather conditions, this limits the data collection and simulation between sunrise and sunset. Thus, the selected building operation profile should be within this time

frame for more accurate results. Therefore, the selected building was an office building that serves an assembly hall within a mixed use/residential complex. Although the full operation profile includes 16 hours, the peak operation hours are between 9 am and 7 pm which falls within the preferred time frame. Besides that, 40% of the selected building walls consists of double-glazed units. As the scope of research focused mainly on glazed walls, the building was suitable for the study. This percentage can represent the situation in most of the UAE buildings which are not fully glazed or fully opaque.

Secondly, in order for the simulation to be accurate and to be verified, full documentation and information regarding this building must be available for the researcher. Due to information availability, the selected building was an ideal choice for the study. Thirdly, as the research covered several ETFE applications with ten different scenarios and various aspects to be covered by the simulation, large buildings could not be selected for the study because of time limitation. For instance, selecting the simulation program along with the simulation process, verification of results, trial and error took almost 60% of the research time.

3.12 Studied Building Description

The studied case will be a reception office building in Abu Dhabi that serves a large residential compound in Yas Island. As agreed with the head of the architectural department, the design consultant name, client's name and the project name will be kept anonymous due to confidentiality agreement with the client. Multiple ETFE/DSF applications and configurations will be studied when used within this building as shown in the following sections. The building consists of 10 rooms. The waiting and reception rooms are the only ones with large windows (almost 1/3 of the total façade area). Refer to figures 3.2, 3.3, 3.4 and 3.5 for basic building details.

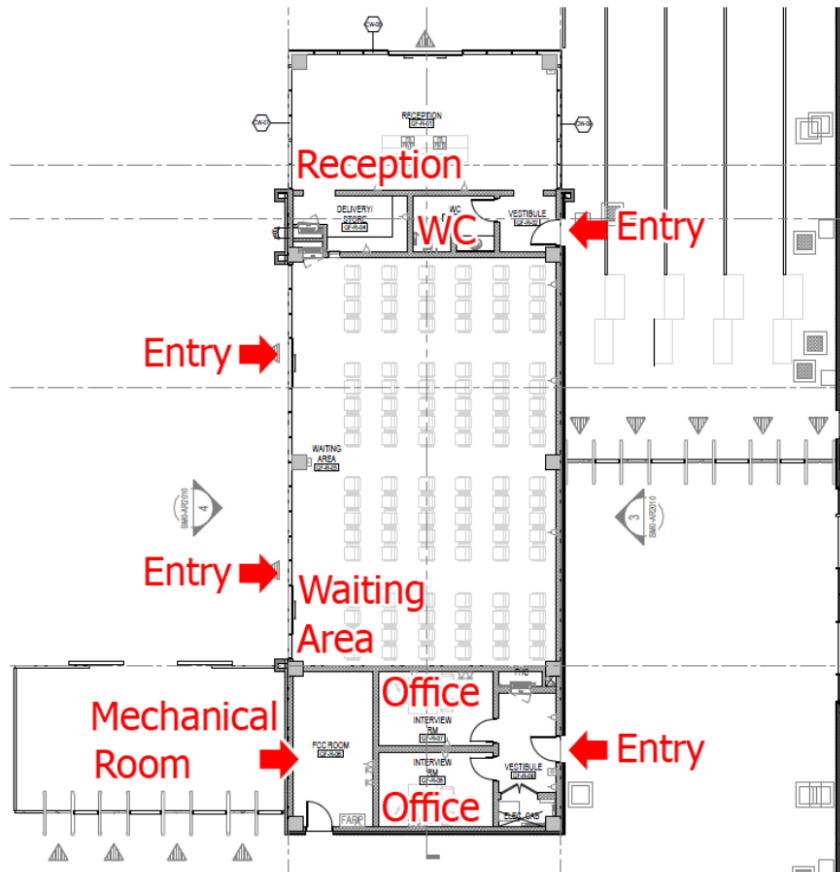


Figure 3.2. Reception building plan (author 2019).

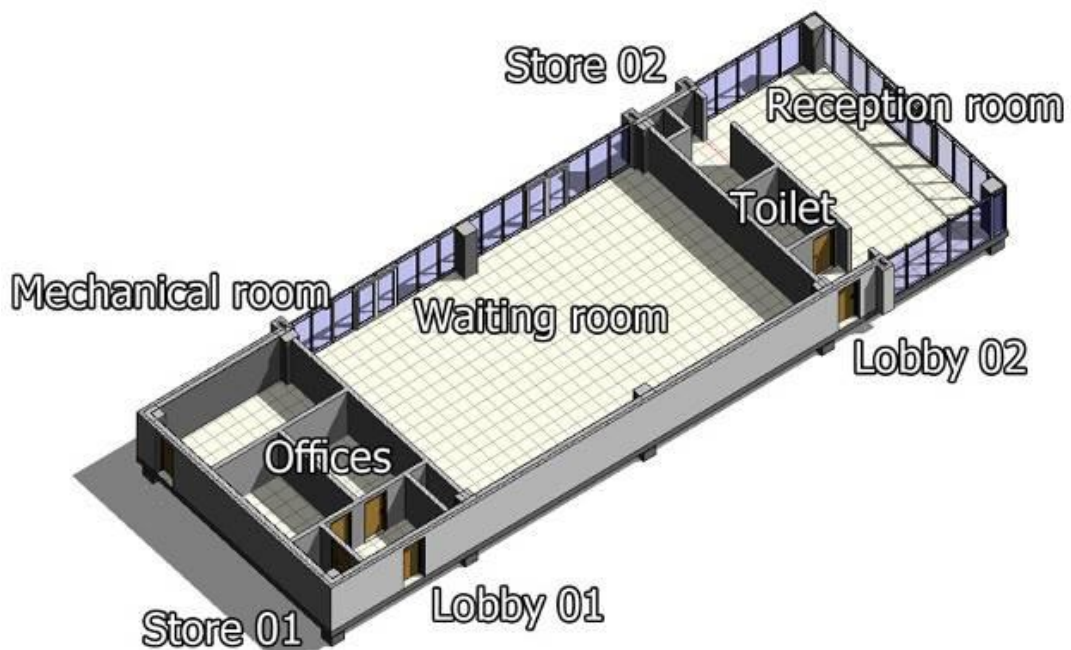


Figure 3.3. Reception building 3D plan from the Revit model (author 2019).

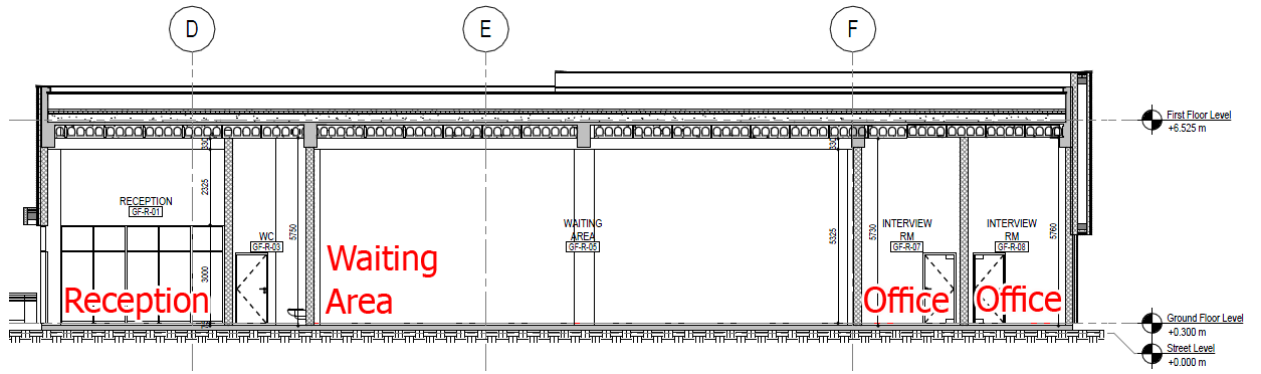


Figure 3.4. Reception building section (author 2019).

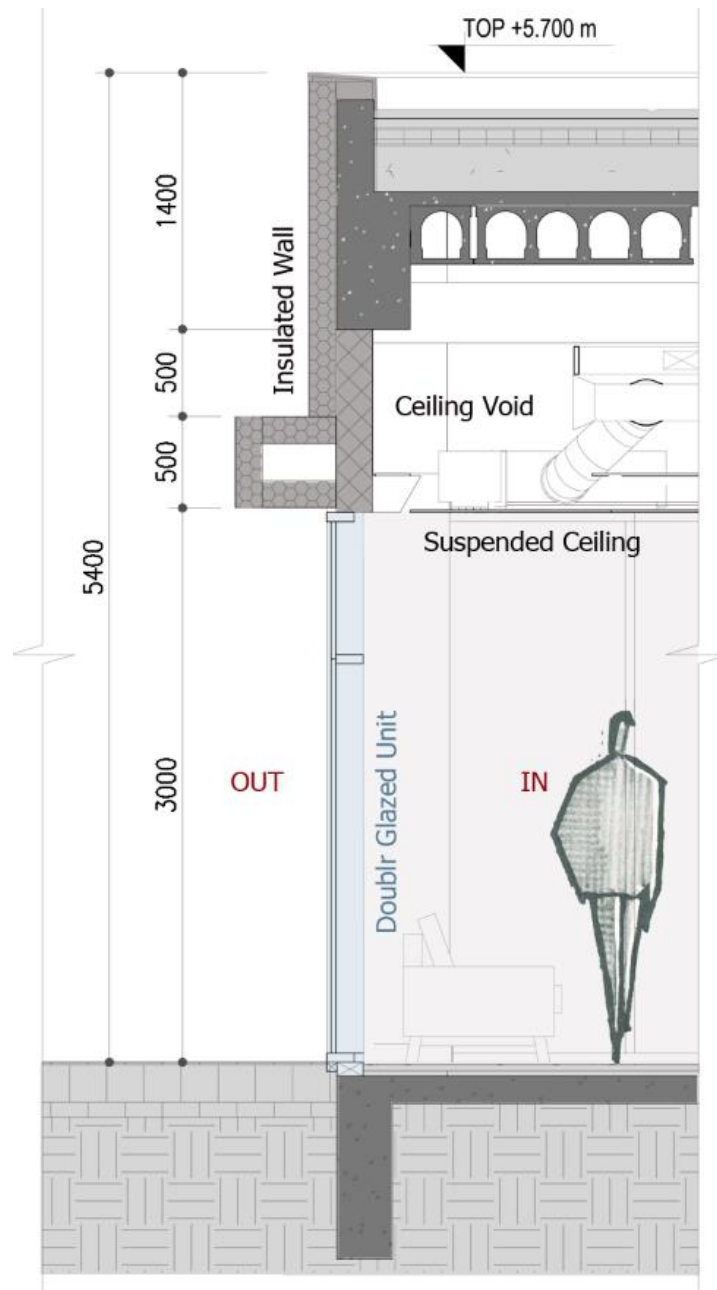


Figure 3.5. Building wall section (author 2019).

3.13 Simulation Software Validation

The annual energy consumption results were verified against the actual electrical loads in the building which were approved by the authorities (Abu Dhabi Distribution Company) as part of the building permit process. The total actual hourly consumption load ,after adding diversity factor, is 16.89 kW (Cherian 2017). As the building operates for 5110 hours annually. But as the load varies from min 20% to maximum 80% from the total load according to the occupancy/operation schedule, the actual full load (100%) operating hours are equal to 7.1 daily hours. Hence the actual total annual consumption, according to the electrical calculations, is 16.89 kW x 7.1 hours daily x 365 operating days = 43770.435 kWh which is equal to 43.770 MWh (Cherian 2017). The IES VE Apache simulation result showed the total annual electricity consumption as 44.5490 MWh (table 3.3). Comparing to the actual building annual consumption, the results bias was +1.80% (figure 3.6).

Table 3.3. Total annual electricity consumption results in IES VE (author 2019).

| | Total electricity (MWh) |
|--------------|-------------------------|
| Date | Basic Model.apr |
| Jan 01-31 | 2.1744 |
| Feb 01-28 | 2.4339 |
| Mar 01-31 | 3.0512 |
| Apr 01-30 | 3.6774 |
| May 01-31 | 4.4261 |
| Jun 01-30 | 4.5822 |
| Jul 01-31 | 4.9159 |
| Aug 01-31 | 4.9626 |
| Sep 01-30 | 4.4772 |
| Oct 01-31 | 4.0166 |
| Nov 01-30 | 3.2288 |
| Dec 01-31 | 2.6027 |
| Summed total | 44.5490 |

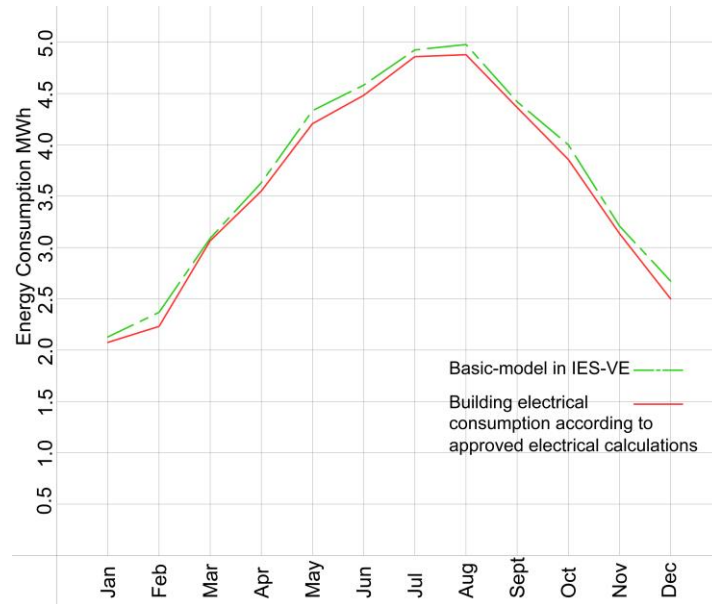


Figure 3.6. Comparison between simulated and actual electrical loads (author 2019).

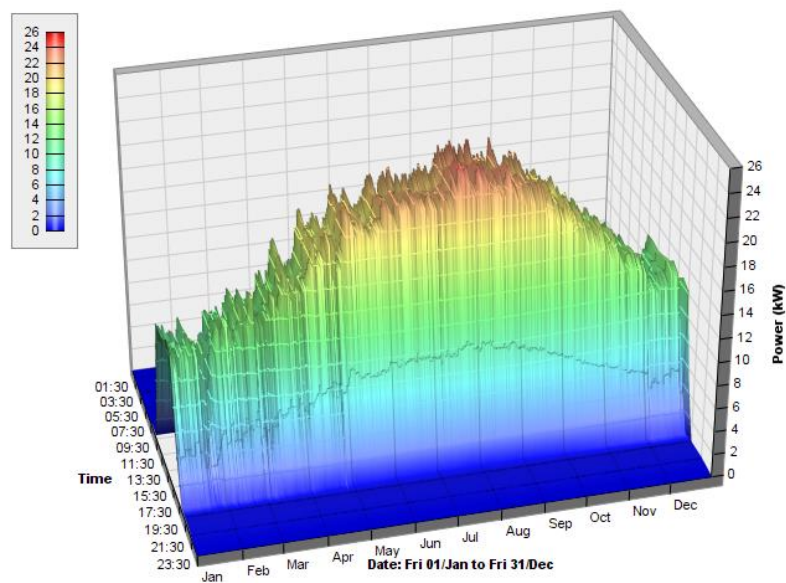


Figure 3.7. Total annual electricity consumption results in IES VE (by the author).

According to the actual electrical loads in the building the maximum connected load is 23.13 kW (Cherian 2017). The predicted maximum electrical load in August in the simulation results was 26 kW (figure 3.7). The results bias was +12.4%. It was noted that the maximum daily electrical consumption in winter was between 10 and 14 kW and it increased in summer to reach the peak point in August.

3.14 Methodological Map and Research Structure

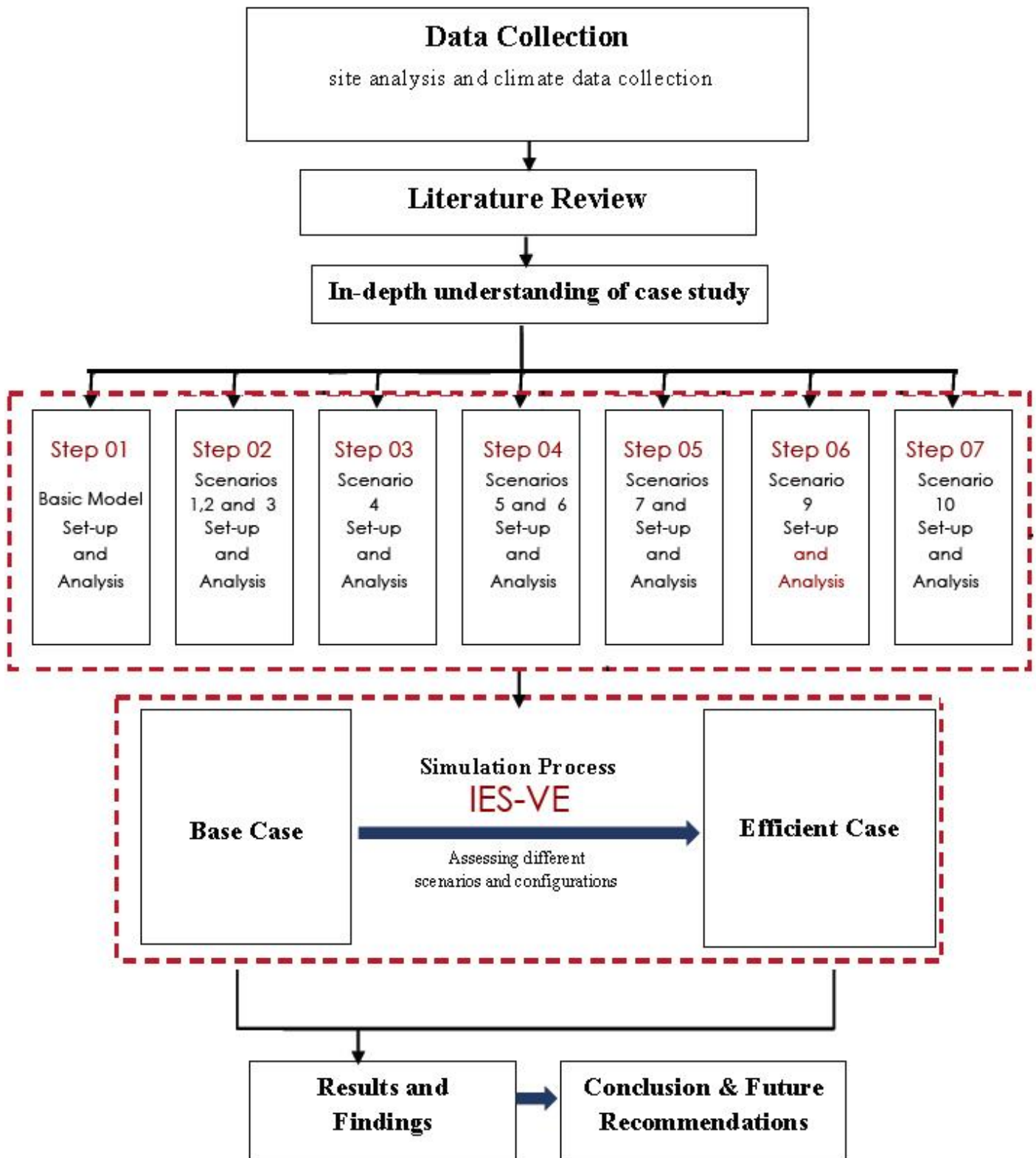


Figure 3.8. Methodological map (author 2019).

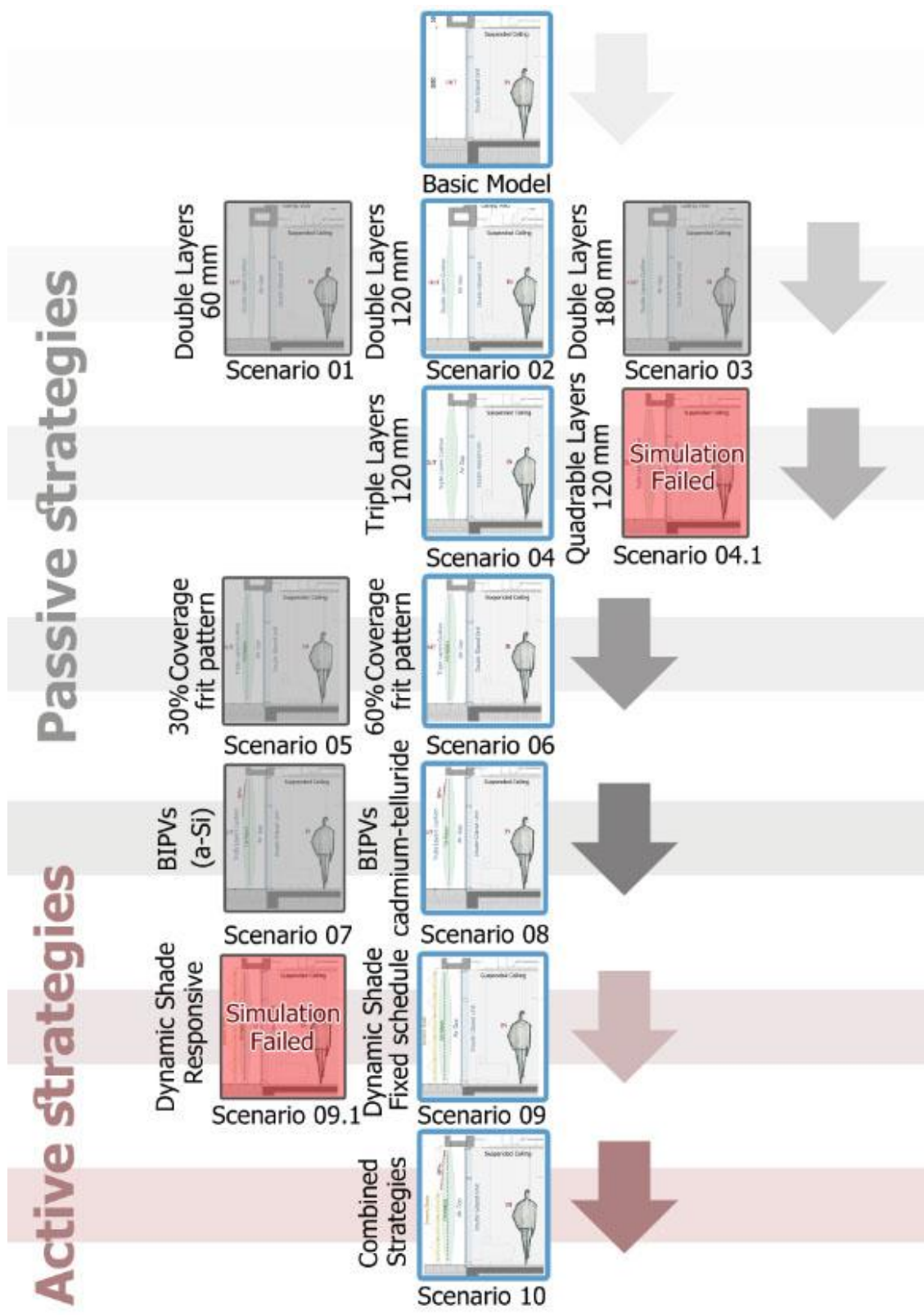


Figure 3.9. Scenarios research structure (author 2019).

The research covered various ETFE/DSF applications including:

1. Using different ETFE types as part of buffer DSF/corridor facade façade with different parameters. This study included investigation of changes in cushion depth and number of layers as shown in scenarios 1,2,3 and 4.
2. Using ETFE cushions with fritted patterns as part of buffer DSF/corridor facade as shown in scenarios 5 and 6.
3. The installation of ETFE cushions with different BIPVs types as part of buffer DSF/corridor facade as shown in scenarios 7 and 8.
4. Utilizing single layer opaque ETFE as light dynamic solar shading system as part of buffer DSF/corridor facade facade as shown in scenarios 9.
5. Applying both BIPVs and dynamic shading devices as part of buffer DSF/corridor facade model as shown in scenarios 10.

For further explanation, next chapter covered the basic description and modelling steps for each of these scenarios.

CHAPTER 04
STUDIED BUILDING AND MODELS'
SETUP

4 Studied building and models' setup

4.1 Basic Model

4.1.1 Basic spaces modelling

The first step in the energy modelling process is building basic modelling in IES VE software (figures 4.1 and 4.2). After adjusting the units and grids, the different rooms were added using the ModelIT application in the software. The rooms height is 4.15 meters. The projected shade elements were added as local shades. Doors and windows were inserted in all related rooms. Also, as the spaces have suspended ceiling, the ceiling void height was inserted (figure 4.3).

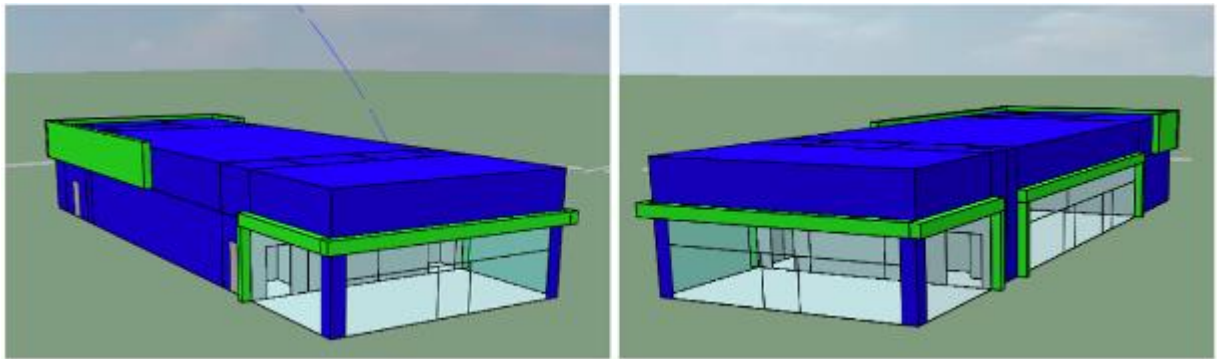


Figure 4.1. Reception-building model in IES VE software (author 2019).

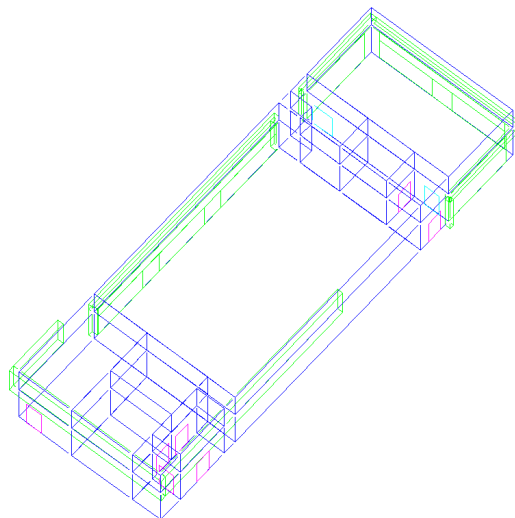


Figure 4.2. Reception-building model in IES VE software (author 2019).

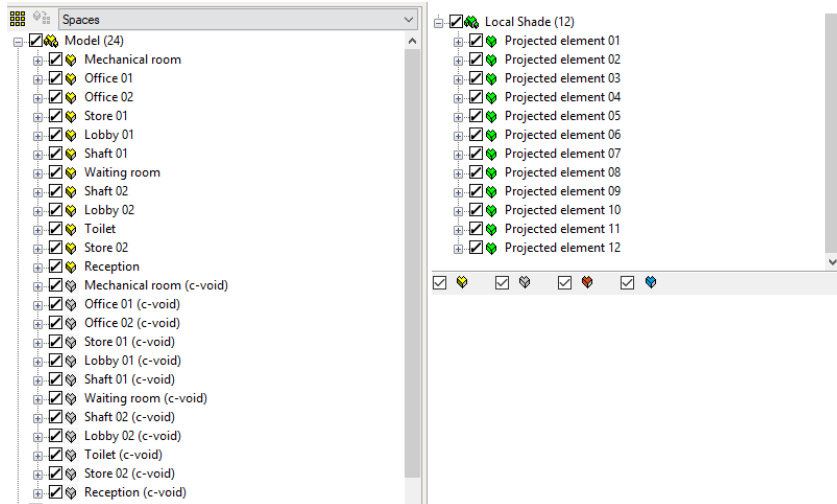


Figure 4.3. Reception-building model components in IES VE software (author 2019).

4.1.2 Project location and weather data

The second step is to select the current location for the building by adjusting the location data. The nearest location in IES VE database to our project is Abu Dhabi international airport (figures 4.4,4.5 and 4.6). The software acquired the data from ASHRAE Fundamental design weather database version six (figures 4.7,4.8,4.9 and 4.10). After selecting the nearest location, the software shows all the data related to the city such as basic weather data and sun path. It is also important to adjust the project north in the software to match the true north which is rotated 17 degrees counter clockwise.



Figure 4.4. Basic location data as shown in the IES VE software (author 2019).

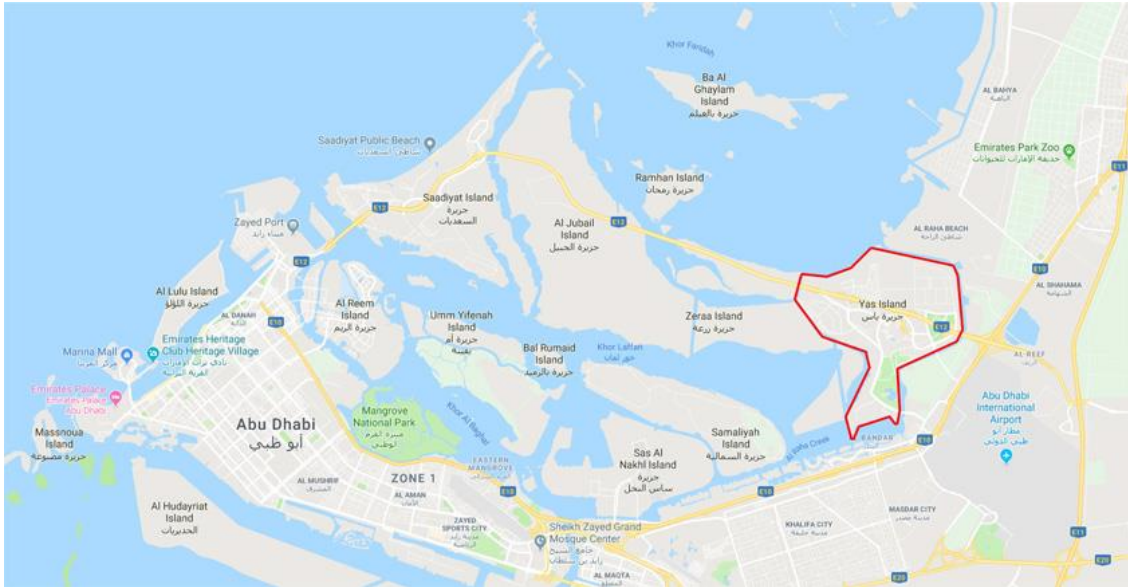


Figure 4.5. Project location in Yas island near the city of Abu Dhabi (Google map 2018).



Figure 4.6. Project location in Yas island and the weather station location (Google map 2018).

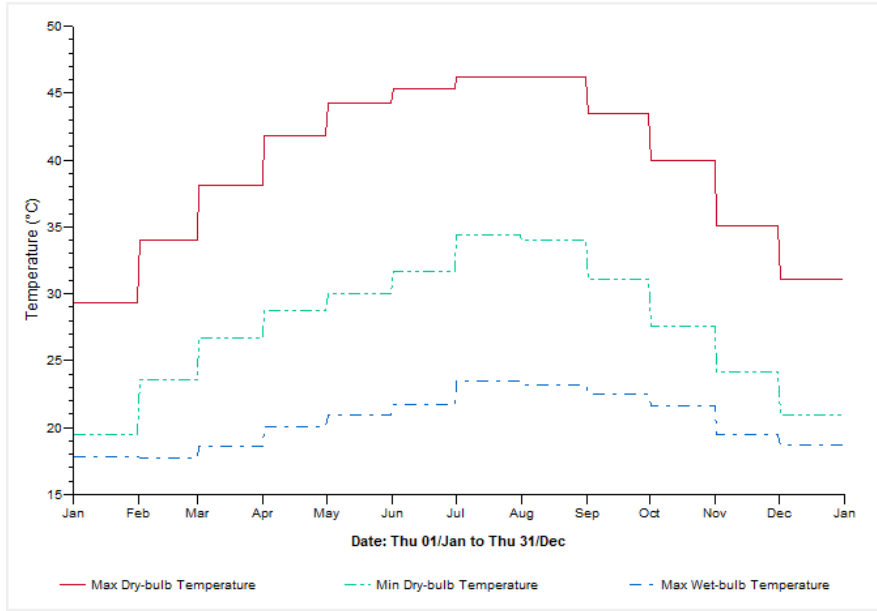


Figure 4.7. Basic design data as shown in the IES VE software (author 2019).

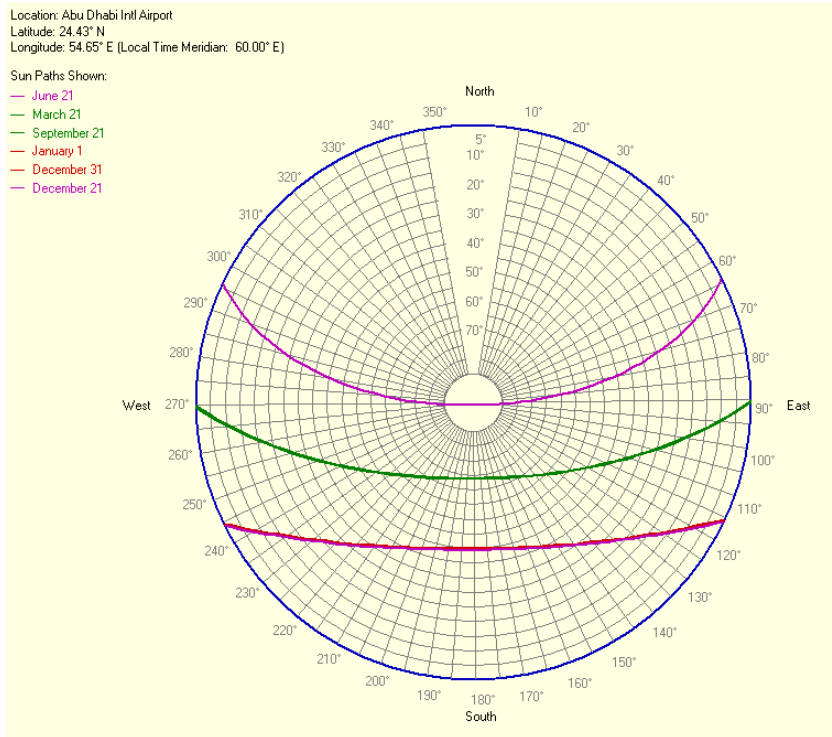


Figure 4.8. Sun path as shown in the IES VE software (author 2019).

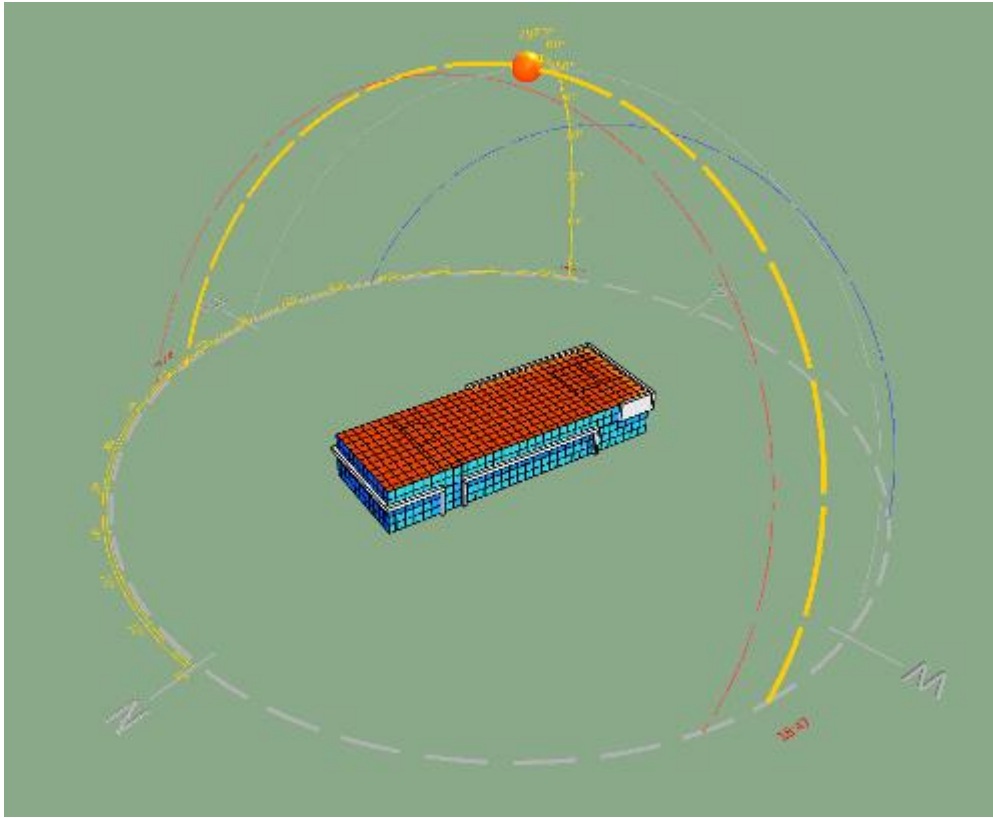


Figure 4.9. Sun path with relation to the building orientation in IES-VE (author 2019).

Cooling Loads Weather Data

Adjust max. outside temps (°C)...

Dry-bulb Wet-bulb

Display: ASHRAE / CIBSE

Hourly temp. variation: Sinusoidal / ASHRAE standard

Plot design day:

-----Temperature----- Humidity-----Solar Radiation

| | Min Tdb (°C) | Max Tdb (°C) | Twb at Max Tdb (°C) |
|-----|--------------|--------------|---------------------|
| Jan | 19.50 | 29.30 | 17.80 |
| Feb | 23.60 | 34.00 | 17.70 |
| Mar | 26.70 | 38.10 | 18.60 |
| Apr | 28.70 | 41.80 | 20.10 |
| May | 30.00 | 44.20 | 20.90 |
| Jun | 31.70 | 45.30 | 21.70 |
| Jul | 34.40 | 47.00 | 23.50 |
| Aug | 34.00 | 46.20 | 23.20 |
| Sep | 31.10 | 43.50 | 22.50 |
| Oct | 27.60 | 40.00 | 21.60 |
| Nov | 24.20 | 35.10 | 19.50 |
| Dec | 20.90 | 31.10 | 18.70 |

Figure 4.10. Basic design data as shown in the IES VE software (author 2019).

4.1.3 Material set-up

One of the most important steps is the set-up of the building materials. According to ESTIDAMA requirements and the building design documents, maximum U-Value of the roof is 0.2 W/m²K, maximum U-Value of the external walls is 0.25 W/m²K, maximum U-Value of the vertical glazing is 2 W/m²K. According to technical specifications, the selected material achieved excellent performance comparing to the requirements. For instance, external wall U-value is 1.75 W/m²K as it consists of autoclaved aerated concrete blocks and external insulation finishing system. The construction template was adjusted according to the drawings and the technical specifications (figures 4.11 to 4.17). It was noted that the g-value cannot drop below 0.27 due to a software error. Hence the double-glazed window g-value was changed from 0.26 to 0.27.

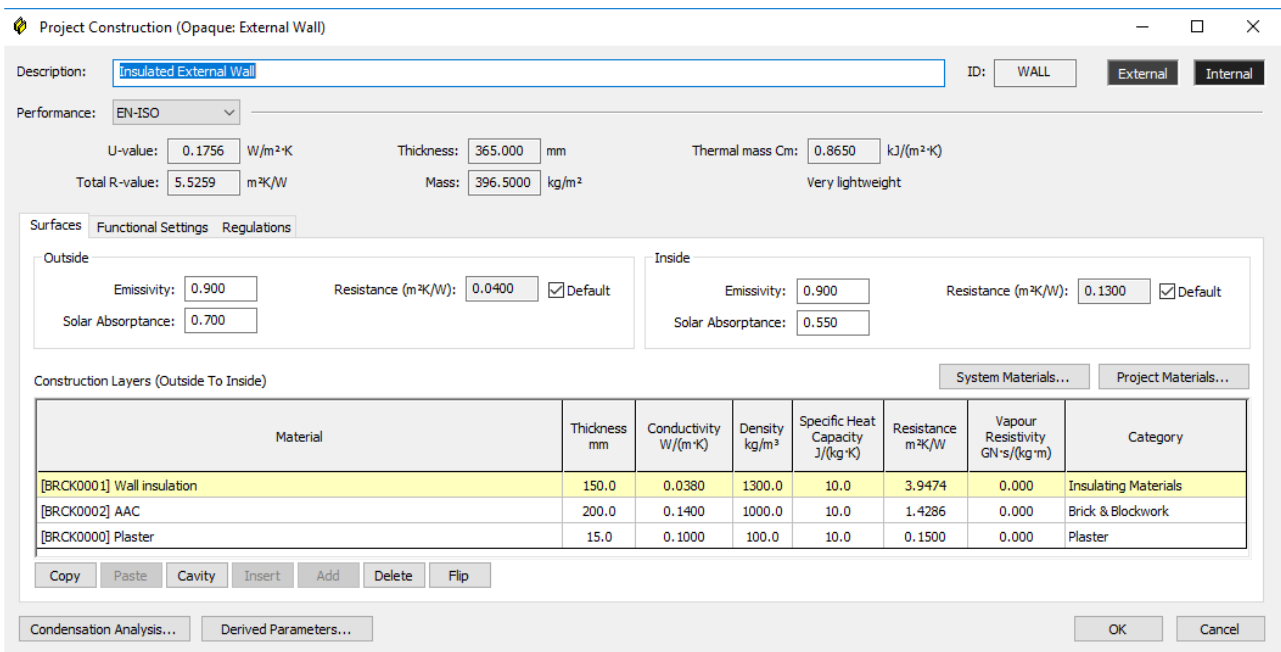


Figure 4.11. Inserted external wall layers in the adjusted construction template in IES-VE (author 2019).

- I. Insulation: Cellular Glass insulation boards complying with the following test data as per EN 13167
 1. Density (+/- 10%) (EN1602): 100 kg/m³
 2. Thickness (EN822): according the drawing or as required to achieve the U Value.
 3. Dimensions: (EN822), +/- 2mm: Length 600 mm; Width 450 mm.
 4. Thermal Conductivity (EN ISO 10456: 0.038 W/(m.K).
 5. Reaction to Fire (EN 13501-1): Euroclass A1
 6. Compressive Strength (EN 826 annexe A): CS> 400 KpA
 7. Tensile Strength (EN 1607): TR > 100 KpA
 8. VOC: Zero.

Figure 4.12. External wall insulation (cellular glass) properties in the technical specs (Dunn et al. 2017).

- A. Autoclaved Aerated Concrete (AAC) Masonry Units produced from quartz sand, cement and lime to extremely narrow dimensioned tolerances suitable for thin-bed mortar (glue) method comply with requirements of ASTM C 1386.
 1. Density: Low density units: 500 kg/m³.
 2. Compressive Strength: 3.2 Mpa.
 3. Thermal conductivity: 0.14 W/mK
 4. Size: Manufacturers' standard block with actual face dimensions 600 mm long x 200 mm high unless otherwise indicated. Thickness as indicated on drawings.
 5. Special Shapes: Provide where required for lintels, corners, jambs, control joints, headers, bonding, scored accented walls and other special conditions.
 6. Lintel Blocks:
 - a. Solid reinforced blocks: Same width as walls.

Figure 4.13. Autoclaved aerated concrete blocks (AAC) properties in the technical specs (Dunn et al. 2017).

The screenshot shows the 'Project Construction (Opaque: Roof)' window in IES-VE. The description is 'Insulated Roof'. Performance metrics include U-value: 0.1347 W/m²K, Total R-value: 7.2852 m²K/W, Thickness: 502.000 mm, Mass: 815.2000 kg/m², and Thermal mass Cm: 149.5000 kJ/(m²K). Surface properties are set for both outside and inside. The construction layers table is as follows:

| Material | Thickness mm | Conductivity W/(m·K) | Density kg/m³ | Specific Heat Capacity J/(kg·K) | Resistance m²K/W | Vapour Resistivity GN·s/(kg·m) | Category |
|--------------------------------------------|--------------|----------------------|---------------|---------------------------------|------------------|--------------------------------|--------------------------|
| [ROOF0001] Roof Tile | 50.0 | 0.8400 | 1900.0 | 80.0 | 0.0595 | 0.000 | Asphalts & Other Roofing |
| [ROOF0002] Geotextile membrane | 1.0 | 0.0600 | 1000.0 | 650.0 | 0.0167 | 0.000 | Asphalts & Other Roofing |
| [ROOF0003] Extruded Polystyrene insulation | 100.0 | 0.0160 | 32.0 | 1050.0 | 6.2500 | 0.000 | Asphalts & Other Roofing |
| [ROOF0004] Water proofing | 1.0 | 0.0600 | 1000.0 | 200.0 | 0.0167 | 0.000 | Asphalts & Other Roofing |
| [ROOF0005] Light concrete | 150.0 | 0.2000 | 1700.0 | 650.0 | 0.7500 | 0.000 | Asphalts & Other Roofing |
| [ROOF0000] Concrete | 200.0 | 1.0400 | 2300.0 | 650.0 | 0.1923 | 0.000 | Asphalts & Other Roofing |

Figure 4.14. Inserted Roof layers in the adjusted construction template in IES-VE (author 2019).

- C. Physical properties of for roofs and cavity walls: (type VII)
1. Thermal conductivity : 0.016 W/m.K (DIN 52612)
– 5 years aged value 0.032 W/m.K (ASTM C177)
 2. Water Absorption : <1% by volume to ASTM D2842
 3. Capillarity : Nil
 4. Density : 32-35 kg/m³.
 5. Compressive strength : 220 – 360 KPA to DIN 53421 or 42 – 65 PSI
to ASTM D-1621
 6. Fire : Class B1 DIN 4102
 7. Thicknesses : 50mm for wall cavity and 75mm for roof
unless otherwise indicated on drawings
 8. Flame Spread/Smoke Developed Values (ASTM E84): 5/165.

Figure 4.15. Roof insulation properties in the technical specs (Dunn et al. 2017).

| Net U-value (including frame): | 1.9140 | W/m ² ·K | U-value (glass only): | 1.6176 | W/m ² ·K | | | | | | | | |
|--------------------------------|--------------|----------------------|-----------------------|--------|--------------------------------------------|--------------------------------|---------------|---------------------|--------------------|------------------|--------------------|-------------------|-------------------------|
| Net R-value: | 0.6182 | m ² ·K/W | g-value (EN 410): | 0.2839 | Visible light normal transmittance: | 0.37 | | | | | | | |
| Material | Thickness mm | Conductivity W/(m·K) | Angular Dependence | Gas | Convection Coefficient W/m ² ·K | Resistance m ² ·K/W | Transmittance | Outside Reflectance | Inside Reflectance | Refractive Index | Outside Emissivity | Inside Emissivity | Visible Light Specified |
| [EXTW.1] SMOKE SILVER | 8.0 | 0.0400 | Constant | - | - | 0.2000 | 0.230 | 0.230 | 0.120 | - | - | - | No |
| Cavity | 16.0 | - | - | Air | 1.6136 | 0.1882 | - | - | - | - | - | - | - |
| [EXTW.] CLEAR FLOAT 6MM | 6.0 | 0.1000 | Constant | - | - | 0.0600 | 0.230 | 0.230 | 0.120 | - | - | - | No |

Figure 4.16. Inserted double glazed unit windows in the adjusted construction template in IES-VE (author 2019).

| | |
|-------------------------------------------------------------------------------------|------------------------------------------------------------------------------------------------------------------------------------------------------|
|  | VISION GLASS BUILD-UP: 8mm COOL-LITE SMOKE SILVER (KNT140) 16mm AIRSPACE 6mm CLEAR FLOAT GLASS |
| | PERFORMANCE: U-VALUE: 1.6W/m2/K LIGHT TRANSMITTANCE: 37% TOTAL SOLAR TRANS: 23% SHADING COEFFICIENT: 0.30 SOLAR HEAT GAIN (LSG): 0.26 |

Figure 4.17. Glazing properties in the technical specs (Dunn et al. 2017).

4.1.4 Profiles database

The reception building serves a large assembly hall (separate building). Thus, occupancy, lighting and power schedule was selected accordingly. So, the building is considered to be working from 7.00 am to 11.00 pm every day with a changing factor (figure 4.17 and 4.18). The schedule was based on one of built-in occupancy schedules in Revit software which is based on ASHRAE fundamental (Autodesk 2018).

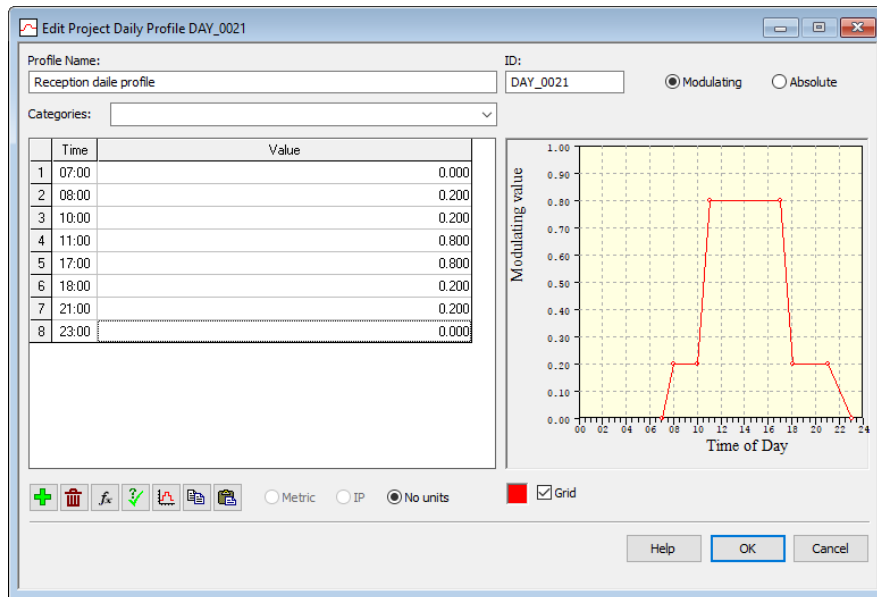


Figure 4.18. Inserted APro daily profile in IES-VE (author 2019).

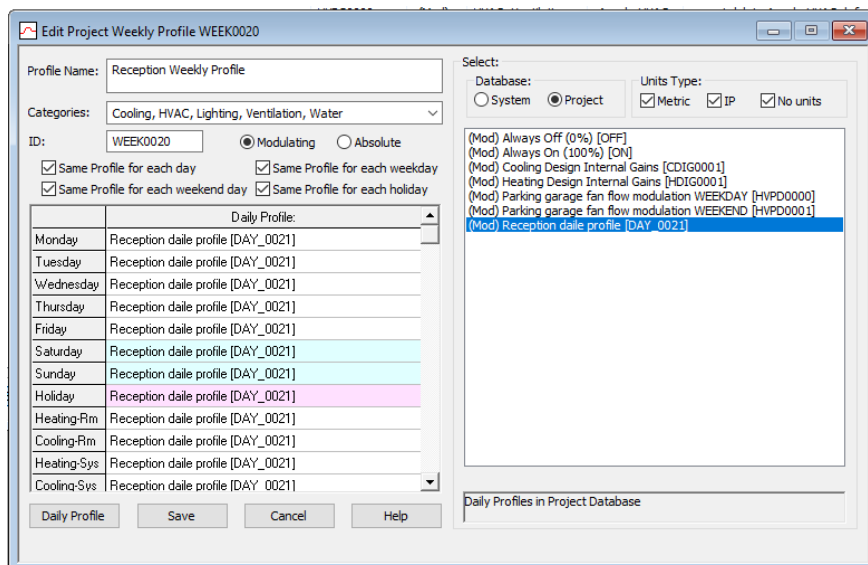


Figure 4.19. Inserted APro weekly profile in IES-VE (author 2019).

4.1.5 Thermal profile

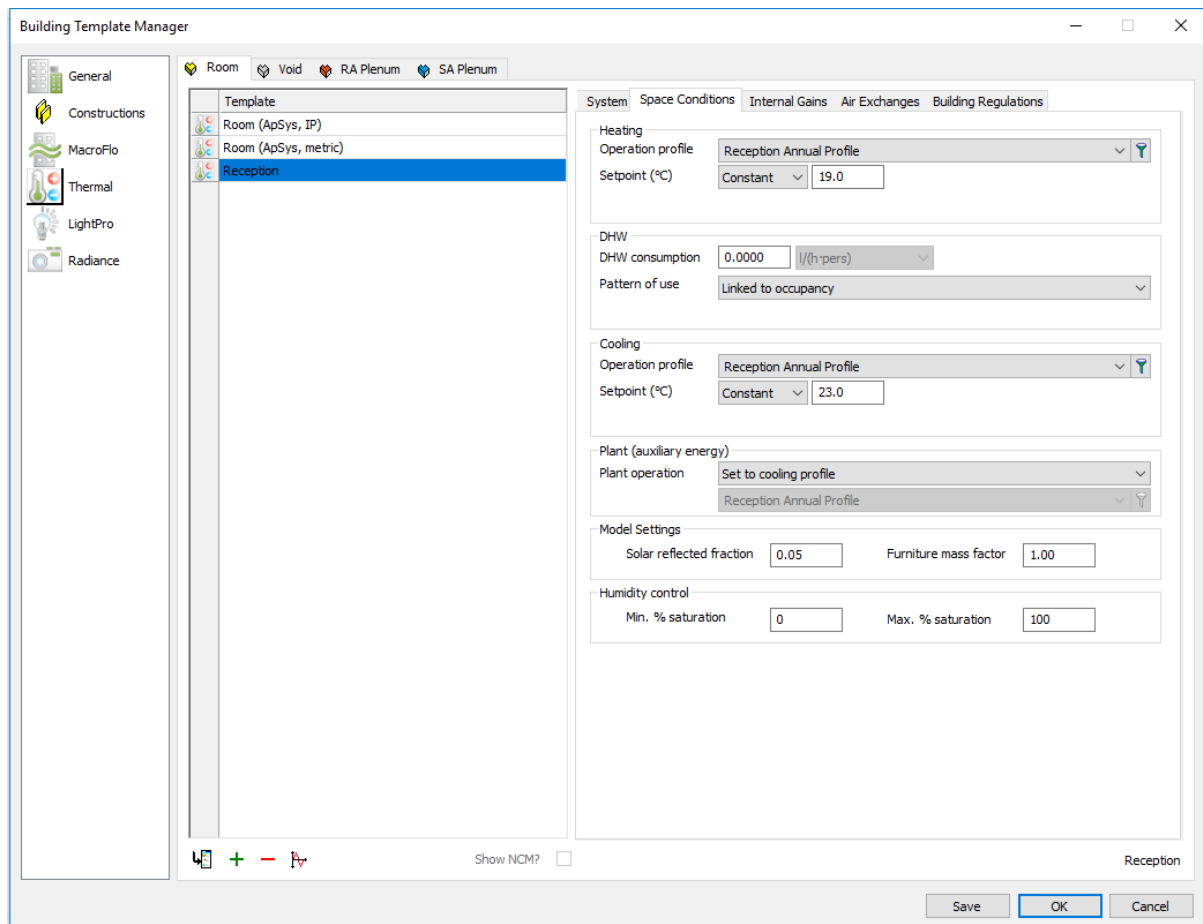


Figure 4.20. Inserted space conditions properties in IES-VE (author 2019).

The next step was the thermal profile setup (figure 4.24). It was assumed that the heating is turned off continuously while cooling and domestic hot water were following the selected occupancy profile. According to the design documents it will come from people, lighting and computers. According to ASHRAE fundamentals (2013) internal gain from computers, printers and similar equipment is 9~13 W/m² for general offices. As the usage of computers is minimal in the building, it was assumed that the heat gain from computers is 9 W/m² only. The offices area is 110 m² and the total building area is 360 m², hence the average heat gain from computers for the whole building is 2.75 W/m² (figure 4.21). According to the HVAC calculations (Hussein 2017) the average

maximum heat gain from people is 68.5 W/person, the average maximum latent gain from people is 41.43 W/person and the maximum sensible heat from light is 10W/m² (figures 4.22 and 4.23). Air exchange comes from infiltration with a maximum flow of 0.25 ach (Fawzy, A.2018,pers. Comm.,16 September) (figures 4.24 and 4.25). Eventually, the thermal profile was assigned to the rooms using the Tabular Space Data tool from Apache application in the software.

| Type | Reference |
|----------------------|----------------------|
| Fluorescent Lighting | Fluorescent Lighting |
| People | People |
| Computers | Computers |

Type:

Reference:

Diversity factor:

Maximum Sensible Gain: W/m²

Maximum Power Consumption: W/m²

Radiant Fraction:

Meter:

Variation Profile:

Allow profile to saturate for loads analysis?

Figure 4.21. Inserted computer (miscellaneous equipment) internal gain data in IES-VE (author 2019).

| Type | Reference |
|----------------------|----------------------|
| Fluorescent Lighting | Fluorescent Lighting |
| People | People |
| Computers | Computers |

Type:

Reference:

Diversity Factor:

Maximum Sensible Gain: W/m²

Maximum Power Consumption: W/m²

Radiant Fraction:

Meter:

Variation Profile:

Dimming Profile:

Ballast/driver fraction:

% of convective gain to RA plenum: %

Allow profile to saturate for loads analysis?

Figure 4.22. Inserted lighting internal gain data in IES-VE (author 2019).

| Type | Reference | |
|----------------------|----------------------|----------------------------------------------------------------------------------|
| Fluorescent Lighting | Fluorescent Lighting | <input type="button" value="Add/Edit"/> <input type="button" value="Remove"/> |
| People | People | |
| Computers | Computers | |

Type:

Reference:

Diversity Factor:

Maximum Sensible Gain: W/person

Maximum Latent Gain: W/person

Occupant Density: m²/person

Variation Profile:

Allow profile to saturate for loads analysis?

Figure 4.23. Inserted people internal gain data in IES-VE (author 2019).

System **Space Conditions** Internal Gains Air Exchanges Building Regulations

| Type | Reference | |
|--------------|--------------|----------------------------------------------------------------------------------|
| Infiltration | Infiltration | <input type="button" value="Add/Edit"/> <input type="button" value="Remove"/> |

Type:

Reference:

Variation Profile:

Adjacent Condition:

Max Flow: ach

Figure 4.24. Inserted air exchange properties in IES-VE (author 2019).

System outside air supply ('system air supply' in Vista)

Flow rate: l/(s·m²)

Variation profile:

Free cooling flow capacity: ach

Figure 4.25. Inserted OA parameters in IES-VE (author 2019).

4.1.6 Apache Sim application - dynamic simulation

Firstly, sun cast simulation was done to add the solar shading analysis to the energy model. Secondly, using the Apache Sim application the final energy simulation was done (figure 4.26). All the previous step was followed for all cases after modelling each scenario. In following scenarios, as the model has an inlet and outlet openings in the DSF, MacroFlo simulation was connected to the Apache simulation. That was not applicable for the basic model as there were not any openings in the envelope.

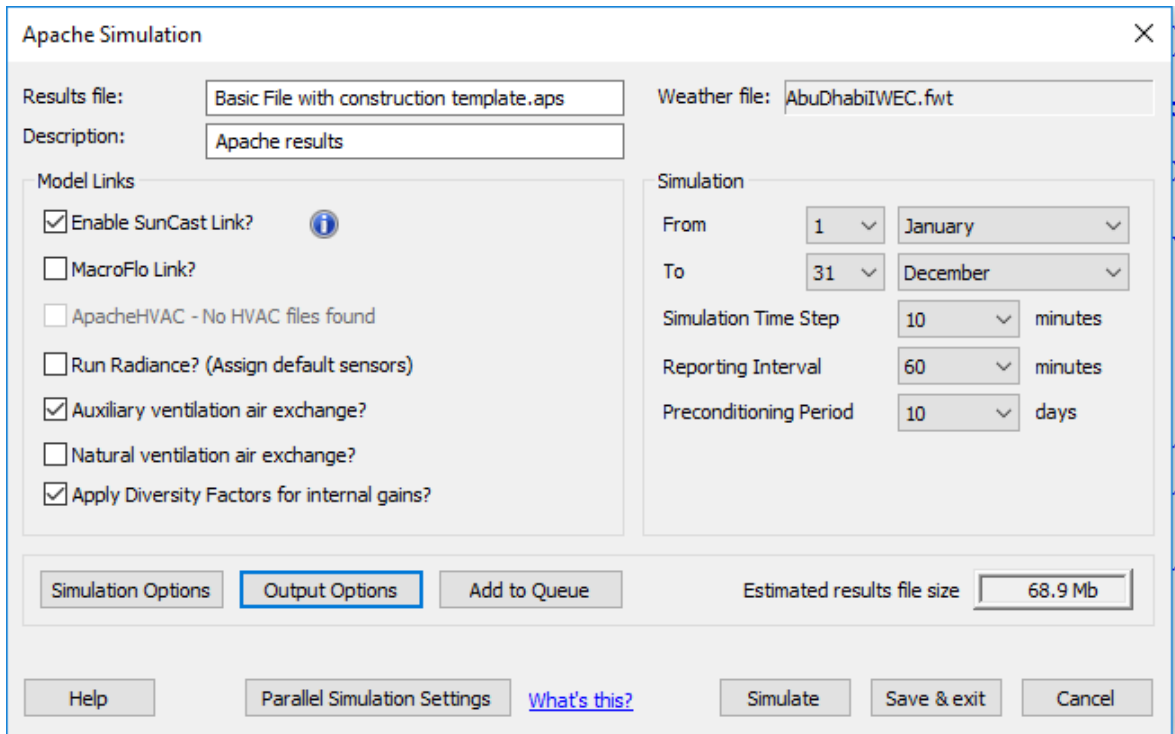


Figure 4.26. Inserted Apache Sim parameters in IES-VE (author 2019).

4.2 Buffer DSF/Corridor Facade- Scenarios-01,02 and 03: Double layers ETFE cushion modelling in IES VE

In the study conducted by Dimitriadou (2013), he concluded that even when IES VE simplifies the ETFE cushion into a flat plane, the software gave accurate results comparing to the physical experiment that he conducted. Cremers and Marx (2016) in their investigation pointed out that the simulation software TRNSYS had the same limitation and modelled the cushion as a flat surface which had a minor impact on the results. When the ETFE layers were added to the model, IES VE didn't accept a layer thickness which is less than 0.3 mm (300 μm). The available ETFE foil thickness is between 50 and 250 μm (0.05 and 0.25 mm) (Dimitriadou 2015). Cremers and Marx (2016) had the same issue in their study and concluded that thickness did not have a significant impact on the results as the cushions thermal properties depended mainly on the air gaps rather than the foil itself. The ETFE was modelled as each foil conductivity is equal to 0.2380 W/m²K (Dimitriadou & Shea 2013) with a 0.3 mm thickness. ETFE foil reflectance is 0.08 and 120mm air gap/chamber thermal resistance is 0.173 m²K/W (Dimitriadou 2015). As thermal resistance (m²K/W) is equal to thickness (m) divided by material conductivity (W/mK) , thermal resistance of the 60 mm air gap/chamber is 0.0865 m²K/W and thermal resistance of the 180 mm air gap/chamber is 0.2595 m²K/W (figures 4.27). In order to study the effect of cushion depth, three scenarios were investigated (table 4.1). ETFE foil offers 95% of visible light transmittance (Lamnatou et al. 2017). Hence, VLT of the cushion is $0.95 \times 0.95 = 0.90$ or 90% and total VLT of the system is $0.95 \times 0.95 \times 0.37 = 0.33$ or 33% (figures 4.27). According to Dimitriadou (2015) the energy used for the inflation unit is not negligible. Its annual average consumption is 0.44kWh for every square meter of ETFE cushion area. As the ETFE cushions area in the studied project is 89 m², the total inflation unit electrical consumption will be 39.16 kWh annually. It was assumed that the inflation unit consumption will be the same for all ETFE types as there is a lack of verified and detailed energy consumption information has been found. The double skin system was modelled with an inlet opening at the bottom and an outlet/exhaust opening at the top. The areas in front of the doors were kept free (figures 4.28,4.29 and 4.30). The

cushions covered 93.3% of the glazed area which is 30% of the total envelope area. The DSF cavity depth was 40 cm from the external face of the glass to the external edge of the cushion which falls in the range recommended by the Belgium Building Research Institute between 20 to 200 cm maximum (Joe et al. 2014).

Table 4.1. investigated scenarios (author 2019).

| Possible Cushions size and depth scenarios | Net U-Value (including frame) of the cushion | G-Value of the cushion | VLT of the cushion | Remarks |
|-------------------------------------------------------------|----------------------------------------------|------------------------|--------------------|----------------------------------------------------------------|
| Scenario-01: Double layer ETFE cushion with 60 mm chamber. | 3.7 W/m ² K | 0.47 | 0.90 | 60 mm air gap/chamber resistance is 0.0865 m ² K/W |
| Scenario-02: Double layer ETFE cushion with 120 mm chamber. | 2.9 W/m ² K | 0.56 | 0.90 | 120 mm air gap/chamber resistance is 0.173 m ² K/W |
| Scenario-02: Double layer ETFE cushion with 180 mm chamber. | 2.4 W/m ² K | 0.61 | 0.90 | 180 mm air gap/chamber resistance is 0.2595 m ² K/W |

| Net U-value (including frame): 3.7085 W/m ² K | | U-value (glass only): 3.8607 W/m ² K | | | | | | | | | | | |
|----------------------------------------------------------|--------------|-------------------------------------------------|--------------------|-----|--------------------------------------------|-------------------------------|---------------|---------------------|--------------------|------------------|--------------------|-------------------|-------------------------|
| Net R-value: 0.2590 m ² K/W | | g-value (EN 410): 0.4702 | | | | | | | | | | | |
| | | Visible light normal transmittance: 0.9 | | | | | | | | | | | |
| Material | Thickness mm | Conductivity W/(m·K) | Angular Dependence | Gas | Convection Coefficient W/m ² ·K | Resistance m ² K/W | Transmittance | Outside Reflectance | Inside Reflectance | Refractive Index | Outside Emissivity | Inside Emissivity | Visible Light Specified |
| [EXTW11] SMOKE SILVER | 0.3 | 0.2380 | Fresnel | - | - | 0.0013 | 0.900 | 0.080 | 0.080 | 1.526 | - | - | No |
| Cavity | 60.0 | - | - | - | - | 0.0865 | - | - | - | - | - | - | - |
| [EXTW2] CLEAR FLOAT 6MM | 0.3 | 0.2380 | Fresnel | - | - | 0.0013 | 0.090 | 0.080 | 0.080 | 1.526 | - | - | No |
| Net U-value (including frame): 2.9353 W/m ² K | | U-value (glass only): 2.8942 W/m ² K | | | | | | | | | | | |
| Net R-value: 0.3455 m ² K/W | | g-value (EN 410): 0.5615 | | | | | | | | | | | |
| | | Visible light normal transmittance: 0.9 | | | | | | | | | | | |
| Material | Thickness mm | Conductivity W/(m·K) | Angular Dependence | Gas | Convection Coefficient W/m ² ·K | Resistance m ² K/W | Transmittance | Outside Reflectance | Inside Reflectance | Refractive Index | Outside Emissivity | Inside Emissivity | Visible Light Specified |
| [EXTW11] SMOKE SILVER | 0.3 | 0.2380 | Fresnel | - | - | 0.0013 | 0.900 | 0.080 | 0.080 | 1.526 | - | - | No |
| Cavity | 120.0 | - | - | - | - | 0.1730 | - | - | - | - | - | - | - |
| [EXTW2] CLEAR FLOAT 6MM | 0.3 | 0.2380 | Fresnel | - | - | 0.0013 | 0.090 | 0.080 | 0.080 | 1.526 | - | - | No |
| Net U-value (including frame): 2.4717 W/m ² K | | U-value (glass only): 2.3147 W/m ² K | | | | | | | | | | | |
| Net R-value: 0.4320 m ² K/W | | g-value (EN 410): 0.6161 | | | | | | | | | | | |
| | | Visible light normal transmittance: 0.9 | | | | | | | | | | | |
| Material | Thickness mm | Conductivity W/(m·K) | Angular Dependence | Gas | Convection Coefficient W/m ² ·K | Resistance m ² K/W | Transmittance | Outside Reflectance | Inside Reflectance | Refractive Index | Outside Emissivity | Inside Emissivity | Visible Light Specified |
| [EXTW11] SMOKE SILVER | 0.3 | 0.2380 | Fresnel | - | - | 0.0013 | 0.900 | 0.080 | 0.080 | 1.526 | - | - | No |
| Cavity | 180.0 | - | - | - | - | 0.2595 | - | - | - | - | - | - | - |
| [EXTW2] CLEAR FLOAT 6MM | 0.3 | 0.2380 | Fresnel | - | - | 0.0013 | 0.090 | 0.080 | 0.080 | 1.526 | - | - | No |

Figure 4.27. ETFE double layers cushion layers parameters as inserted in the construction template (3 scenarios) in IES-VE (author 2019).



Figure 4.28. ETFE Cushions in IES-VE (author 2019).

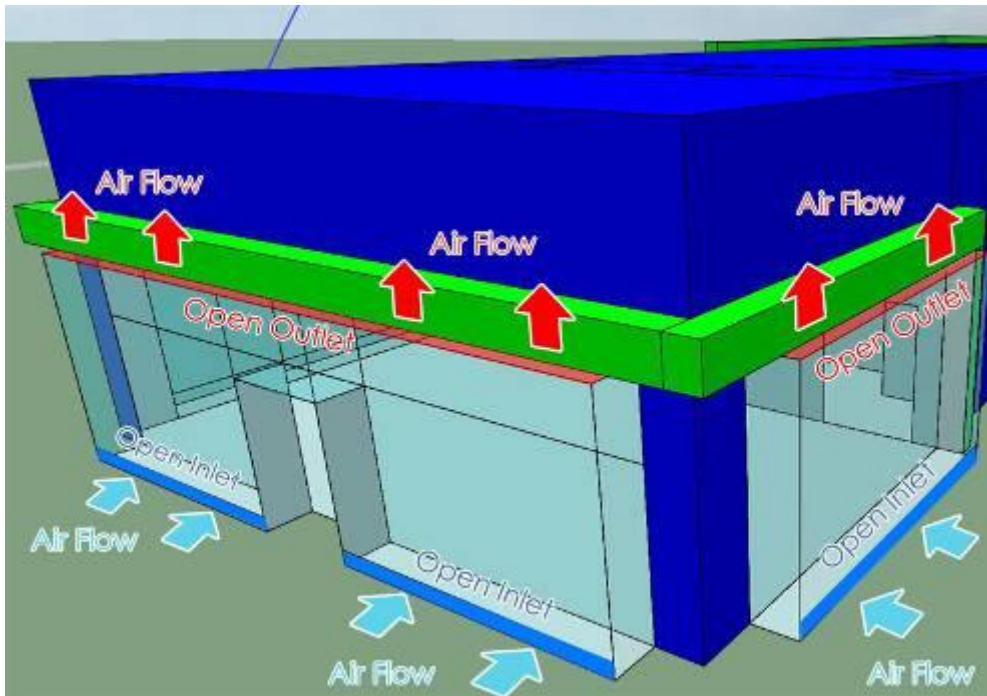


Figure 4.29. ETFE Cushions in IES-VE (author 2019).

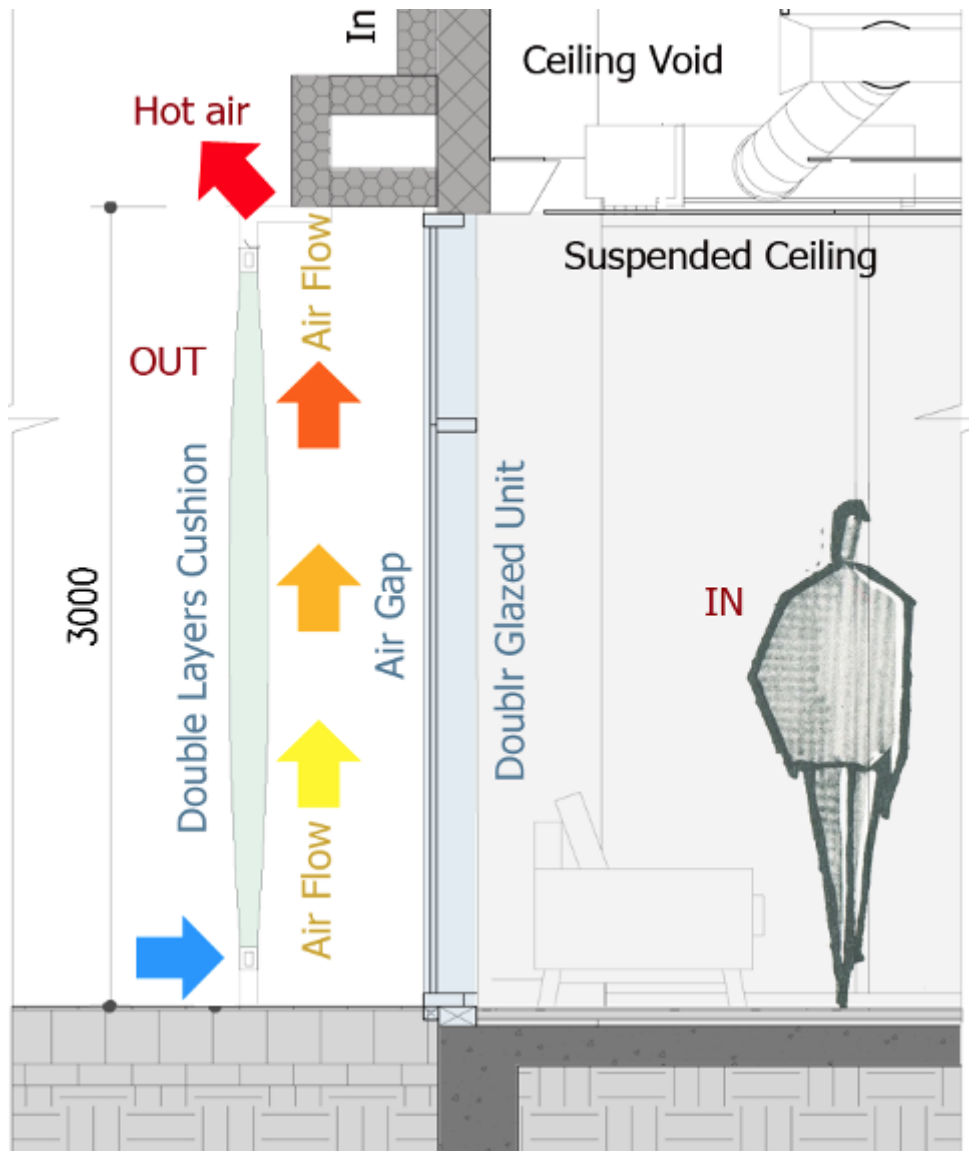


Figure 4.30. Building wall section which shows the cushion and DSF positioning (author 2019).

4.3 Buffer DSF/ Corridor Facade -Scenario 04: Triple layers ETFE cushion modelling in IES VE

As shown in the next section, the variation between the three scenarios results was minimal. In order to continue with the next scenario, the 120 mm chamber width was selected as it is an average width that can give more rigidity to the cushion and it is more common (table 4.2). Thus, the triple layer cushion scenario had 120 mm chambers width. Due to software limitation, quadrable layers could not be tested. The software could not create the required number of layers. VLT of the triple layer cushion is $0.95 \times 0.95 \times 0.95 = 0.85$ or 85% and total VLT of the system (DGU and the triple layers cushion) is $0.85 \times 0.37 = 0.31$ or 31% (figures 4.31 and 4.32).

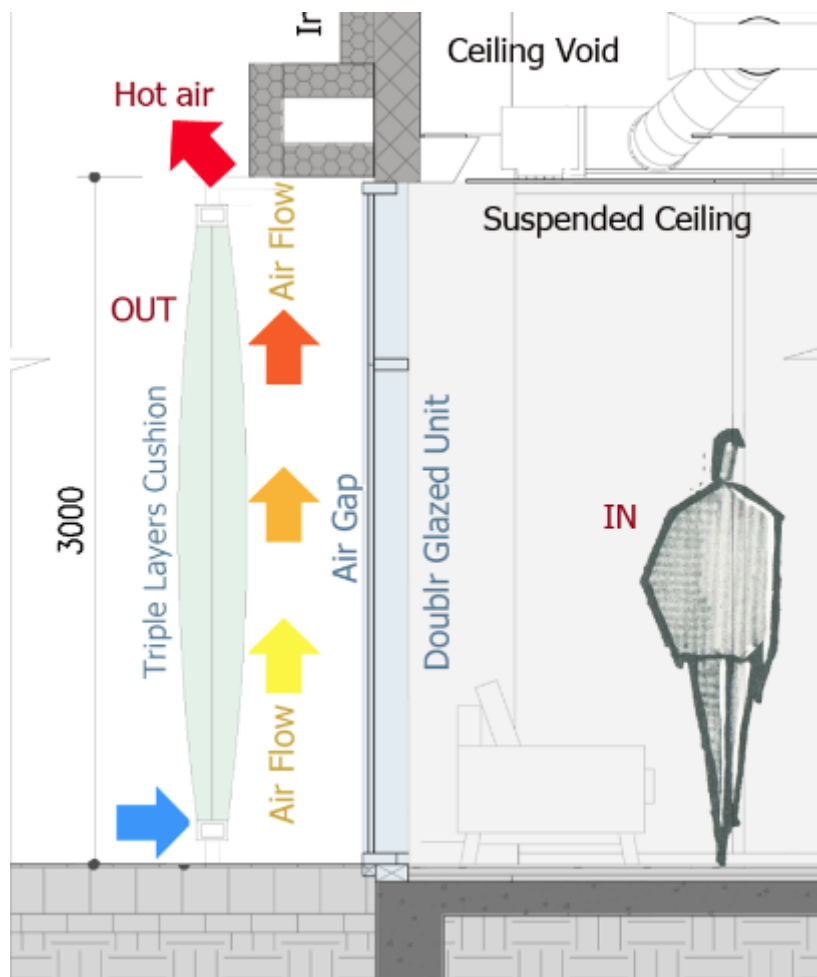


Figure 4.31. Building wall section which shows the cushion positioning (author 2019)

Table 4.2. investigated scenario (author 2019).

| Possible Cushions size and depth scenarios | Net U-Value (including frame) of the cushion | G-Value of the cushion | VLT of the cushion | Remarks |
|--------------------------------------------------------------|----------------------------------------------|------------------------|--------------------|---------------------------------------------------------------|
| Scenario-04: Triple layer ETFE cushion with 120 mm chambers. | 2.1589 W/m ² K | 0.7650 | 0.85 | 120 mm air gap/chamber resistance is 0.173 m ² K/W |

| Net U-value (including frame): <input type="text" value="2.1589"/> W/m ² K | | U-value (glass only): <input type="text" value="1.9237"/> W/m ² K | | | | | | | | | | | |
|---------------------------------------------------------------------------------------|--------------|------------------------------------------------------------------------------|--------------------|-----|-------------------------------------------|-------------------------------|---------------|---------------------|--------------------|------------------|--------------------|-------------------|-------------------------|
| Net R-value: <input type="text" value="0.5198"/> m ² K/W | | g-value (EN 410): <input type="text" value="0.7650"/> | | | | | | | | | | | |
| Visible light normal transmittance: <input type="text" value="0.85"/> | | | | | | | | | | | | | |
| Material | Thickness mm | Conductivity W/(m·K) | Angular Dependence | Gas | Convection Coefficient W/m ² K | Resistance m ² K/W | Transmittance | Outside Reflectance | Inside Reflectance | Refractive Index | Outside Emissivity | Inside Emissivity | Visible Light Specified |
| [EXTW21] ETFE Foil | 0.3 | 0.2300 | Constant | - | - | 0.0013 | 0.900 | 0.080 | 0.080 | - | - | - | No |
| Cavity | 120.0 | - | - | - | - | 0.1730 | - | - | - | - | - | - | - |
| [EXTW2] ETFE Foil | 0.3 | 0.2380 | Constant | - | - | 0.0013 | 0.900 | 0.080 | 0.080 | - | - | - | No |
| Cavity | 120.0 | - | - | - | - | 0.1730 | - | - | - | - | - | - | - |
| [EXTW2] ETFE Foil | 0.3 | 0.2380 | Constant | - | - | 0.0013 | 0.900 | 0.080 | 0.080 | - | - | - | No |

Figure 4.32. ETFE triple layers cushion as inserted in the construction template in IES-VE (author 2019).

4.4 Buffer DSF/ Corridor Facade -Scenarios 05 and 06: Triple layer ETFE cushion with two different frit pattern types modelling in IES VE

In the study conducted by Wilson and Elstner (2018) they concluded that RAL 9010 white full coating frit pattern has VLT of 0.320, external and internal reflectance of 0.623 (table 4.3). The researchers used a device called integrating sphere that provides sensitive recording for direct and sensitive radiation which reflects or travel through the frit pattern. Although there is a variety of frit patterns colours, parameters and arrangements (figure 4.33), the white colour was selected for the study as it matches the building external finishes and it suits Abu Dhabi weather conditions which requires a highly reflective light external colour. Scenario 05 included triple layers ETFE cushion with 30% coverage frit pattern and scenario 06 included triple layers ETFE cushion with 60% coverage frit pattern (table 4.4).

Table 4.3. Frit pattern parameters (Wilson & Elstner 2018).

T = transmittance (= τ in EN 410), R' = reflectance (from the screen-printed side), nh = normal-hemispherical, L = light, e = (solar) energy. Only the first two digits after the decimal point are significant. The third digit is used only to indicate very small differences.

| Screen-Printing Colour | T _{nh,L} [-] | T _{nh,e} [-] | R _{nh,L} [-] | R _{nh,e} [-] | R' _{nh,L} [-] | R' _{nh,e} [-] |
|------------------------|--------------------------|--------------------------|--------------------------|--------------------------|---------------------------|---------------------------|
| White | 0.320 | 0.337 | 0.572 | 0.479 | 0.623 | 0.523 |

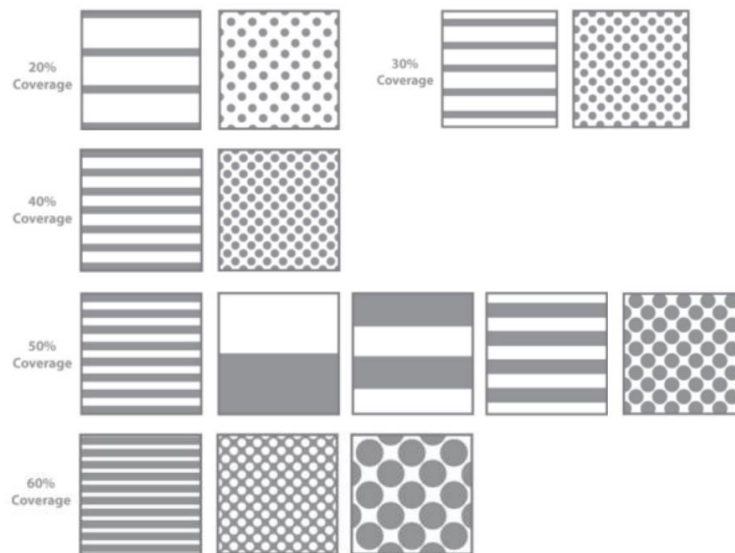


Figure 4.33. Various frit patterns with their coverage ratio (O'Donnell 2015)

Table 4.4. investigated scenario (author 2019).

| Possible Cushions size and depth scenarios | Net U-Value (including frame) of the cushion | G-Value of the cushion | Average reflectance of the middle-fritted layer | Average VLT of the middle-fritted layer | VLT of the cushion | Remarks |
|--------------------------------------------------------------------------------------------------|----------------------------------------------|------------------------|-------------------------------------------------|-----------------------------------------|--------------------|---------------------------------------------------------------|
| Scenario-05: Triple layer ETFE cushion with 30% coverage white frit pattern on the middle layer. | 2.16 W/m ² K | 0.6499 | (0.3x0.623) + (0.7x0.08) = 0.2429 | (0.3x0.320) + (0.7x0.95) = 0.76 | 0.69 | 120 mm air gap/chamber resistance is 0.173 m ² K/W |
| Scenario-06: Triple layer ETFE cushion with 60% coverage white frit pattern on the middle layer. | 2.16 W/m ² K | 0.4815 | (0.6x0.623) + (0.4x0.08) = 0.4058 | (0.6x0.320) + (0.4x0.95) = 0.57 | 0.52 | 120 mm air gap/chamber resistance is 0.173 m ² K/W |

The pattern was modelled on the middle layer. Scenario 05 total VLT of the system (DGU and the triple layers cushion) is $0.69 \times 0.37 = 0.255$ or 25.5%. Scenario 06 total VLT of the system (DGU and the triple layers cushion) is $0.52 \times 0.37 = 0.19$ or 19% (figure 4.34 and 4.35).

| Net U-value (including frame): | | 2.1589 | W/m ² ·K | U-value (glass only): | | 1.9237 | W/m ² ·K | | | | | | |
|--------------------------------|--------------|----------------------|---------------------|-----------------------|--------------------------------------------|--------------------------------|---------------------|------------------------------------------|--------------------|------------------|--------------------|-------------------|-------------------------|
| Net R-value: | | 0.5198 | m ² ·K/W | g-value (EN 410): | | 0.6499 | | Visible light normal transmittance: 0.69 | | | | | |
| Material | Thickness mm | Conductivity W/(m·K) | Angular Dependence | Gas | Convection Coefficient W/m ² ·K | Resistance m ² ·K/W | Transmittance | Outside Reflectance | Inside Reflectance | Refractive Index | Outside Emissivity | Inside Emissivity | Visible Light Specified |
| [EXTW211] ETFE Foil | 0.3 | 0.2300 | Constant | - | - | 0.0013 | 0.900 | 0.080 | 0.080 | - | - | - | No |
| Cavity | 120.0 | - | - | - | - | 0.1730 | - | - | - | - | - | - | - |
| [EXTW231] ETFE Foil | 0.3 | 0.2380 | Constant | - | - | 0.0013 | 0.750 | 0.243 | 0.243 | - | - | - | No |
| Cavity | 120.0 | - | - | - | - | 0.1730 | - | - | - | - | - | - | - |
| [EXTW24] ETFE Foil | 0.3 | 0.2380 | Constant | - | - | 0.0013 | 0.900 | 0.080 | 0.080 | - | - | - | No |
| Net U-value (including frame): | | 2.1589 | W/m ² ·K | U-value (glass only): | | 1.9237 | W/m ² ·K | | | | | | |
| Net R-value: | | 0.5198 | m ² ·K/W | g-value (EN 410): | | 0.4815 | | Visible light normal transmittance: 0.52 | | | | | |
| Material | Thickness mm | Conductivity W/(m·K) | Angular Dependence | Gas | Convection Coefficient W/m ² ·K | Resistance m ² ·K/W | Transmittance | Outside Reflectance | Inside Reflectance | Refractive Index | Outside Emissivity | Inside Emissivity | Visible Light Specified |
| [EXTW211] ETFE Foil | 0.3 | 0.2300 | Constant | - | - | 0.0013 | 0.900 | 0.080 | 0.080 | - | - | - | No |
| Cavity | 120.0 | - | - | - | - | 0.1730 | - | - | - | - | - | - | - |
| [EXTW23] ETFE Foil | 0.3 | 0.2380 | Constant | - | - | 0.0013 | 0.500 | 0.406 | 0.406 | - | - | - | No |
| Cavity | 120.0 | - | - | - | - | 0.1730 | - | - | - | - | - | - | - |
| [EXTW24] ETFE Foil | 0.3 | 0.2380 | Constant | - | - | 0.0013 | 0.900 | 0.080 | 0.080 | - | - | - | No |

Figure 4.34. ETFE triple layers cushion as inserted in the construction template. Scenario05 on the top and scenario 06 on the bottom (author 2019).

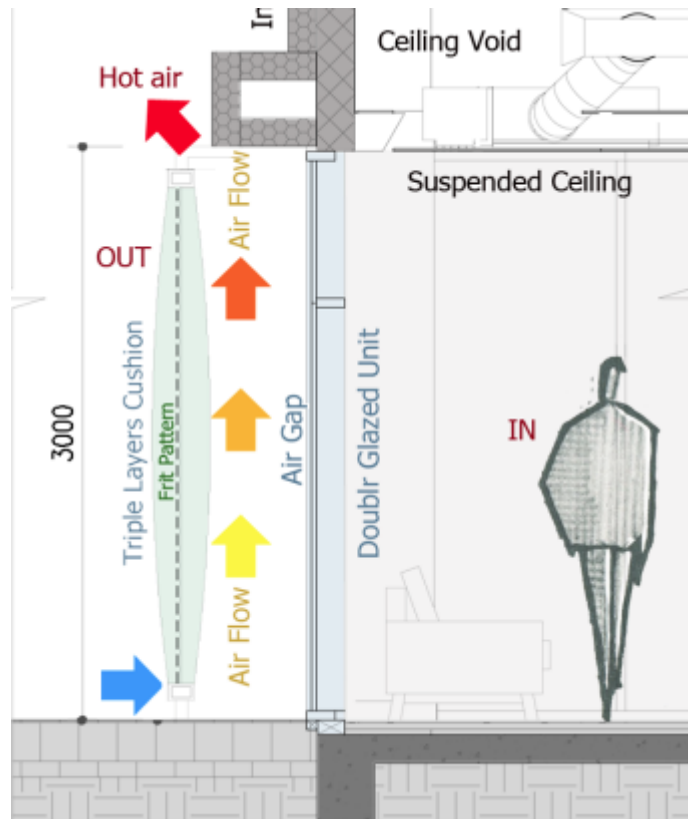


Figure 4.35. Building wall section which shows the cushion positioning (by the author).

4.5 Buffer DSF/ Corridor Facade -Scenarios 07 and 08: BIPVs on the front layer of the cushion

In scenario 07, thin-film amorphous silicon solar cells type (a-Si) was selected as it is a popular type used for exterior architectural application due to its thickness and visual look (figure 4.36). Also, it was used in previous studies on ETFE cushions due to its light weight and flexibility. Hu et al. (2015) concluded that the hottest layer in the cushion was the middle layer. Hence, in these scenarios, the PV panels were located on the external layer of the cushion. Due to the curvature of the cushion the panels, which is located at the top of the cushions were slightly tilted towards the sky by almost 5 degrees. Due to the software limitation, the PV panels could not be curved. To imitate the curvature of the PV panel, the object was titled 5 degrees vertically which had a minimal variation as a shape comparing to the curved PV. The PV type was selected, and the parameters followed the software standard for this type. The height of each panel is 1 m and they cover the top one third of each cushion (figure 4.38). In scenario 08 thin-film cadmium-telluride solar cells type was used due its high efficiency (figure 4.37). The PVs where located on the eastern and western cushions only (figures 4.39 and 4.40). The two scenarios, the BIPVs were added to scenario 06 situation. In both scenarios, the software provided the default parameters for each type such as module nominal efficiency, electrical conversion efficiency, temperature coefficient for module efficiency, etc (figures 4.36 and 4.37).

| Show: All PV Types | | | | | | | | | | | |
|-------------------------------------|-------------|----------|---------|-------------------|---------------------------|-------------------------------------|---------------------------------------------------|-----------------------------------------------------|--------------------|----------------------------------|---------------------------------|
| <input checked="" type="checkbox"/> | Description | Default? | In Use? | Technology | Module Nominal Efficiency | Nominal Cell Temperature (NOCT) (°) | Reference Irradiance for NOCT (W/m ²) | Temperature Coefficient for Module Efficiency (1/K) | Degradation Factor | Electrical Conversion Efficiency | Meter |
| <input checked="" type="checkbox"/> | PV Type | ✓ | Y | Amorphous Silicon | 0.0500 | 50.0 | 800 | 0.0011 | 0.9900 | 0.8500 | Grid Displaced Electricity: ... |

Figure 4.36. Scenario 07 PV panel type in IES-VE (author 2019).

| Show: All PV Types | | | | | | | | | | | |
|-------------------------------------|-------------|----------|---------|-----------------------------|---------------------------|-------------------------------------|---------------------------------------------------|-----------------------------------------------------|--------------------|----------------------------------|---------------------------------|
| <input checked="" type="checkbox"/> | Description | Default? | In Use? | Technology | Module Nominal Efficiency | Nominal Cell Temperature (NOCT) (°) | Reference Irradiance for NOCT (W/m ²) | Temperature Coefficient for Module Efficiency (1/K) | Degradation Factor | Electrical Conversion Efficiency | Meter |
| <input checked="" type="checkbox"/> | PV Type | ✓ | Y | Thin Film Cadmium-Telluride | 0.1300 | 45.0 | 800 | 0.0040 | 0.9900 | 0.8500 | Grid Displaced Electricity: ... |

Figure 4.37. Scenario 08 PV panel type in IES-VE (author 2019).

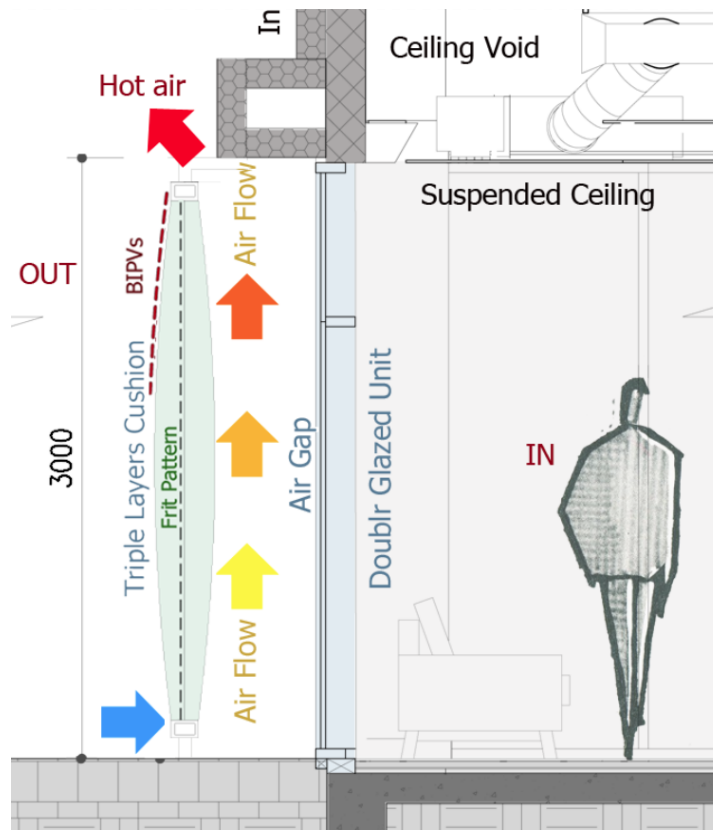


Figure 4.38. Building wall section which shows the cushion positioning (author 2019).



Figure 4.39. BIPVs as modelled on the eastern façade cushions in IES-VE (by the author).



Figure 4.40. BIPVs as modelled on the western façade cushions in IES-VE (author 2019).

4.6 Buffer DSF/ Corridor Facade -Scenario 09: Dynamic opaque ETFE foil shade

In this scenario, the BIPVs were replaced with dynamic opaque shade (figure 4.43). In IES VE dynamic shade is added to the window/cushion parameters with an operation profile. In this profile 100% means that the shade is fully lowered/closed and 0% means that the shade is fully raised/open. The northern windows/cushions will not have any shade. The eastern shade operation was gradually changing from 6 am when the shades were fully closed to 12 pm when the shades were fully open (figure 4.41). The western shade operation was gradually changing from 12 pm when the shades were fully open to 6 pm when the shades were fully closed (figure 4.42). The fixed operation profile method was used as the responsive operation method gave error in the Apache application which failed to run the simulation. Due to the light weight of the ETFE foil, the power which was consumed by the operation motor/actuator was negligible (Haddad, D.2018, pers. Comm.,3 December). In the following figures the shade devices parameters are shown along with the operation profile.

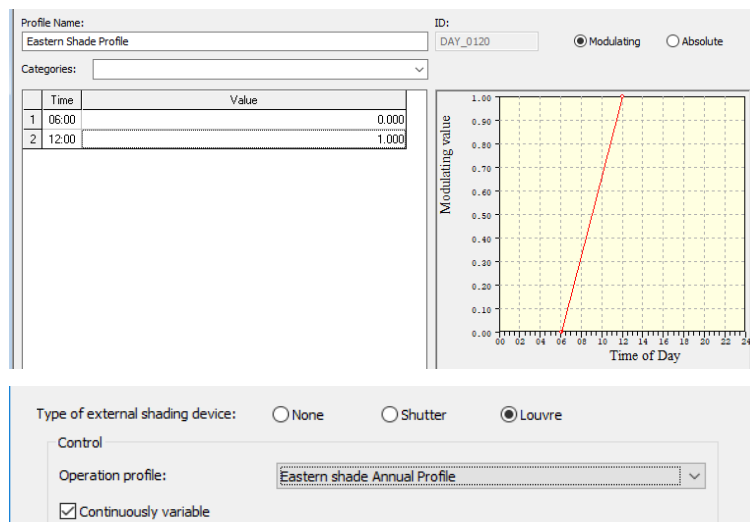


Figure 4.41. Eastern shade operation profile in IES-VE (author 2019).

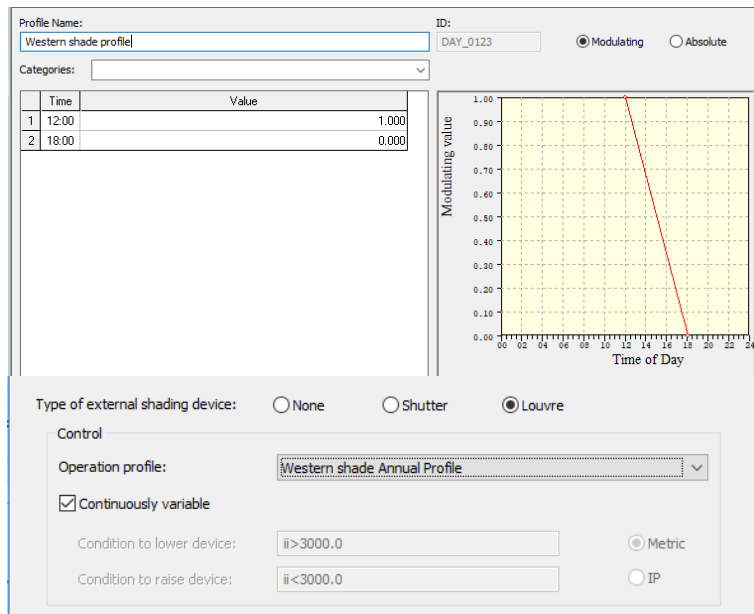


Figure 4.42. Western shade operation profile in IES-VE (author 2019).

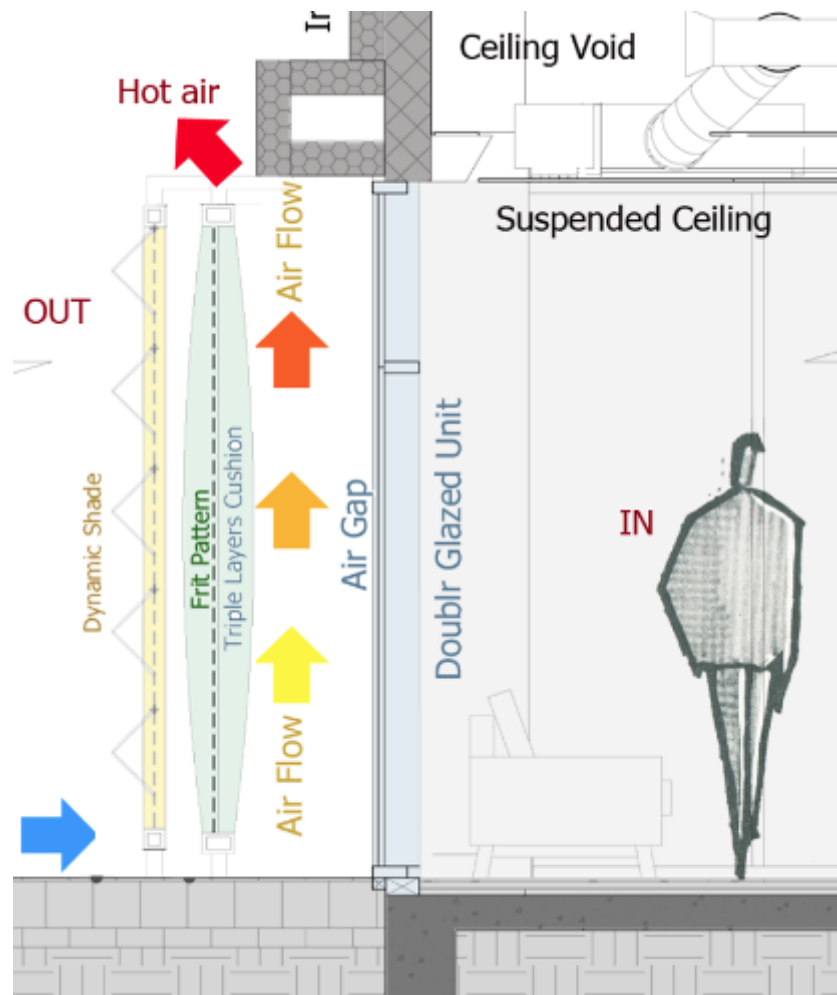


Figure 4.43. Building wall section which shows the cushion positioning (author 2019).

4.7 Buffer DSF/Corridor Façade- Scenario 10: Dynamic opaque ETFE foil shade with BIPVs

In this scenario, the BIPVs were added to the model along with the dynamic opaque shade. As scenario 08 was more efficient comparing to scenario 07, thin-film cadmium-telluride solar cells type was used in this scenario.

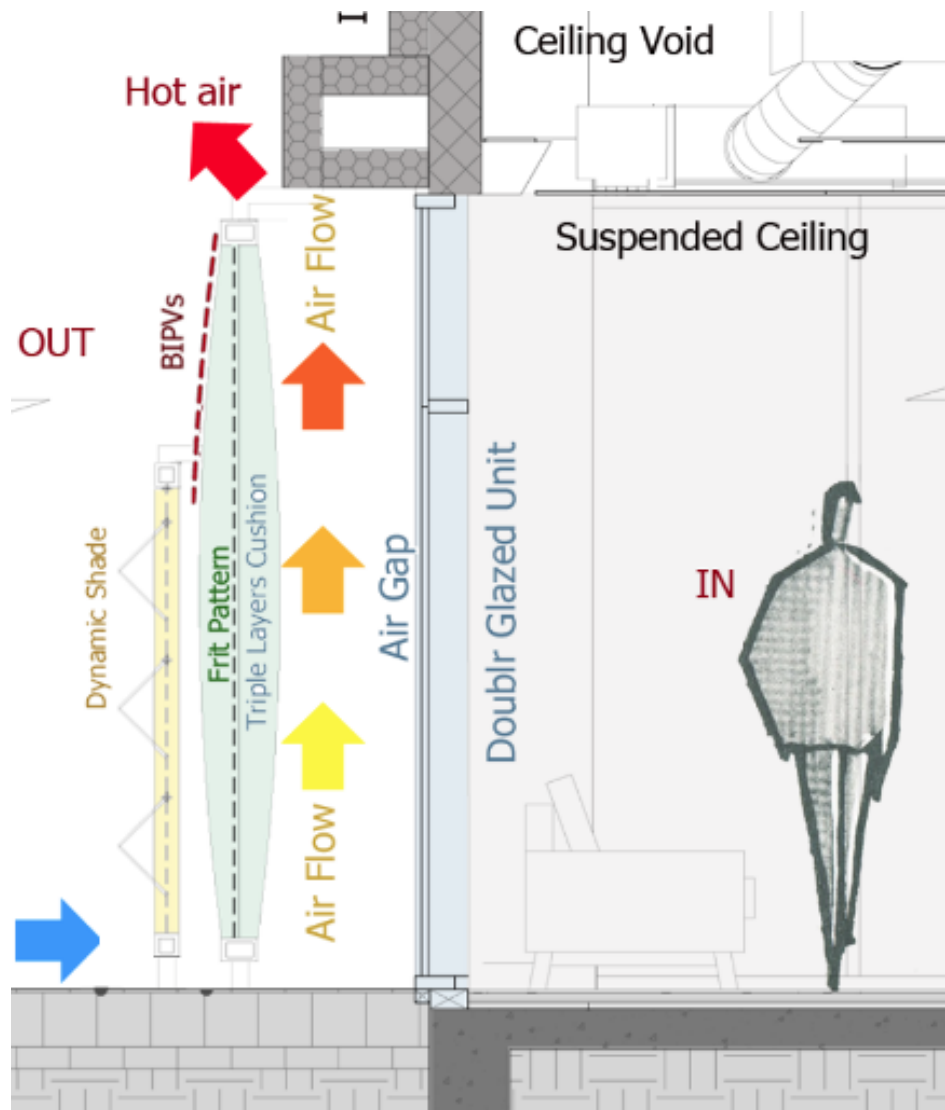


Figure 4.44. Building wall section which shows the cushion positioning (author 2019).

CHAPTER 05
RESULTS AND FINDINGS

5 Results and Findings.

5.1 Basic Model

5.1.1 Basic model thermal comfort results

Table 5.1. Comfort index results (author 2019).

| Var. Name | Location | Filename | Type | Mean |
|---------------|-----------------|-----------------|---------------|------|
| Comfort index | Mechanical room | Basic Model.aps | Comfort index | 9 |
| Comfort index | Office 01 | Basic Model.aps | Comfort index | 9 |
| Comfort index | Office 02 | Basic Model.aps | Comfort index | 9 |
| Comfort index | Store 01 | Basic Model.aps | Comfort index | 9 |
| Comfort index | Lobby 01 | Basic Model.aps | Comfort index | 9 |
| Comfort index | Waiting room | Basic Model.aps | Comfort index | 10 |
| Comfort index | Lobby 02 | Basic Model.aps | Comfort index | 9 |
| Comfort index | Toilet | Basic Model.aps | Comfort index | 9 |
| Comfort index | Store 02 | Basic Model.aps | Comfort index | 10 |
| Comfort index | Reception | Basic Model.aps | Comfort index | 10 |

IES VE uses comfort index, which is similar to the PMV method, to predict the occupant thermal comfort within each room. It ranges from 1 which indicates a very cold situation to 15 which indicates a non-sedentary situation (IES VE 2018). The project mean comfort index varied from 9 (slightly warm/acceptable) to 10 (warm/acceptable) (table 5.1). Although there are only two rooms with windows which will be directly affected by the proposed DSF, considering all rooms for the simulation is necessary to study realistic boundary conditions.

Table 5.2. Mean room temperature (author 2019).

| Var. Name | Location | Filename | Type | Mean |
|-----------------|-----------------|-----------------|------------------|-------|
| Air temperature | Mechanical room | Basic Model.aps | Temperature (°C) | 24.89 |
| Air temperature | Office 01 | Basic Model.aps | Temperature (°C) | 24.62 |
| Air temperature | Office 02 | Basic Model.aps | Temperature (°C) | 24.66 |
| Air temperature | Store 01 | Basic Model.aps | Temperature (°C) | 24.52 |
| Air temperature | Lobby 01 | Basic Model.aps | Temperature (°C) | 24.62 |
| Air temperature | Waiting room | Basic Model.aps | Temperature (°C) | 25.51 |
| Air temperature | Lobby 02 | Basic Model.aps | Temperature (°C) | 25.13 |
| Air temperature | Toilet | Basic Model.aps | Temperature (°C) | 24.94 |
| Air temperature | Store 02 | Basic Model.aps | Temperature (°C) | 25.16 |
| Air temperature | Reception | Basic Model.aps | Temperature (°C) | 26.15 |

Mean room air temperature varied from 25.13 °C in lobby 02 to 26.15 °C in the reception room (table 5.2). Although the AC set-point was 23.00 °C , the rooms temperature was affected by the glazing size.

Table 5.3. People dissatisfied index results (author 2019).

| Var. Name | Location | Filename | Type | Mean |
|---------------------|-----------------|-----------------|----------------|-------|
| People dissatisfied | Mechanical room | Basic Model.aps | Percentage (%) | 29.95 |
| People dissatisfied | Office 01 | Basic Model.aps | Percentage (%) | 26.55 |
| People dissatisfied | Office 02 | Basic Model.aps | Percentage (%) | 26.71 |
| People dissatisfied | Store 01 | Basic Model.aps | Percentage (%) | 26.24 |
| People dissatisfied | Lobby 01 | Basic Model.aps | Percentage (%) | 27.70 |
| People dissatisfied | Waiting room | Basic Model.aps | Percentage (%) | 37.07 |
| People dissatisfied | Lobby 02 | Basic Model.aps | Percentage (%) | 33.21 |
| People dissatisfied | Toilet | Basic Model.aps | Percentage (%) | 29.74 |
| People dissatisfied | Store 02 | Basic Model.aps | Percentage (%) | 32.37 |
| People dissatisfied | Reception | Basic Model.aps | Percentage (%) | 43.40 |

IES VE uses people dissatisfaction index, which is similar to the PDD method, to predict the percentage of users that would express dissatisfaction with thermal conditions in each room (IES VE 2018). The project mean comfort index varied from 26.24% in store 01 to 43.40% in Reception room (table 5.3).

5.1.2 Basic model day light analysis

The simulation was done for four days which were the solstice and equinox days. On summer solstice, which is on June 20th ~ 21st, the earth has the longest day time in the year and receives the most sunlight and on winter solstice, which is on December 21st, the earth has the shortest day time in the year and receives the least sunlight. On equinox days which happens on March 21st and September 22th ~23rd night-time and day-time are almost the same for the whole earth. Moreover, as the four days are the reference for different seasons, they were chosen for the analysis. The analysis was done at 09:00 ,12:00 and 15:00 to represent morning, noon and afternoon conditions. The analysis was done only for the two rooms affected by the daylight which were the reception room and the waiting room. The daylight factor and daylight lux levels were simulated using FlucsDL application in IES VE under over-cast sky conditions. The adequate illuminance levels in the building are 300~400 lux in the reception, waiting and other services rooms and 500 lux for the interview/offices rooms following the CIBSE standards and client requirements (Aledavood,A.2018,pers. Comm.,19 September).

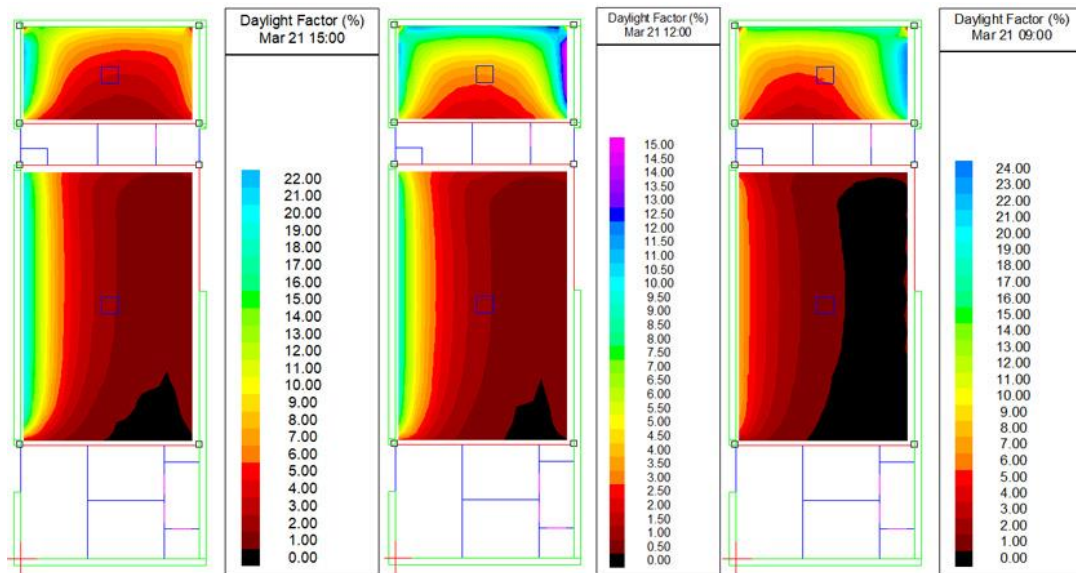


Figure 5.1. Daylight factor simulation results on the 21st of March (author 2019).

Table 5.4. 21st of March results summery (author 2019).

| Room | Date | Hour | Daylight factor | | | Daylight illuminance | | | Uniformity |
|----------------|---------------------------|-------|-----------------|-------|-------|----------------------|-----------|------------|------------|
| | | | Min. | Ave. | Max. | Min. | Ave. | Max. | |
| Waiting room | 21 st of March | 9:00 | 0.5% | 2.1% | 7.7% | 34.6 lux | 156.3 lux | 585.8 lux | 0.22 |
| Reception room | 21 st of March | 9:00 | 2.7% | 10.3% | 24.4% | 204.37 lux | 781.8 lux | 1850.2 lux | 0.26 |
| Waiting room | 21 st of March | 12:00 | 0.4% | 2.1% | 9.4% | 32.3 lux | 181.0 lux | 825.6 lux | 0.18 |
| Reception room | 21 st of March | 12:00 | 1.8% | 6.2% | 15.2% | 164.5 lux | 543.4 lux | 1343.3 lux | 0.30 |
| Waiting room | 21 st of March | 15:00 | 0.6% | 4.4% | 20.6% | 47.4 lux | 370.5 lux | 1719.4 lux | 0.13 |
| Reception room | 21 st of March | 15:00 | 2.1% | 7.2% | 22.1% | 177.1 lux | 592.4 lux | 1841.7 lux | 0.3 |

The results showed that the average daylighting levels in the waiting room are lower than the requirements in first two cases and the daylighting levels in the reception room are exceeding the requirement in the first two cases and within range in the third case. Average DF was within the acceptable range of spaces with supporting artificial light. In all cases daylighting levels and DF were low in half of the waiting room (figure 5.1 and table 5.4).

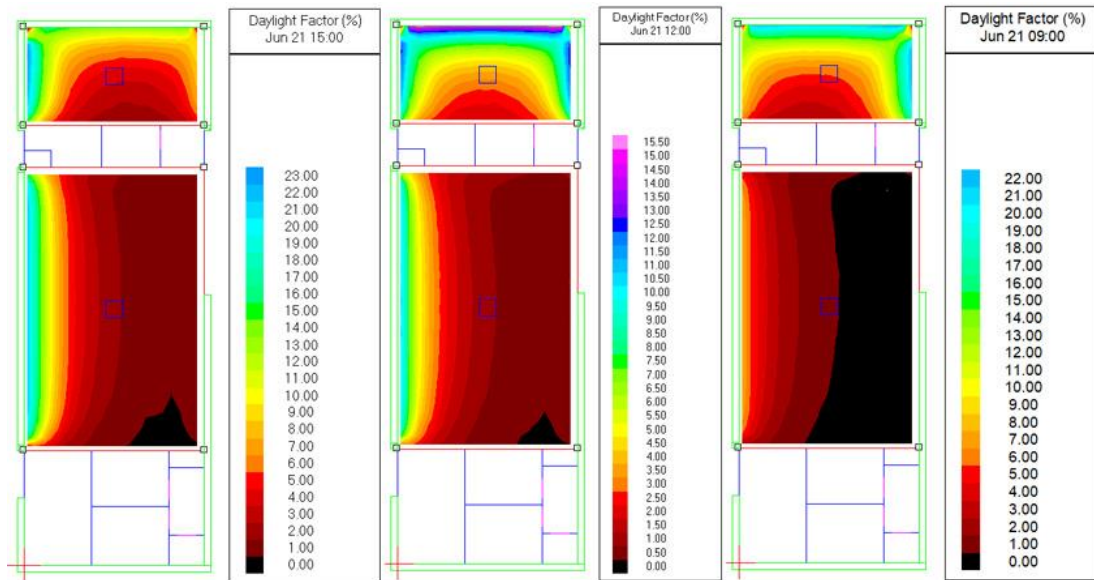


Figure 5.2. Daylight factor simulation results on the 21st of June (author 2019).

Table 5.5 21st of June results summery (author 2019).

| Room | Date | Hour | Daylight factor | | | Daylight illuminance | | | Uniformity |
|----------------|--------------------------|-------|-----------------|-------|-------|----------------------|------------|-------------|------------|
| | | | Min. | Ave. | Max. | Min. | Ave. | Max. | |
| Waiting room | 21 st of June | 9:00 | 0.4% | 1.9% | 7.7% | 33.3 lux | 158.2 lux | 636.3 lux | 0.21 |
| Reception room | 21 st of June | 9:00 | 2.0% | 10.5% | 22.8% | 163.8 lux | 866.8 lux | 1882.1 lux | 0.19 |
| Waiting room | 21 st of June | 12:00 | 0.4% | 2.2% | 10.5% | 74.6 lux | 408.0 lux | 1961.70 lux | 0.18 |
| Reception room | 21 st of June | 12:00 | 1.5% | 6.8% | 15.7% | 274.10 lux | 1259.9 lux | 2925.8 lux | 0.22 |
| Waiting room | 21 st of June | 15:00 | 0.7% | 4.7% | 21.7% | 56.6 lux | 398.6 lux | 1857.4 lux | 0.14 |
| Reception room | 21 st of June | 15:00 | 1.7% | 8.0% | 23.1% | 142.23 lux | 687.87 lux | 1980.0 lux | 0.21 |

The results were similar to the 12st of March results with minimal variation, except for the second case where average lux levels were almost doubled. There were minimal variations in the DF levels. In the first case, in the waiting room, average DF was slightly lower than recommended level (figure 5.2 and table 5.5).

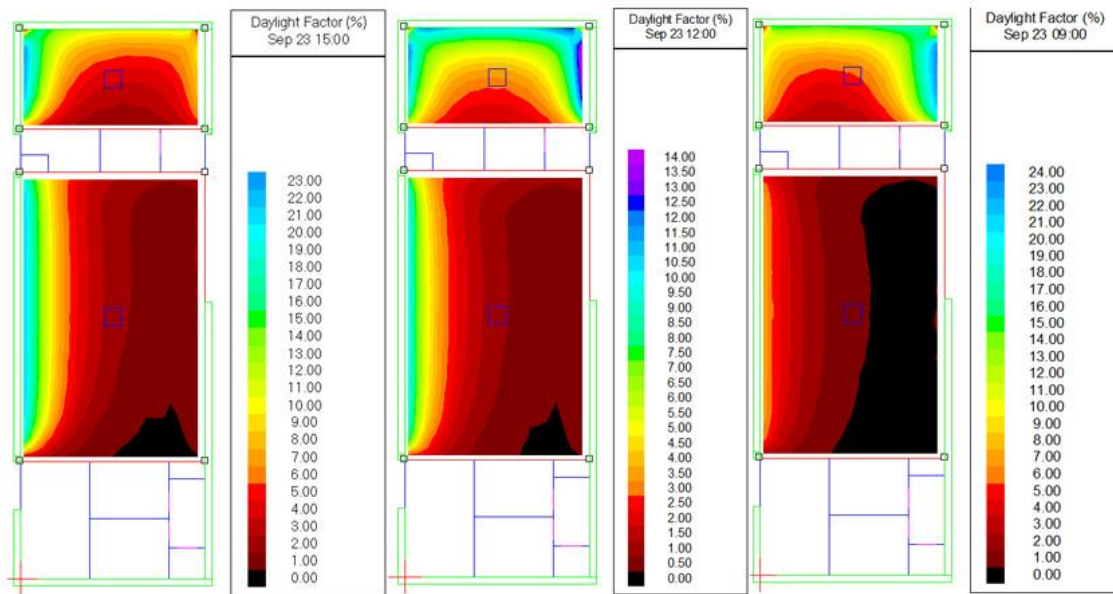


Figure 5.3. Daylight factor simulation results on the 23rd of September (author 2019).

Table 5.6. 23rd of September results summary (author 2019).

| Room | Date | Hour | Daylight factor | | | Daylight illuminance | | | Uniformity |
|----------------|---------------------------|-------|-----------------|-------|-------|----------------------|-----------|-------------|------------|
| | | | Min. | Ave. | Max. | Min. | Ave. | Max. | |
| Waiting room | 23 rd of Sept. | 9:00 | 0.4% | 1.9% | 7.5% | 34.8 lux | 156.8 lux | 605.6 lux | 0.22 |
| Reception room | 23 rd of Sept. | 9:00 | 2.4% | 10.2% | 23.7% | 189.9 lux | 819.7 lux | 1904.7 lux | 0.23 |
| Waiting room | 23 rd of Sept. | 12:00 | 0.4% | 2.1% | 10.0% | 39.05 lux | 220 lux | 1035.8 lux | 0.18 |
| Reception room | 23 rd of Sept. | 12:00 | 1.6% | 6.4% | 13.9% | 169.0 lux | 656.9 lux | 1442.40 lux | 0.26 |
| Waiting room | 23 rd of Sept. | 15:00 | 0.6% | 4.7% | 21.7% | 52.7 lux | 397.6 lux | 1839.1 lux | 0.13 |
| Reception room | 23 rd of Sept. | 15:00 | 2.1% | 7.6% | 23.1% | 174.7 lux | 647.8 lux | 1961.5 lux | 0.27 |

The results were similar to the 12st of June results, except for the second case where average lux levels were reduced to adequate levels. There were minimal variations in the DF levels. In the first case, in the waiting room, average DF was slightly lower than recommended level (figure 5.3 and table 5.6).

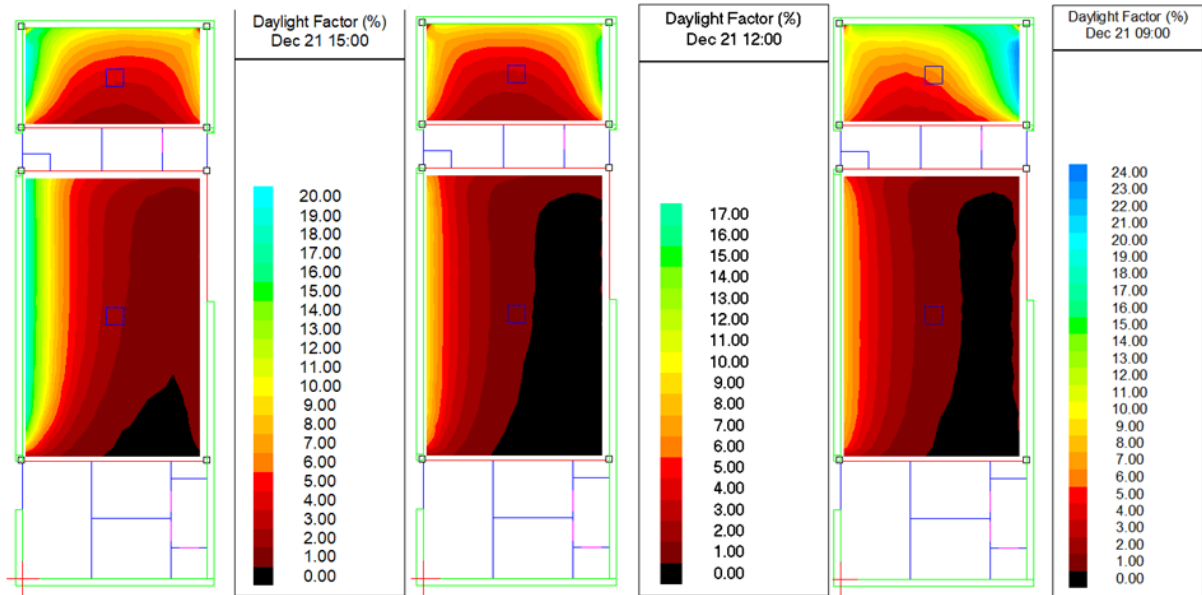


Figure 5.4. Daylight factor simulation results on the 21st of December (author 2019).

Table 5.7. 21st of December results summary (author 2019).

| Room | Date | Hour | Daylight factor | | | Daylight illuminance | | | Uniformity |
|----------------|--------------------------|-------|-----------------|-------|-------|----------------------|-----------|-------------|------------|
| | | | Min. | Ave. | Max. | Min. | Ave. | Max. | |
| Waiting room | 21 st of Dec. | 9:00 | 0.5% | 2.3% | 8.6% | 32.3 lux | 145.8 lux | 536.0 lux | 0.22 |
| Reception room | 21 st of Dec. | 9:00 | 3.2% | 10.2% | 24.3% | 196.0 lux | 630.6 lux | 1505.8 lux | 0.31 |
| Waiting room | 21 st of Dec. | 12:00 | 0.4% | 2.3% | 9.7% | 33.60 lux | 183.5 lux | 790.3 lux | 0.18 |
| Reception room | 21 st of Dec | 12:00 | 2.1% | 6.5% | 17.3% | 170.7 lux | 527.0 lux | 1412.90 lux | 0.32 |
| Waiting room | 21 st of Dec. | 15:00 | 0.5% | 4.4% | 19.3% | 38.0 lux | 307.1 lux | 1349.6 lux | 0.12 |
| Reception room | 21 st of Dec | 15:00 | 2.3% | 7.3% | 20.9% | 163.5 lux | 509.7 lux | 1466.3 lux | 0.32 |

The DF results were similar to other days with minimal variation. Average lux levels were still exceeding the requirements in the reception room while lux levels in waiting room were low in the first two cases. In all cases uniformity varied from low to very low (figure 5.4 and table 5.7). In the following diagrams (figures 5.5 and 5.6) summarize the four days daylighting levels and average DF results.

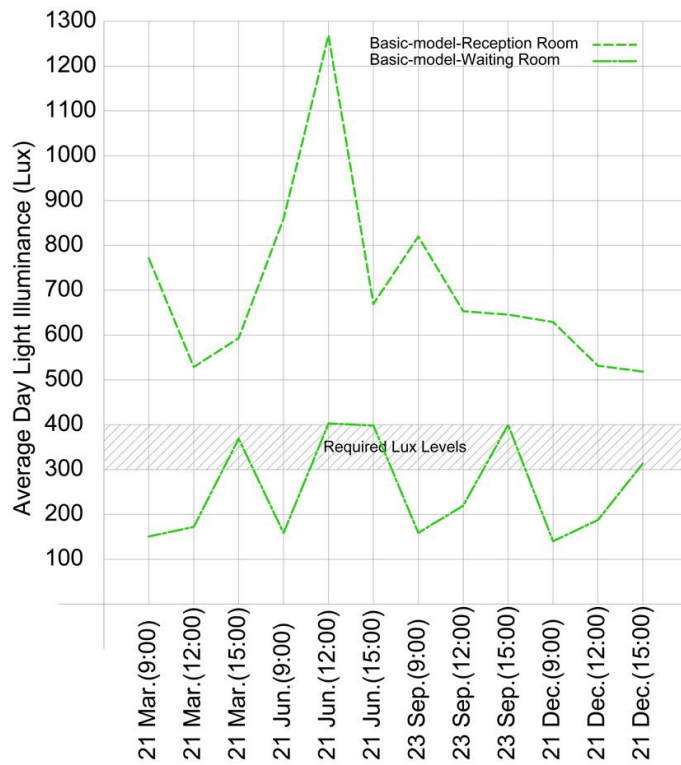


Figure 5.5 Summary of the basic model daylighting illuminance (lux) results (author 2019).

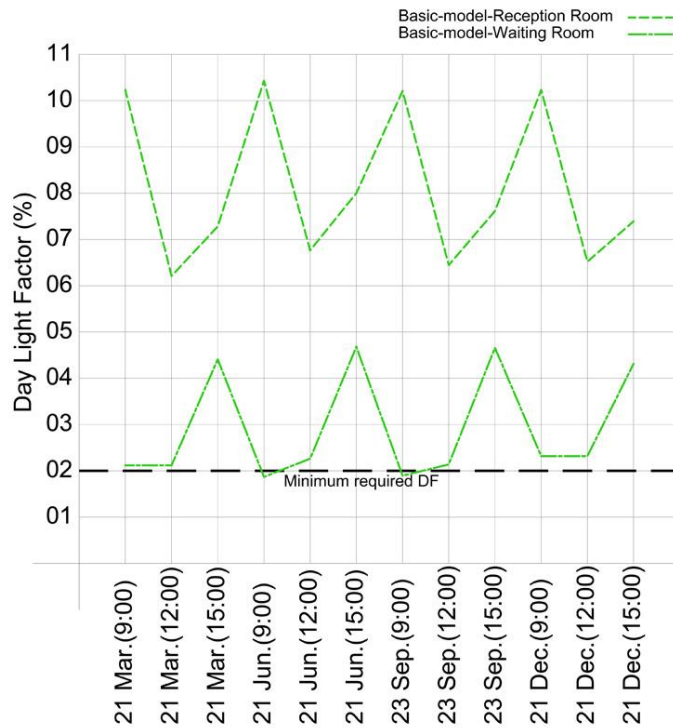


Figure 5.6 Summary of the basic model DF results (author 2019).

5.1.3 Basic model glare analysis

Similar to the daylight analysis the simulation was done for four days only which were the solstice and equinox days. The simulation was done with the RadianceIES application in the software which provided hemispherical fisheye images that showed luminance levels in the room and the associated parameters such as Daylight glare index (DGI) and Guth Visual Comfort Probability (GVSP).

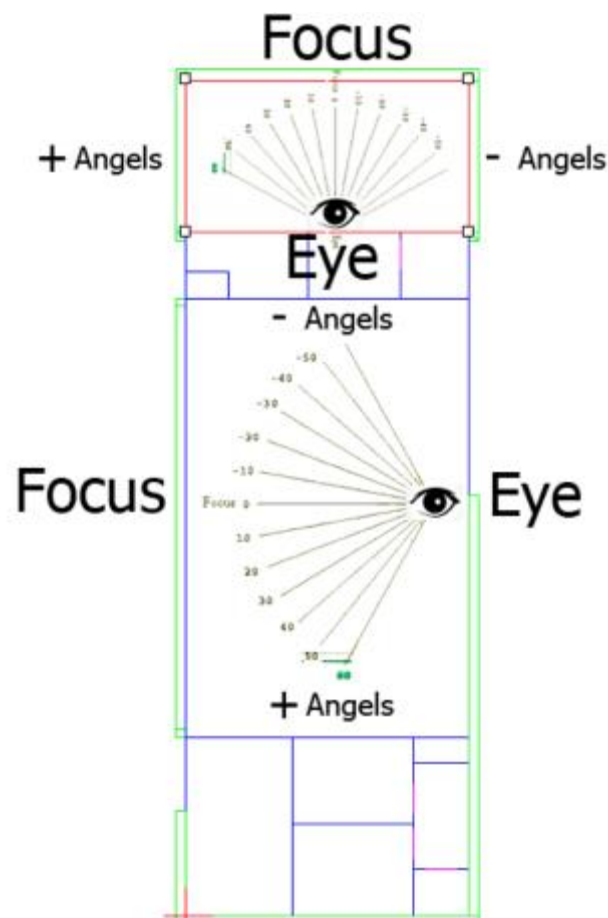


Figure 5.7. Eye/camera location in both rooms. IES VE consider negative angles on the right of nadir and positive angles on left of it (author 2019).

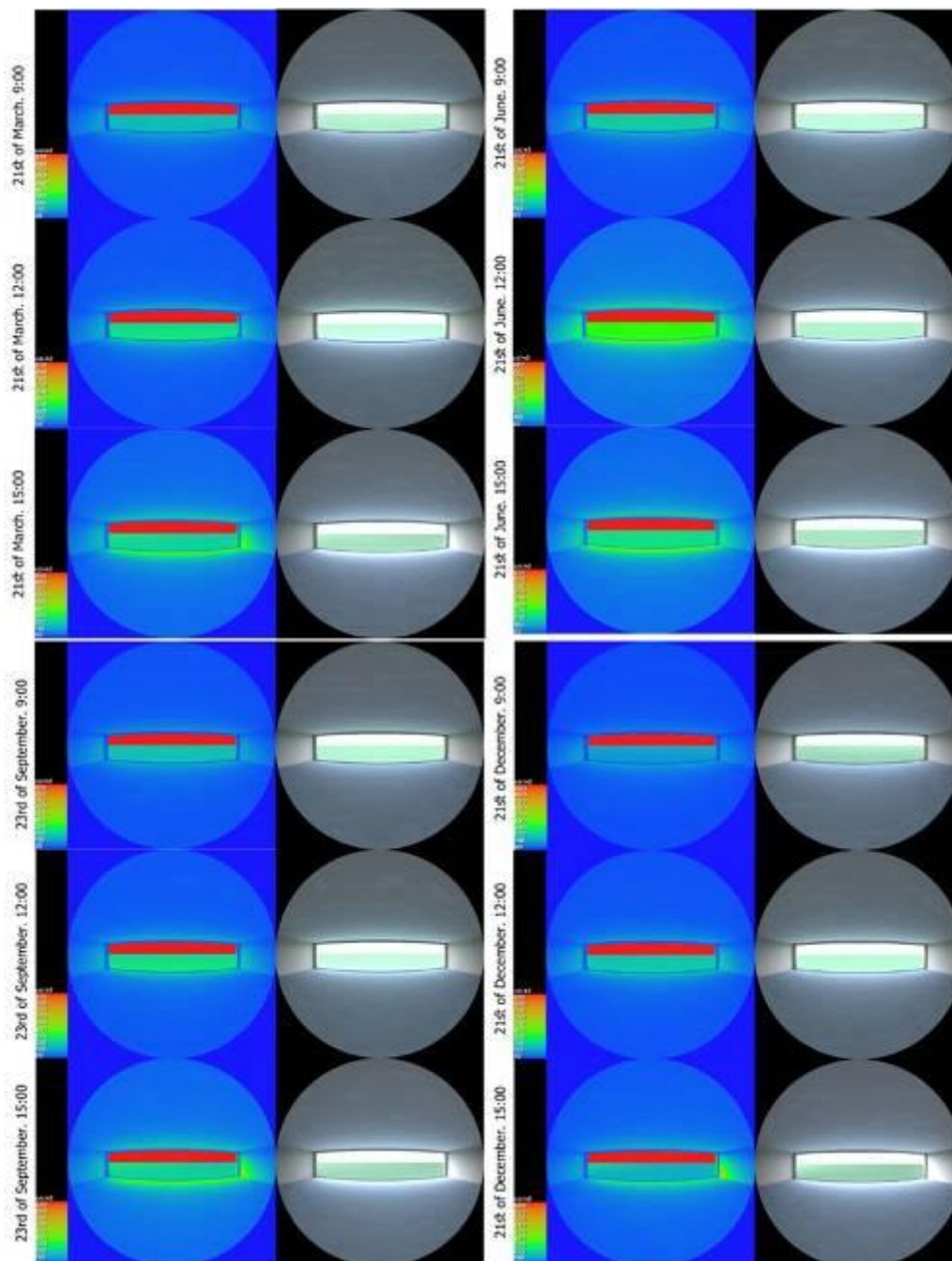


Figure 5.8. Waiting room luminance map in all cases including 21st of March case on the top left, 21st of June case on the top right, 23rd of September case on the bottom left and 21st of December case on the bottom right (author 2019).

In the waiting room, average luminance levels from the glazed wall reached 950 cd/m² in all cases (figure 5.8).

Table 5.8. DGI levels from different angles from nadir for the four days at 9:00,12:00 and 15:00 (author 2019).

| Angle | 60 | 50 | 40 | 30 | 20 | 10 | 0 | -10 | -20 | -30 | -40 | -50 | -60 |
|-------------------------------------------|------|------|------|------|------|------|------|------|------|------|------|------|------|
| 09:00 21 st of March | 14.7 | 16.6 | 18.3 | 19.7 | 20.8 | 21.6 | 21.9 | 21.6 | 20.8 | 19.7 | 18.3 | 16.7 | 14.8 |
| 12:00 21 st of March | 14.6 | 16.5 | 18.1 | 19.5 | 20.6 | 21.4 | 21.7 | 21.4 | 20.6 | 19.5 | 18.2 | 16.5 | 14.6 |
| 15:00 21 st of March | 15.3 | 18.2 | 18.8 | 20.1 | 21.2 | 21.9 | 22.2 | 21.9 | 21.1 | 19.9 | 18.6 | 16.9 | 15.1 |
| 09:00 21 st of June | 14.7 | 15.6 | 18.3 | 19.6 | 20.7 | 21.6 | 21.8 | 21.6 | 20.7 | 19.7 | 18.3 | 16.7 | 14.7 |
| 12:00 21 st of June | 16.1 | 18.1 | 19.7 | 21.1 | 22.1 | 22.9 | 23.2 | 22.9 | 22.1 | 21.1 | 19.7 | 18.1 | 16.2 |
| 15:00 21 st of June | 15.4 | 17.2 | 18.9 | 20.2 | 21.3 | 22.1 | 22.4 | 22.1 | 21.3 | 20.2 | 18.9 | 17.3 | 15.4 |
| 09:00 23 rd of September | 14.7 | 16.7 | 18.4 | 19.7 | 20.8 | 21.6 | 21.9 | 21.6 | 20.9 | 19.8 | 19.4 | 16.7 | 14.8 |
| 12:00 23 rd of September | 14.6 | 16.5 | 18.2 | 19.5 | 20.6 | 21.4 | 21.7 | 21.4 | 10.6 | 19.5 | 18.2 | 16.5 | 14.6 |
| 15:00 23 rd of September | 15.4 | 17.3 | 18.9 | 20.3 | 21.3 | 22.1 | 22.3 | 22.1 | 21.2 | 20.1 | 18.7 | 17.1 | 15.2 |
| 09:00 21 st of December | 14.3 | 16.3 | 17.9 | 19.3 | 20.4 | 21.3 | 21.5 | 21.3 | 20.4 | 19.4 | 18.0 | 16.4 | 14.4 |
| 12:00 21 st of December | 14.4 | 16.4 | 18.1 | 19.4 | 20.4 | 21.3 | 21.5 | 24.3 | 20.4 | 19.4 | 17.9 | 16.4 | 14.4 |
| 15:00 21 st of December | 14.8 | 16.7 | 18.4 | 19.7 | 20.7 | 21.5 | 21.7 | 21.4 | 20.5 | 19.4 | 18.1 | 16.4 | 14.5 |

According to the DGI analysis in the waiting room, there is a perceptible glare in all cases, as it exceeded 18 in the centre of the glazed wall. However, it did not reach the high disturbance level which is above

Table 5.9. GVCP levels from different angles from nadir for the four days at 9:00,12:00 and 15:00 (author 2019).

| Angle | 60 | 50 | 40 | 30 | 20 | 10 | 0 | -10 | -20 | -30 | -40 | -50 | -60 |
|-------------------------------------------|------|------|------|------|-----|-----|-----|-----|-----|------|------|------|------|
| 09:00 21 st of March | 37.8 | 24.4 | 15.4 | 9.8 | 6.5 | 4.7 | 4.2 | 4.7 | 6.5 | 9.8 | 15.4 | 24.4 | 37.9 |
| 12:00 21 st of March | 37.6 | 24.3 | 15.4 | 9.9 | 6.6 | 4.8 | 4.3 | 4.8 | 6.6 | 9.9 | 15.5 | 24.5 | 37.8 |
| 15:00 21 st of March | 30.4 | 18.6 | 11.2 | 6.9 | 4.5 | 3.2 | 2.9 | 3.3 | 4.7 | 7.2 | 11.7 | 19.4 | 31.5 |
| 09:00 21 st of June | 37.7 | 24.3 | 15.3 | 9.8 | 6.6 | 4.7 | 4.2 | 4.7 | 6.6 | 9.8 | 15.4 | 24.4 | 37.8 |
| 12:00 21 st of June | 22.7 | 12.9 | 7.3 | 4.2 | 2.6 | 1.8 | 1.6 | 1.8 | 2.6 | 4.3 | 7.3 | 12.9 | 22.8 |
| 15:00 21 st of June | 28.9 | 17.5 | 10.4 | 6.4 | 4.1 | 2.9 | 2.5 | 2.9 | 4.1 | 6.4 | 10.5 | 17.7 | 29.2 |
| 09:00 23 rd of September | 37.5 | 24.1 | 15.1 | 9.6 | 6.4 | 4.6 | 4.1 | 4.6 | 6.4 | 9.6 | 15.1 | 24.1 | 37.5 |
| 12:00 23 rd of September | 37.5 | 24.2 | 15.3 | 9.8 | 6.6 | 4.7 | 4.3 | 4.8 | 6.6 | 9.9 | 15.5 | 21.4 | 37.8 |
| 15:00 23 rd of September | 29.1 | 19.6 | 10.5 | 6.4 | 4.2 | 2.9 | 2.6 | 3.0 | 4.3 | 6.7 | 11.0 | 18.4 | 30.2 |
| 09:00 21 st of December | 42.4 | 28.2 | 18.3 | 11.9 | 8.1 | 5.9 | 5.3 | 5.9 | 8.1 | 11.9 | 18.2 | 28.1 | 42.3 |
| 12:00 21 st of December | 39.6 | 25.9 | 16.6 | 10.7 | 7.3 | 5.3 | 4.8 | 5.3 | 7.4 | 10.8 | 16.8 | 26.2 | 39.9 |
| 15:00 21 st of December | 35.2 | 22.4 | 13.9 | 8.9 | 6.0 | 4.3 | 3.9 | 4.4 | 6.3 | 9.5 | 15.0 | 23.9 | 37.3 |

GVCP analysis, in the waiting room, showed that minimum percentage of satisfied occupants was 1.55% at 12:00 on 21st of June to and maximum was 5.31% at 9:00 on 21st of December when looking at the middle of the glazed wall. The minimum percentage of satisfied occupants was 22.74% at 12:00 on 21st of June to and maximum was 42.45% at 9:00 on 21st of December when looking at the edges of the glazed wall (table 5.9).

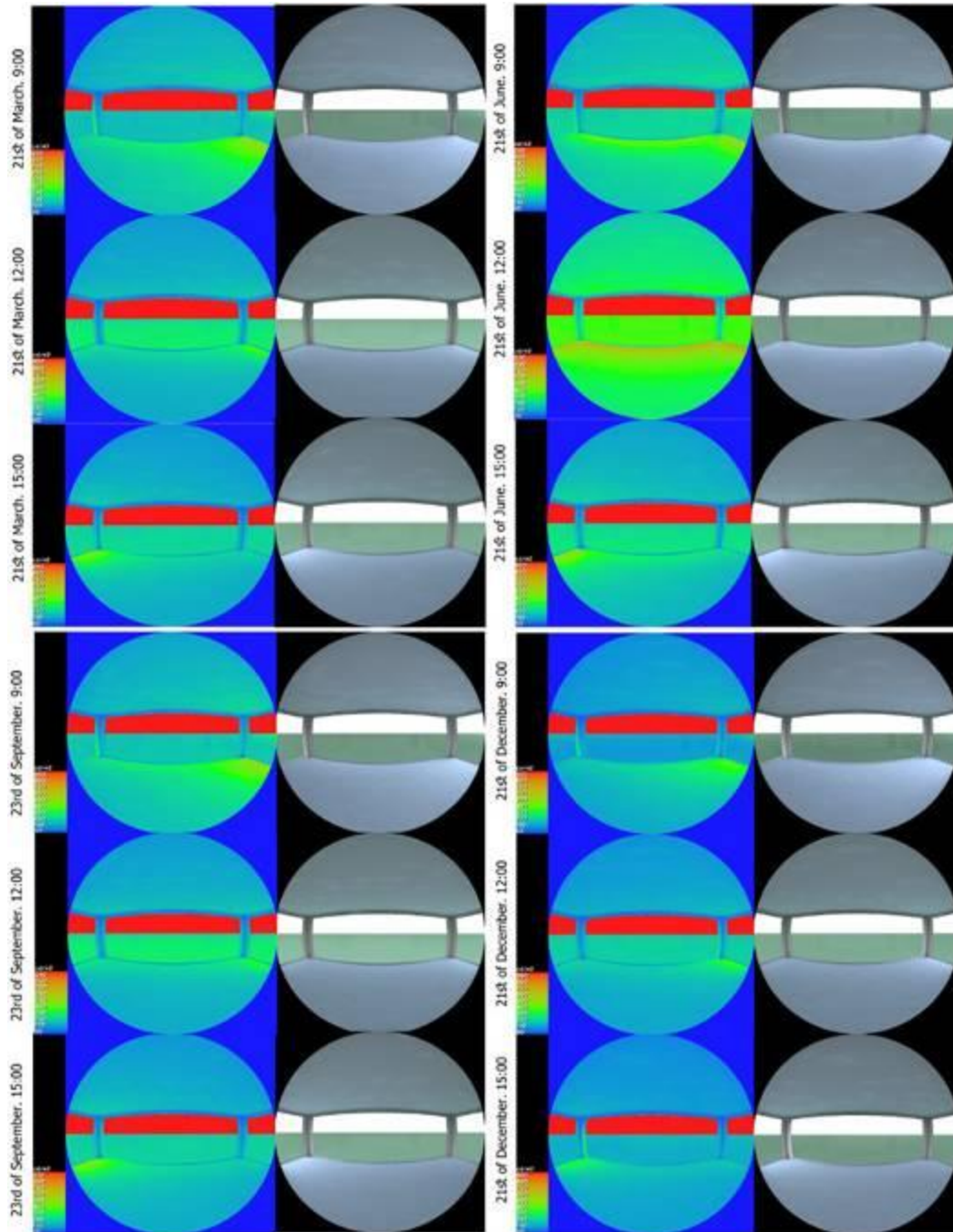


Figure 5.9. Reception room luminance map in all cases including 21st of March case on the top left, 21st of June case on the top right, 23rd of September case on the bottom left and 21st of December case on the bottom right (author 2019).

In the reception room, luminance levels from the glazed wall reached 950 cd/m² in all cases (figure 5.9).

Table 5.10. DGI levels from different angles from nadir for the four days at 9:00,12:00 and 15:00 (author 2019).

| Angle | 60 | 50 | 40 | 30 | 20 | 10 | 0 | -10 | -20 | -30 | -40 | -50 | -60 |
|-------------------------------------------|------|------|------|------|------|------|------|------|------|------|------|------|------|
| 09:00 21 st of March | 11.1 | 10.1 | 8.9 | 8.1 | 8.1 | 8.9 | 10.5 | 11.9 | 14.9 | 15.9 | 16.8 | 17.6 | 14.8 |
| 12:00 21 st of March | 17.6 | 17.5 | 17.4 | 17.4 | 17.3 | 17.2 | 16.9 | 16.8 | 16.6 | 15.8 | 14.8 | 13.6 | 12.1 |
| 15:00 21 st of March | 19.1 | 18.3 | 17.5 | 16.8 | 16.4 | 16.2 | 16.2 | 15.7 | 14.9 | 13.9 | 12.6 | 11.2 | 9.6 |
| 09:00 21 st of June | 2.6 | 5.4 | 7.8 | 10.1 | 11.9 | 13.6 | 14.9 | 16.1 | 16.8 | 17.1 | 16.6 | 15.7 | 14.6 |
| 12:00 21 st of June | 18.5 | 18.3 | 18.1 | 17.7 | 17.4 | 17.3 | 17.5 | 17.6 | 17.5 | 17.0 | 15.9 | 14.8 | 13.3 |
| 15:00 21 st of June | 19.4 | 18.5 | 17.3 | 16.1 | 14.4 | 12.5 | 10.6 | 8.5 | 6.2 | 2.5 | 0.1 | 0 | 0 |
| 09:00 23 rd of September | 13.9 | 12.8 | 11.5 | 10.4 | 9.5 | 9.5 | 10.4 | 11.4 | 12.8 | 13.9 | 14.8 | 15.4 | 16.0 |
| 12:00 23 rd of September | 17.6 | 17.5 | 17.5 | 17.5 | 17.4 | 17.1 | 16.9 | 16.7 | 15.9 | 14.9 | 13.8 | 12.3 | 13.5 |
| 15:00 23 rd of September | 0.0 | 18.8 | 17.9 | 16.7 | 15.9 | 15.1 | 14.7 | 14.5 | 14.5 | 14.3 | 13.7 | 13.1 | 11.9 |
| 09:00 21 st of December | 17.4 | 16.5 | 15.5 | 14.5 | 12.9 | 11.4 | 10.2 | 9.4 | 9.3 | 9.8 | 11.1 | 12.3 | 13.5 |
| 12:00 21 st of December | 18.9 | 18.9 | 18.9 | 18.9 | 18.8 | 18.5 | 18.6 | 18.1 | 17.8 | 16.7 | 15.8 | 14.6 | 13.1 |
| 15:00 21 st of December | 17.1 | 17.1 | 17.2 | 17.6 | 18.1 | 18.1 | 18.1 | 18.1 | 18.1 | 17.8 | 16.8 | 15.7 | 14.4 |

In the reception room, the glare threshold changed because of room orientation. Thus, there was a glare possibility only in five cases as shown in the DGI analysis table. According to the DGI analysis there is a perceptible glare in these cases, as it exceeded 18 in various locations. However, it did not reach the high disturbance level which is above 24 (table 5.10).

Table 5.11. GVCP levels from different angles from nadir for the four days at 9:00,12:00 and 15:00 (author 2019).

| Angle | 60 | 50 | 40 | 30 | 20 | 10 | 0 | -10 | -20 | -30 | -40 | -50 | -60 |
|-------------------------------------------|------|------|------|------|------|------|------|------|------|------|------|------|------|
| 09:00 21 st of March | 71.7 | 80.3 | 83.6 | 85.6 | 88.1 | 87.1 | 83.3 | 74.9 | 65.9 | 52.5 | 44.7 | 38.9 | 34.3 |
| 12:00 21 st of March | 37.3 | 35.9 | 34.5 | 33.8 | 34.2 | 35.3 | 37.7 | 40.4 | 44.3 | 44.9 | 54.1 | 62.6 | 67.9 |
| 15:00 21 st of March | 30.6 | 33.1 | 36.9 | 41.1 | 45.2 | 48.8 | 52 | 55.1 | 62.1 | 61.4 | 50.1 | 61.3 | 73.3 |
| 09:00 21 st of June | 96.1 | 89.1 | 77.3 | 62.6 | 48.1 | 35.9 | 26.6 | 20.1 | 16.5 | 18.6 | 18.6 | 23.7 | 31.4 |
| 12:00 21 st of June | 26.2 | 25.7 | 25.8 | 26.5 | 27.9 | 29.2 | 30.2 | 25.7 | 28.2 | 33.9 | 33.3 | 42.2 | 40.1 |
| 15:00 21 st of June | 12.9 | 16.1 | 20.8 | 27.9 | 38.5 | 51.6 | 65.9 | 79.4 | 89.5 | 98.5 | 99.9 | 99.9 | 100 |
| 09:00 23 rd of September | 53.7 | 66.6 | 72.1 | 16.8 | 80.1 | 83.2 | 82.4 | 76.6 | 69.5 | 57.1 | 50.3 | 45.6 | 41.8 |
| 12:00 23 rd of September | 37.2 | 35.6 | 34.2 | 33.3 | 33.5 | 34.4 | 36.6 | 39.2 | 42.8 | 43.6 | 51.7 | 61.2 | 66.6 |
| 15:00 23 rd of September | 30.1 | 35.9 | 40.1 | 44.9 | 50.8 | 56.3 | 61.1 | 62.9 | 66.1 | 64.3 | 61.1 | 66.6 | 66.7 |
| 09:00 21 st of December | 22.8 | 40.6 | 45.8 | 52.9 | 61.3 | 74.1 | 81.2 | 83.6 | 84.1 | 81.5 | 76.9 | 71.9 | 62.1 |
| 12:00 21 st of December | 32.1 | 30.4 | 29.5 | 29.1 | 29.6 | 31.4 | 33.9 | 36.7 | 35.9 | 36.8 | 36.8 | 47.1 | 59.1 |
| 15:00 21 st of December | 40.1 | 38.3 | 36.2 | 33.8 | 31.8 | 31.3 | 31.9 | 26.6 | 28.5 | 23.7 | 29.9 | 38.9 | 50.1 |

In the reception room, GVCP analysis showed that minimum percentage of satisfied occupants was 25.69% at 12:00 on 21st of June to and the maximum was 81.24% at 9:00 on 21st of December when looking at various directions (as the room has three windows). The results were expected as the room largest window is oriented to the north (table 5.11).

5.1.4 Basic model daylight harvesting potential analysis

Artificial lighting is also a massive consumer of energy, especially in office buildings. Recently, it is expected that LEDs will become the preponderant technology in the market in future due to their durability, efficiency and efficacy. Nevertheless, almost 80% of the total power consumption by LEDs is converted into convective thermal power that eventually increases the cooling demand in the space (Cao, Dai & Liu 2016). IES software is capable of calculating artificial light saving potential due to usage of daylight. The simulation was done between RadianceIES application and Apache application in the software. Two light sensors at ceiling level pointing down were added to reception and waiting room spaces. Following IES developers' instructions, a daily dimming profile was created following a ramp profile formula. The profile changes as if the day light illuminance is equal or lower that 5 foot candles or 53.8 lux, 100 % of artificial light is on and if it is equal or higher than 50 foot candle or 538 lux, artificial lights would be dimmed until its level reaches 20% of the total lighting power (figures 5.10 and 5.11).

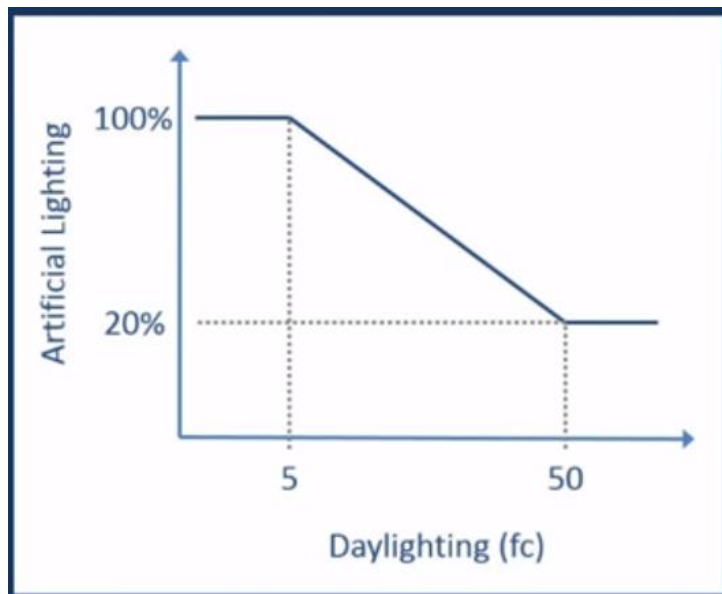


Figure 5.10. Recommended dimming profile which is associated with daylight sensors (IES 2018).

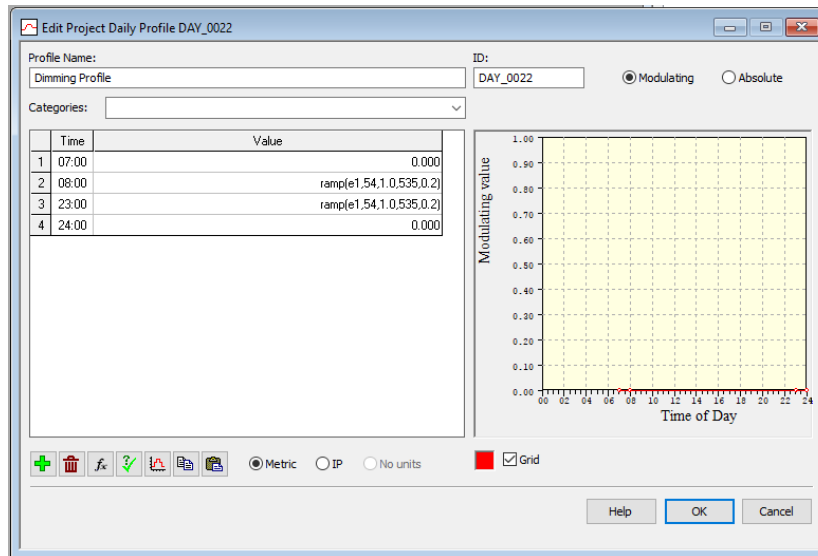


Figure 5.11. Formula daily profile as inserted in IES VE (author 2019).

Table 5.12. Total annual electricity consumption Results summary (author 2019).

| | Total electricity (MWh) | Total electricity (MWh) |
|--------------|---------------------------|-------------------------|
| Date | Basic Model with Daylight | Basic Model.aps |
| Jan 01-31 | 2.1298 | 2.1744 |
| Feb 01-28 | 2.3670 | 2.4339 |
| Mar 01-31 | 2.9213 | 3.0512 |
| Apr 01-30 | 3.5473 | 3.6774 |
| May 01-31 | 4.3064 | 4.4261 |
| Jun 01-30 | 4.4735 | 4.5822 |
| Jul 01-31 | 4.7856 | 4.9159 |
| Aug 01-31 | 4.8492 | 4.9626 |
| Sep 01-30 | 4.3747 | 4.4772 |
| Oct 01-31 | 3.9378 | 4.0166 |
| Nov 01-30 | 3.1782 | 3.2288 |
| Dec 01-31 | 2.5626 | 2.6027 |
| Summed total | 43.4334 | 44.5490 |

After adding the dimming profile to the two spaces, the IES-VE Apache simulation was done, and results were checked against the original results in order to evaluate the daylight harvesting potential (table 5.12). According to the results, the daylight sensors managed to reduce total annual electrical consumption from 44.5490 MWh to 43.4334 MWh. Total achieved annual saving is 1.1156 MWh which is equal to 340.3 UAE Dirhams based residential buildings tariff, as the building is a part of a residential complex, of 30.5 UAE Fils for 1 kW of electricity as the building exceed the green allowance of 20 kWh/day.

5.2 Buffer DSF/Corridor Facade- Scenarios-01,02 and 03: Double Layers Cushion with Three Different Gap depths

5.2.1 Scenarios 01,02 and 03 CFD simulation and analysis

The vertical buoyancy flow on the proposed DSF systems was simulated by Computational Fluid Dynamic (CFD) MicroFlo application in IES-VE software. The studied day represented the worst-case scenario on 10th of August at 3:00 when the building had the highest energy consumption rate. The external boundary situation was extracted from the Apache sim application for a suburban condition in Abu Dhabi as the building is located in Yas island. The application analysed the DSF behaviour and possibilities.

Table 5.13. Air temperature within the DSF cavity from Microflo results (author 2019).

| Location | Date | Hour | Minimum DSF cavity air temperature (°C) | Maximum DSF cavity air temperature (°C) | Mean DSF cavity air temperature (°C) | Comparison between ambient temperature (47°C) and mean DSF cavity air temperature |
|---------------------|--------------------------|-------|-----------------------------------------|-----------------------------------------|--------------------------------------|-----------------------------------------------------------------------------------|
| Eastern DSF cavity | 10 th of Aug. | 15:00 | 28.21 | 48.35 | 36.95 | -21.4% |
| Western DSF cavity | 10 th of Aug. | 12:00 | 28.39 | 47.61 | 36.78 | -21.6% |
| Northern DSF cavity | 10 th of Aug. | 15:00 | 28.51 | 47.54 | 36.89 | -21.5% |

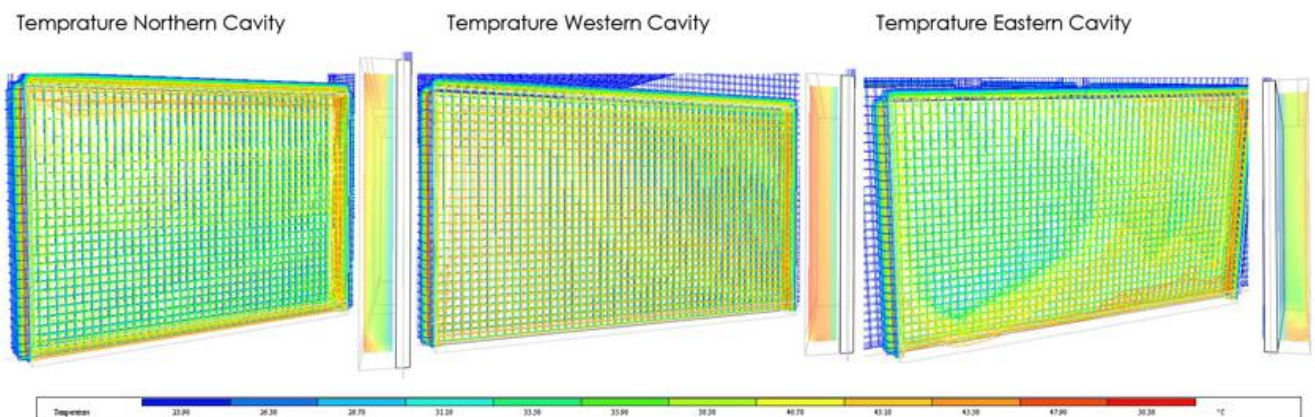


Figure 5.12. CFD analysis of Norther, Eastern and Western cushions in Microflo (author 2019).

Scenarios 01,02 and 03 simulations showed similar results with minimal variation where the stack effect caused air flow with higher velocity comparing to the ambient conditions. The temperature analysis (table 5.12 and figure 5.12) showed that when the ambient temperature reached 47.0 °C at the building level , the temperature in the DSF cavity near the cushion was maximum 48.35 °C in eastern DSF, maximum 47.61 °C in western DSF and maximum 47.54 °C in northern DSF. Thus, the temperature near the external DSF layer was higher than ambient temperature. The temperature in the DSF cavity near the DGU was minimum 28.21 °C in eastern DSF, minimum 28.39 °C in western DSF and minimum 28.51 °C in northern DSF. Due to the natural air flow, hot air was discharged and average reduction in mean cavity air temperature, comparing to ambient temperature, was 21.4% in eastern DSF, 21.6% in western DSF and 21.5% in northern DSF.

Table 5.14. Air velocity within the DSF cavity from Microflo results (author 2019).

| Location | Date | Hour | Air velocity within the cavity near the bottom inlet (m/s) | Air velocity within the cavity near the top outlet (m/s) | Mean air velocity within the cavity (m/s) |
|---------------------|--------------------------|-------|------------------------------------------------------------|----------------------------------------------------------|-------------------------------------------|
| Eastern DSF cavity | 10 th of Aug. | 15:00 | 0.62~0.72 | 1.03~1.13 | 0.62 |
| Western DSF cavity | 10 th of Aug. | 12:00 | 0.51~0.62 | 0.93~1.03 | 0.51 |
| Northern DSF cavity | 10 th of Aug. | 15:00 | 0.21 | 0.41~0.72 | 0.31 |

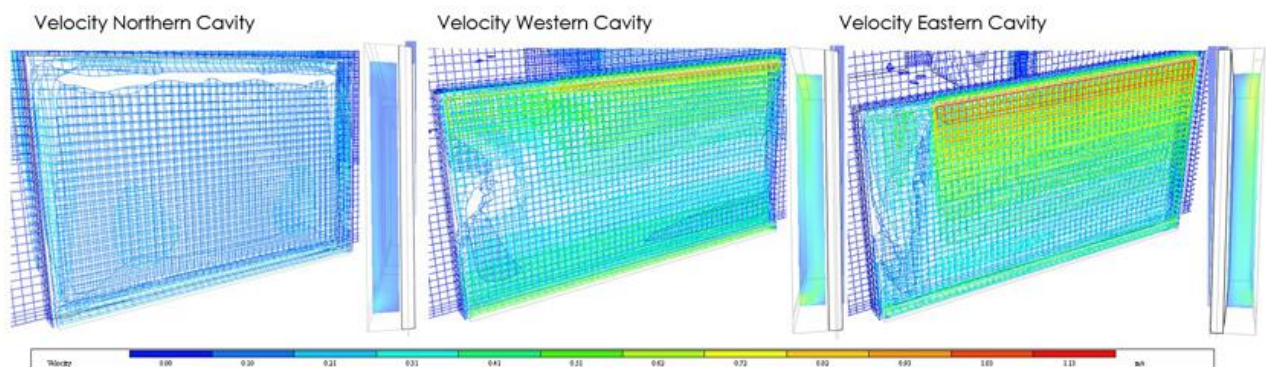


Figure 5.13. CFD analysis of the eastern cushions in IES VE (author 2019).

The analysis proved that air flow was from bottom to top which helped to discharge hot air from the DSF cavity (table 5.14 and figure 5.13). The maximum air velocity was near the top exhaust/outlet. Average air velocity in the eastern DSF was 0.62 while the maximum velocity was 1.13 m/s near the top and the inlet air velocity was 0.67 m/s. Average air velocity in the western DSFs was 0.51 while the maximum velocity was 0.97 m/s near the top and the inlet air velocity was 0.67 m/s. It was noted that the sun location affects the air flow in the DSF cavity, that is why the lowest air velocity was recorded in the northern DSF. However, as the northern ones are not exposed to direct solar irradiance, the temperature within the cavity was lower than other DSFs. The impact of the of the stack effect on the DSF was evaluated in the following sections where additional investigations on the internal conditions within the building were provided.

5.2.2 Scenarios 01,02 and 03 annual electrical consumption results

Table 5.15. Total annual electricity consumption of the basic model and the three scenarios (author 2019).

| | Electricity (MWh) | Electricity (MWh) | Electricity (MWh) | Electricity (MWh) |
|--------------|-------------------|-------------------|-------------------|-------------------|
| Date | Scenario 03.aps | Scenario 02.aps | Scenario 01.aps | Basic Model.aps |
| Jan 01-31 | 1.9502 | 1.9443 | 1.9374 | 2.1744 |
| Feb 01-28 | 2.1265 | 2.1204 | 2.1133 | 2.4339 |
| Mar 01-31 | 2.6390 | 2.6331 | 2.6262 | 3.0512 |
| Apr 01-30 | 3.2019 | 3.2002 | 3.1981 | 3.6774 |
| May 01-31 | 3.8501 | 3.8523 | 3.8550 | 4.4261 |
| Jun 01-30 | 4.0059 | 4.0103 | 4.0156 | 4.5822 |
| Jul 01-31 | 4.3264 | 4.3335 | 4.3420 | 4.9159 |
| Aug 01-31 | 4.3931 | 4.4009 | 4.4102 | 4.9626 |
| Sep 01-30 | 3.9878 | 3.9939 | 4.0012 | 4.4772 |
| Oct 01-31 | 3.6004 | 3.6028 | 3.6057 | 4.0166 |
| Nov 01-30 | 2.9156 | 2.9137 | 2.9115 | 3.2288 |
| Dec 01-31 | 2.3434 | 2.3370 | 2.3295 | 2.6027 |
| Summed total | 39.3406 | 39.3426 | 39.3457 | 44.5490 |

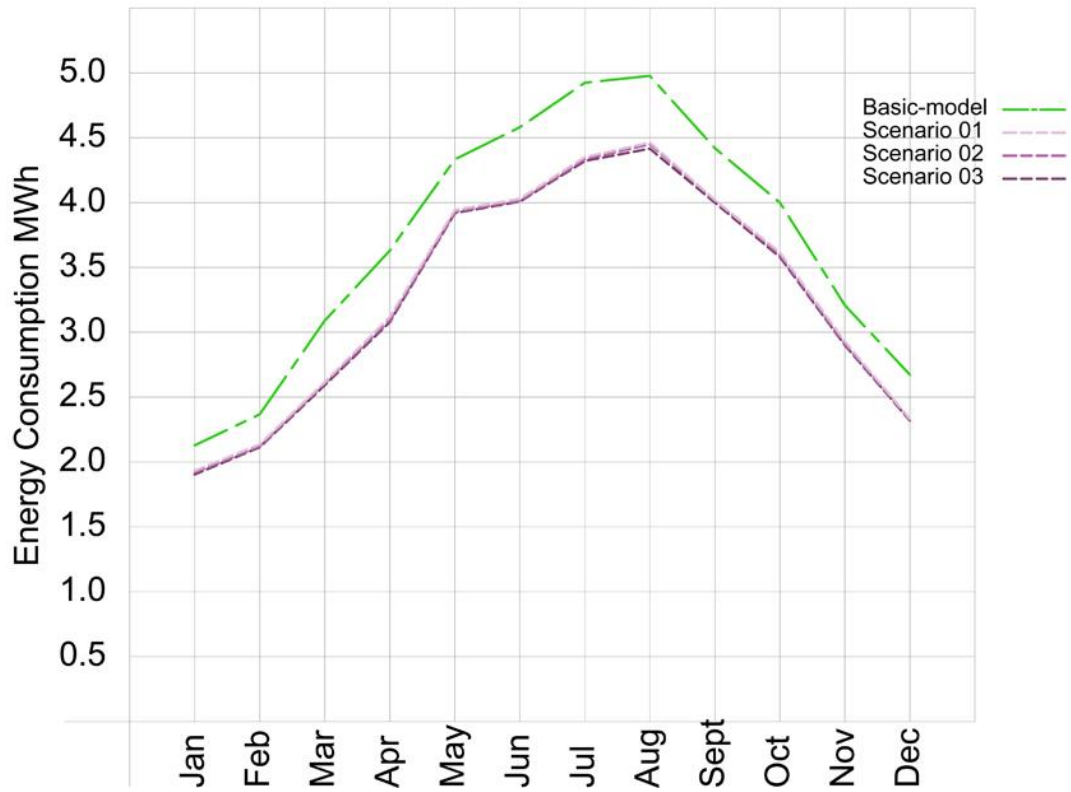


Figure 5.14. Combined diagram of the basic model results and the three scenarios results (author 2019)

The three scenarios showed good improvement comparing to the basic-model. It was noticed that changes in the air gap thickness had minor effect on the electricity consumption (table 5.15 and figure 5.14). Comparing to the basic model results, the total electrical consumption reduction, with consideration of the inflation unit consumption, was almost 5.2 MWh or 11.6% in all cases with minimal variations (table 5.16). Thus, the cushion chamber or cavity depth did not have any major impact on its performance as a DSF component.

Table 5.16. Results summary and comparison with the basic model (by the author).

| Scenario | Total annual electrical consumption saving comparing to the basic model (MWh) | Inflation unit annual electricity consumption (MWh) | Total annual electrical consumption saving considering inflation unit annual consumption (MWh) | Total annual electrical consumption saving considering inflation unit annual consumption (%) | Cost saving based on tariff of 30.5 Fils for every KW (ADDC 2018). |
|-------------|-------------------------------------------------------------------------------|-----------------------------------------------------|------------------------------------------------------------------------------------------------|----------------------------------------------------------------------------------------------|--------------------------------------------------------------------|
| Scenario-01 | 5.2033 | 0.03916 | 5.16414 | 11.594% | 1575.1 UAE Dirhams |
| Scenario-02 | 5.2064 | 0.03916 | 5.16724 | 11.600% | 1576.0 UAE Dirhams |
| Scenario-03 | 5.2084 | 0.03916 | 5.16924 | 11.603% | 1576.6 UAE Dirhams |

5.2.3 Scenarios 01,02 and 03 thermal comfort results

Table 5.17. Comfort index results comparison between three scenarios and the basic model (author 2019).

| Var. Name | Location | Filename | Type | Mean |
|---------------|-----------------|-----------------|---------------|------|
| Comfort index | Mechanical room | Scenario 03.aps | Comfort index | 9 |
| Comfort index | Office 01 | Scenario 03.aps | Comfort index | 9 |
| Comfort index | Office 02 | Scenario 03.aps | Comfort index | 9 |
| Comfort index | Store 01 | Scenario 03.aps | Comfort index | 9 |
| Comfort index | Lobby 01 | Scenario 03.aps | Comfort index | 9 |
| Comfort index | Waiting room | Scenario 03.aps | Comfort index | 10 |
| Comfort index | Lobby 02 | Scenario 03.aps | Comfort index | 9 |
| Comfort index | Toilet | Scenario 03.aps | Comfort index | 9 |
| Comfort index | Store 02 | Scenario 03.aps | Comfort index | 9 |
| Comfort index | Reception | Scenario 03.aps | Comfort index | 9 |
| Comfort index | Mechanical room | Scenario 02.aps | Comfort index | 9 |
| Comfort index | Office 01 | Scenario 02.aps | Comfort index | 9 |
| Comfort index | Office 02 | Scenario 02.aps | Comfort index | 9 |
| Comfort index | Store 01 | Scenario 02.aps | Comfort index | 9 |
| Comfort index | Lobby 01 | Scenario 02.aps | Comfort index | 9 |
| Comfort index | Waiting room | Scenario 02.aps | Comfort index | 10 |
| Comfort index | Lobby 02 | Scenario 02.aps | Comfort index | 9 |
| Comfort index | Toilet | Scenario 02.aps | Comfort index | 9 |
| Comfort index | Store 02 | Scenario 02.aps | Comfort index | 9 |
| Comfort index | Reception | Scenario 02.aps | Comfort index | 9 |
| Comfort index | Mechanical room | Scenario 01.aps | Comfort index | 9 |
| Comfort index | Office 01 | Scenario 01.aps | Comfort index | 9 |
| Comfort index | Office 02 | Scenario 01.aps | Comfort index | 9 |
| Comfort index | Store 01 | Scenario 01.aps | Comfort index | 9 |
| Comfort index | Lobby 01 | Scenario 01.aps | Comfort index | 9 |
| Comfort index | Waiting room | Scenario 01.aps | Comfort index | 9 |
| Comfort index | Lobby 02 | Scenario 01.aps | Comfort index | 9 |
| Comfort index | Toilet | Scenario 01.aps | Comfort index | 9 |
| Comfort index | Store 02 | Scenario 01.aps | Comfort index | 9 |
| Comfort index | Reception | Scenario 01.aps | Comfort index | 9 |
| Comfort index | Mechanical room | Basic Model.aps | Comfort index | 9 |
| Comfort index | Office 01 | Basic Model.aps | Comfort index | 9 |
| Comfort index | Office 02 | Basic Model.aps | Comfort index | 9 |
| Comfort index | Store 01 | Basic Model.aps | Comfort index | 9 |
| Comfort index | Lobby 01 | Basic Model.aps | Comfort index | 9 |
| Comfort index | Waiting room | Basic Model.aps | Comfort index | 10 |
| Comfort index | Lobby 02 | Basic Model.aps | Comfort index | 9 |
| Comfort index | Toilet | Basic Model.aps | Comfort index | 9 |
| Comfort index | Store 02 | Basic Model.aps | Comfort index | 10 |
| Comfort index | Reception | Basic Model.aps | Comfort index | 10 |

The three scenarios had the same comfort index result with a minor change in scenario 01 (table 5.17). Comparing to the basic model, the mean index in all rooms was improved in store 02 and reception in scenario 02 and 03 and waiting room, store 02 and reception in scenario 01. Comfort index in those rooms changed from 10 (warm/acceptable) to 9 (slightly warm/acceptable).

Table 5.18. Mean room temperature (author 2019).

| Var. Name | Location | Filename | Type | Mean |
|-----------------|-----------------|-----------------|------------------|-------|
| Air temperature | Mechanical room | Scenario 03.aps | Temperature (°C) | 24.83 |
| Air temperature | Office 01 | Scenario 03.aps | Temperature (°C) | 24.59 |
| Air temperature | Office 02 | Scenario 03.aps | Temperature (°C) | 24.58 |
| Air temperature | Store 01 | Scenario 03.aps | Temperature (°C) | 24.50 |
| Air temperature | Lobby 01 | Scenario 03.aps | Temperature (°C) | 24.59 |
| Air temperature | Waiting room | Scenario 03.aps | Temperature (°C) | 25.16 |
| Air temperature | Lobby 02 | Scenario 03.aps | Temperature (°C) | 24.77 |
| Air temperature | Toilet | Scenario 03.aps | Temperature (°C) | 24.62 |
| Air temperature | Store 02 | Scenario 03.aps | Temperature (°C) | 24.75 |
| Air temperature | Reception | Scenario 03.aps | Temperature (°C) | 25.16 |
| Air temperature | Mechanical room | Scenario 02.aps | Temperature (°C) | 24.83 |
| Air temperature | Office 01 | Scenario 02.aps | Temperature (°C) | 24.59 |
| Air temperature | Office 02 | Scenario 02.aps | Temperature (°C) | 24.58 |
| Air temperature | Store 01 | Scenario 02.aps | Temperature (°C) | 24.50 |
| Air temperature | Lobby 01 | Scenario 02.aps | Temperature (°C) | 24.59 |
| Air temperature | Waiting room | Scenario 02.aps | Temperature (°C) | 25.17 |
| Air temperature | Lobby 02 | Scenario 02.aps | Temperature (°C) | 24.78 |
| Air temperature | Toilet | Scenario 02.aps | Temperature (°C) | 24.63 |
| Air temperature | Store 02 | Scenario 02.aps | Temperature (°C) | 24.76 |
| Air temperature | Reception | Scenario 02.aps | Temperature (°C) | 25.19 |
| Air temperature | Mechanical room | Scenario 01.aps | Temperature (°C) | 24.83 |
| Air temperature | Office 01 | Scenario 01.aps | Temperature (°C) | 24.59 |
| Air temperature | Office 02 | Scenario 01.aps | Temperature (°C) | 24.59 |
| Air temperature | Store 01 | Scenario 01.aps | Temperature (°C) | 24.50 |
| Air temperature | Lobby 01 | Scenario 01.aps | Temperature (°C) | 24.59 |
| Air temperature | Waiting room | Scenario 01.aps | Temperature (°C) | 25.18 |
| Air temperature | Lobby 02 | Scenario 01.aps | Temperature (°C) | 24.79 |
| Air temperature | Toilet | Scenario 01.aps | Temperature (°C) | 24.64 |
| Air temperature | Store 02 | Scenario 01.aps | Temperature (°C) | 24.77 |
| Air temperature | Reception | Scenario 01.aps | Temperature (°C) | 25.21 |
| Air temperature | Mechanical room | Basic Model.aps | Temperature (°C) | 24.89 |
| Air temperature | Office 01 | Basic Model.aps | Temperature (°C) | 24.62 |
| Air temperature | Office 02 | Basic Model.aps | Temperature (°C) | 24.66 |
| Air temperature | Store 01 | Basic Model.aps | Temperature (°C) | 24.52 |
| Air temperature | Lobby 01 | Basic Model.aps | Temperature (°C) | 24.62 |
| Air temperature | Waiting room | Basic Model.aps | Temperature (°C) | 25.51 |
| Air temperature | Lobby 02 | Basic Model.aps | Temperature (°C) | 25.13 |
| Air temperature | Toilet | Basic Model.aps | Temperature (°C) | 24.94 |
| Air temperature | Store 02 | Basic Model.aps | Temperature (°C) | 25.16 |
| Air temperature | Reception | Basic Model.aps | Temperature (°C) | 26.15 |

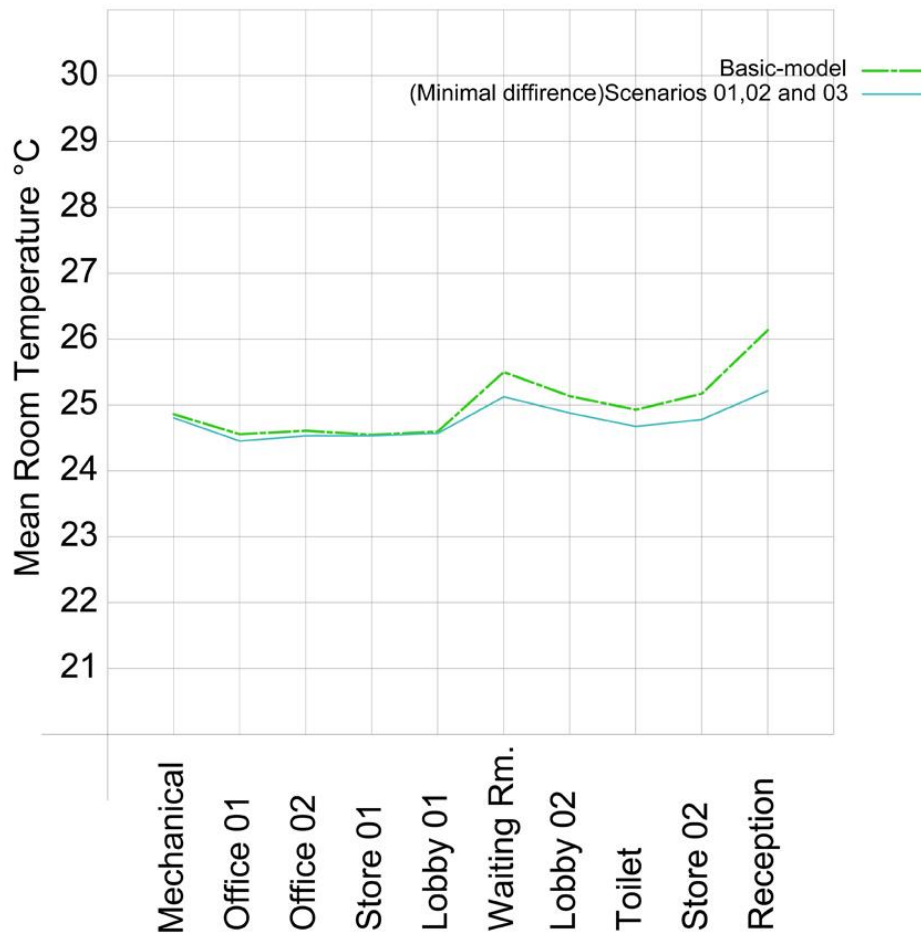


Figure 5.15. Combined diagram of the basic model results and the three scenarios results (author 2019)

The rooms air temperature results in the three scenarios were similar with slight variation. Comparing to the basic model, the average overall improvement/reduction in the mean room temperature was 1.00% in scenario 01, 1.03% in scenario 02 and 1.04% in scenario 03 (table 5.18 and figure 5.15). The improvement/reduction in the mean waiting room temperature was 1.3% in scenario 01, 1.3% in scenario 02 and 1.4% in scenario 03. The improvement/reduction in the mean reception room temperature was 3.6% in scenario 01, 3.7% in scenario 02 and 3.8% in scenario 03. Other than the targeted rooms with windows, temperature was reduced also in adjacent rooms which were lobby 02, toilet and store 02.

Table 5.19. People dissatisfied index results comparison between the three scenarios and the basic model (author 2019).

| Var. Name | Location | Filename | Type | Mean |
|---------------------|-----------------|-----------------|----------------|-------|
| People dissatisfied | Mechanical room | Scenario 03.aps | Percentage (%) | 29.43 |
| People dissatisfied | Office 01 | Scenario 03.aps | Percentage (%) | 26.33 |
| People dissatisfied | Office 02 | Scenario 03.aps | Percentage (%) | 26.00 |
| People dissatisfied | Store 01 | Scenario 03.aps | Percentage (%) | 26.10 |
| People dissatisfied | Lobby 01 | Scenario 03.aps | Percentage (%) | 27.40 |
| People dissatisfied | Waiting room | Scenario 03.aps | Percentage (%) | 33.42 |
| People dissatisfied | Lobby 02 | Scenario 03.aps | Percentage (%) | 30.02 |
| People dissatisfied | Toilet | Scenario 03.aps | Percentage (%) | 26.87 |
| People dissatisfied | Store 02 | Scenario 03.aps | Percentage (%) | 28.63 |
| People dissatisfied | Reception | Scenario 03.aps | Percentage (%) | 35.67 |
| People dissatisfied | Mechanical room | Scenario 02.aps | Percentage (%) | 29.44 |
| People dissatisfied | Office 01 | Scenario 02.aps | Percentage (%) | 26.33 |
| People dissatisfied | Office 02 | Scenario 02.aps | Percentage (%) | 26.00 |
| People dissatisfied | Store 01 | Scenario 02.aps | Percentage (%) | 26.10 |
| People dissatisfied | Lobby 01 | Scenario 02.aps | Percentage (%) | 27.40 |
| People dissatisfied | Waiting room | Scenario 02.aps | Percentage (%) | 33.45 |
| People dissatisfied | Lobby 02 | Scenario 02.aps | Percentage (%) | 30.04 |
| People dissatisfied | Toilet | Scenario 02.aps | Percentage (%) | 26.90 |
| People dissatisfied | Store 02 | Scenario 02.aps | Percentage (%) | 28.66 |
| People dissatisfied | Reception | Scenario 02.aps | Percentage (%) | 35.74 |
| People dissatisfied | Mechanical room | Scenario 01.aps | Percentage (%) | 29.44 |
| People dissatisfied | Office 01 | Scenario 01.aps | Percentage (%) | 26.33 |
| People dissatisfied | Office 02 | Scenario 01.aps | Percentage (%) | 26.01 |
| People dissatisfied | Store 01 | Scenario 01.aps | Percentage (%) | 26.10 |
| People dissatisfied | Lobby 01 | Scenario 01.aps | Percentage (%) | 27.40 |
| People dissatisfied | Waiting room | Scenario 01.aps | Percentage (%) | 33.49 |
| People dissatisfied | Lobby 02 | Scenario 01.aps | Percentage (%) | 30.07 |
| People dissatisfied | Toilet | Scenario 01.aps | Percentage (%) | 26.92 |
| People dissatisfied | Store 02 | Scenario 01.aps | Percentage (%) | 28.69 |
| People dissatisfied | Reception | Scenario 01.aps | Percentage (%) | 35.81 |
| People dissatisfied | Mechanical room | Basic Model.aps | Percentage (%) | 29.95 |
| People dissatisfied | Office 01 | Basic Model.aps | Percentage (%) | 26.55 |
| People dissatisfied | Office 02 | Basic Model.aps | Percentage (%) | 26.71 |
| People dissatisfied | Store 01 | Basic Model.aps | Percentage (%) | 26.24 |
| People dissatisfied | Lobby 01 | Basic Model.aps | Percentage (%) | 27.70 |
| People dissatisfied | Waiting room | Basic Model.aps | Percentage (%) | 37.07 |
| People dissatisfied | Lobby 02 | Basic Model.aps | Percentage (%) | 33.21 |
| People dissatisfied | Toilet | Basic Model.aps | Percentage (%) | 29.74 |
| People dissatisfied | Store 02 | Basic Model.aps | Percentage (%) | 32.37 |
| People dissatisfied | Reception | Basic Model.aps | Percentage (%) | 43.40 |

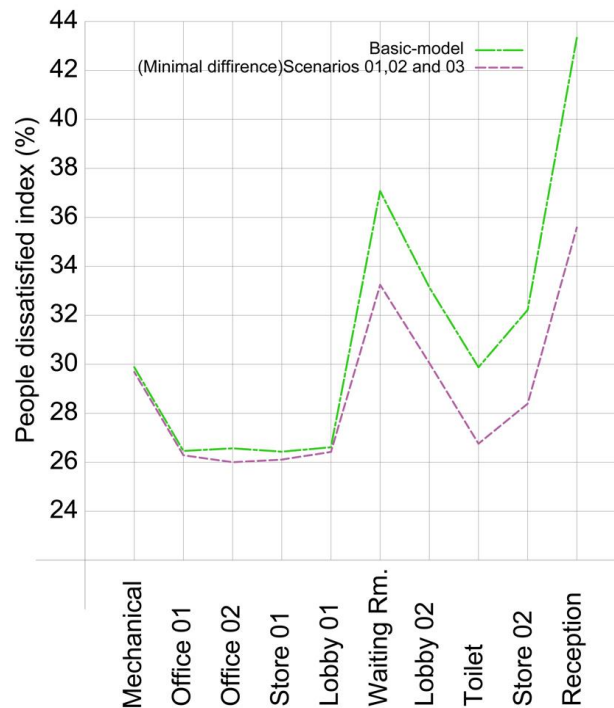


Figure 5.16. Combined diagram of the basic model results and the three scenarios results (author 2019)

Moreover, the typical mean dissatisfied index value of three scenarios had slight variation comparing to each other (table 5.19 and figure 5.16). Comparing to the basic model, the mean values had an average improvement of 7.18% in scenario 01, 7.37% in scenario 02 and 7.54% in scenario 03. In the waiting room, the mean values had an average improvement of 9.7% in scenario 01, 9.8% in scenario 02 and 9.85% in scenario 03. In the reception room, the mean value had an average improvement of 17.5% in scenario 01, 17.6% in scenario 02 and 17.8% in scenario 03. Other than the targeted rooms with windows, mean value was improved also in adjacent rooms which were lobby 02, toilet and store 02.

5.2.4 Scenarios 01,02 and 03 daylight analysis

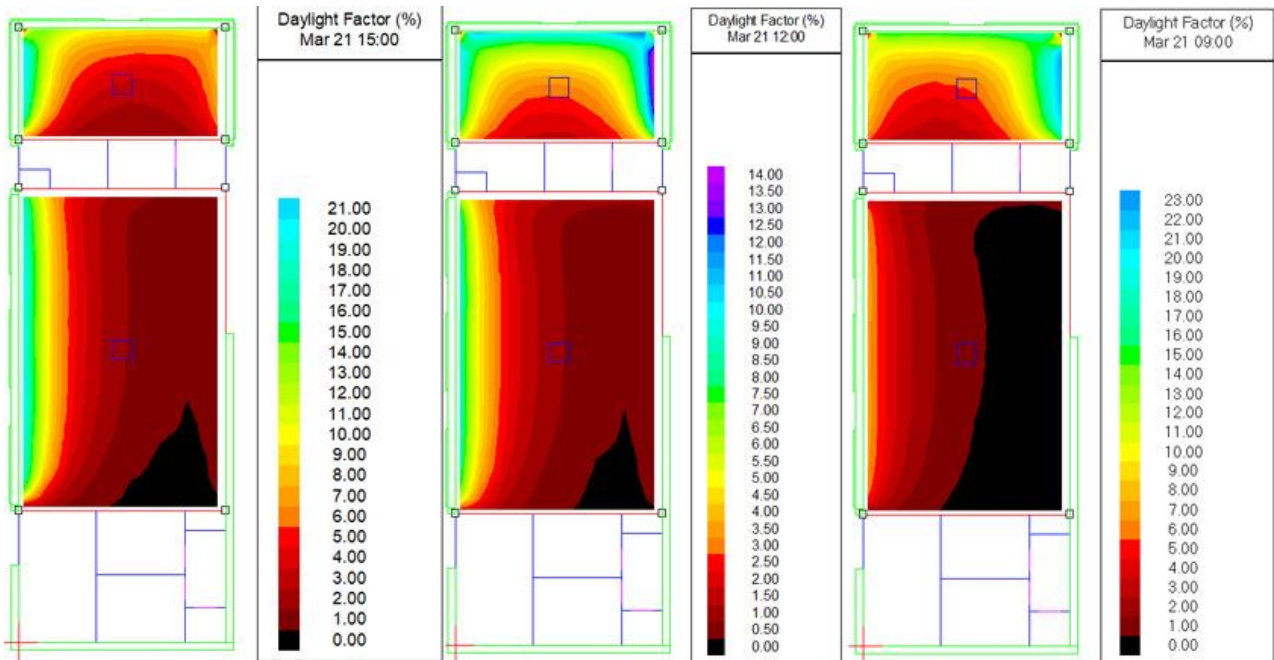


Figure 5.17. Scenarios 01,02 and 03 daylight factor simulation results on the 21st of March (author 2019).

Table 5.20. Scenarios 01,02 and 03 21st of March results summery (author 2019).

| Room | Date | Hour | Daylight factor | | | Daylight illuminance | | | Uniformity |
|----------------|---------------------------|-------|-----------------|------|-------|----------------------|------------|-------------|------------|
| | | | Min. | Ave. | Max. | Min. | Ave. | Max. | |
| Waiting room | 21 st of March | 9:00 | 0.4% | 2.0% | 7.5% | 31.8 lux | 149.35 lux | 569.85 lux | 0.21 |
| Reception room | 21 st of March | 9:00 | 2.6% | 9.8% | 23.2% | 197.23 lux | 746.23 lux | 1758.74 lux | 0.26 |
| Waiting room | 21 st of March | 12:00 | 0.3% | 2.0% | 9.1% | 30.80 lux | 173.17 lux | 806.31 lux | 0.18 |
| Reception room | 21 st of March | 12:00 | 1.8% | 5.9% | 14.5% | 161.4 lux | 519.08 lux | 1277.09 lux | 0.31 |
| Waiting room | 21 st of March | 15:00 | 0.5% | 4.3% | 20.3% | 42.63 lux | 354.58 lux | 1694.06 lux | 0.12 |
| Reception room | 21 st of March | 15:00 | 2.0% | 6.9% | 21.0% | 168.97 lux | 571.03 lux | 1749.83 lux | 0.30 |

On 21st of March, the results show that the average daylighting levels in the waiting room are lower than the requirements in first two cases while it is within the acceptable range in the third case and the average daylighting levels in the reception room are exceeding the requirement in all cases. Average DF was within the acceptable range which is above 2% (figures 5.17,5.21,5.22,5.23,5.24 and table 5.20).

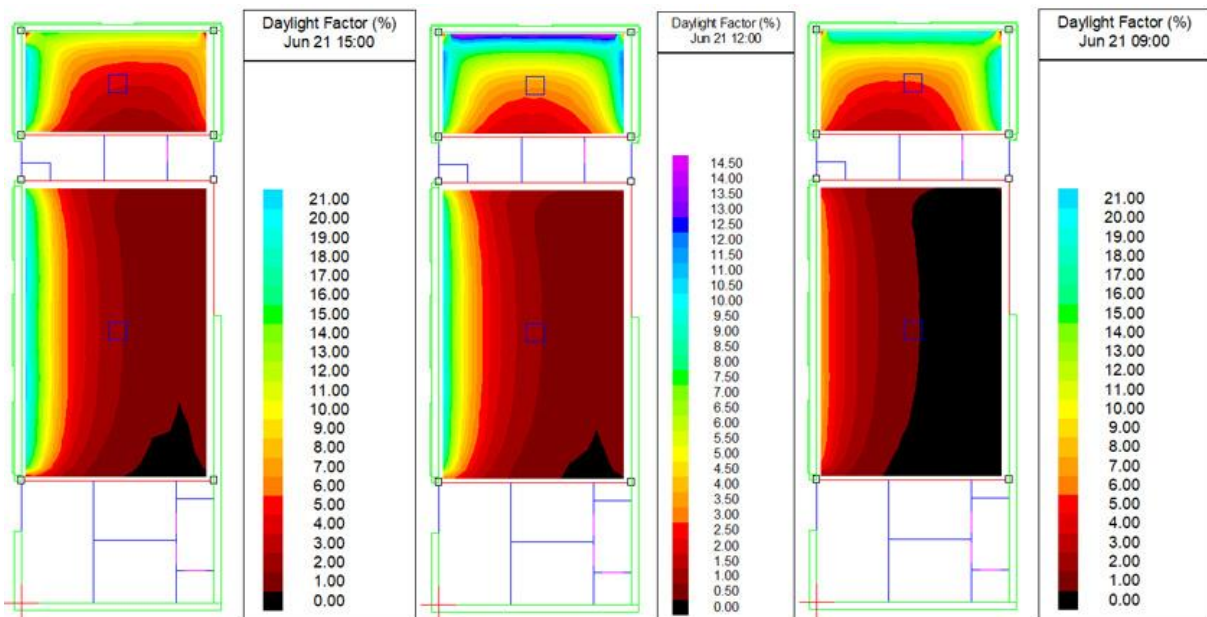


Figure 5.18. Scenarios 01,02 and 03 daylight factor simulation results on the 21st of June (author 2019).

Table 5.21. Scenarios 01,02 and 03 21st of June results summery (author 2019).

| Room | Date | Hour | Daylight factor | | | Daylight illuminance | | | Uniformity |
|----------------|--------------------------|-------|-----------------|-------|-------|----------------------|------------|-------------|------------|
| | | | Min. | Ave. | Max. | Min. | Ave. | Max. | |
| Waiting room | 21 st of June | 9:00 | 0.4% | 1.8% | 7.5% | 33.2 lux | 150.78 lux | 616.01 lux | 0.22 |
| Reception room | 21 st of June | 9:00 | 2.0% | 10.0% | 21.7% | 161.76 lux | 828.22 lux | 1789.94 lux | 0.20 |
| Waiting room | 21 st of June | 12:00 | 0.4% | 2.1% | 10.3% | 70.49 lux | 390.64 lux | 1919.86 lux | 0.18 |
| Reception room | 21 st of June | 12:00 | 1.5% | 6.5% | 14.9% | 274.70 lux | 1203.9 lux | 2783.58 lux | 0.23 |
| Waiting room | 21 st of June | 15:00 | 0.6% | 4.5% | 21.4% | 53.12 lux | 381.43 lux | 1834.3 lux | 0.14 |
| Reception room | 21 st of June | 15:00 | 1.6% | 7.7% | 22.0% | 138.03 lux | 656.84 lux | 1881.78 lux | 0.21 |

On 21st of June, the results were similar to the 12st of March results with slight differences, except for the second case where lux levels were almost doubled. There were minimal variations in the average DF levels. In the first case, in the waiting room, average DF was slightly lower than recommended level (figures 5.18,5.21,5.22,5.23,5.24 and table 5.21).

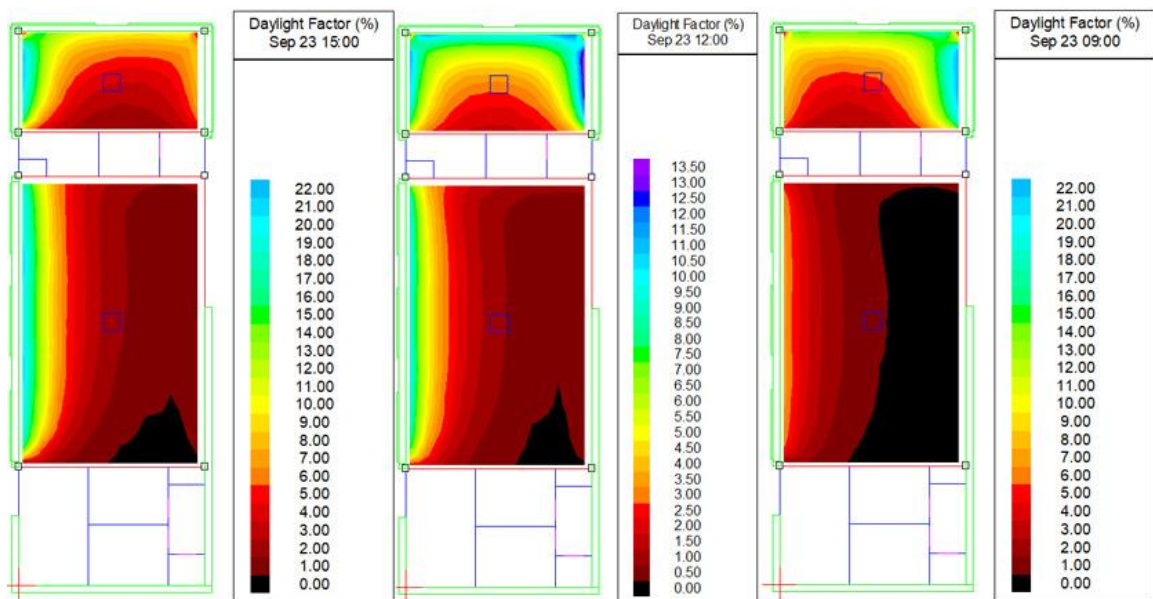


Figure 5.19. Scenarios 01,02 and 03 daylight factor simulation results on the 23 rd of September (author 2019).

Table 5.22. Scenarios 01,02 and 03 23rd of September results summary (author 2019).

| Room | Date | Hour | Daylight factor | | | Daylight illuminance | | | Uniformity |
|----------------|---------------------------|-------|-----------------|------|-------|----------------------|------------|-------------|------------|
| | | | Min. | Ave. | Max. | Min. | Ave. | Max. | |
| Waiting room | 23 rd of Sept. | 9:00 | 0.4% | 1.9% | 7.4% | 32.32 lux | 150.43 lux | 577.88 lux | 0.21 |
| Reception room | 23 rd of Sept. | 9:00 | 2.5% | 9.3% | 23.0% | 197.71 lux | 731.60 lux | 1800.99 lux | 0.27 |
| Waiting room | 23 rd of Sept. | 12:00 | 0.4% | 2.1% | 9.9% | 31.37 lux | 184.74 lux | 875.75 lux | 0.17 |
| Reception room | 23 rd of Sept. | 12:00 | 1.8% | 5.9% | 13.7% | 162.99 lux | 519.27 lux | 1215.85 lux | 0.31 |
| Waiting room | 23 rd of Sept. | 15:00 | 0.6% | 4.7% | 21.4% | 45.60 lux | 385.12 lux | 1756.21 lux | 0.12 |
| Reception room | 23 rd of Sept. | 15:00 | 2.0% | 6.8% | 20.8% | 175.71 lux | 596.96 lux | 1700.63 lux | 0.29 |

On 23rd of September, the results were similar to the 21st of June results, except for the second case where average lux levels were reduced to adequate levels. There were minimal variations in the DF levels. In the first case, in the waiting room, average DF was slightly lower than recommended level (figures 5.19,5.21,5.22,5.23,5.24 and table 5.22).

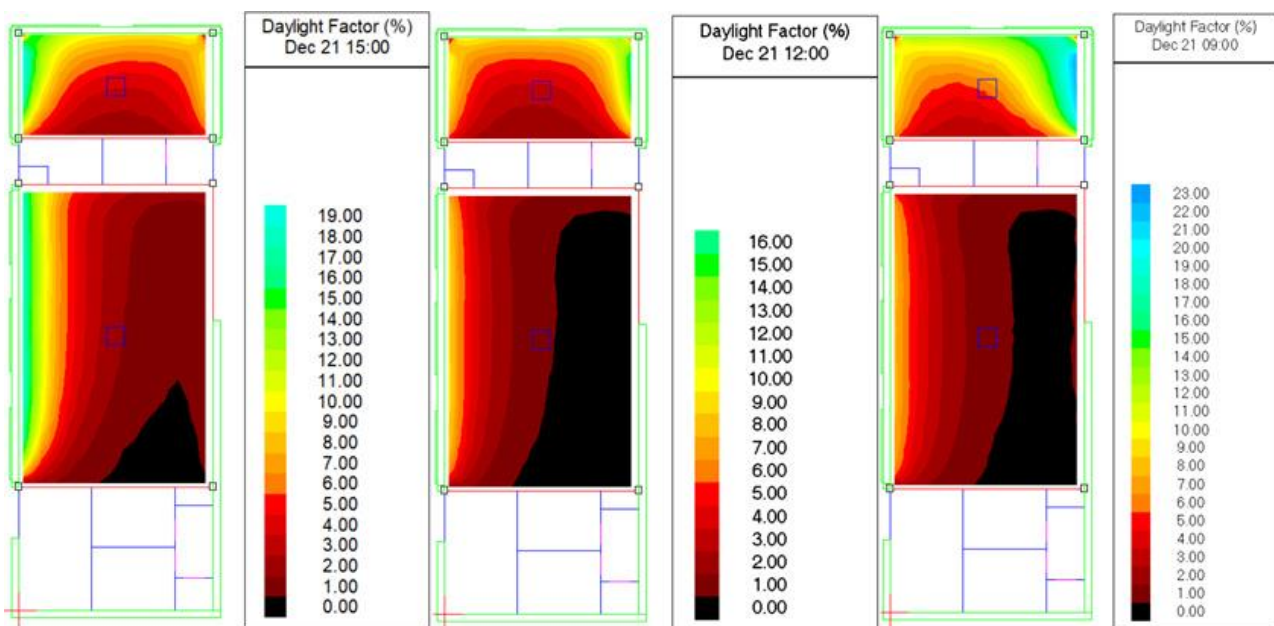


Figure 5.20 Scenarios 01,02 and 03 daylight factor simulation results on the 21st of December (author 2019).

Table 5.23. Scenarios 01,02 and 03 21st of December results summery (author 2019).

| Room | Date | Hour | Daylight factor | | | Daylight illuminance | | | Uniformity |
|----------------|--------------------------|-------|-----------------|------|-------|----------------------|------------|-------------|------------|
| | | | Min. | Ave. | Max. | Min. | Ave. | Max. | |
| Waiting room | 21 st of Dec. | 9:00 | 0.5% | 2.2% | 8.4% | 30.60 lux | 139.39 lux | 522.94 lux | 0.22 |
| Reception room | 21 st of Dec. | 9:00 | 3.0% | 9.7% | 23.1% | 187.04 lux | 601.45 lux | 1431.43 lux | 0.31 |
| Waiting room | 21 st of Dec. | 12:00 | 0.4% | 2.1% | 9.4% | 31.44 lux | 175.30 lux | 768.47 lux | 0.18 |
| Reception room | 21 st of Dec | 12:00 | 2.0% | 6.2% | 16.5% | 162.90 lux | 503.49 lux | 1342.86 lux | 0.32 |
| Waiting room | 21 st of Dec. | 15:00 | 0.5% | 4.2% | 18.8% | 35.35 lux | 294.39 lux | 1320.02 lux | 0.12 |
| Reception room | 21 st of Dec | 15:00 | 2.2% | 6.9% | 19.9% | 155.98 lux | 486.90 lux | 1394.73 lux | 0.32 |

In all cases average daylighting levels and average DF were low in half of the waiting room area. On 21st of December, the average DF results were similar to other days with minimal variation. Average lux levels were still exceeding the requirements in the reception room while lux levels in waiting room were low in all cases. In all cases uniformity varied from low to very low (figures 5.20,5.21,5.22,5.23,5.24 and table 5.23).

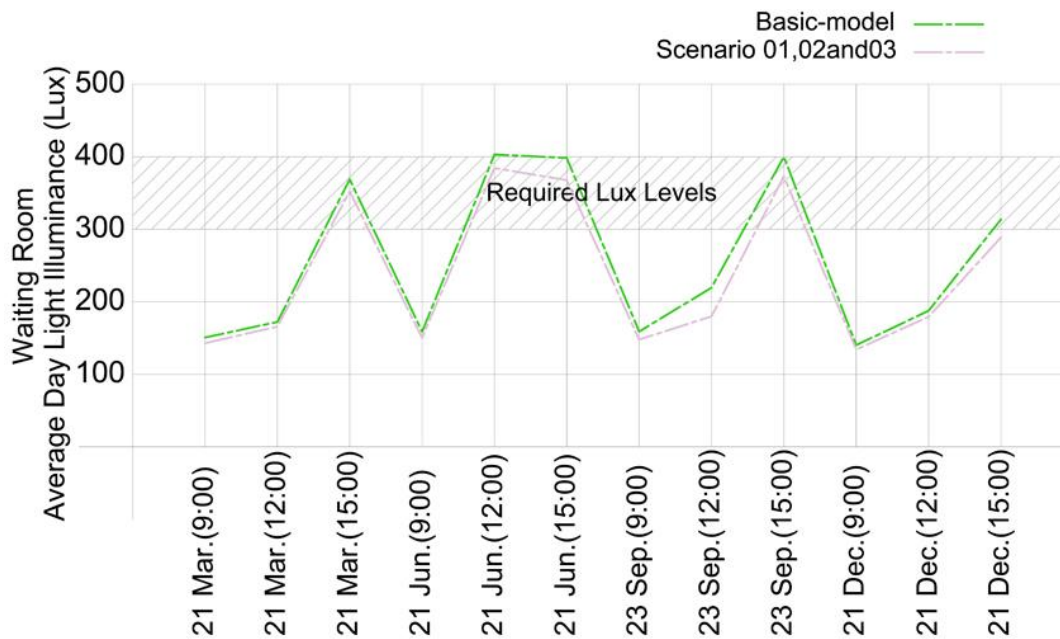


Figure 5.21. Combined diagram of the basic model DI results and the three scenarios DI results in waiting room (author 2019).

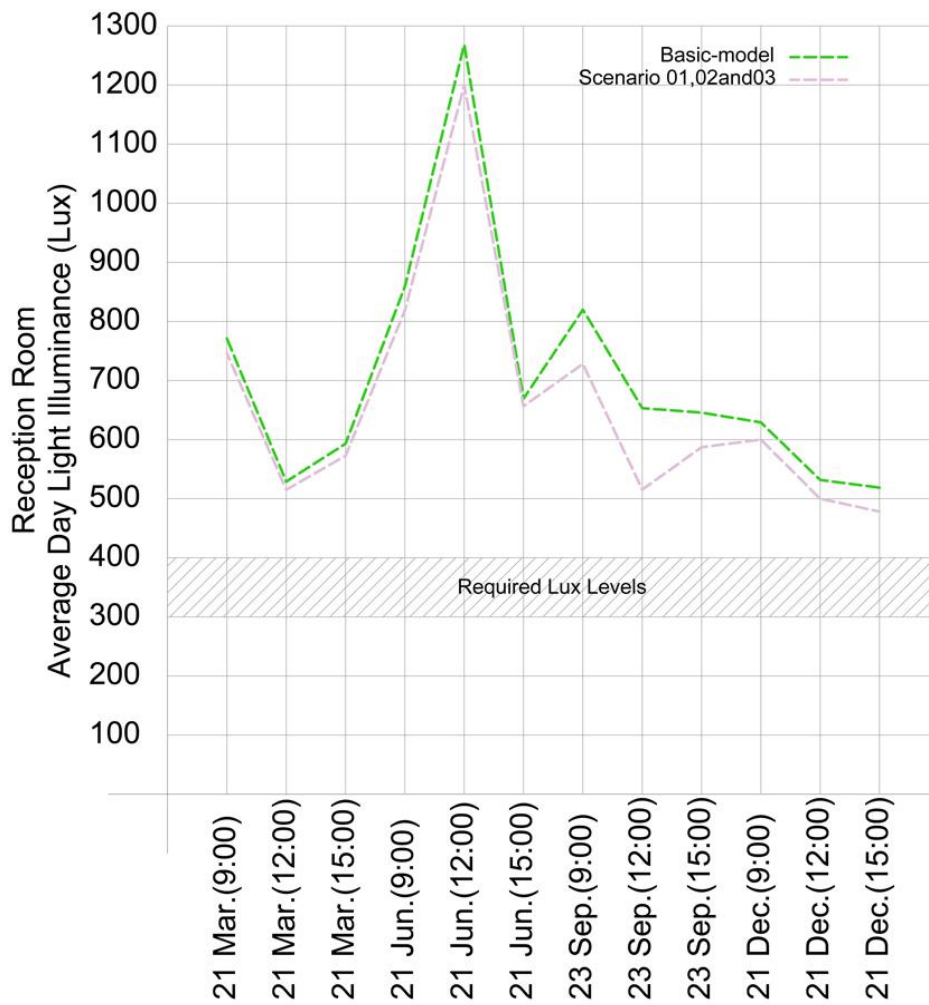


Figure 5.22. Combined diagram of the basic model DI results and the three scenarios DI results in reception room (author 2019).

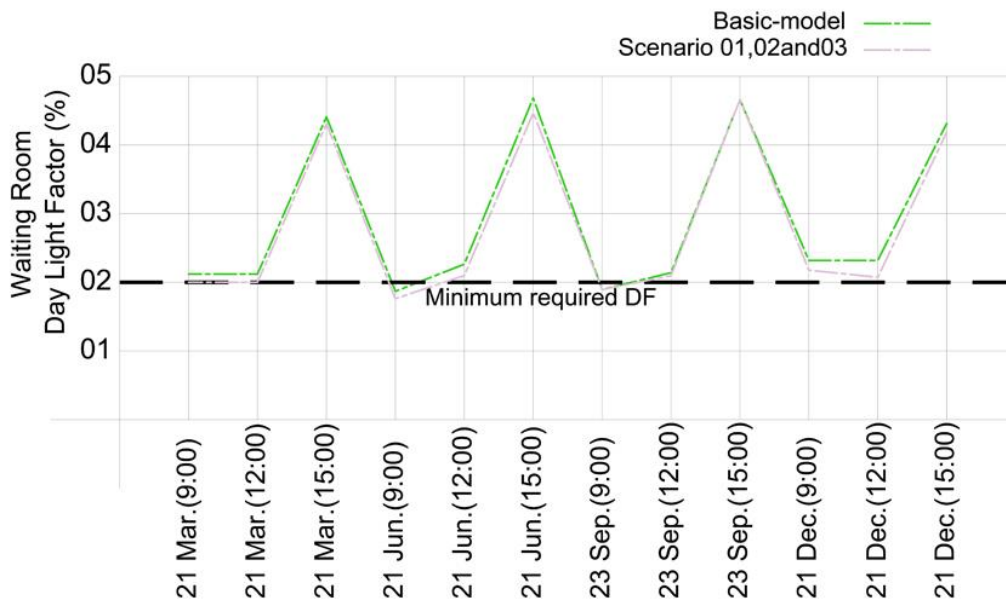


Figure 5.23. Combined diagram of the basic model DF results and the three scenarios DF results in the waiting room (author 2019)

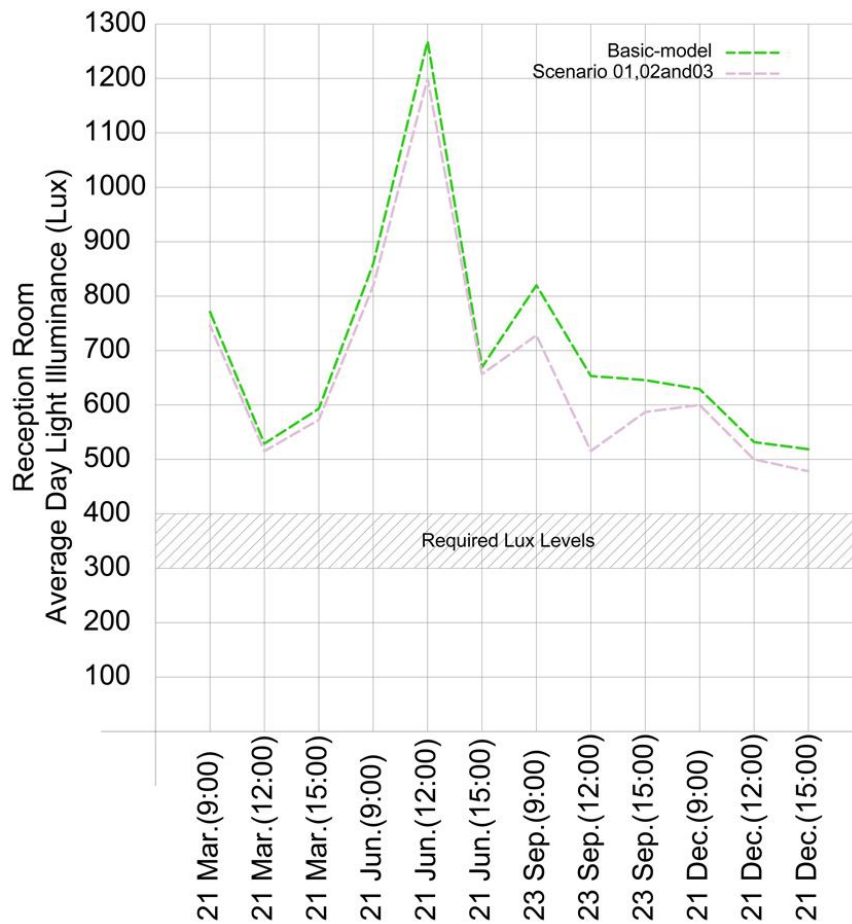


Figure 5.24. Combined diagram of the basic model DF results and the three scenarios DF results in reception room (author 2019)

Comparing to the basic-model, the addition of the double-layers cushions reduced daylighting lux levels by minimum 3.0% and maximum 20.9%. Furthermore, the change reduced average DF by minimum 0.0% and maximum 10.5%. Uniformity changes varied from 0.0% to -7.7% (figures 5.21,5.22,5.23,5.24 and table 5.24).

Table 5.24. Final comparison between Scenarios 01,02 and 03 and basic model (author 2019).

| Scenario | Date | Hour | Average daylight factor reduction | Average daylight illuminance reduction | Uniformity increment |
|--------------------|---------------------------|-------|-------------------------------------------|--------------------------------------------|---------------------------------------------|
| Scenario 1,2and 3. | 21 st of Mar. | 9:00 | Waiting room 4.7% Reception room 4.8% | Waiting room 4.4% Reception room 4.5% | Waiting room -4.5% Reception room 0.0% |
| Scenario 1,2and 3. | 21 st of Mar. | 12:00 | Waiting room 4.7% Reception room 4.8% | Waiting room 4.4% Reception room 4.4% | Waiting room 0.0% Reception room 3.3% |
| Scenario 1,2and 3. | 21 st of Mar. | 15:00 | Waiting room 2.3% Reception room 4.2% | Waiting room 4.3% Reception room 3.5% | Waiting room -7.6% Reception room 0.0% |
| Scenario 1,2and 3. | 21 st of Jun. | 9:00 | Waiting room 5.2% Reception room 4.8% | Waiting room 5.0% Reception room 4.40% | Waiting room 4.7% Reception room 5.2% |
| Scenario 1,2and 3. | 21 st of Jun. | 12:00 | Waiting room 4.5% Reception room 4.4% | Waiting room 4.4% Reception room 4.5% | Waiting room 5.5% Reception room 4.5% |
| Scenario 1,2and 3. | 21 st of Jun. | 15:00 | Waiting room 4.3% Reception room 3.8% | Waiting room 4.3% Reception room 4.7% | Waiting room 0.00% Reception room 0.00% |
| Scenario 1,2and 3. | 23 rd of Sept. | 9:00 | Waiting room 0.0% Reception room 8.8% | Waiting room 3.8% Reception room 8.8% | Waiting room 0.00% Reception room 17.40% |
| Scenario 1,2and 3. | 23 rd of Sept. | 12:00 | Waiting room 0.0% Reception room 7.8% | Waiting room 16.4% Reception room 20.9% | Waiting room 0.00% Reception room 16.13% |
| Scenario 1,2and 3. | 23 rd of Sept. | 15:00 | Waiting room 0.0% Reception room 10.5% | Waiting room 3.0% Reception room 7.8% | Waiting room -7.70% Reception room 7.40% |
| Scenario 1,2and 3. | 21 st of Dec. | 9:00 | Waiting room 4.3% Reception room 4.9% | Waiting room 4.1% Reception room 4.7% | Waiting room 0.0% Reception room 0.0% |
| Scenario 1,2and 3. | 21 st of Dec. | 12:00 | Waiting room 8.6% Reception room 4.5% | Waiting room 4.30% Reception room 4.6% | Waiting room 0.0% Reception room 0.0% |
| Scenario 1,2and 3. | 21 st of Dec. | 15:00 | Waiting room 4.8% Reception room 0.4% | Waiting room 3.9% Reception room 4.5% | Waiting room 0.0% Reception room 0.0% |

5.2.5 Scenarios 01,02 and 03 glare analysis

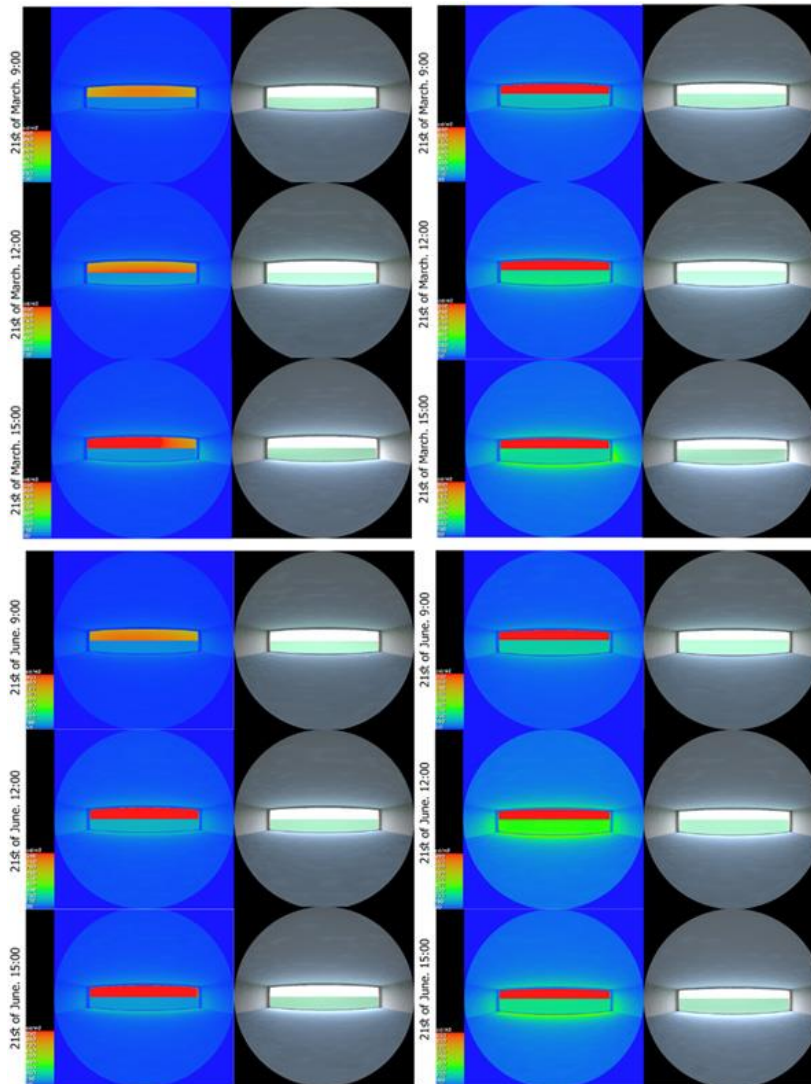


Figure 5.25. Waiting room luminance maps on the 21st of March (top images) and 21st of June (bottom images). The images on the left show scenarios 01, 02 and 03 results and the images on the right show the basic model results (author 2019).

On 21st of March, in the waiting room, average luminance levels from the glazed wall reached 800 cd/m² in first two cases and 900 cd/m² in third case. Comparing to the basic model, this is considered 15.7% reduction in the first two cases and 5.2% reduction in the third case. On 21st of June, in the waiting room, average luminance levels from the glazed wall reached 800 cd/m² in first case and 900 cd/m² in second and third case. Comparing to the basic model, this is considered 15.7% reduction in the first cases and 5.2% reduction in the second and third case (figure 5.25 and table 5.27).

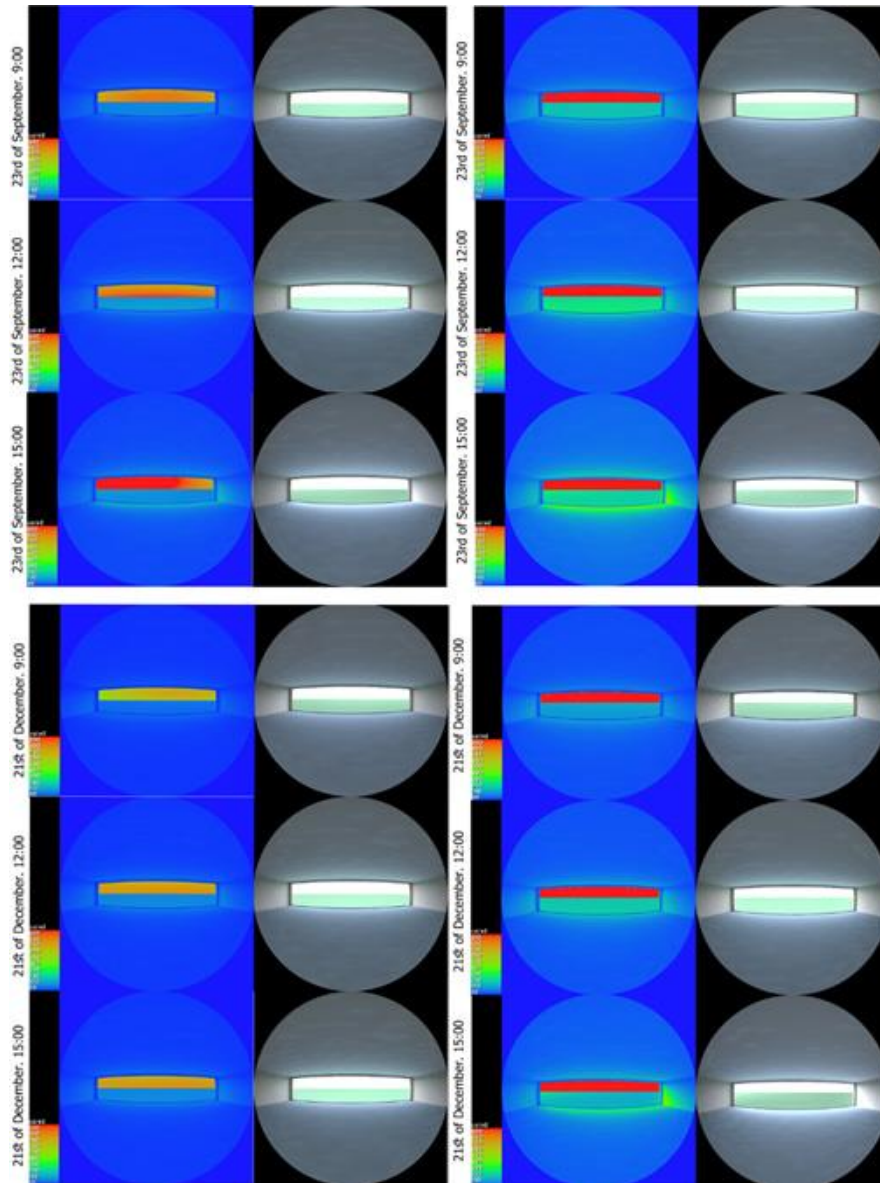


Figure 5.26. Waiting room luminance maps on the 23rd of September (top images) and 21st of December (bottom images). The images on the left show scenarios01,02 and 03 results and the images on the right show the basic model results (author 2019).

On 23rd of September, in the waiting room, average luminance levels from the glazed wall reached 800 cd/m² in first two cases and 900 cd/m² in third case. Comparing to the basic model, this is considered 15.7% reduction in the first two cases and 5.2% reduction in the third case. On 21st of December, in the waiting room, average luminance levels from the glazed wall reached 750 cd/m² in all cases which is, comparing to the basic model, is equal to 21% reduction (figure 5.26 and table 5.27).

Table 5.25. DGI levels from different angles from nadir for the four days at 9:00,12:00 and 15:00 (author 2019).

| Angle | 60 | 50 | 40 | 30 | 20 | 10 | 0 | -10 | -20 | -30 | -40 | -50 | -60 |
|-------------------------------------------|------|------|------|------|------|------|------|------|------|------|------|------|------|
| 09:00 21 st of March | 12.6 | 14.5 | 16. | 17.6 | 18.7 | 19.5 | 19.8 | 19.5 | 18.7 | 17.6 | 16.2 | 14.6 | 12.6 |
| 12:00 21 st of March | 12.5 | 14.4 | 16.1 | 17.4 | 18.5 | 19.3 | 19.6 | 19.3 | 18.5 | 17.4 | 16.1 | 14.4 | 12.5 |
| 15:00 21 st of March | 13.1 | 15.1 | 16.7 | 18.0 | 19.1 | 19.9 | 20.1 | 19.9 | 18.9 | 17.9 | 16.5 | 14.9 | 12.9 |
| 09:00 21 st of June | 12.5 | 14.5 | 16.1 | 17.5 | 18.6 | 19.5 | 19.7 | 19.5 | 18.6 | 17.5 | 16.2 | 14.5 | 12.6 |
| 12:00 21 st of June | 14.0 | 15.9 | 17.5 | 18.9 | 20.1 | 20.8 | 21.1 | 20.8 | 20.1 | 18.9 | 17.6 | 16.9 | 14.1 |
| 15:00 21 st of June | 13.2 | 15.1 | 16.8 | 18.1 | 19.1 | 20.1 | 20.3 | 20.1 | 19.1 | 18.1 | 16.8 | 15.1 | 13.2 |
| 09:00 23 rd of September | 12.6 | 14.5 | 16.2 | 17.6 | 18.7 | 19.5 | 19.8 | 19.5 | 18.7 | 17.6 | 16.2 | 14.6 | 12.6 |
| 12:00 23 rd of September | 12.5 | 14.4 | 16.1 | 17.4 | 18.5 | 19.3 | 19.6 | 19.3 | 18.5 | 17.4 | 16.1 | 14.1 | 12.5 |
| 15:00 23 rd of September | 13.2 | 15.2 | 16.8 | 18.1 | 19.2 | 19.9 | 20.2 | 19.9 | 19.1 | 17.9 | 16.6 | 14.9 | 13.1 |
| 09:00 21 st of December | 12.2 | 14.1 | 15.8 | 17.2 | 18.3 | 19.2 | 19.4 | 19.2 | 18.3 | 17.2 | 15.9 | 14.2 | 12.2 |
| 12:00 21 st of December | 12.3 | 14.3 | 15.9 | 17.3 | 18.4 | 19.2 | 19.5 | 19.2 | 18.3 | 17.2 | 15.9 | 14.3 | 12.3 |
| 15:00 21 st of December | 12.7 | 14.6 | 16.3 | 17.6 | 18.6 | 19.4 | 19.6 | 19.3 | 18.5 | 17.3 | 15.9 | 14.3 | 12.4 |

According to the DGI analysis there is a perceptible glare in all cases, as it exceeded 18 in the centre of the glazed wall. However, it did not reach the high disturbance level which is above 24 (table 5.25).

Table 5.26. GVCP levels from different angles from nadir for the four days at 9:00,12:00 and 15:00 (author 2019).

| Angle | 60 | 50 | 40 | 30 | 20 | 10 | 0 | -10 | -20 | -30 | -40 | -50 | -60 |
|-------------------------------------------|------|------|------|------|------|------|------|------|------|------|------|------|------|
| 09:00 21 st of March | 62.5 | 47.4 | 34.7 | 25.3 | 18.9 | 14.9 | 13.5 | 14.7 | 18.9 | 25.3 | 34.9 | 49.4 | 62.5 |
| 12:00 21 st of March | 62.3 | 47.2 | 34.7 | 25.3 | 19.0 | 14.9 | 13.7 | 14.9 | 19.1 | 25.5 | 34.9 | 47.4 | 62.5 |
| 15:00 21 st of March | 54.7 | 39.6 | 27.9 | 19.7 | 14.4 | 11.1 | 10.1 | 11.2 | 14.6 | 20.2 | 28.7 | 40.6 | 55.8 |
| 09:00 21 st of June | 62.4 | 47.3 | 34.6 | 25.3 | 18.9 | 14.8 | 14.0 | 14.8 | 18.9 | 25.3 | 34.7 | 47.3 | 62.5 |
| 12:00 21 st of June | 45.4 | 30.9 | 20.5 | 13.9 | 9.5 | 7.1 | 6.3 | 7.1 | 9.5 | 13.7 | 20.5 | 30.9 | 45.4 |
| 15:00 21 st of June | 52.9 | 37.9 | 26.4 | 18.5 | 13.3 | 10.1 | 9.2 | 10.2 | 13.4 | 18.5 | 26.6 | 38.2 | 53.2 |
| 09:00 23 rd of September | 62.2 | 47.1 | 34.4 | 25.1 | 18.6 | 14.5 | 13.4 | 14.5 | 18.6 | 25.1 | 34.4 | 47.1 | 62.2 |
| 12:00 23 rd of September | 62.2 | 47.2 | 34.6 | 25.3 | 18.9 | 14.9 | 13.7 | 14.9 | 19.1 | 25.5 | 34.8 | 47.4 | 62.4 |
| 15:00 23 rd of September | 53.7 | 38.7 | 27.1 | 19.1 | 13.8 | 10.6 | 9.7 | 10.7 | 14.1 | 19.6 | 27.9 | 39.8 | 54.9 |
| 09:00 21 st of December | 67.1 | 52.1 | 39.2 | 29.2 | 22.2 | 17.6 | 16.2 | 17.6 | 22.1 | 29.1 | 39.1 | 52.1 | 66.9 |
| 12:00 21 st of December | 64.3 | 49.3 | 36.6 | 27.1 | 20.4 | 16.1 | 14.9 | 16.2 | 20.5 | 27.2 | 36.9 | 49.6 | 46.6 |
| 15:00 21 st of December | 60.1 | 44.9 | 32.7 | 23.8 | 17.8 | 13.9 | 12.9 | 14.3 | 18.4 | 24.8 | 34.2 | 46.9 | 62.0 |

GVCP analysis showed that minimum percentage of satisfied occupants was 6.34% at 12:00 on 21st of June to and maximum was 16.22% at 9:00 on 21st of December when looking at the middle of the glazed wall. The minimum percentage of satisfied occupants was 45.34% at 12:00 on 21st of June to and maximum was 67.03% at 9:00 on 21st of December when looking at the edges of the glazed wall (table 5.26).

Table 5.27. Final comparison of the waiting room results between Scenarios 01,02 and 03 and basic model (author 2019).

| Scenario | Date | Hour | Average DGI reduction | Average GVCP increment |
|-------------------|---------------------------|-------|-----------------------|------------------------|
| Scenarios 1,2and3 | 21 st of Mar. | 9:00 | 10.5% | 109.4% |
| Scenarios 1,2and3 | 21 st of Mar. | 12:00 | 11.2% | 108.4% |
| Scenarios 1,2and3 | 21 st of Mar. | 15:00 | 10.6% | 126.2% |
| Scenarios 1,2and3 | 21 st of Jun. | 9:00 | 11.5% | 109.8% |
| Scenarios 1,2and3 | 21 st of Jun. | 12:00 | 10.7% | 144.8% |
| Scenarios 1,2and3 | 21 st of Jun. | 15:00 | 10.7% | 128.7% |
| Scenarios 1,2and3 | 23 rd of Sept. | 9:00 | 13.4% | 111.5% |
| Scenarios 1,2and3 | 23 rd of Sept. | 12:00 | 12.3% | 135.8% |
| Scenarios 1,2and3 | 23 rd of Sept. | 15:00 | 7.0% | 132.8% |
| Scenarios 1,2and3 | 21 st of Dec. | 9:00 | 14% | 101.9% |
| Scenarios 1,2and3 | 21 st of Dec. | 12:00 | 18.8% | 104.8% |
| Scenarios 1,2and3 | 21 st of Dec. | 15:00 | 11.6% | 114.4% |

Comparing to the basic model minimum DGI reduction was 7% and maximum DGI reduction was 18.8% while the minimum GVCP improvement was 101.9% and maximum GVCP improvement was 135.8% (table 5.27).

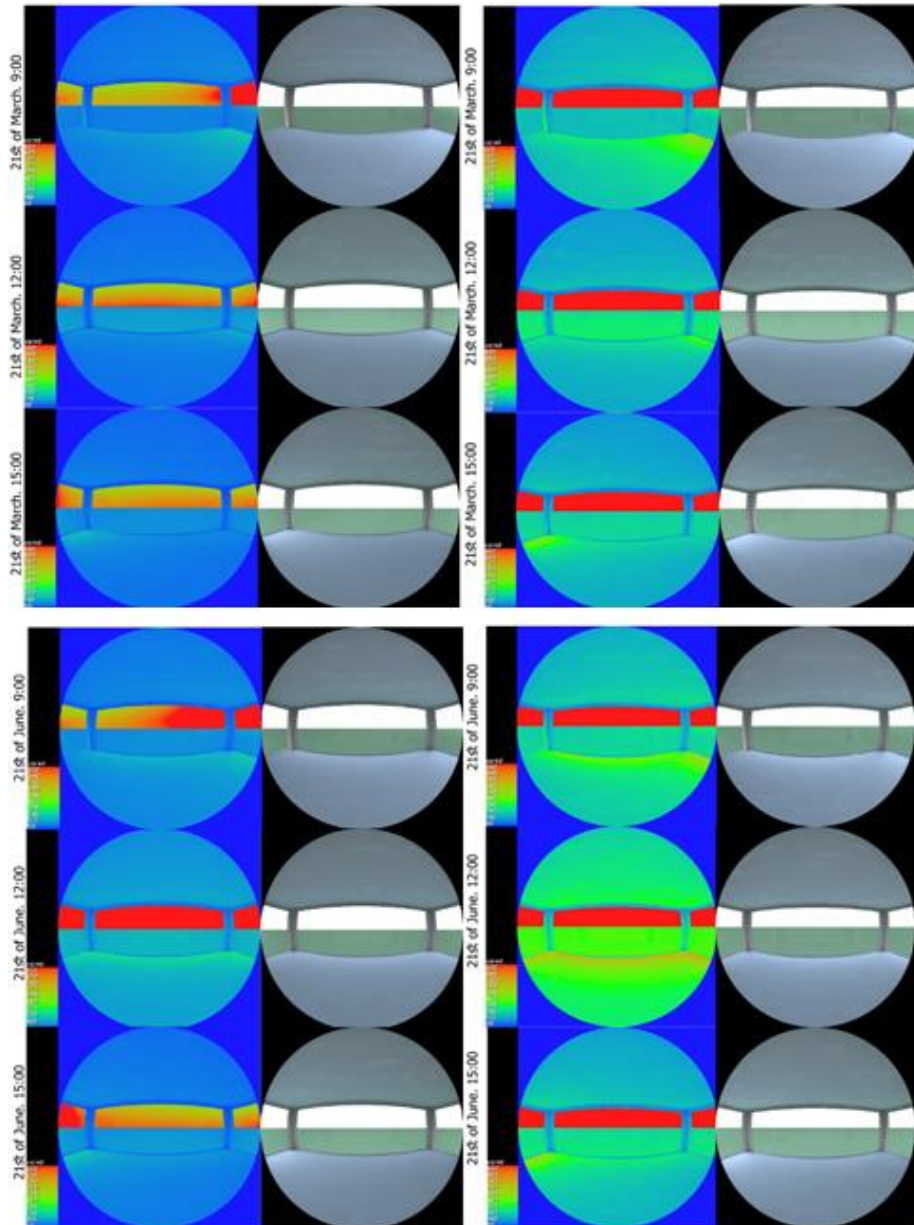


Figure 5.27. Reception room luminance maps on the 21st of March (top images) and 21st of June (bottom images). The images on the left show scenarios01,02 and 03 results and the images on the right show the basic model results (author 2019).

On 21st of March, in the reception room, average luminance levels from the glazed wall reached 700 cd/m² in all cases. Thus, comparing to the basic model results, there was 26.3% reduction. On 21st of June, in the reception room, average luminance levels from the glazed wall reached 800 cd/m² in the first case, 900 cd/m² in second case and 750 cd/m² in the third case. Hence, comparing to the basic model results, the reduction was 15.7%, 5.2% and 21% respectively (figure 5.27).

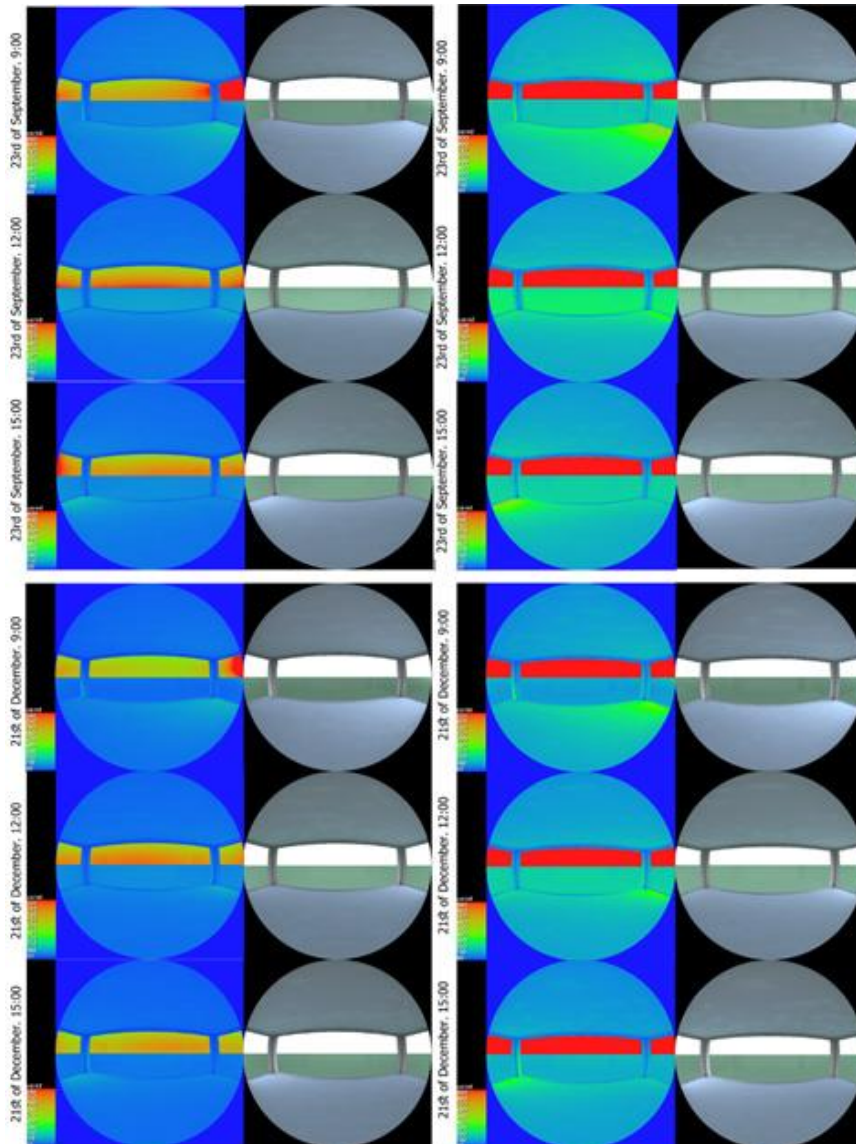


Figure 5.28. Reception room luminance maps on the 23rd of September (top images) and 21st of December (bottom images). The images on the left show scenarios01,02 and 03 results and the images on the right show the basic model results (author 2019).

On 23rd of September and 21st of December, in the reception room, average luminance levels from the glazed wall reached 700 cd/m² in all cases. Thus, comparing to the basic model results, there was 26.3% reduction (figure 5.28).

Table 5.28. DGI levels from different angles from nadir for the four days at 9:00,12:00 and 15:00 (author 2019).

| Angle | 60 | 50 | 40 | 30 | 20 | 10 | 0 | -10 | -20 | -30 | -40 | -50 | -60 |
|-------------------------------------------|------|------|------|------|------|------|------|------|------|------|------|------|------|
| 09:00 21 st of March | 0.00 | 0.00 | 0.00 | 0.00 | 1.48 | 4.6 | 7.5 | 10.1 | 12.4 | 14.4 | 16.2 | 17.7 | 18.9 |
| 12:00 21 st of March | 11.1 | 10.6 | 10.4 | 10.5 | 10.8 | 0.00 | 11.5 | 11.1 | 10.8 | 10.8 | 11.1 | 11.7 | 12.4 |
| 15:00 21 st of March | 13.9 | 12.4 | 10.6 | 8.5 | 3.7 | 1.5 | 1.6 | 0.00 | 0.00 | 0.14 | 2.2 | 3.9 | 5.5 |
| 09:00 21 st of June | 0.00 | 0.00 | 1.5 | 3.9 | 7.1 | 9.3 | 11.3 | 13.2 | 14.8 | 16.2 | 17.4 | 18.3 | 19.1 |
| 12:00 21 st of June | 0.00 | 0.00 | 0.00 | 0.00 | 0.00 | 0.00 | 0.00 | 0.00 | 0.00 | 0.00 | 0.00 | 0.00 | 0.00 |
| 15:00 21 st of June | 15.5 | 14.2 | 12.6 | 10.6 | 8.5 | 3.4 | 0.4 | 0.00 | 0.00 | 0.00 | 0.00 | 0.00 | 0.00 |
| 09:00 23 rd of September | 0.00 | 0.00 | 0.00 | 0.00 | 0.00 | 3.8 | 6.7 | 9.3 | 11.6 | 13.7 | 15.5 | 17.0 | 18.3 |
| 12:00 23 rd of September | 11.1 | 10.6 | 10.5 | 10.6 | 10.9 | 11.4 | 11.7 | 11.4 | 10.9 | 10.9 | 11.0 | 11.5 | 12.2 |
| 15:00 23 rd of September | 14.4 | 12.9 | 11.1 | 9.1 | 6.8 | 4.3 | 1.5 | 0.00 | 0.00 | 0.00 | 0.00 | 0.00 | 0.00 |
| 09:00 21 st of December | 0.00 | 0.00 | 0.00 | 0.00 | 0.00 | 0.81 | 3.93 | 6.8 | 9.3 | 11.6 | 13.6 | 15.4 | 16.8 |
| 12:00 21 st of December | 9.1 | 9.7 | 10.4 | 11.1 | 11.6 | 11.8 | 11.2 | 10.4 | 9.6 | 8.9 | 8.6 | 8.8 | 9.4 |
| 15:00 21 st of December | 8.8 | 8.1 | 8.1 | 8.6 | 9.5 | 10.5 | 11.4 | 12.1 | 12.2 | 11.7 | 10.1 | 9.7 | 8.3 |

According to the DGI analysis there is an imperceptible glare in all cases, as DGI levels were lower than 18 in the centre of the glazed wall (table 5.28).

Table 5.29. GVCP levels from different angles from nadir for the four days at 9:00,12:00 and 15:00 (author 2019).

| Angle | 60 | 50 | 40 | 30 | 20 | 10 | 0 | -10 | -20 | -30 | -40 | -50 | -60 |
|-------------------------------------------|------|------|------|------|------|------|------|------|------|------|------|------|------|
| 09:00 21 st of March | 100 | 100 | 100 | 100 | 97.6 | 91.6 | 79.9 | 63.7 | 46.7 | 32.3 | 21.6 | 14.6 | 10.4 |
| 12:00 21 st of March | 79.2 | 79.1 | 79.8 | 79.6 | 82.9 | 81.8 | 82.8 | 83.4 | 80.9 | 79.6 | 77.8 | 75.6 | 73.0 |
| 15:00 21 st of March | 64.8 | 73.3 | 81.7 | 89.1 | 94.7 | 97.8 | 99.1 | 99.8 | 99.8 | 99.1 | 98.1 | 98.0 | 96.3 |
| 09:00 21 st of June | 100 | 99.8 | 99.2 | 97.6 | 90.9 | 82.4 | 71.2 | 59.1 | 47.5 | 38.4 | 31.7 | 27.1 | 24.1 |
| 12:00 21 st of June | 100 | 100 | 100 | 100 | 100 | 100 | 100 | 100 | 100 | 100 | 100 | 100 | 100 |
| 15:00 21 st of June | 29.9 | 38.7 | 50.3 | 65.8 | 77.5 | 88.7 | 95.7 | 98.8 | 100 | 100 | 100 | 100 | 100 |
| 09:00 23 rd of September | 100 | 100 | 100 | 100 | 100 | 93.9 | 84.1 | 69.2 | 52.5 | 37.4 | 25.8 | 17.8 | 12.8 |
| 12:00 23 rd of September | 79.1 | 79.3 | 79.2 | 78.9 | 82.2 | 80.9 | 82.0 | 82.7 | 80.3 | 79.5 | 77.9 | 76.1 | 73.9 |
| 15:00 23 rd of September | 61.9 | 70.6 | 79.5 | 85.5 | 93.7 | 97.4 | 99.2 | 99.9 | 100 | 100 | 100 | 100 | 100 |
| 09:00 21 st of December | 100 | 100 | 100 | 100 | 100 | 98.5 | 94.3 | 85.6 | 72.5 | 57.5 | 43.5 | 32.2 | 24.1 |
| 12:00 21 st of December | 85.9 | 83.6 | 81.1 | 78.6 | 74.5 | 76.1 | 83.2 | 81.8 | 84.2 | 86.1 | 87.2 | 87.5 | 87.0 |
| 15:00 21 st of December | 84.5 | 89.6 | 88.9 | 87.1 | 84.3 | 80.9 | 77.3 | 62.1 | 61.3 | 65.6 | 71.9 | 79.1 | 86.2 |

GVCP analysis showed that minimum was 71.23% at 9:00 on 21st of June and maximum percentage of satisfied occupants was 100% at 12:00 on 21st of June when looking at the middle of the northern glazed wall. The minimum percentage of satisfied occupants was 29.99% at 15:00 on 21st of June and maximum was 100% at 12:00 on 21st of June when looking at the eastern and western glazed walls (table 5.29).

Comparing to the basic model minimum DGI reduction was 20.7% and maximum DGI reduction was 100% while the minimum GVCP improvement was 3.7% and maximum GVCP improvement was 230.0% (table 5.30).

Table 5.30. Final comparison between Scenarios 01,02 and 03 and basic model (author 2019).

| Scenario | Date | Hour | Average DGI reduction | Average GVCP increment |
|-------------------|---------------------------|-------|-----------------------|------------------------|
| Scenarios 1,2and3 | 21 st of Mar. | 9:00 | 35.0% | 3.7% |
| Scenarios 1,2and3 | 21 st of Mar. | 12:00 | 36.8% | 84.8% |
| Scenarios 1,2and3 | 21 st of Mar. | 15:00 | 65.3% | 82.9% |
| Scenarios 1,2and3 | 21 st of Jun. | 9:00 | 20.7% | 54.7% |
| Scenarios 1,2and3 | 21 st of Jun. | 12:00 | 100% | 230.0% |
| Scenarios 1,2and3 | 21 st of Jun. | 15:00 | 43.1% | 30.1% |
| Scenarios 1,2and3 | 23 rd of Sept. | 9:00 | 40.3% | 4.4% |
| Scenarios 1,2and3 | 23 rd of Sept. | 12:00 | 31.0% | 86.1% |
| Scenarios 1,2and3 | 23 rd of Sept. | 15:00 | 67.0% | 83.2% |
| Scenarios 1,2and3 | 21 st of Dec. | 9:00 | 51.4% | 19.3% |
| Scenarios 1,2and3 | 21 st of Dec. | 12:00 | 43.5% | 130.8% |
| Scenarios 1,2and3 | 21 st of Dec. | 15:00 | 42.4% | 132.2% |

5.2.6 Scenarios 01,02 and 03 daylight harvesting potential analysis

Similar to the basic model simulation, the analysis was done using both RadianceIES and Apache applications. The daylight harvesting potential for the three scenarios was measured by the annual electrical consumption saving which happened after using the sensors (table 5.31). Due to the reduction of the average illuminance levels, the daylight harvesting potential was reduced by 31.07% in scenario 01, 30.98% in scenario 02 and 30.7% in scenario 03. Although the light uniformity improved in the three scenarios by an average of 4.6% in the waiting room and 4.0% on the reception room, that didn't improve the daylight harvesting potential (table 5.32).

Table 5.31. Total annual electricity consumption Results summary. On the left the three scenarios annual electricity consumption and on the right the day light harvesting scenario (author 2019).

| | Total electricity (MWh) | Total electricity (MWh) | Total electricity (MWh) | Total electricity (MWh) | Total electricity (MWh) | Total electricity (MWh) |
|--------------|--------------------------|--------------------------|--------------------------|-------------------------|-------------------------|-------------------------|
| Date | Scenario 03 With DH. aps | Scenario 02 With DH. aps | Scenario 01 With DH. aps | Scenario 03. aps | Scenario 02. aps | Scenario 01. aps |
| Jan 01-31 | 1.9012 | 1.9014 | 1.9016 | 1.9502 | 1.9443 | 1.9374 |
| Feb 01-28 | 2.1070 | 2.1073 | 2.1074 | 2.1265 | 2.1204 | 2.1133 |
| Mar 01-31 | 2.6007 | 2.6010 | 2.6013 | 2.6390 | 2.6331 | 2.6262 |
| Apr 01-30 | 3.1513 | 3.1517 | 3.1521 | 3.2019 | 3.2002 | 3.1981 |
| May 01-31 | 3.8171 | 3.8176 | 3.8180 | 3.8501 | 3.8523 | 3.8550 |
| Jun 01-30 | 3.9675 | 3.9679 | 3.9684 | 4.0059 | 4.0103 | 4.0156 |
| Jul 01-31 | 4.2417 | 4.2421 | 4.2426 | 4.3264 | 4.3335 | 4.3420 |
| Aug 01-31 | 4.2953 | 4.2956 | 4.2963 | 4.3931 | 4.4009 | 4.4102 |
| Sep 01-30 | 3.8803 | 3.8808 | 3.8812 | 3.9878 | 3.9939 | 4.0012 |
| Oct 01-31 | 3.4947 | 3.4951 | 3.4955 | 3.6004 | 3.6028 | 3.6057 |
| Nov 01-30 | 2.8259 | 2.8262 | 2.8265 | 2.9156 | 2.9137 | 2.9115 |
| Dec 01-31 | 2.2850 | 2.2853 | 2.2855 | 2.3434 | 2.3370 | 2.3295 |
| Summed total | 38.5679 | 38.5723 | 38.5767 | 39.3406 | 39.3426 | 39.3457 |

Table 5.32. Final comparison (by the author 2019).

| Scenario | Total annual artificial lighting electrical consumption saving | Cost saving based on tariff of 30.5 Fils for every KW (ADDC 2018). | Reduction in daylight harvesting potential comparing to basic model potential |
|--------------|----------------------------------------------------------------|--------------------------------------------------------------------|-------------------------------------------------------------------------------|
| Basic-model | 1.1156 MWh | 340.3 UAE Dirhams | - |
| Scenario-01: | 0.769 MWh | 234.5 UAE Dirhams | 31.07% |
| Scenario-02: | 0.770 MWh | 234.9 UAE Dirhams | 30.98% |
| Scenario-03: | 0.773 MWh | 235.8 UAE Dirhams | 30.71% |

5.3 Buffer DSF/ Corridor Facade -Scenario 04: Triple Layers Cushions.

5.3.1 Scenarios 04 CFD simulation and analysis

Table 5.31. Air temperature within the DSF cavity from Microflo results (author 2019).

| Location | Date | Hour | Minimum DSF cavity air temperature (°C) | Maximum DSF cavity air temperature (°C) | Mean DSF cavity air temperature (°C) | Comparison between ambient temperature (47°C) and mean DSF cavity air temperature | Reduction in average air temperature comparing to scenarios 01,02 and 03. |
|---------------------|--------------------------|-------|-----------------------------------------|-----------------------------------------|--------------------------------------|-----------------------------------------------------------------------------------|---------------------------------------------------------------------------|
| Eastern DSF cavity | 10 th of Aug. | 15:00 | 28.19 | 47.44 | 36.64 | -22.0% | 0.8% |
| Western DSF cavity | 10 th of Aug. | 12:00 | 28.36 | 46.81 | 36.50 | -22.3% | 1.0% |
| Northern DSF cavity | 10 th of Aug. | 15:00 | 28.48 | 46.98 | 36.60 | -22.1% | 0.8% |

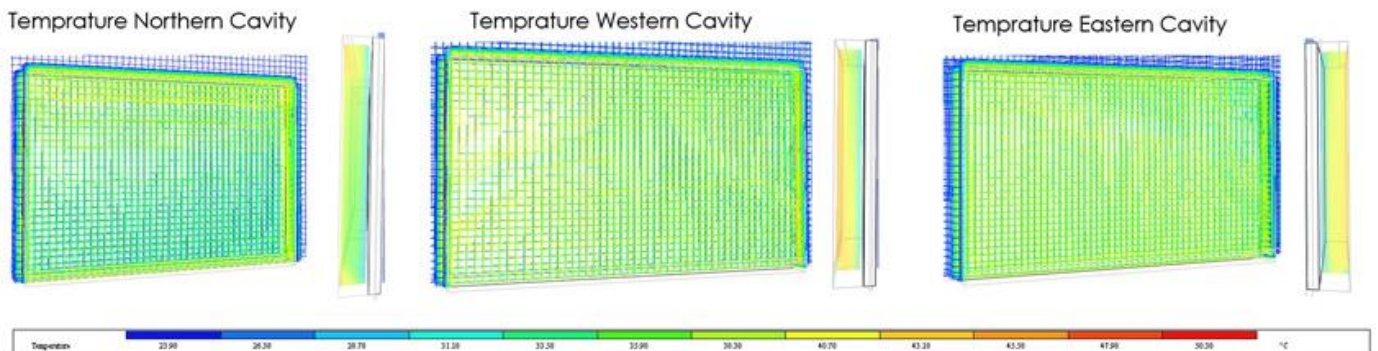


Figure 5.29. CFD analysis of Norther, Eastern and Western cushions in Microflo (author 2019).

The temperature analysis showed that when the ambient temperature reached 47.0 °C at the building level , the temperature in the DSF cavity near the cushion was maximum 47.44 °C in eastern DSF, maximum 46.81 °C in western DSF and maximum 46.98 °C in northern DSF (table 5.31 and figure 5.29). Thus, the temperature near the external DSF layer was higher than ambient temperature only in the western DSF. The temperature in the DSF cavity near the DGU was minimum 28.19 °C in eastern DSF,

minimum 28.36 °C in western DSF and minimum 28.48 °C in northern DSF. Due to the natural air flow, hot air was discharged and average reduction in mean cavity air temperature, comparing to ambient temperature, was 21.4% in eastern DSF, 21.6% in western DSF and 21.5% in northern DSF. Comparing to scenarios 01,02 and 03, the average air temperature was reduced by 1% in western DSF cavity and 0.8% in northern and eastern DSFs cavities.

Table 5.32. Air velocity within the DSF cavity from Microflo results (author 2019).

| Location | Date | Hour | Air velocity within the cavity near the bottom inlet (m/s) | Air velocity within the cavity near the top outlet (m/s) | Mean air velocity within the cavity (m/s) |
|---------------------|--------------------------|-------|------------------------------------------------------------|----------------------------------------------------------|-------------------------------------------|
| Eastern DSF cavity | 10 th of Aug. | 15:00 | 0.51~0.62 | 0.72 | 0.51 |
| Western DSF cavity | 10 th of Aug. | 12:00 | 0.72 | 1.03~1.13 | 0.72 |
| Northern DSF cavity | 10 th of Aug. | 15:00 | 0.21 | 0.41~0.72 | 0.31 |

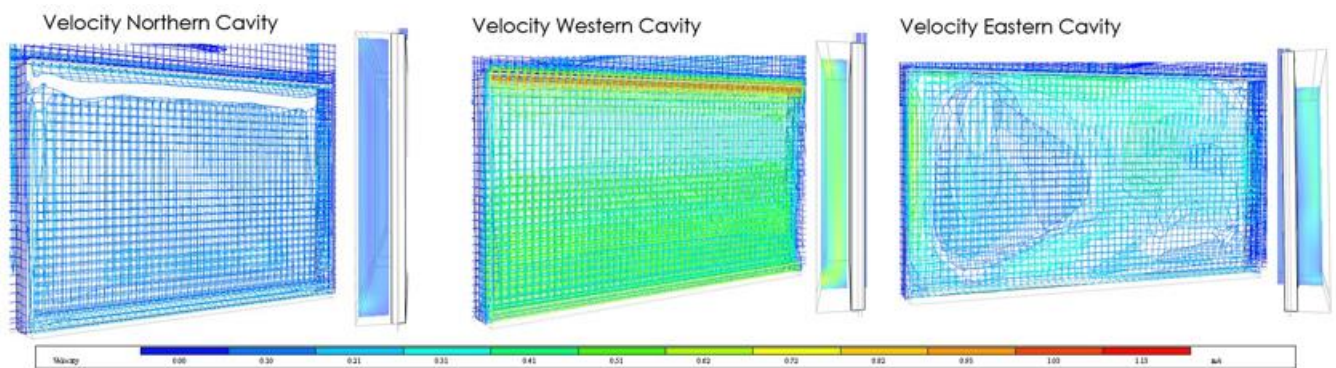


Figure 5.30. CFD analysis of the eastern cushions in IES VE (author 2019).

The analysis proved that air flow was from bottom to top which helped to discharge hot air from the DSF cavity. The maximum air velocity was near the top exhaust/outlet. Average air velocity in the eastern DSF was 0.51 while the maximum velocity was 0.72 m/s near the top and the inlet air velocity was 0.57 m/s. Average air velocity in the western DSFs was 0.72 m/s while the maximum velocity was 1.13 m/s near the top and the inlet air velocity was 0.72 m/s (table 5.32 and figure 5.30). It was

noted that the lowest air velocity and temperature was simulated in the northern DSF. The impact of the of the stack effect on the DSF was evaluated in the following sections where additional investigations on the internal conditions within the building were provided.

5.3.2 Scenarios 04 annual electrical consumption results

Table 5.33. Total annual electricity consumption for scenarios-04 and the basic model (author 2019).

| | Total electricity (MWh) | Total electricity (MWh) |
|--------------|-------------------------|-------------------------|
| | | |
| Date | Scenario 04.aps | Basic Model.aps |
| Jan 01-31 | 1.9450 | 2.1744 |
| Feb 01-28 | 2.1150 | 2.4339 |
| Mar 01-31 | 2.6196 | 3.0512 |
| Apr 01-30 | 3.1707 | 3.6774 |
| May 01-31 | 3.8051 | 4.4261 |
| Jun 01-30 | 3.9571 | 4.5822 |
| Jul 01-31 | 4.2717 | 4.9159 |
| Aug 01-31 | 4.3387 | 4.9626 |
| Sep 01-30 | 3.9420 | 4.4772 |
| Oct 01-31 | 3.5662 | 4.0166 |
| Nov 01-30 | 2.8960 | 3.2288 |
| Dec 01-31 | 2.3358 | 2.6027 |
| Summed total | 38.9627 | 44.5490 |

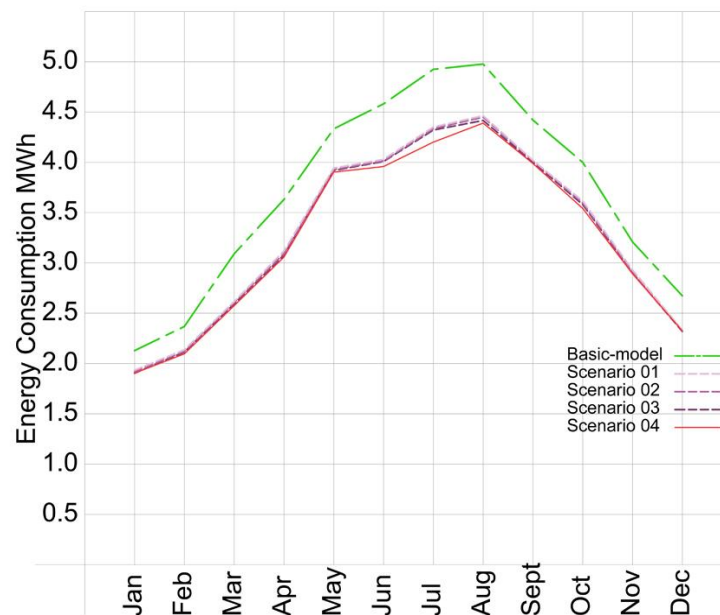


Figure 5.31. Combined diagram of the basic model results and the first four scenarios results (author 2019)

The fourth scenarios showed good improvement comparing to the basic-model. The total electrical consumption reduction, with consideration of the inflation unit, was 12.45% (table 5.33 and figure 5.31). The results were better than the first three scenarios specially in the period from May up to August. Comparing to the first three scenarios, the energy saving was improved by 0.85% (from 11.6% to 12.45%) when the third foil was added (table 5.34).

Table 5.34. Final comparison between the first four scenarios (author 2019).

| Scenario | Total annual electrical consumption saving comparing to the basic model (MWh) | Inflation unit annual electricity consumption (MWh) | Total annual electrical consumption saving considering inflation unit annual consumption (MWh) | Total annual electrical consumption saving considering inflation unit annual consumption (%) | Cost saving based on tariff of 30.5 Fils for every KW (ADDC 2018) |
|--------------|-------------------------------------------------------------------------------|-----------------------------------------------------|------------------------------------------------------------------------------------------------|----------------------------------------------------------------------------------------------|-------------------------------------------------------------------|
| Scenario-01 | 5.2033 | 0.03916 | 5.16414 | 11.594% | 1575.1 UAE Dirhams |
| Scenario-02 | 5.2064 | 0.03916 | 5.16724 | 11.600% | 1576.0 UAE Dirhams |
| Scenario-03 | 5.2084 | 0.03916 | 5.16924 | 11.603% | 1576.6 UAE Dirhams |
| Scenario 04. | 5.5863 | 0.03916 | 5.54714 | 12.45% | 1691.9 UAE Dirhams |

5.3.3 Scenarios 04 thermal comfort results

Table 5.35. Comfort index results comparison between scenario 04 and the basic model (author 2019).

| Var. Name | Location | Filename | Type | Mean |
|---------------|-----------------|-----------------|---------------|------|
| Comfort index | Mechanical room | Scenario 04.aps | Comfort index | 9 |
| Comfort index | Office 01 | Scenario 04.aps | Comfort index | 9 |
| Comfort index | Office 02 | Scenario 04.aps | Comfort index | 9 |
| Comfort index | Store 01 | Scenario 04.aps | Comfort index | 9 |
| Comfort index | Lobby 01 | Scenario 04.aps | Comfort index | 9 |
| Comfort index | Waiting room | Scenario 04.aps | Comfort index | 10 |
| Comfort index | Lobby 02 | Scenario 04.aps | Comfort index | 9 |
| Comfort index | Toilet | Scenario 04.aps | Comfort index | 9 |
| Comfort index | Store 02 | Scenario 04.aps | Comfort index | 9 |
| Comfort index | Reception | Scenario 04.aps | Comfort index | 9 |
| Comfort index | Mechanical room | Basic Model.aps | Comfort index | 9 |
| Comfort index | Office 01 | Basic Model.aps | Comfort index | 9 |
| Comfort index | Office 02 | Basic Model.aps | Comfort index | 9 |
| Comfort index | Store 01 | Basic Model.aps | Comfort index | 9 |
| Comfort index | Lobby 01 | Basic Model.aps | Comfort index | 9 |
| Comfort index | Waiting room | Basic Model.aps | Comfort index | 10 |
| Comfort index | Lobby 02 | Basic Model.aps | Comfort index | 9 |
| Comfort index | Toilet | Basic Model.aps | Comfort index | 9 |
| Comfort index | Store 02 | Basic Model.aps | Comfort index | 10 |
| Comfort index | Reception | Basic Model.aps | Comfort index | 10 |

The fourth scenarios had the same comfort index result as scenario 02 and 03. Comparing to the basic model, Comfort index in store 02 and the reception changed from 10 (warm/acceptable) to 9 (slightly warm/acceptable) (table 5.35).

Table 5.36. Mean room temperature results of basic-model and scenario 04 (author 2019).

| Var. Name | Location | Filename | Type | Mean |
|-----------------|-----------------|-----------------|------------------|-------|
| Air temperature | Mechanical room | Scenario 04.aps | Temperature (°C) | 24.83 |
| Air temperature | Office 01 | Scenario 04.aps | Temperature (°C) | 24.59 |
| Air temperature | Office 02 | Scenario 04.aps | Temperature (°C) | 24.58 |
| Air temperature | Store 01 | Scenario 04.aps | Temperature (°C) | 24.50 |
| Air temperature | Lobby 01 | Scenario 04.aps | Temperature (°C) | 24.59 |
| Air temperature | Waiting room | Scenario 04.aps | Temperature (°C) | 25.17 |
| Air temperature | Lobby 02 | Scenario 04.aps | Temperature (°C) | 24.78 |
| Air temperature | Toilet | Scenario 04.aps | Temperature (°C) | 24.62 |
| Air temperature | Store 02 | Scenario 04.aps | Temperature (°C) | 24.75 |
| Air temperature | Reception | Scenario 04.aps | Temperature (°C) | 25.18 |
| Air temperature | Mechanical room | Basic Model.aps | Temperature (°C) | 24.89 |
| Air temperature | Office 01 | Basic Model.aps | Temperature (°C) | 24.62 |
| Air temperature | Office 02 | Basic Model.aps | Temperature (°C) | 24.66 |
| Air temperature | Store 01 | Basic Model.aps | Temperature (°C) | 24.52 |
| Air temperature | Lobby 01 | Basic Model.aps | Temperature (°C) | 24.62 |
| Air temperature | Waiting room | Basic Model.aps | Temperature (°C) | 25.51 |
| Air temperature | Lobby 02 | Basic Model.aps | Temperature (°C) | 25.13 |
| Air temperature | Toilet | Basic Model.aps | Temperature (°C) | 24.94 |
| Air temperature | Store 02 | Basic Model.aps | Temperature (°C) | 25.16 |
| Air temperature | Reception | Basic Model.aps | Temperature (°C) | 26.15 |

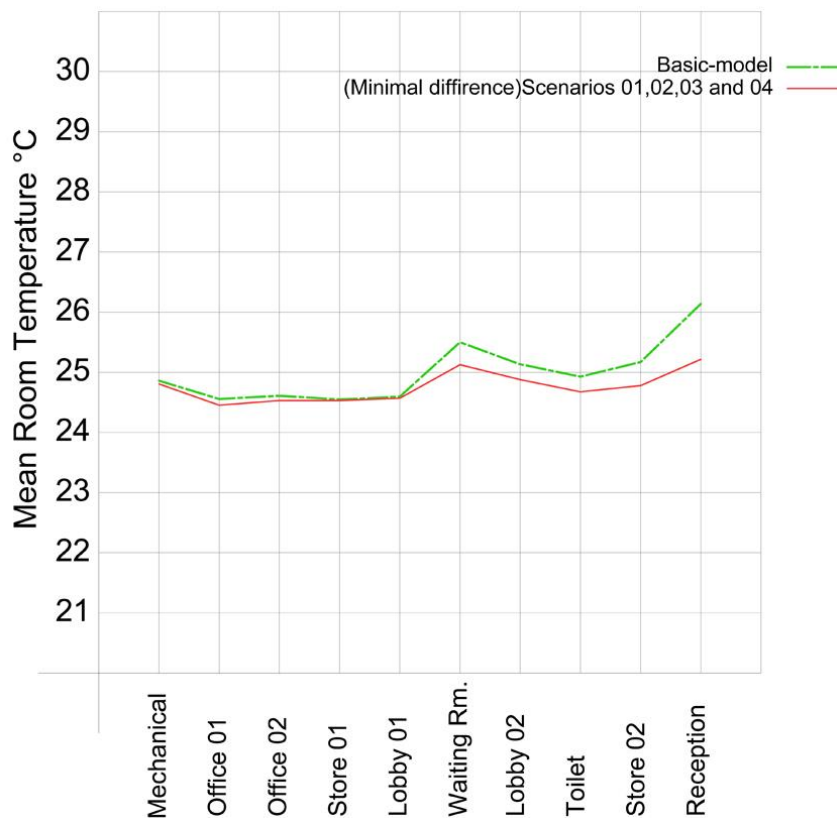


Figure 5.32. Combined diagram of the basic model results and the first four scenarios results (author 2019)

Comparing to the basic model, the average overall improvement/reduction in the mean room temperature was 1.043% in scenario 04. The improvement/reduction in the mean room temperature in waiting room was 1.3% and the improvement/reduction in mean room temperature in the reception room was 3.7%. In general, scenarios 01,02,03 and 04 results were almost the same (table 5.36 and figure 5.32).

| Var. Name | Location | Filename | Type | Min. Val. | Min. Time | Max. Val. | Max. Time | Mean |
|-----------|-----------------|------------------|----------------|-----------|--------------|-----------|--------------|-------|
| People | Mechanical room | Triple Layer-120 | Percentage (%) | 5.00 | 03:30,29/Jan | 86.96 | 09:30,12/Aug | 29.61 |
| People | Office 01 | Triple Layer-120 | Percentage (%) | 5.11 | 06:30,29/Jan | 77.12 | 09:30,12/Aug | 26.40 |
| People | Office 02 | Triple Layer-120 | Percentage (%) | 5.41 | 06:30,29/Jan | 75.14 | 09:30,12/Aug | 26.25 |
| People | Store 01 | Triple Layer-120 | Percentage (%) | 5.00 | 05:30,30/Jan | 80.59 | 09:30,12/Aug | 26.15 |
| People | Lobby 01 | Triple Layer-120 | Percentage (%) | 5.00 | 06:30,21/Jan | 84.52 | 09:30,12/Aug | 27.50 |
| People | Waiting room | Triple Layer-120 | Percentage (%) | 5.00 | 04:30,09/Jan | 97.35 | 09:30,12/Aug | 34.74 |
| People | Lobby 02 | Triple Layer-120 | Percentage (%) | 5.00 | 07:30,13/Dec | 93.10 | 09:30,12/Aug | 30.80 |
| People | Toilet | Triple Layer-120 | Percentage (%) | 5.06 | 06:30,29/Jan | 81.57 | 09:30,12/Aug | 27.63 |
| People | Store 02 | Triple Layer-120 | Percentage (%) | 5.00 | 07:30,28/Jan | 87.82 | 09:30,12/Aug | 29.55 |
| People | Reception | Triple Layer-120 | Percentage (%) | 5.00 | 23:30,07/Feb | 100.00 | 09:30,03/Jul | 37.42 |
| People | Mechanical room | Basic Model.aps | Percentage (%) | 5.00 | 04:30,30/Jan | 87.50 | 09:30,12/Aug | 29.95 |
| People | Office 01 | Basic Model.aps | Percentage (%) | 5.12 | 06:30,29/Jan | 77.50 | 09:30,12/Aug | 26.55 |
| People | Office 02 | Basic Model.aps | Percentage (%) | 5.46 | 06:30,29/Jan | 76.30 | 09:30,12/Aug | 26.71 |
| People | Store 01 | Basic Model.aps | Percentage (%) | 5.00 | 05:30,30/Jan | 80.82 | 09:30,12/Aug | 26.24 |
| People | Lobby 01 | Basic Model.aps | Percentage (%) | 5.00 | 03:30,29/Jan | 84.89 | 09:30,12/Aug | 27.70 |
| People | Waiting room | Basic Model.aps | Percentage (%) | 5.00 | 06:30,23/Jan | 98.36 | 09:30,12/Aug | 37.07 |
| People | Lobby 02 | Basic Model.aps | Percentage (%) | 5.00 | 07:30,18/Feb | 96.18 | 09:30,12/Aug | 33.21 |
| People | Toilet | Basic Model.aps | Percentage (%) | 5.16 | 06:30,29/Jan | 85.33 | 09:30,12/Aug | 29.74 |
| People | Store 02 | Basic Model.aps | Percentage (%) | 5.00 | 07:30,29/Jan | 92.59 | 09:30,12/Aug | 32.37 |
| People | Reception | Basic Model.aps | Percentage (%) | 5.00 | 05:30,20/Mar | 100.00 | 09:30,14/Apr | 43.40 |

Table 5.36. People dissatisfied index results of scenario 04 and the basic model (author 2019).

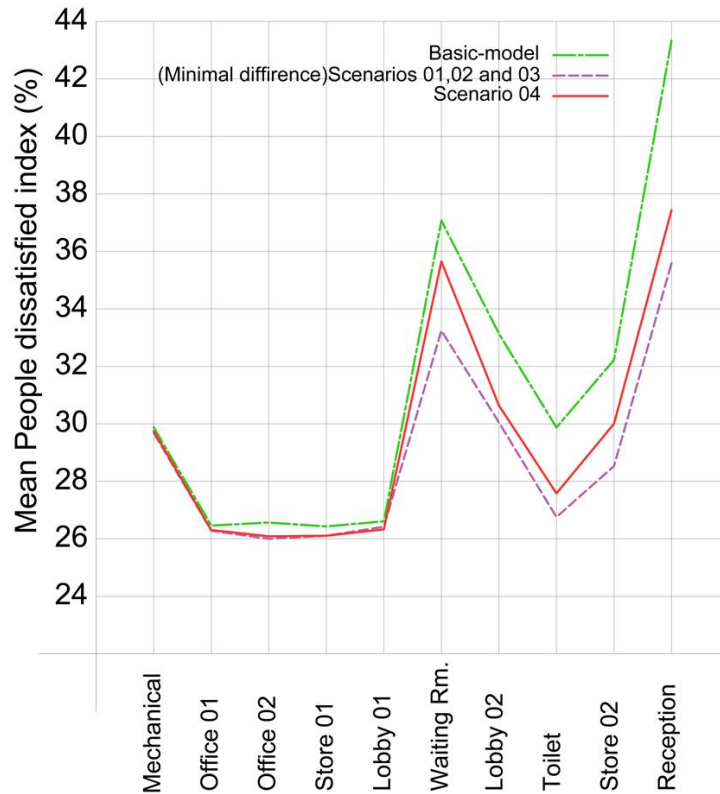


Figure 5.33. Combined diagram of the basic model results and the first four scenarios results (author 2019).

Comparing to basic model results, the mean people dissatisfied index in scenario 04 had an average improvement of 7.85%. In the waiting room, the mean values had an average improvement of 6.3 % and in the reception room, the mean value had an average improvement of 13.8%. However, as shown in the diagram, the first three scenarios results were better than scenario 04 results (table 5.36 and figure 5.33).

5.3.4 Scenario 04 daylight analysis

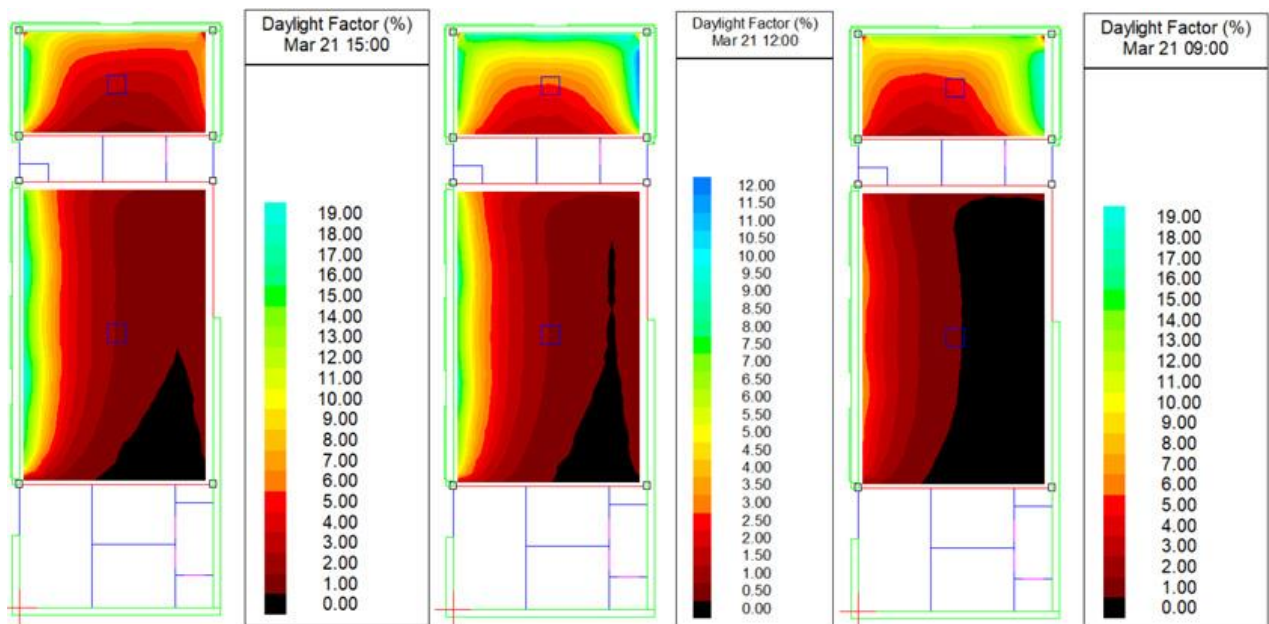


Figure 5.34. Scenario 04 daylight factor simulation results on the 21st of March (author 2019).

Table 5.37. Scenario 04 21st of March results summery (author 2019).

| Room | Date | Hour | Daylight factor | | | Daylight illuminance | | | Uniformity |
|----------------|---------------------------|-------|-----------------|------|-------|----------------------|------------|-------------|------------|
| | | | Min. | Ave. | Max. | Min. | Ave. | Max. | |
| Waiting room | 21 st of March | 9:00 | 0.4% | 1.7% | 7.1% | 29.19 lux | 132.37 lux | 539.43 lux | 0.22 |
| Reception room | 21 st of March | 9:00 | 2.4% | 8.4% | 19.6% | 179.00 lux | 639.92 lux | 1482.92 lux | 0.28 |
| Waiting room | 21 st of March | 12:00 | 0.3% | 1.7% | 8.7% | 28.16 lux | 153.48 lux | 763.69 lux | 0.18 |
| Reception room | 21 st of March | 12:00 | 1.6% | 5.1% | 12.2% | 139.53 lux | 446.22 lux | 1077.51 lux | 0.31 |
| Waiting room | 21 st of March | 15:00 | 0.5% | 3.8% | 19.6% | 38.19 lux | 314.08 lux | 1631.79 lux | 0.12 |
| Reception room | 21 st of March | 15:00 | 1.8% | 5.9% | 17.7% | 145.95 lux | 489.82 lux | 1475.85 lux | 0.30 |

In all cases average daylighting levels and average DF levels in the reception room were exceeding the requirements. In the waiting room, the daylighting levels were within the acceptable range at 15:00 on the 21st of March and low in the other cases. In all cases average daylighting levels and average DF were low in half of the waiting room area. Also, average DF was higher than the requirement at 15:00 while it was low in the other timings (figures 5.34,5.38,5.39,5.40,5.41 and table 5.37).

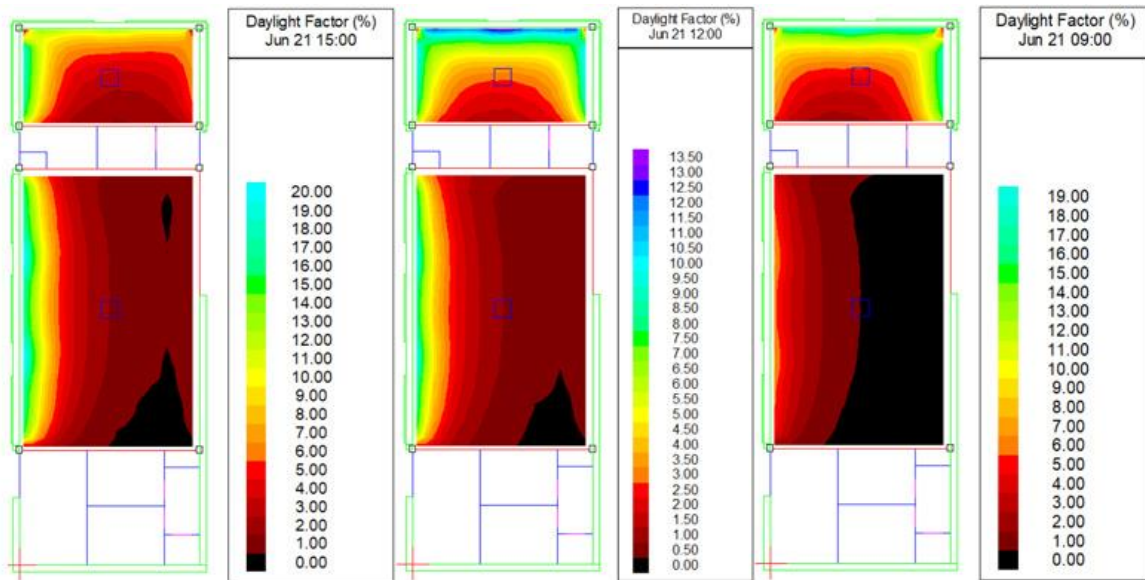


Figure 5.35. Scenario 04 daylight factor simulation results on the 21st of June (author 2019).

Table 5.38. Scenario 04 21st of June results summary (author 2019).

| Room | Date | Hour | Daylight factor | | | Daylight illuminance | | | Uniformity |
|----------------|--------------------------|-------|-----------------|-------|-------|----------------------|------------|-------------|------------|
| | | | Min. | Ave. | Max. | Min. | Ave. | Max. | |
| Waiting room | 21 st of June | 9:00 | 0.4% | 1.6% | 7.1% | 29.76 lux | 133.87 lux | 483.54 lux | 0.22 |
| Reception room | 21 st of June | 9:00 | 1.8% | 8.60% | 19.9% | 146.73 lux | 713.53 lux | 1638.78 lux | 0.21 |
| Waiting room | 21 st of June | 12:00 | 0.3% | 1.9% | 9.8% | 64.31 lux | 346.57 lux | 1831.12 lux | 0.19 |
| Reception room | 21 st of June | 12:00 | 1.3% | 5.6% | 13.7% | 239.43 lux | 1037.9 lux | 2555.76 lux | 0.23 |
| Waiting room | 21 st of June | 15:00 | 0.6% | 4.0% | 20.8% | 48.09 lux | 338.33 lux | 1777.99 lux | 0.14 |
| Reception room | 21 st of June | 15:00 | 1.4% | 6.6% | 18.5% | 122.91 lux | 564.13 lux | 1586.48 lux | 0.22 |

In all cases average daylighting levels and average DF levels in the reception room were exceeding the requirements. In the waiting room, the daylighting levels were within the acceptable range at 12:00 and 15:00 on 21st of June and low in the other cases. In all cases average daylighting levels and average DF were low in half of

the waiting room area. Also, average DF was higher than the requirement at 15:00 while it was low in the other timings (figures 5.35,5.38,5.39,5.40,5.41 and table 5.38).

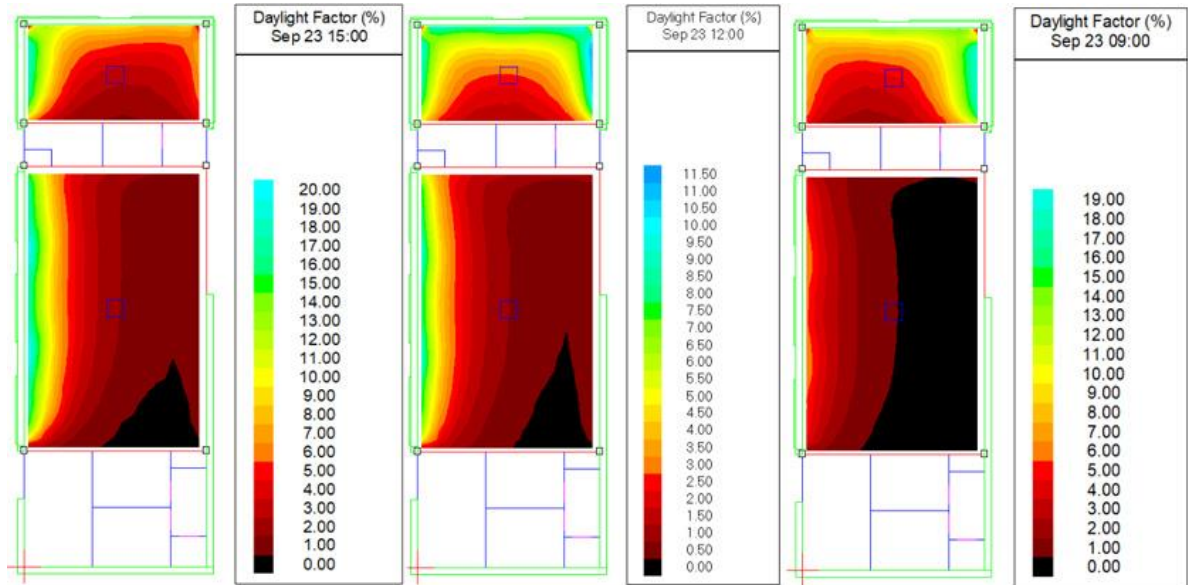


Figure 5.36. Scenario 04 daylight factor simulation results on the 23rd of September (author 2019).

Table 5. 39. Scenario 04 23rd of September results summery (author 2019).

| Room | Date | Hour | Daylight factor | | | Daylight illuminance | | | Uniformity |
|----------------|---------------------------|-------|-----------------|------|-------|----------------------|------------|-------------|------------|
| | | | Min. | Ave. | Max. | Min. | Ave. | Max. | |
| Waiting room | 23 rd of Sept. | 9:00 | 0.4% | 1.7% | 7.0% | 29.27 lux | 133.19 lux | 549.10 lux | 0.22 |
| Reception room | 23 rd of Sept. | 9:00 | 2.2% | 8.0% | 19.4% | 174.93 lux | 627.14 lux | 1518.84 lux | 0.28 |
| Waiting room | 23 rd of Sept. | 12:00 | 0.3% | 1.9% | 9.4% | 29.10 lux | 164.14 lux | 830.57 lux | 0.18 |
| Reception room | 23 rd of Sept. | 12:00 | 1.6% | 5.0% | 11.6% | 140.86 lux | 446.74 lux | 1026.36 lux | 0.32 |
| Waiting room | 23 rd of Sept. | 15:00 | 0.5% | 4.2% | 20.7% | 41.63 lux | 341.57 lux | 1693.38 lux | 0.12 |
| Reception room | 23 rd of Sept. | 15:00 | 1.9% | 6.2% | 18.6% | 151.86 lux | 512.01 lux | 1527.47 lux | 0.30 |

In all cases average daylighting levels and average DF levels in the reception room were exceeding the requirements. In the waiting room, the average daylighting levels were within the acceptable range at 15:00 on 23rd of September and low in the other cases. In all cases daylighting levels and average DF were low in half of the waiting room area. Also, average DF was higher than the requirement at 15:00 while it was low in the other timings (figures 5.36,5.38,5.39,5.40,5.41 and table 5.39).

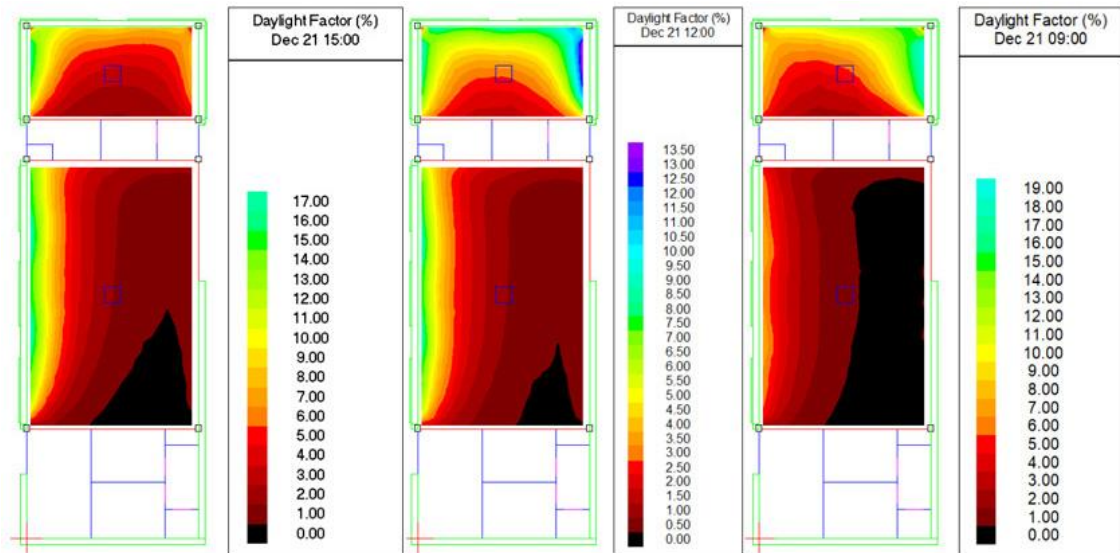


Figure 5.37. Scenarios-04 daylight factor simulation results on the 21st of December (author 2019).

Table 5.40. Scenarios 04 21st of December results summary (author 2019).

| Room | Date | Hour | Daylight factor | | | Daylight illuminance | | | Uniformity |
|----------------|--------------------------|-------|-----------------|------|-------|----------------------|------------|-------------|------------|
| | | | Min. | Ave. | Max. | Min. | Ave. | Max. | |
| Waiting room | 21 st of Dec. | 9:00 | 0.4% | 2.0% | 8.0% | 27.44 lux | 124.00 lux | 493.88 lux | 0.22 |
| Reception room | 21 st of Dec. | 9:00 | 2.6% | 8.3% | 19.5% | 160.38 lux | 515.33 lux | 1207.48 lux | 0.31 |
| Waiting room | 21 st of Dec. | 12:00 | 0.3% | 1.9% | 8.9% | 28.37 lux | 155.98 lux | 723.34 lux | 0.18 |
| Reception room | 21 st of Dec | 12:00 | 1.7% | 5.3% | 13.9% | 141.15 lux | 432.32 lux | 1133.09 lux | 0.33 |
| Waiting room | 21 st of Dec. | 15:00 | 0.5% | 3.7% | 17.7% | 32.60 lux | 261.48 lux | 1242.34 lux | 0.12 |
| Reception room | 21 st of Dec | 15:00 | 1.9% | 6.0% | 16.8% | 135.12 lux | 417.96 lux | 1175.98 lux | 0.32 |

In all cases average daylighting levels and average DF levels in the reception room were exceeding the requirements. In the waiting room, the daylighting levels were low in the other cases. In all cases daylighting levels and average DF were low in half of the waiting room area. Also, average DF was higher than the requirement at 15:00 while it was low in the other timings (figures 5.37,5.38,5.39,5.40,5.41 and table 5.40).

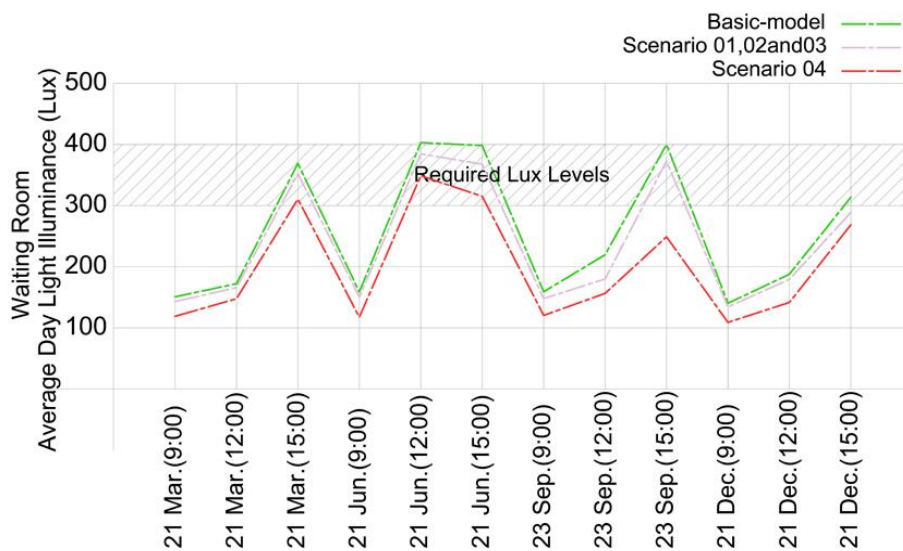


Figure 5.38. Combined diagram of the basic model DI results and the four scenarios DI results in waiting room (author 2019)

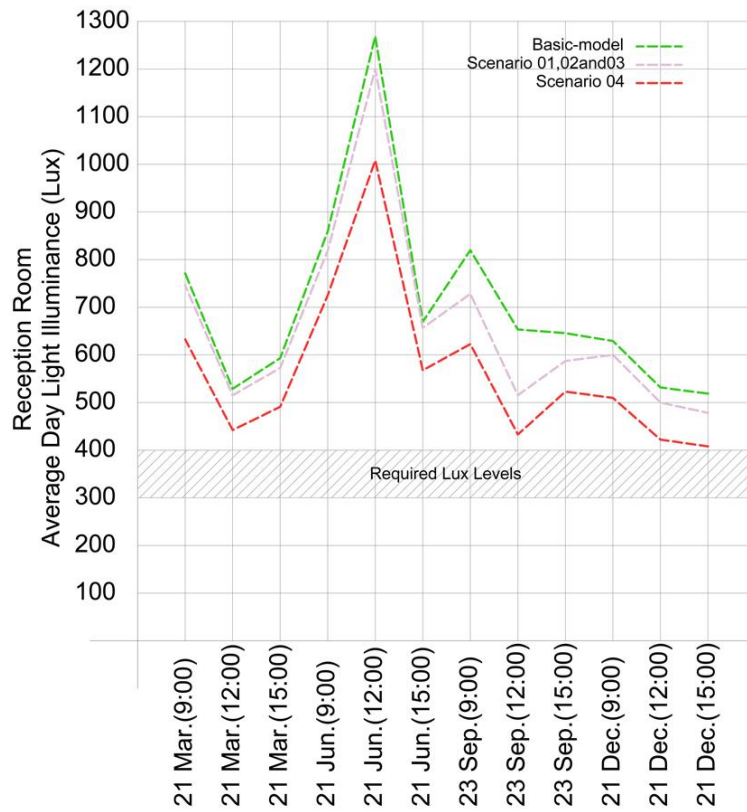


Figure 5.39. Combined diagram of the basic model DI results and the four scenarios DI results in reception room (author 2019)

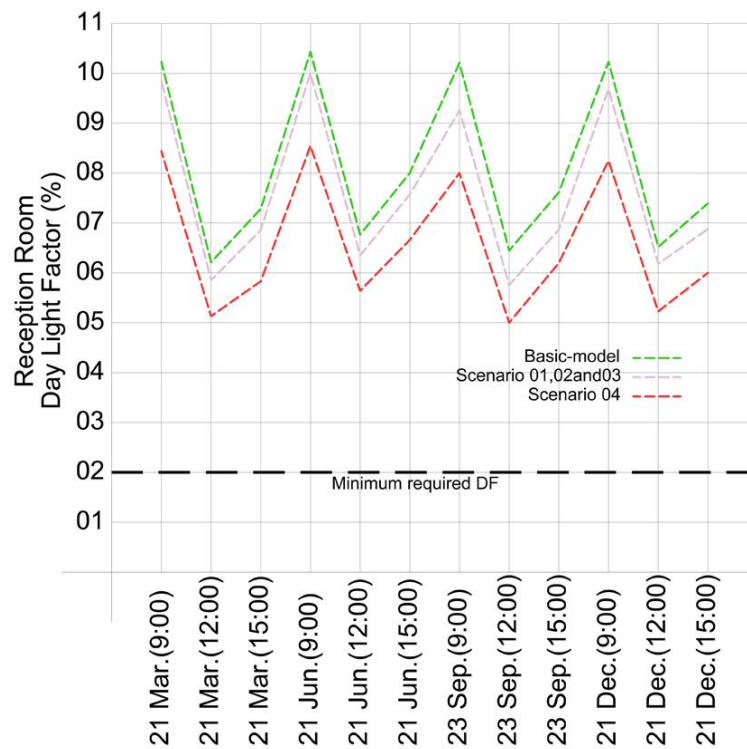


Figure 5.40. Combined diagram of the basic model DF results and the four scenarios DF results in reception room (author 2019)

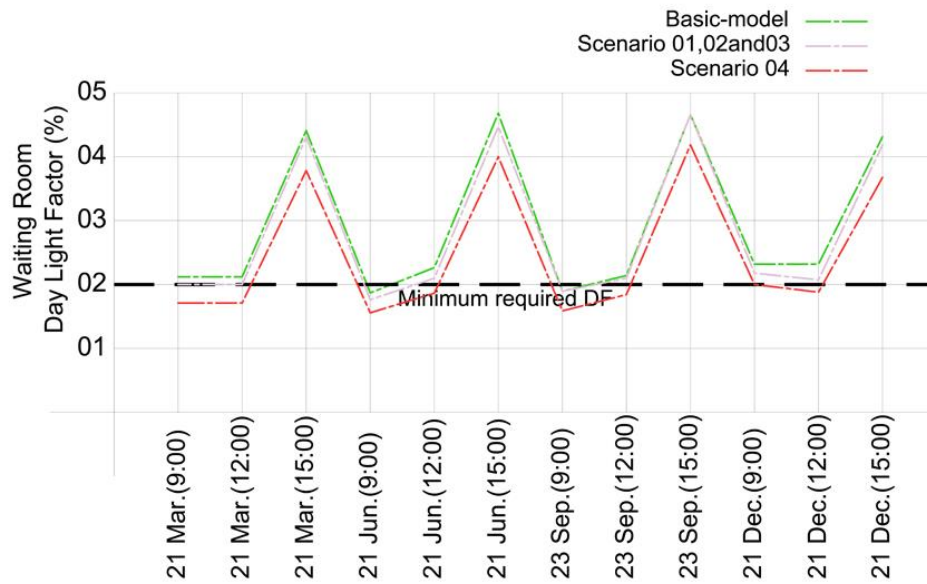


Figure 5.41. Combined diagram of the basic model DF results and the four scenarios DF results in the waiting room (author 2019).

Comparing to the basic-model, the addition of the triple layers cushions reduced daylighting lux levels by minimum 14.0% and maximum 32%. Furthermore, the change reduced average DF by minimum 9.5% and maximum 21.8%. Uniformity changes varied from 11.1% to -7.7%. Refer to the final comparison table for full details. Due to changes in VLT transmittance, scenarios 01.02 and 03 results were better as shown in the previous diagrams. Comparing to them, the additional foil reduced the daylighting levels by an average of 14.4% in the reception room and 9.3% in the waiting room. Also, the average DF reduction was 13.75% in the reception room and 12.2% in the waiting room (figures 5.38,5.39,5.40,5.41 and table 5.41).

Table 5.41. Final comparison between Scenario 04 results and basic model results (author 2019).

| Scenario | Date | Hour | Average daylight factor reduction | Average daylight illuminance reduction | Uniformity increment |
|-------------|---------------------------|-------|--------------------------------------------|--------------------------------------------|---------------------------------------------|
| Scenario 4. | 21 st of Mar. | 9:00 | Waiting room 19.0% Reception room 18.4% | Waiting room 15.4% Reception room 18.2% | Waiting room 0.0% Reception room 7.7% |
| Scenario 4. | 21 st of Mar. | 12:00 | Waiting room 19.0% Reception room 17.7% | Waiting room 15.5% Reception room 17.8% | Waiting room 0.0% Reception room 3.3% |
| Scenario 4. | 21 st of Mar. | 15:00 | Waiting room 13.6% Reception room 18.1% | Waiting room 15.1% Reception room 17.3% | Waiting room -7.6% Reception room 0.0% |
| Scenario 4. | 21 st of Jun. | 9:00 | Waiting room 15.7% Reception room 18.1% | Waiting room 15.8% Reception room 17.7% | Waiting room 4.7% Reception room 10.5% |
| Scenario 4. | 21 st of Jun. | 12:00 | Waiting room 13.6% Reception room 17.6% | Waiting room 15.1% Reception room 17.6% | Waiting room 5.5% Reception room 4.5% |
| Scenario 4. | 21 st of Jun. | 15:00 | Waiting room 14.9% Reception room 18.4% | Waiting room 14.0% Reception room 20.8% | Waiting room -7.6% Reception room 11.1% |
| Scenario 4. | 23 rd of Sept. | 9:00 | Waiting room 10.7% Reception room 21.5% | Waiting room 14.7% Reception room 23.4% | Waiting room 0.00% Reception room 17.0% |
| Scenario 4. | 23 rd of Sept. | 12:00 | Waiting room 9.5% Reception room 21.8% | Waiting room 25.4% Reception room 32.0% | Waiting room 0.00% Reception room 23.0% |
| Scenario 4. | 23 rd of Sept. | 15:00 | Waiting room 10.6% Reception room 18.4% | Waiting room 14.1% Reception room 20.8% | Waiting room -7.70% Reception room 11.1% |
| Scenario 4. | 21 st of Dec. | 9:00 | Waiting room 13.0% Reception room 18.6% | Waiting room 14.5% Reception room 18.3% | Waiting room 0.0% Reception room 0.0% |
| Scenario 4. | 21 st of Dec. | 12:00 | Waiting room 17.4% Reception room 18.4% | Waiting room 14.8% Reception room 18.0% | Waiting room 0.0% Reception room 3.1% |
| Scenario 4. | 21 st of Dec. | 15:00 | Waiting room 15.9% Reception room 17.8% | Waiting room 15.0% Reception room 18.1% | Waiting room 0.0% Reception room 0.0% |

5.3.5 Scenario 04 glare analysis

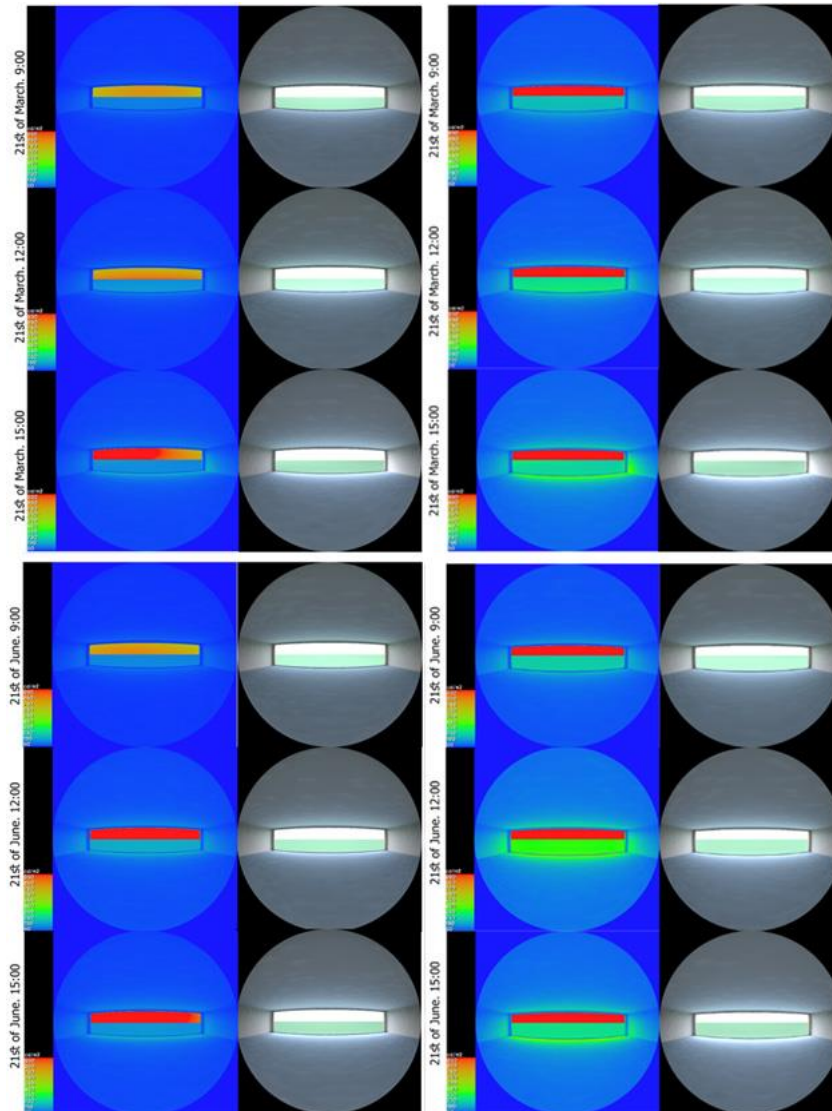


Figure 5.42. Waiting room luminance maps on the 21st of March (top images) and 21st of June (bottom images). The images on the left show scenario 04 results and the images on the right show the basic model results (author 2019).

On 21st of March, in the waiting room, average luminance levels from the glazed wall reached 700 cd/m² in first two cases and 850 cd/m² in third case. Which, comparing to basic model, were considered as 26.3% and 10.5% reduction. On 21st of June, average luminance levels from the glazed wall reached 700 cd/m² in first case and 850 cd/m² in second and third case. Which, comparing to basic model, were considered as 26.3% and 10.5% reduction respectively (figure 5.42).

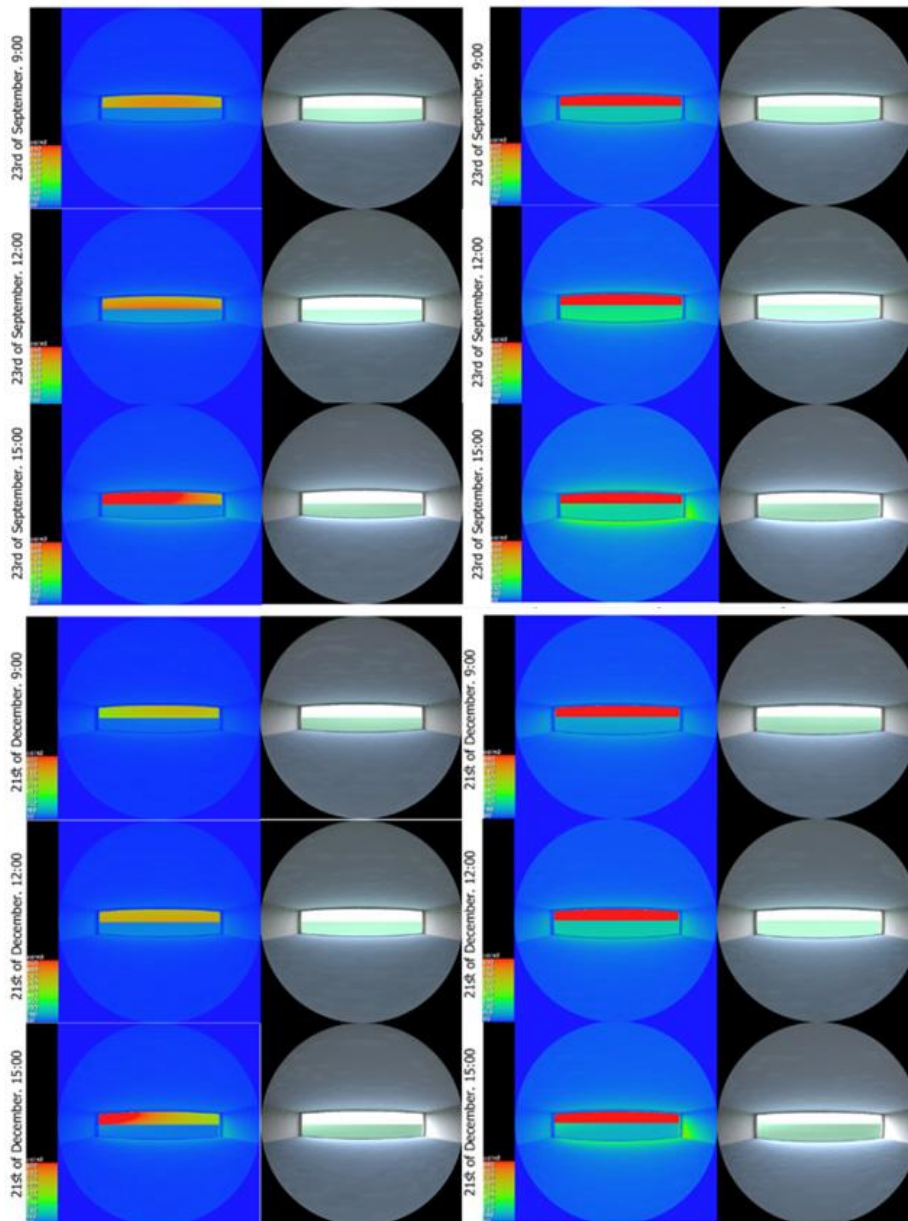


Figure 5.43. Waiting room luminance maps on the 23rd of September (top images) and 21st of December (bottom images). The images on the left show scenario 04 results and the images on the right show the basic model results (author 2019).

On 23rd of September, in the waiting room, average luminance levels from the glazed wall reached 700 cd/m² in first two cases and 850 cd/m² in third case. Which, comparing to basic model, were considered as 26.3% and 10.5% reduction. On 21st of December, average luminance levels from the glazed wall reached 650 cd/m² in the first two cases and 750 cd/m² in the third case. Which, comparing to basic model, were considered as 31.5% and 10.5% reduction respectively (figure 5.43).

Table 5.42. DGI levels from different angles from nadir for the four days at 9:00,12:00 and 15:00 (author 2019).

| Angle | 60 | 50 | 40 | 30 | 20 | 10 | 0 | -10 | -20 | -30 | -40 | -50 | -60 |
|-------------------------------------------|------|------|------|------|------|------|------|------|------|------|------|------|------|
| 09:00 21 st of March | 12.4 | 14.3 | 16.0 | 17.4 | 18.5 | 19.3 | 19.5 | 19.3 | 18.5 | 17.4 | 16.1 | 14.4 | 12.4 |
| 12:00 21 st of March | 12.3 | 14.2 | 15.9 | 17.2 | 18.3 | 19.1 | 19.4 | 19.2 | 18.4 | 18.3 | 17.2 | 15.9 | 14.2 |
| 15:00 21 st of March | 12.9 | 14.9 | 16.5 | 17.8 | 18.9 | 19.7 | 19.9 | 19.6 | 18.8 | 17.7 | 16.3 | 14.7 | 12.7 |
| 09:00 21 st of June | 12.4 | 14.3 | 15.9 | 17.6 | 18.4 | 19.3 | 19.5 | 19.3 | 18.4 | 17.4 | 15.9 | 14.3 | 12.4 |
| 12:00 21 st of June | 13.8 | 15.7 | 17.4 | 18.7 | 19.8 | 20.6 | 20.9 | 20.7 | 19.8 | 18.8 | 17.4 | 15.8 | 13.8 |
| 15:00 21 st of June | 13.1 | 14.9 | 15.6 | 17.9 | 19.1 | 19.8 | 20.1 | 19.8 | 19.1 | 17.9 | 16.6 | 14.9 | 13.1 |
| 09:00 23 rd of September | 12.4 | 14.3 | 16.1 | 17.4 | 18.5 | 19.3 | 19.6 | 19.4 | 18.5 | 17.4 | 16.1 | 14.1 | 12.5 |
| 12:00 23 rd of September | 12.3 | 14.2 | 15.8 | 17.2 | 18.2 | 19.1 | 19.4 | 19.1 | 18.3 | 17.2 | 15.9 | 14.2 | 12.3 |
| 15:00 23 rd of September | 13.1 | 15.1 | 16.6 | 17.9 | 19.1 | 19.8 | 20.1 | 19.8 | 18.9 | 17.8 | 16.5 | 14.8 | 12.9 |
| 09:00 21 st of December | 11.9 | 13.9 | 15.6 | 17.1 | 18.2 | 18.9 | 19.3 | 18.9 | 18.2 | 17.1 | 15.7 | 14.1 | 12.1 |
| 12:00 21 st of December | 12.1 | 14.1 | 15.7 | 17.1 | 18.2 | 18.9 | 19.3 | 18.9 | 18.2 | 17.1 | 15.7 | 14.1 | 12.1 |
| 15:00 21 st of December | 12.5 | 14.4 | 16.1 | 17.4 | 18.4 | 19.2 | 19.4 | 19.1 | 18.3 | 17.2 | 15.7 | 14.1 | 12.1 |

According to the DGI analysis there is a perceptible glare in all cases, as it exceeded 18 in the centre of the glazed wall. However, it did not reach the high disturbance level which is above 24 (table 5.42).

Table 5.43. GVCP levels from different angles from nadir for the four days at 9:00,12:00 and 15:00 (author 2019).

| Angle | 60 | 50 | 40 | 30 | 20 | 10 | 0 | -10 | -20 | -30 | -40 | -50 | -60 |
|-------------------------------------------|------|------|------|------|------|------|------|------|------|------|------|------|------|
| 09:00 21 st of March | 65.0 | 50.1 | 37.3 | 27.5 | 20.8 | 16.4 | 15.1 | 16.4 | 20.8 | 27.5 | 37.3 | 50.1 | 65.1 |
| 12:00 21 st of March | 64.7 | 49.9 | 37.1 | 27.5 | 20.8 | 16.5 | 15.2 | 16.5 | 20.9 | 27.6 | 37.3 | 50.1 | 64.9 |
| 15:00 21 st of March | 57.4 | 42.3 | 30.3 | 21.7 | 15.9 | 12.4 | 11.4 | 12.6 | 16.3 | 22.2 | 31.1 | 43.4 | 58.5 |
| 09:00 21 st of June | 60.8 | 49.9 | 37.1 | 28.4 | 20.7 | 16.4 | 15.1 | 16.4 | 20.7 | 27.5 | 37.2 | 49.9 | 64.9 |
| 12:00 21 st of June | 47.9 | 33.4 | 22.4 | 15.2 | 7.9 | 7.5 | 7.2 | 10.9 | 15.2 | 22.4 | 33.3 | 33.3 | 48.1 |
| 15:00 21 st of June | 55.6 | 40.5 | 28.6 | 20.3 | 14.7 | 11.4 | 10.4 | 11.4 | 14.9 | 20.4 | 28.8 | 40.7 | 55.8 |
| 09:00 23 rd of September | 64.6 | 49.7 | 36.9 | 27.2 | 20.5 | 16.2 | 14.8 | 16.2 | 20.5 | 27.2 | 36.9 | 49.7 | 64.7 |
| 12:00 23 rd of September | 64.7 | 49.8 | 37.1 | 27.5 | 20.8 | 16.5 | 15.2 | 16.5 | 20.9 | 27.6 | 39.3 | 50.1 | 64.9 |
| 15:00 23 rd of September | 55.9 | 40.7 | 28.9 | 20.5 | 15.1 | 11.6 | 10.9 | 11.8 | 15.4 | 21.1 | 29.8 | 41.9 | 57.1 |
| 09:00 21 st of December | 69.5 | 54.9 | 41.9 | 31.7 | 24.3 | 19.5 | 18.1 | 19.5 | 24.3 | 31.6 | 41.8 | 54.8 | 69.4 |
| 12:00 21 st of December | 66.7 | 51.9 | 39.1 | 29.3 | 22.3 | 17.8 | 16.4 | 17.9 | 17.9 | 22.4 | 29.4 | 39.4 | 52.3 |
| 15:00 21 st of December | 62.7 | 47.9 | 35.2 | 25.9 | 19.6 | 15.6 | 15.6 | 14.5 | 15.9 | 20.3 | 27.1 | 36.7 | 64.6 |

GVCP analysis showed that minimum percentage of satisfied occupants was 7.20% at 12:00 on 21st of June to and maximum was 18.01% at 9:00 on 21st of December when looking at the middle of the glazed wall. The minimum percentage of satisfied occupants was 48.01% at 12:00 on 21st of June to and maximum was 69.49% at 9:00 on 21st of December when looking at the edges of the glazed wall (table 5.43).

Comparing to the basic model minimum DGI reduction was 7.1% and maximum DGI reduction was 18.9% while the minimum GVCP improvement was 114.8% and maximum GVCP improvement was 157.3%. Refer to final comparison table 5.44 for full details including comparison with the basic model and first three scenarios.

Table 5.44. Final comparison between the first four scenarios results and the basic model results in the waiting room (author 2019).

| Date | Hour | Average DGI reduction comparing to the basic model results (scenario 04) | Average DGI reduction comparing to the basic model results (scenarios 01,02 and 03) | Average GVCP increment comparing to the basic model results (scenario 04) | Average GVCP increment comparing to the basic model results (scenarios 01,02 and 03) |
|---------------------------|-------|--------------------------------------------------------------------------|-------------------------------------------------------------------------------------|---------------------------------------------------------------------------|--------------------------------------------------------------------------------------|
| 21 st of Mar. | 9:00 | 13.7% | 10.5% | 122.8% | 109.4% |
| 21 st of Mar. | 12:00 | 13.2% | 11.2% | 123.3% | 108.4% |
| 21 st of Mar. | 15:00 | 11.5% | 10.6% | 141.1% | 126.2% |
| 21 st of Jun. | 9:00 | 13.3% | 11.5% | 123.3% | 109.8% |
| 21 st of Jun. | 12:00 | 10.8% | 10.7% | 131.7% | 144.8% |
| 21 st of Jun. | 15:00 | 11.4% | 10.7% | 157.3% | 128.7% |
| 23 rd of Sept. | 9:00 | 15.5% | 13.4% | 125.2% | 111.5% |
| 23 rd of Sept. | 12:00 | 14.2% | 12.3% | 152.7% | 135.8% |
| 23 rd of Sept. | 15:00 | 7.1% | 7.0% | 146.4% | 132.8% |
| 21 st of Dec. | 9:00 | 16.4% | 14% | 114.8% | 101.9% |
| 21 st of Dec. | 12:00 | 18.9% | 18.8% | 117.8% | 104.8% |
| 21 st of Dec. | 15:00 | 13.2% | 11.6% | 129.7% | 114.4% |

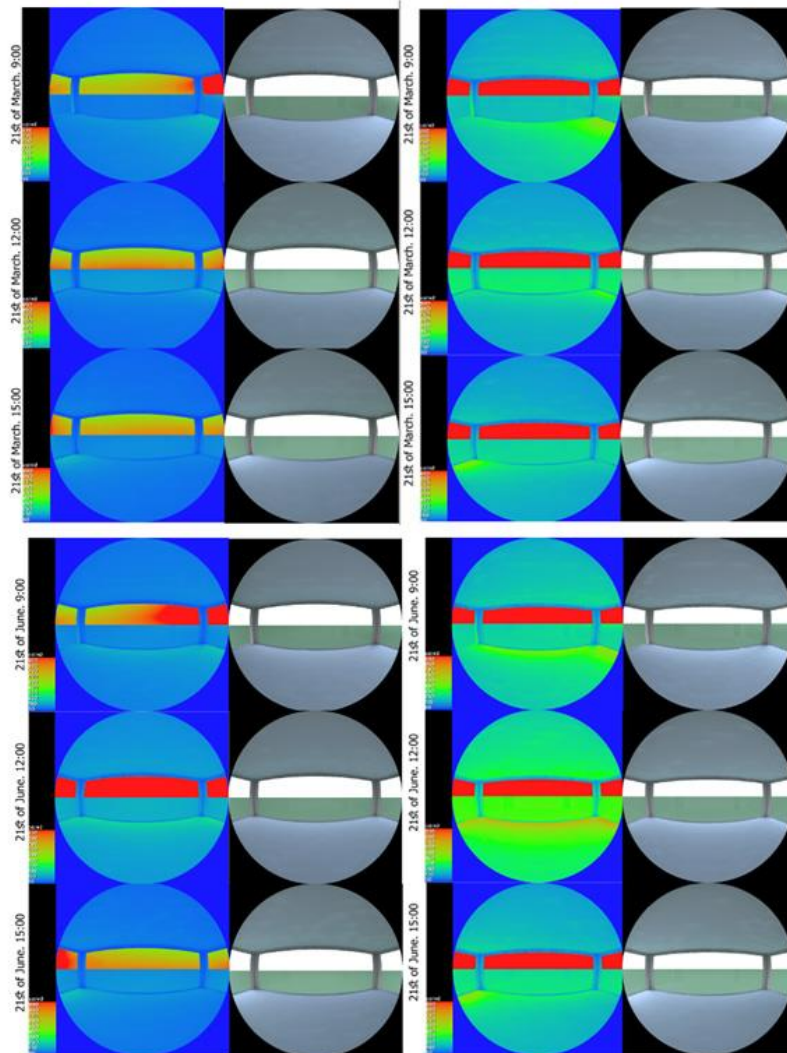


Figure 5.44. Reception room luminance maps on the 21st of March (top images) and 21st of June (bottom images). The images on the left show scenarios01,02 and 03 results and the images on the right show the basic model results (author 2019).

On 21st of March, in the reception room, luminance levels from the glazed wall reached 630 cd/m² in all cases. Comparing to basic model, installation of the triple-layers cushions reduced luminance levels on that day by 33.7%. On 21st of June, in the reception room, luminance levels from the glazed wall reached 700 cd/m² in the first case, 850 cd/m² in second case and 650 cd/m² in the third case which, comparing to the basic model, indicates 26.3%,10.5% and 31.5% reduction (figure 5.44).

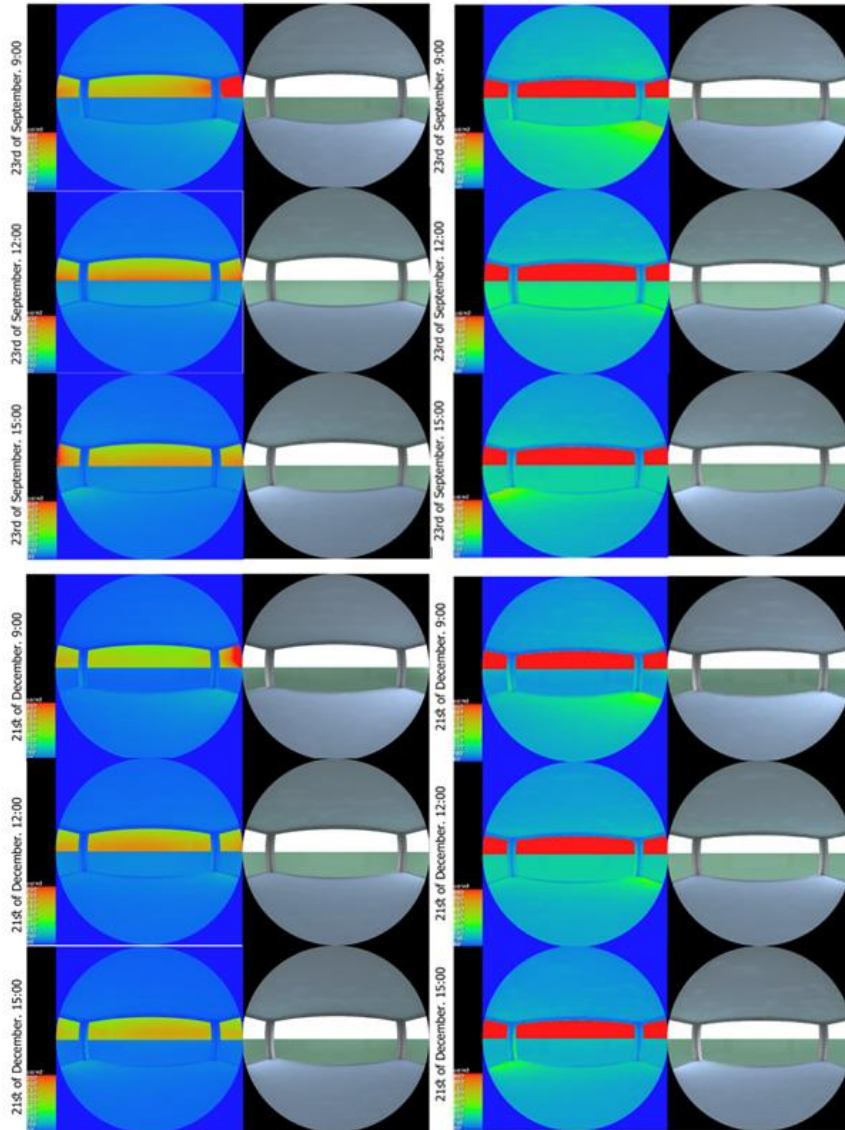


Figure 5.45. Reception room luminance maps on the 23rd of September (top images) and 21st of December (bottom images). The images on the left show scenarios 01, 02 and 03 results and the images on the right show the basic model results (author 2019).

On 23rd of September and 21st of December, in the reception room, luminance levels from the glazed wall reached 630 cd/m² in all cases. Comparing to basic model, installation of the triple-layers cushions reduced luminance levels on that day by 33.7% (figure 5.45).

Table 5.45. DGI levels from different angles from nadir for the four days at 9:00,12:00 and 15:00 (author 2019).

| Angle | 60 | 50 | 40 | 30 | 20 | 10 | 0 | -10 | -20 | -30 | -40 | -50 | -60 |
|-------------------------------------------|------|------|------|------|------|------|------|------|------|------|------|------|------|
| 09:00 21 st of March | 0.00 | 0.00 | 0.00 | 0.00 | 3.7 | 6.7 | 9.4 | 11.8 | 13.9 | 15.8 | 15.9 | 17.4 | 18.6 |
| 12:00 21 st of March | 9.6 | 9.1 | 8.8 | 8.8 | 0.00 | 9.4 | 9.4 | 9.0 | 8.7 | 8.9 | 9.5 | 10.4 | 11.3 |
| 15:00 21 st of March | 13.6 | 11.9 | 10.2 | 8.0 | 5.6 | 3.1 | 0.00 | 0.00 | 0.00 | 0.00 | 0.00 | 0.00 | 0.00 |
| 09:00 21 st of June | 0.00 | 0.00 | 0.7 | 3.2 | 0.00 | 8.7 | 10.8 | 12.7 | 14.4 | 15.8 | 16.9 | 17.9 | 18.9 |
| 12:00 21 st of June | 0.00 | 0.00 | 0.00 | 0.00 | 0.00 | 0.00 | 0.00 | 0.00 | 0.00 | 0.00 | 0.00 | 0.00 | 0.00 |
| 15:00 21 st of June | 15.2 | 13.7 | 12.1 | 10.1 | 7.8 | 5.3 | 2.5 | 0.00 | 0.00 | 0.00 | 0.00 | 0.00 | 0.00 |
| 09:00 23 rd of September | 0.00 | 0.00 | 0.00 | 0.00 | 0.00 | 3.1 | 6.1 | 8.7 | 11.1 | 13.3 | 15.1 | 16.7 | 17.9 |
| 12:00 23 rd of September | 9.8 | 9.4 | 9.1 | 9.2 | 0.00 | 9.9 | 10.3 | 9.9 | 9.5 | 9.4 | 9.7 | 10.3 | 11.1 |
| 15:00 23 rd of September | 14.1 | 12.5 | 10.6 | 8.5 | 6.2 | 3.5 | 0.1 | 0.00 | 0.00 | 0.00 | 0.00 | 0.00 | 0.00 |
| 09:00 21 st of December | 0.00 | 0.00 | 0.00 | 0.00 | 0.00 | 0.6 | 3.7 | 6.6 | 9.2 | 11.4 | 13.5 | 15.2 | 16.6 |
| 12:00 21 st of December | 3.3 | 4.9 | 6.3 | 7.4 | 8.2 | 0.00 | 0.00 | 8.2 | 7.7 | 7.5 | 7.7 | 8.4 | 9.4 |
| 15:00 21 st of December | 9.5 | 8.4 | 7.8 | 7.8 | 8.3 | 9.2 | 9.9 | 10.7 | 10.8 | 10.3 | 10.3 | 9.4 | 6.8 |

According to the DGI analysis there is an imperceptible glare in all cases, as it DGI level was lower than 18 in the centre of the glazed wall (table 5.45).

Table 5.46. GVCP levels from different angles from nadir for the four days at 9:00,12:00 and 15:00 (author 2019).

| Angle | 60 | 50 | 40 | 30 | 20 | 10 | 0 | -10 | -20 | -30 | -40 | -50 | -60 |
|-------------------------------------------|------|------|------|------|------|------|------|------|------|------|------|------|------|
| 09:00 21 st of March | 100 | 100 | 100 | 100 | 100 | 93.8 | 83.5 | 67.9 | 50.9 | 35.2 | 23.5 | 15.7 | 10.9 |
| 12:00 21 st of March | 86.3 | 87.1 | 87.1 | 87.9 | 88.1 | 89.7 | 90.9 | 91.1 | 89.3 | 87.8 | 85.6 | 82.8 | 79.5 |
| 15:00 21 st of March | 66.8 | 75.5 | 83.9 | 90.9 | 95.8 | 93.5 | 99.7 | 99.9 | 100 | 100 | 100 | 100 | 100 |
| 09:00 21 st of June | 100 | 99.9 | 99.5 | 98.3 | 95.8 | 85.3 | 74.8 | 62.8 | 51.1 | 41.5 | 33.9 | 28.8 | 25.3 |
| 12:00 21 st of June | 100 | 100 | 100 | 100 | 100 | 100 | 100 | 100 | 100 | 100 | 100 | 100 | 100 |
| 15:00 21 st of June | 32.2 | 41.7 | 54.1 | 67.9 | 81.1 | 91.2 | 96.9 | 99.3 | 100 | 100 | 100 | 100 | 100 |
| 09:00 23 rd of September | 100 | 100 | 100 | 100 | 100 | 95.5 | 86.9 | 73.1 | 56.4 | 40.6 | 28.1 | 19.2 | 13.5 |
| 12:00 23 rd of September | 85.3 | 85.9 | 86.3 | 86.3 | 86.1 | 87.9 | 88.7 | 89.1 | 87.3 | 86.3 | 84.6 | 82.5 | 79.9 |
| 15:00 23 rd of September | 64.1 | 72.9 | 81.9 | 89.5 | 95.1 | 98.1 | 99.6 | 99.9 | 100 | 100 | 100 | 100 | 100 |
| 09:00 21 st of December | 100 | 100 | 100 | 100 | 100 | 98.8 | 95.2 | 87.1 | 74.3 | 59.1 | 44.4 | 32.5 | 23.8 |
| 12:00 21 st of December | 98.7 | 97.1 | 94.8 | 92.1 | 89.3 | 86.9 | 91.4 | 93.3 | 93.2 | 92.7 | 91.7 | 89.9 | 87.5 |
| 15:00 21 st of December | 87.9 | 90.1 | 91.4 | 91.7 | 91.4 | 90.3 | 85.9 | 74.9 | 74.3 | 77.9 | 82.8 | 88.0 | 92.8 |

GVCP analysis showed that minimum percentage was 74.79% at 9:00 on 21st of June and maximum percentage was 100% at 12:00 on 21st of June when looking at the middle of the northern glazed wall. The minimum percentage of satisfied occupants was 32.20% at 15:00 on 21st of June and maximum was 100% at 12:00 on 21st of June when looking the eastern and western glazed walls (table 5.46).

Comparing to the basic model minimum DGI reduction was 26.7% and maximum DGI reduction was 100% while the minimum GVCP improvement was 3.8% and maximum GVCP improvement was 230.0%. Refer to final comparison table. Refer to final comparison table for full details including comparison with the basic model and first three scenarios (table 5.47).

Table 5.47. Final comparison between the first four scenarios results and the basic model results in the waiting room (author 2019).

| Date | Hour | Average DGI reduction comparing to the basic model results (scenario 04) | Average DGI reduction comparing to the basic model results (scenarios 01,02 and 03) | Average GVCP increment comparing to the basic model results (scenario 04) | Average GVCP increment comparing to the basic model results (scenarios 01,02 and 03) |
|---------------------------|-------|--------------------------------------------------------------------------|-------------------------------------------------------------------------------------|---------------------------------------------------------------------------|--------------------------------------------------------------------------------------|
| 21 st of Mar. | 9:00 | 37.7% | 35.0% | 3.8% | 3.7% |
| 21 st of Mar. | 12:00 | 46.8% | 36.8% | 101.9% | 84.8% |
| 21 st of Mar. | 15:00 | 73.4% | 65.3% | 85.6% | 82.9% |
| 21 st of Jun. | 9:00 | 26.7% | 20.7% | 59.7% | 54.7% |
| 21 st of Jun. | 12:00 | 100% | 100% | 230.0% | 230.0% |
| 21 st of Jun. | 15:00 | 46.3% | 43.1% | 32.4% | 30.1% |
| 23 rd of Sept. | 9:00 | 43.4% | 40.3% | 6.6% | 4.4% |
| 23 rd of Sept. | 12:00 | 45.3% | 31.0% | 86.2% | 86.1% |
| 23 rd of Sept. | 15:00 | 69.2% | 67.0% | 84.9% | 83.2% |
| 21 st of Dec. | 9:00 | 52.6% | 51.4% | 20.0% | 19.3% |
| 21 st of Dec. | 12:00 | 66.5% | 43.5% | 156.0% | 130.8% |
| 21 st of Dec. | 15:00 | 48.1% | 42.4% | 153.9% | 132.2% |

5.3.6 Scenario 04 daylight harvesting potential analysis

Table 5.48. Total annual electricity consumption Results summery. On the left the fourth scenario annual electricity consumption and on the right the day light harvesting scenario (author 2019).

| | Total electricity (MWh) | Total electricity (MWh) |
|--------------|-------------------------|-------------------------|
| Date | Scenario 04 With DH.aps | Scenario 04.aps |
| Jan 01-31 | 1.8971 | 1.9450 |
| Feb 01-28 | 2.0979 | 2.1150 |
| Mar 01-31 | 2.5893 | 2.6196 |
| Apr 01-30 | 3.1307 | 3.1707 |
| May 01-31 | 3.7931 | 3.8051 |
| Jun 01-30 | 3.9407 | 3.9571 |
| Jul 01-31 | 4.2085 | 4.2717 |
| Aug 01-31 | 4.2641 | 4.3387 |
| Sep 01-30 | 3.8537 | 3.9420 |
| Oct 01-31 | 3.4742 | 3.5662 |
| Nov 01-30 | 2.8150 | 2.8960 |
| Dec 01-31 | 2.2766 | 2.3358 |
| Summed total | 38.3412 | 38.9627 |

Table 5.49. Final comparison between the first four scenarios (author 2019).

| Scenario | Total annual artificial lighting electrical consumption saving | Cost saving based on tariff of 30.5 Fils for every KW (ADDC 2018). | Reduction in daylight harvesting potential comparing to basic model potential |
|--------------|----------------------------------------------------------------|--------------------------------------------------------------------|-------------------------------------------------------------------------------|
| Basic-model | 1.1156 MWh | 340.3 UAE Dirhams | - |
| Scenario-01: | 0.769 MWh | 234.5 UAE Dirhams | 31.07% |
| Scenario-02: | 0.770 MWh | 234.9 UAE Dirhams | 30.98% |
| Scenario-03: | 0.773 MWh | 235.8 UAE Dirhams | 30.71% |
| Scenario-04 | 0.6215 MWh | 189.6 UAE Dirhams | 55.7% |

Similar to the basic model simulation, the analysis was done using both RadianceIES and Apache applications. The daylight harvesting potential for the fourth scenario was measured by the annual electrical consumption saving which happened after using the sensors (table 5.48). Due to the reduction of the average illuminance levels, the day light harvesting potential was reduced by an average of 55.7% in this scenario (table 5.49). Refer to final comparison table for full details including comparison with the basic model and first three scenarios.

5.4 Buffer DSF/ Corridor Facade -Scenarios 05 and 06 Analysis

5.4.1 Scenario 05 CFD simulation and analysis

Table 5.50. Air temperature within the DSF cavity from Microflo results (author 2019).

| Location | Date | Hour | Minimum DSF cavity air temperature (°C) | Maximum DSF cavity air temperature (°C) | Mean DSF cavity air temperature (°C) | Comparison between ambient temperature (47°C) and mean DSF cavity air temperature | Reduction in average air temperature comparing to scenarios 04. |
|---------------------|--------------------------|-------|-----------------------------------------|-----------------------------------------|--------------------------------------|-----------------------------------------------------------------------------------|-----------------------------------------------------------------|
| Eastern DSF cavity | 10 th of Aug. | 15:00 | 28.11 | 46.71 | 36.36 | -22.6% | 0.8% |
| Western DSF cavity | 10 th of Aug. | 12:00 | 28.18 | 46.54 | 36.17 | -23.0% | 0.9% |
| Northern DSF cavity | 10 th of Aug. | 15:00 | 28.19 | 46.62 | 36.26 | -22.9% | 0.9% |

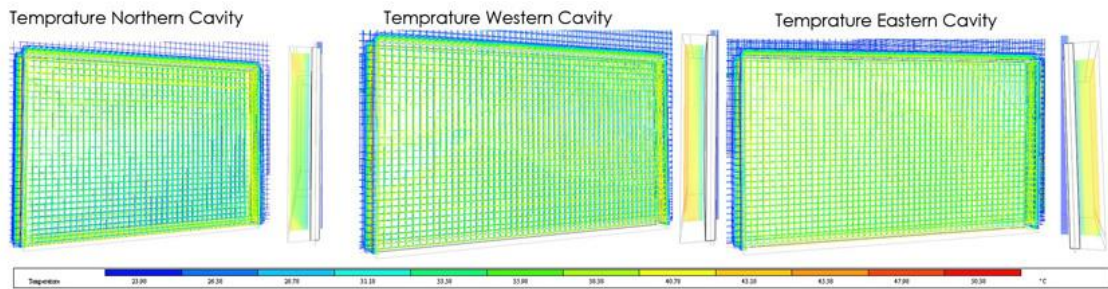


Figure 5.46. CFD analysis of Norther, Eastern and Western cushions in Microflo (author 2019).

The temperature analysis showed that when the ambient temperature reached 47.0 °C at the building level , the temperature in the DSF cavity near the cushion was maximum 46.71 °C in eastern DSF, maximum 46.54 °C in western DSF and maximum 46.62 °C in northern DSF. Thus, the temperature near the external DSF layer was slightly lower than ambient temperature in all cases. The temperature in the DSF cavity near the DGU was minimum 28.11 °C in eastern DSF, minimum 28.18 °C in western

DSF and minimum 28.19 °C in northern DSF. Due to the natural air flow, hot air was discharged and average reduction in mean cavity air temperature, comparing to ambient temperature, was 22.6% in eastern DSF, 23.0% in western DSF and 22.9% in northern DSF. Comparing to scenario 04, the average air temperature was reduced by 0.8% in eastern DSF cavity and 0.9% in western and northern DSFs cavities (table 5.50 and figure 5.46).

Table 5.51. Air velocity within the DSF cavity from Microflo results (author 2019).

| Location | Date | Hour | Air velocity within the cavity near the bottom inlet (m/s) | Air velocity within the cavity near the top outlet (m/s) | Mean air velocity within the cavity (m/s) |
|---------------------|--------------------------|-------|------------------------------------------------------------|----------------------------------------------------------|-------------------------------------------|
| Eastern DSF cavity | 10 th of Aug. | 15:00 | 0.51 | 0.62 | 0.57 |
| Western DSF cavity | 10 th of Aug. | 12:00 | 0.72 | 1.03~1.13 | 0.72 |
| Northern DSF cavity | 10 th of Aug. | 15:00 | 0.21 | 0.41~0.72 | 0.31 |

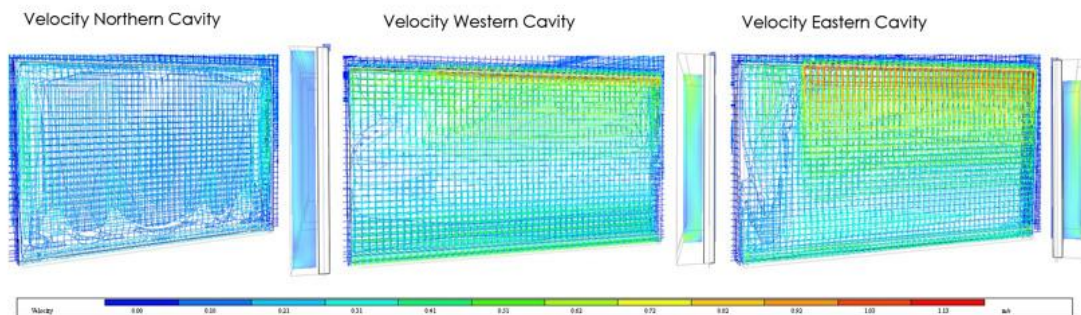


Figure 5.47. CFD analysis of the eastern cushions in IES VE (author 2019).

The analysis proved that air flow was from bottom to top which helped to discharge hot air from the DSF cavity. The maximum air velocity was near the top exhaust/outlet. Average air velocity in the eastern DSF was 0.57 while the maximum velocity was 0.62 m/s near the top and the inlet air velocity was 0.51 m/s. Average air velocity in the western DSFs was 0.72 m/s while the maximum velocity was 1.13 m/s near the top and the inlet air velocity was 0.72 m/s. Similar to previous scenarios the lowest air velocity and temperature was simulated in the northern DSF. The impact of the stack effect on the DSF was evaluated in the following sections where additional investigations on the internal conditions within the building were provided (table 5.51 and figure 5.47).

5.4.2 Scenario 06 CFD simulation and analysis

Table 5.52. Air temperature within the DSF cavity from Microflo results (author 2019).

| Location | Date | Hour | Minimum DSF cavity air temperature (°C) | Maximum DSF cavity air temperature (°C) | Mean DSF cavity air temperature (°C) | Comparison between ambient temperature (47°C) and mean DSF cavity air temperature | Reduction in average air temperature comparing to scenarios 04. |
|---------------------|--------------------------|-------|-----------------------------------------|-----------------------------------------|--------------------------------------|-----------------------------------------------------------------------------------|-----------------------------------------------------------------|
| Eastern DSF cavity | 10 th of Aug. | 15:00 | 28.02 | 46.24 | 36.00 | -23.4% | 1.8% |
| Western DSF cavity | 10 th of Aug. | 12:00 | 28.04 | 46.12 | 35.85 | -23.7% | 1.8% |
| Northern DSF cavity | 10 th of Aug. | 15:00 | 28.05 | 46.20 | 35.9 | -23.6% | 1.9% |

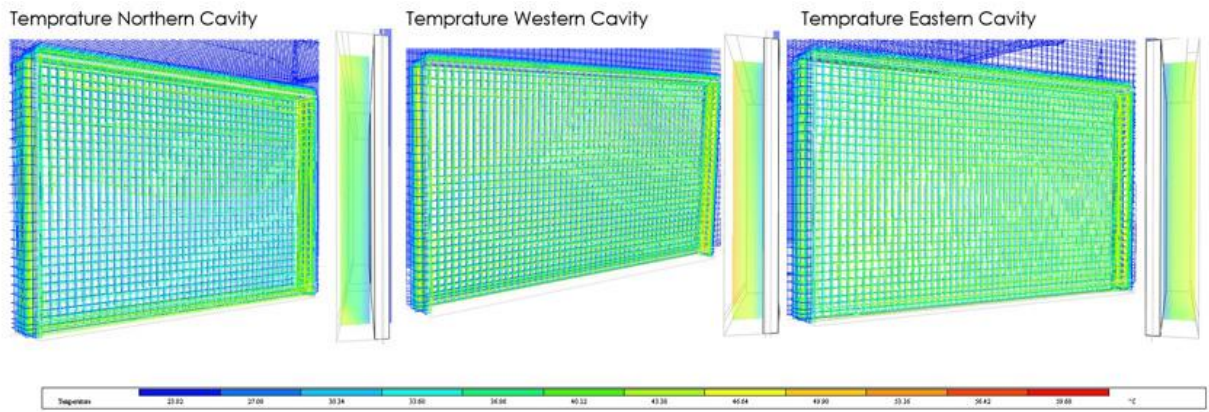


Figure 5.48. CFD analysis of Northern, Eastern and Western cushions in Microflo (author 2019).

The temperature analysis showed that when the ambient temperature reached 47.0 °C at the building level, the temperature in the DSF cavity near the cushion was maximum 46.24 °C in eastern DSF, maximum 46.12 °C in western DSF and maximum 46.20 °C in northern DSF. Thus, the temperature near the external DSF layer was slightly lower than ambient temperature in all cases. The temperature in the DSF cavity near the DGU was minimum 28.02 °C in eastern DSF, minimum 28.04 °C in western DSF and minimum 28.05 °C in northern DSF. Due to the natural air flow, hot air was discharged and average reduction in mean cavity air temperature, comparing to ambient temperature, was 23.4% in eastern DSF, 23.7% in western DSF and 23.6% in northern DSF. Comparing to scenario 04, the average air temperature was reduced by 1.9% in Northern DSF cavity and 1.8% in western and Eastern DSFs cavities (table 5.52 and figure 5.48).

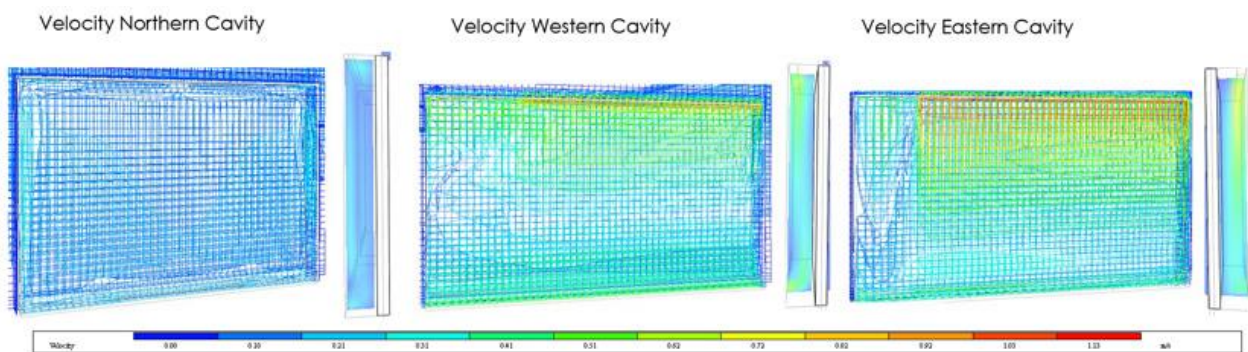


Figure 5.49. CFD analysis of the eastern cushions in IES VE (author 2019).

Table 5.53. Air velocity within the DSF cavity from Microflo results (author 2019).

| Location | Date | Hour | Air velocity within the cavity near the bottom inlet (m/s) | Air velocity within the cavity near the top outlet (m/s) | Mean air velocity within the cavity (m/s) |
|---------------------|--------------------------|-------|------------------------------------------------------------|----------------------------------------------------------|-------------------------------------------|
| Eastern DSF cavity | 10 th of Aug. | 15:00 | 0.51 | 1.03~1.13 | 0.79 |
| Western DSF cavity | 10 th of Aug. | 12:00 | 0.62 | 0.92 | 0.72 |
| Northern DSF cavity | 10 th of Aug. | 15:00 | 0.21 | 0.62 | 0.41 |

The analysis proved that air flow was from bottom to top which helped to discharge hot air from the DSF cavity. The maximum air velocity was near the top exhaust/outlet. Average air velocity in the eastern DSF was 0.79 while the maximum velocity was 1.13 m/s near the top and the inlet air velocity was 0.51 m/s. Average air velocity in the western DSFs was 0.72 m/s while the maximum velocity was 0.92 m/s near the top and the inlet air velocity was 0.62 m/s. Similar to previous scenarios the lowest air velocity and temperature was simulated in the northern DSF. The impact of the stack effect on the DSF was evaluated in the following sections where additional investigations on the internal conditions within the building were provided (table 5.53 and figure 5.49).

5.4.3 Scenarios 05 and 06 electrical consumption

Table 5.54. Total annual electricity consumption for scenario-02 comparing to the basic model (author 2019).

| | Total electricity (MWh) | Total electricity (MWh) | Total electricity (MWh) |
|--------------|-------------------------|-------------------------|-------------------------|
| Date | Scenario 06.aps | Scenario 05.aps | Basic Model.aps |
| Jan 01-31 | 1.9410 | 1.9420 | 2.1744 |
| Feb 01-28 | 2.1094 | 2.1108 | 2.4339 |
| Mar 01-31 | 2.6119 | 2.6139 | 3.0512 |
| Apr 01-30 | 3.1623 | 3.1643 | 3.6774 |
| May 01-31 | 3.7951 | 3.7975 | 4.4261 |
| Jun 01-30 | 3.9465 | 3.9491 | 4.5822 |
| Jul 01-31 | 4.2607 | 4.2633 | 4.9159 |
| Aug 01-31 | 4.3288 | 4.3310 | 4.9626 |
| Sep 01-30 | 3.9334 | 3.9354 | 4.4772 |
| Oct 01-31 | 3.5596 | 3.5613 | 4.0166 |
| Nov 01-30 | 2.8903 | 2.8920 | 3.2288 |
| Dec 01-31 | 2.3313 | 2.3324 | 2.6027 |
| Summed total | 38.8702 | 38.8930 | 44.5490 |

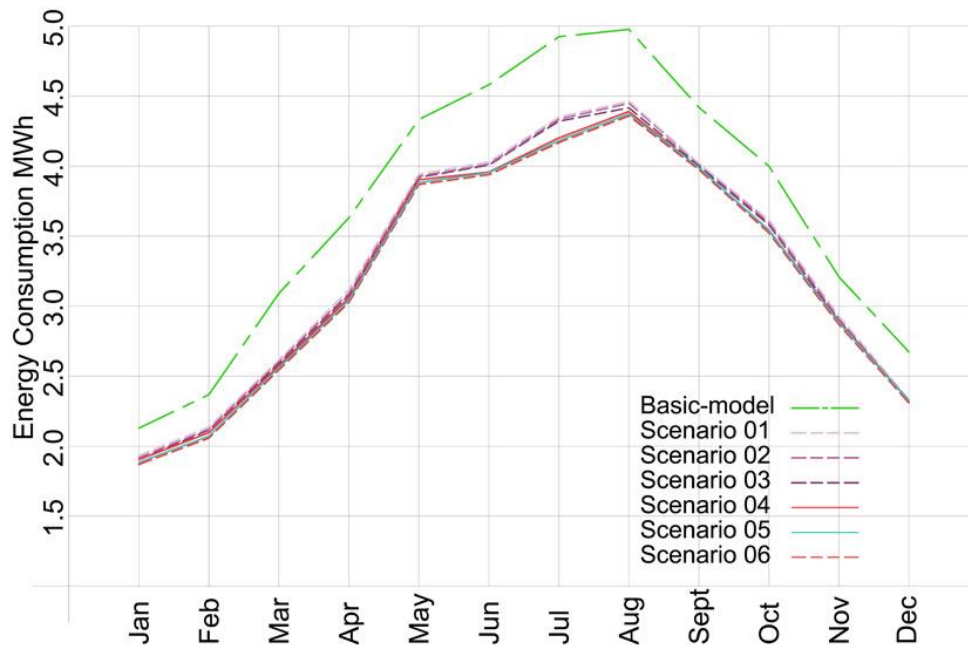


Figure 5.50. Combined diagram of the basic model results and the first six scenarios results (author 2019)

In scenario 05 and 06, the total electrical consumption reduction, with consideration of the inflation unit consumption, was 12.6% and 12.7% respectively. The results were better than the first four scenarios. Comparing to the fourth scenarios, the energy saving was improved by 0.15% and 0.25% when the different frit patterns were added (from 12.45% to 12.6% and 12.7%) (tables 5.54,5.55 and figure 5.50).

Table 5.55. Final comparison between the first five scenarios (author 2019).

| Scenario | Total annual electrical consumption saving comparing to the basic model (MWh) | Inflation unit annual electricity consumption (MWh) | Total annual electrical consumption saving considering inflation unit annual consumption (MWh) | Total annual electrical consumption saving considering inflation unit annual consumption (%) | Cost saving based on tariff of 30.5 Fils for every KW (ADDC 2018) |
|-------------|-------------------------------------------------------------------------------|-----------------------------------------------------|------------------------------------------------------------------------------------------------|----------------------------------------------------------------------------------------------|-------------------------------------------------------------------|
| Scenario-01 | 5.2033 | 0.03916 | 5.16414 | 11.594% | 1575.1 UAE Dirhams |
| Scenario-02 | 5.2064 | 0.03916 | 5.16724 | 11.600% | 1576.0 UAE Dirhams |
| Scenario-03 | 5.2084 | 0.03916 | 5.16924 | 11.603% | 1576.6 UAE Dirhams |
| Scenario-04 | 5.5863 | 0.03916 | 5.54714 | 12.45% | 1691.9 UAE Dirhams |
| Scenario-05 | 5.656 | 0.03916 | 5.61684 | 12.6% | 1713.1 UAE Dirhams |
| Scenario-06 | 5.6788 | 0.03916 | 5.63964 | 12.7% | 1720.1 UAE Dirhams |

5.4.4 Scenarios 05 and 06 thermal comfort results

Table 5.56. Comfort index results comparison between two scenarios and the basic model (author 2019).

| Var. Name | Location | Filename | Type | Mean |
|---------------|-----------------|-----------------|---------------|------|
| Comfort index | Mechanical room | Scenario 06.aps | Comfort index | 9 |
| Comfort index | Office 01 | Scenario 06.aps | Comfort index | 9 |
| Comfort index | Office 02 | Scenario 06.aps | Comfort index | 9 |
| Comfort index | Store 01 | Scenario 06.aps | Comfort index | 9 |
| Comfort index | Lobby 01 | Scenario 06.aps | Comfort index | 9 |
| Comfort index | Waiting room | Scenario 06.aps | Comfort index | 10 |
| Comfort index | Lobby 02 | Scenario 06.aps | Comfort index | 9 |
| Comfort index | Toilet | Scenario 06.aps | Comfort index | 9 |
| Comfort index | Store 02 | Scenario 06.aps | Comfort index | 9 |
| Comfort index | Reception | Scenario 06.aps | Comfort index | 9 |
| Comfort index | Mechanical room | Scenario 05.aps | Comfort index | 9 |
| Comfort index | Office 01 | Scenario 05.aps | Comfort index | 9 |
| Comfort index | Office 02 | Scenario 05.aps | Comfort index | 9 |
| Comfort index | Store 01 | Scenario 05.aps | Comfort index | 9 |
| Comfort index | Lobby 01 | Scenario 05.aps | Comfort index | 9 |
| Comfort index | Waiting room | Scenario 05.aps | Comfort index | 10 |
| Comfort index | Lobby 02 | Scenario 05.aps | Comfort index | 9 |
| Comfort index | Toilet | Scenario 05.aps | Comfort index | 9 |
| Comfort index | Store 02 | Scenario 05.aps | Comfort index | 9 |
| Comfort index | Reception | Scenario 05.aps | Comfort index | 9 |
| Comfort index | Mechanical room | Basic Model.aps | Comfort index | 9 |
| Comfort index | Office 01 | Basic Model.aps | Comfort index | 9 |
| Comfort index | Office 02 | Basic Model.aps | Comfort index | 9 |
| Comfort index | Store 01 | Basic Model.aps | Comfort index | 9 |
| Comfort index | Lobby 01 | Basic Model.aps | Comfort index | 9 |
| Comfort index | Waiting room | Basic Model.aps | Comfort index | 10 |
| Comfort index | Lobby 02 | Basic Model.aps | Comfort index | 9 |
| Comfort index | Toilet | Basic Model.aps | Comfort index | 9 |
| Comfort index | Store 02 | Basic Model.aps | Comfort index | 10 |
| Comfort index | Reception | Basic Model.aps | Comfort index | 10 |

In the two scenarios, the comfort index results were exactly the same as scenarios 02,03 and 04. Comparing to the basic model, Comfort index in store 02 and the reception changed from 10 (warm/acceptable) to 9 (slightly warm/acceptable). Thus, scenarios 05 and 06 results are similar to scenarios 02,03 and 04 results (table 5.56)

Table 5.57. Mean room temperature comparison between two scenarios and the basic model (author 2019).

| Var. Name | Location | Filename | Type | Mean |
|-----------------|-----------------|-----------------|------------------|-------|
| Air temperature | Mechanical room | Scenario 06.aps | Temperature (°C) | 24.83 |
| Air temperature | Office 01 | Scenario 06.aps | Temperature (°C) | 24.59 |
| Air temperature | Office 02 | Scenario 06.aps | Temperature (°C) | 24.58 |
| Air temperature | Store 01 | Scenario 06.aps | Temperature (°C) | 24.50 |
| Air temperature | Lobby 01 | Scenario 06.aps | Temperature (°C) | 24.59 |
| Air temperature | Waiting room | Scenario 06.aps | Temperature (°C) | 25.17 |
| Air temperature | Lobby 02 | Scenario 06.aps | Temperature (°C) | 24.77 |
| Air temperature | Toilet | Scenario 06.aps | Temperature (°C) | 24.62 |
| Air temperature | Store 02 | Scenario 06.aps | Temperature (°C) | 24.75 |
| Air temperature | Reception | Scenario 06.aps | Temperature (°C) | 25.16 |
| Air temperature | Mechanical room | Scenario 05.aps | Temperature (°C) | 24.83 |
| Air temperature | Office 01 | Scenario 05.aps | Temperature (°C) | 24.59 |
| Air temperature | Office 02 | Scenario 05.aps | Temperature (°C) | 24.58 |
| Air temperature | Store 01 | Scenario 05.aps | Temperature (°C) | 24.50 |
| Air temperature | Lobby 01 | Scenario 05.aps | Temperature (°C) | 24.59 |
| Air temperature | Waiting room | Scenario 05.aps | Temperature (°C) | 25.17 |
| Air temperature | Lobby 02 | Scenario 05.aps | Temperature (°C) | 24.77 |
| Air temperature | Toilet | Scenario 05.aps | Temperature (°C) | 24.62 |
| Air temperature | Store 02 | Scenario 05.aps | Temperature (°C) | 24.75 |
| Air temperature | Reception | Scenario 05.aps | Temperature (°C) | 25.17 |
| Air temperature | Mechanical room | Basic Model.aps | Temperature (°C) | 24.89 |
| Air temperature | Office 01 | Basic Model.aps | Temperature (°C) | 24.62 |
| Air temperature | Office 02 | Basic Model.aps | Temperature (°C) | 24.66 |
| Air temperature | Store 01 | Basic Model.aps | Temperature (°C) | 24.52 |
| Air temperature | Lobby 01 | Basic Model.aps | Temperature (°C) | 24.62 |
| Air temperature | Waiting room | Basic Model.aps | Temperature (°C) | 25.51 |
| Air temperature | Lobby 02 | Basic Model.aps | Temperature (°C) | 25.13 |
| Air temperature | Toilet | Basic Model.aps | Temperature (°C) | 24.94 |
| Air temperature | Store 02 | Basic Model.aps | Temperature (°C) | 25.16 |
| Air temperature | Reception | Basic Model.aps | Temperature (°C) | 26.15 |

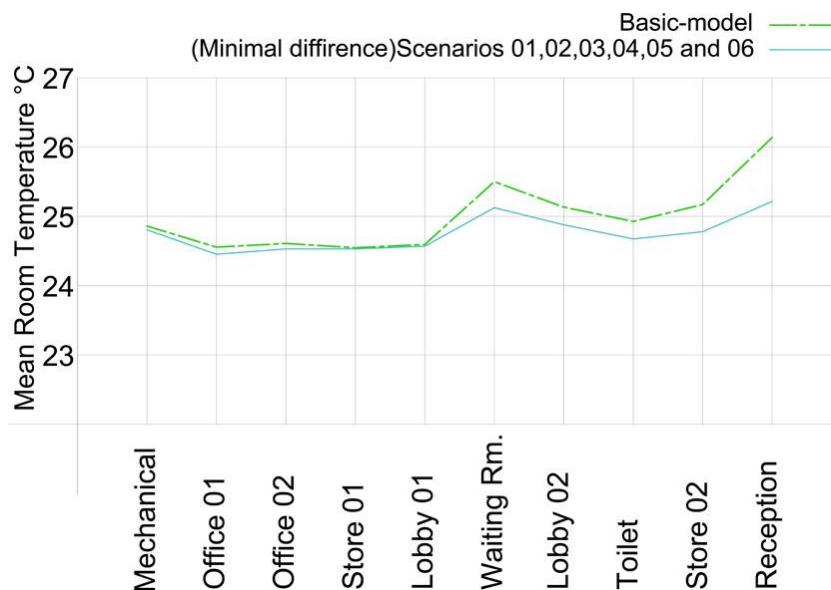


Figure 5.51. Combined diagram of the basic model results and the first six scenarios results (author 2019)

The rooms air temperature results in the two scenarios were similar with slight variation. Comparing to the basic model, the overall improvement/reduction in the mean room temperature was 1.06% in scenario 05 and 1.063% in scenario 06. The improvement/reduction in the mean waiting room temperature was 1.33% in scenario 05 and 1.33% in scenario 06. The improvement/reduction in the mean reception room temperature was 3.7% in scenario 05 and 3.8% in scenario 06. In general, scenarios 01,02,03,04,05 and 06 results were almost the same (table 5.57 and figure 5.51).

Table 5.58. People dissatisfied index results comparison between the two scenarios and the basic model (author 2019).

| Var. Name | Location | Filename | Type | Mean |
|---------------------|-----------------|-----------------|----------------|-------|
| People dissatisfied | Mechanical room | Scenario 06.aps | Percentage (%) | 29.41 |
| People dissatisfied | Office 01 | Scenario 06.aps | Percentage (%) | 26.32 |
| People dissatisfied | Office 02 | Scenario 06.aps | Percentage (%) | 25.96 |
| People dissatisfied | Store 01 | Scenario 06.aps | Percentage (%) | 26.10 |
| People dissatisfied | Lobby 01 | Scenario 06.aps | Percentage (%) | 27.38 |
| People dissatisfied | Waiting room | Scenario 06.aps | Percentage (%) | 33.26 |
| People dissatisfied | Lobby 02 | Scenario 06.aps | Percentage (%) | 29.82 |
| People dissatisfied | Toilet | Scenario 06.aps | Percentage (%) | 26.70 |
| People dissatisfied | Store 02 | Scenario 06.aps | Percentage (%) | 28.41 |
| People dissatisfied | Reception | Scenario 06.aps | Percentage (%) | 35.07 |
| People dissatisfied | Mechanical room | Scenario 05.aps | Percentage (%) | 29.41 |
| People dissatisfied | Office 01 | Scenario 05.aps | Percentage (%) | 26.32 |
| People dissatisfied | Office 02 | Scenario 05.aps | Percentage (%) | 25.96 |
| People dissatisfied | Store 01 | Scenario 05.aps | Percentage (%) | 26.10 |
| People dissatisfied | Lobby 01 | Scenario 05.aps | Percentage (%) | 27.38 |
| People dissatisfied | Waiting room | Scenario 05.aps | Percentage (%) | 33.26 |
| People dissatisfied | Lobby 02 | Scenario 05.aps | Percentage (%) | 29.84 |
| People dissatisfied | Toilet | Scenario 05.aps | Percentage (%) | 26.72 |
| People dissatisfied | Store 02 | Scenario 05.aps | Percentage (%) | 28.43 |
| People dissatisfied | Reception | Scenario 05.aps | Percentage (%) | 35.13 |
| People dissatisfied | Mechanical room | Basic Model.aps | Percentage (%) | 29.95 |
| People dissatisfied | Office 01 | Basic Model.aps | Percentage (%) | 26.55 |
| People dissatisfied | Office 02 | Basic Model.aps | Percentage (%) | 26.71 |
| People dissatisfied | Store 01 | Basic Model.aps | Percentage (%) | 26.24 |
| People dissatisfied | Lobby 01 | Basic Model.aps | Percentage (%) | 27.70 |
| People dissatisfied | Waiting room | Basic Model.aps | Percentage (%) | 37.07 |
| People dissatisfied | Lobby 02 | Basic Model.aps | Percentage (%) | 33.21 |
| People dissatisfied | Toilet | Basic Model.aps | Percentage (%) | 29.74 |
| People dissatisfied | Store 02 | Basic Model.aps | Percentage (%) | 32.37 |
| People dissatisfied | Reception | Basic Model.aps | Percentage (%) | 43.40 |

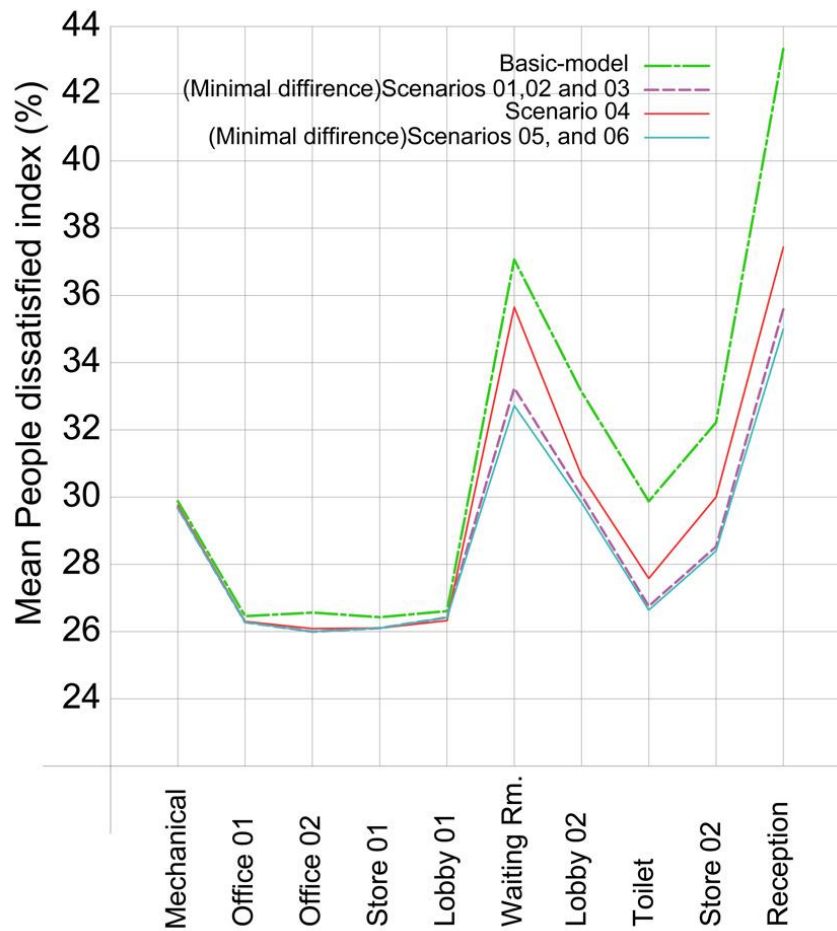


Figure 5.52. Combined diagram of the basic model results and the first six scenarios results (author 2019)

The typical mean dissatisfied index value of three scenarios had slight variation comparing to each other. Furthermore, comparing to the basic model, the mean values had an average improvement of 7.96% in scenario 05 and 8.0% in scenario 06. In the waiting room, the mean values had an average improvement of 10.3% in scenario 05 and 10.3% in scenario 06. In the reception room, the mean value had an average improvement of 19.0% in scenario 05 and 19.1% in scenario 06. As shown in the diagram, scenario 05 and 06 results were better than the first four scenarios results (table 5.58 and figure 5.52).

5.4.5 Scenarios 05 daylight analysis

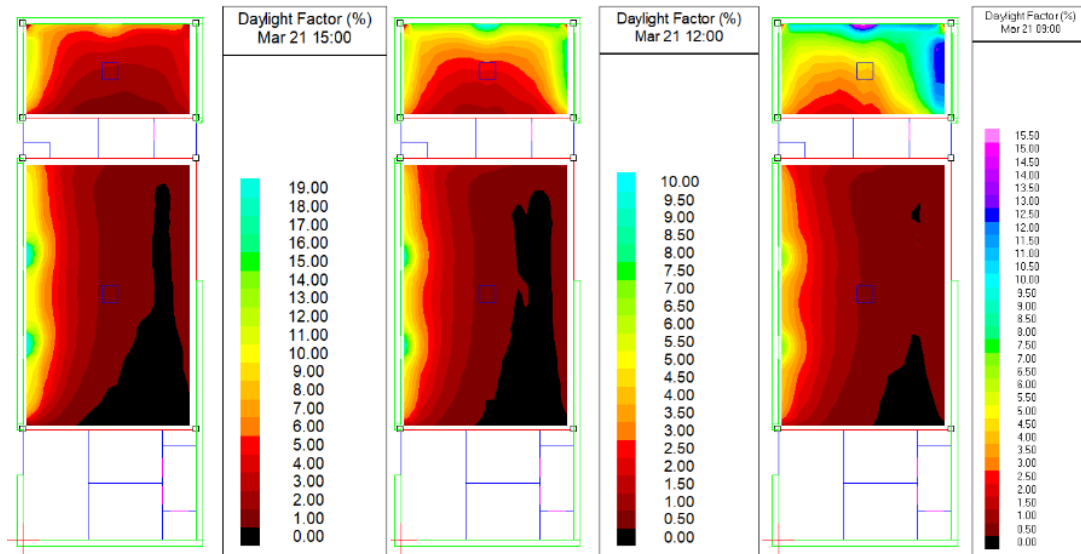


Figure 5.53. Scenario 05 daylight factor simulation results on the 21st of March (author 2019).

Table 5.59. Scenario 05 21st of March results summary (author 2019).

| Room | Date | Hour | Daylight factor | | | Daylight illuminance | | | Uniformity |
|----------------|---------------------------|-------|-----------------|------|-------|----------------------|------------|-------------|------------|
| | | | Min. | Ave. | Max. | Min. | Ave. | Max. | |
| Waiting room | 21 st of March | 9:00 | 0.3% | 1.4% | 7.1% | 26.06 lux | 105.84 lux | 538.46 lux | 0.25 |
| Reception room | 21 st of March | 9:00 | 1.6% | 6.6% | 15.6% | 118.65 lux | 498.3 lux | 1181 lux | 0.24 |
| Waiting room | 21 st of March | 12:00 | 0.3% | 1.4% | 8.8% | 24.4 lux | 121.85 lux | 772.79 lux | 0.20 |
| Reception room | 21 st of March | 12:00 | 1.1% | 3.9% | 10.1% | 98.75 lux | 343.66 lux | 894.07 lux | 0.29 |
| Waiting room | 21 st of March | 15:00 | 0.4% | 3.0% | 19.9% | 33.71 lux | 246.76 lux | 1654.11 lux | 0.14 |
| Reception room | 21 st of March | 15:00 | 1.5% | 4.5% | 11.6% | 120.95 lux | 374.14 lux | 966.12 lux | 0.32 |

In all cases, average daylighting level in the waiting room was lower than required while in the reception room, daylighting levels were higher than required at 9:00 on 21st of March. However, in all other cases, daylighting levels were within the

acceptable range. In all cases daylighting levels and DF were low in 60% to 75% of the waiting room area. Also, Average DF was lower than 2% in all the waiting room cases except at 15:00. Average DF was higher than 2% in all the reception room cases (figures 5.53 ,5.57,5.58,5.59,5.60 and table 5.59).

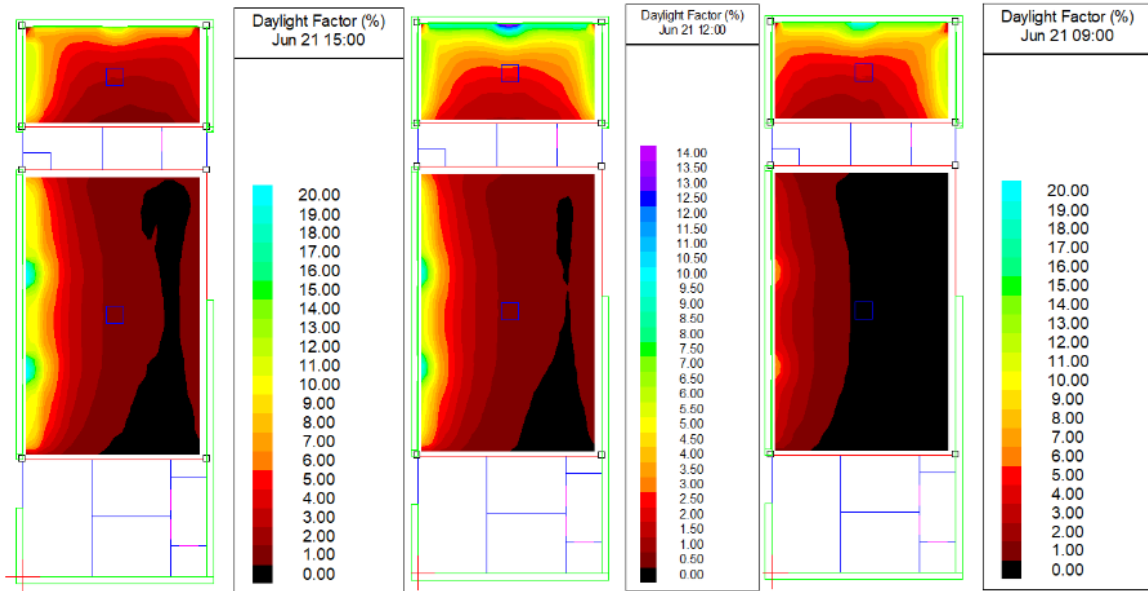


Figure 5.54. Scenario 05 daylight factor simulation results on the 21st of June (author 2019).

Table 5.60. Scenario 05 21st of June results summary (author 2019).

| Room | Date | Hour | Daylight factor | | | Daylight illuminance | | | Uniformity |
|----------------|--------------------------|-------|-----------------|------|-------|----------------------|------------|-------------|------------|
| | | | Min. | Ave. | Max. | Min. | Ave. | Max. | |
| Waiting room | 21 st of June | 9:00 | 0.3% | 1.3% | 7.0% | 25.18 lux | 106.50 lux | 580.56 lux | 0.24 |
| Reception room | 21 st of June | 9:00 | 1.2% | 6.8% | 20.6% | 99.55 lux | 558.34 lux | 1704.05 lux | 0.18 |
| Waiting room | 21 st of June | 12:00 | 0.3% | 1.5% | 9.9% | 56.85 lux | 275.48 lux | 1843.08 lux | 0.21 |
| Reception room | 21 st of June | 12:00 | 0.8% | 4.3% | 14.1% | 155.96 lux | 798.66 lux | 2629.01 lux | 0.20 |
| Waiting room | 21 st of June | 15:00 | 0.5% | 3.1% | 21.0% | 41.28 lux | 264.14 lux | 1795.59 lux | 0.16 |
| Reception room | 21 st of June | 15:00 | 1.0% | 5.0% | 13.1% | 81.97 lux | 429.48 lux | 1122.84 lux | 0.19 |

In all cases, average daylighting level in the waiting room was lower than required while in the reception room, daylighting levels were higher than required in all 21st of June cases. In all cases average daylighting levels and DF were low in 60% to 75% of the waiting room area. Also, Average DF was lower than 2% in all the waiting room cases except at 15:00. Average DF was higher than 2% in all the reception room cases (figures 5.54 ,5.57,5.58,5.59,5.60 and table 5.60).

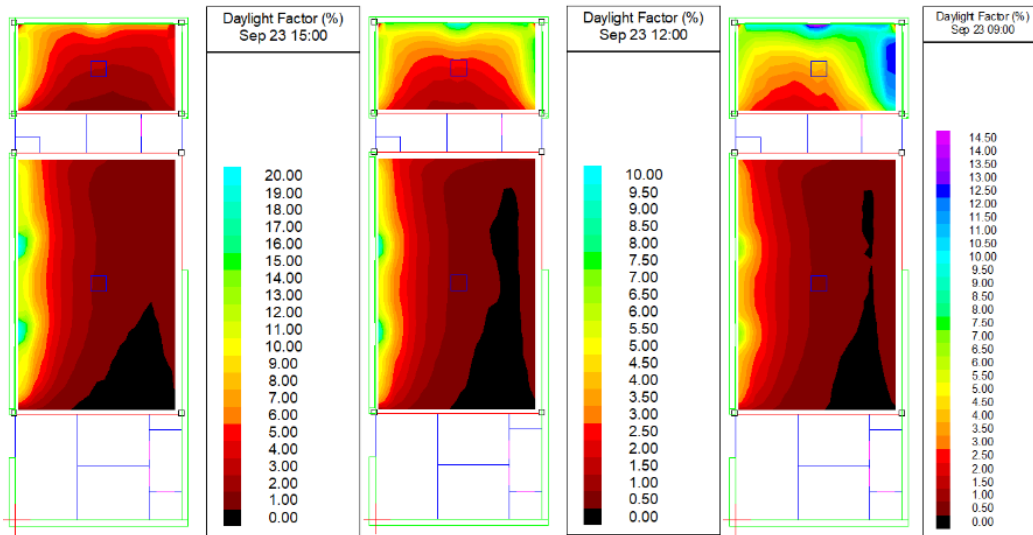


Figure 5.55. Scenario 05 daylight factor simulation results on the 23rd of September (author 2019).

Table 5.61. Scenario 05 23rd of September results summary (author 2019).

| Room | Date | Hour | Daylight factor | | | Daylight illuminance | | | Uniformity |
|----------------|---------------------------|-------|-----------------|------|-------|----------------------|------------|-------------|------------|
| | | | Min. | Ave. | Max. | Min. | Ave. | Max. | |
| Waiting room | 23 rd of Sept. | 9:00 | 0.3% | 1.4% | 7.0% | 25.64 lux | 106.58 lux | 548.55 lux | 0.24 |
| Reception room | 23 rd of Sept. | 9:00 | 1.6% | 6.2% | 14.8% | 124.94 lux | 487.00 lux | 1157.05 lux | 0.26 |
| Waiting room | 23 rd of Sept. | 12:00 | 0.3% | 1.5% | 9.5% | 25.17 lux | 129.89 lux | 840.82 lux | 0.19 |
| Reception room | 23 rd of Sept. | 12:00 | 1.1% | 3.9% | 10.0% | 101.66 lux | 343.74 lux | 889.89 lux | 0.30 |
| Waiting room | 23 rd of Sept. | 15:00 | 0.4% | 3.3% | 20.9% | 36.43 lux | 268.42 lux | 1715.11 lux | 0.14 |
| Reception room | 23 rd of Sept. | 15:00 | 1.5% | 4.8% | 12.2% | 121.93 lux | 390.90 lux | 997.08 lux | 0.31 |

In all cases, average daylighting level in the waiting room was lower than required while in the reception room, daylighting levels were higher than required at 9:00 on 23rd of September. However, in all other cases, average daylighting levels were within the acceptable range. In all cases daylighting levels and DF were low in 60% to 75% of the waiting room area. Also, Average DF was lower than 2% in all the waiting room cases except at 15:00 in all days. Average DF was higher than 2% in all the reception room cases (figures 5.55 ,5.57,5.58,5.59,5.60 and table 5.61).

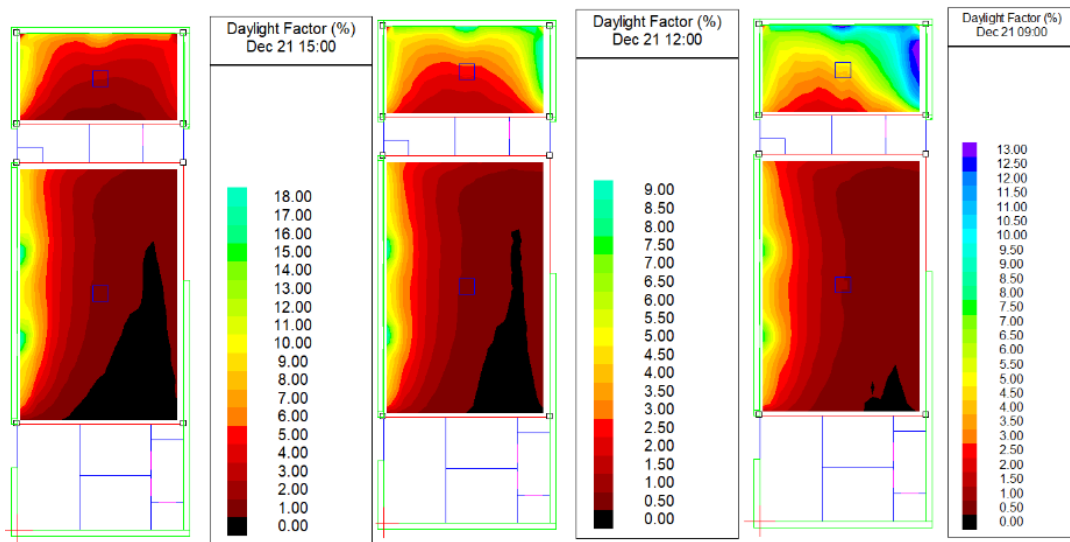


Figure 5.56. Scenarios-05 daylight factor simulation results on the 21st of December (author 2019).

Table 5.62. Scenarios 05 21st of December results summary (author 2019).

| Room | Date | Hour | Daylight factor | | | Daylight illuminance | | | Uniformity |
|----------------|--------------------------|-------|-----------------|------|-------|----------------------|------------|-------------|------------|
| | | | Min. | Ave. | Max. | Min. | Ave. | Max. | |
| Waiting room | 21 st of Dec. | 9:00 | 0.4% | 1.6% | 7.9% | 24.39 lux | 99.05 lux | 492.35 lux | 0.25 |
| Reception room | 21 st of Dec. | 9:00 | 2.1% | 6.5% | 13.4% | 129.55 lux | 402.28 lux | 830.8 lux | 0.32 |
| Waiting room | 21 st of Dec. | 12:00 | 0.3% | 1.5% | 8.9% | 25.18 lux | 124.46 lux | 727.98 lux | 0.20 |
| Reception room | 21 st of Dec | 12:00 | 1.5% | 4.1% | 9.5% | 121.6 lux | 333.97 lux | 772.36 lux | 0.36 |
| Waiting room | 21 st of Dec. | 15:00 | 0.4% | 3.0% | 18.0% | 28.37 lux | 207.10 lux | 1262.93 lux | 0.14 |
| Reception room | 21 st of Dec | 15:00 | 1.7% | 4.6% | 11.3% | 117.55 lux | 322.01 lux | 791.3 lux | 0.37 |

In all cases, average daylighting level in the waiting room was lower than required while in the reception room, in all cases, daylighting levels were within the acceptable range. In all cases daylighting levels and DF were low in 60% to 75% of the waiting room area. Also, Average DF was lower than 2% in all the waiting room cases except at 15:00. Average DF was higher than 2% in all the reception room cases (figures 5.56 ,5.57,5.58,5.59,5.60 and table 5.62).

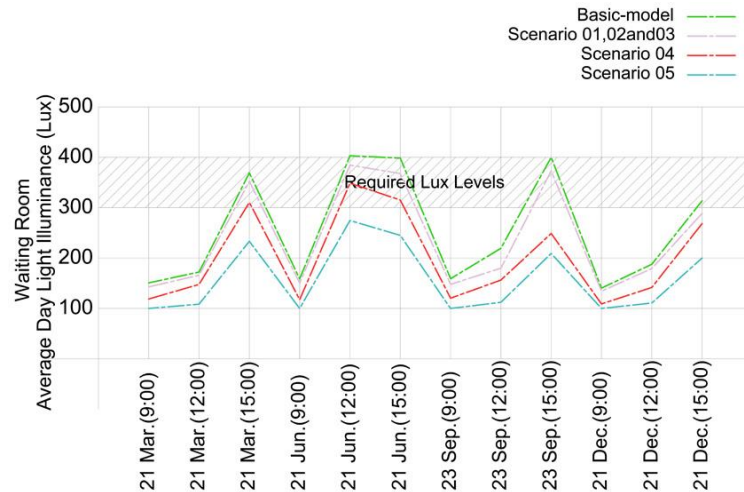


Figure 5.57. Combined diagram of the basic model DI results and the six scenarios DI results in waiting room (author 2019).

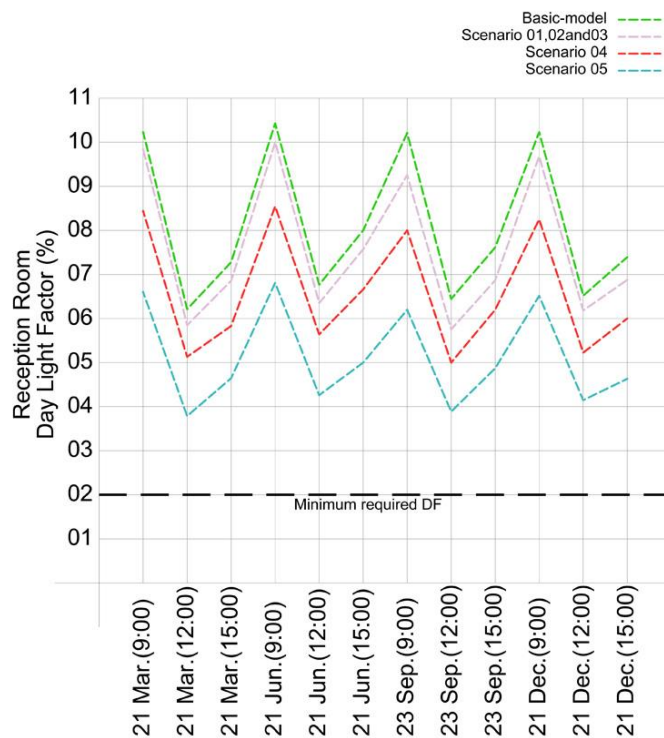


Figure 5.58. Combined diagram of the basic model DI results and the six scenarios DI results in reception room (author 2019).

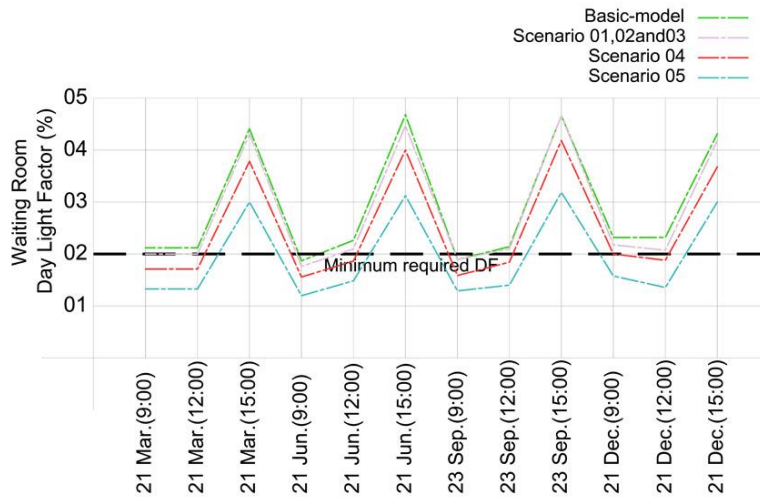


Figure 5.59. Combined diagram of the basic model DF results and the six scenarios DF results in the waiting room (author 2019).

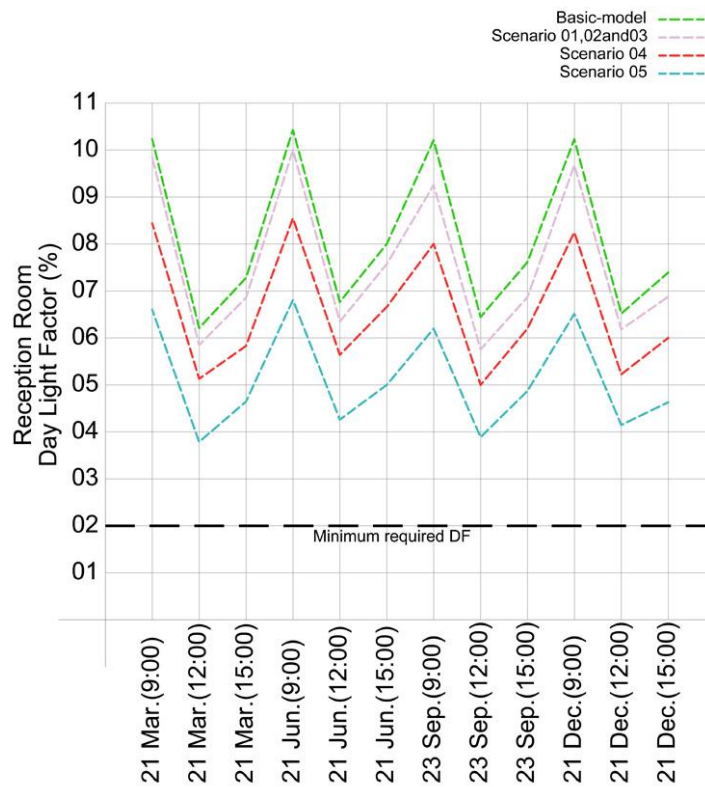


Figure 5.60. Combined diagram of the basic model DF results and the six scenarios DF results in reception room (author 2019).

Table 5.63. Final comparison between Scenario 05 and basic model (author 2019).

| Scenario | Date | Hour | Average daylight factor reduction | Average daylight illuminance reduction | Uniformity increment |
|-------------|---------------------------|-------|--------------------------------------------|--------------------------------------------|----------------------------------------------|
| Scenario 05 | 21 st of Mar. | 9:00 | Waiting room 33.3% Reception room 35.9% | Waiting room 32.6% Reception room 36.2% | Waiting room 13.6% Reception room -7.7% |
| Scenario 05 | 21 st of Mar. | 12:00 | Waiting room 33.3% Reception room 37.1% | Waiting room 33.2% Reception room 36.8% | Waiting room 11.1% Reception room -3.3% |
| Scenario 05 | 21 st of Mar. | 15:00 | Waiting room 31.8% Reception room 37.5% | Waiting room 33.5% Reception room 36.8% | Waiting room 7.7% Reception room 6.6% |
| Scenario 05 | 21 st of Jun. | 9:00 | Waiting room 31.5% Reception room 35.2% | Waiting room 32.9% Reception room 35.5% | Waiting room 14.3% Reception room -5.3% |
| Scenario 05 | 21 st of Jun. | 12:00 | Waiting room 31.8% Reception room 36.8% | Waiting room 32.6% Reception room 36.6% | Waiting room 16.7% Reception room -9.1% |
| Scenario 05 | 21 st of Jun. | 15:00 | Waiting room 34.0% Reception room 37.5% | Waiting room 33.7% Reception room 37.6% | Waiting room -14.2% Reception room -14.3% |
| Scenario 05 | 23 rd of Sept. | 9:00 | Waiting room 26.3% Reception room 39.2% | Waiting room 32.1% Reception room 40.6% | Waiting room 9.0% Reception room 13.0% |
| Scenario 05 | 23 rd of Sept. | 12:00 | Waiting room 28.6% Reception room 39.1% | Waiting room 41.4% Reception room 47.7% | Waiting room 5.5% Reception room 15.3% |
| Scenario 05 | 23 rd of Sept. | 15:00 | Waiting room 29.8% Reception room 36.8% | Waiting room 32.5% Reception room 39.7% | Waiting room 7.7% Reception room 14.8% |
| Scenario 05 | 21 st of Dec. | 9:00 | Waiting room 30.4% Reception room 36.3% | Waiting room 31.7% Reception room 36.2% | Waiting room 13.6% Reception room 3.2% |
| Scenario 05 | 21 st of Dec. | 12:00 | Waiting room 34.8% Reception room 36.9% | Waiting room 32.2% Reception room 36.8% | Waiting room 11.1% Reception room 12.5% |
| Scenario 05 | 21 st of Dec. | 15:00 | Waiting room 31.8% Reception room 37.0% | Waiting room 32.6% Reception room 36.7% | Waiting room 16.6% Reception room 15.6% |

Comparing to the basic-model, the changes in scenario 05 reduced daylighting lux levels by minimum 32.1% and maximum 41.4%. Furthermore, the change reduced average DF by minimum 26.3% and maximum 34.8%. Uniformity changes varied from 16.7% to -9.7%. Refer to the final comparison table. Due to changes in VLT transmittance, scenarios 0.4 results were better as shown in the previous diagrams. Comparing to them, the additional frit pattern reduced the daylighting levels by an average of 19.8% in the reception room and 24.8% in the waiting room. Also, the average DF reduction was 20.3% in the reception room and 20.6% in the waiting room (figures 5.57,5.58,5.59,5.60, tables 5.62 and 5.63).

5.4.6 Scenarios 06 daylight analysis

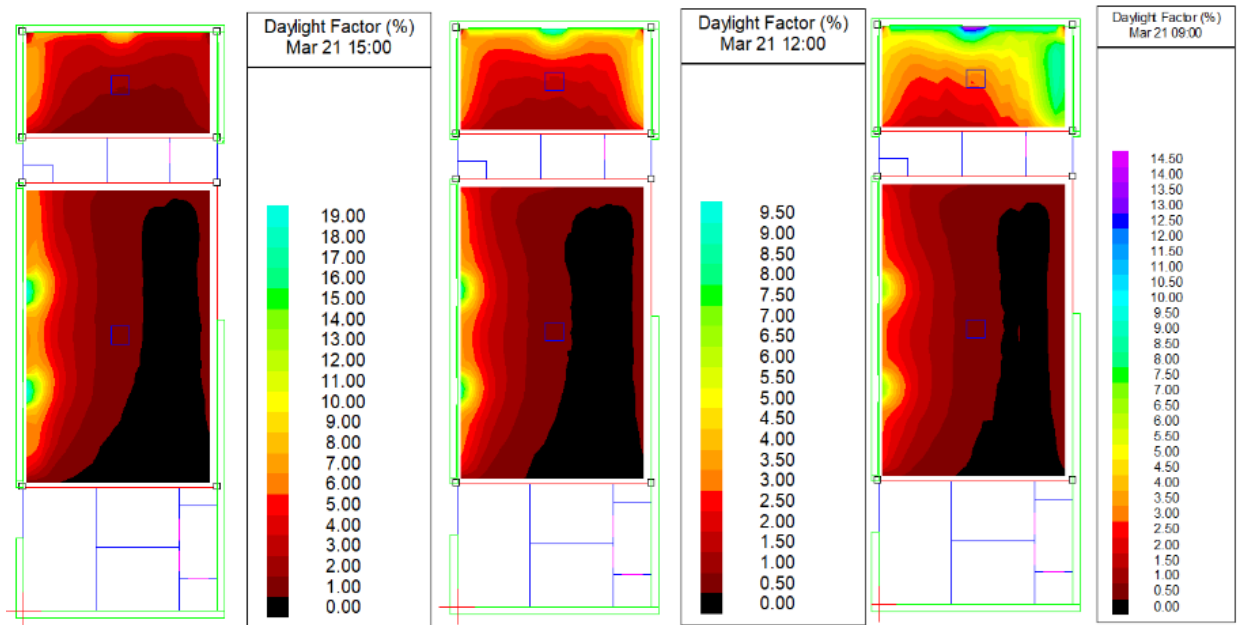


Figure 5.61. Scenario 06 daylight factor simulation results on the 21st of March (author 2019).

Table 5.64. Scenario 06 21st of March results summery (author 2019).

| Room | Date | Hour | Daylight factor | | | Daylight illuminance | | | Uniformity |
|----------------|---------------------------|-------|-----------------|------|-------|----------------------|------------|-------------|------------|
| | | | Min. | Ave. | Max. | Min. | Ave. | Max. | |
| Waiting room | 21 st of March | 9:00 | 0.3% | 1.1% | 6.9% | 21.07 lux | 84.25 lux | 524.84 lux | 0.25 |
| Reception room | 21 st of March | 9:00 | 1.1% | 4.8% | 15.0% | 83.89 lux | 366.93 lux | 1135.60 lux | 0.23 |
| Waiting room | 21 st of March | 12:00 | 0.2% | 1.1% | 8.6% | 20.28 lux | 97.17 lux | 757.85 lux | 0.21 |
| Reception room | 21 st of March | 12:00 | 0.9% | 2.9% | 9.9% | 80.73 lux | 255.11 lux | 870.63 lux | 0.32 |
| Waiting room | 21 st of March | 15:00 | 0.3% | 2.4% | 19.6% | 28.73 lux | 196.40 lux | 1635.27 lux | 0.15 |
| Reception room | 21 st of March | 15:00 | 1.0% | 3.3% | 96.6% | 87.35 lux | 275.75 lux | 797.84 lux | 0.32 |

In all cases, average daylighting level in the waiting room was lower than required while in the reception room, average daylighting levels were within acceptable range at 9:00 on 21st of March. In the rest of the cases, it was lower than required. In all cases average daylighting levels and DF were low in 70% to 80% of the waiting room area. Also, Average DF was lower than 2% in all the waiting room cases except at 15:00. Average DF was higher than 2% in all the reception room cases (figures 5.61 ,5.65,5.66,5.67,5.68 and table 5.64).

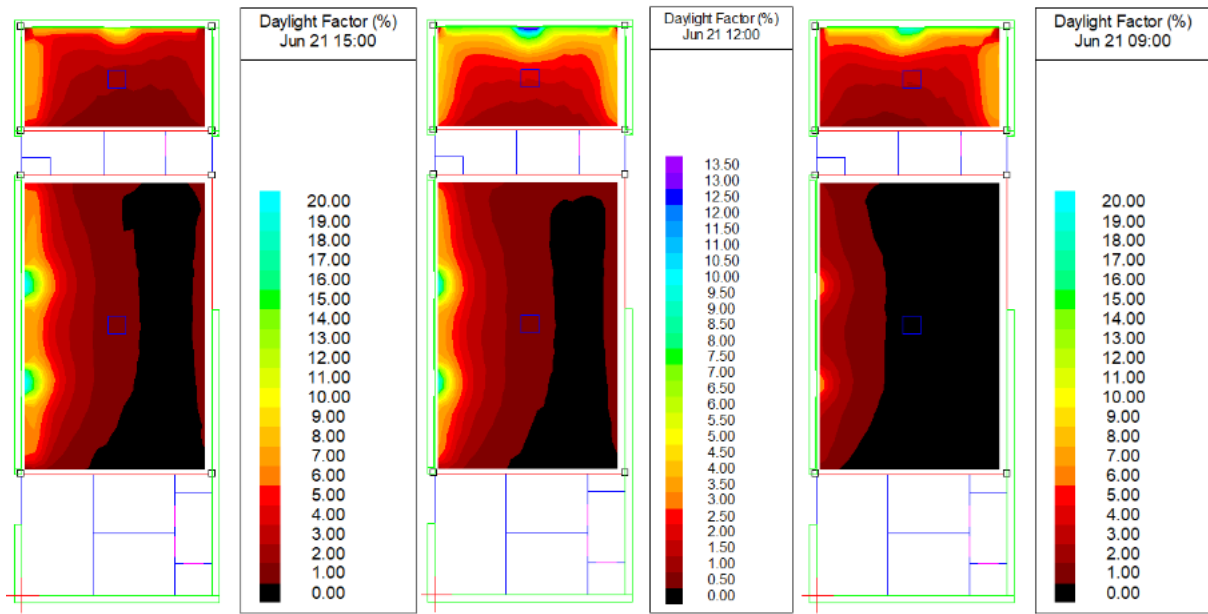


Figure 5.62. Scenario 06 daylight factor simulation results on the 21st of June (author 2019).

Table 5.65. Scenario 06 21st of June results summery (author 2019).

| Room | Date | Hour | Daylight factor | | | Daylight illuminance | | | Uniformity |
|----------------|--------------------------|-------|-----------------|------|-------|----------------------|------------|-------------|------------|
| | | | Min. | Ave. | Max. | Min. | Ave. | Max. | |
| Waiting room | 21 st of June | 9:00 | 0.3% | 1.0% | 6.8% | 20.99 lux | 84.57 lux | 564.81 lux | 0.25 |
| Reception room | 21 st of June | 9:00 | 0.9% | 5.1% | 20.3% | 72.15 lux | 419.81 lux | 1674.25 lux | 0.17 |
| Waiting room | 21 st of June | 12:00 | 0.3% | 1.2% | 9.7% | 46.62 lux | 220.77 lux | 1808.03 lux | 0.21 |
| Reception room | 21 st of June | 12:00 | 0.8% | 3.2% | 13.9% | 141.32 lux | 599.22 lux | 2586.44 lux | 0.24 |
| Waiting room | 21 st of June | 15:00 | 0.4% | 2.4% | 20.8% | 33.34 lux | 208.62 lux | 1776.34 lux | 0.16 |
| Reception room | 21 st of June | 15:00 | 0.8% | 3.7% | 12.8% | 67.03 lux | 317.29 lux | 1096.85 lux | 0.21 |

In all cases, average daylighting level in the waiting room was lower than required while in the reception room, average daylighting level was higher than required at 12:00 on 21st of June and within acceptable range at 9:00 and 12:00 on the 21st of June. In all cases average daylighting levels and DF were low in 70% to 80% of the waiting room area. Also, Average DF was lower than 2% in all the waiting room cases except at 15:00. Average DF was higher than 2% in all the reception room cases (figures 5.62 ,5.65,5.66,5.67,5.68 and table 5.65).

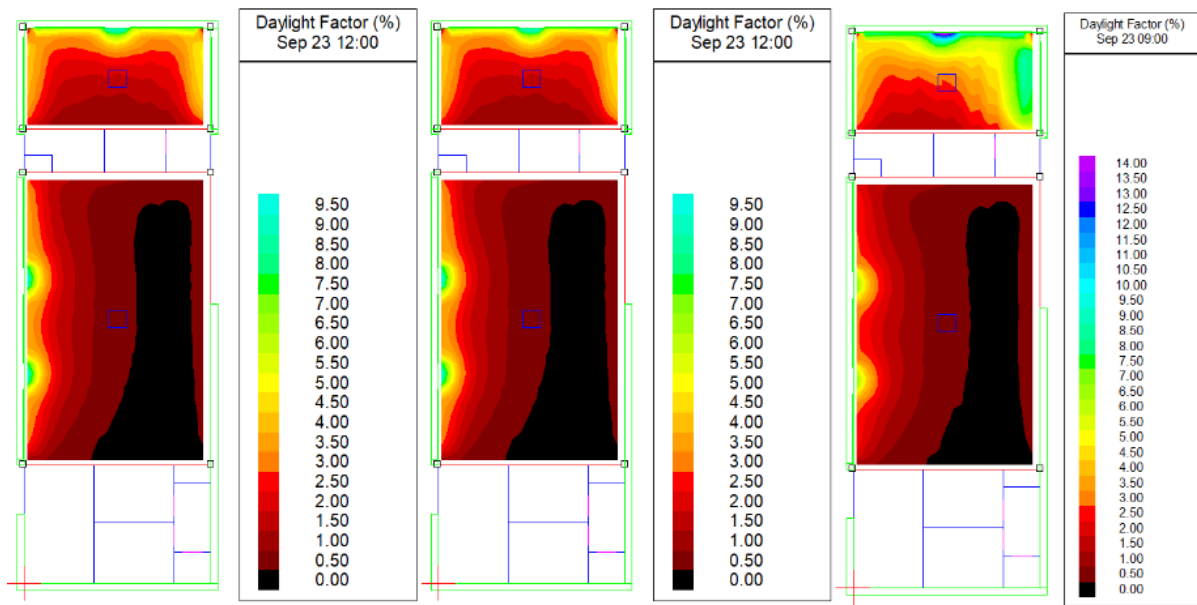


Figure 5.63. Scenario 06 daylight factor simulation results on the 23rd of September (author 2019).

Table 5.66. Scenario 06 23rd of September results summary (author 2019).

| Room | Date | Hour | Daylight factor | | | Daylight illuminance | | | Uniformity |
|----------------|---------------------------|-------|-----------------|------|-------|----------------------|------------|-------------|------------|
| | | | Min. | Ave. | Max. | Min. | Ave. | Max. | |
| Waiting room | 23 rd of Sept. | 9:00 | 0.3% | 1.1% | 6.8% | 20.91 lux | 85.01 lux | 535.38 lux | 0.25 |
| Reception room | 23 rd of Sept. | 9:00 | 1.1% | 4.6% | 14.2% | 88.22 lux | 358.32 lux | 1112.83 lux | 0.25 |
| Waiting room | 23 rd of Sept. | 12:00 | 0.2% | 1.2% | 9.3% | 21.01 lux | 103.48 lux | 824.75 lux | 0.20 |
| Reception room | 23 rd of Sept. | 12:00 | 1.0% | 2.9% | 9.8% | 88.88 lux | 255.42 lux | 866.73 lux | 0.35 |
| Waiting room | 23 rd of Sept. | 15:00 | 0.4% | 2.6% | 20.7% | 30.61 lux | 214.05 lux | 1695.95 lux | 0.14 |
| Reception room | 23 rd of Sept. | 15:00 | 1.1% | 3.5% | 9.9% | 89.78 lux | 288.38 lux | 811.56 lux | 0.31 |

In all cases, average daylighting levels in both rooms were lower than required. In all cases average daylighting levels and DF were low in 70% to 80% of the waiting room area. Also, Average DF was lower than 2% in all the waiting room cases except at 15:00 in all days. Average DF was higher than 2% in all the reception room cases (figures 5.63 ,5.65,5.66,5.67,5.68 and table 5.66).

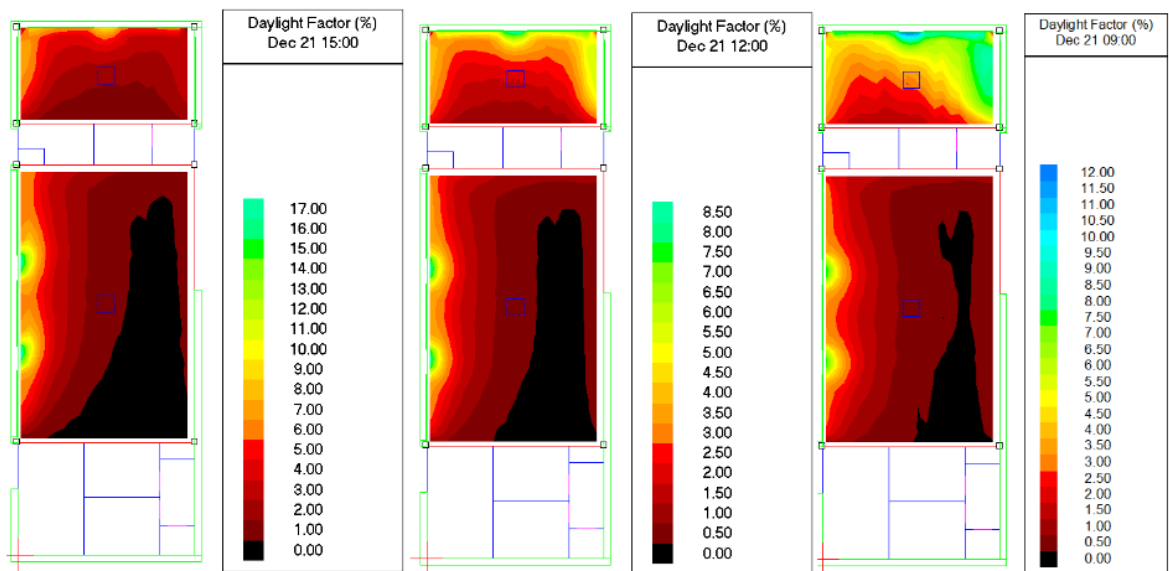


Figure 5.64. Scenarios 06 daylight factor simulation results on the 21st of December (author 2019).

Table 5.67. Scenarios 06 21st of December results summary (author 2019).

| Room | Date | Hour | Daylight factor | | | Daylight illuminance | | | Uniformity |
|----------------|--------------------------|-------|-----------------|------|-------|----------------------|------------|-------------|------------|
| | | | Min. | Ave. | Max. | Min. | Ave. | Max. | |
| Waiting room | 21 st of Dec. | 9:00 | 0.3% | 1.3% | 7.7% | 19.92 lux | 78.7 lux | 478.25 lux | 0.25 |
| Reception room | 21 st of Dec. | 9:00 | 1.6% | 4.8% | 12.5% | 97.57 lux | 294.92 lux | 774.55 lux | 0.33 |
| Waiting room | 21 st of Dec. | 12:00 | 0.3% | 1.2% | 8.7% | 21.36 lux | 100.09 lux | 711.66 lux | 0.21 |
| Reception room | 21 st of Dec | 12:00 | 1.1% | 3.0% | 8.8% | 89.35 lux | 247.43 lux | 714.73 lux | 0.36 |
| Waiting room | 21 st of Dec. | 15:00 | 0.3% | 2.4% | 17.7% | 24.20 lux | 165.45 lux | 1238.83 lux | 0.15 |
| Reception room | 21 st of Dec | 15:00 | 1.2% | 3.4% | 9.3% | 85.11 lux | 239.03 lux | 651.82 lux | 0.36 |

In all cases, average daylighting levels in both rooms were lower than required. In all cases average daylighting levels and DF were low in 70% to 80% of the waiting room area. Also, Average DF was lower than 2% in all the waiting room cases except at 15:00 in all days. Average DF was higher than 2% in all the reception room cases (figures 5.64 ,5.65,5.66,5.67,5.68 and table 5.67).

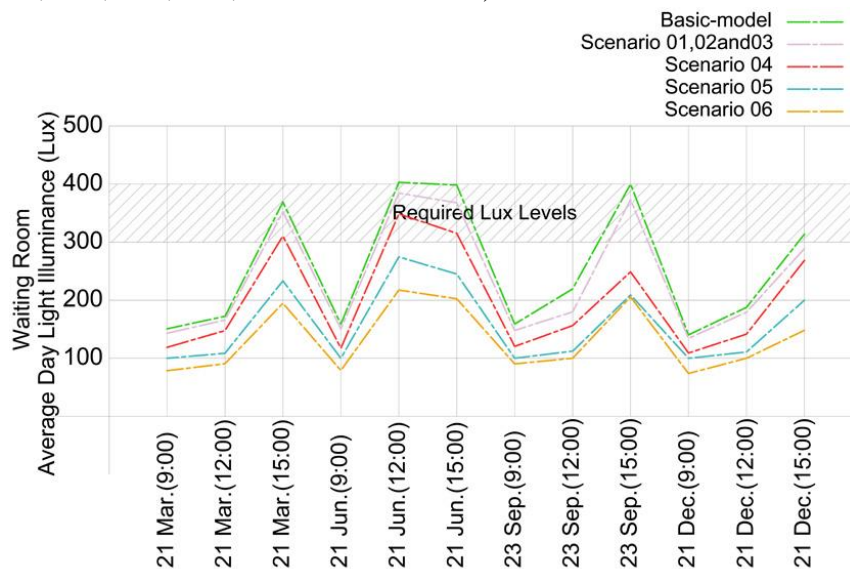


Figure 5.65. Combined diagram of the basic model DI results and the six scenarios DI results in waiting room (author 2019).

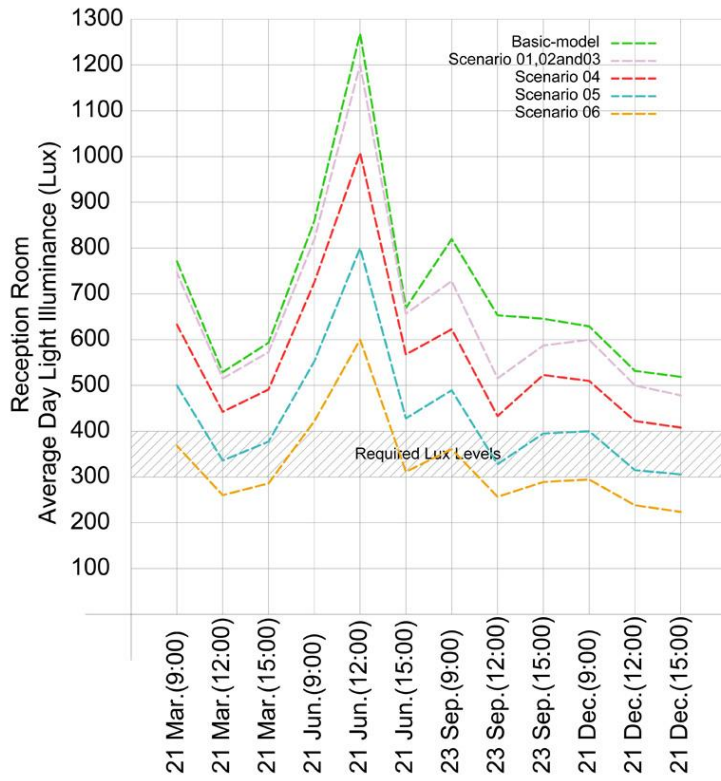


Figure 5.66. Combined diagram of the basic model DI results and the six scenarios DI results in reception room (author 2019).

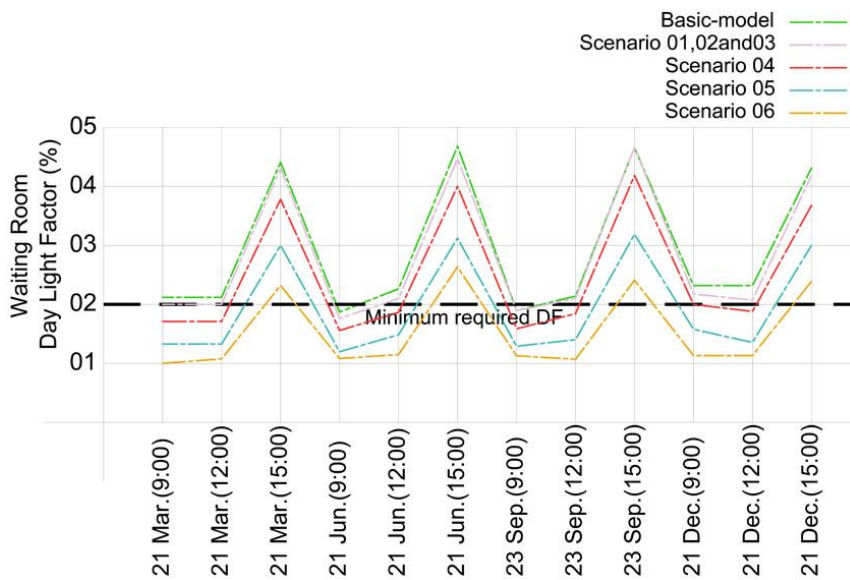


Figure 5.67. Combined diagram of the basic model DF results and the six scenarios DF results in the waiting room (author 2019).

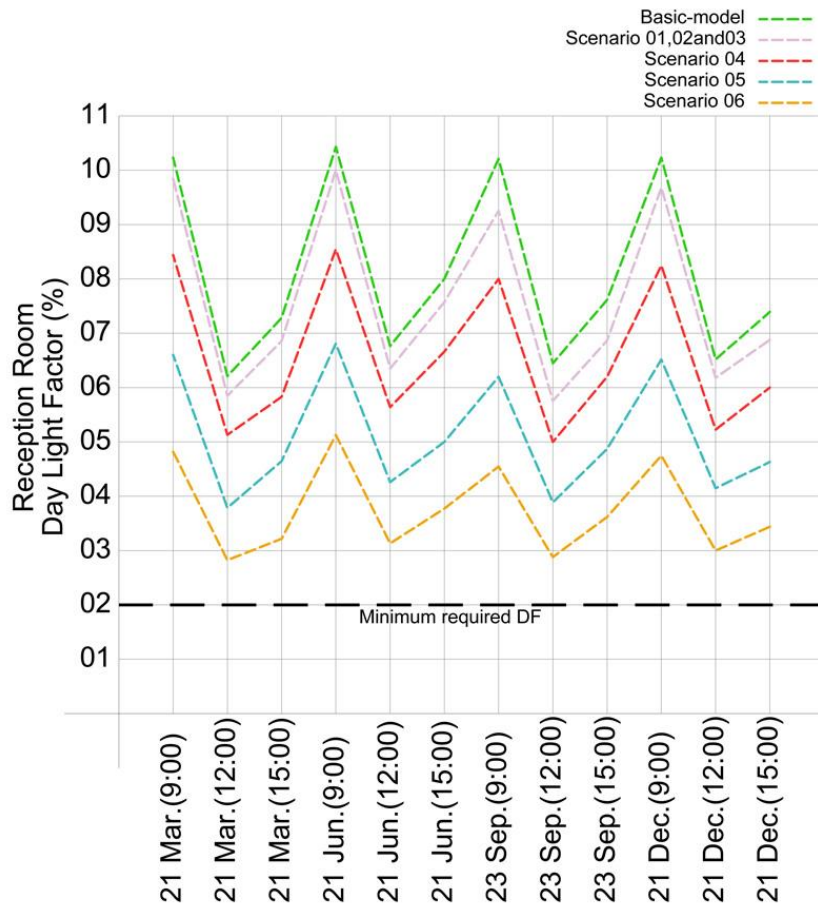


Figure 5.68. Combined diagram of the basic model DF results and the six scenarios DF results in reception room (author 2019).

Comparing to the basic-model, the changes in scenario 06 reduced daylighting lux levels by minimum 44.4% and maximum 60.1%. Furthermore, the change reduced average DF by minimum 42.1% and maximum 54.7%. Uniformity changes varied from 34.6% to -11.5%. Refer to the final comparison table. Due to changes in VLT transmittance, scenarios 04 results were better as shown in the previous diagrams. Comparing to them, the additional frit pattern reduced the daylighting levels by an average of 39.9% in the reception room and 37.3% in the waiting room. Also, the average DF reduction was 44.8% in the reception room and 38.6% in the waiting room (figures 5.65,5.66,5.67,5.68 and table 5.68).

Table 5.68. Final comparison between Scenario 06 and basic model (author 2019).

| Scenario | Date | Hour | Average daylight factor reduction | Average daylight illuminance reduction | Uniformity increment |
|-------------|---------------------------|-------|--------------------------------------------|--------------------------------------------|---------------------------------------------|
| Scenario 06 | 21 st of Mar. | 9:00 | Waiting room 47.6% Reception room 53.4% | Waiting room 46.1% Reception room 53.1% | Waiting room 13.6% Reception room -11.5% |
| Scenario 06 | 21 st of Mar. | 12:00 | Waiting room 47.6% Reception room 53.2% | Waiting room 46.4% Reception room 53.0% | Waiting room 16.7% Reception room 6.6% |
| Scenario 06 | 21 st of Mar. | 15:00 | Waiting room 45.5% Reception room 54.2% | Waiting room 47.0% Reception room 53.5% | Waiting room 15.4% Reception room 6.6% |
| Scenario 06 | 21 st of Jun. | 9:00 | Waiting room 47.4% Reception room 51.4% | Waiting room 46.8% Reception room 51.6% | Waiting room 19.0% Reception room -10.5% |
| Scenario 06 | 21 st of Jun. | 12:00 | Waiting room 45.5% Reception room 52.9% | Waiting room 46.0% Reception room 52.5% | Waiting room 16.7% Reception room 9.1% |
| Scenario 06 | 21 st of Jun. | 15:00 | Waiting room 48.9% Reception room 53.8% | Waiting room 47.7% Reception room 53.9% | Waiting room -14.2% Reception room 0.00% |
| Scenario 06 | 23 rd of Sept. | 9:00 | Waiting room 42.1% Reception room 52.8% | Waiting room 44.5% Reception room 56.3% | Waiting room 13.6% Reception room 8.7% |
| Scenario 06 | 23 rd of Sept. | 12:00 | Waiting room 42.9% Reception room 54.7% | Waiting room 53.2% Reception room 60.1% | Waiting room 11.1% Reception room 34.6% |
| Scenario 06 | 23 rd of Sept. | 15:00 | Waiting room 44.6% Reception room 53.9% | Waiting room 46.1% Reception room 55.5% | Waiting room 7.7% Reception room 14.8% |
| Scenario 06 | 21 st of Dec. | 9:00 | Waiting room 43.5% Reception room 52.9% | Waiting room 46.2% Reception room 53.3% | Waiting room 13.6% Reception room 6.4% |
| Scenario 06 | 21 st of Dec. | 12:00 | Waiting room 47.8% Reception room 53.8% | Waiting room 45.4% Reception room 53.1% | Waiting room 16.7% Reception room 12.5% |
| Scenario 06 | 21 st of Dec. | 15:00 | Waiting room 45.4% Reception room 53.4% | Waiting room 46.3% Reception room 53.1% | Waiting room 25.0% Reception room 12.5% |

5.4.7 Scenario 05 glare analysis

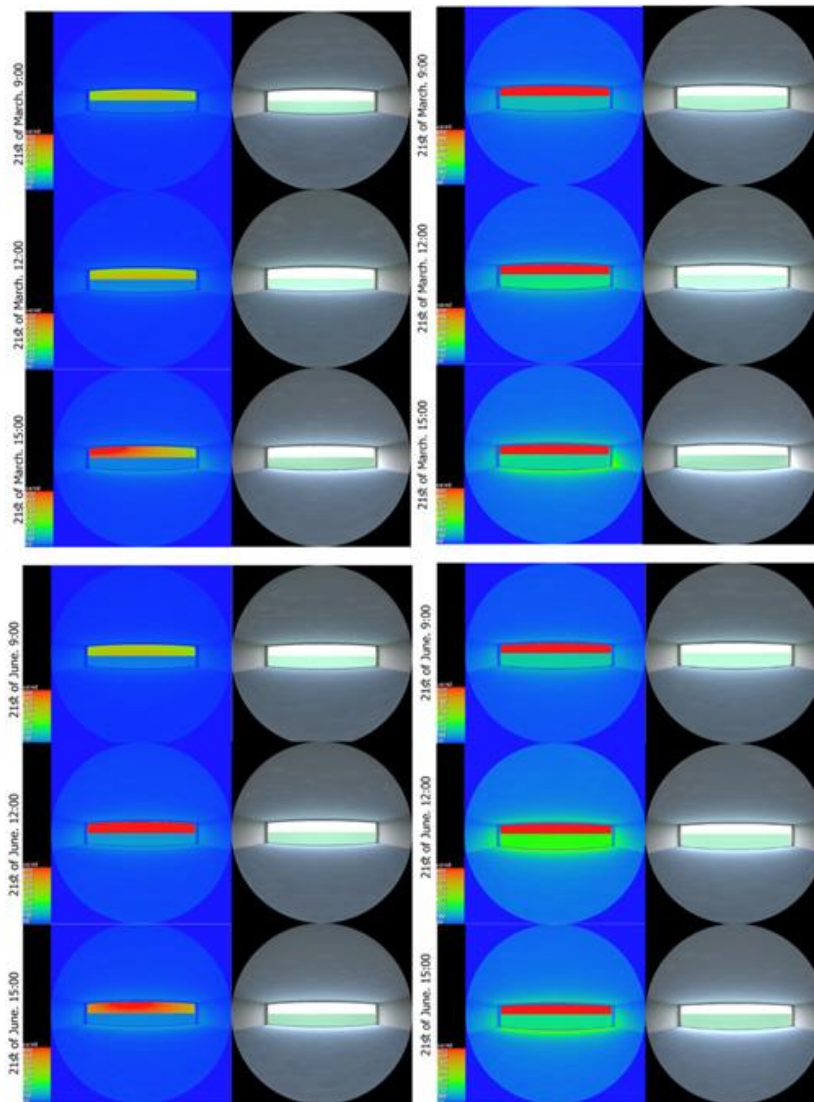


Figure 5.69. Waiting room luminance maps on the 21st of March (top images) and 21st of June (bottom images). The images on the left show scenario 04 results and the images on the right show the basic model results (author 2019).

On 21st of March, average luminance levels from the glazed wall reached 600 cd/m² in first two cases and 750 cd/m² in third case which, comparing to the basic model results, indicated 36.8% and 21.0% luminance level reduction. On 21st of June, in the waiting room, average luminance levels from the glazed wall reached 600 cd/m² in first case and 850 cd/m² in second and third case which, comparing to the basic model results, indicated 36.8% 10.5% luminance level reduction (figure 5.69).

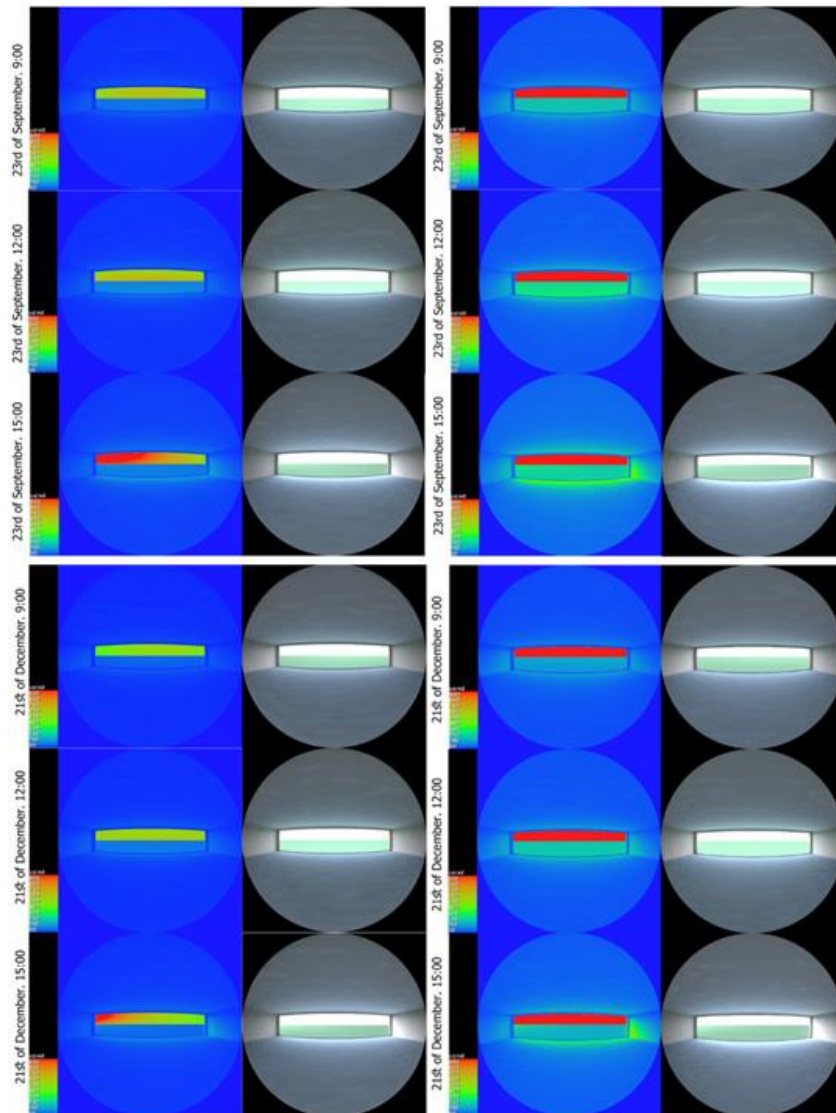


Figure 5.70. Waiting room luminance maps on the 23rd of September (top images) and 21st of December (bottom images). The images on the left show scenario 04 results and the images on the right show the basic model results (author 2019).

On 23rd of September, in the waiting room, average luminance levels from the glazed wall reached 600 cd/m² in first two cases and 750 cd/m² in third case which, comparing to the basic model results, indicated 36.8% and 21.0% luminance level reduction. 21st of December, in the waiting room, average luminance levels from the glazed wall reached 550 cd/m² in the first two cases and 700 cd/m² in the third case which, comparing to the basic model results, indicated 42.1% 26.3% luminance level reduction (figure 5.70).

Table 5.69. DGI levels from different angles from nadir for the four days at 9:00,12:00 and 15:00 (author 2019).

| Angle | 60 | 50 | 40 | 30 | 20 | 10 | 0 | -10 | -20 | -30 | -40 | -50 | -60 |
|-------------------------------------------|------|------|------|------|------|------|------|------|------|------|------|------|------|
| 09:00 21 st of March | 11.8 | 13.8 | 15.4 | 16.8 | 17.9 | 18.8 | 19.1 | 18.8 | 17.9 | 16.9 | 15.5 | 13.8 | 11.9 |
| 12:00 21 st of March | 11.7 | 13.7 | 15.3 | 16.7 | 17.8 | 18.6 | 18.8 | 18.6 | 17.8 | 16.7 | 15.3 | 13.7 | 11.7 |
| 15:00 21 st of March | 12.4 | 14.3 | 15.9 | 17.3 | 18.3 | 19.1 | 19.4 | 19.1 | 18.3 | 17.1 | 15.8 | 14.1 | 12.2 |
| 09:00 21 st of June | 11.8 | 13.8 | 15.4 | 16.8 | 17.9 | 18.7 | 18.9 | 18.7 | 17.9 | 16.8 | 15.4 | 13.8 | 11.8 |
| 12:00 21 st of June | 13.3 | 15.2 | 16.8 | 18.2 | 19.3 | 20.1 | 20.4 | 20.1 | 19.3 | 18.2 | 16.9 | 15.2 | 13.3 |
| 15:00 21 st of June | 12.5 | 14.4 | 16.1 | 17.4 | 18.5 | 19.3 | 19.6 | 19.3 | 18.5 | 17.4 | 16.1 | 14.4 | 12.5 |
| 09:00 23 rd of September | 11.8 | 13.8 | 15.5 | 16.8 | 17.9 | 18.8 | 19.0 | 18.8 | 17.9 | 16.9 | 15.5 | 13.8 | 11.9 |
| 12:00 23 rd of September | 11.7 | 13.7 | 15.3 | 16.6 | 17.1 | 18.6 | 18.8 | 18.6 | 17.7 | 16.7 | 15.3 | 13.7 | 11.7 |
| 15:00 23 rd of September | 12.5 | 14.4 | 16.1 | 17.4 | 18.5 | 19.3 | 19.5 | 19.2 | 18.4 | 17.3 | 15.9 | 14.3 | 12.3 |
| 09:00 21 st of December | 11.4 | 13.4 | 15.1 | 16.4 | 17.5 | 18.4 | 18.7 | 18.4 | 17.6 | 16.5 | 15.1 | 13.4 | 11.5 |
| 12:00 21 st of December | 11.6 | 13.5 | 15.2 | 16.5 | 17.6 | 18.4 | 18.7 | 18.4 | 17.6 | 16.5 | 16.1 | 13.5 | 11.6 |
| 15:00 21 st of December | 11.7 | 13.9 | 15.5 | 16.8 | 17.9 | 18.7 | 18.9 | 18.6 | 17.7 | 16.7 | 15.2 | 13.5 | 11.6 |

According to the DGI analysis there is a perceptible glare in all cases, as it exceeded 18 in the centre of the glazed wall. However, it did not reach the high disturbance level which is above 24 (table 5.69).

Table 5.70. GVCP levels from different angles from nadir for the four days at 9:00,12:00 and 15:00 (author 2019).

| Angle | 60 | 50 | 40 | 30 | 20 | 10 | 0 | -10 | -20 | -30 | -40 | -50 | -60 |
|-------------------------------------------|------|------|------|------|------|------|------|------|------|------|------|------|------|
| 09:00 21 st of March | 70.8 | 56.5 | 43.5 | 33.1 | 25.7 | 20.7 | 19.2 | 20.7 | 25.7 | 33.1 | 43.5 | 56.5 | 70.8 |
| 12:00 21 st of March | 70.5 | 56.3 | 43.4 | 33.1 | 25.7 | 20.8 | 19.3 | 20.8 | 25.8 | 33.3 | 43.6 | 56.5 | 70.7 |
| 15:00 21 st of March | 63.5 | 48.6 | 36.1 | 26.7 | 20.2 | 15.9 | 14.8 | 16.2 | 20.5 | 27.3 | 36.9 | 49.7 | 64.6 |
| 09:00 21 st of June | 70.6 | 56.3 | 43.3 | 32.9 | 25.6 | 20.6 | 19.1 | 20.6 | 25.6 | 33.0 | 43.4 | 56.3 | 70.7 |
| 12:00 21 st of June | 54.4 | 39.2 | 27.5 | 19.3 | 13.9 | 10.6 | 9.7 | 10.6 | 13.9 | 19.3 | 27.5 | 39.3 | 54.4 |
| 15:00 21 st of June | 61.8 | 46.8 | 34.4 | 25.1 | 18.8 | 14.8 | 13.6 | 14.8 | 18.9 | 25.3 | 34.6 | 47.1 | 62.1 |
| 09:00 23 rd of September | 70.4 | 56.1 | 43.1 | 32.7 | 25.3 | 20.4 | 18.9 | 20.4 | 25.3 | 32.7 | 43.1 | 56.1 | 70.4 |
| 12:00 23 rd of September | 70.4 | 56.1 | 43.3 | 33.1 | 25.7 | 20.7 | 19.2 | 20.8 | 25.7 | 33.2 | 43.5 | 56.4 | 70.6 |
| 15:00 23 rd of September | 62.1 | 47.1 | 34.6 | 25.4 | 19.1 | 15.1 | 13.9 | 15.2 | 19.5 | 26.1 | 35.5 | 48.2 | 63.2 |
| 09:00 21 st of December | 74.8 | 61.1 | 48.2 | 37.5 | 29.6 | 24.2 | 22.5 | 24.1 | 29.5 | 37.4 | 48.1 | 61.1 | 74.7 |
| 12:00 21 st of December | 72.3 | 58.3 | 45.4 | 34.9 | 27.4 | 22.3 | 20.7 | 22.3 | 27.5 | 35.2 | 45.6 | 58.6 | 72.5 |
| 15:00 21 st of December | 68.6 | 54.1 | 41.3 | 31.4 | 24.3 | 19.7 | 18.4 | 20.0 | 25.1 | 32.6 | 42.9 | 55.9 | 70.4 |

GVCP analysis showed that minimum percentage of satisfied occupants was 9.67% at 12:00 on 21st of June and maximum was 22.46% at 9:00 on 21st of December when looking at the middle of the northern glazed wall. The minimum percentage of satisfied occupants was 54.37% at 12:00 on 21st of June to and maximum was 74.83% at 9:00 on 21st of December when looking at the eastern and western glazed walls (table 5.70).

Comparing to the basic model minimum DGI reduction was 11.4% and maximum DGI reduction was 20.4% while the minimum GVCP improvement was 141.9% and maximum GVCP improvement was 218.9%. Refer to final comparison table 5.71 for full details including comparison with the basic model and fourth scenario.

Table 5.71. Final comparison between Scenarios 04,05 and basic model (author 2019).

| Date | Hour | Average DGI reduction comparing to the basic model results (scenario 05) | Average DGI reduction comparing to the basic model results (scenario 04) | Average GVCP increment comparing to the basic model results (scenario 05) | Average GVCP increment comparing to the basic model results (scenario 04) |
|---------------------------|-------|--------------------------------------------------------------------------|--------------------------------------------------------------------------|---------------------------------------------------------------------------|---------------------------------------------------------------------------|
| 21 st of Mar. | 9:00 | 15.0% | 13.7% | 158.1% | 122.8% |
| 21 st of Mar. | 12:00 | 14.0% | 13.2% | 157.6% | 123.3% |
| 21 st of Mar. | 15:00 | 15.5% | 11.5% | 186.4% | 141.1% |
| 21 st of Jun. | 9:00 | 14.9% | 13.3% | 159.2% | 123.3% |
| 21 st of Jun. | 12:00 | 15.1% | 10.8% | 218.9% | 131.7% |
| 21 st of Jun. | 15:00 | 15.9% | 11.4% | 193.0% | 157.3% |
| 23 rd of Sept. | 9:00 | 16.7% | 15.5% | 159.6% | 125.2% |
| 23 rd of Sept. | 12:00 | 14.9% | 14.2% | 190.8% | 152.7% |
| 23 rd of Sept. | 15:00 | 11.4% | 7.1% | 188.6% | 146.4% |
| 21 st of Dec. | 9:00 | 18.2% | 16.4% | 146.2% | 114.8% |
| 21 st of Dec. | 12:00 | 20.4% | 18.9% | 141.9% | 117.8% |
| 21 st of Dec. | 15:00 | 14.5% | 13.2% | 165.5% | 129.7% |

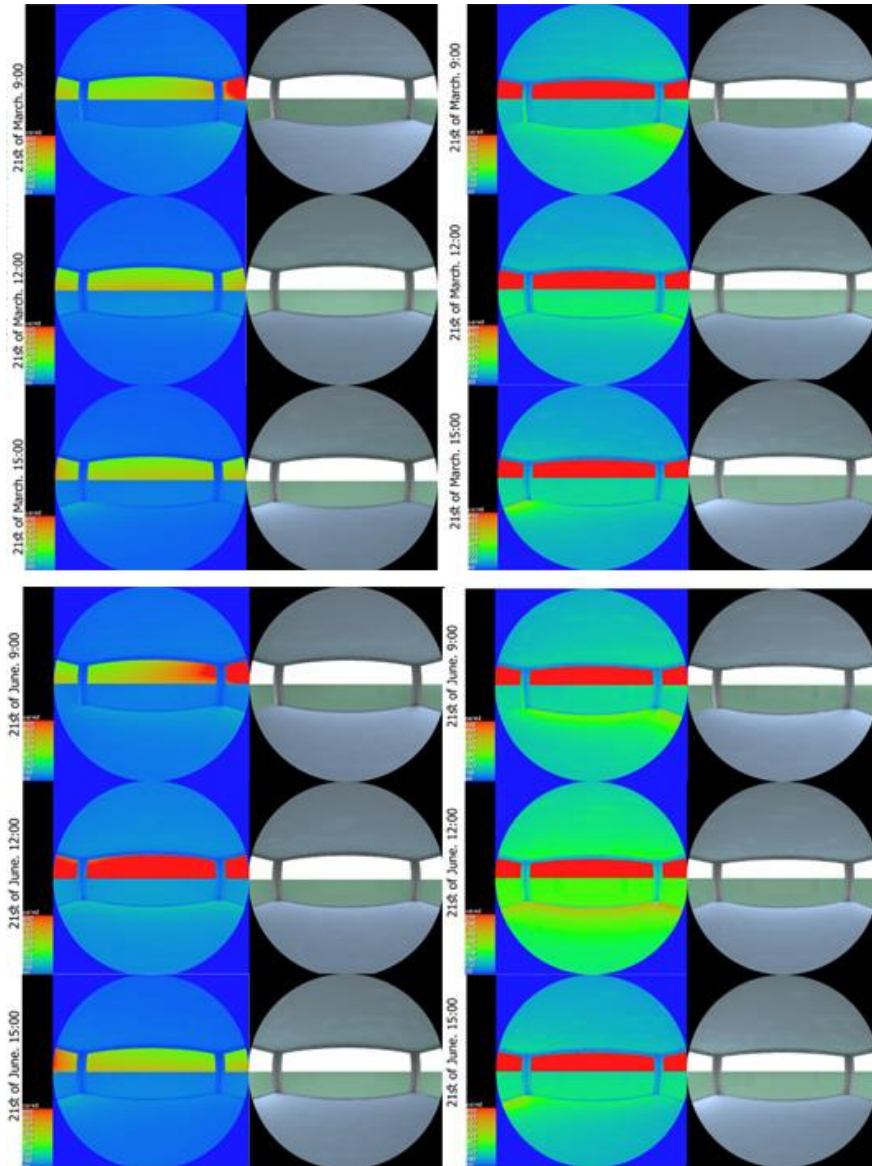


Figure 5.71. Reception room luminance maps on the 21st of March (top images) and 21st of June (bottom images). The images on the left show scenarios01,02 and 03 results and the images on the right show the basic model results (author 2019).

On 21st of March, in the reception room, luminance levels from the glazed wall reached 450 cd/m² in all cases which, comparing to the basic model results, indicated 52.6% luminance level reduction. On 21st of June, in the reception room, luminance levels from the glazed wall reached 650 cd/m² in the first case, 800 cd/m² in second case and 550 cd/m² in the third case which, comparing to the basic model results, indicated 31.6% ,15.7% and 42.1% luminance level reduction (figure 5.71).

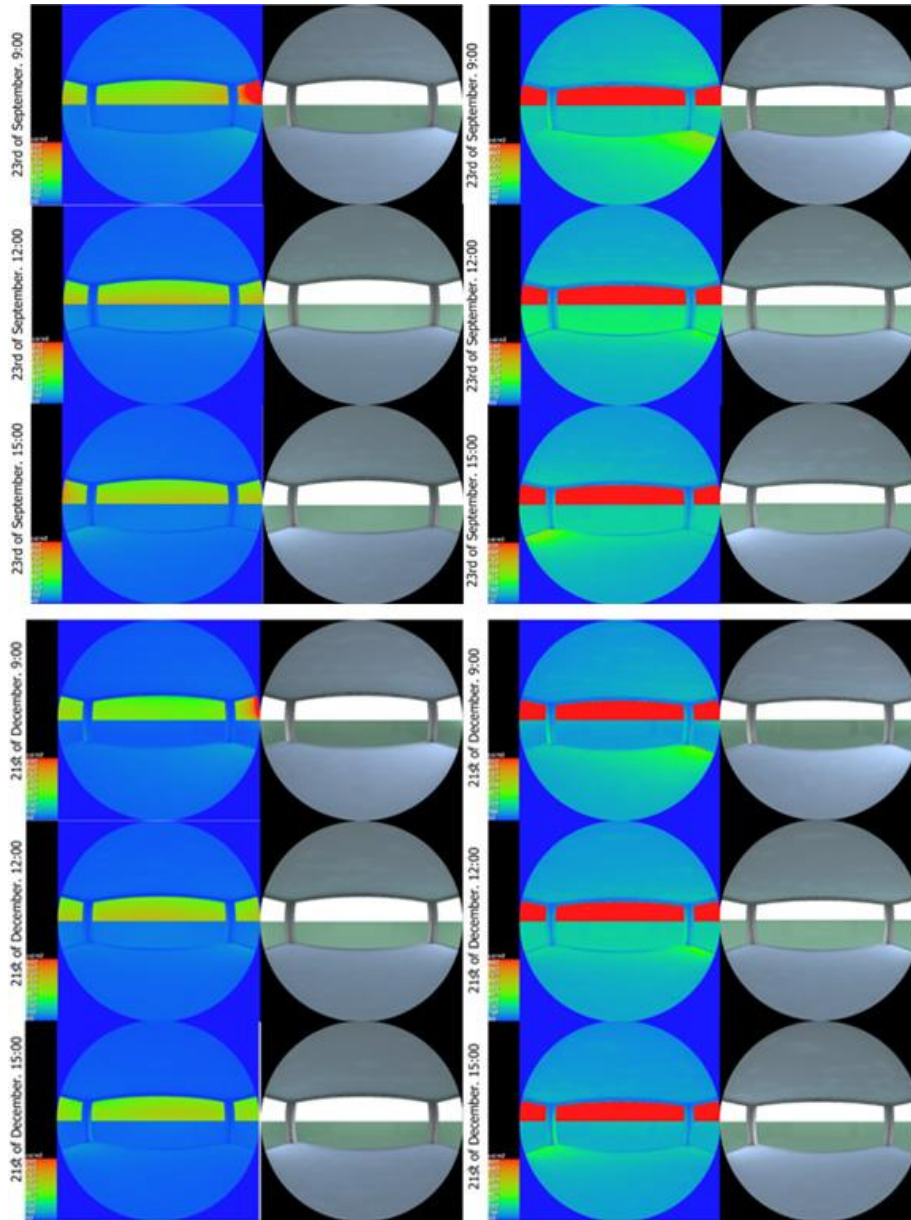


Figure 5.72. Reception room luminance maps on the 23rd of September (top images) and 21st of December (bottom images). The images on the left show scenarios01,02 and 03 results and the images on the right show the basic model results (author 2019).

On 23rd of September and 21st of December, in the reception room, luminance levels from the glazed wall reached 450 cd/m² in all cases which, comparing to the basic model results, indicated 52.6% luminance level reduction (5.72).

Table 5.72. DGI levels from different angles from nadir for the four days at 9:00,12:00 and 15:00 (author 2019).

| Angle | 60 | 50 | 40 | 30 | 20 | 10 | 0 | -10 | -20 | -30 | -40 | -50 | -60 |
|-------------------------------------------|------|------|------|------|------|------|------|------|------|------|------|------|------|
| 09:00 21 st of March | 0.00 | 0.00 | 0.00 | 0.00 | 0.00 | 3.12 | 6.1 | 8.8 | 11.2 | 13.3 | 15.2 | 16.8 | 18.1 |
| 12:00 21 st of March | 9.1 | 8.7 | 8.4 | 8.4 | 0.00 | 9.1 | 9.2 | 8.8 | 8.6 | 8.7 | 9.2 | 9.9 | 10.9 |
| 15:00 21 st of March | 12.4 | 14.3 | 15.9 | 17.3 | 18.3 | 19.1 | 19.4 | 19.1 | 18.3 | 17.2 | 15.8 | 14.2 | 12.2 |
| 09:00 21 st of June | 0.00 | 0.00 | 0.2 | 2.9 | 0.00 | 8.1 | 10.1 | 12.1 | 13.7 | 15.2 | 16.4 | 17.4 | 18.2 |
| 12:00 21 st of June | 0.00 | 0.00 | 0.00 | 0.00 | 0.00 | 0.00 | 0.00 | 0.00 | 0.00 | 0.00 | 0.00 | 0.00 | 0.00 |
| 15:00 21 st of June | 14.6 | 13.2 | 11.5 | 9.5 | 7.2 | 4.7 | 1.9 | 0.00 | 0.00 | 0.00 | 0.00 | 0.00 | 0.00 |
| 09:00 23 rd of September | 0.00 | 0.00 | 0.00 | 0.00 | 0.00 | 2.6 | 5.3 | 8.1 | 10.5 | 12.6 | 14.5 | 16.1 | 17.4 |
| 12:00 23 rd of September | 9.7 | 9.3 | 9.1 | 9.1 | 0.00 | 9.9 | 10.3 | 9.9 | 9.5 | 9.4 | 9.7 | 10.2 | 10.9 |
| 15:00 23 rd of September | 13.8 | 12.2 | 10.4 | 8.3 | 5.9 | 3.3 | 0.00 | 0.00 | 0.00 | 0.00 | 0.00 | 0.00 | 0.00 |
| 09:00 21 st of December | 0.00 | 0.00 | 0.00 | 0.00 | 0.00 | 0.1 | 3.2 | 6.0 | 8.6 | 10.9 | 12.9 | 14.6 | 16.1 |
| 12:00 21 st of December | 3.9 | 5.6 | 6.9 | 8.1 | 8.9 | 0.00 | 0.00 | 9.0 | 8.5 | 8.1 | 8.1 | 8.7 | 9.4 |
| 15:00 21 st of December | 9.4 | 8.4 | 7.8 | 7.8 | 8.3 | 9.2 | 9.9 | 10.5 | 10.4 | 9.7 | 8.7 | 7.5 | 6.1 |

According to the DGI analysis there is an imperceptible glare in all cases except at 15:00 on 21st of March (table 5.72).

Table 5.73. GVCP levels from different angles from nadir for the four days at 9:00,12:00 and 15:00 (author 2019).

| Angle | 60 | 50 | 40 | 30 | 20 | 10 | 0 | -10 | -20 | -30 | -40 | -50 | -60 |
|-------------------------------------------|------|------|------|------|------|------|------|------|------|------|------|------|------|
| 09:00 21 st of March | 100 | 100 | 100 | 100 | 100 | 95.6 | 87.4 | 73.8 | 57.4 | 41.7 | 29.2 | 20.2 | 14.5 |
| 12:00 21 st of March | 88.9 | 89.6 | 89.9 | 90.2 | 90.2 | 91.5 | 92.2 | 92.4 | 90.9 | 89.7 | 89.7 | 85.4 | 82.6 |
| 15:00 21 st of March | 72.1 | 79.9 | 87.3 | 93.1 | 96.9 | 98.9 | 99.7 | 99.9 | 100 | 100 | 100 | 100 | 100 |
| 09:00 21 st of June | 100 | 99.9 | 99.7 | 98.6 | 97.0 | 88.5 | 79.4 | 68.4 | 57.2 | 47.7 | 39.9 | 34.4 | 30.5 |
| 12:00 21 st of June | 100 | 100 | 100 | 100 | 100 | 100 | 100 | 100 | 100 | 100 | 100 | 100 | 100 |
| 15:00 21 st of June | 38.3 | 48.3 | 60.6 | 73.6 | 85.3 | 93.5 | 97.9 | 99.5 | 100 | 100 | 100 | 100 | 100 |
| 09:00 23 rd of September | 100 | 100 | 100 | 100 | 100 | 96.9 | 90.4 | 78.6 | 63.3 | 47.6 | 34.3 | 24.4 | 17.8 |
| 12:00 23 rd of September | 86.6 | 87.1 | 87.4 | 87.3 | 86.9 | 88.7 | 89.3 | 89.8 | 88.1 | 87.2 | 85.9 | 84.1 | 81.8 |
| 15:00 23 rd of September | 67.4 | 75.8 | 84.1 | 91.0 | 95.8 | 98.5 | 99.7 | 100 | 100 | 100 | 100 | 100 | 100 |
| 09:00 21 st of December | 100 | 100 | 100 | 100 | 100 | 99.2 | 96.6 | 90.2 | 79.3 | 65.2 | 50.9 | 38.6 | 29.2 |
| 12:00 21 st of December | 98.9 | 97.5 | 94.9 | 92.8 | 89.5 | 87.0 | 91.8 | 93.5 | 93.4 | 92.9 | 91.9 | 90.1 | 87.8 |
| 15:00 21 st of December | 89.2 | 91.0 | 92.1 | 92.3 | 92.9 | 91.1 | 85.9 | 77.1 | 77.7 | 81.5 | 86.2 | 90.9 | 94.9 |

GVCP analysis showed that minimum percentage was 79.40% at 9:00 on 21st of June and maximum percentage was 100% at 12:00 on 21st of June when looking at the middle of the northern glazed wall. The minimum percentage of satisfied occupants was 38.93% at 15:00 on 21st of June and maximum was 100% at 12:00 on 21st of June when looking at the eastern and western glazed walls (table 5.73).

Comparing to the basic model minimum DGI reduction was 41.5% and maximum DGI reduction was 100% while the minimum GVCP improvement was 2.5% and maximum GVCP improvement was 230.0%. Refer to final comparison table 5.74 for full details including comparison with the basic model and fourth scenario.

Table 5.74. Final comparison between Scenario 05 and basic model (author 2019).

| Date | Hour | Average DGI reduction comparing to the basic model results (scenario 05) | Average DGI reduction comparing to the basic model results (scenario 04) | Average GVCP increment comparing to the basic model results (scenario 05) | Average GVCP increment comparing to the basic model results (scenario 04) |
|---------------------------|-------|--------------------------------------------------------------------------|--------------------------------------------------------------------------|---------------------------------------------------------------------------|---------------------------------------------------------------------------|
| 21 st of Mar. | 9:00 | 41.5% | 37.7% | 2.5% | 3.8% |
| 21 st of Mar. | 12:00 | 47.0% | 46.8% | 106.7% | 101.9% |
| 21 st of Mar. | 15:00 | 74.0% | 73.4% | 87.8% | 85.6% |
| 21 st of Jun. | 9:00 | 31.6% | 26.7% | 67.7% | 59.7% |
| 21 st of Jun. | 12:00 | 100% | 100% | 230.0% | 230.0% |
| 21 st of Jun. | 15:00 | 48.7% | 46.3% | 36.7% | 32.4% |
| 23 rd of Sept. | 9:00 | 47.1% | 43.4% | 11.2% | 6.6% |
| 23 rd of Sept. | 12:00 | 45.4% | 45.3% | 120.3% | 86.2% |
| 23 rd of Sept. | 15:00 | 70.8% | 69.2% | 86.4% | 84.9% |
| 21 st of Dec. | 9:00 | 55.1% | 52.6% | 24.1% | 20.0% |
| 21 st of Dec. | 12:00 | 66.8% | 66.5% | 156.2% | 156.0% |
| 21 st of Dec. | 15:00 | 49.5% | 48.1% | 138.7% | 153.9% |

5.4.8 Scenario 06 glare analysis

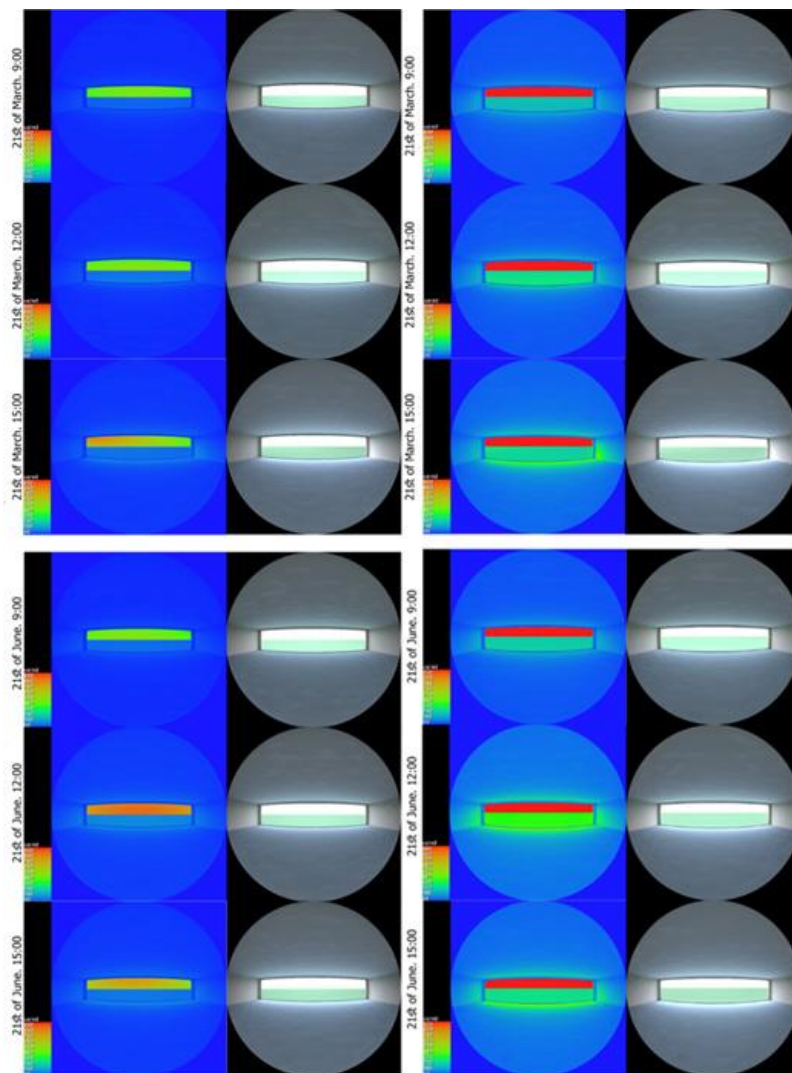


Figure 5.73. Waiting room luminance maps on the 21st of March (top images) and 21st of June (bottom images). The images on the left show scenario 04 results and the images on the right show the basic model results (author 2019).

On 21st of March, in the waiting room, average luminance levels from the glazed wall reached 300 cd/m² in first two cases and 450 cd/m² in third case which, comparing to the basic model results, indicated 68.4% and 52.6% luminance level reduction. On 21st of June, in the waiting room, average luminance levels from the glazed wall reached 600 cd/m² in first case and 850 cd/m² in second and third case which, comparing to the basic model results, indicated 36.8% and 10.5% luminance level reduction (figure 5.73).

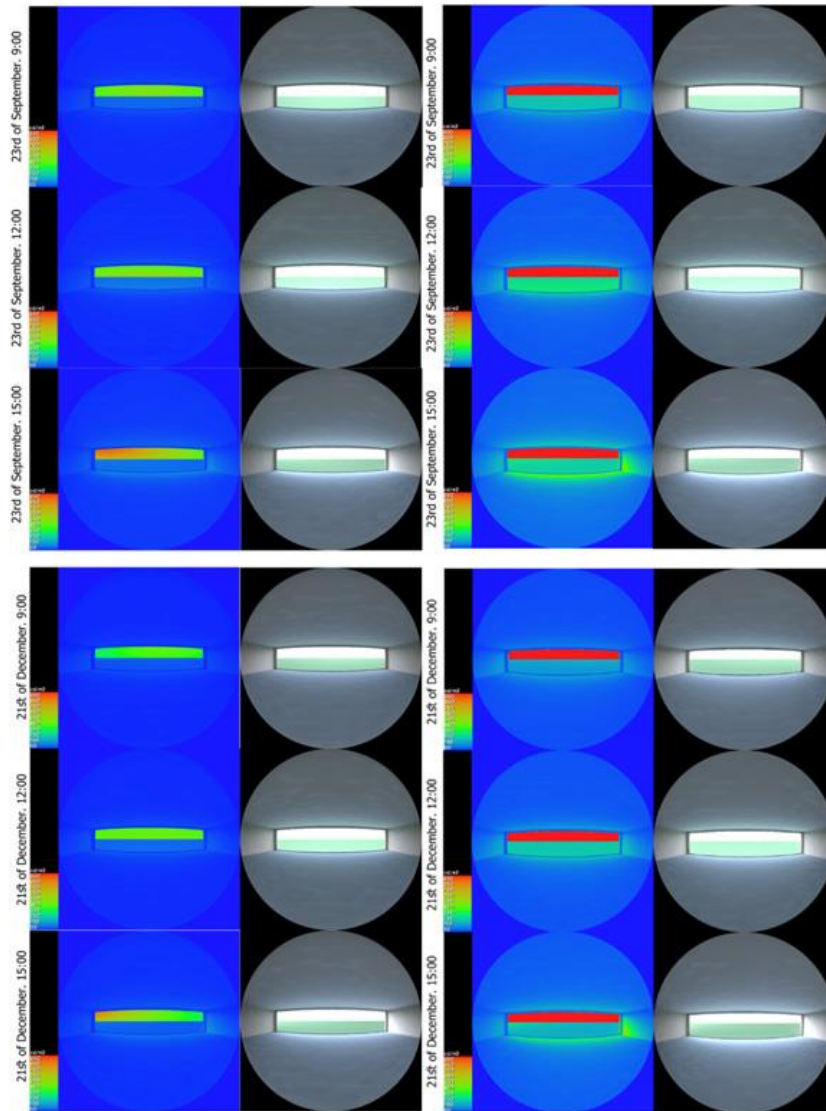


Figure 5.74. Waiting room luminance maps on the 23rd of September (top images) and 21st of December (bottom images). The images on the left show scenario 04 results and the images on the right show the basic model results (author 2019).

On 23rd of September, in the waiting room, average luminance levels from the glazed wall reached 300 cd/m² in first two cases and 450 cd/m² in third case which, comparing to the basic model results, indicated 68.4% and 52.6% luminance level reduction. On 21st of December, in the waiting room, average luminance levels from the glazed wall reached 350 cd/m² in the first case, 600 cd/m² in the first case and 550 cd/m² in the third case which, comparing to the basic model results, indicated 63.2% ,36.8% and 42.1% luminance level reduction (figure 5.74).

Table 5.75. DGI levels from different angles from nadir for the four days at 9:00,12:00 and 15:00 (author 2019).

| Angle | 60 | 50 | 40 | 30 | 20 | 10 | 0 | -10 | -20 | -30 | -40 | -50 | -60 |
|-------------------------------------------|------|------|------|------|------|------|------|------|------|------|------|------|------|
| 09:00 21 st of March | 11.2 | 13.1 | 14.7 | 16.1 | 17.2 | 18.1 | 18.3 | 18.1 | 17.2 | 16.1 | 14.8 | 13.1 | 11.2 |
| 12:00 21 st of March | 11.0 | 12.9 | 14.6 | 15.6 | 17.1 | 17.8 | 18.1 | 17.9 | 17.1 | 15.9 | 14.6 | 12.9 | 11.1 |
| 15:00 21 st of March | 11.7 | 13.6 | 15.2 | 16.6 | 17.6 | 18.4 | 18.7 | 18.4 | 17.6 | 16.4 | 15.3 | 13.4 | 11.5 |
| 09:00 21 st of June | 11.1 | 13.1 | 14.9 | 16.1 | 17.2 | 17.9 | 18.3 | 17.9 | 17.2 | 16.1 | 14.9 | 13.1 | 11.1 |
| 12:00 21 st of June | 12.5 | 14.5 | 16.1 | 17.5 | 18.5 | 19.4 | 19.4 | 18.6 | 17.5 | 16.1 | 14.5 | 12.5 | 12.3 |
| 15:00 21 st of June | 11.8 | 13.7 | 15.3 | 16.7 | 17.8 | 18.6 | 18.9 | 18.6 | 17.8 | 16.7 | 15.3 | 13.7 | 11.8 |
| 09:00 23 rd of September | 11.1 | 13.1 | 14.8 | 16.1 | 17.2 | 18.1 | 18.4 | 18.1 | 17.2 | 16.2 | 14.8 | 13.1 | 11.2 |
| 12:00 23 rd of September | 11.1 | 12.9 | 14.6 | 15.9 | 17.1 | 17.9 | 18.1 | 17.9 | 17.1 | 15.9 | 14.6 | 12.9 | 11.1 |
| 15:00 23 rd of September | 11.8 | 13.7 | 15.4 | 16.7 | 17.8 | 18.6 | 18.8 | 18.5 | 17.7 | 16.6 | 15.2 | 13.6 | 11.6 |
| 09:00 21 st of December | 10.7 | 12.7 | 14.3 | 15.7 | 16.8 | 17.7 | 17.9 | 17.7 | 16.8 | 15.7 | 14.4 | 12.7 | 10.8 |
| 12:00 21 st of December | 10.9 | 12.8 | 14.4 | 15.8 | 16.9 | 17.7 | 17.9 | 17.7 | 16.9 | 15.8 | 14.4 | 12.8 | 10.8 |
| 15:00 21 st of December | 11.2 | 13.2 | 14.8 | 16.2 | 17.2 | 17.9 | 18.2 | 17.9 | 17.1 | 15.9 | 14.5 | 12.8 | 10.9 |

According to the DGI analysis there is a perceptible glare in all cases, as it exceeded 18 in the centre of the glazed wall except at 9:00 on 21st of December. However, it did not reach the high disturbance level which is above 24 (table 5.75).

Table 5.76. GVCP levels from different angles from nadir for the four days at 9:00,12:00 and 15:00 (author 2019).

| Angle | 60 | 50 | 40 | 30 | 20 | 10 | 0 | -10 | -20 | -30 | -40 | -50 | -60 |
|-------------------------------------------|------|------|------|------|------|------|------|------|------|------|------|------|------|
| 09:00 21 st of March | 77.5 | 64.4 | 51.7 | 60.8 | 32.7 | 27.1 | 25.3 | 27.1 | 32.7 | 40.9 | 51.7 | 64.5 | 72.5 |
| 12:00 21 st of March | 77.2 | 64.2 | 51.6 | 40.9 | 32.8 | 27.2 | 25.4 | 27.2 | 32.9 | 41.1 | 51.7 | 64.4 | 77.4 |
| 15:00 21 st of March | 71.1 | 56.9 | 44.1 | 33.9 | 26.5 | 21.5 | 20.1 | 21.7 | 26.9 | 32.5 | 44.9 | 57.9 | 71.9 |
| 09:00 21 st of June | 77.3 | 64.3 | 51.6 | 40.9 | 32.7 | 27.1 | 25.3 | 27.1 | 32.7 | 40.9 | 51.7 | 64.4 | 77.4 |
| 12:00 21 st of June | 62.5 | 47.4 | 34.8 | 25.5 | 19.1 | 14.9 | 13.7 | 14.9 | 19.1 | 19.1 | 25.5 | 34.9 | 62.4 |
| 15:00 21 st of June | 69.3 | 54.9 | 42.2 | 32.1 | 24.8 | 19.9 | 18.5 | 20.1 | 24.8 | 32.2 | 42.4 | 55.2 | 69.6 |
| 09:00 23 rd of September | 77.2 | 64.1 | 51.3 | 40.6 | 32.4 | 26.8 | 25.0 | 26.8 | 32.4 | 40.6 | 51.4 | 64.1 | 77.2 |
| 12:00 23 rd of September | 77.4 | 64.2 | 51.5 | 40.9 | 32.8 | 27.2 | 25.4 | 27.2 | 32.8 | 40.9 | 51.6 | 64.3 | 77.3 |
| 15:00 23 rd of September | 69.9 | 55.3 | 42.5 | 32.4 | 25.2 | 20.4 | 18.9 | 20.6 | 25.6 | 33.2 | 43.5 | 56.4 | 70.7 |
| 09:00 21 st of December | 80.9 | 68.8 | 56.4 | 45.6 | 37.1 | 31.1 | 29.2 | 31.1 | 37.1 | 15.5 | 56.3 | 68.7 | 80.9 |
| 12:00 21 st of December | 78.8 | 66.2 | 53.7 | 42.9 | 34.7 | 28.9 | 27.1 | 28.9 | 34.8 | 43.1 | 53.8 | 66.4 | 79.0 |
| 15:00 21 st of December | 75.5 | 62.2 | 49.5 | 39.1 | 31.2 | 25.9 | 24.3 | 26.3 | 31.9 | 40.2 | 51.1 | 63.9 | 77.1 |

GVCP analysis showed that minimum percentage of satisfied occupants was 18.99% at 15:00 on 23rd of September and maximum was 27.11% at 12:00 on 21st of December when looking at the middle of the glazed wall. The minimum percentage of satisfied occupants was 62.48% at 12:00 on 21st of June to and maximum was 80.96% at 9:00 on 21st of December when looking at the edges of the glazed wall (table 5.76).

Comparing to the basic model minimum DGI reduction was 13.1% and maximum DGI reduction was 24.6% while the minimum GVCP improvement was 179.4% and maximum GVCP improvement was 266.8%. Refer to final comparison table 5.77 for full details including comparison with the basic model and fourth scenario.

Table 5.77. Final comparison between Scenario 04,06 and basic model (author 2019).

| Date | Hour | Average DGI reduction comparing to the basic model results (scenario 06) | Average DGI reduction comparing to the basic model results (scenario 04) | Average GVCP increment comparing to the basic model results (scenario 06) | Average GVCP increment comparing to the basic model results (scenario 04) |
|---------------------------|-------|--------------------------------------------------------------------------|--------------------------------------------------------------------------|---------------------------------------------------------------------------|---------------------------------------------------------------------------|
| 21 st of Mar. | 9:00 | 19.8% | 13.7% | 205.2% | 122.8% |
| 21 st of Mar. | 12:00 | 18.5% | 13.2% | 179.4% | 123.3% |
| 21 st of Mar. | 15:00 | 18.2% | 11.5% | 243.9% | 141.1% |
| 21 st of Jun. | 9:00 | 19.4% | 13.3% | 173.2% | 123.3% |
| 21 st of Jun. | 12:00 | 18.2% | 10.8% | 266.8% | 131.7% |
| 21 st of Jun. | 15:00 | 17.1% | 11.4% | 253.8% | 157.3% |
| 23 rd of Sept. | 9:00 | 21.6% | 15.5% | 208.2% | 125.2% |
| 23 rd of Sept. | 12:00 | 19.4% | 14.2% | 244.2% | 152.7% |
| 23 rd of Sept. | 15:00 | 13.1% | 7.1% | 234.9% | 146.4% |
| 21 st of Dec. | 9:00 | 19.8% | 16.4% | 186.6% | 114.8% |
| 21 st of Dec. | 12:00 | 24.6% | 18.9% | 195.6% | 117.8% |
| 21 st of Dec. | 15:00 | 19.0% | 13.2% | 215.1% | 129.7% |

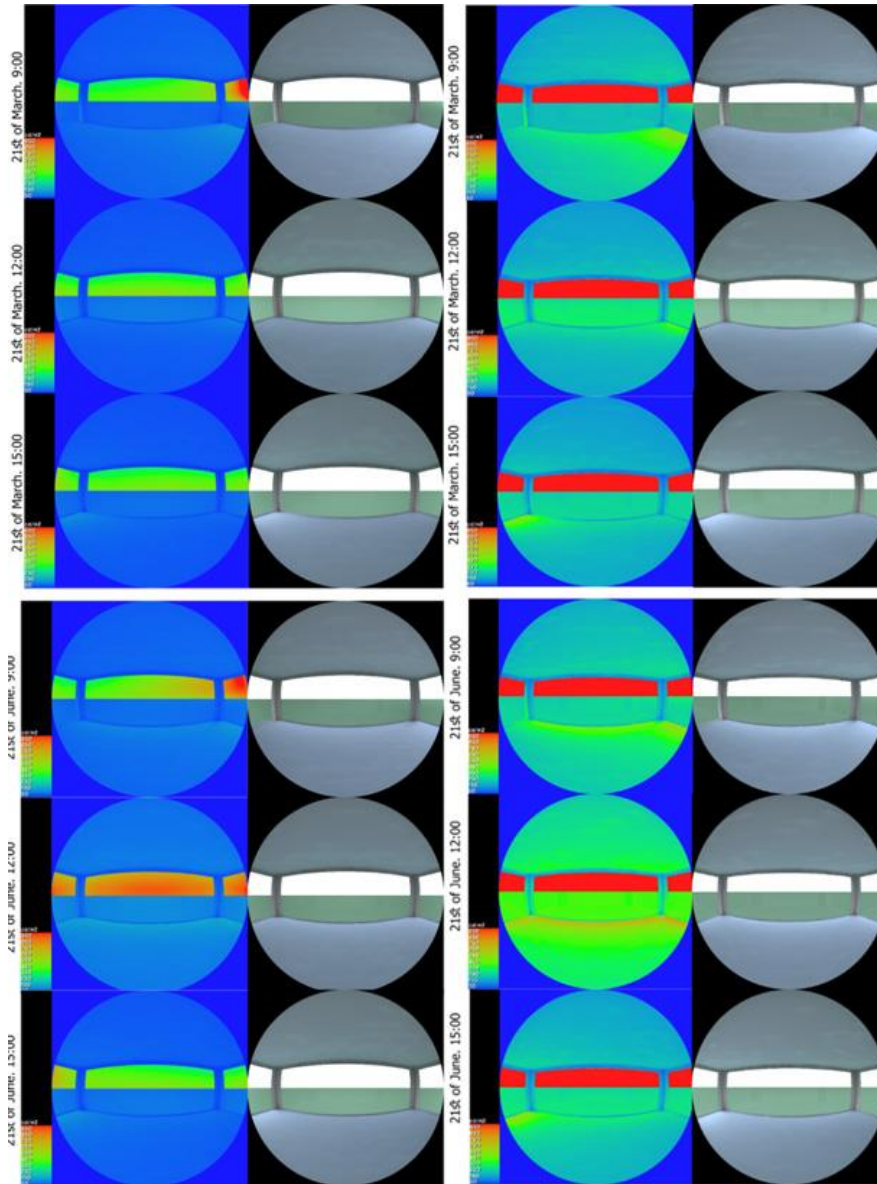


Figure 5.75. Reception room luminance maps on the 21st of March (top images) and 21st of June (bottom images). The images on the left show scenarios 01, 02 and 03 results and the images on the right show the basic model results (author 2019).

On 21st of March, in the reception room, luminance levels from the glazed wall reached 450 cd/m² in all cases which, comparing to the basic model results, indicated 52.6% luminance level reduction. On 21st of June, in the reception room, luminance levels from the glazed wall reached 500 cd/m² in the first case, 750 cd/m² in second case and 550 cd/m² in the third case which, comparing to the basic model results, indicated 47.3%, 21.1% and 42.1% luminance level reduction (figure 5.75).

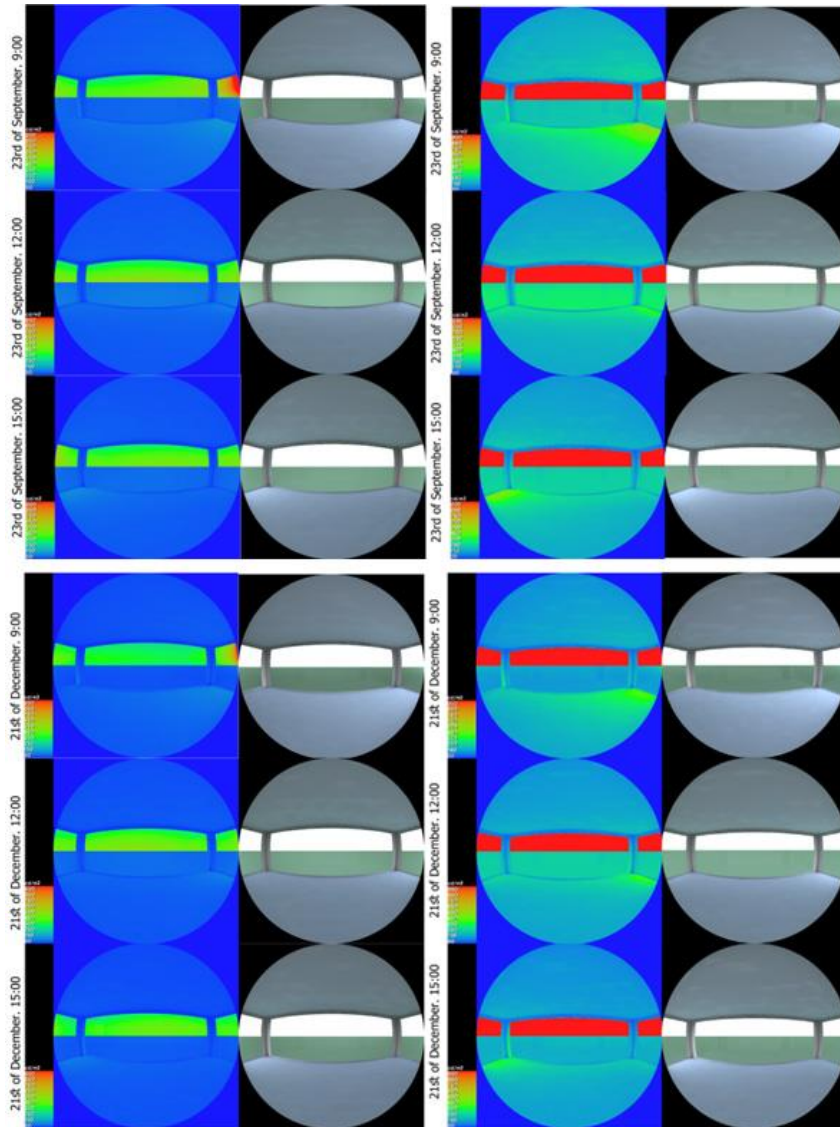


Figure 5.76. Reception room luminance maps on the 23rd of September (top images) and 21st of December (bottom images). The images on the left show scenarios01,02 and 03 results and the images on the right show the basic model results (author 2019).

On 23rd of September and 21st of December, in the reception room, luminance levels from the glazed wall reached 450 cd/m² in all cases which, comparing to the basic model results, indicated 52.6% luminance level reduction.

Table 5.78. DGI levels from different angles from nadir for the four days at 9:00,12:00 and 15:00 (author 2019).

| Angle | 60 | 50 | 40 | 30 | 20 | 10 | 0 | -10 | -20 | -30 | -40 | -50 | -60 |
|-------------------------------------------|------|------|------|------|------|------|------|------|------|------|------|------|------|
| 09:00 21 st of March | 0.00 | 0.00 | 0.00 | 0.00 | 0.00 | 2.2 | 5.2 | 7.9 | 10.3 | 12.5 | 14.4 | 16.0 | 17.3 |
| 12:00 21 st of March | 8.7 | 8.3 | 8.1 | 8.1 | 0.00 | 8.8 | 9.1 | 8.7 | 8.4 | 8.5 | 8.8 | 9.6 | 10.5 |
| 15:00 21 st of March | 12.5 | 10.9 | 9.1 | 6.9 | 4.6 | 1.9 | 0.00 | 0.00 | 0.00 | 0.00 | 0.61 | 2.42 | 3.9 |
| 09:00 21 st of June | 0.00 | 0.00 | 0.00 | 0.9 | 0.00 | 6.7 | 8.8 | 10.8 | 12.6 | 14.1 | 15.4 | 16.4 | 17.3 |
| 12:00 21 st of June | 0.00 | 0.00 | 0.00 | 0.00 | 0.00 | 0.00 | 0.00 | 0.00 | 0.00 | 0.00 | 0.00 | 0.00 | 0.00 |
| 15:00 21 st of June | 13.9 | 12.4 | 10.7 | 8.7 | 6.5 | 3.9 | 1.2 | 0.00 | 0.00 | 0.00 | 0.00 | 0.00 | 0.00 |
| 09:00 23 rd of September | 0.00 | 0.00 | 0.00 | 0.00 | 0.00 | 1.7 | 4.7 | 7.4 | 9.8 | 11.9 | 13.8 | 15.4 | 16.7 |
| 12:00 23 rd of September | 9.1 | 8.6 | 8.4 | 8.5 | 0.00 | 9.4 | 9.8 | 9.3 | 8.9 | 8.8 | 9.1 | 9.6 | 10.4 |
| 15:00 23 rd of September | 13.2 | 11.6 | 9.7 | 7.6 | 5.3 | 2.7 | 0.00 | 0.00 | 0.00 | 0.00 | 0.00 | 0.75 | 2.33 |
| 09:00 21 st of December | 0.00 | 0.00 | 0.00 | 0.00 | 0.00 | 0.00 | 2.6 | 5.4 | 7.9 | 10.3 | 12.3 | 14.1 | 15.5 |
| 12:00 21 st of December | 7.3 | 7.6 | 8.2 | 8.8 | 9.5 | 0.00 | 10.0 | 9.4 | 8.8 | 8.4 | 8.3 | 8.7 | 9.4 |
| 15:00 21 st of December | 9.2 | 8.4 | 7.9 | 8.1 | 8.6 | 9.2 | 9.9 | 10.4 | 10.2 | 9.5 | 8.5 | 7.2 | 5.7 |

According to the DGI analysis there is an imperceptible glare in all cases, as it DGI level was lower than 18 in the centre of the glazed wall. At 12:00 on 21st of June DGI level was zero (table 5.78).

Table 5.79. GVCP levels from different angles from nadir for the four days at 9:00,12:00 and 15:00 (author 2019).

| Angle | 60 | 50 | 40 | 30 | 20 | 10 | 0 | -10 | -20 | -30 | -40 | -50 | -60 |
|-------------------------------------------|------|------|------|------|------|------|------|------|------|------|------|------|------|
| 09:00 21 st of March | 100 | 100 | 100 | 100 | 100 | 97.5 | 91.6 | 80.8 | 66.1 | 50.7 | 37.2 | 26.9 | 19.9 |
| 12:00 21 st of March | 91.2 | 91.7 | 91.9 | 91.9 | 91.8 | 92.9 | 93.4 | 93.6 | 92.3 | 91.4 | 90.1 | 88.1 | 85.8 |
| 15:00 21 st of March | 76.9 | 82.9 | 90.2 | 94.9 | 97.9 | 99.1 | 99.9 | 99.9 | 100 | 100 | 100 | 100 | 100 |
| 09:00 21 st of June | 100 | 99.9 | 99.9 | 99.3 | 98.7 | 92.2 | 84.3 | 73.8 | 64.1 | 51.4 | 42.6 | 35.9 | 31.2 |
| 12:00 21 st of June | 100 | 100 | 100 | 100 | 100 | 100 | 100 | 100 | 100 | 100 | 100 | 100 | 100 |
| 15:00 21 st of June | 46.8 | 56.9 | 68.6 | 80.2 | 89.7 | 95.9 | 98.9 | 99.8 | 100 | 100 | 100 | 100 | 100 |
| 09:00 23 rd of September | 100 | 100 | 100 | 100 | 100 | 98.1 | 93.4 | 84.1 | 70.6 | 55.7 | 42.1 | 31.2 | 23.6 |
| 12:00 23 rd of September | 90.1 | 90.2 | 90.7 | 90.6 | 90.3 | 91.6 | 92.1 | 92.4 | 91.2 | 90.5 | 89.5 | 87.9 | 86.1 |
| 15:00 23 rd of September | 73.5 | 81.1 | 88.1 | 93.6 | 97.2 | 99.1 | 99.8 | 99.9 | 100 | 100 | 100 | 100 | 100 |
| 09:00 21 st of December | 100 | 100 | 100 | 100 | 100 | 99.5 | 97.8 | 93.1 | 84.2 | 91.8 | 58.3 | 45.8 | 35.8 |
| 12:00 21 st of December | 98.9 | 97.7 | 94.6 | 92.9 | 89.8 | 87.5 | 91.9 | 93.4 | 93.8 | 92.9 | 92.0 | 90.5 | 87.9 |
| 15:00 21 st of December | 90.4 | 91.8 | 92.6 | 92.6 | 92.1 | 91.2 | 87.1 | 78.1 | 79.2 | 83.2 | 87.8 | 92.2 | 95.8 |

GVCP analysis showed that minimum percentage was 87.01% at 15:00 on 21st of December and maximum percentage was 100% at 12:00 on 21st of June when looking at the middle of the northern glazed wall. The minimum percentage of satisfied occupants was 46.83% at 15:00 on 21st of June and maximum was 100% at 12:00 on 21st of June when looking at the eastern and western glazed walls (table 5.79).

Comparing to the basic model minimum DGI reduction was 38.2% and maximum DGI reduction was 100% while the minimum GVCP improvement was 8.7% and maximum GVCP improvement was 230.0%. Refer to final comparison table. Refer to final comparison table for full details including comparison with the basic model and fourth scenario (table 5.80).

Table 5.80. Final comparison between Scenario 04,06 and basic model (author 2019).

| Date | Hour | Average DGI reduction comparing to the basic model results (scenario 06) | Average DGI reduction comparing to the basic model results (scenario 04) | Average GVCP increment comparing to the basic model results (scenario 06) | Average GVCP increment comparing to the basic model results (scenario 04) |
|---------------------------|-------|--------------------------------------------------------------------------|--------------------------------------------------------------------------|---------------------------------------------------------------------------|---------------------------------------------------------------------------|
| 21 st of Mar. | 9:00 | 46.0% | 37.7% | 8.7% | 3.8% |
| 21 st of Mar. | 12:00 | 49.7% | 46.8% | 110.2% | 101.9% |
| 21 st of Mar. | 15:00 | 73.0% | 73.4% | 89.4% | 85.6% |
| 21 st of Jun. | 9:00 | 38.2% | 26.7% | 73.1% | 59.7% |
| 21 st of Jun. | 12:00 | 100% | 100% | 230.0% | 230.0% |
| 21 st of Jun. | 15:00 | 53.3% | 46.3% | 41.6% | 32.4% |
| 23 rd of Sept. | 9:00 | 49.5% | 43.4% | 16.6% | 6.6% |
| 23 rd of Sept. | 12:00 | 48.1% | 45.3% | 111.8% | 86.2% |
| 23 rd of Sept. | 15:00 | 70.3% | 69.2% | 89.6% | 84.9% |
| 21 st of Dec. | 9:00 | 58.8% | 52.6% | 28.8% | 20.0% |
| 21 st of Dec. | 12:00 | 61.0% | 66.5% | 156.3% | 156.0% |
| 21 st of Dec. | 15:00 | 49.5% | 48.1% | 161.9% | 153.9% |

5.4.9 Scenarios 05 and 06 daylight harvesting potential analysis

Similar to the basic model simulation, the analysis was done using both RadianceIES and Apache applications. The daylight harvesting potential was measured by the annual electrical consumption saving which happened after using the sensors (table 5.81). Due to the reduction of the average illuminance levels, the daylight harvesting potential was reduced by 78.5% in the fifth scenario and 87.1% in the sixth scenario (table 5.81).

Table 5.81. Total annual electricity consumption Results summary (author 2019).

| | Total electricity (MWh) | Total electricity (MWh) | Total electricity (MWh) | Total electricity (MWh) |
|--------------|-------------------------|-------------------------|-------------------------|-------------------------|
| Date | Scenario 06 With DH.aps | Scenario 06.aps | Scenario 05 With DH.aps | Scenario 05.aps |
| Jan 01-31 | 1.9569 | 1.9410 | 1.9295 | 1.9420 |
| Feb 01-28 | 2.1377 | 2.1094 | 2.1251 | 2.1108 |
| Mar 01-31 | 2.6342 | 2.6119 | 2.6182 | 2.6139 |
| Apr 01-30 | 3.1641 | 3.1623 | 3.1576 | 3.1643 |
| May 01-31 | 3.8097 | 3.7951 | 3.8156 | 3.7975 |
| Jun 01-30 | 3.9499 | 3.9465 | 3.9536 | 3.9491 |
| Jul 01-31 | 4.2266 | 4.2607 | 4.2357 | 4.2633 |
| Aug 01-31 | 4.2798 | 4.3288 | 4.2853 | 4.3310 |
| Sep 01-30 | 3.8671 | 3.9334 | 3.8752 | 3.9354 |
| Oct 01-31 | 3.5045 | 3.5596 | 3.5019 | 3.5613 |
| Nov 01-30 | 2.8588 | 2.8903 | 2.8444 | 2.8920 |
| Dec 01-31 | 2.3370 | 2.3313 | 2.3114 | 2.3324 |
| Summed total | 38.7263 | 38.8702 | 38.6533 | 38.8930 |

Table 5.82. Final comparison (author 2019).

| Scenario | Total annual artificial lighting electrical consumption saving | Cost saving based on tariff of 30.5 Fils for every KW (ADDC 2018). | Reduction in daylight harvesting potential comparing to basic model potential |
|--------------|----------------------------------------------------------------|--------------------------------------------------------------------|-------------------------------------------------------------------------------|
| Basic-model | 1.1156 MWh | 340.3 UAE Dirhams | - |
| Scenario-01: | 0.769 MWh | 234.5 UAE Dirhams | 31.07% |
| Scenario-02: | 0.770 MWh | 234.9 UAE Dirhams | 30.98% |
| Scenario-03: | 0.773 MWh | 235.8 UAE Dirhams | 30.71% |
| Scenario-04 | 0.6215 MWh | 189.6 UAE Dirhams | 55.7% |
| Scenario-05: | 0.2397 MWh | 73.1 UAE Dirhams | 78.5% |
| Scenario-06: | 0.1439 MWh | 43.9 UAE Dirhams | 87.1% |

5.5 Buffer DSF/ Corridor Facade -Scenarios 07 and 08 Analysis

5.5.1 Scenarios 07 and 08 CFD simulation and analysis

Table 5.82. Air temperature within the DSF cavity from Microflo results (author 2019).

| Location | Date | Hour | Minimum DSF cavity air temperature (°C) | Maximum DSF cavity air temperature (°C) | Mean DSF cavity air temperature (°C) | Comparison between ambient temperature (47°C) and mean DSF cavity air temperature | Reduction in average air temperature comparing to scenarios 06. |
|---------------------|--------------------------|-------|-----------------------------------------|-----------------------------------------|--------------------------------------|-----------------------------------------------------------------------------------|-----------------------------------------------------------------|
| Eastern DSF cavity | 10 th of Aug. | 15:00 | 27.96 | 46.00 | 35.90 | -23.6% | 0.3% |
| Western DSF cavity | 10 th of Aug. | 12:00 | 27.95 | 45.93 | 35.80 | -23.8% | 0.2% |
| Northern DSF cavity | 10 th of Aug. | 15:00 | 28.04 | 46.19 | 35.90 | -23.6% | 0.0% |

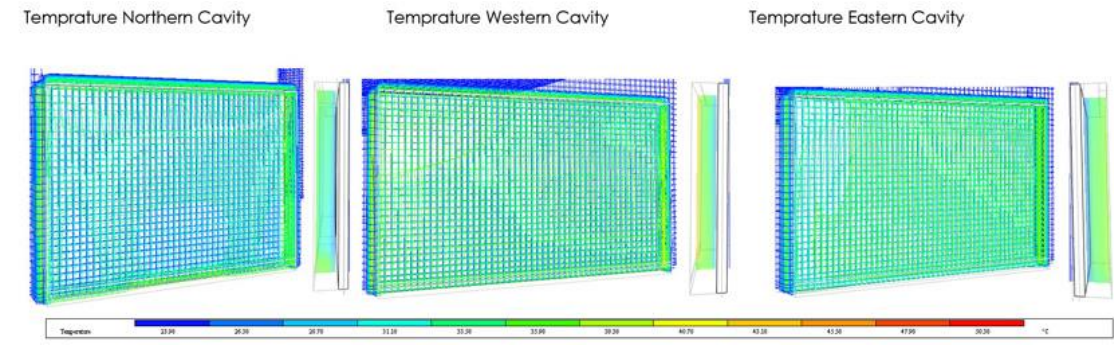


Figure 5.77. CFD analysis of Norther, Eastern and Western cushions in Microflo (author 2019).

The temperature analysis showed that when the ambient temperature reached 47.0 °C at the building level , the temperature in the DSF cavity near the cushion was maximum 46.00 °C in eastern DSF, maximum 45.93 °C in western DSF and maximum 46.19 °C in northern DSF. Thus, the temperature near the external DSF layer was slightly lower than ambient temperature in all cases. The temperature in the DSF cavity near the DGU was minimum 27.96 °C in eastern DSF, minimum 27.95 °C in western

DSF and minimum 28.04 °C in northern DSF. Due to the natural air flow, hot air was discharged and average reduction in mean cavity air temperature, comparing to ambient temperature, was 23.6% in eastern DSF, 23.8% in western DSF and 23.6% in northern DSF. Comparing to scenario 06, the average air temperature was reduced by 0.2~0.3% in eastern and western DSF cavities while it was the same in the northern DSF cavity (table 5.82 and figure 5.77).

Table 5.83. Air velocity within the DSF cavity from Microflo results (suthor 2019).

| Location | Date | Hour | Air velocity within the cavity near the bottom inlet (m/s) | Air velocity within the cavity near the top outlet (m/s) | Mean air velocity within the cavity (m/s) |
|---------------------|--------------------------|-------|------------------------------------------------------------|----------------------------------------------------------|-------------------------------------------|
| Eastern DSF cavity | 10 th of Aug. | 15:00 | 0.72 | 1.03~1.13 | 0.90 |
| Western DSF cavity | 10 th of Aug. | 12:00 | 0.62 | 0.92 | 0.72 |
| Northern DSF cavity | 10 th of Aug. | 15:00 | 0.21 | 0.62 | 0.41 |

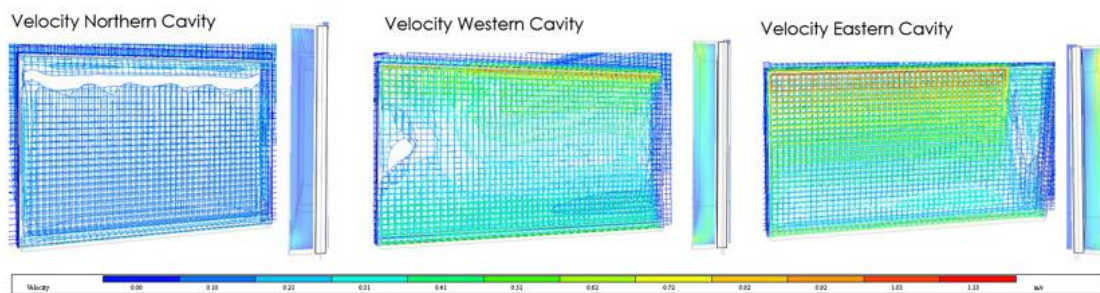


Figure 5.78. CFD analysis of the eastern cushions in IES VE (suthor 2019).

The analysis proved that air flow was from bottom to top which helped to discharge hot air from the DSF cavity. The maximum air velocity was near the top exhaust/outlet. Average air velocity in the eastern DSF was 0.90 while the maximum velocity was 1.13 m/s near the top and the inlet air velocity was 0.72 m/s. Average air velocity in the western DSFs was 0.72 m/s while the maximum velocity was 0.92 m/s

near the top and the inlet air velocity was 0.62 m/s. Similar to previous scenarios the lowest air velocity and temperature was simulated in the northern DSF. The impact of the of the stack effect on the DSF was evaluated in the following sections where additional investigations on the internal conditions within the building were provided (table 5.83 and figure 5.78).

5.5.2 Scenarios 07 and 08 electrical/energy consumption

Table 5.84. Total annual electricity/energy consumption for scenarios 07 and 08 comparing to the basic model (author 2019).

| | Total Energy (MWh) | Total Energy (MWh) | Total Energy (MWh) |
|--------------|--------------------|--------------------|--------------------|
| Date | Scenario 08.aps | Scenario 07.aps | Basic Model.aps |
| Jan 01-31 | 1.8248 | 1.8893 | 2.1744 |
| Feb 01-28 | 1.9664 | 2.0442 | 2.4339 |
| Mar 01-31 | 2.4371 | 2.5315 | 3.0512 |
| Apr 01-30 | 2.9830 | 3.0799 | 3.6774 |
| May 01-31 | 3.5849 | 3.6984 | 4.4261 |
| Jun 01-30 | 3.7426 | 3.8524 | 4.5822 |
| Jul 01-31 | 4.0644 | 4.1686 | 4.9159 |
| Aug 01-31 | 4.1385 | 4.2394 | 4.9626 |
| Sep 01-30 | 3.7641 | 3.8537 | 4.4772 |
| Oct 01-31 | 3.4076 | 3.4892 | 4.0166 |
| Nov 01-30 | 2.7614 | 2.8305 | 3.2288 |
| Dec 01-31 | 2.2251 | 2.2822 | 2.6027 |
| Summed total | 36.8998 | 37.9594 | 44.5490 |

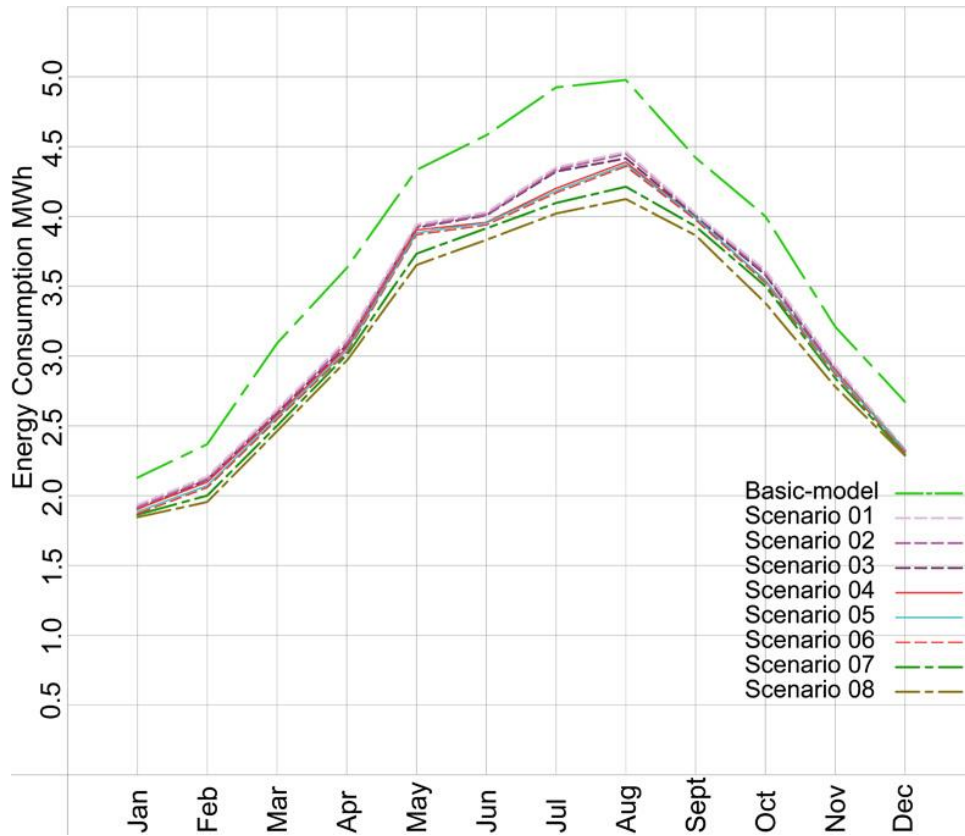


Figure 5.79. Combined diagram of the basic model results and the first eight scenarios results (author 2019)

In IES VE when PVs and are used, the generation is not considered in the total electricity consumption, but in the total energy consumption. Note that in previous scenarios, total annual energy consumption was equal to the total electricity consumption as they didn't include any PVs. In the software, the generation is calculated as a negative value as it is considered as a negative contribution (saving) in the total energy consumption. In scenarios 07 and 08, the total electrical consumption reduction, with consideration of the inflation unit consumption, was 14.7% and 17.1% respectively (table 5.84 and figure 5.79). The total PV electricity generation reached 0.7328 MWh in scenario 07 and 1.7924 MWh in scenario 08 (table 5.85). Comparing to the sixth scenario, the energy saving was improved by 2% and 4.4% (from 12.7% to 14.7% and 17.1%) when the two BIPV types were added (figure 5.79 and table 5.86).

Table 5.84. Total annual electricity generation in scenarios 07 and 08 (author 2019).

| | PV generated electricity (MWh) | PV generated electricity (MWh) |
|--------------|--------------------------------|--------------------------------|
| Date | Scenario 08.aps | Scenario 07.aps |
| Jan 01-31 | -0.1061 | -0.0416 |
| Feb 01-28 | -0.1292 | -0.0514 |
| Mar 01-31 | -0.1572 | -0.0628 |
| Apr 01-30 | -0.1635 | -0.0666 |
| May 01-31 | -0.1942 | -0.0806 |
| Jun 01-30 | -0.1885 | -0.0788 |
| Jul 01-31 | -0.1793 | -0.0750 |
| Aug 01-31 | -0.1737 | -0.0728 |
| Sep 01-30 | -0.1533 | -0.0636 |
| Oct 01-31 | -0.1380 | -0.0564 |
| Nov 01-30 | -0.1153 | -0.0461 |
| Dec 01-31 | -0.0943 | -0.0371 |
| Summed total | -1.7924 | -0.7328 |

Table 5.85. Final comparison between the first eight scenarios (author 2019).

| Scenario | Total annual electrical consumption saving comparing to the basic model (MWh) | Inflation unit annual electricity consumption (MWh) | Total annual electrical consumption saving considering inflation unit annual consumption (MWh) | Total annual electrical consumption saving considering inflation unit annual consumption (%) | Cost saving based on tariff of 30.5 Fils for every KW (ADDC 2018) |
|-------------|-------------------------------------------------------------------------------|-----------------------------------------------------|------------------------------------------------------------------------------------------------|----------------------------------------------------------------------------------------------|-------------------------------------------------------------------|
| Scenario-01 | 5.2033 | 0.03916 | 5.16414 | 11.594% | 1575.1 UAE Dirhams |
| Scenario-02 | 5.2064 | 0.03916 | 5.16724 | 11.600% | 1576.0 UAE Dirhams |
| Scenario-03 | 5.2084 | 0.03916 | 5.16924 | 11.603% | 1576.6 UAE Dirhams |
| Scenario-04 | 5.5863 | 0.03916 | 5.54714 | 12.45% | 1691.9 UAE Dirhams |
| Scenario-05 | 5.656 | 0.03916 | 5.61684 | 12.6% | 1713.1 UAE Dirhams |
| Scenario-06 | 5.6788 | 0.03916 | 5.63964 | 12.7% | 1720.1 UAE Dirhams |
| Scenario-07 | 6.5896 | 0.03916 | 6.55044 | 14.7% | 1997.9 UAE Dirhams |
| Scenario-08 | 7.6492 | 0.03916 | 7.61004 | 17.1% | 2333.0 UAE Dirhams |

5.5.3 Scenarios 07 and 08 thermal comfort results

Table 5.86. Comfort index results comparison between two scenarios and the basic model (author 2019).

| Var. Name | Location | Filename | Type | Mean |
|---------------|-----------------|-----------------|---------------|------|
| Comfort index | Mechanical room | Scenario 08.apr | Comfort index | 9 |
| Comfort index | Office 01 | Scenario 08.apr | Comfort index | 9 |
| Comfort index | Office 02 | Scenario 08.apr | Comfort index | 9 |
| Comfort index | Store 01 | Scenario 08.apr | Comfort index | 9 |
| Comfort index | Lobby 01 | Scenario 08.apr | Comfort index | 9 |
| Comfort index | Waiting room | Scenario 08.apr | Comfort index | 10 |
| Comfort index | Lobby 02 | Scenario 08.apr | Comfort index | 9 |
| Comfort index | Toilet | Scenario 08.apr | Comfort index | 9 |
| Comfort index | Store 02 | Scenario 08.apr | Comfort index | 9 |
| Comfort index | Reception | Scenario 08.apr | Comfort index | 9 |
| Comfort index | Mechanical room | Scenario 07.apr | Comfort index | 9 |
| Comfort index | Office 01 | Scenario 07.apr | Comfort index | 9 |
| Comfort index | Office 02 | Scenario 07.apr | Comfort index | 9 |
| Comfort index | Store 01 | Scenario 07.apr | Comfort index | 9 |
| Comfort index | Lobby 01 | Scenario 07.apr | Comfort index | 9 |
| Comfort index | Waiting room | Scenario 07.apr | Comfort index | 10 |
| Comfort index | Lobby 02 | Scenario 07.apr | Comfort index | 9 |
| Comfort index | Toilet | Scenario 07.apr | Comfort index | 9 |
| Comfort index | Store 02 | Scenario 07.apr | Comfort index | 9 |
| Comfort index | Reception | Scenario 07.apr | Comfort index | 9 |
| Comfort index | Mechanical room | Basic Model.apr | Comfort index | 9 |
| Comfort index | Office 01 | Basic Model.apr | Comfort index | 9 |
| Comfort index | Office 02 | Basic Model.apr | Comfort index | 9 |
| Comfort index | Store 01 | Basic Model.apr | Comfort index | 9 |
| Comfort index | Lobby 01 | Basic Model.apr | Comfort index | 9 |
| Comfort index | Waiting room | Basic Model.apr | Comfort index | 10 |
| Comfort index | Lobby 02 | Basic Model.apr | Comfort index | 9 |
| Comfort index | Toilet | Basic Model.apr | Comfort index | 9 |
| Comfort index | Store 02 | Basic Model.apr | Comfort index | 10 |
| Comfort index | Reception | Basic Model.apr | Comfort index | 10 |

In the two scenarios, the comfort index results were the same as it was affected only by the shade of the opaque PVs. Comparing to the basic model, Comfort index in store 02 and the reception changed from 10 (warm/acceptable) to 9 (slightly warm/acceptable). Thus, scenarios 07 and 08 results are similar to scenarios 02,03,04,05 and 06 results (table 5.86).

Table 5.87. Mean room temperature results comparison between two scenarios and the basic model (author 2019).

| Var. Name | Location | Filename | Type | Mean |
|-----------------|-----------------|-----------------|------------------|-------|
| Air temperature | Mechanical room | Scenario 08.apr | Temperature (°C) | 24.83 |
| Air temperature | Office 01 | Scenario 08.apr | Temperature (°C) | 24.59 |
| Air temperature | Office 02 | Scenario 08.apr | Temperature (°C) | 24.58 |
| Air temperature | Store 01 | Scenario 08.apr | Temperature (°C) | 24.50 |
| Air temperature | Lobby 01 | Scenario 08.apr | Temperature (°C) | 24.59 |
| Air temperature | Waiting room | Scenario 08.apr | Temperature (°C) | 25.16 |
| Air temperature | Lobby 02 | Scenario 08.apr | Temperature (°C) | 24.76 |
| Air temperature | Toilet | Scenario 08.apr | Temperature (°C) | 24.61 |
| Air temperature | Store 02 | Scenario 08.apr | Temperature (°C) | 24.73 |
| Air temperature | Reception | Scenario 08.apr | Temperature (°C) | 25.11 |
| Air temperature | Mechanical room | Scenario 07.apr | Temperature (°C) | 24.83 |
| Air temperature | Office 01 | Scenario 07.apr | Temperature (°C) | 24.59 |
| Air temperature | Office 02 | Scenario 07.apr | Temperature (°C) | 24.58 |
| Air temperature | Store 01 | Scenario 07.apr | Temperature (°C) | 24.50 |
| Air temperature | Lobby 01 | Scenario 07.apr | Temperature (°C) | 24.59 |
| Air temperature | Waiting room | Scenario 07.apr | Temperature (°C) | 25.16 |
| Air temperature | Lobby 02 | Scenario 07.apr | Temperature (°C) | 24.76 |
| Air temperature | Toilet | Scenario 07.apr | Temperature (°C) | 24.61 |
| Air temperature | Store 02 | Scenario 07.apr | Temperature (°C) | 24.73 |
| Air temperature | Reception | Scenario 07.apr | Temperature (°C) | 25.11 |
| Air temperature | Mechanical room | Basic Model.apr | Temperature (°C) | 24.89 |
| Air temperature | Office 01 | Basic Model.apr | Temperature (°C) | 24.62 |
| Air temperature | Office 02 | Basic Model.apr | Temperature (°C) | 24.66 |
| Air temperature | Store 01 | Basic Model.apr | Temperature (°C) | 24.52 |
| Air temperature | Lobby 01 | Basic Model.apr | Temperature (°C) | 24.62 |
| Air temperature | Waiting room | Basic Model.apr | Temperature (°C) | 25.51 |
| Air temperature | Lobby 02 | Basic Model.apr | Temperature (°C) | 25.13 |
| Air temperature | Toilet | Basic Model.apr | Temperature (°C) | 24.94 |
| Air temperature | Store 02 | Basic Model.apr | Temperature (°C) | 25.16 |
| Air temperature | Reception | Basic Model.apr | Temperature (°C) | 26.15 |

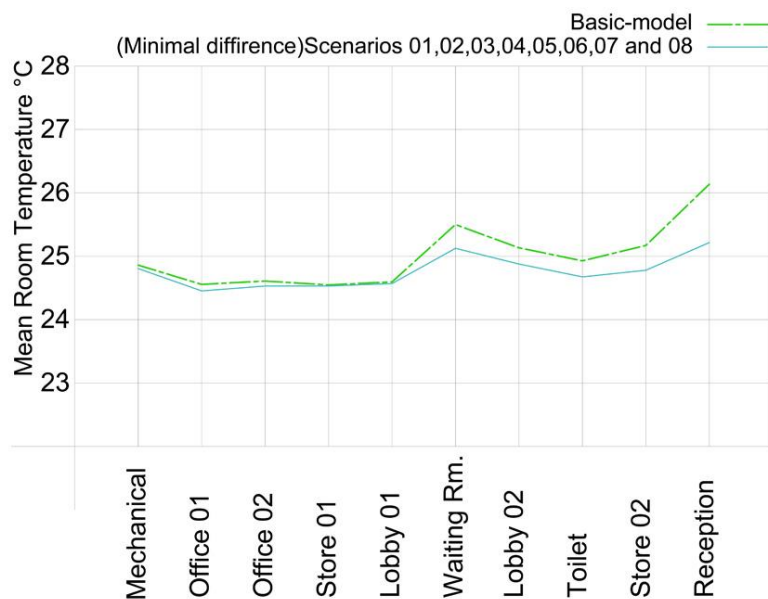


Figure 5.80. Combined diagram of the basic model results and the first eight scenarios results (author 2019)

The rooms air temperature results in the two scenarios were the same as it was affected only by the shade of the opaque PVs. Comparing to the basic model, the overall improvement/reduction in the mean room temperature was 1.09%. The improvement/reduction in the mean waiting room temperature was 1.37%. The improvement/reduction in the mean reception room temperature was 4.0%. In general, scenarios 01,02,03,04,05,06,07 and 08 results were almost the same (table 5.87 and figure 5.80).

Table 5.88. People dissatisfied index results comparison between the two scenarios and the basic model (author 2019).

| Var. Name | Location | Filename | Type | Mean |
|---------------------|-----------------|-----------------|----------------|-------|
| People dissatisfied | Mechanical room | Scenario 08.aps | Percentage (%) | 29.39 |
| People dissatisfied | Office 01 | Scenario 08.aps | Percentage (%) | 26.31 |
| People dissatisfied | Office 02 | Scenario 08.aps | Percentage (%) | 25.94 |
| People dissatisfied | Store 01 | Scenario 08.aps | Percentage (%) | 26.09 |
| People dissatisfied | Lobby 01 | Scenario 08.aps | Percentage (%) | 27.37 |
| People dissatisfied | Waiting room | Scenario 08.aps | Percentage (%) | 33.16 |
| People dissatisfied | Lobby 02 | Scenario 08.aps | Percentage (%) | 29.71 |
| People dissatisfied | Toilet | Scenario 08.aps | Percentage (%) | 26.61 |
| People dissatisfied | Store 02 | Scenario 08.aps | Percentage (%) | 28.28 |
| People dissatisfied | Reception | Scenario 08.aps | Percentage (%) | 34.71 |
| People dissatisfied | Mechanical room | Scenario 07.aps | Percentage (%) | 29.39 |
| People dissatisfied | Office 01 | Scenario 07.aps | Percentage (%) | 26.31 |
| People dissatisfied | Office 02 | Scenario 07.aps | Percentage (%) | 25.94 |
| People dissatisfied | Store 01 | Scenario 07.aps | Percentage (%) | 26.09 |
| People dissatisfied | Lobby 01 | Scenario 07.aps | Percentage (%) | 27.37 |
| People dissatisfied | Waiting room | Scenario 07.aps | Percentage (%) | 33.16 |
| People dissatisfied | Lobby 02 | Scenario 07.aps | Percentage (%) | 29.71 |
| People dissatisfied | Toilet | Scenario 07.aps | Percentage (%) | 26.61 |
| People dissatisfied | Store 02 | Scenario 07.aps | Percentage (%) | 28.28 |
| People dissatisfied | Reception | Scenario 07.aps | Percentage (%) | 34.71 |
| People dissatisfied | Mechanical room | Basic Model.aps | Percentage (%) | 29.95 |
| People dissatisfied | Office 01 | Basic Model.aps | Percentage (%) | 26.55 |
| People dissatisfied | Office 02 | Basic Model.aps | Percentage (%) | 26.71 |
| People dissatisfied | Store 01 | Basic Model.aps | Percentage (%) | 26.24 |
| People dissatisfied | Lobby 01 | Basic Model.aps | Percentage (%) | 27.70 |
| People dissatisfied | Waiting room | Basic Model.aps | Percentage (%) | 37.07 |
| People dissatisfied | Lobby 02 | Basic Model.aps | Percentage (%) | 33.21 |
| People dissatisfied | Toilet | Basic Model.aps | Percentage (%) | 29.74 |
| People dissatisfied | Store 02 | Basic Model.aps | Percentage (%) | 32.37 |
| People dissatisfied | Reception | Basic Model.aps | Percentage (%) | 43.40 |

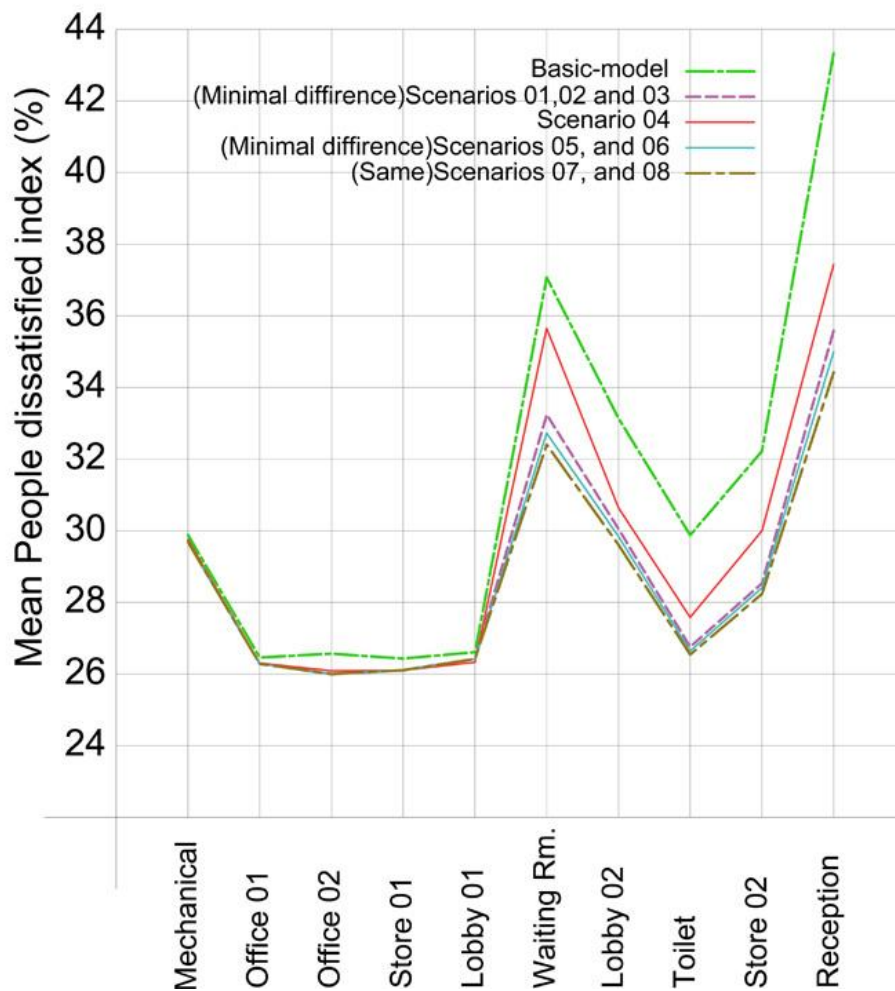


Figure 5.81. Combined diagram of the basic model results and the first eight scenarios results (author 2019).

The typical mean dissatisfied index values of the two scenarios were the same. Furthermore, comparing to the basic model, the mean values had an average improvement of 8.1%. In the waiting room, the mean values had an average improvement of 10.6%. In the reception room, the mean value had an average improvement of 20.0%. As shown in the diagram, scenario 07 and 08 results were better than the first six scenarios results (table 5.88 and figure 5.81).

5.5.4 Scenarios 07 and 08 daylight analysis

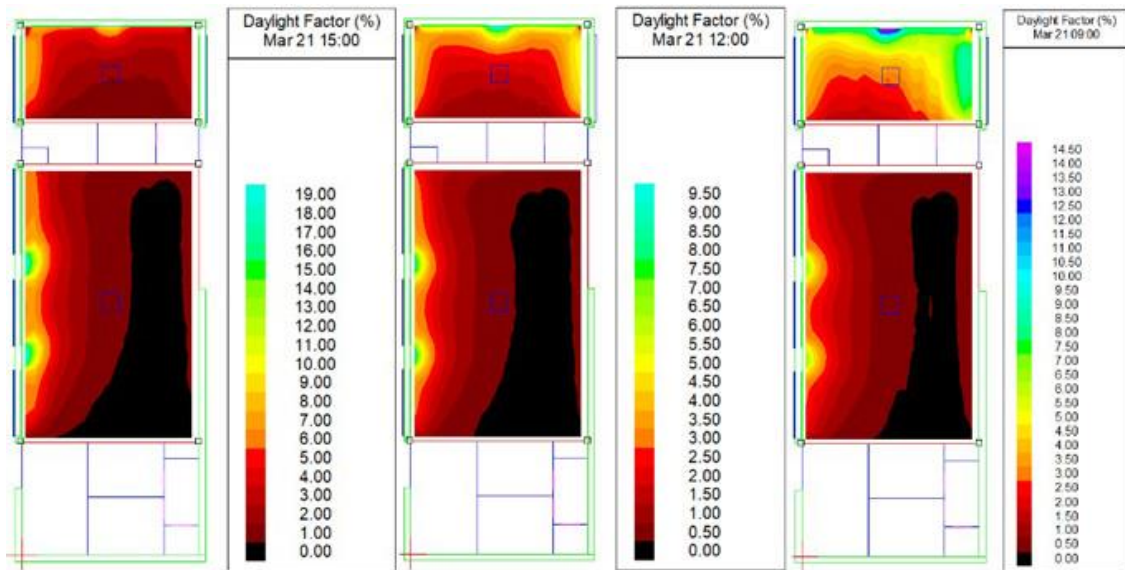


Figure 5.82. Scenarios 07 and 08 daylight factor simulation results on the 21st of March (author 2019).

Table 5.89. Scenarios 07 and 08 21st of March results summary (author 2019).

| Room | Date | Hour | Daylight factor | | | Daylight illuminance | | | Uniformity |
|----------------|---------------------------|-------|-----------------|------|-------|----------------------|------------|-------------|------------|
| | | | Min. | Ave. | Max. | Min. | Ave. | Max. | |
| Waiting room | 21 st of March | 9:00 | 0.3% | 1.1% | 7.0% | 26.93 lux | 85.62 lux | 526.78 lux | 0.24 |
| Reception room | 21 st of March | 9:00 | 1.1% | 4.9% | 15.0% | 84.40 lux | 368.66 lux | 1135.96 lux | 0.23 |
| Waiting room | 21 st of March | 12:00 | 0.2% | 1.1% | 8.6% | 20.80 lux | 97.96 lux | 758.66 lux | 0.21 |
| Reception room | 21 st of March | 12:00 | 0.9% | 2.9% | 9.9% | 80.46 lux | 256.62 lux | 870.88 lux | 0.31 |
| Waiting room | 21 st of March | 15:00 | 0.3% | 2.4% | 19.6% | 28.95 lux | 196.98 lux | 1636.04 lux | 0.15 |
| Reception room | 21 st of March | 15:00 | 1.1% | 3.3% | 9.6% | 88.50 lux | 277.96 lux | 798.38 lux | 0.32 |

In all cases, daylighting level in the waiting room was lower than required while in the reception room, average daylighting levels were within acceptable range at 9:00 on 21st of March. In the rest of the cases, it was lower than required. In all cases daylighting levels and DF were low in 75% to 85% of the waiting room area. Also, Average DF was lower than 2% in all the waiting room cases except at 15:00. Average DF was higher than 2% in all the reception room cases (figures 5.82,5.86,5.87,5.88,5.89 and table 5.89).

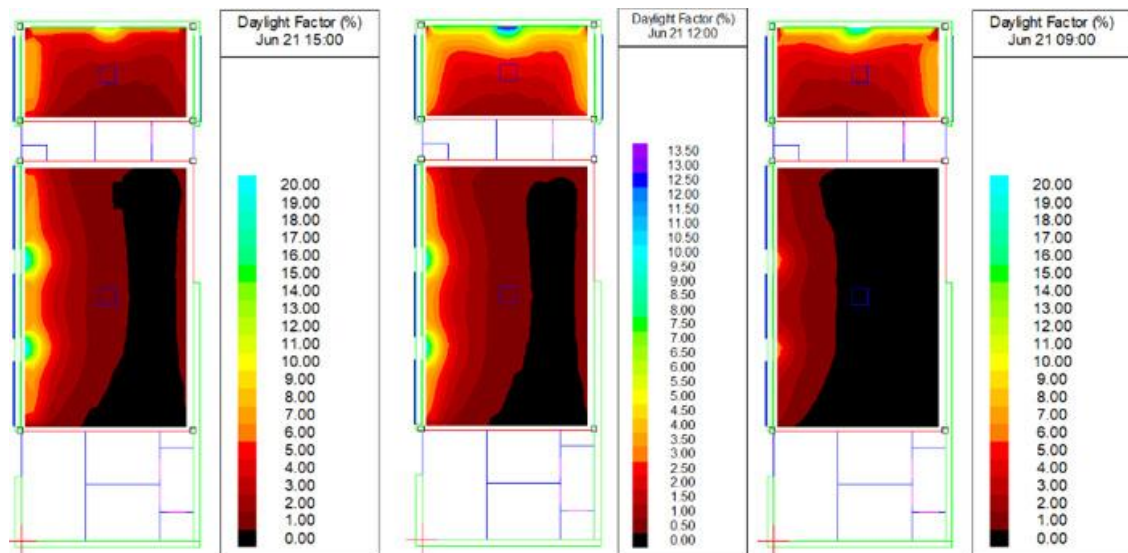


Figure 5.83. Scenarios 07 and 08 daylight factor simulation results on the 21st of June (author 2019).

In all cases, daylighting level in the waiting room was lower than required while in the reception room, daylighting levels were higher than required at 12:00 and within acceptable range at 9:00 and 15:00 on the 21st of June. In all cases daylighting levels and DF were low in 75% to 85% of the waiting room area. Also, Average DF was lower than 2% in all the waiting room cases except at 15:00 in all days. Average DF was higher than 2% in all the reception room cases (figures 5.83,5.86,5.87,5.88,5.89 and table 5.90).

Table 5.90. Scenarios 07 and 08 21st of June results summery (author 2019).

| Room | Date | Hour | Daylight factor | | | Daylight illuminance | | | Uniformity |
|----------------|--------------------------|-------|-----------------|------|-------|----------------------|------------|-------------|------------|
| | | | Min. | Ave. | Max. | Min. | Ave. | Max. | |
| Waiting room | 21 st of June | 9:00 | 0.3% | 1.0% | 6.9% | 22.84 lux | 85.83 lux | 566.04 lux | 0.27 |
| Reception room | 21 st of June | 9:00 | 0.9% | 5.1% | 20.3% | 72.74 lux | 421.20 lux | 1674.44 lux | 0.17 |
| Waiting room | 21 st of June | 12:00 | 0.3% | 1.2% | 9.7% | 47.11 lux | 222.40 lux | 1810.19 lux | 0.21 |
| Reception room | 21 st of June | 12:00 | 0.7% | 3.2% | 13.9% | 127.54 lux | 600.99 lux | 2586.48 lux | 0.21 |
| Waiting room | 21 st of June | 15:00 | 0.4% | 2.4% | 20.8% | 34.52 lux | 209.36 lux | 1776.92 lux | 0.16 |
| Reception room | 21 st of June | 15:00 | 0.8% | 3.7% | 12.8% | 67.82 lux | 318.65 lux | 1097.16 lux | 0.21 |

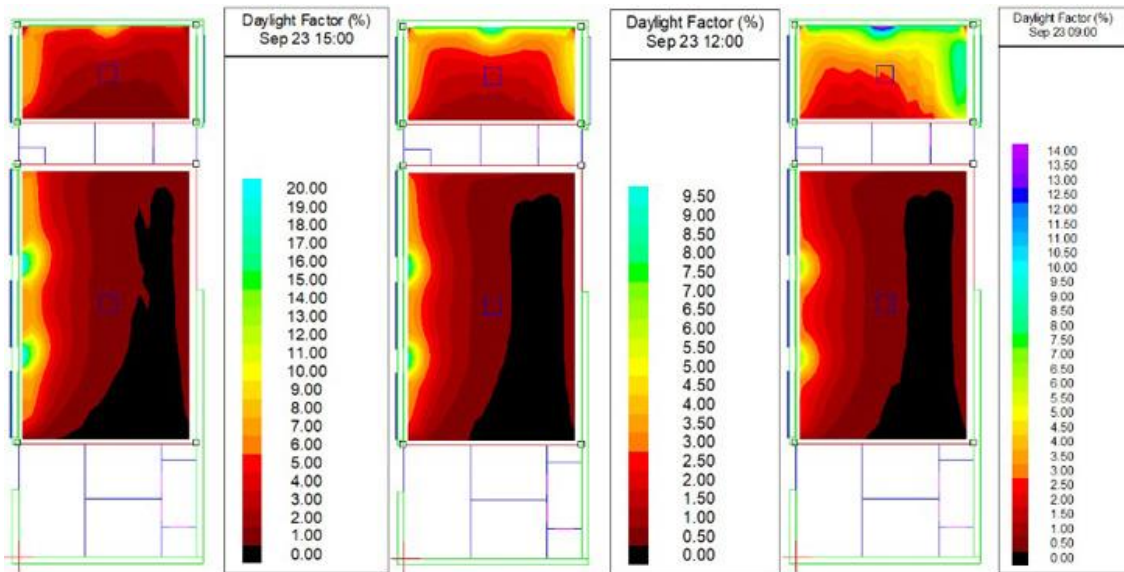


Figure 5.84. Scenarios 07 and 08 daylight factor simulation results on the 23rd of September (author 2019).

Table 5.91. Scenarios 07 and 08 23rd of September results summary (author 2019).

| Room | Date | Hour | Daylight factor | | | Daylight illuminance | | | Uniformity |
|----------------|---------------------------|-------|-----------------|------|-------|----------------------|------------|-------------|------------|
| | | | Min. | Ave. | Max. | Min. | Ave. | Max. | |
| Waiting room | 23 rd of Sept. | 9:00 | 0.3% | 1.1% | 6.8% | 21.22 lux | 86.19 lux | 536.41 lux | 0.25 |
| Reception room | 23 rd of Sept. | 9:00 | 1.1% | 4.6% | 14.2% | 88.08 lux | 359.84 lux | 1113.10 lux | 0.24 |
| Waiting room | 23 rd of Sept. | 12:00 | 0.2% | 1.2% | 9.3% | 21.25 lux | 104.62 lux | 825.98 lux | 0.20 |
| Reception room | 23 rd of Sept. | 12:00 | 1.0% | 2.9% | 9.8% | 84.81 lux | 257.09 lux | 867.12 lux | 0.33 |
| Waiting room | 23 rd of Sept. | 15:00 | 0.4% | 2.6% | 20.7% | 30.91 lux | 214.68 lux | 1696.73 lux | 0.14 |
| Reception room | 23 rd of Sept. | 15:00 | 1.1% | 3.5% | 9.9% | 92.21 lux | 290.05 lux | 811.94 lux | 0.32 |

On 23rd of September, daylighting level in both rooms was lower than required. In all timings daylighting levels and DF were low in 75% to 85% of the waiting room area. Also, Average DF was lower than 2% in all the waiting room cases except at 15:00. Average DF was higher than 2% in all the reception room cases (figures 5.84,5.86,5.87,5.88,5.89 and table 5.91).

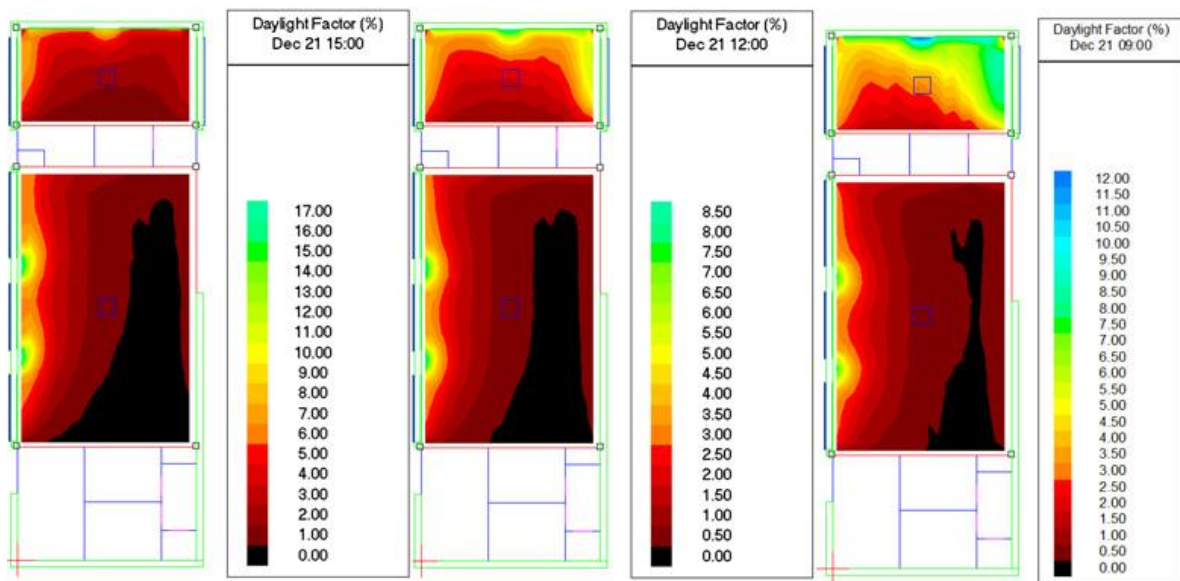


Figure 5.85. Scenarios 07 and 08 daylight factor simulation results on the 21st of December (author 2019).

Table 5.92. Scenarios 07 and 08 21st of December results summery (author 2019).

| Room | Date | Hour | Daylight factor | | | Daylight illuminance | | | Uniformity |
|----------------|--------------------------|-------|-----------------|------|-------|----------------------|------------|-------------|------------|
| | | | Min. | Ave. | Max. | Min. | Ave. | Max. | |
| Waiting room | 21 st of Dec. | 9:00 | 0.3% | 1.3% | 7.7% | 19.9 lux | 80.16 lux | 480.74 lux | 0.25 |
| Reception room | 21 st of Dec. | 9:00 | 1.6% | 4.8% | 12.5% | 97.87 lux | 296.43 lux | 774.92 lux | 0.33 |
| Waiting room | 21 st of Dec. | 12:00 | 0.3% | 1.2% | 8.7% | 21.25 lux | 100.93 lux | 711.75 lux | 0.21 |
| Reception room | 21 st of Dec | 12:00 | 1.1% | 3.1% | 8.8% | 90.33 lux | 249.59 lux | 715.62 lux | 0.36 |
| Waiting room | 21 st of Dec. | 15:00 | 0.3% | 2.4% | 17.7% | 23.96 lux | 166.22 lux | 1239.54 lux | 0.14 |
| Reception room | 21 st of Dec | 15:00 | 1.2% | 3.4% | 9.3% | 86.35 lux | 240.79 lux | 652.2 lux | 0.36 |

On 21st of December, daylighting level in both rooms was lower than required. In all timings daylighting levels and DF were low in 75% to 85% of the waiting room area. Also, Average DF was lower than 2% in all the waiting room cases except at 15:00. Average DF was higher than 2% in all the reception room cases (figures 5.85,5.86,5.87,5.88,5.89 and table 5.92).

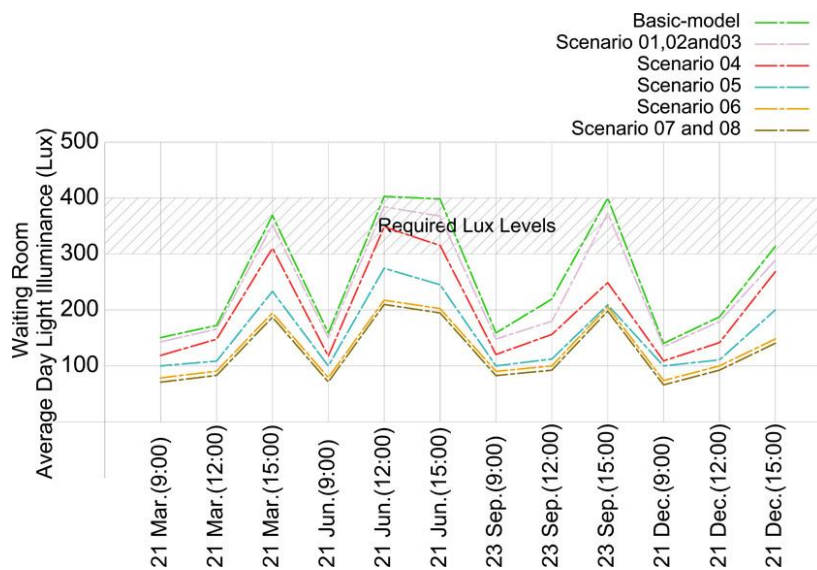


Figure 5.86. Combined diagram of the basic model DI results and the eight scenarios DI results in waiting room (author 2019)

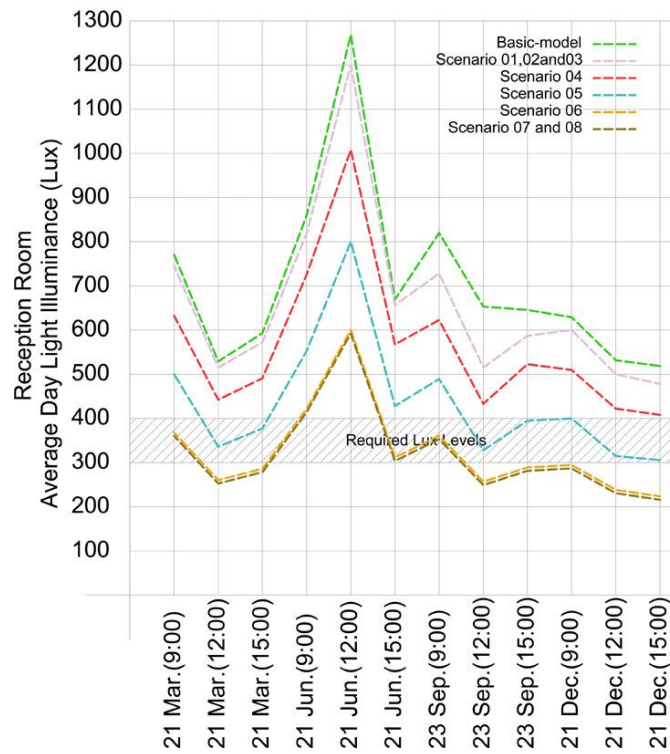


Figure 5.87. Combined diagram of the basic model DI results and the eight scenarios DI results in reception room (author 2019)

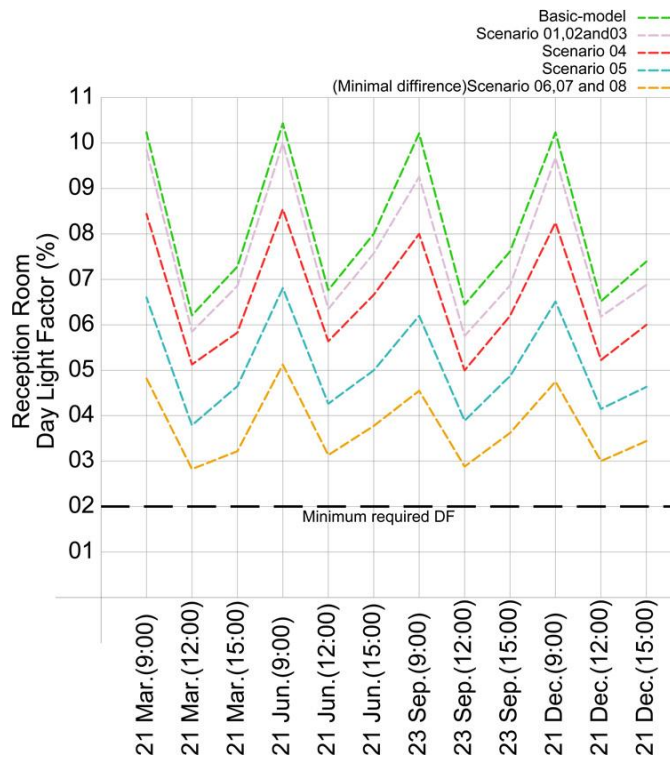


Figure 5.88. Combined diagram of the basic model DF results and the eight scenarios DF results in reception room (author 2019)

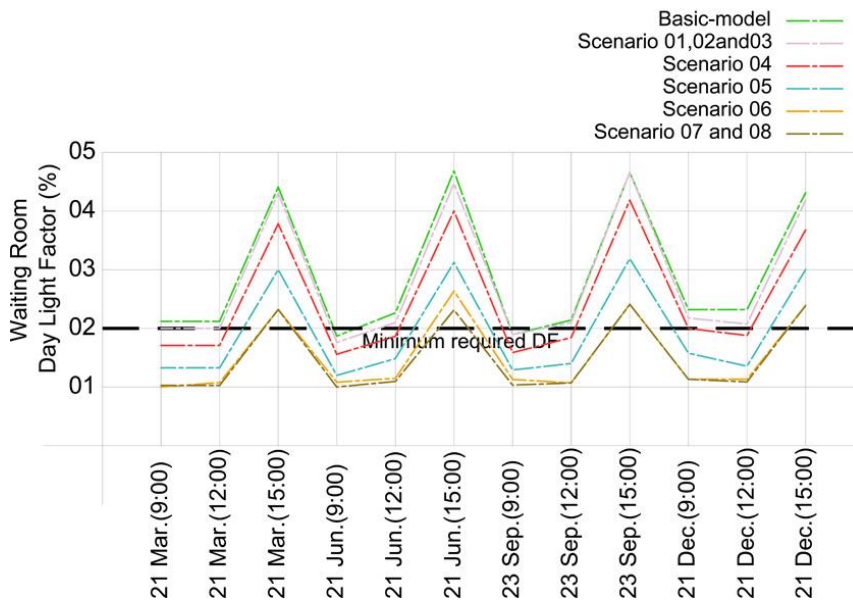


Figure 5.89. Combined diagram of the basic model DF results and the eight scenarios DF results in the waiting room (author 2019).

Comparing to the basic-model, the changes in scenarios 07 and 08 reduced daylighting lux levels by minimum 44.8% and maximum 61.1%. Furthermore, the change reduced average DF by minimum 42.1% and maximum 56.0%. Uniformity changes varied from 26.9% to -11.5%. Refer to the final comparison table. Due to changes in VLT transmittance, scenarios 06 results were better as shown in the previous diagrams. Comparing to them, the additional opaque PVs reduced the daylighting levels by an average of 5.8% in the reception room and 4.3% in the waiting room. Also, the average DF reduction was 0.00% in the reception room and 2.5% in the waiting room (figures 5.86,5.87,5.88,5.89 and table 5.93).

Table 5.93. Final comparison between Scenarios 07,08 and basic model (author 2019).

| Scenario | Date | Hour | Average daylight factor reduction | Average daylight illuminance reduction | Uniformity increment |
|------------------|---------------------------|-------|--------------------------------------------|--------------------------------------------|---------------------------------------------|
| Scenario 7 and 8 | 21 st of Mar. | 9:00 | Waiting room 47.6% Reception room 52.4% | Waiting room 45.2% Reception room 52.8% | Waiting room 9.1% Reception room -11.5% |
| Scenario 7 and 8 | 21 st of Mar. | 12:00 | Waiting room 47.6% Reception room 53.2% | Waiting room 45.9% Reception room 52.9% | Waiting room 16.6% Reception room 3.3% |
| Scenario 7 and 8 | 21 st of Mar. | 15:00 | Waiting room 45.5% Reception room 54.2% | Waiting room 46.8% Reception room 52.9% | Waiting room 15.4% Reception room 6.6% |
| Scenario 7 and 8 | 21 st of Jun. | 9:00 | Waiting room 47.4% Reception room 51.4% | Waiting room 46.2% Reception room 51.4% | Waiting room 28.6% Reception room -10.5% |
| Scenario 7 and 8 | 21 st of Jun. | 12:00 | Waiting room 45.5% Reception room 52.9% | Waiting room 45.6% Reception room 52.3% | Waiting room 16.7% Reception room -4.5% |
| Scenario 7 and 8 | 21 st of Jun. | 15:00 | Waiting room 48.9% Reception room 53.7% | Waiting room 47.6% Reception room 53.7% | Waiting room -14.2% Reception room 0.00% |
| Scenario 7 and 8 | 23 rd of Sept. | 9:00 | Waiting room 42.1% Reception room 56.0% | Waiting room 44.8% Reception room 56.0% | Waiting room 13.6% Reception room 4.3% |
| Scenario 7 and 8 | 23 rd of Sept. | 12:00 | Waiting room 42.9% Reception room 54.7% | Waiting room 52.7% Reception room 60.8% | Waiting room 11.1% Reception room 26.9% |
| Scenario 7 and 8 | 23 rd of Sept. | 15:00 | Waiting room 44.7% Reception room 53.9% | Waiting room 46.1% Reception room 55.2% | Waiting room 7.7% Reception room 18.5% |
| Scenario 7 and 8 | 21 st of Dec. | 9:00 | Waiting room 43.5% Reception room 52.9% | Waiting room 44.8% Reception room 53.0% | Waiting room 13.6% Reception room 6.4% |
| Scenario 7 and 8 | 21 st of Dec. | 12:00 | Waiting room 47.8% Reception room 52.3% | Waiting room 45.3% Reception room 52.7% | Waiting room 16.7% Reception room 12.5% |
| Scenario 7 and 8 | 21 st of Dec. | 15:00 | Waiting room 45.5% Reception room 53.4% | Waiting room 45.9% Reception room 52.8% | Waiting room 16.6% Reception room 12.5% |

5.5.5 Scenarios 07 and 08 glare analysis

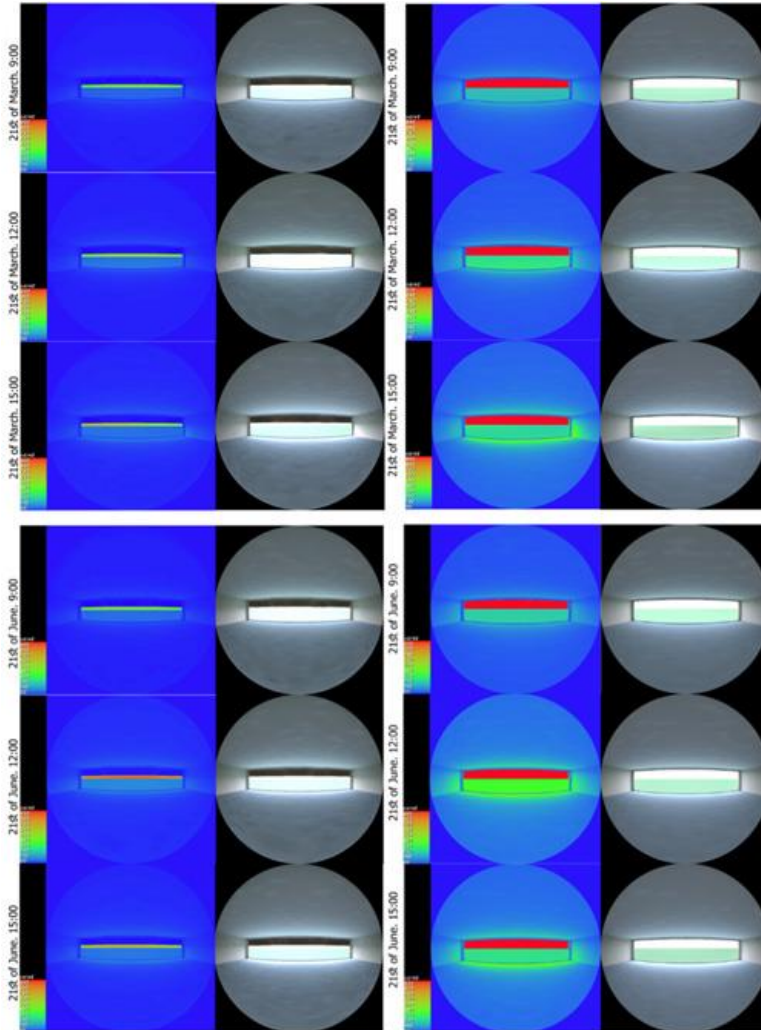


Figure 5.90. Waiting room luminance maps on the 21st of March (top images) and 21st of June (bottom images). The images on the left show scenario 04 results and the images on the right show the basic model results (author 2019).

On 21st of March, in the waiting room, average luminance levels from the glazed wall reached 300 cd/m² in first two cases and 450 cd/m² in third case which, comparing to the basic model results, indicated 68.4% and 52.6% luminance level reduction. On 21st of June, in the waiting room, average luminance levels from the glazed wall reached 600 cd/m² in first case and 850 cd/m² in second and third case which, comparing to the basic model results, indicated 36.8% and 10.5% luminance level reduction (figure 5.90).

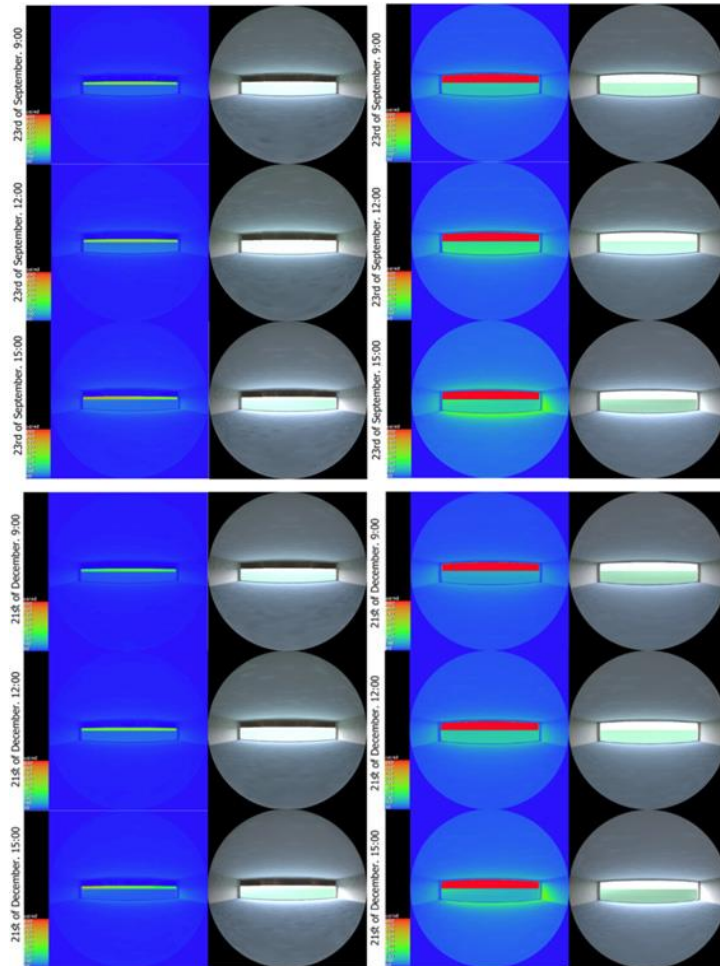


Figure 5.91. Waiting room luminance maps on the 23rd of September (top images) and 21st of December (bottom images). The images on the left show scenario 04 results and the images on the right show the basic model results (author 2019).

On 23rd of September, in the waiting room, average luminance levels from the glazed wall reached 300 cd/m² in first two cases and 450 cd/m² in third case which, comparing to the basic model results, indicated 68.4% and 52.6% luminance level reduction. On 21st of December, in the waiting room, average luminance levels from the glazed wall reached 350 cd/m² in the first case, 600 cd/m² in the first case and 550 cd/m² in the third case which, comparing to the basic model results, indicated 63.2%, 36.8% and 42.1% luminance level reduction (figure 5.91).

Table 5.94. DGI levels from different angles from nadir for the four days at 9:00,12:00 and 15:00 (author 2019).

| Angle | 60 | 50 | 40 | 30 | 20 | 10 | 0 | -10 | -20 | -30 | -40 | -50 | -60 |
|-------------------------------------------|------|------|------|------|------|------|------|------|------|------|------|------|------|
| 09:00 21 st of March | 10.4 | 12.3 | 13.9 | 15.3 | 16.4 | 17.2 | 17.6 | 17.2 | 16.4 | 15.3 | 13.9 | 12.3 | 10.4 |
| 12:00 21 st of March | 10.5 | 12.4 | 13.6 | 15.3 | 16.3 | 17.2 | 17.5 | 17.2 | 16.3 | 15.3 | 13.9 | 12.3 | 10.4 |
| 15:00 21 st of March | 10.9 | 12.8 | 14.4 | 15.7 | 16.7 | 17.5 | 17.9 | 17.5 | 16.7 | 15.6 | 14.3 | 12.6 | 10.8 |
| 09:00 21 st of June | 10.5 | 12.4 | 13.9 | 15.3 | 16.4 | 17.2 | 17.6 | 17.2 | 16.4 | 15.3 | 13.9 | 12.3 | 10.4 |
| 12:00 21 st of June | 11.8 | 13.7 | 15.3 | 16.7 | 17.7 | 18.6 | 18.9 | 18.6 | 17.7 | 16.7 | 15.4 | 13.7 | 11.9 |
| 15:00 21 st of June | 11.1 | 12.9 | 14.5 | 15.8 | 16.9 | 17.7 | 18.1 | 17.7 | 16.9 | 15.8 | 14.5 | 12.9 | 11.1 |
| 09:00 23 rd of September | 10.5 | 12.4 | 14.0 | 15.4 | 16.4 | 17.3 | 17.6 | 17.3 | 16.3 | 15.4 | 14.1 | 12.4 | 10.5 |
| 12:00 23 rd of September | 10.5 | 12.4 | 13.9 | 12.3 | 16.3 | 17.2 | 17.2 | 16.3 | 15.3 | 13.9 | 12.3 | 12.4 | 10.4 |
| 15:00 23 rd of September | 11.1 | 12.9 | 14.5 | 15.8 | 16.8 | 17.6 | 17.9 | 17.6 | 16.7 | 15.7 | 14.3 | 12.9 | 10.8 |
| 09:00 21 st of December | 9.9 | 11.8 | 13.5 | 14.8 | 15.9 | 16.7 | 17.1 | 16.7 | 15.9 | 14.8 | 13.5 | 11.9 | 9.9 |
| 12:00 21 st of December | 10.2 | 12.1 | 13.7 | 15.1 | 16.1 | 16.9 | 17.3 | 16.9 | 16.1 | 15.1 | 13.7 | 12.1 | 10.2 |
| 15:00 21 st of December | 10.4 | 12.3 | 13.8 | 15.1 | 16.2 | 16.9 | 17.3 | 16.9 | 16.1 | 14.9 | 13.6 | 11.9 | 10.1 |

According to the DGI analysis there is an imperceptible glare in all cases except at 12:00 and 15:00 on 21st of June where there was perceptible glare (table 5.94).

Table 5.95. GVCP levels from different angles from nadir for the four days at 9:00,12:00 and 15:00 (author 2019).

| Angle | 60 | 50 | 40 | 30 | 20 | 10 | 0 | -10 | -20 | -30 | -40 | -50 | -60 |
|-------------------------------------------|------|------|------|------|------|------|------|------|------|------|------|------|------|
| 09:00 21 st of March | 86.7 | 77.1 | 66.5 | 56.5 | 48.2 | 41.9 | 38.9 | 41.9 | 48.6 | 56.6 | 66.6 | 77.2 | 86.8 |
| 12:00 21 st of March | 85.9 | 76.1 | 65.5 | 55.5 | 47.2 | 40.9 | 38.1 | 41.1 | 47.3 | 55.6 | 65.6 | 76.3 | 86.1 |
| 15:00 21 st of March | 82.6 | 71.7 | 60.4 | 50.3 | 42.1 | 36.2 | 33.5 | 36.4 | 42.6 | 51.0 | 61.3 | 72.6 | 83.4 |
| 09:00 21 st of June | 86.4 | 76.7 | 66.1 | 56.1 | 47.7 | 41.4 | 38.5 | 41.5 | 47.8 | 56.1 | 66.1 | 76.7 | 86.4 |
| 12:00 21 st of June | 75.2 | 62.3 | 49.9 | 39.7 | 31.9 | 26.5 | 24.1 | 26.5 | 31.9 | 39.8 | 50.1 | 62.3 | 75.2 |
| 15:00 21 st of June | 81.2 | 69.8 | 58.3 | 48.1 | 39.9 | 33.9 | 31.3 | 34.1 | 40.1 | 18.3 | 58.5 | 70.1 | 81.4 |
| 09:00 23 rd of September | 86.4 | 76.6 | 65.9 | 55.9 | 47.6 | 41.2 | 38.3 | 41.2 | 47.5 | 55.9 | 65.9 | 76.6 | 86.4 |
| 12:00 23 rd of September | 85.8 | 76.1 | 65.4 | 55.5 | 47.2 | 40.9 | 38.1 | 41.1 | 47.3 | 55.6 | 65.6 | 76.3 | 86.1 |
| 15:00 23 rd of September | 81.8 | 70.6 | 59.2 | 49.1 | 40.9 | 35.1 | 32.4 | 35.4 | 41.5 | 49.9 | 60.2 | 71.7 | 82.7 |
| 09:00 21 st of December | 89.5 | 91.1 | 71.4 | 61.8 | 53.6 | 47.2 | 44.2 | 47.2 | 53.6 | 51.8 | 71.3 | 81.1 | 89.4 |
| 12:00 21 st of December | 87.6 | 78.4 | 68.2 | 58.5 | 50.3 | 43.9 | 40.8 | 40.8 | 43.8 | 50.4 | 58.6 | 68.4 | 87.7 |
| 15:00 21 st of December | 86.4 | 76.9 | 66.4 | 56.7 | 48.6 | 42.5 | 39.8 | 42.9 | 39.8 | 42.9 | 57.9 | 78.2 | 87.5 |

GVCP analysis showed that minimum percentage of satisfied occupants was 24.06% at 12:00 on 21st of June and maximum was 40.98% at 12:00 on 21st of December when looking at the middle of the glazed wall. The minimum percentage of satisfied occupants was 75.18% at 12:00 on 21st of June to and maximum was 89.49% at 9:00 on 21st of December when looking at the edges of the glazed wall (table 5.95).

Comparing to the basic model minimum DGI reduction was 21.3% and maximum DGI reduction was 28.8% while the minimum GVCP improvement was 266.1% and maximum GVCP improvement was 457.0%. Refer to final comparison table 5.96 for full details including comparison with the basic model and sixth scenario.

Table 5.96. Final comparison between Scenarios 07 and 08 and basic model in the waiting room (author 2019).

| Date | Hour | Average DGI reduction comparing to the basic model results (scenarios 07 and 08) | Average DGI reduction comparing to the basic model results (scenario 06) | Average GVCP increment comparing to the basic model results (scenarios 07 and 08) | Average GVCP increment comparing to the basic model results (scenario 06) |
|---------------------------|-------|----------------------------------------------------------------------------------|--------------------------------------------------------------------------|-----------------------------------------------------------------------------------|---------------------------------------------------------------------------|
| 21 st of Mar. | 9:00 | 24.6% | 19.8% | 294.5% | 205.2% |
| 21 st of Mar. | 12:00 | 23.4% | 18.5% | 287.6% | 179.4% |
| 21 st of Mar. | 15:00 | 21.8% | 18.2% | 368.0% | 243.9% |
| 21 st of Jun. | 9:00 | 24.2% | 19.4% | 293.1% | 173.2% |
| 21 st of Jun. | 12:00 | 20.8% | 18.2% | 457.0% | 266.8% |
| 21 st of Jun. | 15:00 | 21.9% | 17.1% | 385.3% | 253.8% |
| 23 rd of Sept. | 9:00 | 26.2% | 21.6% | 297.7% | 208.2% |
| 23 rd of Sept. | 12:00 | 24.3% | 19.4% | 338.0% | 244.2% |
| 23 rd of Sept. | 15:00 | 21.3% | 13.1% | 384.0% | 234.9% |
| 21 st of Dec. | 9:00 | 25.5% | 19.8% | 266.1% | 186.6% |
| 21 st of Dec. | 12:00 | 28.8% | 24.6% | 277.2% | 195.6% |
| 21 st of Dec. | 15:00 | 24.3% | 19.0% | 323.1% | 215.1% |

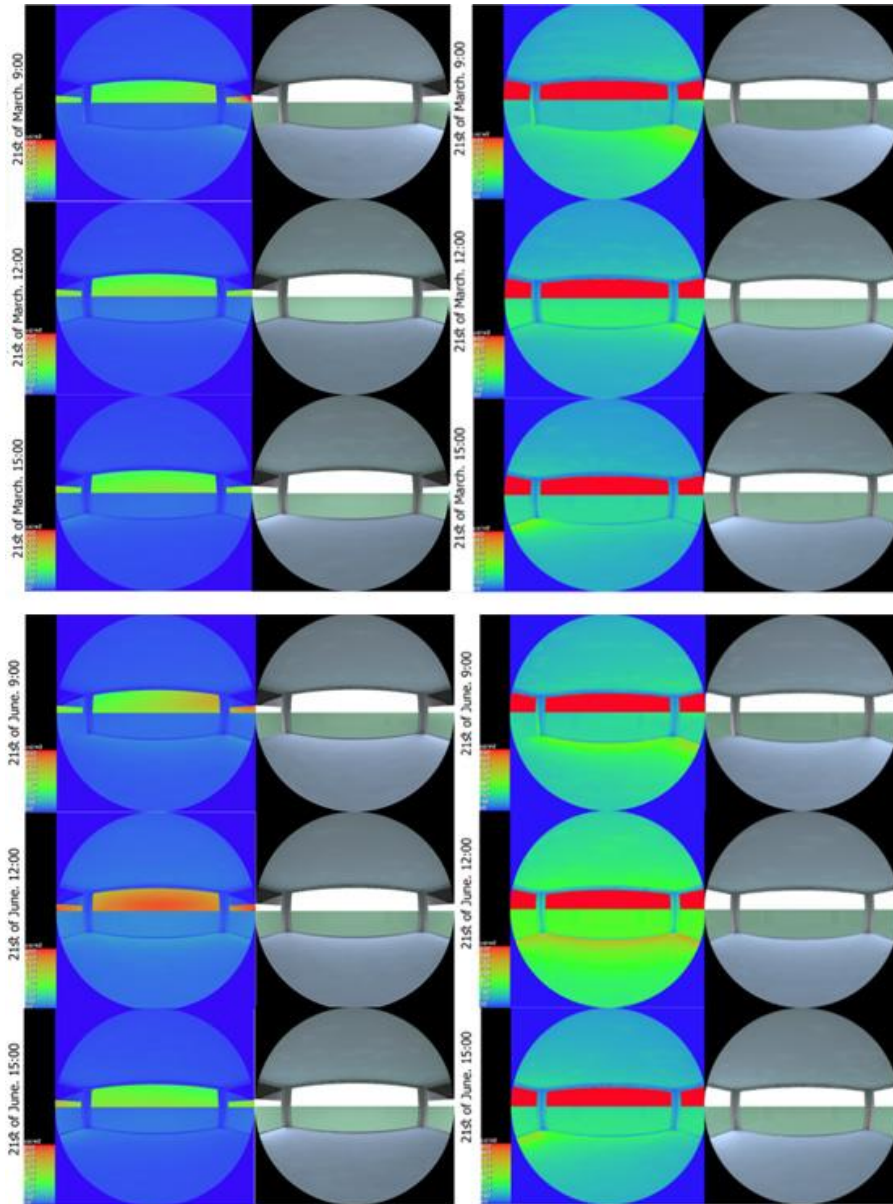


Figure 5.92. Reception room luminance maps on the 21st of March (top images) and 21st of June (bottom images). The images on the left show scenarios01,02 and 03 results and the images on the right show the basic model results (author 2019).

On 21st of March, in the reception room, luminance levels from the glazed wall reached 450 cd/m² in all cases which, comparing to the basic model results, indicated 42.1% luminance level reduction. On 21st of June, in the reception room, luminance levels from the glazed wall reached 500 cd/m² in the first case, 750 cd/m² in second case and 550 cd/m² in the third case which, comparing to the basic model results, indicated 47.4%,21.1% and 42.1% luminance level reduction (figure 5.92).

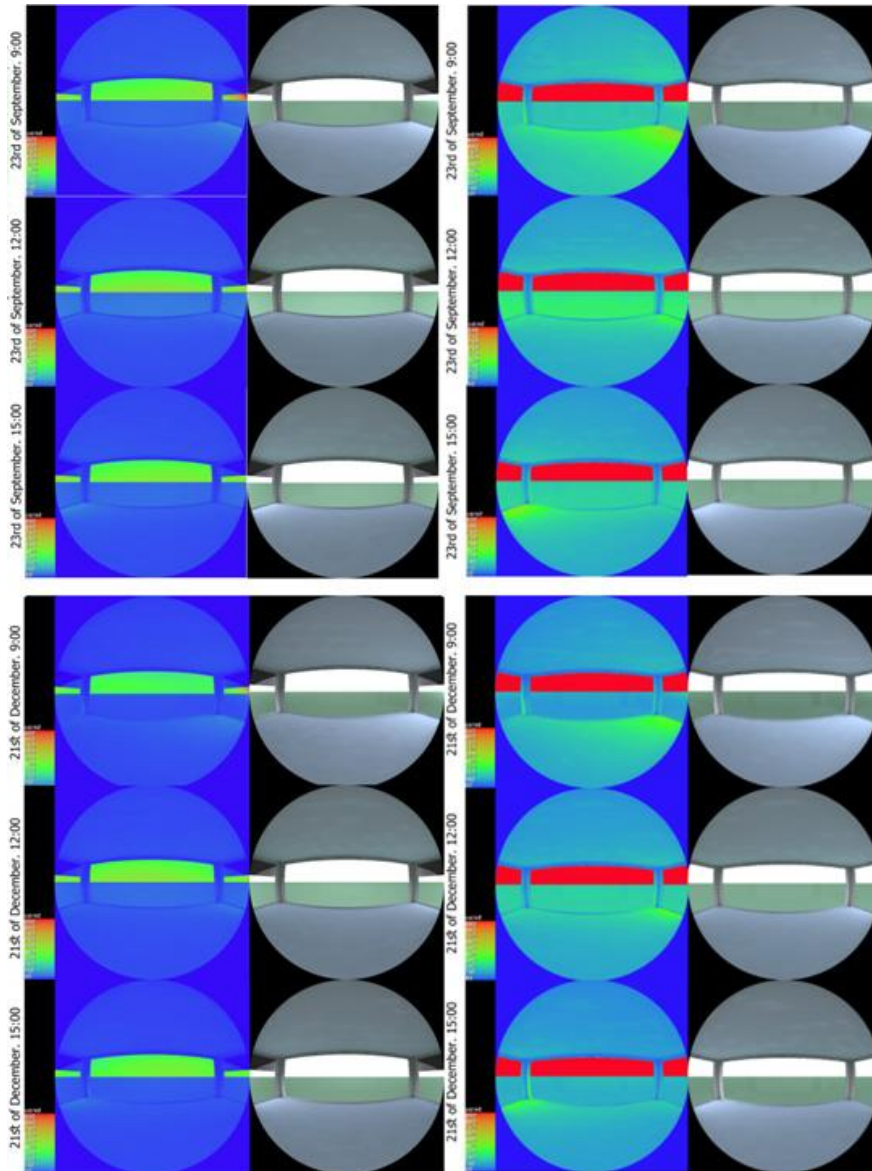


Figure 5.93. Reception room luminance maps on the 23rd of September (top images) and 21st of December (bottom images). The images on the left show scenarios01,02 and 03 results and the images on the right show the basic model results (author 2019).

On 23rd of September and 21st of December, in the reception room, luminance levels from the glazed wall reached 450 cd/m² in all cases which, comparing to the basic model results, indicated 42.1% luminance level reduction. On 21st of June, in the reception room, luminance levels from the glazed wall reached 500 cd/m² in the first case, 750 cd/m² in second case and 550 cd/m² in the third case which, comparing to the basic model results, indicated 47.4%,21.1% and 42.1% luminance level reduction (figure 5.93).

Table 5.97. DGI levels from different angles from nadir for the four days at 9:00,12:00 and 15:00 (author 2019).

| Angle | 60 | 50 | 40 | 30 | 20 | 10 | 0 | -10 | -20 | -30 | -40 | -50 | -60 |
|-------------------------------------------|------|------|------|------|------|------|------|------|------|------|------|------|------|
| 09:00 21 st of March | 0.00 | 0.00 | 0.00 | 0.00 | 0.00 | 0.00 | 0.00 | 7.9 | 10.3 | 10.5 | 14.4 | 16.0 | 16.3 |
| 12:00 21 st of March | 8.7 | 8.3 | 0.00 | 0.00 | 0.00 | 8.8 | 9.1 | 8.7 | 8.4 | 8.5 | 8.8 | 9.6 | 9.5 |
| 15:00 21 st of March | 12.5 | 9.9 | 9.1 | 4.5 | 0.00 | 0.00 | 0.00 | 0.00 | 0.00 | 0.00 | 0.00 | 2.4 | 3.9 |
| 09:00 21 st of June | 0.00 | 0.00 | 0.00 | 0.00 | 0.00 | 0.00 | 8.8 | 10.8 | 12.6 | 14.1 | 14.4 | 14.4 | 17.3 |
| 12:00 21 st of June | 0.00 | 0.00 | 0.00 | 0.00 | 0.00 | 0.00 | 0.00 | 0.00 | 0.00 | 0.00 | 0.00 | 0.00 | 0.00 |
| 15:00 21 st of June | 12.8 | 12.4 | 10.7 | 6.74 | 6.5 | 0.00 | 0.00 | 0.00 | 0.00 | 0.00 | 0.00 | 0.00 | 0.00 |
| 09:00 23 rd of September | 0.00 | 0.00 | 0.00 | 0.00 | 0.00 | 0.00 | 0.00 | 0.00 | 9.7 | 9.9 | 13.8 | 15.4 | 15.7 |
| 12:00 23 rd of September | 8.1 | 8.6 | 8.4 | 7.5 | 0.00 | 9.4 | 7.8 | 9.3 | 8.9 | 7.7 | 9.1 | 8.8 | 9.9 |
| 15:00 23 rd of September | 13.2 | 11.6 | 7.7 | 5.6 | 5.3 | 0.00 | 0.00 | 0.00 | 0.00 | 0.00 | 0.00 | 0.75 | 2.33 |
| 09:00 21 st of December | 0.00 | 0.00 | 0.00 | 0.00 | 0.00 | 0.00 | 0.00 | 0.00 | 5.9 | 7.9 | 10.3 | 14.1 | 14.5 |
| 12:00 21 st of December | 7.2 | 7.5 | 8.1 | 8.8 | 0.00 | 0.00 | 0.00 | 7.8 | 7.4 | 7.3 | 7.7 | 7.7 | 9.5 |
| 15:00 21 st of December | 7.3 | 7.4 | 7.9 | 8.1 | 8.6 | 9.2 | 10.0 | 10.4 | 10.2 | 7.5 | 7.5 | 7.2 | 5.6 |

According to the DGI analysis there is an imperceptible glare in all cases, as it DGI level was lower than 18 in the centre of the glazed wall. In several cases DGI level was zero (table 5.97).

Table 5.98. GVCP levels from different angles from nadir for the four days at 9:00,12:00 and 15:00 (author 2019).

| Angle | 60 | 50 | 40 | 30 | 20 | 10 | 0 | -10 | -20 | -30 | -40 | -50 | -60 |
|-------------------------------------------|------|------|------|------|------|------|------|------|------|------|------|------|------|
| 09:00 21 st of March | 100 | 100 | 100 | 100 | 100 | 100 | 100 | 100 | 66.1 | 50.7 | 50.2 | 26.9 | 19.9 |
| 12:00 21 st of March | 100 | 100 | 100 | 91.9 | 92.8 | 92.8 | 93.4 | 93.6 | 92.3 | 91.4 | 90.1 | 88.1 | 85.8 |
| 15:00 21 st of March | 100 | 100 | 90.1 | 94.9 | 97.9 | 99.3 | 99.8 | 100 | 100 | 100 | 100 | 100 | 100 |
| 09:00 21 st of June | 100 | 99.9 | 99.9 | 99.6 | 92.2 | 84.3 | 84.3 | 84.3 | 62.1 | 51.4 | 52.6 | 55.9 | 51.2 |
| 12:00 21 st of June | 100 | 100 | 100 | 100 | 100 | 100 | 100 | 100 | 100 | 100 | 100 | 100 | 100 |
| 15:00 21 st of June | 46.8 | 56.9 | 68.6 | 80.2 | 100 | 100 | 100 | 100 | 100 | 100 | 100 | 100 | 100 |
| 09:00 23 rd of September | 100 | 100 | 100 | 100 | 100 | 100 | 100 | 100 | 70.6 | 55.7 | 65.5 | 61.2 | 73.6 |
| 12:00 23 rd of September | 91.1 | 91.5 | 91.7 | 90.6 | 90.3 | 91.6 | 92.5 | 92.4 | 92.1 | 90.5 | 90.5 | 87.9 | 86.1 |
| 15:00 23 rd of September | 81.5 | 81.1 | 88.1 | 93.6 | 97.2 | 99.1 | 99.8 | 99.9 | 100 | 100 | 100 | 100 | 100 |
| 09:00 21 st of December | 100 | 100 | 100 | 100 | 100 | 100 | 100 | 100 | 84.2 | 71.8 | 68.3 | 55.8 | 55.8 |
| 12:00 21 st of December | 98.9 | 97.7 | 94.7 | 93.0 | 90.1 | 87.5 | 92.5 | 94.5 | 93.8 | 92.9 | 93.0 | 91.0 | 88.8 |
| 15:00 21 st of December | 100 | 100 | 100 | 100 | 100 | 91.2 | 91.1 | 78.1 | 79.2 | 83.2 | 87.8 | 92.2 | 95.8 |

GVCP analysis showed that minimum percentage was 84.30% at 9:00 on 21st of June and maximum percentage was 100% at 12:00 on 21st of June when looking at the middle of the northern glazed wall. The minimum percentage of satisfied occupants was 46.83% at 15:00 on 21st of June and maximum was 100% at 12:00 on 21st of June when looking at the eastern and western glazed walls (table 5.98).

Comparing to the basic model minimum DGI reduction was 44.3% and maximum DGI reduction was 100% while the minimum GVCP improvement was 13.5% and maximum GVCP improvement was 230.0%. Refer to final comparison table 5.99 for full details including comparison with the basic model and sixth scenario.

Table 5.99. Final comparison between Scenarios 06, 07,08 and basic model in the reception room (author 2019).

| Date | Hour | Average DGI reduction comparing to the basic model results (scenarios 07 and 08) | Average DGI reduction comparing to the basic model results (scenario 06) | Average GVCP increment comparing to the basic model results (scenarios 07 and 08) | Average GVCP increment comparing to the basic model results (scenario 06) |
|---------------------------|-------|----------------------------------------------------------------------------------|--------------------------------------------------------------------------|-----------------------------------------------------------------------------------|---------------------------------------------------------------------------|
| 21 st of Mar. | 9:00 | 52.3% | 46.0% | 13.5% | 8.7% |
| 21 st of Mar. | 12:00 | 57.7% | 49.7% | 116.0% | 110.2% |
| 21 st of Mar. | 15:00 | 78.3% | 73.0% | 96.3% | 89.4% |
| 21 st of Jun. | 9:00 | 44.3% | 38.2% | 75.7% | 73.1% |
| 21 st of Jun. | 12:00 | 100% | 100% | 230.4% | 230.0% |
| 21 st of Jun. | 15:00 | 60.0% | 53.3% | 43.5% | 41.6% |
| 23 rd of Sept. | 9:00 | 69.2% | 49.5% | 21.1% | 16.6% |
| 23 rd of Sept. | 12:00 | 69.3% | 48.1% | 112.7% | 111.8% |
| 23 rd of Sept. | 15:00 | 75.8% | 70.3% | 90.9% | 89.6% |
| 21 st of Dec. | 9:00 | 68.0% | 58.8% | 29.7% | 28.8% |
| 21 st of Dec. | 12:00 | 69.1% | 61.0% | 157.0% | 156.3% |
| 21 st of Dec. | 15:00 | 52.2% | 49.5% | 171.8% | 161.9% |

5.5.6 Scenarios 07 and 08 daylight harvesting potential analysis

Similar to the basic model simulation, the analysis was done using both RadianceIES and Apache applications. The daylight harvesting potential was measured by the annual electrical consumption saving which happened after using the sensors. Due to the reduction of the average illuminance levels, the daylight harvesting potential was reduced by 98.8% in both scenarios. It was noticed that the software gave higher results for specific months. That was a possible error with the software (tables 5.100 and 5.101).

Table 5.100. Total annual electricity consumption Results summary (author 2019).

| | Total energy (MWh) | Total energy (MWh) | Total Energy (MWh) | Total Energy (MWh) |
|--------------|-------------------------|--------------------|-------------------------|--------------------|
| Date | Scenario 08 With DH.aps | Scenario 08.aps | Scenario 07 With DH.aps | Scenario 07.aps |
| Jan 01-31 | 1.8748 | 1.8248 | 1.9286 | 1.8893 |
| Feb 01-28 | 2.0340 | 1.9664 | 2.0924 | 2.0442 |
| Mar 01-31 | 2.5020 | 2.4371 | 2.5739 | 2.5315 |
| Apr 01-30 | 3.0088 | 2.9830 | 3.0951 | 3.0799 |
| May 01-31 | 3.6075 | 3.5849 | 3.7110 | 3.6984 |
| Jun 01-30 | 3.7357 | 3.7426 | 3.8429 | 3.8524 |
| Jul 01-31 | 4.0206 | 4.0644 | 4.1335 | 4.1686 |
| Aug 01-31 | 4.0731 | 4.1385 | 4.1900 | 4.2394 |
| Sep 01-30 | 3.6902 | 3.7641 | 3.7961 | 3.8537 |
| Oct 01-31 | 3.3556 | 3.4076 | 3.4520 | 3.4892 |
| Nov 01-30 | 2.7410 | 2.7614 | 2.8197 | 2.8305 |
| Dec 01-31 | 2.2429 | 2.2251 | 2.3072 | 2.2822 |
| Summed total | 36.8863 | 36.8998 | 37.9452 | 37.9594 |

Table 5.101. Final comparison (author 2019).

| Scenario | Total annual artificial lighting electrical consumption saving | Cost saving based on tariff of 30.5 Fils for every KW (ADDC 2018). | Reduction in daylight harvesting potential comparing to basic model potential |
|--------------|----------------------------------------------------------------|--------------------------------------------------------------------|-------------------------------------------------------------------------------|
| Basic-model | 1.1156 MWh | 340.3 UAE Dirhams | - |
| Scenario-01: | 0.769 MWh | 234.5 UAE Dirhams | 31.07% |
| Scenario-02: | 0.770 MWh | 234.9 UAE Dirhams | 30.98% |
| Scenario-03: | 0.773 MWh | 235.8 UAE Dirhams | 30.71% |
| Scenario-04 | 0.6215 MWh | 189.6 UAE Dirhams | 55.7% |
| Scenario-05: | 0.2397 MWh | 73.1 UAE Dirhams | 78.5% |
| Scenario-06: | 0.1439 MWh | 43.9 UAE Dirhams | 87.1% |
| Scenario 07 | 0.0140 MWh | 4.27 UAE Dirhams | 98.8% |
| Scenario 08 | 0.0135 MWh | 4.11 UAE Dirhams | 98.8% |

5.6 Buffer DSF/ Corridor Facade -Scenario 09 Analysis

5.6.1 Scenario 09 CFD simulation and analysis

Table 5.102. Air temperature within the DSF cavity from Microflo results (author 2019).

| Location | Date | Hour | Minimum DSF cavity air temperature (°C) | Maximum DSF cavity air temperature (°C) | Mean DSF cavity air temperature (°C) | Comparison between ambient temperature (47°C) and mean DSF cavity air temperature | Reduction in average air temperature comparing to scenarios 06. |
|---------------------|--------------------------|-------|-----------------------------------------|-----------------------------------------|--------------------------------------|-----------------------------------------------------------------------------------|-----------------------------------------------------------------|
| Eastern DSF cavity | 10 th of Aug. | 15:00 | 27.90 | 45.96 | 35.86 | -23.7% | 0.4% |
| Western DSF cavity | 10 th of Aug. | 12:00 | 27.93 | 45.90 | 35.78 | -23.9% | 0.3% |
| Northern DSF cavity | 10 th of Aug. | 15:00 | 28.04 | 46.19 | 35.90 | -23.6% | 0.0% |

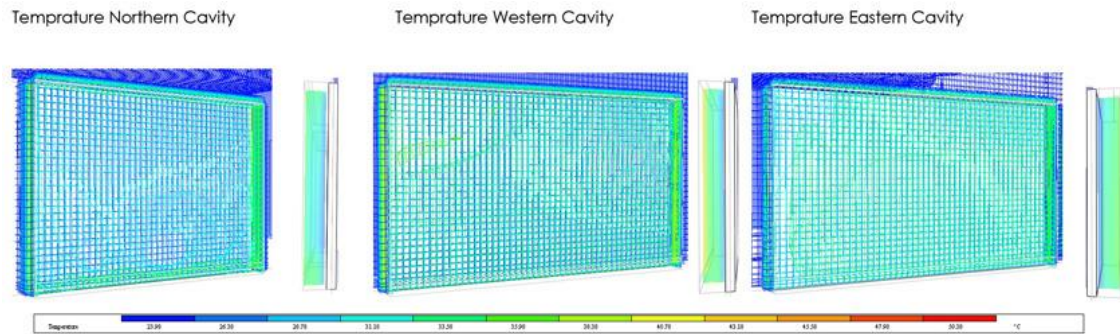


Figure 5.93. CFD analysis of Norther, Eastern and Western cushions in Microflo (author 2019).

The temperature analysis showed that when the ambient temperature reached 47.0 °C at the building level , the temperature in the DSF cavity near the cushion was maximum 45.96 °C in eastern DSF, maximum 45.90 °C in western DSF and maximum 46.19 °C in northern DSF. Thus, the temperature near the external DSF layer was slightly lower than ambient temperature in all cases. The temperature in the DSF cavity near the DGU was minimum 27.90 °C in eastern DSF, minimum 27.93 °C in western

DSF and minimum 28.04 °C in northern DSF. Due to the natural air flow, hot air was discharged and average reduction in mean cavity air temperature, comparing to ambient temperature, was 23.7% in eastern DSF, 23.9% in western DSF and 23.6% in northern DSF. Comparing to scenario 06, the average air temperature was reduced by 0.3~0.4% in eastern and western DSF cavities while it was the same in the northern DSF cavity (table 5.102 and figure 5.93).

Table 5.103. Air velocity within the DSF cavity from Microflo results (author 2019).

| Location | Date | Hour | Air velocity within the cavity near the bottom inlet (m/s) | Air velocity within the cavity near the top outlet (m/s) | Mean air velocity within the cavity (m/s) |
|---------------------|--------------------------|-------|------------------------------------------------------------|----------------------------------------------------------|-------------------------------------------|
| Eastern DSF cavity | 10 th of Aug. | 15:00 | 0.62 | 1.13 | 0.88 |
| Western DSF cavity | 10 th of Aug. | 12:00 | 0.62 | 1.03 | 0.83 |
| Northern DSF cavity | 10 th of Aug. | 15:00 | 0.21 | 0.62 | 0.41 |

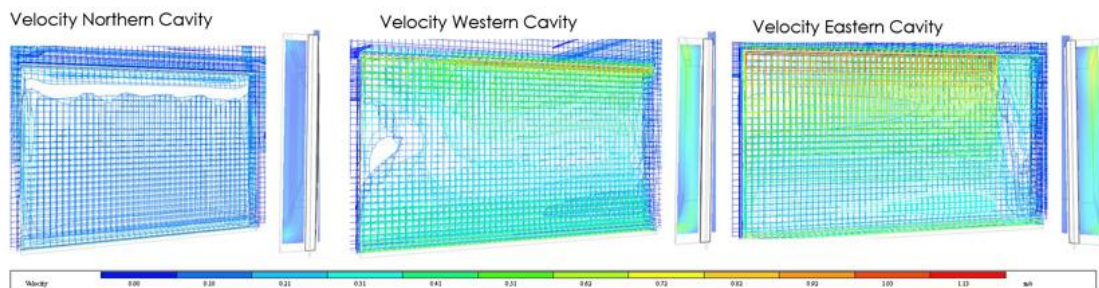


Figure 5.94. CFD analysis of the eastern cushions in IES VE (author 2019).

The analysis proved that air flow was from bottom to top which helped to discharge hot air from the DSF cavity. The maximum air velocity was near the top exhaust/outlet. Average air velocity in the eastern DSF was 0.88 while the maximum velocity was 1.13 m/s near the top and the inlet air velocity was 0.62 m/s. Average air velocity in the western DSFs was 0.83 m/s while the maximum velocity was 1.03 m/s near the top and the inlet air velocity was 0.62 m/s. Similar to previous scenarios the lowest air velocity and temperature was simulated in the northern DSF. The impact of the stack effect on the DSF was evaluated in the following sections where additional investigations on the internal conditions within the building were provided (table 5.103 and figure 5.94).

5.6.2 Scenario 09 electrical/energy consumption

Table 5.104. Total annual electricity/energy consumption for scenarios 07 and 08 comparing to the basic model (author 2019).

| | Total electricity (MWh) | Total electricity (MWh) |
|--------------|-------------------------|-------------------------|
| Date | Scenario 09.aps | Basic Model.aps |
| Jan 01-31 | 1.8888 | 2.1744 |
| Feb 01-28 | 2.0382 | 2.4339 |
| Mar 01-31 | 2.5273 | 3.0512 |
| Apr 01-30 | 3.0734 | 3.6774 |
| May 01-31 | 3.6990 | 4.4261 |
| Jun 01-30 | 3.8540 | 4.5822 |
| Jul 01-31 | 4.1643 | 4.9159 |
| Aug 01-31 | 4.2350 | 4.9626 |
| Sep 01-30 | 3.8459 | 4.4772 |
| Oct 01-31 | 3.4785 | 4.0166 |
| Nov 01-30 | 2.8205 | 3.2288 |
| Dec 01-31 | 2.2700 | 2.6027 |
| Summed total | 37.8950 | 44.5490 |

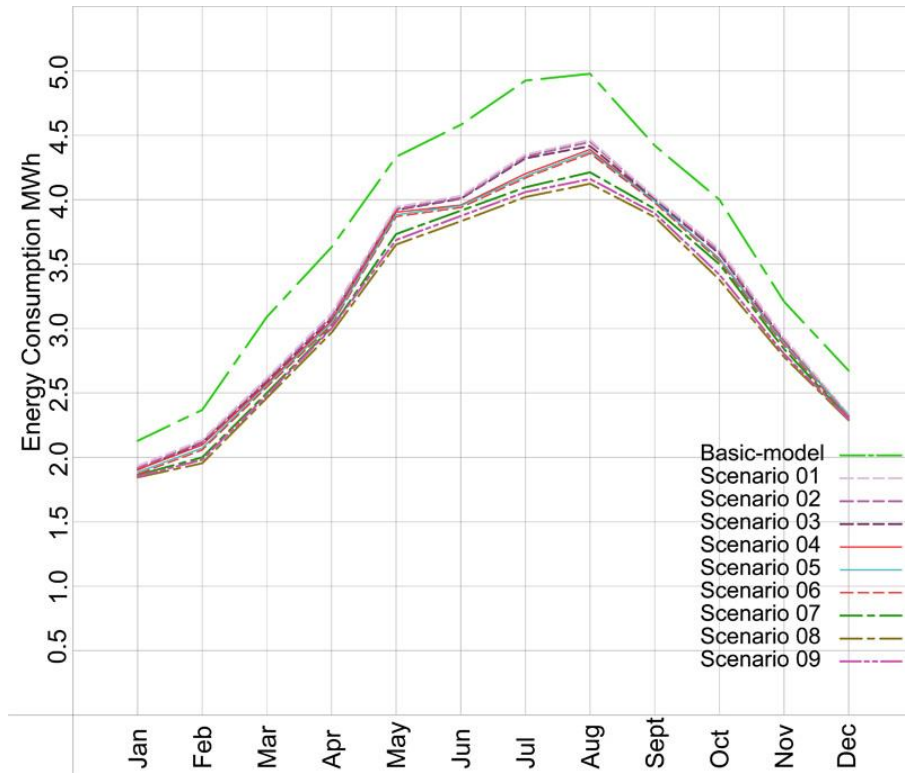


Figure 5.95. Combined diagram of the basic model results and the first nine scenarios results (author 2019)

In scenario 09, the total electrical consumption reduction, with consideration of the inflation unit consumption, was 14.9% which was better than savings from scenario 07 (14.7%) but was low comparing to scenario 08 (17.1%). Comparing to the sixth scenario (as dynamic shades were added to this scenario), the energy saving was improved by 2.2% (from 12.7% to 14.9%) when the shade was installed (table 5.104 and figure 5.95). Refer to table 5.105 for complete comparison

Table 5.105. Final comparison between the first nine scenarios (author 2019).

| Scenario | Total annual electrical consumption saving comparing to the basic model (MWh) | Inflation unit annual electricity consumption (MWh) | Total annual electrical consumption saving considering inflation unit annual consumption (MWh) | Total annual electrical consumption saving considering inflation unit annual consumption (%) | Cost saving based on tariff of 30.5 Fils for every KW (ADDC 2018) |
|-------------|-------------------------------------------------------------------------------|-----------------------------------------------------|------------------------------------------------------------------------------------------------|----------------------------------------------------------------------------------------------|-------------------------------------------------------------------|
| Scenario-01 | 5.2033 | 0.03916 | 5.16414 | 11.594% | 1575.1 UAE Dirhams |
| Scenario-02 | 5.2064 | 0.03916 | 5.16724 | 11.600% | 1576.0 UAE Dirhams |
| Scenario-03 | 5.2084 | 0.03916 | 5.16924 | 11.603% | 1576.6 UAE Dirhams |
| Scenario-04 | 5.5863 | 0.03916 | 5.54714 | 12.45% | 1691.9 UAE Dirhams |
| Scenario-05 | 5.656 | 0.03916 | 5.61684 | 12.6% | 1713.1 UAE Dirhams |
| Scenario-06 | 5.6788 | 0.03916 | 5.63964 | 12.7% | 1720.1 UAE Dirhams |
| Scenario-07 | 6.5896 | 0.03916 | 6.55044 | 14.7% | 1997.9 UAE Dirhams |
| Scenario-08 | 7.6492 | 0.03916 | 7.61004 | 17.1% | 2333.0 UAE Dirhams |
| Scenario 09 | 6.654 | 0.03916 | 6.61484 | 14.9% | 2029.5 UAE Dirhams |

5.6.3 Scenario 09 thermal comfort results

Table 5.106. Comfort index results comparison between scenario 09 and the basic model (author 2019).

| Var. Name | Location | Filename | Type | Mean |
|---------------|-----------------|-----------------|---------------|------|
| Comfort index | Mechanical room | Scenario 09.aps | Comfort index | 9 |
| Comfort index | Office 01 | Scenario 09.aps | Comfort index | 9 |
| Comfort index | Office 02 | Scenario 09.aps | Comfort index | 9 |
| Comfort index | Store 01 | Scenario 09.aps | Comfort index | 9 |
| Comfort index | Lobby 01 | Scenario 09.aps | Comfort index | 9 |
| Comfort index | Waiting room | Scenario 09.aps | Comfort index | 9 |
| Comfort index | Lobby 02 | Scenario 09.aps | Comfort index | 9 |
| Comfort index | Toilet | Scenario 09.aps | Comfort index | 9 |
| Comfort index | Store 02 | Scenario 09.aps | Comfort index | 9 |
| Comfort index | Reception | Scenario 09.aps | Comfort index | 9 |
| Comfort index | Mechanical room | Basic Model.aps | Comfort index | 9 |
| Comfort index | Office 01 | Basic Model.aps | Comfort index | 9 |
| Comfort index | Office 02 | Basic Model.aps | Comfort index | 9 |
| Comfort index | Store 01 | Basic Model.aps | Comfort index | 9 |
| Comfort index | Lobby 01 | Basic Model.aps | Comfort index | 9 |
| Comfort index | Waiting room | Basic Model.aps | Comfort index | 10 |
| Comfort index | Lobby 02 | Basic Model.aps | Comfort index | 9 |
| Comfort index | Toilet | Basic Model.aps | Comfort index | 9 |
| Comfort index | Store 02 | Basic Model.aps | Comfort index | 10 |
| Comfort index | Reception | Basic Model.aps | Comfort index | 10 |

In scenario 09, comparing to the basic model, Comfort index in store 02, waiting room and the reception changed from 10 (warm/acceptable) to 9 (slightly warm/acceptable) (table 5.106). Thus, scenario 09 results are the same as scenario 01 results.

Table 5.107. Mean room temperature results comparison between scenario 09 and the basic model (author 2019).

| Var. Name | Location | Filename | Type | Mean |
|-----------------|-----------------|-----------------|------------------|-------|
| Air temperature | Mechanical room | Scenario 09.aps | Temperature (°C) | 24.82 |
| Air temperature | Office 01 | Scenario 09.aps | Temperature (°C) | 24.59 |
| Air temperature | Office 02 | Scenario 09.aps | Temperature (°C) | 24.57 |
| Air temperature | Store 01 | Scenario 09.aps | Temperature (°C) | 24.50 |
| Air temperature | Lobby 01 | Scenario 09.aps | Temperature (°C) | 24.58 |
| Air temperature | Waiting room | Scenario 09.aps | Temperature (°C) | 25.09 |
| Air temperature | Lobby 02 | Scenario 09.aps | Temperature (°C) | 24.70 |
| Air temperature | Toilet | Scenario 09.aps | Temperature (°C) | 24.56 |
| Air temperature | Store 02 | Scenario 09.aps | Temperature (°C) | 24.67 |
| Air temperature | Reception | Scenario 09.aps | Temperature (°C) | 24.94 |
| Air temperature | Mechanical room | Basic Model.aps | Temperature (°C) | 24.89 |
| Air temperature | Office 01 | Basic Model.aps | Temperature (°C) | 24.62 |
| Air temperature | Office 02 | Basic Model.aps | Temperature (°C) | 24.66 |
| Air temperature | Store 01 | Basic Model.aps | Temperature (°C) | 24.52 |
| Air temperature | Lobby 01 | Basic Model.aps | Temperature (°C) | 24.62 |
| Air temperature | Waiting room | Basic Model.aps | Temperature (°C) | 25.51 |
| Air temperature | Lobby 02 | Basic Model.aps | Temperature (°C) | 25.13 |
| Air temperature | Toilet | Basic Model.aps | Temperature (°C) | 24.94 |
| Air temperature | Store 02 | Basic Model.aps | Temperature (°C) | 25.16 |
| Air temperature | Reception | Basic Model.aps | Temperature (°C) | 26.15 |

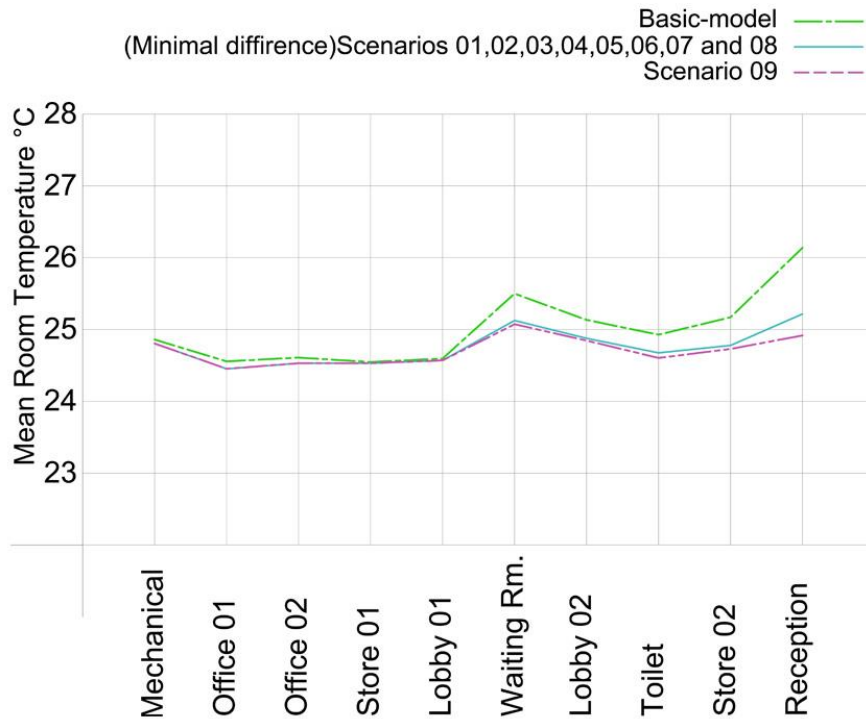


Figure 5.96. Combined diagram of the basic model results and the first nine scenarios results (author 2019)

Comparing to the basic model, the overall improvement/reduction in the mean room temperature was 1.27%. The improvement/reduction in the mean waiting room temperature was 1.65%. The improvement/reduction in the mean reception room temperature was 4.6% (table 5.107 and figure 5.96). Hence, Scenario 09 results were better than previous scenarios in 5 rooms.

Table 5.108. People dissatisfied index results comparison between scenario 09 and the basic model (author 2019).

| Var. Name | Location | Filename | Type | Mean |
|---------------------|-----------------|-----------------|----------------|-------|
| People dissatisfied | Mechanical room | Scenario 09.aps | Percentage (%) | 29.30 |
| People dissatisfied | Office 01 | Scenario 09.aps | Percentage (%) | 26.27 |
| People dissatisfied | Office 02 | Scenario 09.aps | Percentage (%) | 25.82 |
| People dissatisfied | Store 01 | Scenario 09.aps | Percentage (%) | 26.07 |
| People dissatisfied | Lobby 01 | Scenario 09.aps | Percentage (%) | 27.32 |
| People dissatisfied | Waiting room | Scenario 09.aps | Percentage (%) | 32.45 |
| People dissatisfied | Lobby 02 | Scenario 09.aps | Percentage (%) | 29.27 |
| People dissatisfied | Toilet | Scenario 09.aps | Percentage (%) | 26.19 |
| People dissatisfied | Store 02 | Scenario 09.aps | Percentage (%) | 27.75 |
| People dissatisfied | Reception | Scenario 09.aps | Percentage (%) | 33.41 |
| People dissatisfied | Mechanical room | Basic Model.aps | Percentage (%) | 29.95 |
| People dissatisfied | Office 01 | Basic Model.aps | Percentage (%) | 26.55 |
| People dissatisfied | Office 02 | Basic Model.aps | Percentage (%) | 26.71 |
| People dissatisfied | Store 01 | Basic Model.aps | Percentage (%) | 26.24 |
| People dissatisfied | Lobby 01 | Basic Model.aps | Percentage (%) | 27.70 |
| People dissatisfied | Waiting room | Basic Model.aps | Percentage (%) | 37.07 |
| People dissatisfied | Lobby 02 | Basic Model.aps | Percentage (%) | 33.21 |
| People dissatisfied | Toilet | Basic Model.aps | Percentage (%) | 29.74 |
| People dissatisfied | Store 02 | Basic Model.aps | Percentage (%) | 32.37 |
| People dissatisfied | Reception | Basic Model.aps | Percentage (%) | 43.40 |

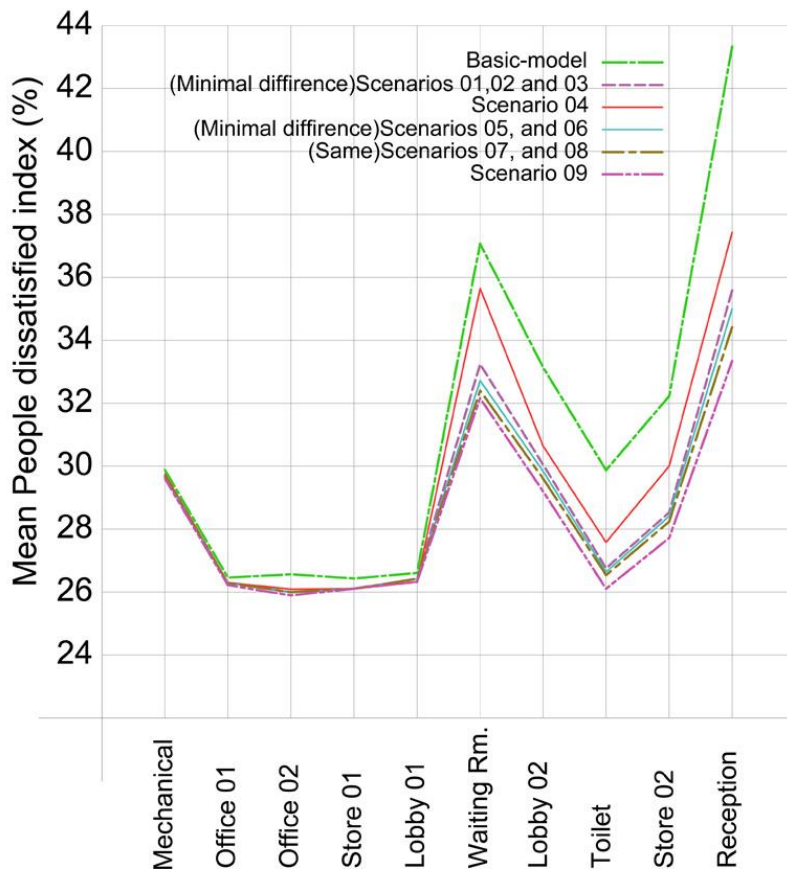


Figure 5.97. Combined diagram of the basic model results and the first nine scenarios results (author 2019)

Comparing to the basic model, the mean people dissatisfaction index had an average improvement of 9.3%. In the waiting room, the mean values had an average improvement of 12.5%. In the reception room, the mean value had an average improvement of 23.0% (table 5.108 and figure 5.97). Thus, scenario 09 results were better than all previous scenarios results.

5.6.4 Scenarios 09 daylight analysis

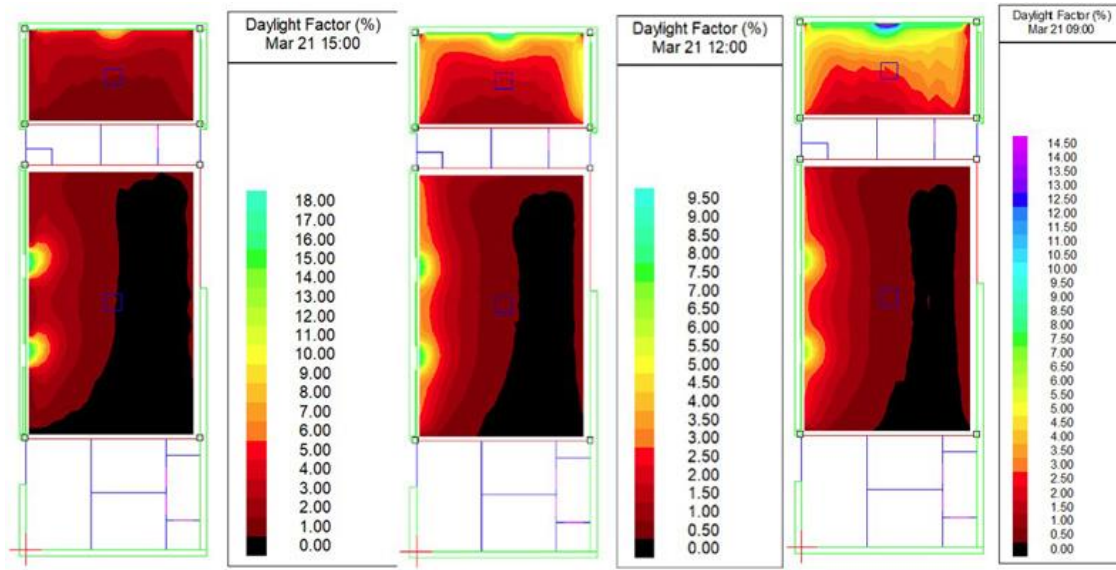


Figure 5.98. Scenario 09 daylight factor simulation results on the 21st of March (author 2019).

Table 5.109. Scenario 09 21st of March results summary (author 2019).

| Room | Date | Hour | Daylight factor | | | Daylight illuminance | | | Uniformity |
|----------------|---------------------------|-------|-----------------|------|-------|----------------------|------------|-------------|------------|
| | | | Min. | Ave. | Max. | Min. | Ave. | Max. | |
| Waiting room | 21 st of March | 9:00 | 0.3% | 1.1% | 6.9% | 21.36 lux | 85.20 lux | 524.84 lux | 0.25 |
| Reception room | 21 st of March | 9:00 | 0.6% | 3.9% | 14.8% | 42.35 lux | 297.07 lux | 1119.94 lux | 0.14 |
| Waiting room | 21 st of March | 12:00 | 0.2% | 1.1% | 8.6% | 20.28 lux | 97.17 lux | 757.85 lux | 0.21 |
| Reception room | 21 st of March | 12:00 | 0.9% | 2.9% | 9.9% | 80.73 lux | 255.11 lux | 870.63 lux | 0.32 |
| Waiting room | 21 st of March | 15:00 | 0.3% | 1.6% | 18.1% | 23.73 lux | 137.04 lux | 1507.74 lux | 0.17 |
| Reception room | 21 st of March | 15:00 | 0.5% | 2.7% | 9.4% | 41.43 lux | 224.42 lux | 786.07 lux | 0.18 |

In all cases, daylighting level in the waiting room was lower than required while in the reception room, average daylighting levels were within acceptable range at 9:00 on 21st of March. In the rest of the cases, it was lower than required. In all cases daylighting levels and DF were low in 75% to 90% of the waiting room area. Also, Average DF was lower than 2% in all the waiting room cases. Average DF was higher than 2% in all the reception room cases (figures 5.98,5.102,5.103,5.104,5.105 and table 5.109).

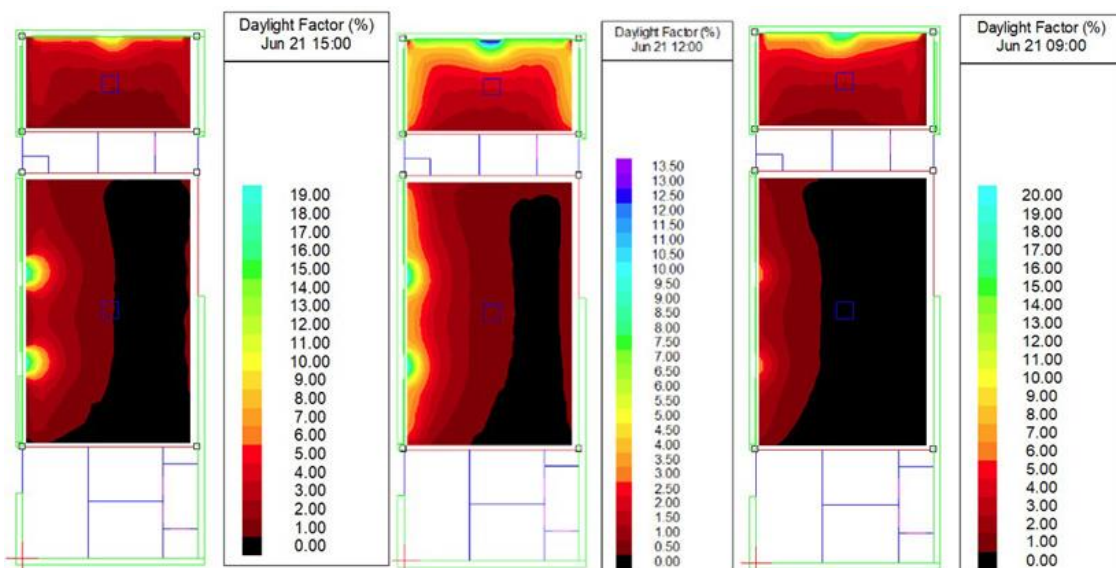


Figure 5.99. Scenario 09 daylight factor simulation results on the 21st of June (author 2019).

In all cases, average daylighting levels in the waiting room were lower than required while in the reception room, daylighting levels were higher than required at 12:00 and within acceptable range at 9:00 and 15:00 on the 21st of June. In all cases daylighting levels and DF were low in 75% to 90% of the waiting room area. Also, Average DF was lower than 2% in all the waiting room cases. Average DF was higher than 2% in all the reception room cases (figures 5.99,5.102,5.103,5.104,5.105 and table 5.110).

Table 5.110. Scenario 09 21st of June results summary (author 2019).

| Room | Date | Hour | Daylight factor | | | Daylight illuminance | | | Uniformity |
|----------------|--------------------------|-------|-----------------|------|-------|----------------------|------------|-------------|------------|
| | | | Min. | Ave. | Max. | Min. | Ave. | Max. | |
| Waiting room | 21 st of June | 9:00 | 0.3% | 1.0% | 6.8% | 20.99 lux | 84.57 lux | 564.81 lux | 0.25 |
| Reception room | 21 st of June | 9:00 | 0.5% | 4.4% | 20.2% | 40.62 lux | 362.64 lux | 1665.22 lux | 0.11 |
| Waiting room | 21 st of June | 12:00 | 0.3% | 1.2% | 9.7% | 46.62 lux | 220.77 lux | 1808.03 lux | 0.21 |
| Reception room | 21 st of June | 12:00 | 0.8% | 3.2% | 13.9% | 141.32 lux | 599.22 lux | 2586.44 lux | 0.24 |
| Waiting room | 21 st of June | 15:00 | 0.3% | 1.7% | 19.4% | 28.37 lux | 145.27 lux | 1659 lux | 0.20 |
| Reception room | 21 st of June | 15:00 | 0.5% | 3.1% | 12.7% | 43.76 lux | 261.07 lux | 1086.64 lux | 0.17 |

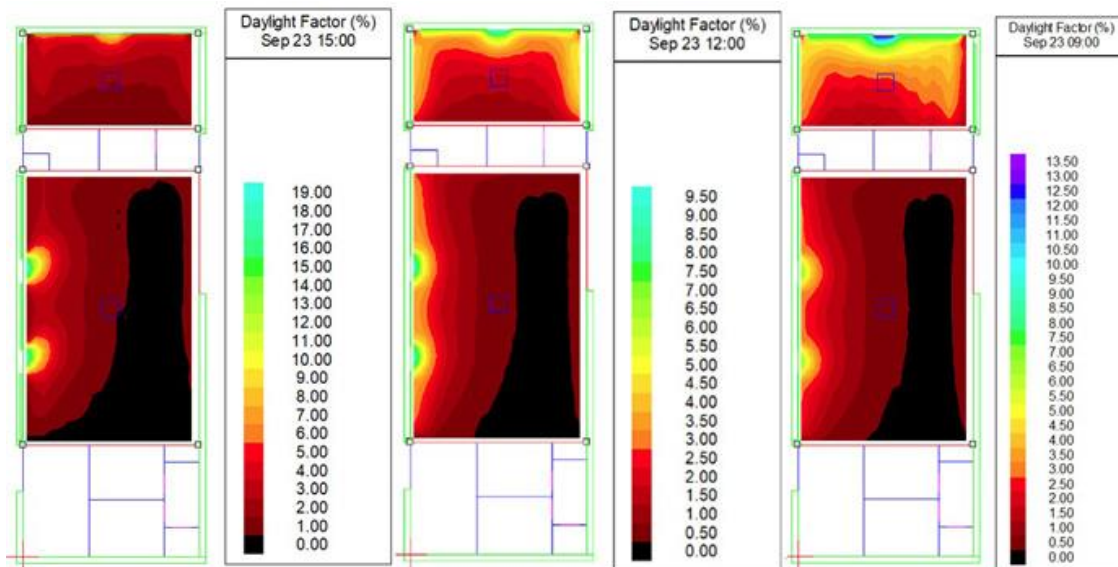


Figure 5.100. Scenario 06 daylight factor simulation results on the 23rd of September (author 2019).

Table 5.111. Scenario 06 23rd of September results summery (author 2019).

| Room | Date | Hour | Daylight factor | | | Daylight illuminance | | | Uniformity |
|----------------|---------------------------|-------|-----------------|------|-------|----------------------|------------|-------------|------------|
| | | | Min. | Ave. | Max. | Min. | Ave. | Max. | |
| Waiting room | 23 rd of Sept. | 9:00 | 0.3% | 1.1% | 6.8% | 20.91 lux | 85.01 lux | 535.38 lux | 0.25 |
| Reception room | 23 rd of Sept. | 9:00 | 1.1% | 4.6% | 14.2% | 88.22 lux | 358.32 lux | 1112.83 lux | 0.25 |
| Waiting room | 23 rd of Sept. | 12:00 | 0.2% | 1.2% | 9.3% | 21.01 lux | 103.48 lux | 824.75 lux | 0.20 |
| Reception room | 23 rd of Sept. | 12:00 | 1.0% | 2.9% | 9.8% | 88.88 lux | 255.42 lux | 866.73 lux | 0.35 |
| Waiting room | 23 rd of Sept. | 15:00 | 0.3% | 1.8% | 19.1% | 23.56 lux | 148.60 lux | 1567.99 lux | 0.16 |
| Reception room | 23 rd of Sept. | 15:00 | 0.5% | 2.8% | 9.7% | 40.93 lux | 232.23 lux | 798.05 lux | 0.18 |

In all cases, average daylighting levels in both rooms were lower than required. In all cases daylighting levels and DF were low in 75% to 90% of the waiting room area. Also, Average DF was lower than 2% in all the waiting room cases. Average DF was higher than 2% in all the reception room cases (figures 5.100,5.102,5.103,5.104,5.105 and table 5.111).

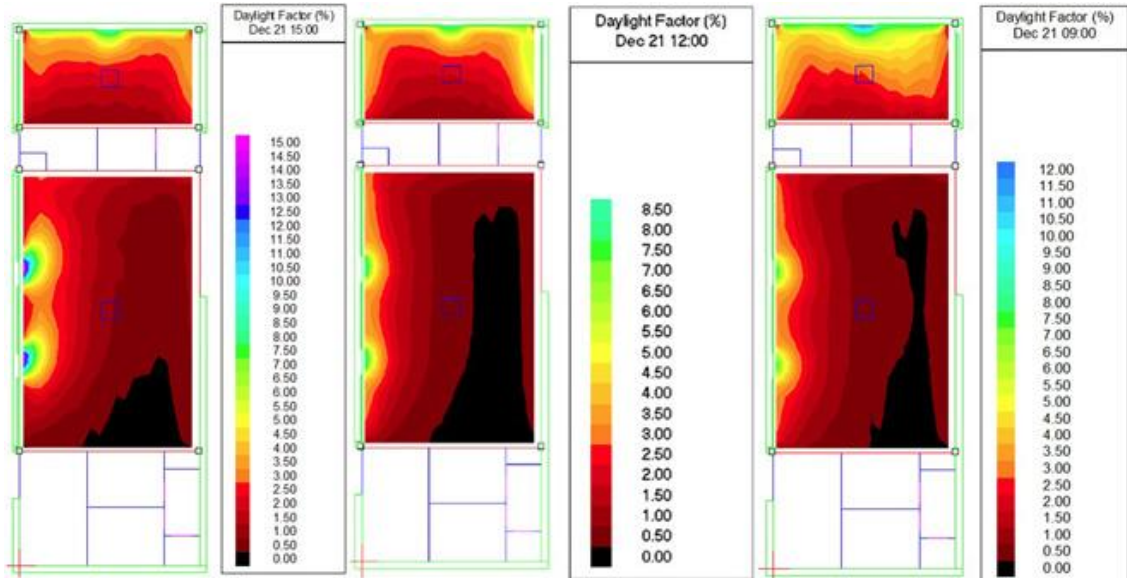


Figure 5.101. Scenarios 06 daylight factor simulation results on the 21st of December (author 2019).

Table 5.112. Scenarios 06 21st of December results summery (author 2019).

| Room | Date | Hour | Daylight factor | | | Daylight illuminance | | | Uniformity |
|----------------|--------------------------|-------|-----------------|------|-------|----------------------|------------|-------------|------------|
| | | | Min. | Ave. | Max. | Min. | Ave. | Max. | |
| Waiting room | 21 st of Dec. | 9:00 | 0.3% | 1.3% | 7.7% | 19.92 lux | 78.7 lux | 478.25 lux | 0.25 |
| Reception room | 21 st of Dec. | 9:00 | 0.5% | 3.7% | 12.1% | 41.24 lux | 232.04 lux | 750.15 lux | 0.15 |
| Waiting room | 21 st of Dec. | 12:00 | 0.3% | 1.2% | 8.7% | 21.36 lux | 100.09 lux | 711.66 lux | 0.21 |
| Reception room | 21 st of Dec | 12:00 | 1.1% | 3.0% | 8.8% | 89.35 lux | 247.43 lux | 714.73 lux | 0.36 |
| Waiting room | 21 st of Dec. | 15:00 | 0.3% | 1.6% | 15.2% | 19.93 lux | 114.70 lux | 1062.20 lux | 0.17 |
| Reception room | 21 st of Dec | 15:00 | 0.6% | 2.8% | 9.1% | 44.05 lux | 198.46 lux | 640.82 lux | 0.22 |

In all cases, average daylighting levels in both rooms were lower than required. In all cases daylighting levels and DF were low in 75% to 90% of the waiting room area. Also, Average DF was lower than 2% in all the waiting room cases. Average DF was higher than 2% in all the reception room cases (figures 5.101,5.102,5.103,5.104,5.105 and table 5.112).

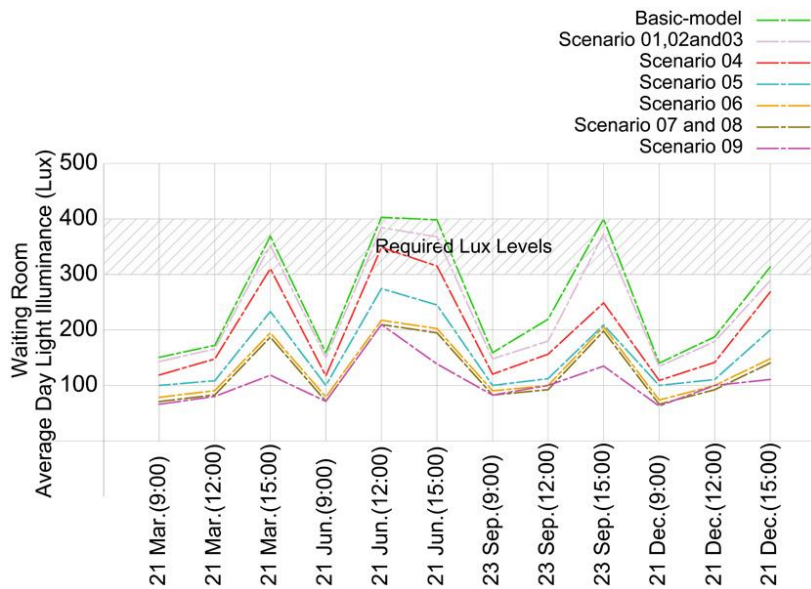


Figure 5.102. Combined diagram of the basic model DI results and the nine scenarios DI results in waiting room (author 2019).

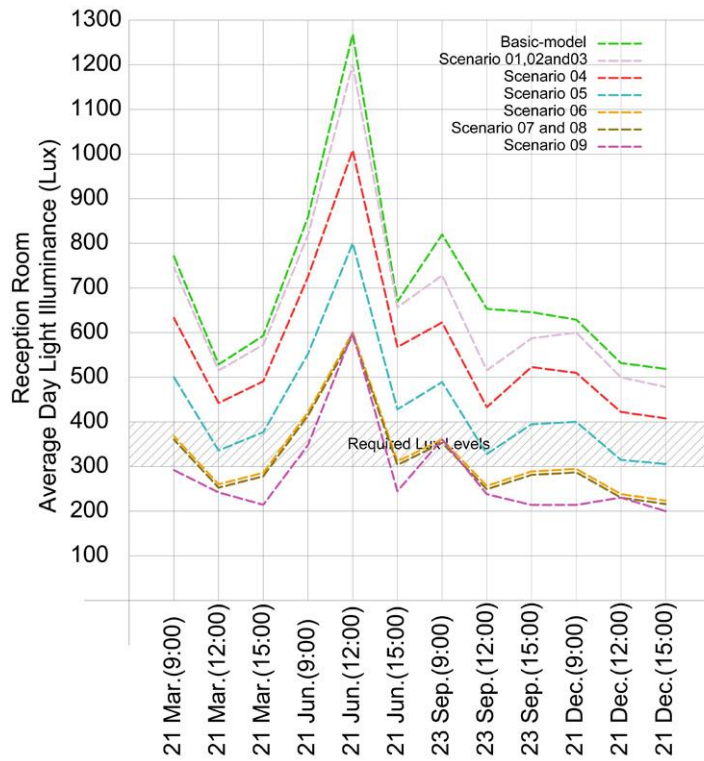


Figure 5.103. Combined diagram of the basic model DI results and the nine scenarios DI results in reception room (author 2019)

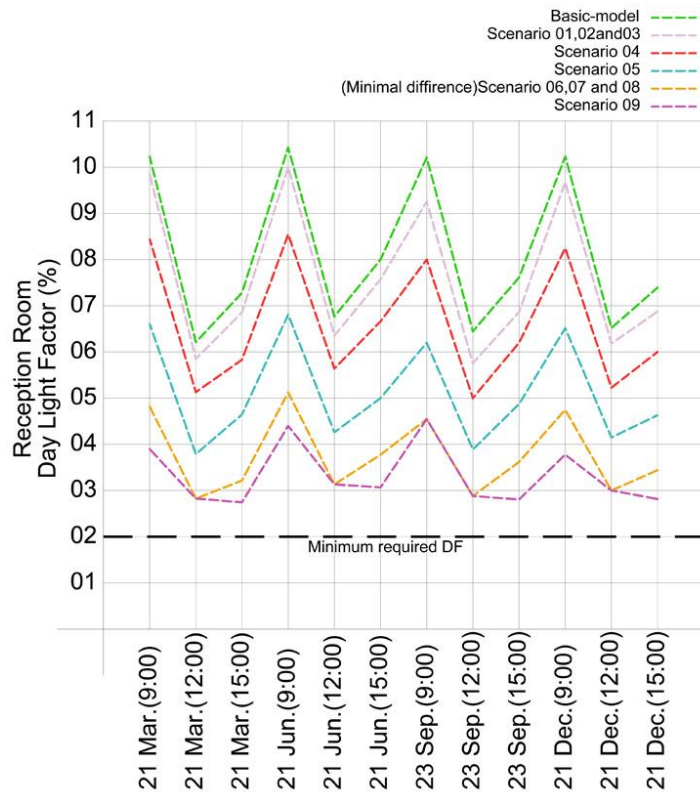


Figure 5.104. Combined diagram of the basic model DF results and the nine scenarios DF results in reception room (author 2019)

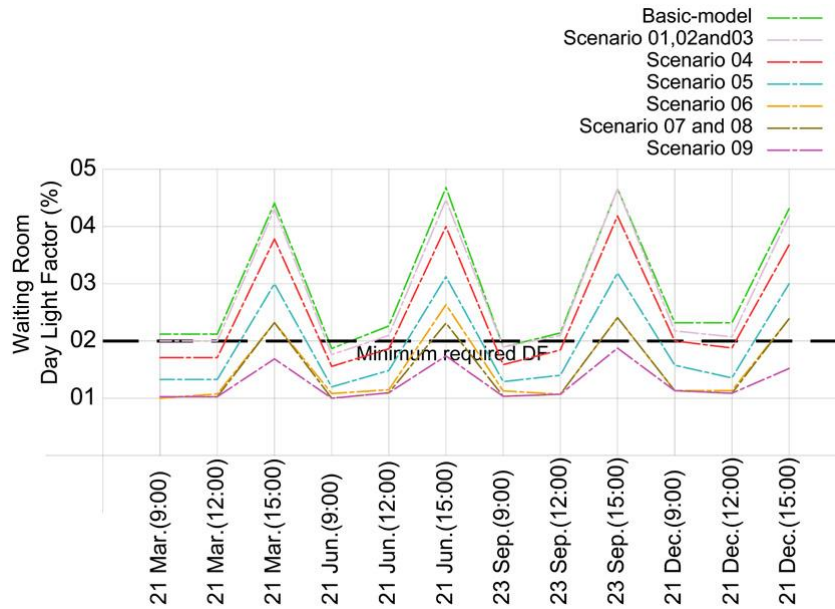


Figure 5.105. Combined diagram of the basic model DF results and the nine scenarios DF results in the waiting room (author 2019).

Comparing to the basic-model, the changes in scenario 09 reduced daylighting lux levels by minimum 45.5% and maximum 63.7%. Furthermore, the change reduced average DF by minimum 42.1% and maximum 63.7%. Uniformity changes varied from 42.8% to -46.2%. Refer to the final comparison table. Due to changes in VLT transmittance, scenarios 06 results were better as shown in the previous diagrams. Comparing to them, the additional dynamic shades reduced the daylighting levels by an average of 8.3% in the reception room and 13.3% in the waiting room. Also, the average DF reduction was 11.00% in the reception room and 12.8% in the waiting room (figures 5.102,5.103,5.104,5.105 and table 5.113).

Table 5.113. Final comparison between Scenario 09 and basic model (author 2019).

| Scenario | Date | Hour | Average daylight factor reduction | Average daylight illuminance reduction | Uniformity increment |
|------------|---------------------------|-------|---------------------------------------------|--------------------------------------------|----------------------------------------------|
| Scenario 9 | 21 st of Mar. | 9:00 | Waiting room 47.6% Reception room 62.13% | Waiting room 46.1% Reception room 62.0% | Waiting room 13.6% Reception room -46.2% |
| Scenario 9 | 21 st of Mar. | 12:00 | Waiting room 47.6% Reception room 53.2% | Waiting room 46.4% Reception room 53.0% | Waiting room 16.7% Reception room 6.6% |
| Scenario 9 | 21 st of Mar. | 15:00 | Waiting room 63.6% Reception room 62.5% | Waiting room 63.0% Reception room 62.1% | Waiting room 30.8% Reception room -40.0% |
| Scenario 9 | 21 st of Jun. | 9:00 | Waiting room 47.4% Reception room 58.1% | Waiting room 46.8% Reception room 58.2% | Waiting room 19.0% Reception room -42.1% |
| Scenario 9 | 21 st of Jun. | 12:00 | Waiting room 45.5% Reception room 52.9% | Waiting room 46.0% Reception room 52.5% | Waiting room 16.7% Reception room 9.1% |
| Scenario 9 | 21 st of Jun. | 15:00 | Waiting room 63.8% Reception room 61.3% | Waiting room 63.6% Reception room 62.0% | Waiting room -42.8% Reception room -19.1% |
| Scenario 9 | 23 rd of Sept. | 9:00 | Waiting room 42.2% Reception room 54.9% | Waiting room 45.5% Reception room 56.5% | Waiting room 13.6% Reception room 8.7% |
| Scenario 9 | 23 rd of Sept. | 12:00 | Waiting room 42.9% Reception room 54.7% | Waiting room 53.2% Reception room 61.1% | Waiting room 11.1% Reception room 34.6% |
| Scenario 9 | 23 rd of Sept. | 15:00 | Waiting room 61.7% Reception room 63.2% | Waiting room 62.7% Reception room 64.1% | Waiting room 23.1% Reception room -33.3% |
| Scenario 9 | 21 st of Dec. | 9:00 | Waiting room 43.5% Reception room 63.7% | Waiting room 46.2% Reception room 63.7% | Waiting room 13.6% Reception room -51.6% |
| Scenario 9 | 21 st of Dec. | 12:00 | Waiting room 47.8% Reception room 53.8% | Waiting room 45.4% Reception room 53.1% | Waiting room 16.7% Reception room 12.5% |
| Scenario 9 | 21 st of Dec. | 15:00 | Waiting room 63.6% Reception room 61.6% | Waiting room 62.5% Reception room 61.2% | Waiting room 41.6% Reception room -31.25% |

5.6.5 Scenario 09 glare analysis

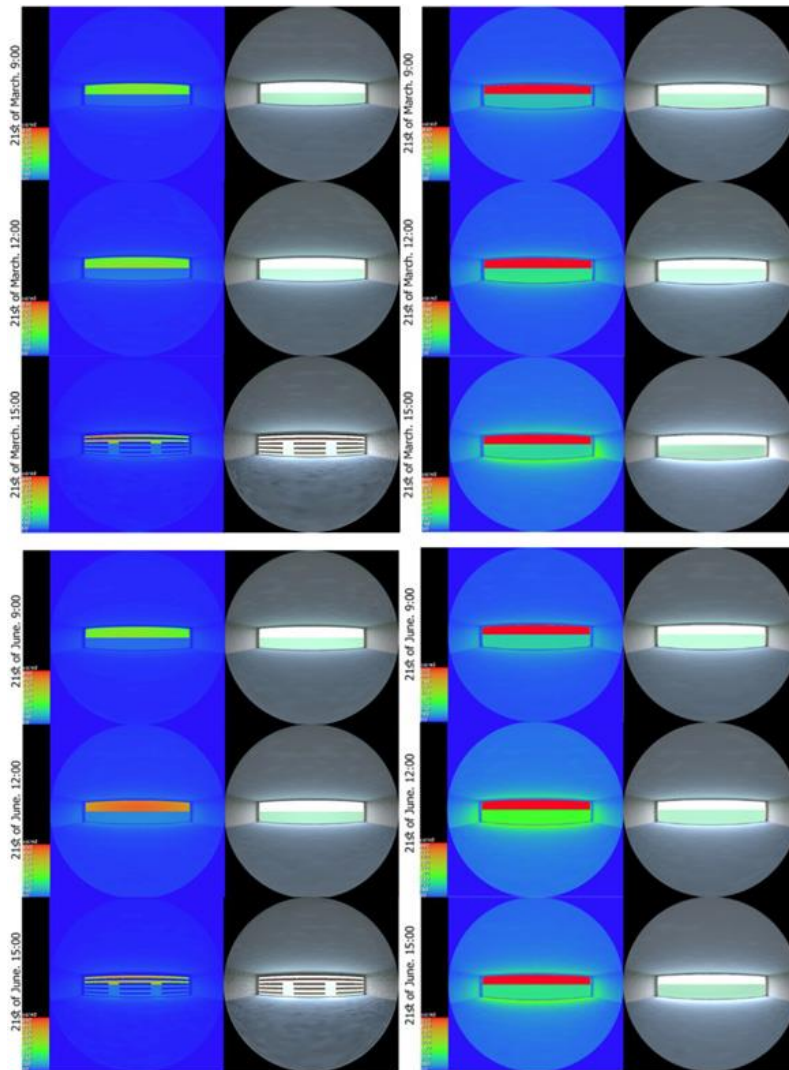


Figure 5.106. Waiting room luminance maps on the 21st of March (top images) and 21st of June (bottom images). The images on the left show scenario 04 results and the images on the right show the basic model results (author 2019).

On 21st of March, in the waiting room, average luminance levels from the glazed wall reached 300 cd/m² in first two cases and 450 cd/m² in third case which, comparing to the basic model results, indicated 68.4% and 52.6% luminance level reduction. On 21st of June, in the waiting room, average luminance levels from the glazed wall reached 600 cd/m² in first case and 850 cd/m² in second and third case which, comparing to the basic model results, indicated 36.8% and 10.5% luminance level reduction (figure 5.106).

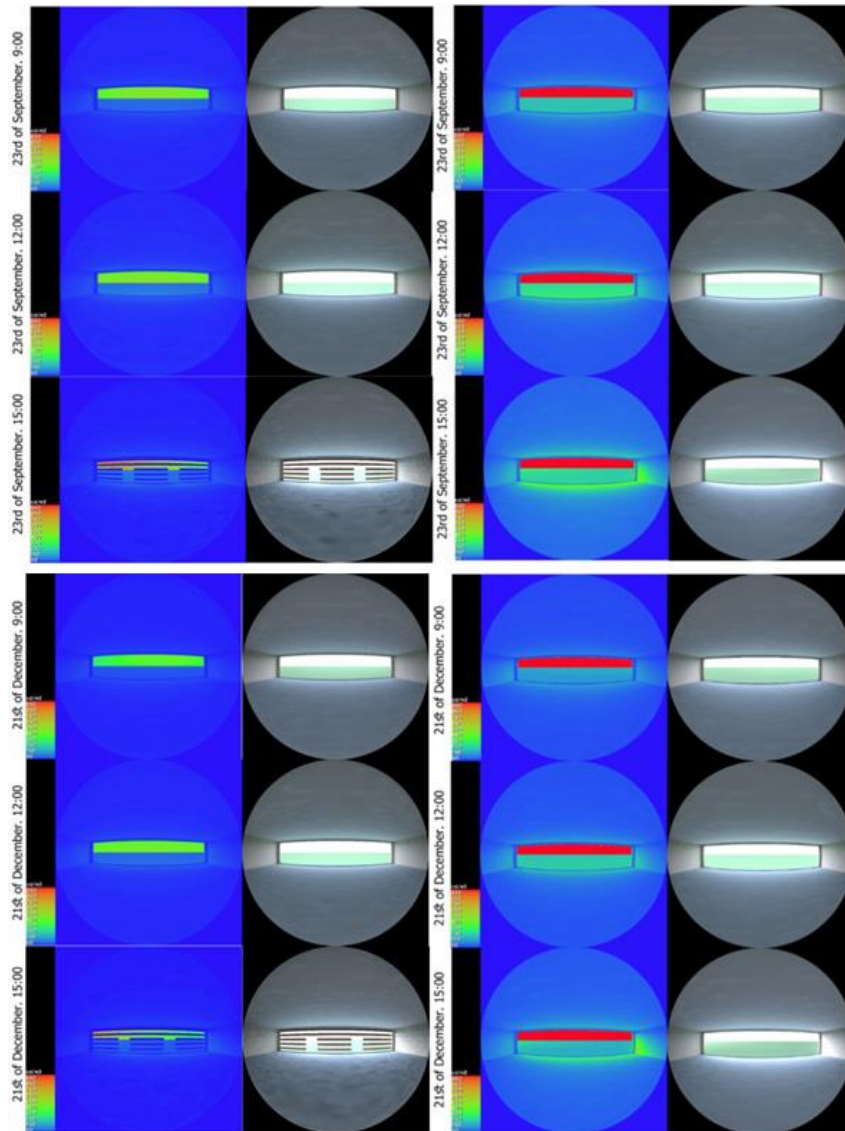


Figure 5.107. Waiting room luminance maps on the 23rd of September (top images) and 21st of December (bottom images). The images on the left show scenario 04 results and the images on the right show the basic model results (author 2019).

On 23rd of September, in the waiting room, average luminance levels from the glazed wall reached 300 cd/m² in first two cases and 450 cd/m² in third case which, comparing to the basic model results, indicated 68.4% and 52.6% luminance level reduction. On 21st of December, in the waiting room, average luminance levels from the glazed wall reached 350 cd/m² in the first case, 600 cd/m² in the first case and 550 cd/m² in the third case which, comparing to the basic model results, indicated 63.2%, 36.8% and 42.1% luminance level reduction (figure 5.107).

Table 5.114. DGI levels from different angles from nadir for the four days at 9:00,12:00 and 15:00 in waiting room (author 2019).

| Angle | 60 | 50 | 40 | 30 | 20 | 10 | 0 | -10 | -20 | -30 | -40 | -50 | -60 |
|-------------------------------------------|------|------|------|------|------|------|------|------|------|------|------|------|------|
| 09:00 21 st of March | 11.8 | 13.8 | 15.4 | 16.8 | 17.9 | 18.8 | 19.1 | 18.8 | 17.9 | 16.8 | 15.5 | 13.8 | 11.9 |
| 12:00 21 st of March | 11.7 | 13.7 | 15.3 | 16.7 | 17.7 | 18.6 | 18.8 | 18.6 | 17.7 | 16.7 | 15.3 | 13.7 | 11.7 |
| 15:00 21 st of March | 11.9 | 12.5 | 13.8 | 16.8 | 18.3 | 19.1 | 19.4 | 19.1 | 18.2 | 16.9 | 14.4 | 13.8 | 11.9 |
| 09:00 21 st of June | 11.8 | 13.8 | 15.4 | 16.8 | 17.9 | 18.7 | 18.9 | 18.7 | 17.9 | 16.8 | 15.4 | 13.8 | 11.8 |
| 12:00 21 st of June | 13.3 | 15.2 | 16.8 | 18.2 | 19.2 | 20.1 | 20.4 | 20.1 | 19.3 | 18.2 | 16.9 | 15.2 | 13.3 |
| 15:00 21 st of June | 11.4 | 12.5 | 13.9 | 15.3 | 18.5 | 19.3 | 19.5 | 19.3 | 18.5 | 17.4 | 15.4 | 13.4 | 11.8 |
| 09:00 23 rd of September | 11.9 | 13.8 | 15.5 | 16.9 | 17.9 | 18.9 | 19.1 | 18.8 | 17.8 | 16.9 | 15.5 | 13.4 | 11.9 |
| 12:00 23 rd of September | 11.9 | 13.8 | 15.5 | 16.9 | 17.9 | 18.8 | 19.1 | 18.8 | 17.9 | 16.9 | 15.5 | 13.9 | 11.9 |
| 15:00 23 rd of September | 11.7 | 13.8 | 15.3 | 16.7 | 17.7 | 18.6 | 18.8 | 18.6 | 17.7 | 16.7 | 15.3 | 13.7 | 11.7 |
| 09:00 21 st of December | 11.4 | 13.4 | 15.1 | 16.4 | 17.5 | 18.4 | 18.7 | 18.4 | 17.6 | 16.5 | 15.2 | 13.5 | 11.5 |
| 12:00 21 st of December | 11.6 | 13.5 | 15.2 | 16.5 | 17.6 | 18.4 | 18.7 | 18.4 | 17.6 | 16.5 | 15.2 | 13.5 | 11.6 |
| 15:00 21 st of December | 11.4 | 12.5 | 13.5 | 15.3 | 17.9 | 18.9 | 18.6 | 17.7 | 16.6 | 13.4 | 12.5 | 12.4 | 11.6 |

According to the DGI analysis there is a perceptible glare in all cases (table 5.114).

Table 5.115. GVCP levels from different angles from nadir for the four days at 9:00,12:00 and 15:00 in the waiting room (author 2019).

| Angle | 60 | 50 | 40 | 30 | 20 | 10 | 0 | -10 | -20 | -30 | -40 | -50 | -60 |
|-------------------------------------------|------|------|------|------|------|------|------|------|------|------|------|------|------|
| 09:00 21 st of March | 77.5 | 64.4 | 51.7 | 40.9 | 32.9 | 27.1 | 25.3 | 27.1 | 32.7 | 40.9 | 51.7 | 64.5 | 77.5 |
| 12:00 21 st of March | 77.2 | 64.2 | 51.6 | 40.9 | 32.8 | 27.2 | 25.4 | 27.2 | 32.9 | 41.1 | 51.7 | 64.4 | 77.4 |
| 15:00 21 st of March | 77.1 | 64.9 | 44.1 | 40.9 | 32.5 | 21.5 | 20.1 | 21.7 | 26.9 | 40.5 | 44.9 | 64.9 | 77.9 |
| 09:00 21 st of June | 77.1 | 64.3 | 51.6 | 40.9 | 32.7 | 27.1 | 25.3 | 27.1 | 32.9 | 40.9 | 51.7 | 64.4 | 77.4 |
| 12:00 21 st of June | 62.5 | 47.4 | 34.8 | 25.5 | 19.1 | 14.9 | 13.7 | 14.9 | 19.1 | 25.5 | 34.9 | 47.5 | 62.5 |
| 15:00 21 st of June | 77.4 | 64.9 | 51.2 | 40.1 | 24.8 | 19.9 | 18.5 | 20.1 | 24.9 | 32.2 | 51.4 | 64.2 | 77.6 |
| 09:00 23 rd of September | 77.2 | 64.1 | 51.3 | 40.6 | 32.4 | 26.7 | 25.0 | 26.8 | 32.4 | 20.6 | 21.3 | 64.1 | 77.2 |
| 12:00 23 rd of September | 77.2 | 64.2 | 51.5 | 40.9 | 32.8 | 27.2 | 25.4 | 27.2 | 32.8 | 40.9 | 51.6 | 64.3 | 77.3 |
| 15:00 23 rd of September | 77.6 | 64.3 | 51.5 | 32.4 | 32.2 | 20.4 | 18.9 | 20.6 | 32.6 | 33.1 | 51.5 | 64.4 | 77.9 |
| 09:00 21 st of December | 80.9 | 68.8 | 56.4 | 45.6 | 37.1 | 31.1 | 29.1 | 31.1 | 37.1 | 45.5 | 56.3 | 68.7 | 80.9 |
| 12:00 21 st of December | 78.8 | 66.2 | 53.7 | 42.9 | 34.8 | 28.9 | 27.1 | 28.9 | 34.8 | 43.2 | 53.9 | 66.4 | 79.1 |
| 15:00 21 st of December | 80.5 | 68.2 | 56.5 | 45.1 | 31.2 | 25.9 | 24.3 | 26.2 | 37.9 | 45.2 | 56.1 | 63.9 | 80.1 |

GVCP analysis showed that minimum percentage of satisfied occupants was 13.72% at 12:00 on 21st of June and maximum was 29.14% at 09:00 on 21st of December when looking at the middle of the glazed wall. The minimum percentage of satisfied occupants was 62.48% at 12:00 on 21st of June to and maximum was 80.96% at 9:00 on 21st of December when looking at the edges of the glazed wall (table 5.115).

Comparing to the basic model minimum DGI reduction was 13.3% and maximum DGI reduction was 24.6% while the minimum GVCP improvement was 186.6% and maximum GVCP improvement was 269.5%. Refer to final comparison table. Refer to table 5.116 for full details including comparison with the basic model and sixth scenario.

Table 5.116. Final comparison between Scenarios 06, 09 and basic model (author 2019).

| Date | Hour | Average DGI reduction comparing to the basic model results (scenario 09) | Average DGI reduction comparing to the basic model results (scenario 06) | Average GVCP increment comparing to the basic model results (scenario 09) | Average GVCP increment comparing to the basic model results (scenario 09) |
|---------------|-------|--------------------------------------------------------------------------|--------------------------------------------------------------------------|---------------------------------------------------------------------------|---------------------------------------------------------------------------|
| 21st of Mar. | 9:00 | 19.8% | 19.8% | 205.2% | 205.2% |
| 21st of Mar. | 12:00 | 18.5% | 18.5% | 179.4% | 179.4% |
| 21st of Mar. | 15:00 | 18.7% | 18.2% | 274.3% | 243.9% |
| 21st of Jun. | 9:00 | 19.4% | 19.4% | 173.2% | 173.2% |
| 21st of Jun. | 12:00 | 18.2% | 18.2% | 266.8% | 266.8% |
| 21st of Jun. | 15:00 | 19.5% | 17.1% | 296.5% | 253.8% |
| 23rd of Sept. | 9:00 | 21.6% | 21.6% | 208.2% | 208.2% |
| 23rd of Sept. | 12:00 | 19.4% | 19.4% | 244.2% | 244.2% |
| 23rd of Sept. | 15:00 | 13.3% | 13.1% | 292.1% | 234.9% |
| 21st of Dec. | 9:00 | 19.8% | 19.8% | 186.6% | 186.6% |
| 21st of Dec. | 12:00 | 24.6% | 24.6% | 195.6% | 195.6% |
| 21st of Dec. | 15:00 | 19.5% | 19.0% | 237.7% | 215.1% |

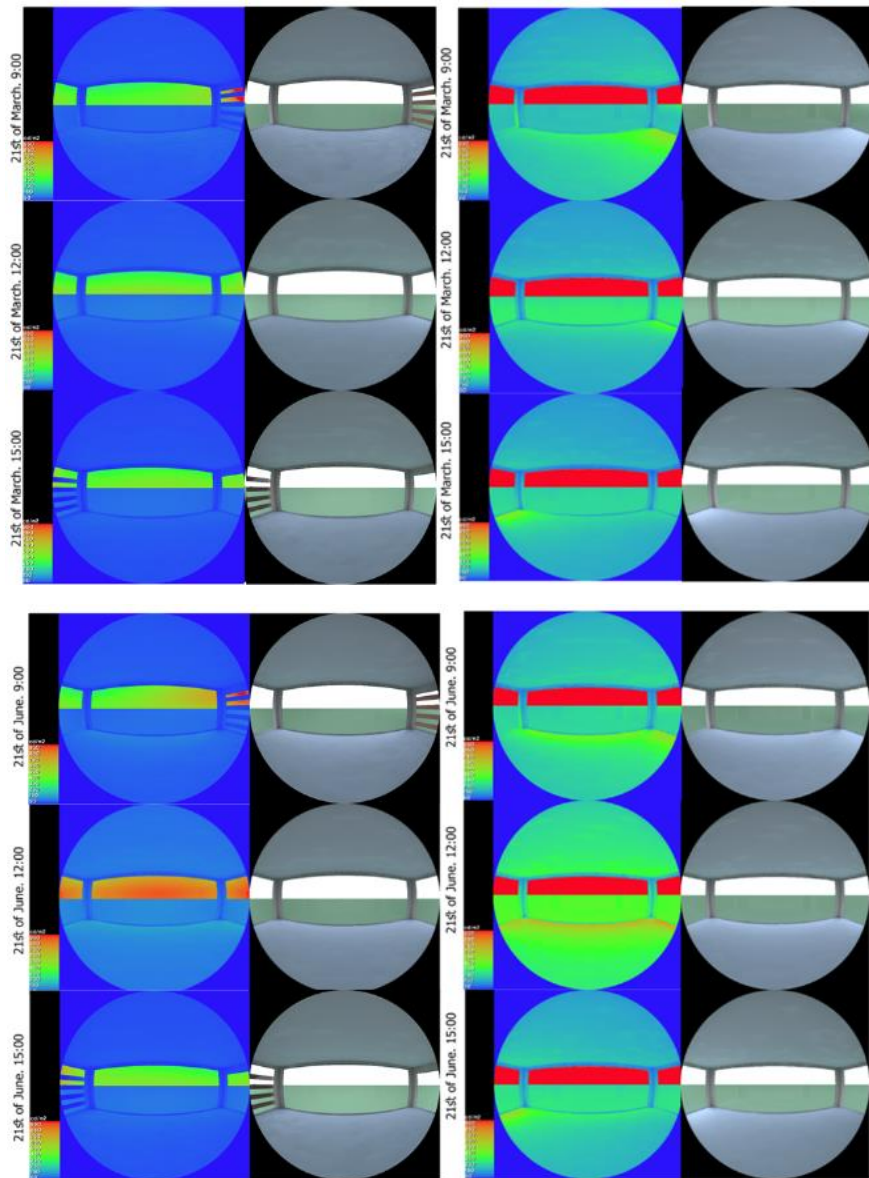


Figure 5.108. Reception room luminance maps on the 21st of March (top images) and 21st of June (bottom images). The images on the left show scenarios01,02 and 03 results and the images on the right show the basic model results (author 2019).

On 21st of March, in the reception room, luminance levels from the glazed wall reached 450 cd/m² in all cases which, comparing to the basic model results, indicated 42.1% luminance level reduction. On 21st of June, in the reception room, luminance levels from the glazed wall reached 500 cd/m² in the first case, 750 cd/m² in second case and 550 cd/m² in the third case which, comparing to the basic model results, indicated 47.4%,21.1% and 42.1% luminance level reduction (figure 5.108).

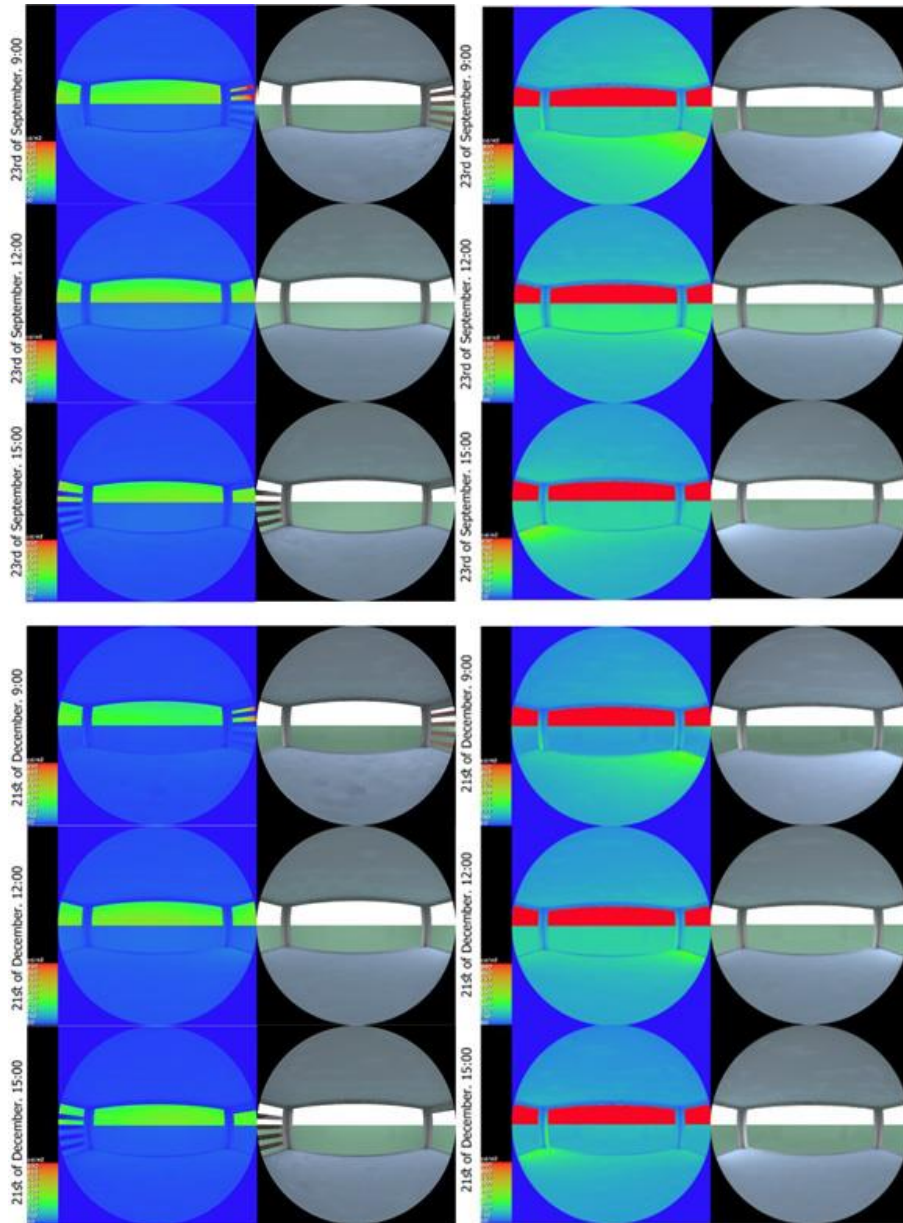


Figure 5.109. Reception room luminance maps on the 23rd of September (top images) and 21st of December (bottom images). The images on the left show scenarios01,02 and 03 results and the images on the right show the basic model results (author 2019).

On 23rd of September and 21st of December, in the reception room, luminance levels from the glazed wall reached 450 cd/m² in all cases which, comparing to the basic model results, indicated 42.1% luminance level reduction (figure 5.109).

Table 5.117. DGI levels from different angles from nadir for the four days at 9:00,12:00 and 15:00 (author 2019).

| Angle | 60 | 50 | 40 | 30 | 20 | 10 | 0 | -10 | -20 | -30 | -40 | -50 | -60 |
|-------------------------------------------|------|------|------|------|------|------|------|------|------|------|------|------|------|
| 09:00 21 st of March | 0.00 | 0.00 | 0.00 | 0.00 | 0.00 | 2.26 | 5.2 | 7.9 | 10.4 | 12.5 | 8.8 | 0.9 | 0.00 |
| 12:00 21 st of March | 8.7 | 8.3 | 8.0 | 8.1 | 0.00 | 8.8 | 9.1 | 8.7 | 8.4 | 8.5 | 8.8 | 9.6 | 10.5 |
| 15:00 21 st of March | 0.00 | 0.00 | 6.7 | 6.9 | 4.6 | 1.9 | 0.00 | 0.00 | 0.00 | 0.00 | 0.61 | 2.4 | 3.9 |
| 09:00 21 st of June | 0.00 | 0.00 | 0.00 | 0.93 | 0.00 | 6.7 | 8.8 | 10.8 | 12.6 | 10.4 | 8.7 | 3.9 | 0.00 |
| 12:00 21 st of June | 0.00 | 0.00 | 0.00 | 0.00 | 0.00 | 0.00 | 0.00 | 0.00 | 0.00 | 0.00 | 0.00 | 0.00 | 0.00 |
| 15:00 21 st of June | 0.00 | 0.00 | 6.9 | 8.7 | 6.5 | 3.9 | 1.2 | 0.00 | 0.00 | 0.00 | 0.00 | 0.00 | 0.00 |
| 09:00 23 rd of September | 0.00 | 0.00 | 0.00 | 0.00 | 0.00 | 1.7 | 4.7 | 7.4 | 9.8 | 11.9 | 10.8 | 6.7 | 0.00 |
| 12:00 23 rd of September | 9.1 | 8.6 | 8.4 | 8.5 | 0.00 | 9.4 | 9.7 | 9.3 | 8.9 | 8.8 | 9.0 | 9.5 | 10.4 |
| 15:00 23 rd of September | 0.00 | 0.00 | 7.4 | 7.6 | 5.3 | 2.7 | 0.00 | 0.00 | 0.00 | 0.00 | 0.00 | 0.75 | 2.33 |
| 09:00 21 st of December | 0.00 | 0.00 | 0.00 | 0.00 | 0.00 | 0.00 | 2.6 | 5.4 | 7.9 | 10.3 | 9.8 | 9.4 | 0.00 |
| 12:00 21 st of December | 7.3 | 7.6 | 8.2 | 8.8 | 9.5 | 0.00 | 10.0 | 9.4 | 8.8 | 8.4 | 8.3 | 8.7 | 9.5 |
| 15:00 21 st of December | 0.00 | 0.00 | 4.6 | 8.1 | 8.6 | 9.4 | 10.1 | 10.4 | 10.3 | 9.5 | 8.5 | 7.3 | 5.7 |

According to the DGI analysis there is an imperceptible glare in all cases, as it DGI level was lower than 18 in the centre of the glazed wall. In several cases DGI level was zero (table 5.117).

Table 5.118. GVCP levels from different angles from nadir for the four days at 9:00,12:00 and 15:00 (author 2019).

| Angle | 60 | 50 | 40 | 30 | 20 | 10 | 0 | -10 | -20 | -30 | -40 | -50 | -60 |
|-------------------------------------------|------|------|------|------|------|------|------|------|------|------|------|------|------|
| 09:00 21 st of March | 100 | 100 | 100 | 100 | 100 | 97.4 | 91.6 | 80.8 | 66.1 | 50.7 | 37.3 | 93.4 | 100. |
| 12:00 21 st of March | 91.2 | 91.7 | 91.9 | 91.9 | 91.8 | 92.9 | 93.4 | 93.6 | 92.4 | 91.4 | 90.1 | 88.1 | 85.9 |
| 15:00 21 st of March | 100 | 100 | 90.1 | 94.9 | 97.9 | 99.3 | 99.8 | 99.9 | 99.9 | 99.9 | 99.8 | 99.4 | 98.7 |
| 09:00 21 st of June | 100 | 99.9 | 99.9 | 99.6 | 98.7 | 92.2 | 84.3 | 73.8 | 62.1 | 51.4 | 90.1 | 97.9 | 100 |
| 12:00 21 st of June | 100 | 100 | 100 | 100 | 100 | 100 | 100 | 100 | 100 | 100 | 100 | 100 | 100 |
| 15:00 21 st of June | 100 | 100 | 92.2 | 80.2 | 89.7 | 95.8 | 98.8 | 99.8 | 100 | 100 | 100 | 100 | 100 |
| 09:00 23 rd of September | 100 | 100 | 100 | 100 | 100 | 98.1 | 84.1 | 70.6 | 55.7 | 73.8 | 55.7 | 100 | 100 |
| 12:00 23 rd of September | 90.1 | 90.5 | 90.7 | 90.6 | 90.3 | 91.6 | 92.1 | 92.4 | 91.1 | 90.5 | 89.5 | 97.9 | 86.1 |
| 15:00 23 rd of September | 100 | 100 | 90.5 | 93.6 | 97.2 | 99.1 | 99.8 | 99.9 | 100 | 99.9 | 99.9 | 99.7 | 99.3 |
| 09:00 21 st of December | 100 | 100 | 100 | 100 | 100 | 99.6 | 97.8 | 93.1 | 84.2 | 71.8 | 80.2 | 100 | 100 |
| 12:00 21 st of December | 93.9 | 93.1 | 91.8 | 90.4 | 88.9 | 87.8 | 92.1 | 91.4 | 91.8 | 91.8 | 91.9 | 91.6 | 89.2 |
| 15:00 21 st of December | 100 | 100 | 97.1 | 92.6 | 92.1 | 91.2 | 87.1 | 78.1 | 79.2 | 83.1 | 87.8 | 92.2 | 95.9 |

GVCP analysis showed that minimum percentage was 84.30% at 9:00 on 21st of June and maximum percentage was 100% at 12:00 on 21st of June when looking at the middle of the northern glazed wall. The minimum percentage of satisfied occupants was 91.08% at 15:00 on 21st of June and maximum was 100% at 12:00 on 21st of June when looking at the eastern and western glazed wall (table 5.118).

Comparing to the basic model minimum DGI reduction was 48.1% and maximum DGI reduction was 100% while the minimum GVCP improvement was 25.0% and maximum GVCP improvement was 230.0%. Refer to table 5.119 for full details including comparison with the basic model and sixth scenario

Table 5.119. Final comparison between Scenarios 06, 09 and basic model in the reception room (author 2019).

| Date | Hour | Average DGI reduction comparing to the basic model results (scenario 09) | Average DGI reduction comparing to the basic model results (scenario 06) | Average GVCP increment comparing to the basic model results (scenario 09) | Average GVCP increment comparing to the basic model results (scenario 06) |
|---------------------------|-------|--------------------------------------------------------------------------|--------------------------------------------------------------------------|---------------------------------------------------------------------------|---------------------------------------------------------------------------|
| 21 st of Mar. | 9:00 | 69.5% | 46.0% | 25.0% | 8.7% |
| 21 st of Mar. | 12:00 | 49.7% | 49.7% | 110.2% | 110.2% |
| 21 st of Mar. | 15:00 | 85.9% | 73.0% | 96.1% | 89.4% |
| 21 st of Jun. | 9:00 | 61.2% | 38.2% | 104.8% | 73.1% |
| 21 st of Jun. | 12:00 | 100% | 100% | 230.0% | 230.0% |
| 21 st of Jun. | 15:00 | 77.6% | 53.3% | 56.5% | 41.6% |
| 23 rd of Sept. | 9:00 | 68.0% | 49.5% | 37.2% | 16.6% |
| 23 rd of Sept. | 12:00 | 48.1% | 48.1% | 111.8% | 111.8% |
| 23 rd of Sept. | 15:00 | 85.7% | 70.3% | 96.8% | 89.6% |
| 21 st of Dec. | 9:00 | 73.5% | 58.8% | 45.2% | 28.8% |
| 21 st of Dec. | 12:00 | 61.0% | 61.0% | 156.3% | 156.3% |
| 21 st of Dec. | 15:00 | 58.4% | 49.5% | 166.8% | 161.9% |

5.6.6 Scenario 09 daylight harvesting potential analysis

Similar to the basic model simulation, the analysis was done using both RadianceIES and Apache applications. The daylight harvesting potential was measured by the annual electrical consumption saving which happened after using the sensors. Due to the reduction of the average illuminance levels, the daylight harvesting potential was reduced by 95.0% in scenario 09 (tables 5.120 and 5.121).

Table 5.120. Total annual electricity consumption Results summary (author 2019).

| | Total electricity (MWh) | Total electricity (MWh) |
|--------------|-------------------------|-------------------------|
| Date | Scenario 09 With DH.aps | Scenario 09.aps |
| Jan 01-31 | 1.8887 | 1.8888 |
| Feb 01-28 | 2.0381 | 2.0382 |
| Mar 01-31 | 2.5272 | 2.5273 |
| Apr 01-30 | 3.0734 | 3.0734 |
| May 01-31 | 3.6880 | 3.6990 |
| Jun 01-30 | 3.8099 | 3.8540 |
| Jul 01-31 | 4.1642 | 4.1643 |
| Aug 01-31 | 4.2350 | 4.2350 |
| Sep 01-30 | 3.8458 | 3.8459 |
| Oct 01-31 | 3.4784 | 3.4785 |
| Nov 01-30 | 2.8205 | 2.8205 |
| Dec 01-31 | 2.2700 | 2.2700 |
| Summed total | 37.8392 | 37.8950 |

Table 5.121. Final comparison (author 2019).

| Scenario | Total annual artificial lighting electrical consumption saving | Cost saving based on tariff of 30.5 Fils for every KW (ADDC 2018). | Reduction in daylight harvesting potential comparing to basic model potential |
|--------------|----------------------------------------------------------------|--------------------------------------------------------------------|-------------------------------------------------------------------------------|
| Basic-model | 1.1156 MWh | 340.3 UAE Dirhams | - |
| Scenario-01: | 0.769 MWh | 234.5 UAE Dirhams | 31.07% |
| Scenario-02: | 0.770 MWh | 234.9 UAE Dirhams | 30.98% |
| Scenario-03: | 0.773 MWh | 235.8 UAE Dirhams | 30.71% |
| Scenario-04 | 0.6215 MWh | 189.6 UAE Dirhams | 55.7% |
| Scenario-05: | 0.2397 MWh | 73.1 UAE Dirhams | 78.5% |
| Scenario-06: | 0.1439 MWh | 43.9 UAE Dirhams | 87.1% |
| Scenario 07 | 0.0140 MWh | 4.27 UAE Dirhams | 98.8% |
| Scenario 08 | 0.0135 MWh | 4.11 UAE Dirhams | 98.8% |
| Scenario 09 | 0.0558 MWh | 17.0 UAE Dirhams | 95.0% |

5.7 Buffer DSF/ Corridor Facade -Scenario 10 Analysis

5.7.1 Scenario 10 CFD simulation and analysis

Table 5.122. Air temperature within the DSF cavity from Microflo results (author 2019).

| Location | Date | Hour | Minimum DSF cavity air temperature (°C) | Maximum DSF cavity air temperature (°C) | Mean DSF cavity air temperature (°C) | Comparison between ambient temperature (47°C) and mean DSF cavity air temperature | Reduction in average air temperature comparing to scenarios 06. |
|---------------------|--------------------------|-------|-----------------------------------------|-----------------------------------------|--------------------------------------|-----------------------------------------------------------------------------------|-----------------------------------------------------------------|
| Eastern DSF cavity | 10 th of Aug. | 15:00 | 27.85 | 45.90 | 35.82 | -23.8% | 0.5% |
| Western DSF cavity | 10 th of Aug. | 12:00 | 27.87 | 45.86 | 35.74 | -24.0% | 0.4% |
| Northern DSF cavity | 10 th of Aug. | 15:00 | 28.03 | 46.19 | 35.89 | -23.6% | 0.0% |

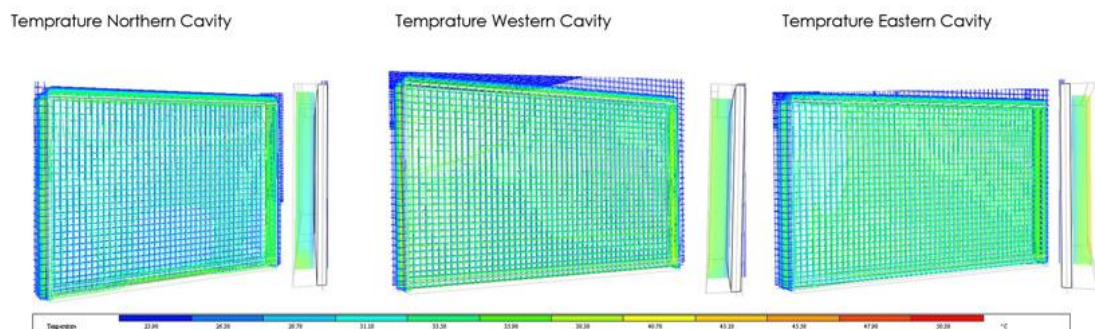


Figure 5.110. CFD analysis of Norther, Eastern and Western cushions in Microflo (author 2019).

The temperature analysis showed that when the ambient temperature reached 47.0 °C at the building level , the temperature in the DSF cavity near the cushion was maximum 45.90 °C in eastern DSF, maximum 45.86 °C in western DSF and maximum 46.19 °C in northern DSF. Thus, the temperature near the external DSF layer was slightly lower than ambient temperature in all cases. The temperature in the DSF cavity

near the DGU was minimum 27.85 °C in eastern DSF, minimum 27.87 °C in western DSF and minimum 28.03 °C in northern DSF. Due to the natural air flow, hot air was discharged and average reduction in mean cavity air temperature, comparing to ambient temperature, was 23.8% in eastern DSF, 24.0% in western DSF and 23.6% in northern DSF. Comparing to scenario 06, the average air temperature was reduced by 0.4~0.5% in eastern and western DSF cavities while it was the same in the northern DSF cavity (table 5.122 and figure 5.110).

Table 5.123. Air velocity within the DSF cavity from Microflo results (author 2019).

| Location | Date | Hour | Air velocity within the cavity near the bottom inlet (m/s) | Air velocity within the cavity near the top outlet (m/s) | Mean air velocity within the cavity (m/s) |
|---------------------|--------------------------|-------|------------------------------------------------------------|----------------------------------------------------------|-------------------------------------------|
| Eastern DSF cavity | 10 th of Aug. | 15:00 | 0.62 | 1.03 | 0.83 |
| Western DSF cavity | 10 th of Aug. | 12:00 | 0.72 | 0.92 | 0.82 |
| Northern DSF cavity | 10 th of Aug. | 15:00 | 0.21 | 0.62 | 0.41 |

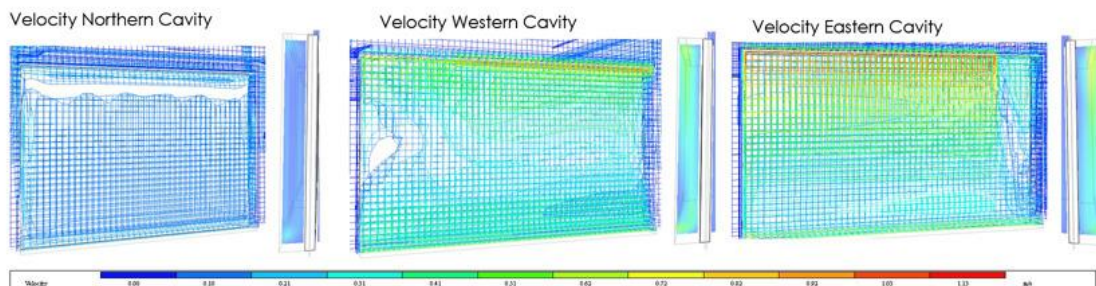


Figure 5.111. CFD analysis of the eastern cushions in IES VE (author 2019).

The analysis proved that air flow was from bottom to top which helped to discharge hot air from the DSF cavity. The maximum air velocity was near the top exhaust/outlet. Average air velocity in the eastern DSF was 0.83 while the maximum velocity was 1.03 m/s near the top and the inlet air velocity was 0.62 m/s. Average air velocity in the western DSFs was 0.82 m/s while the maximum velocity was 0.92 m/s near the top and the inlet air velocity was 0.72 m/s. Similar to previous scenarios the lowest air velocity and temperature was simulated in the northern DSF. The impact of the stack effect on the DSF was evaluated in the following sections where additional investigations on the internal conditions within the building were provided (table 5.123 and figure 5.111).

5.7.2 Scenario 10 electrical/energy consumption

Table 5.124. Total annual electricity/energy consumption for scenario 10 comparing to the basic model (author 2019).

| | Total Energy (MWh) | Total energy (MWh) |
|--------------|--------------------|--------------------|
| Date | Scenario 10.aps | Basic Model.aps |
| Jan 01-31 | 1.6963 | 2.1744 |
| Feb 01-28 | 1.9275 | 2.4339 |
| Mar 01-31 | 2.2960 | 3.0512 |
| Apr 01-30 | 2.9407 | 3.6774 |
| May 01-31 | 3.5392 | 4.4261 |
| Jun 01-30 | 3.5998 | 4.5822 |
| Jul 01-31 | 4.0199 | 4.9159 |
| Aug 01-31 | 4.0925 | 4.9626 |
| Sep 01-30 | 3.7177 | 4.4772 |
| Oct 01-31 | 3.2628 | 4.0166 |
| Nov 01-30 | 2.7233 | 3.2288 |
| Dec 01-31 | 2.1934 | 2.6027 |
| Summed total | 36.0094 | 44.5490 |

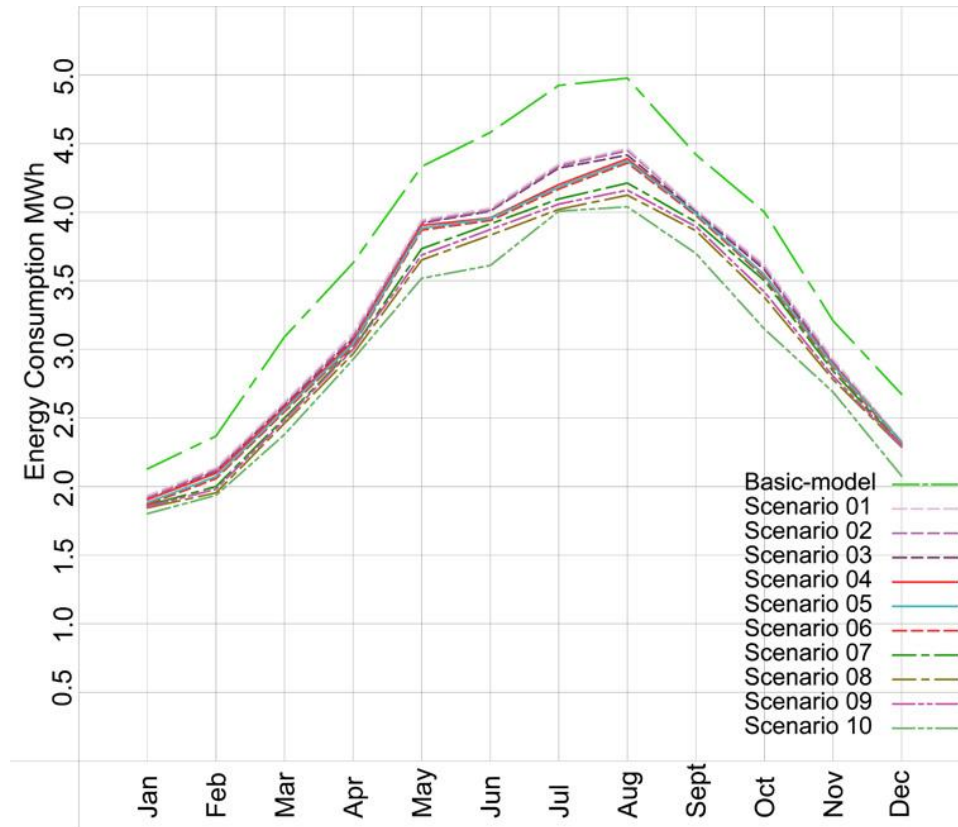


Figure 5.112. Combined diagram of all scenarios results (author 2019).

In scenario 10, as the ultimate efficient option that combined all effective strategies, the total electrical consumption reduction, with consideration of the inflation unit consumption, was 19.1% which was the best results comparing to all previous scenarios. The total PV electricity generation reached 1.7924 MWh like scenario 08. As mentioned in the previous section thin-film cadmium-telluride BIPVs, from scenario 08, and dynamic shades, from scenario 09, were added to scenario 06 to form the final most efficient case. Comparing to the sixth scenario, the energy saving was improved by 6.4% (from 12.7% to 19.1%) when both strategies were added to the system. Comparing to the eighth scenario, the energy saving was improved by 2.0% (from 17.1% to 19.1%). Comparing to the ninth scenario, the energy saving was improved by 4.2% (from 14.9% to 19.1%) (table 5.124 and figure 5.112). Refer to table 5.125 for complete comparison.

Table 5.125. Final comparison between all scenarios (author 2019).

| Scenario | Total annual electrical consumption saving comparing to the basic model (MWh) | Inflation unit annual electricity consumption (MWh) | Total annual electrical consumption saving considering inflation unit annual consumption (MWh) | Total annual electrical consumption saving considering inflation unit annual consumption (%) | Cost saving based on tariff of 30.5 Fils for every KW (ADDC 2018) |
|-------------|-------------------------------------------------------------------------------|-----------------------------------------------------|------------------------------------------------------------------------------------------------|----------------------------------------------------------------------------------------------|-------------------------------------------------------------------|
| Scenario-01 | 5.2033 | 0.03916 | 5.16414 | 11.594% | 1575.1 UAE Dirhams |
| Scenario-02 | 5.2064 | 0.03916 | 5.16724 | 11.600% | 1576.0 UAE Dirhams |
| Scenario-03 | 5.2084 | 0.03916 | 5.16924 | 11.603% | 1576.6 UAE Dirhams |
| Scenario-04 | 5.5863 | 0.03916 | 5.54714 | 12.45% | 1691.9 UAE Dirhams |
| Scenario-05 | 5.656 | 0.03916 | 5.61684 | 12.6% | 1713.1 UAE Dirhams |
| Scenario-06 | 5.6788 | 0.03916 | 5.63964 | 12.7% | 1720.1 UAE Dirhams |
| Scenario-07 | 6.5896 | 0.03916 | 6.55044 | 14.7% | 1997.9 UAE Dirhams |
| Scenario-08 | 7.6492 | 0.03916 | 7.61004 | 17.1% | 2333.0 UAE Dirhams |
| Scenario 09 | 6.654 | 0.03916 | 6.61484 | 14.9% | 2029.5 UAE Dirhams |
| Scenario 10 | 8.5396 | 0.03916 | 8.5 | 19.1% | 2592.6 UAE Dirhams |

5.7.3 Scenario 10 thermal comfort results

Table 5.126. Comfort index results comparison between scenario 10 and the basic model (author 2019).

| Var. Name | Location | Filename | Type | Mean |
|---------------|-----------------|-----------------|---------------|------|
| Comfort index | Mechanical room | Scenario 10.apr | Comfort index | 9 |
| Comfort index | Office 01 | Scenario 10.apr | Comfort index | 9 |
| Comfort index | Office 02 | Scenario 10.apr | Comfort index | 9 |
| Comfort index | Store 01 | Scenario 10.apr | Comfort index | 9 |
| Comfort index | Lobby 01 | Scenario 10.apr | Comfort index | 9 |
| Comfort index | Waiting room | Scenario 10.apr | Comfort index | 9 |
| Comfort index | Lobby 02 | Scenario 10.apr | Comfort index | 9 |
| Comfort index | Toilet | Scenario 10.apr | Comfort index | 9 |
| Comfort index | Store 02 | Scenario 10.apr | Comfort index | 9 |
| Comfort index | Reception | Scenario 10.apr | Comfort index | 9 |
| Comfort index | Mechanical room | Basic Model.apr | Comfort index | 9 |
| Comfort index | Office 01 | Basic Model.apr | Comfort index | 9 |
| Comfort index | Office 02 | Basic Model.apr | Comfort index | 9 |
| Comfort index | Store 01 | Basic Model.apr | Comfort index | 9 |
| Comfort index | Lobby 01 | Basic Model.apr | Comfort index | 9 |
| Comfort index | Waiting room | Basic Model.apr | Comfort index | 10 |
| Comfort index | Lobby 02 | Basic Model.apr | Comfort index | 9 |
| Comfort index | Toilet | Basic Model.apr | Comfort index | 9 |
| Comfort index | Store 02 | Basic Model.apr | Comfort index | 10 |
| Comfort index | Reception | Basic Model.apr | Comfort index | 10 |

In scenario 10, comparing to the basic model, Comfort index in store 02, waiting room and the reception changed from 10 (warm/acceptable) to 9 (slightly warm/acceptable) (table 5.126). These results are the same as scenario 01 and scenario 09 results. Thus, these three scenarios had the best results among all scenarios.

Table 5.127. Mean room temperature results comparison between scenario 10 and the basic model (author 2019).

| Var. Name | Location | Filename | Type | Mean |
|-----------------|-----------------|-----------------|------------------|-------|
| Air temperature | Mechanical room | Scenario 10.aps | Temperature (°C) | 24.82 |
| Air temperature | Office 01 | Scenario 10.aps | Temperature (°C) | 24.59 |
| Air temperature | Office 02 | Scenario 10.aps | Temperature (°C) | 24.57 |
| Air temperature | Store 01 | Scenario 10.aps | Temperature (°C) | 24.50 |
| Air temperature | Lobby 01 | Scenario 10.aps | Temperature (°C) | 24.58 |
| Air temperature | Waiting room | Scenario 10.aps | Temperature (°C) | 24.80 |
| Air temperature | Lobby 02 | Scenario 10.aps | Temperature (°C) | 24.74 |
| Air temperature | Toilet | Scenario 10.aps | Temperature (°C) | 24.59 |
| Air temperature | Store 02 | Scenario 10.aps | Temperature (°C) | 24.71 |
| Air temperature | Reception | Scenario 10.aps | Temperature (°C) | 24.90 |
| Air temperature | Mechanical room | Basic Model.aps | Temperature (°C) | 24.89 |
| Air temperature | Office 01 | Basic Model.aps | Temperature (°C) | 24.62 |
| Air temperature | Office 02 | Basic Model.aps | Temperature (°C) | 24.66 |
| Air temperature | Store 01 | Basic Model.aps | Temperature (°C) | 24.52 |
| Air temperature | Lobby 01 | Basic Model.aps | Temperature (°C) | 24.62 |
| Air temperature | Waiting room | Basic Model.aps | Temperature (°C) | 25.51 |
| Air temperature | Lobby 02 | Basic Model.aps | Temperature (°C) | 25.13 |
| Air temperature | Toilet | Basic Model.aps | Temperature (°C) | 24.94 |
| Air temperature | Store 02 | Basic Model.aps | Temperature (°C) | 25.16 |
| Air temperature | Reception | Basic Model.aps | Temperature (°C) | 26.15 |

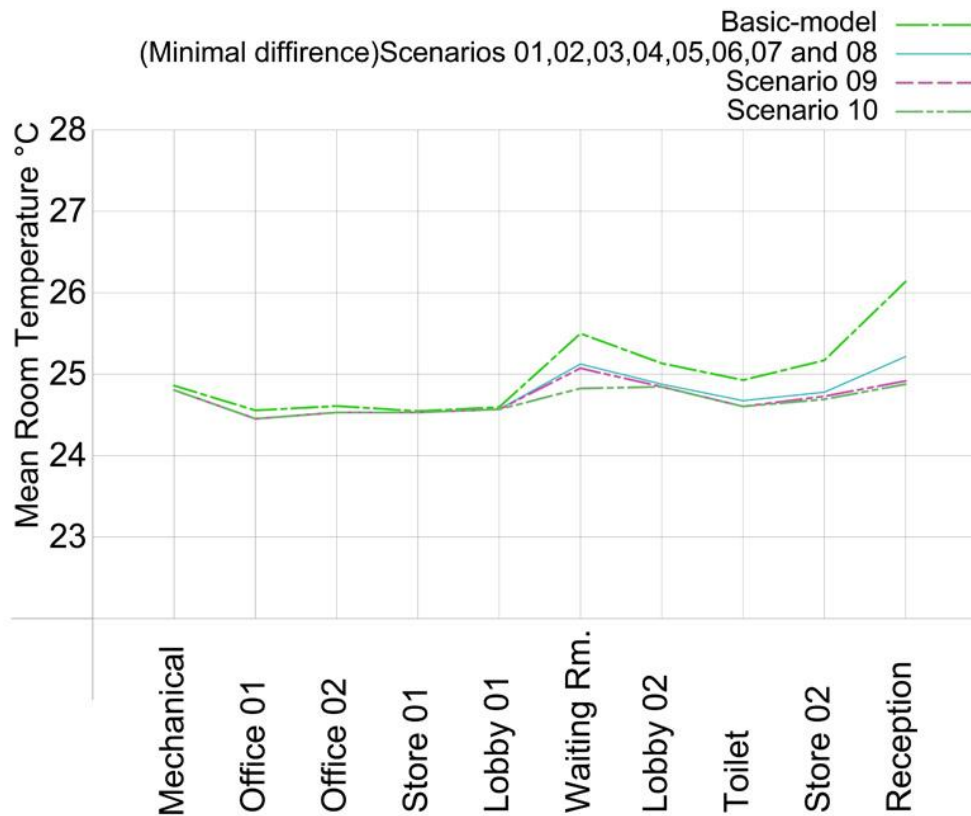


Figure 5.113. Combined diagram of the basic model results and all scenarios results (author 2019)

Comparing to the basic model, the overall improvement/reduction in the mean room temperature was 1.33%. The improvement/reduction in the mean waiting room temperature was 2.8%. The improvement/reduction in the mean reception room temperature was 4.8% (table 5.127 and figure 5.113). Thus, this scenario gave the maximum temperature reduction among other scenarios specially in the waiting room.

Table 5.128. People dissatisfied index results comparison between scenario 10 and the basic model (author 2019).

| Var. Name | Location | Filename | Type | Mean |
|---------------------|-----------------|-----------------|----------------|-------|
| People dissatisfied | Mechanical room | Scenario 10.aps | Percentage (%) | 29.31 |
| People dissatisfied | Office 01 | Scenario 10.aps | Percentage (%) | 26.28 |
| People dissatisfied | Office 02 | Scenario 10.aps | Percentage (%) | 25.83 |
| People dissatisfied | Store 01 | Scenario 10.aps | Percentage (%) | 26.07 |
| People dissatisfied | Lobby 01 | Scenario 10.aps | Percentage (%) | 27.33 |
| People dissatisfied | Waiting room | Scenario 10.aps | Percentage (%) | 31.94 |
| People dissatisfied | Lobby 02 | Scenario 10.aps | Percentage (%) | 29.57 |
| People dissatisfied | Toilet | Scenario 10.aps | Percentage (%) | 26.45 |
| People dissatisfied | Store 02 | Scenario 10.aps | Percentage (%) | 28.11 |
| People dissatisfied | Reception | Scenario 10.aps | Percentage (%) | 32.96 |
| People dissatisfied | Mechanical room | Basic Model.aps | Percentage (%) | 29.95 |
| People dissatisfied | Office 01 | Basic Model.aps | Percentage (%) | 26.55 |
| People dissatisfied | Office 02 | Basic Model.aps | Percentage (%) | 26.71 |
| People dissatisfied | Store 01 | Basic Model.aps | Percentage (%) | 26.24 |
| People dissatisfied | Lobby 01 | Basic Model.aps | Percentage (%) | 27.70 |
| People dissatisfied | Waiting room | Basic Model.aps | Percentage (%) | 37.07 |
| People dissatisfied | Lobby 02 | Basic Model.aps | Percentage (%) | 33.21 |
| People dissatisfied | Toilet | Basic Model.aps | Percentage (%) | 29.74 |
| People dissatisfied | Store 02 | Basic Model.aps | Percentage (%) | 32.37 |
| People dissatisfied | Reception | Basic Model.aps | Percentage (%) | 43.40 |

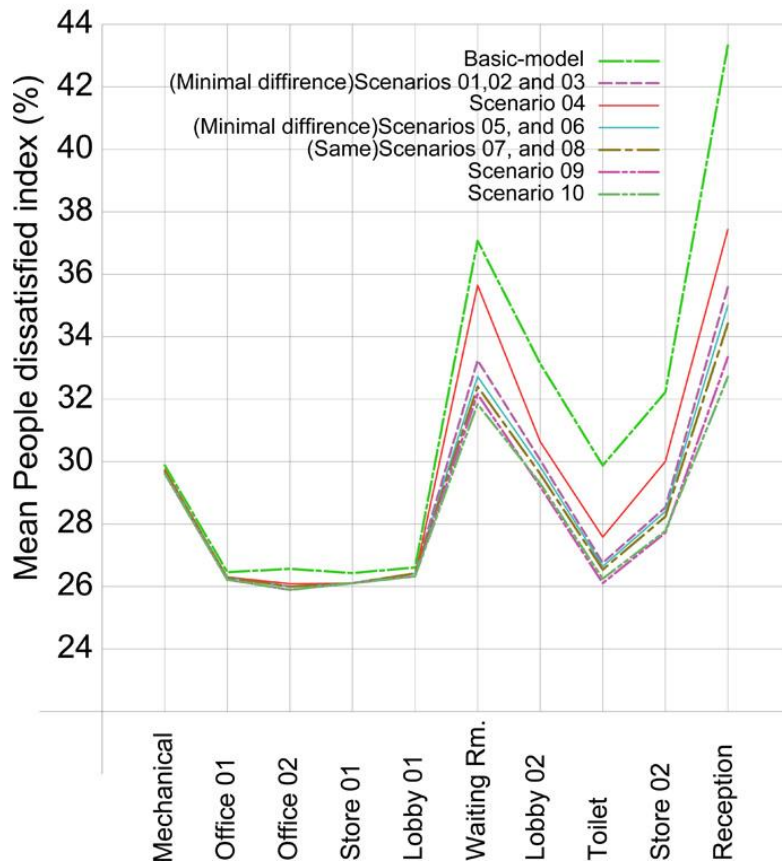


Figure 5.114. Combined diagram of the basic model results and all scenarios results (author 2019)

Comparing to the basic model, the mean values had an average improvement of 9.6%. In the waiting room, the mean values had an average improvement of 13.8%. In the reception room, the mean value had an average improvement of 24.1% (table 5.128 and figure 5.114). Hence, this scenario gave the best results. However, there were minimal variation between them and the ninth scenario results. So, the most effective strategy when it comes to thermal comfort was dynamic shade as it was the common strategy between the two scenarios.

5.7.4 Scenario 10 daylight analysis

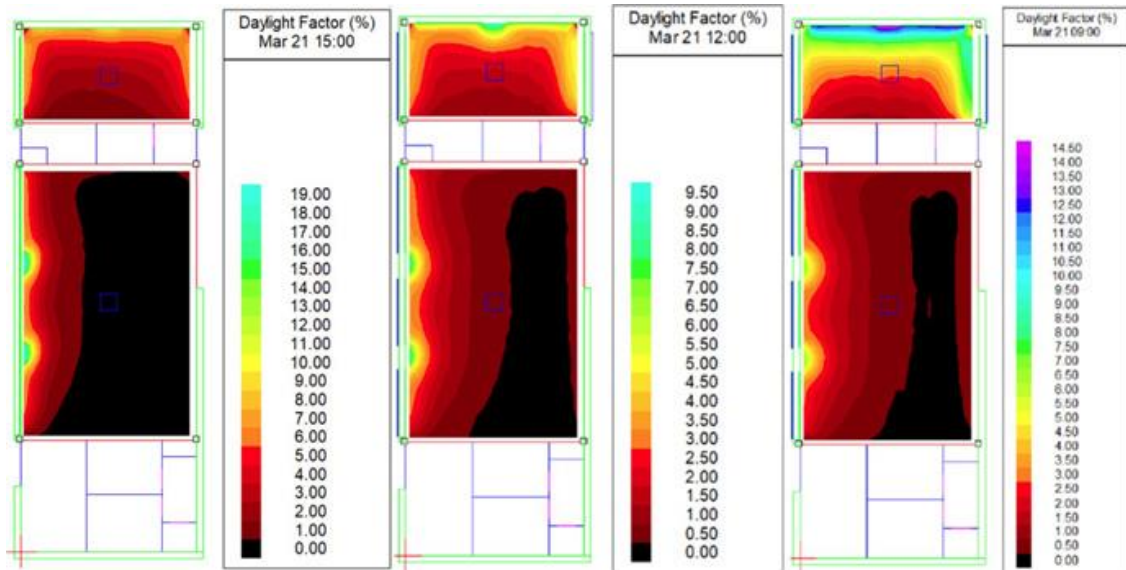


Figure 5.115. Scenario 10 daylight factor simulation results on the 21st of March (author 2019).

Table 5.129. Scenario 10 and 08 21st of March results summery (author 2019).

| Room | Date | Hour | Daylight factor | | | Daylight illuminance | | | Uniformity |
|----------------|---------------------------|-------|-----------------|------|-------|----------------------|------------|------------|------------|
| | | | Min. | Ave. | Max. | Min. | Ave. | Max. | |
| Waiting room | 21 st of March | 9:00 | 0.3% | 1.1% | 7.0% | 26.93 lux | 85.62 lux | 526.78 lux | 0.24 |
| Reception room | 21 st of March | 9:00 | 0.4% | 3.2% | 14.8% | 30.45 lux | 250.48 lux | 920.00 lux | 0.25 |
| Waiting room | 21 st of March | 12:00 | 0.2% | 1.1% | 8.6% | 20.80 lux | 97.96 lux | 758.66 lux | 0.21 |
| Reception room | 21 st of March | 12:00 | 0.9% | 2.9% | 9.9% | 80.46 lux | 256.62 lux | 870.88 lux | 0.31 |
| Waiting room | 21 st of March | 15:00 | 0.2% | 1.5% | 19.7% | 15.35 lux | 128.2 lux | 1640.2 lux | 0.12 |
| Reception room | 21 st of March | 15:00 | 0.4% | 2.5% | 9.4% | 33.56 lux | 189.25 lux | 722.85 lux | 0.30 |

In all cases, average daylighting levels in the waiting room were lower than required while in the reception room, average daylighting levels were within acceptable range at 9:00 on 21st of March. In the rest of the cases, it was lower than required. In all cases daylighting levels and DF were low in 75% to 95% of the waiting room area. Also, Average DF was lower than 2% in all the waiting room cases. Average DF was higher than 2% in all the reception room cases (figures 5.115,5.119,5.120,5.121,5.122 and table 5.129).

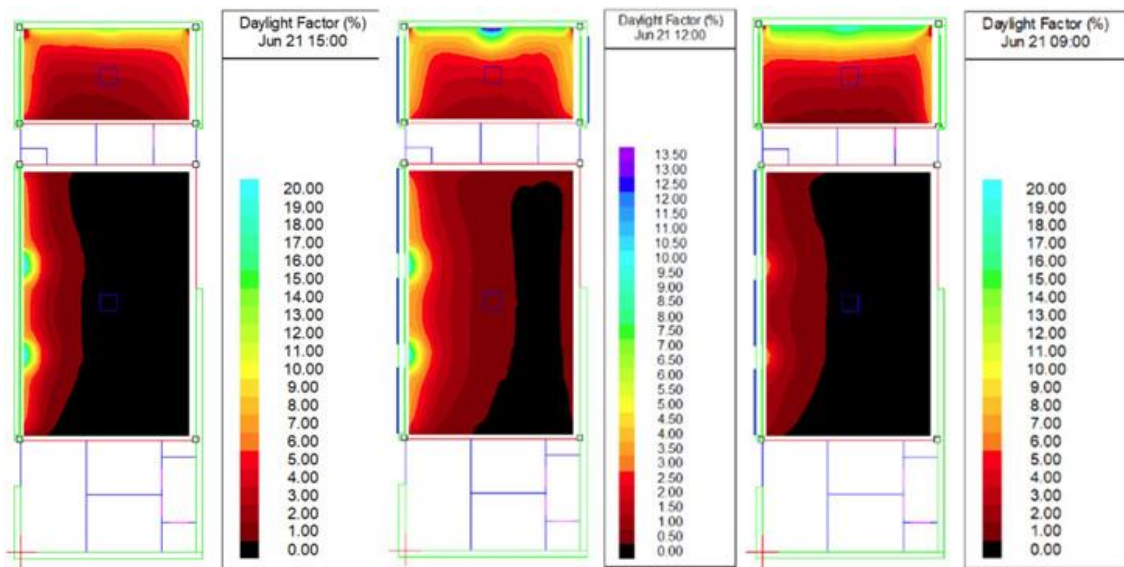


Figure 5.116. Scenario 10 daylight factor simulation results on the 21st of June (author 2019).

Table 5.130. Scenario 10 21st of June results summery (author 2019).

| Room | Date | Hour | Daylight factor | | | Daylight illuminance | | | Uniformity |
|----------------|--------------------------|-------|-----------------|------|-------|----------------------|------------|-------------|------------|
| | | | Min. | Ave. | Max. | Min. | Ave. | Max. | |
| Waiting room | 21 st of June | 9:00 | 0.3% | 1.0% | 6.9% | 22.84 lux | 85.83 lux | 566.04 lux | 0.27 |
| Reception room | 21 st of June | 9:00 | 0.4% | 4.0% | 20.0% | 30.22 lux | 310.50 lux | 1450.44 lux | 0.18 |
| Waiting room | 21 st of June | 12:00 | 0.3% | 1.2% | 9.7% | 47.11 lux | 222.40 lux | 1810.19 lux | 0.21 |
| Reception room | 21 st of June | 12:00 | 0.7% | 3.2% | 13.9% | 127.54 lux | 600.99 lux | 2586.48 lux | 0.21 |
| Waiting room | 21 st of June | 15:00 | 0.2% | 1.6% | 20.0% | 17.69 lux | 134.07 lux | 1781.08 lux | 0.13 |
| Reception room | 21 st of June | 15:00 | 0.4% | 2.8% | 12.5% | 33.75 lux | 201.70 lux | 1008.14 lux | 0.19 |

In all cases, average daylighting levels in the waiting room were lower than required while in the reception room, average daylighting levels were higher than required at 12:00 and within acceptable range at 9:00 and 15:00 on the 21st of June. In all cases daylighting levels and DF were low in 75% to 95% of the waiting room area. Also, Average DF was lower than 2% in all the waiting room cases. Average DF was higher than 2% in all the reception room cases (figures 5.116,5.119,5.120,5.121,5.122 and table 5.130).

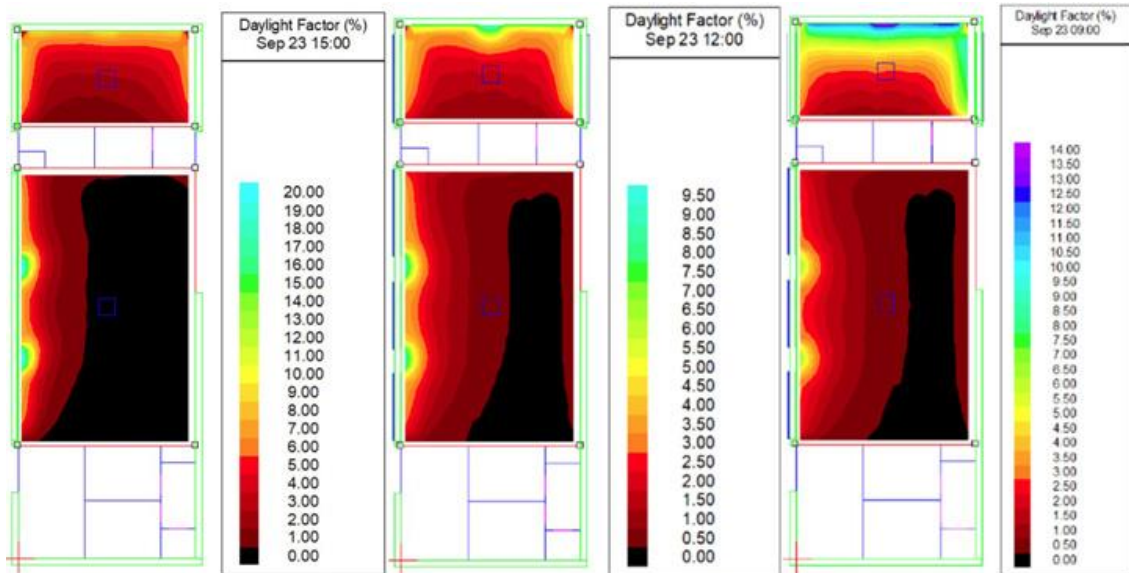


Figure 5.117. Scenario 10 daylight factor simulation results on the 23rd of September (author 2019).

Table 5.131. Scenario 10 23rd of September results summery (author 2019).

| Room | Date | Hour | Daylight factor | | | Daylight illuminance | | | Uniformity |
|----------------|---------------------------|-------|-----------------|------|-------|----------------------|------------|-------------|------------|
| | | | Min. | Ave. | Max. | Min. | Ave. | Max. | |
| Waiting room | 23 rd of Sept. | 9:00 | 0.3% | 1.1% | 6.8% | 21.22 lux | 86.19 lux | 536.41 lux | 0.25 |
| Reception room | 23 rd of Sept. | 9:00 | 1.1% | 4.2% | 14.0% | 76.10 lux | 322.85 lux | 1052.40 lux | 0.26 |
| Waiting room | 23 rd of Sept. | 12:00 | 0.2% | 1.2% | 9.3% | 21.25 lux | 104.62 lux | 825.98 lux | 0.20 |
| Reception room | 23 rd of Sept. | 12:00 | 1.0% | 2.9% | 9.8% | 84.81 lux | 257.09 lux | 867.12 lux | 0.33 |
| Waiting room | 23 rd of Sept. | 15:00 | 0.2% | 1.7% | 20.7% | 17.17 lux | 138.98 lux | 1500.47 lux | 0.12 |
| Reception room | 23 rd of Sept. | 15:00 | 1.1% | 3.2% | 9.9% | 29.20 lux | 201.22 lux | 775.92 lux | 0.29 |

In all cases, average daylighting levels in both rooms were lower than required. In all cases daylighting levels and DF were low in 75% to 95% of the waiting room area. Also, Average DF was lower than 2% in all the waiting room cases. Average DF was higher than 2% in all the reception room cases (figures 5.117,5.119,5.120,5.121,5.122 and table 5.131).

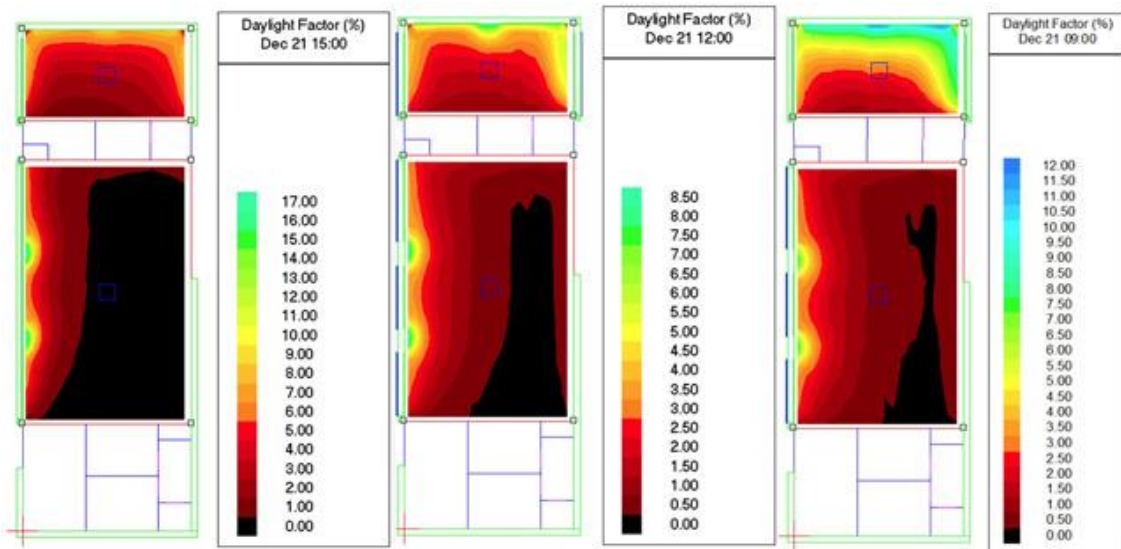


Figure 5.118. Scenario 10 daylight factor simulation results on the 21st of December (author 2019).

Table 5.132. Scenario 10 and 08 21st of December results summery (author 2019).

| Room | Date | Hour | Daylight factor | | | Daylight illuminance | | | Uniformity |
|----------------|--------------------------|-------|-----------------|------|-------|----------------------|------------|-------------|------------|
| | | | Min. | Ave. | Max. | Min. | Ave. | Max. | |
| Waiting room | 21 st of Dec. | 9:00 | 0.3% | 1.3% | 7.7% | 19.9 lux | 80.16 lux | 480.74 lux | 0.25 |
| Reception room | 21 st of Dec. | 9:00 | 0.4% | 3.5% | 12.0% | 31.56 lux | 210.33 lux | 690.66 lux | 0.27 |
| Waiting room | 21 st of Dec. | 12:00 | 0.3% | 1.2% | 8.7% | 21.25 lux | 100.93 lux | 711.75 lux | 0.21 |
| Reception room | 21 st of Dec | 12:00 | 1.1% | 3.1% | 8.8% | 90.33 lux | 249.59 lux | 715.62 lux | 0.36 |
| Waiting room | 21 st of Dec. | 15:00 | 0.2% | 1.5% | 17.7% | 13.51 lux | 101.84 lux | 1044.17 lux | 0.12 |
| Reception room | 21 st of Dec | 15:00 | 0.5% | 2.6% | 8.7% | 34.36 lux | 175.81 lux | 630.2 lux | 0.32 |

In all cases, average daylighting levels in both rooms were lower than required. In all cases daylighting levels and DF were low in 75% to 95% of the waiting room area. Also, Average DF was lower than 2% in all the waiting room cases. Average DF was higher than 2% in all the reception room cases (figures 5.118,5.119,5.120,5.121,5.122 and table 5.132).

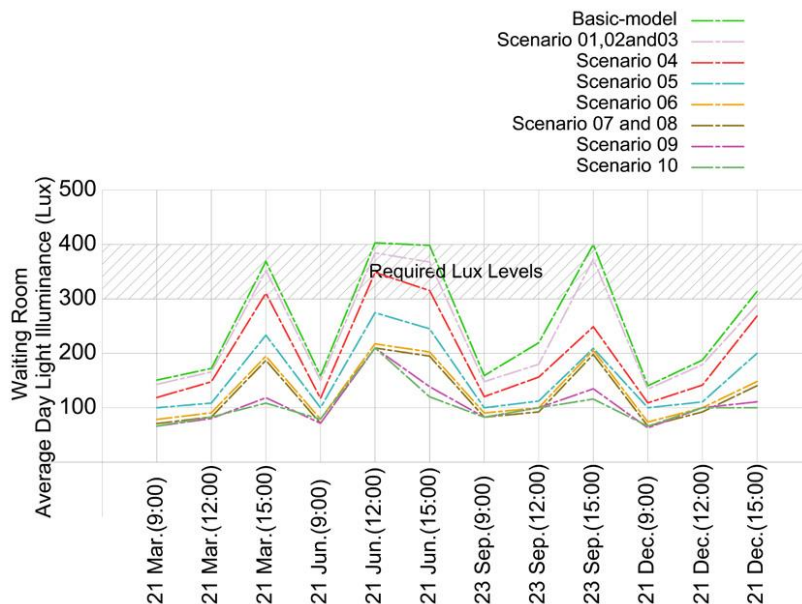


Figure 5.119. Combined diagram of the basic model DI results and all scenarios DI results in the waiting room (author 2019)

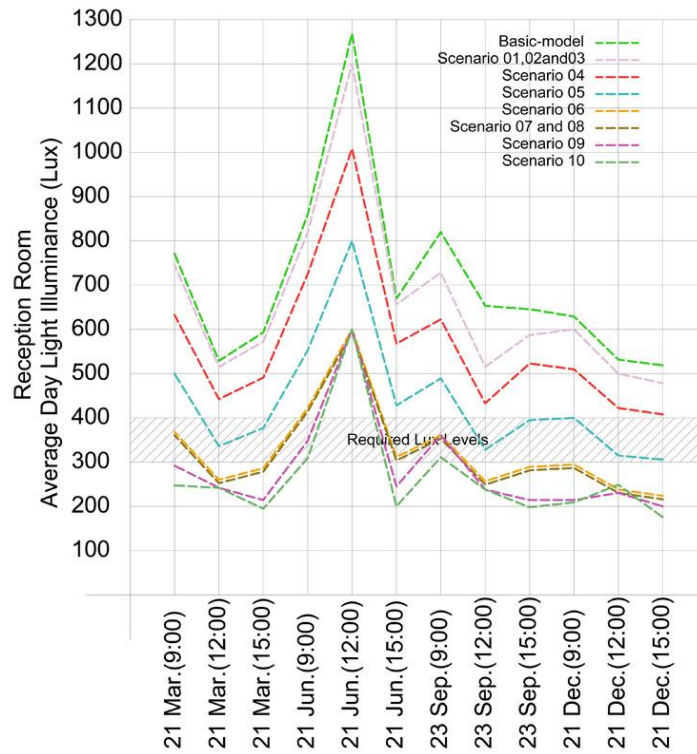


Figure 5.120. Combined diagram of the basic model DI results and all scenarios DI results in reception room (author 2019)

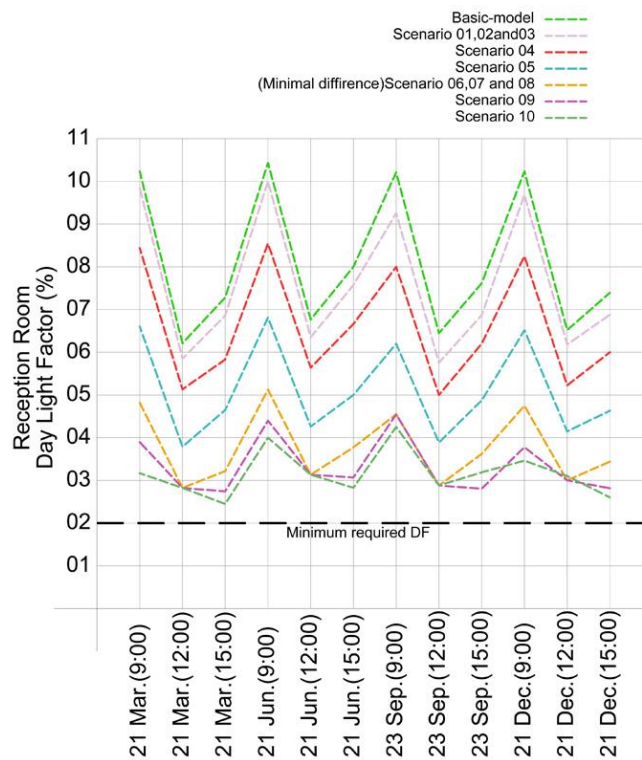


Figure 5.121. Combined diagram of the basic model DF results and all scenarios DF results in reception room (author 2019)

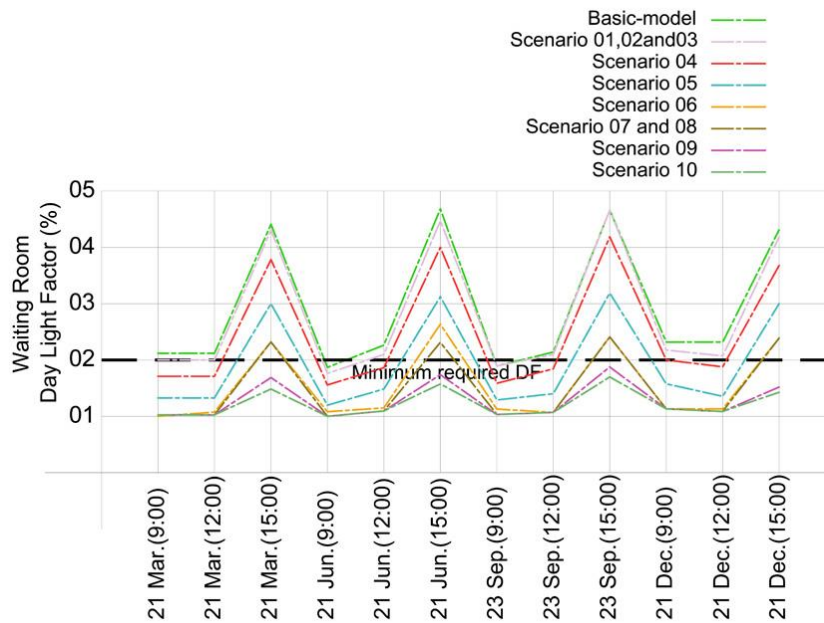


Figure 5.122. Combined diagram of the basic model DF results and all scenarios DF results in the waiting room (author 2019).

Comparing to the basic-model, the changes in scenario 10 reduced daylighting lux levels by minimum 45.5% and maximum 63.7%. Furthermore, the change reduced average DF by minimum 42.1% and maximum 67.1%. Uniformity changes varied from 42.8% to -46.2%. Refer to the final comparison table. Due to changes in VLT transmittance, scenarios 06 results were better as shown in the previous diagrams. Comparing to them, the additional dynamic shades and BIPVs reduced the daylighting levels by an average of 9.6% in the reception room and 15.2% in the waiting room. Also, the average DF reduction was 12.30% in the reception room and 13.4% in the waiting room (figures 5.119,5.120,5.121,5.122 and table 5.134).

Table 5.134. Final comparison between Scenario 10 and basic model (author 2019).

| Scenario | Date | Hour | Average daylight factor reduction | Average daylight illuminance reduction | Uniformity increment |
|-------------|---------------------------|-------|--------------------------------------------|--------------------------------------------|---------------------------------------------|
| Scenario 10 | 21 st of Mar. | 9:00 | Waiting room 47.6% Reception room 68.9% | Waiting room 45.g% Reception room 67.9% | Waiting room 9.1% Reception room -3.8% |
| Scenario 10 | 21 st of Mar. | 12:00 | Waiting room 47.6% Reception room 53.2% | Waiting room 45.9% Reception room 52.9% | Waiting room 16.6% Reception room 3.3% |
| Scenario 10 | 21 st of Mar. | 15:00 | Waiting room 65.5% Reception room 65.3% | Waiting room 46.8% Reception room 52.9% | Waiting room -7.6% Reception room 0.00% |
| Scenario 10 | 21 st of Jun. | 9:00 | Waiting room 47.4% Reception room 61.9% | Waiting room 65.4% Reception room 64.2% | Waiting room 28.6% Reception room -5.2% |
| Scenario 10 | 21 st of Jun. | 12:00 | Waiting room 45.5% Reception room 52.9% | Waiting room 45.6% Reception room 52.3% | Waiting room 16.7% Reception room -4.5% |
| Scenario 10 | 21 st of Jun. | 15:00 | Waiting room 65.9% Reception room 65.0% | Waiting room 66.3% Reception room 70.7% | Waiting room -7.1% Reception room -9.5% |
| Scenario 10 | 23 rd of Sept. | 9:00 | Waiting room 42.1% Reception room 58.8% | Waiting room 45.5% Reception room 60.7% | Waiting room 13.6% Reception room 13.0% |
| Scenario 10 | 23 rd of Sept. | 12:00 | Waiting room 42.9% Reception room 54.7% | Waiting room 52.7% Reception room 60.8% | Waiting room 11.1% Reception room 26.9% |
| Scenario 10 | 23 rd of Sept. | 15:00 | Waiting room 63.8% Reception room 57.9% | Waiting room 64.9% Reception room 68.9% | Waiting room -7.7% Reception room 7.5% |
| Scenario 10 | 21 st of Dec. | 9:00 | Waiting room 43.5% Reception room 65.7% | Waiting room 45.5% Reception room 66.7% | Waiting room 13.6% Reception room -12.9% |
| Scenario 10 | 21 st of Dec. | 12:00 | Waiting room 47.8% Reception room 52.3% | Waiting room 45.5% Reception room 52.7% | Waiting room 16.7% Reception room 12.5% |
| Scenario 10 | 21 st of Dec. | 15:00 | Waiting room 65.9% Reception room 64.4% | Waiting room 67.1% Reception room 65.6% | Waiting room 0.00% Reception room 0.00% |

5.7.5 Scenario 10 glare analysis

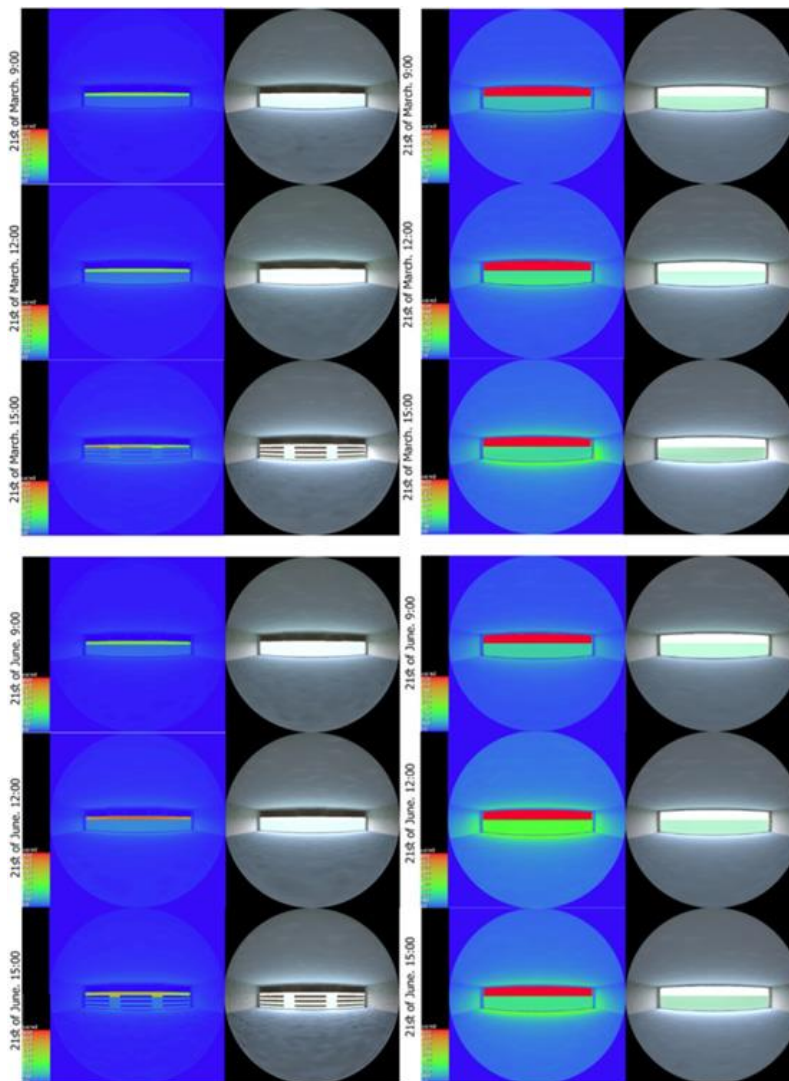


Figure 5.123. Waiting room luminance maps on the 21st of March (top images) and 21st of June (bottom images). The images on the left show scenario 04 results and the images on the right show the basic model results (author 2019).

On 21st of March, in the waiting room, average luminance levels from the glazed wall reached 300 cd/m² in first two cases and 450 cd/m² in third case which, comparing to the basic model results, indicated 68.4% and 52.6% luminance level reduction. On 21st of June, in the waiting room, average luminance levels from the glazed wall reached 600 cd/m² in first case and 850 cd/m² in second and third case which, comparing to the basic model results, indicated 36.8% and 10.5% luminance level reduction (figure 5.123).

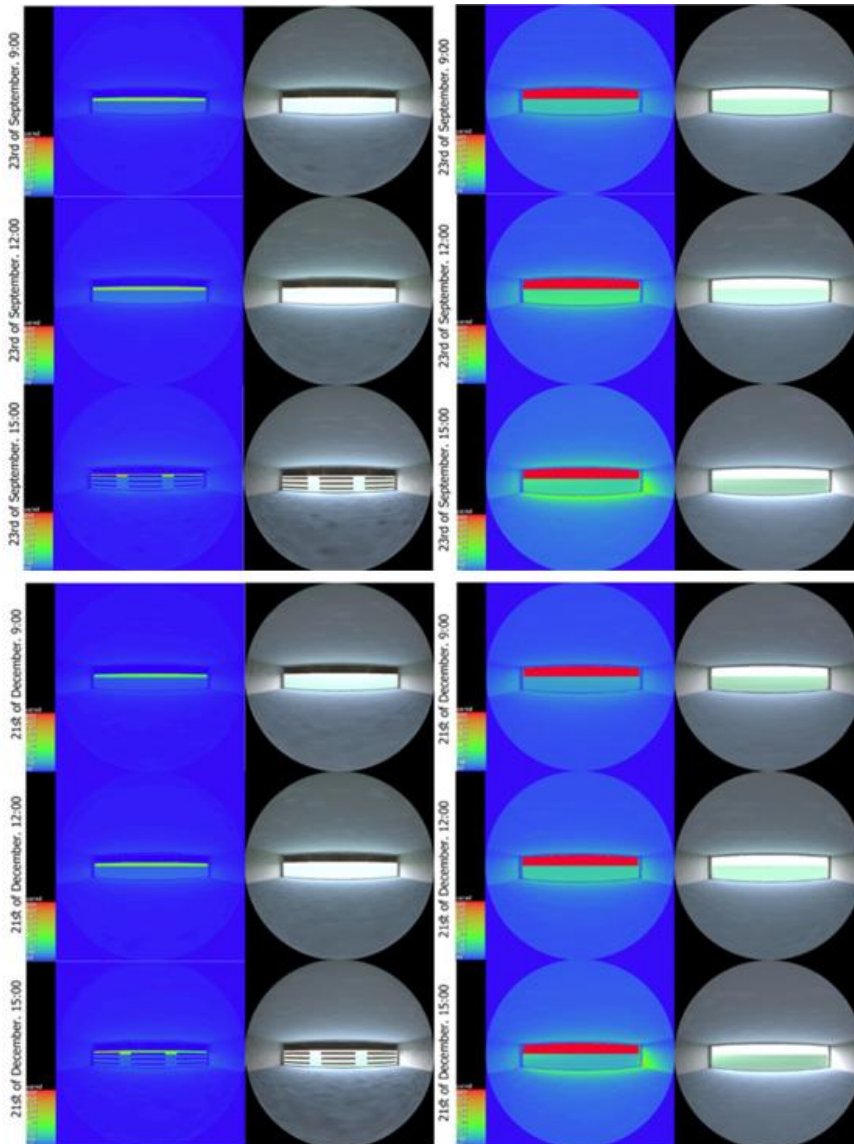


Figure 5.124. Waiting room luminance maps on the 23rd of September (top images) and 21st of December (bottom images). The images on the left show scenario 04 results and the images on the right show the basic model results (author 2019).

On 23rd of September, in the waiting room, average luminance levels from the glazed wall reached 300 cd/m² in first two cases and 450 cd/m² in third case which, comparing to the basic model results, indicated 68.4% and 52.6% luminance level reduction. On 21st of December, in the waiting room, average luminance levels from the glazed wall reached 350 cd/m² in the first case, 600 cd/m² in the first case and 550 cd/m² in the third case which, comparing to the basic model results, indicated 63.2%, 36.8% and 42.1% luminance level reduction (figure 5.124).

Table 5.135. DGI levels from different angles from nadir for the four days at 9:00,12:00 and 15:00 (author 2019).

| Angle | 60 | 50 | 40 | 30 | 20 | 10 | 0 | -10 | -20 | -30 | -40 | -50 | -60 |
|-------------------------------------------|------|------|------|------|------|------|------|------|------|------|------|------|------|
| 09:00 21 st of March | 10.4 | 12.3 | 13.9 | 15.3 | 16.3 | 17.2 | 17.5 | 17.2 | 16.4 | 15.2 | 13.9 | 12.3 | 10.4 |
| 12:00 21 st of March | 10.5 | 12.4 | 13.9 | 15.2 | 16.3 | 17.1 | 17.5 | 17.1 | 16.3 | 15.2 | 13.9 | 12.3 | 10.4 |
| 15:00 21 st of March | 10.4 | 11.4 | 11.8 | 15.3 | 16.7 | 19.1 | 18.4 | 18.1 | 18.2 | 14.9 | 14.4 | 11.8 | 11.9 |
| 09:00 21 st of June | 10.4 | 11.4 | 11.8 | 15.3 | 16.7 | 19.1 | 18.4 | 18.1 | 18.2 | 14.9 | 14.4 | 11.8 | 11.9 |
| 12:00 21 st of June | 10.4 | 12.4 | 13.9 | 15.3 | 16.4 | 17.2 | 17.6 | 17.2 | 16.4 | 15.3 | 13.9 | 12.3 | 10.4 |
| 15:00 21 st of June | 11.9 | 13.7 | 15.4 | 16.7 | 17.7 | 18.6 | 18.9 | 18.6 | 17.7 | 16.7 | 15.4 | 13.8 | 11.9 |
| 09:00 23 rd of September | 10.4 | 12.4 | 14.0 | 15.2 | 16.3 | 17.2 | 17.5 | 17.1 | 16.3 | 15.2 | 13.9 | 12.3 | 10.4 |
| 12:00 23 rd of September | 9.9 | 11.8 | 13.4 | 14.9 | 15.9 | 16.7 | 17.1 | 16.7 | 15.9 | 14.8 | 13.5 | 11.9 | 9.9 |
| 15:00 23 rd of September | 10.8 | 11.8 | 15.5 | 15.3 | 15.5 | 18.2 | 18.5 | 19.2 | 18.4 | 17.3 | 11.9 | 11.8 | 11.4 |
| 09:00 21 st of December | 9.9 | 11.9 | 13.5 | 14.9 | 15.9 | 16.7 | 17.2 | 16.8 | 15.9 | 14.9 | 13.5 | 11.8 | 9.9 |
| 12:00 21 st of December | 10.2 | 12.1 | 13.7 | 15.1 | 16.1 | 16.9 | 17.3 | 16.9 | 16.1 | 15.1 | 13.7 | 12.1 | 10.2 |
| 15:00 21 st of December | 10.4 | 10.5 | 10.5 | 12.3 | 12.9 | 16.7 | 16.9 | 16.6 | 16.7 | 16.6 | 12.6 | 12.5 | 11.6 |

According to the DGI analysis there is a perceptible glare in only four cases and imperceptible glare in the rest of the cases (table 5.135).

Table 5.136. GVCP levels from different angles from nadir for the four days at 9:00,12:00 and 15:00 (author 2019).

| Angle | 60 | 50 | 40 | 30 | 20 | 10 | 0 | -10 | -20 | -30 | -40 | -50 | -60 |
|-------------------------------------------|------|------|------|------|------|------|------|------|------|------|------|------|------|
| 09:00 21 st of March | 86.7 | 77.1 | 66.5 | 56.5 | 48.2 | 41.9 | 38.9 | 41.9 | 48.3 | 56.6 | 66.6 | 77.2 | 86.7 |
| 12:00 21 st of March | 85.9 | 76.1 | 65.5 | 55.5 | 47.2 | 40.9 | 38.1 | 41.1 | 47.3 | 55.6 | 65.6 | 76.2 | 86.1 |
| 15:00 21 st of March | 76.7 | 76.2 | 56.6 | 40.9 | 38.9 | 38.5 | 26.5 | 21.7 | 26.9 | 40.5 | 47.7 | 76.1 | 86.9 |
| 09:00 21 st of June | 86.4 | 76.7 | 66.1 | 56.1 | 47. | 41.4 | 38.5 | 41.5 | 47.8 | 56.4 | 66.1 | 76.7 | 86.4 |
| 12:00 21 st of June | 75.2 | 62.3 | 49.9 | 39.7 | 31.9 | 26.5 | 24.1 | 26.5 | 31.9 | 39.8 | 50.1 | 62.3 | 75.2 |
| 15:00 21 st of June | 86.4 | 76.3 | 56.1 | 49.9 | 47.7 | 19.9 | 18.5 | 20.1 | 24.9 | 31.9 | 56.1 | 76.6 | 86.4 |
| 09:00 23 rd of September | 86.4 | 76.6 | 65.9 | 55.9 | 47.6 | 41.2 | 38.3 | 41.2 | 47.6 | 55.9 | 65.9 | 76.6 | 86.4 |
| 12:00 23 rd of September | 85.8 | 76.1 | 65.4 | 55.4 | 47.2 | 40.9 | 38.1 | 41.1 | 47.5 | 55.6 | 65.6 | 76.2 | 86.1 |
| 15:00 23 rd of September | 86.4 | 76.6 | 76.2 | 47.6 | 38.3 | 20.4 | 20.2 | 20.6 | 32.6 | 33.1 | 51.5 | 64.4 | 86.4 |
| 09:00 21 st of December | 89.5 | 81.1 | 71.4 | 61.9 | 53.6 | 47.2 | 44.2 | 47.2 | 53.6 | 61.8 | 71.3 | 81.1 | 89.4 |
| 12:00 21 st of December | 87.5 | 78.4 | 68.2 | 58.5 | 50.2 | 43.9 | 40.9 | 43.9 | 50.3 | 58.6 | 68.4 | 78.6 | 87.7 |
| 15:00 21 st of December | 87.7 | 87.2 | 76.4 | 64.5 | 53.9 | 38.3 | 37.3 | 37.6 | 37.9 | 45.2 | 86.1 | 86.3 | 86.4 |

GVCP analysis showed that minimum percentage of satisfied occupants was 18.52% at 15:00 on 21st of June and maximum was 44.19% at 09:00 on 21st of December when looking at the middle of the glazed wall. The minimum percentage of satisfied occupants was 75.18% at 12:00 on 21st of June to and maximum was 89.49% at 9:00 on 21st of December when looking at the edges of the glazed wall (table 5.136).

Comparing to the basic model minimum DGI reduction was 18.9% and maximum DGI reduction was 28.8% while the minimum GVCP improvement was 266.1% and maximum GVCP improvement was 457.0%. Refer to final comparison table. Refer to table 5.137 for full details including comparison with the basic model and sixth scenario

Table 5.137. Final comparison between Scenarios 06, 10 and basic model (author 2019).

| Date | Hour | Average DGI reduction comparing to the basic model results (scenario 10) | Average DGI reduction comparing to the basic model results (scenario 06) | Average GVCP increment comparing to the basic model results (scenario 10) | Average GVCP increment comparing to the basic model results (scenario 09) |
|---------------|-------|--------------------------------------------------------------------------|--------------------------------------------------------------------------|---------------------------------------------------------------------------|---------------------------------------------------------------------------|
| 21st of Mar. | 9:00 | 24.6% | 19.8% | 294.5% | 205.2% |
| 21st of Mar. | 12:00 | 23.4% | 18.5% | 287.6% | 179.4% |
| 21st of Mar. | 15:00 | 23.5% | 18.2% | 324.0% | 243.9% |
| 21st of Jun. | 9:00 | 24.2% | 19.4% | 293.1% | 173.2% |
| 21st of Jun. | 12:00 | 20.8% | 18.2% | 457.0% | 266.8% |
| 21st of Jun. | 15:00 | 23.5% | 17.1% | 376.9% | 253.8% |
| 23rd of Sept. | 9:00 | 26.2% | 21.6% | 297.7% | 208.2% |
| 23rd of Sept. | 12:00 | 24.3% | 19.4% | 338.0% | 244.2% |
| 23rd of Sept. | 15:00 | 18.9% | 13.1% | 344.52% | 234.9% |
| 21st of Dec. | 9:00 | 25.5% | 19.8% | 266.1% | 186.6% |
| 21st of Dec. | 12:00 | 28.8% | 24.6% | 277.2% | 195.6% |
| 21st of Dec. | 15:00 | 27.2% | 19.0% | 334.1% | 215.1% |

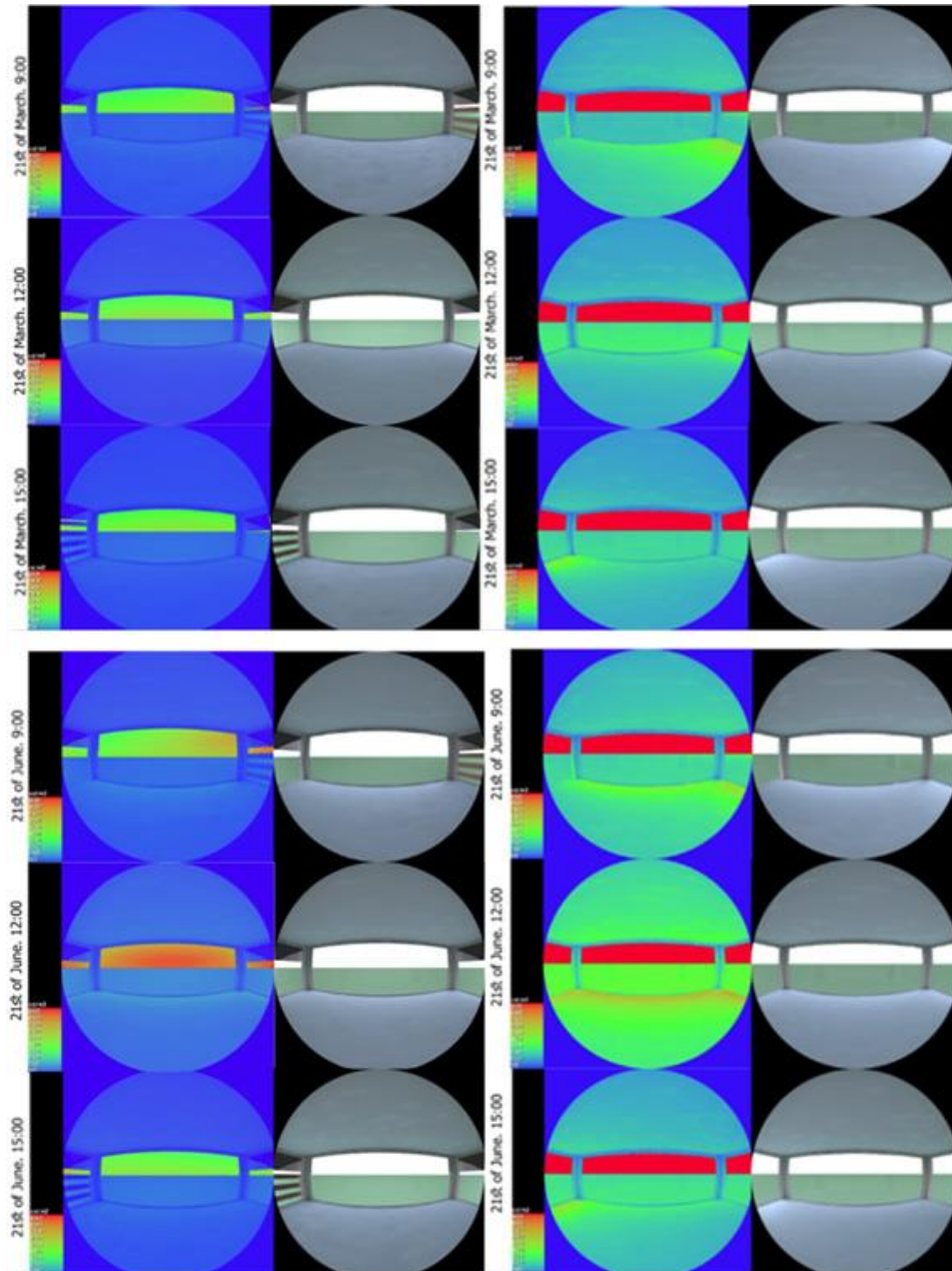


Figure 5.125. Reception room luminance maps on the 21st of March (top images) and 21st of June (bottom images). The images on the left show scenarios01,02 and 03 results and the images on the right show the basic model results (author 2019).

On 21st of March, in the reception room, luminance levels from the glazed wall reached 450 cd/m² in all cases which, comparing to the basic model results, indicated 52.6% luminance level reduction. On 21st of June, in the reception room, luminance levels from the glazed wall reached 500 cd/m² in the first case, 750 cd/m² in second case and 550 cd/m² in the third case which, comparing to the basic model results, indicated 47.3%, 21.1% and 42.1% luminance level reduction (figure 5.125).

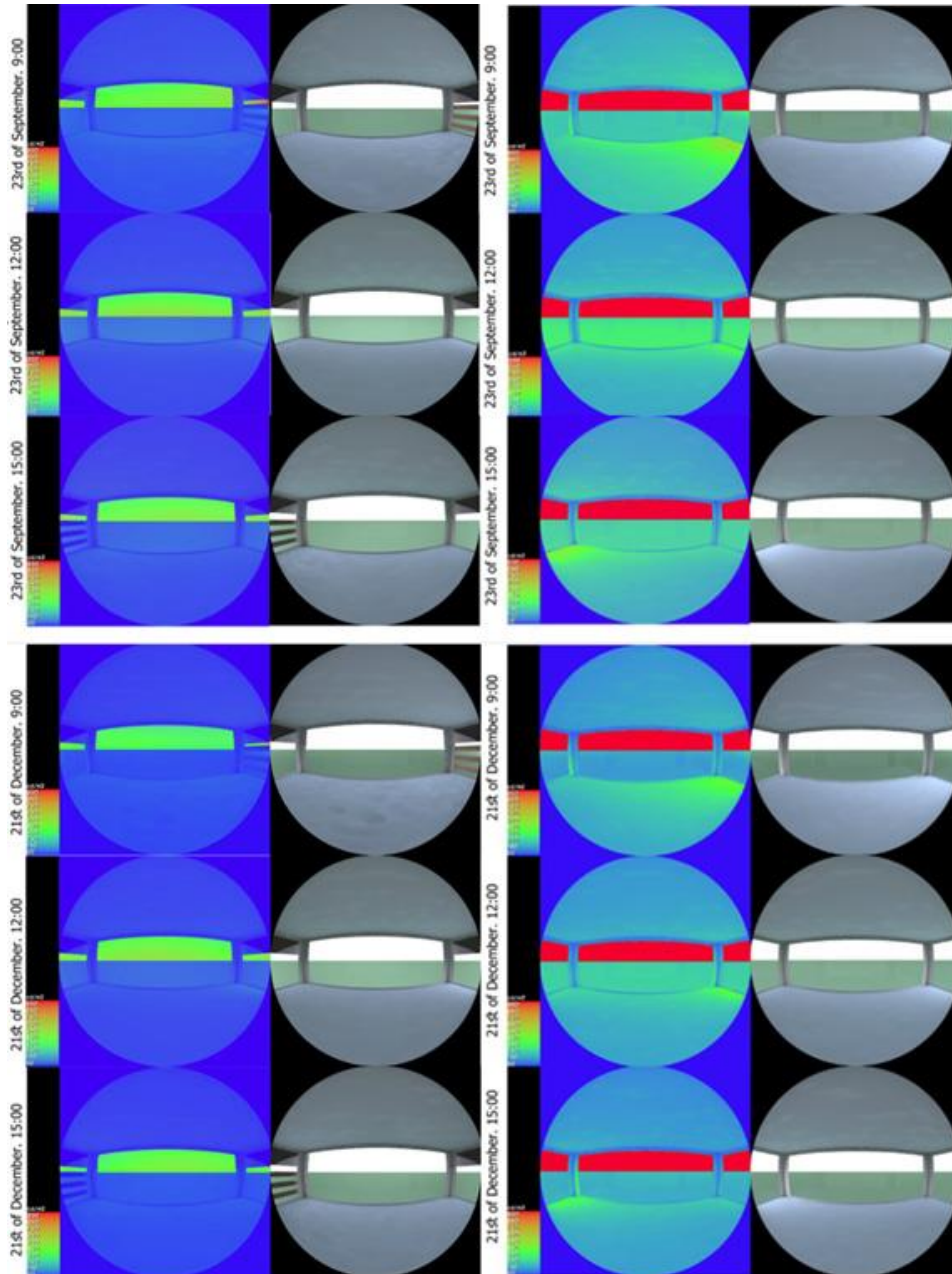


Figure 5.126. Reception room luminance maps on the 23rd of September (top images) and 21st of December (bottom images). The images on the left show scenarios01,02 and 03 results and the images on the right show the basic model results (author 2019).

On 23rd of September and 21st of December, in the reception room, luminance levels from the glazed wall reached 450 cd/m² in all cases which, comparing to the basic model results, indicated 52.6% luminance level reduction (figure 5.126).

Table 5.138. DGI levels from different angles from nadir for the four days at 9:00,12:00 and 15:00 (author 2019).

| Angle | 60 | 50 | 40 | 30 | 20 | 10 | 0 | -10 | -20 | -30 | -40 | -50 | -60 |
|-------------------------------------------|------|------|------|------|------|------|------|------|------|------|------|------|------|
| 09:00 21 st of March | 0.00 | 0.00 | 0.00 | 0.00 | 0.00 | 0.00 | 0.00 | 2.3 | 3.9 | 1.9 | 0.00 | 0.00 | 0.00 |
| 12:00 21 st of March | 8.7 | 8.3 | 0.00 | 0.00 | 0.00 | 8.8 | 9.1 | 8.7 | 8.4 | 8.5 | 8.8 | 9.6 | 9.5 |
| 15:00 21 st of March | 0.00 | 0.00 | 2.2 | 3.9 | 1.9 | 0.00 | 0.00 | 0.00 | 0.00 | 0.00 | 0.00 | 0.00 | 0.00 |
| 09:00 21 st of June | 0.00 | 0.00 | 0.00 | 0.93 | 0.00 | 0.00 | 0.00 | 8.7 | 3.9 | 0.00 | 0.00 | 0.00 | 0.00 |
| 12:00 21 st of June | 0.00 | 0.00 | 0.00 | 0.00 | 0.00 | 0.00 | 0.00 | 0.00 | 0.00 | 0.00 | 0.00 | 0.00 | 0.00 |
| 15:00 21 st of June | 0.00 | 0.00 | 3.9 | 1.2 | 0.00 | 0.00 | 0.00 | 0.00 | 0.00 | 0.00 | 0.00 | 0.00 | 0.00 |
| 09:00 23 rd of September | 0.00 | 0.00 | 0.00 | 0.00 | 0.00 | 0.00 | 0.00 | 0.00 | 1.7 | 4.7 | 7.4 | 0.00 | 0.00 |
| 12:00 23 rd of September | 0.00 | 0.00 | 0.00 | 0.00 | 0.00 | 0.00 | 0.00 | 0.00 | 9.8 | 9.9 | 13.8 | 15.4 | 15.7 |
| 15:00 23 rd of September | 0.00 | 0.00 | 5.3 | 2.9 | 0.00 | 0.00 | 0.00 | 0.00 | 0.00 | 0.00 | 0.00 | 0.00 | 0.00 |
| 09:00 21 st of December | 0.00 | 0.00 | 0.00 | 0.00 | 0.00 | 0.00 | 0.00 | 0.00 | 7.8 | 7.4 | 7.3 | 7.7 | 9.5 |
| 12:00 21 st of December | 7.2 | 7.6 | 8.1 | 8.8 | 0.00 | 0.00 | 0.00 | 0.00 | 7.8 | 7.4 | 7.3 | 7.7 | 9.5 |
| 15:00 21 st of December | 0.00 | 0.00 | 0.00 | 0.00 | 0.00 | 0.00 | 0.00 | 8.6 | 8.5 | 8.0 | 5.7 | 0.00 | 0.00 |

According to the DGI analysis there is an imperceptible glare in all cases, as it DGI level was lower than 18 in the centre of the glazed wall. In several cases DGI level was zero (table 5.138).

Table 5.139. GVCP levels from different angles from nadir for the four days at 9:00,12:00 and 15:00 (author 2019).

| Angle | 60 | 50 | 40 | 30 | 20 | 10 | 0 | -10 | -20 | -30 | -40 | -50 | -60 |
|-------------------------------------------|------|------|------|------|------|------|------|------|------|------|------|------|------|
| 09:00 21 st of March | 100 | 100 | 100 | 100 | 100 | 99.8 | 99.9 | 80.8 | 66.1 | 62.1 | 51.4 | 99.4 | 100. |
| 12:00 21 st of March | 100 | 100 | 100 | 91.9 | 92.8 | 92.9 | 92.9 | 93.4 | 92.3 | 91.4 | 91.1 | 88.1 | 85.8 |
| 15:00 21 st of March | 100 | 100 | 100 | 100 | 100 | 99.3 | 99.8 | 99.9 | 99.9 | 99.9 | 100 | 100 | 100 |
| 09:00 21 st of June | 100 | 100 | 100 | 100 | 100 | 98.7 | 92.2 | 73.8 | 62.1 | 92.2 | 100 | 100 | 100 |
| 12:00 21 st of June | 100 | 100 | 100 | 100 | 100 | 100 | 100 | 100 | 100 | 100 | 100 | 100 | 100 |
| 15:00 21 st of June | 100 | 100 | 100 | 100 | 92.2 | 99.8 | 100 | 100 | 100 | 100 | 100 | 100 | 100 |
| 09:00 23 rd of September | 100 | 100 | 100 | 100 | 100 | 100 | 100 | 100 | 98.1 | 84.1 | 70.6 | 100 | 100 |
| 12:00 23 rd of September | 91.1 | 91.5 | 91.7 | 90.6 | 90.3 | 91.6 | 92.1 | 92.4 | 92.1 | 90.5 | 90.5 | 87.9 | 86.1 |
| 15:00 23 rd of September | 100 | 100 | 90.5 | 93.6 | 97.2 | 99.1 | 100 | 100 | 100 | 100 | 100 | 100 | 100 |
| 09:00 21 st of December | 100 | 100 | 100 | 100 | 100 | 100 | 100 | 100 | 100 | 93.1 | 84.2 | 100 | 100 |
| 12:00 21 st of December | 94.0 | 93.1 | 91.8 | 91.4 | 88.9 | 87.8 | 92.1 | 91.4 | 91.9 | 91.9 | 91.9 | 91.6 | 89.2 |
| 15:00 21 st of December | 100 | 100 | 100 | 100 | 100 | 97.2 | 87.1 | 78.1 | 79.2 | 92.2 | 95.8 | 100 | 100 |

GVCP analysis showed that minimum percentage was 87.01% at 15:00 on 21st of December and maximum percentage was 100% at 12:00 on 21st of June when looking at the middle of the northern glazed wall. The minimum percentage of satisfied occupants was 91.08% at 12:00 on 23rd of September and maximum was 100% at 12:00 on 21st of June when looking at the eastern and western glazed wall (table 5.139).

Comparing to the basic model minimum DGI reduction was 48.1% and maximum DGI reduction was 100% while the minimum GVCP improvement was 57.7% and maximum GVCP improvement was 230.0% (table 5.140).

Table 5.140. Final comparison between Scenarios 06, 10 and basic model in the reception room (author 2019).

| Date | Hour | Average DGI reduction comparing to the basic model results (scenario 10) | Average DGI reduction comparing to the basic model results (scenario 06) | Average GVCP increment comparing to the basic model results (scenario 10) | Average GVCP increment comparing to the basic model results (scenario 06) |
|---------------------------|-------|--------------------------------------------------------------------------|--------------------------------------------------------------------------|---------------------------------------------------------------------------|---------------------------------------------------------------------------|
| 21 st of Mar. | 9:00 | 94.9% | 46.0% | 29.9% | 8.7% |
| 21 st of Mar. | 12:00 | 57.7% | 49.7% | 116.0% | 110.2% |
| 21 st of Mar. | 15:00 | 96.0% | 73.0% | 99.2% | 89.4% |
| 21 st of Jun. | 9:00 | 92.1% | 38.2% | 117.1% | 73.1% |
| 21 st of Jun. | 12:00 | 100% | 100% | 230.0% | 230.0% |
| 21 st of Jun. | 15:00 | 95.9% | 53.3% | 60.8% | 41.6% |
| 23 rd of Sept. | 9:00 | 91.3% | 49.5% | 46.1% | 16.6% |
| 23 rd of Sept. | 12:00 | 69.3% | 48.1% | 112.7% | 111.8% |
| 23 rd of Sept. | 15:00 | 96.2% | 70.3% | 98.3% | 89.6% |
| 21 st of Dec. | 9:00 | 92.0% | 58.8% | 51.1% | 28.8% |
| 21 st of Dec. | 12:00 | 69.1% | 61.0% | 157.0% | 156.3% |
| 21 st of Dec. | 15:00 | 85.7% | 49.5% | 178.9% | 161.9% |

5.7.6 Scenario 10 daylight harvesting potential analysis

In scenario 10, the day light harvesting potential was reduced by 100% as energy consumption after installing the daylighting sensors was exactly the same before installing them (tables 5.141 and 5.142).

Table 5.141. Total annual electricity consumption Results summery (author 2019).

| | Total Energy (MWh) | Total energy (MWh) |
|--------------|--------------------|--------------------|
| Date | Scenario 10.aps | Scenario 10-1 aps |
| Jan 01-31 | 1.6963 | 1.6963 |
| Feb 01-28 | 1.9275 | 1.9275 |
| Mar 01-31 | 2.2960 | 2.2960 |
| Apr 01-30 | 2.9407 | 2.9407 |
| May 01-31 | 3.5392 | 3.5392 |
| Jun 01-30 | 3.5998 | 3.5998 |
| Jul 01-31 | 4.0199 | 4.0199 |
| Aug 01-31 | 4.0925 | 4.0925 |
| Sep 01-30 | 3.7177 | 3.7177 |
| Oct 01-31 | 3.2628 | 3.2628 |
| Nov 01-30 | 2.7233 | 2.7233 |
| Dec 01-31 | 2.1934 | 2.1934 |
| Summed total | 36.0094 | 36.0094 |

Table 5.142. Final comparison (author 2019).

| Scenario | Total annual artificial lighting electrical consumption saving | Cost saving based on tariff of 30.5 Fils for every KW (ADDC 2018). | Reduction in daylight harvesting potential comparing to basic model potential |
|--------------|----------------------------------------------------------------|--------------------------------------------------------------------|-------------------------------------------------------------------------------|
| Basic-model | 1.1156 MWh | 340.3 UAE Dirhams | - |
| Scenario-01: | 0.769 MWh | 234.5 UAE Dirhams | 31.07% |
| Scenario-02: | 0.770 MWh | 234.9 UAE Dirhams | 30.98% |
| Scenario-03: | 0.773 MWh | 235.8 UAE Dirhams | 30.71% |
| Scenario-04 | 0.6215 MWh | 189.6 UAE Dirhams | 55.7% |
| Scenario-05: | 0.2397 MWh | 73.1 UAE Dirhams | 78.5% |
| Scenario-06: | 0.1439 MWh | 43.9 UAE Dirhams | 87.1% |
| Scenario 07 | 0.0140 MWh | 4.27 UAE Dirhams | 98.8% |
| Scenario 08 | 0.0135 MWh | 4.11 UAE Dirhams | 98.8% |
| Scenario 09 | 0.0558 MWh | 17.0 UAE Dirhams | 95.0% |
| Scenario 10 | - | - | 100.00% |

CHAPTER 06
CONCLUSION

6 Conclusion

6.1 Concluding remarks

Global warming phenomena is the main challenge facing architects when designing building envelopes specially in hot arid and hot humid regions. Future envelope designs and existing facades renovations must consider advanced and smart design options which respects the country's climatic characteristics and comply with the environmental and sustainable needs. The main objective is to reduce energy consumption and the overall carbon footprint of buildings while improving both thermal and visual comfort of the occupants.

In order to investigate possible building façade development strategies, it is required to study different scenarios and designs to evaluate their over-all performance. These options can be simulated using virtual modelling programs that can imitate realistic environmental conditions and building parameters. Advanced simulation software facilitates scholars' investigations when studying innovative design strategies, saves time and cost of the research.

The software which was used to investigate the basic model and the ten scenarios was IES-VE. In the initial stages two other simulation programs were tested for the study which were Autodesk Green Building Studio and Autodesk Insight, but both programs gave unrealistic results. However, IES-VE was verified against the approved building energy consumption parameters and proved to be accurate with minimal bias. The software was used to study ten different scenarios and compare them to the basic building model in order to investigate the effects of ETFE cushion width, ETFE number of layers, different frit pattern coverage ratios, addition of different BIPV types to the system and addition of light weight dynamic ETFE shades to the system. The studied factors were annual electricity consumption, BIPVs annual electrical generation, comfort index, mean room temperature, people dissatisfied index, day light factor, day light illuminance levels, luminance maps, DGI, GVCP and day light harvesting potential. These factors were used to evaluate each design scenario comprehensively.

The CFD analysis of all scenarios proved that there was a vertical air flow with different rates within the cavity of the corridor DSF which helped to discharge the hot air from the top outlet. The maximum air velocity at the inlet was 0.72 m/s while the maximum air velocity at the outlet was 1.13 m/s. The system managed to reduce the mean cavity air temperature, comparing to ambient temperature, by 21.4% to 23.8% in eastern DSF, 21.6% to 24.0% in western DSF and 21.5% to 23.6% in northern DSF. It was noted that the performance of corridor DSF is better than multiple-storey facade DSF as, according to the literature review, the second type can cause accumulation of hot air within the cavity, specially near the outlet, which could form a heat sink that could increase the cooling loads in the building. Hence, the corridor DSF is more suitable to hot weather conditions. Also, corridor DSF follows the updated UAE fire and life safety regulations as it can separate between different building floors and thus, prevent fire spreading across the façade.

In the first three scenarios, it was found out that the changes in the thickness of the air chamber made minimal and negligible changes in the three cases results. In general, the addition of the double layer ETFE cushions as a second envelope layer improved most of the factors with a minor reduction in both daylight factor and daylight illumination levels as shown in the detailed results. It only had a noticeable negative impact on the daylight harvesting potential. However, daylight sensors usage was a secondary option added to investigate the potential of full utilization of daylight in the building. Comparing to the second scenario, the addition of ETFE layer to the cushion in scenario 04 reduced the total energy consumption by 0.85% while maintaining similar thermal comfort analysis results, it almost doubled the reduction of daylight factor, daylight illumination levels and daylight harvesting potential. On the other hand, it had a noteworthy improvement in glare analysis results. Comparing to scenario 04, the addition of 30% coverage white frit pattern reduced the total annual electricity consumption by 0.15% while the addition of 60% coverage white frit pattern reduced the total annual electricity consumption by 0.25%. Both scenarios had similar thermal comfort results which had a remarkable reduction in people dissatisfied index in areas with large windows by 39.5% comparing to the previous scenario. Also, they had a major impact on daylight analysis factors that were reduced massively.

Nevertheless, the frit pattern options reduced the DGI by an average of 10.1% and 44.2% and improved GVCP by an average of 30.1% and 70.4% respectively.

In scenarios 07 and 08, where IBPVs were covering one third of the cushions, the thin-film amorphous silicon solar cells type (a-Si), that had 5% module nominal efficiency, generated 1.6% of the required power for the building while the thin-film cadmium-telluride solar cells, that had 13% module nominal efficiency, generated 4% of the required power. Comparing to scenario 06, the shade of the opaque cells reduced the annual electricity consumption by 0.18 MWh which is equal to 0.4% of the basic building consumption. There was minor reduction in the rooms temperature and people dissatisfied index levels. In both scenarios the shade of the opaque BIPVs reduced daylight factor and illumination levels by an average of 2% only. However, it reduced DGI by an average of 23% and improved GVCP by an average of 50%. Also, it almost eliminated the daylight harvesting potential.

Comparing to scenario 06, the addition of dynamic shade in scenario 09 reduced the overall annual consumption by 2.2% and the people dissatisfied index by an average of 2% in the targeted rooms. The effect of shade, when it is active, reduced daylight factor and illumination by an average of 5.1%, reduced DGI by an average of 11% and improved GVCP by an average of 10.5%.

Scenario 10, which represents the most optimal scenario, achieved a total electricity consumption reduction of 19.1% comparing to the basic model. It also, comparing to the basic model, had the best thermal comfort results with 2.8% and 4.8% reduction in the waiting and reception room mean temperature and 9.6% and 13% improvement in the mean people dissatisfied index in both rooms. Reduction in DGI and improvement in GVCP were associated with massive reduction in average daylighting and DF levels and total elimination of daylighting harvesting potential.

To sum up, the addition of the double layer cushion managed to improve all the studied parameters with a minor change in the daylight parameters. It can work along with daylight harvesting strategies. The changes in number of layers had a noticeable impact on daylight and visual comfort parameters and lower impact on energy saving. The addition of frit pattern did not have a major impact on the energy consumption, but it improved both thermal and visual comfort in the spaces. The pattern density had positive effect on the visual comfort parameters with massive reduction of daylighting levels. Highly efficient IBPVs managed to produce an amount of power that was equal to almost one third of the power saving resulted from the installation of the basic double skin option. The dynamic shade effect on the energy consumption was half the effect of the fixed shade of the proposed IBPVs. It was noted that comfort index results had only slight variation between the studied scenarios. However, scenarios 02,09 and 10 had the best results. Also, daylight uniformity was randomly changing without a specific pattern. In scenario 10, both dynamic shading and IBPVs were combined to propose the ultimate efficient option. Although it provided best energy saving, thermal comfort and visual comfort results, it greatly reduced the utilization of daylight in the building. However, when the research juxtaposed the reduction in energy consumption and improvement in thermal and visual comfort against daylighting quality deep within the building, the first factors were more important as HVAC services consumes 47% to 60% of the energy in UAE buildings while artificial lighting consumes 7% to 15% of the energy depending on building type.

These findings address the study question, as all the studied strategies influenced building carbon footprint by affecting total electrical consumption, thermal comfort, daylight utilization potential and visual comfort, room air temperature, people dissatisfied index, daylight factor level, daylight illumination level, DGI, GVCP and daylight harvesting potential. These results gave a direct evaluation for each of the proposed options.

Throughout the research stages, it was revealed that UAE is setting high standard sustainability regulations for building design. This will encourage designers to investigate innovative and sustainable building materials and design options.

6.2 Linking research results to previous studies

- According to the simulation results, the temperature immediately behind the double-layer ETFE cushion was $+0.54 \sim +1.35$ °C (scenarios 0.1,0.2 and 03) higher than ambient temperature while the temperature immediately behind the triple-layer ETFE cushion was $-0.19 \sim +0.44$ °C comparing to ambient temperature. According to Afrin, Chilton and Lau (2017) the temperature immediately below the ETFE layers was typically 9°C higher than the external temperature when the double layer ETFE is used and 7°C higher when the triple layer ETFE is used. The reason of this difference is that the dissertation research covered a vertical ETFE cushion application while their study covered a horizontal ETFE cushion roof application with more exposure to direct solar irradiance. However, both the dissertation research and the study proved that the additional layers increased the insulation effect of the cushions and reduced the temperature behind the cushion by almost 2°C comparing to the double-layers cushions.

- In the simulation results, the basic DSF options (scenarios 01,02 and 03) and the triple-layer ETFE DSF option (scenario 04) the air flow within the DSF cavity helped to save 11.594%~12.45% of the building energy consumption. According to Peng et al. (2016) when they studied similar DSF option, air flow helped to reduce cooling load by almost 15%.

- In the simulation results, the BIPV/DSF option (scenarios 07 and 08) saved 14.7%~17.1% of the building energy consumption. According to Luo et al. (2017) the BIPV/DSF option in their study managed to save 12.16%~25.57% when the same BIPVs types were used. The reason of this difference is the diverse conditions of the studies.

- According to the simulation results, the dynamic shade/DSF option (scenario 09) saved 14.9% of the building energy consumption. According to Hammad and Abu-Hijleh (2010) a similar system managed to save 28.57%~34.02%. Also, Alotaibi (2015) in his study of the dynamic shade of Al-Bahar tower stated that this design option reduced energy consumption in the building by 50%. The reason of this difference is that in the two studies dynamic shade devices were covering 80% to 90% of the fully

glazed façade while in the dissertation research the system was covering only 26% of the façade (western and eastern glazed walls/windows only).

- In the simulation results, the BIPV/DSF option (scenarios 07 and 08), the cadmium telluride thin film PVs generated double the electrical output of a-Si PVs. This matches what Pend et al. (2016) showed in their study.

- According to the simulation results, the addition of the shading device (comparison between scenarios 06 and 09) reduced the mean temperature within the DSF cavity by an average of 0.15°C while in the study conducted by Yang et.al (2016), the shading device reduced the mean temperature by 1.0 °C. The reason of this difference could be the diverse conditions of the studies.

- In the simulation results, when the dynamic shades were installed (comparison between scenarios 06 and 09), average daylighting levels were reduced by 14% and average DF was reduced by 15%. In the study conducted by Mahmoud and Alghazi they concluded that dynamic shade improved daylighting quality by 50% in summer and winter. The reason of this difference could be the diverse conditions of the studies. Also, they considered unique designs for the shading which cannot be modelled in IES-VE.

6.3 Recommendations for future study

The findings of this research set a strong base for future investigation that could enhance the overall results. These future researches should cover:

- 1- Explore the potential of installing the proposed applications on an existing old building. The studied building original design followed ESTIDAMA requirements and had a good performance that was enhanced by the proposed design strategies. It is assumed that if these applications are applied to an old building, it will give much better results. As the EFTE systems are very light comparing to similar double skin façade options, it can be applied to an existing building depending on regulations and structural recommendations.

- 2- Due to lack of verified and detailed manufacturing, installation and maintenance cost of the proposed systems in the UAE, a further cost-benefit analysis study is recommended to evaluate the overall advantages of the systems and if the benefits exceed the cost.
- 3- A life cycle assessment of the system should be conducted to evaluate the environmental impacts that are associated with all the phases of system component life in the UAE.
6. Investigation of the advantages of similar systems that can be combined with ETFE double skin façade system such as integrated photovoltaics with thermal collector system (PVT) and responsive dynamic shades. These systems were not covered by the research due to software limitation.
7. In future studies, innovative ETFE changes can be investigated. This includes usage of IR absorbing materials, air circulation within the cushion's cavity and new environmental products such as ECTFE. Due to software limitation and lack of information, these items were not covered by the study.

7 References

Abdolzadeh, M., Sadeqkhani, M. & Ahmadi, A. (2017). Computational modeling of a BIPV/T ethylene tetrafluoroethylen (ETFE) cushion structure roof. *Energy*, vol. 133, pp. 998-1012.

Abu Dhabi Statistics Centre. (2015). *Energy and Water Statistics*. Abu Dhabi: Abu Dhabi Statistics Centre. [Accessed 23 June 2018]. Available at: <https://www.scad.ae/Release%20Documents/Energy%20and%20Water%20-%20Cover%20-%20EN-v2.pdf>

Abu Dhabi Statistics Centre. (2015). *Energy and Water Statistics*. Abu Dhabi: Abu Dhabi Statistics Centre. [Accessed 23 June 2018]. Available at: <https://www.scad.ae/Release%20Documents/Energy%20and%20Water%20-%20Cover%20-%20EN-v2.pdf>

"AADC Rates and Tariffs 2018". (2018). [Accessed 09 September 2018]. Available at: <https://www.addc.ae/en-US/residential/Pages/RatesAndTariffs2018.aspx>

ADUPC (2010). *The Pearl Rating System for Estidama Emirate of Abu Dhabi*. Abu Dhabi: ADUPC.

Afrin, S., Chilton, J. & Lau, B. (2015). Evaluation and comparison of thermal environment of atria enclosed with ETFE foil cushion envelope. *Energy Procedia*, vol. 78, pp. 477-482.

Agrawal, B. & Tiwari, G. (2011). *Building integrated photovoltaic thermal systems*. Cambridge, UK:RSC Pub.

Al-Saleh, Y. & Taleb, H. (2014). Applying Energy-efficient Water Heating Practices on the Residential Buildings of the United Arab Emirates. *The International Journal of Environmental Sustainability*, vol. 9 (2), pp. 35-51.

Alotaibi, F. (2015). The Role of Kinetic Envelopes to Improve Energy Performance in Buildings . *Architectural Engineering Technology*, vol. 04, pp. 01-05.

"Architonic". (2018). [Accessed 28 July 2018]. Available at: <https://www.architonic.com/en/project/ernst-giselbrecht-partner-dynamic-facade-kiefer-technic-showroom/5100449>

Aristizábal Cardona, A., Páez Chica, C. & Ospina Barragán, D. (2018). *Building-integrated photovoltaic systems (BIPVS)*. Springer International Publishing: Switzerland.

Attia, S., Hensen, J., Beltrán, L. & De Herde, A. (2012). Selection criteria for building performance simulation tools: contrasting architects' and engineers' needs. *Journal of Building Performance Simulation*, vol. 5 (3), pp. 155-169.

Barbosa, S., Ip, K. & Southall, R. (2015). Thermal comfort in naturally ventilated buildings with double skin facade under tropical climate conditions: The influence of key design parameters. *Energy and Buildings*, vol. 109, pp. 397-406.

Bellia, L. & Fragliasso, F. (2018). Evaluating performance of daylight-linked building controls during preliminary design. *Automation in Construction*, vol. 93, pp. 293-314.

- "BREEAM". (2018). [Accessed 17 September 2018]. Available at: https://www.breeam.com/BREEAMUK2014SchemeDocument/content/05_health/hea01_nc.htm
- "BIRDAIR". (2018). [Accessed 11 September 2018]. Available at: <http://www.birdair.com/tensile-architecture/benefits/energy-lighting>
- Cao, X., Dai, X. & Liu, J. (2016). Building energy-consumption status worldwide and the state-of-the-art technologies for zero-energy buildings during the past decade. *Energy and Buildings*, vol. 128, pp. 198-213.
- Carlucci, S., Causone, F., De Rosa, F., & Pagliano, L. (2015). A review of indices for assessing visual comfort with a view to their use in optimization processes to support building integrated design. *Renewable and Sustainable Energy Reviews*, vol. 47 (2015), pp. 1016-1033.
- Chan, A., & Chow, T. (2014). Calculation of overall thermal transfer value (OTTV) for commercial buildings constructed with naturally ventilated double skin facade in subtropical Hong Kong. *Energy and Buildings*, vol. 69, pp. 14-21.
- Cherian, B. (2017). *Residential Village, Electrical Load Schedule*. Abu Dhabi: Anonymous Design Firm.
- Clarke, K. (2016). *80% Energy Consumed by Buildings*. [online]. [Accessed 12 January 2019]. Available at: <https://www.khaleejtimes.com/nation/abu-dhabi/80-energy-consumed-by-buildings>
- "Construction Week Online". (2010). [Accessed 19 January 2010]. Available at: <https://www.constructionweekonline.com/article-9719-first-residents-move-into-22bn-masdar-city>
- "Council on Tall Buildings and Urban Habitat". (2018) . [online]. [Accessed 30 July 2018]. Available at: <http://www.skyscrapercenter.com/building/debis-tower/10075>
- "Council on Tall Buildings and Urban Habitat". (2018). [Accessed 28 July 2018]. Available at: <http://www.skyscrapercenter.com/complex/674>
- Cremers, J. & Marx, H. (2017). 3D-ETFE: Development and evaluation of a new printed and spatially transformed foil improving shading, light quality, thermal comfort and energy demand for membrane cushion structures. *Energy Procedia*, vol. 122, pp. 115-120.
- Cremers, J. & Marx, H. (2016). Comparative study of a new IR-absorbing film to improve solar shading and thermal comfort for ETFE structures. *Energy Procedia*, vol. 155, pp. 113-120.
- "Daylight Analysis in BIM | Sustainability Workshop". (2017). [Accessed 24 November 2017]. Available at: <https://sustainabilityworkshop.autodesk.com/buildings/daylight-analysis-bim>
- Das, A. (2014). *A Guide to Solar Power Generation in the United Arab Emirates*. Dubai: Middle East Solar Industry Association.
- Debbarma, M., Sudhakar, K. & Baredar, P. (2017). Comparison of BIPV and BIPVT: a review. *Resource Efficient Technologies*, vol. 2017, pp. 1-9.
- Dimitriadou, E. (2013). Computational modelling of the thermal behavior of an ETFE cushion using IES. *Sustainable Building*, vol. 1, pp. 175-481.
- Dimitriadou, E. (2015). *Experimental Assessment and Thermal Characterisation of Lightweight Co-Polymer Building Envelope Materials* [online]. Ph.D. Thesis. University of Bath. [Accessed 23 June 2018]. Available at: <https://purehost.bath.ac.uk/ws/portalfiles/portal/114139236>

- Dimitriadou, E., & Shea, A. (2013). Computational modelling of the thermal behaviour of an ETFE cushion using IES. *Sustain Build*, vol. 1 (2013), pp. 175-81.
- Dubey, S., Sarvaiya, J. & Seshadri, B. (2013). Temperature Dependent Photovoltaic (PV) Efficiency and Its Effect on PV Production in the World A Review. *Energy Procedia*, vol. 33 (2013), pp. 311-321.
- Dunn, C., Dehleiah, A., Lerin, C., Cherian, B., Joseph, J., Abdul-Fattah, A., Ibrahim, H., & Hewitt, T. (2017). *Residential Village, Technical Specifications – Section 01 : Volume 2 Division 02 -14*. Abu Dhabi: Anonymous Design Firm
- "EPA". (2019). [Accessed 11 January 2019]. Available at: <https://archive.epa.gov/greenbuilding/web/html/whybuild.html>
- Etheridge, D. (2012). *Natural ventilation of buildings*. Chichester, West Sussex, UK: John Wiley & Sons.
- Gao, A. (2012). *Building skin and details*. Shenyang [China]: Liaoning Science & Technology Pub. House.
- Hamou, S., Zine, S. & Abdellah, R. (2014). Efficiency of PV module under real working conditions. *Energy Procedia*, vol. 50 (2014), pp. 553-558.
- Healy, E. (2015). [Accessed 28 July 2018]. Available at: <https://history.libraries.wsu.edu/spring2015/2015/01/18/carbon-emissions-since-the-time-of-the-industrial-revolution/>
- Hu, J., Chen, W. Qiu, Z. Zhao, B. Zhou, J. & Qu, Y. (2015). Thermal performances of ETFE cushion roof integrated amorphous silicon photovoltaic. *Energy Conversion and Management*, vol. 106, pp. 1201-1211.
- Hu, J., Chen, W. Yang, B. Zhao, W. Song, H. & Ge, B. (2016). Energy performance of ETFE cushion roof integrated photovoltaic/thermal system on hot and cold days. *Applied Energy*, vol. 173, pp. 40-51.
- Hu, J., Chen, W. Zhao, B. & Song, H. (2014). Experimental studies on summer performance and feasibility of a BIPV/T ethylene tetrafluoroethylene (ETFE) cushion structure system. *Energy and Buildings*, vol. 69, pp. 394-406.
- Hu, J., Chen, W., Zhao, B. & Yang, D. (2017). Buildings with ETFE foils: A review on material properties, architectural performance and structural behavior. *Construction and Building Materials*, vol. 131, pp. 411-422.
- Hu, J., Chen, W. Liu, Y. Zhao, B. Yang, D. & Ge, B. (2017). Two-layer ETFE cushions integrated flexible photovoltaics: Prototype development and thermal performance assessment. *Energy and Buildings*, vol. 141, pp. 238-246.
- Hussein, M. (2017). *Residential Village, HAP HVAC calculations*. Abu Dhabi: Anonymous Design Firm.
- Ibrahim, H., Wagdy, A., Beccarelli, P., Carpenter, R. & Chilton, J. (2016). Applicability of flexible photovoltaic modules onto membrane structures using grasshopper integrative model. *Procedia Engineering*, vol. 155, pp. 379-387.
- "IES VE". (2018). [Accessed 15 September 2018]. Available at: <http://www.iesve.com/downloads/help/Thermal/VistaPro.pdf>

"Illuminating Engineering Society". (2018). [Accessed 21 September 2018]. Available at: <https://www.ies.org/definitions/visual-comfort-probability-vcp/>

International Energy Agency (IEA). (2014). *Technology Roadmap-Energy Efficient Building Envelop.* Paris: IEA. [Accessed 26 June 2018]. Available at: <https://www.iea.org/publications/freepublications/publication/TechnologyRoadmapEnergyEfficientBuildingEnvelopes.pdf>

Joe, J., Choi, W., Kwak, Y. & Huh, J. (2014). Optimal design of a multi-story double skin facade. *Energy and Buildings*, vol. 76, pp. 143-150.

Johnsena, K. & Wintherb, F. (2015). Dynamic facades, the smart way of meeting the energy requirements. *Energy Procedia*, vol. 78 (2015), pp. 1568-1573.

Khalifa, I., Ernez, L., Znouda, E., & Bouden, C. (2017). Assessment of the inner skin composition impact on the double-skin façade energy performance in the Mediterranean climate. *Energy Procedia*, vol. 111, pp. 195-204.

Kim, D., Cox, S., Cho, H. & Yoon, J. (2018). Comparative investigation on building energy performance of double skin façade (DSF) with interior or exterior slat blinds. *Journal of Building Engineering*, vol. 20, pp. 411-423.

Kim, J. Lim, H., Cho, S. & Yun, G. (2015). Development of the adaptive PMV model for improving prediction performances. *Energy and Buildings*, vol. 98 (2015), pp. 100-105.

Kittler, R. Kocifaj, M. & Darula, S. (2012). *Daylight Science and Daylighting Technology*. London: Springer Science +Business Media.

Knaack, U., Klein, T. Bilow, M. & Auer, T. (2007). *Principles of Construction*. Medialis: Berlin.

Lamnatou, C., Morenoa, A., Chemisana, D., Reitsma, F. & Clariá, F.(2017). Ethylene tetrafluoroethylene (ETFE) material: critical issues and applications with emphasis on buildings. *Renewable and Sustainable Energy Reviews*, vol. 1, pp. 1364-0321.

Lau, B., Masih, D. Ademakinwa, A. Low, S. & Chilton, J. (2016). Understanding light in lightweight fabric (ETFE foil) structures through field studies. *Procedia Engineering*, vol. 155, pp. 479-485.

Lechner, N. (2015). *Heating, cooling, lighting*. Hoboken (NJ):Wiley.

LeCuyer, A. & Böhme, C. (2013). *ETFE - Technology and Design*. Basel:De Gruyter.

LeCuyer, A. (2008). *ETFE - Technology and Design*. Basel:Birkhäuser.

Lightweight Structure Association (LSA). (2015). *Lightweight Structures for Efficient and Sustainable Building Solutions*. United States Lightweight Structure Association.

Liu, H., Li, B. Chena, Z. Zhoub, T. & Zhang, Q. (2016). Solar radiation properties of common membrane roofs used in building structures. *Materials and Design*, vol. 105, pp. 268-277.

Luo, Y., Zhang, L., Wang, X., Xie, L., Liu, Z., Wu, J., Zhang, Y., & He, X. (2017). A comparative study on thermal performance evaluation of a new double skin façade system integrated with photovoltaic blinds. *Applied Energy*, vol. 199, pp. 281-293.

Mahmod, R. (2011). *Existing Building Re-Skin Thesis Applicative research in Building Technology* [online]. MSc. Thesis. University of Helwan. [Accessed 28 July 2018]. Available at: http://www.cpas-egypt.com/pdf/Riam_elmorshedy/Research/5.pdf

- Maltais, L. & Gosselin, L. (2017). Daylighting 'energy and comfort' performance in office buildings: analysis, metamodel and pareto front sensitivity. *Journal of Building Engineering*, vol. 14 (2017), pp. 61-72.
- Masih, D., Lau, B. & Chilton, J. (2015). Daylighting performance in an atrium with ETFE cushion roof and in an ETFE-encapsulated panel structure. *Energy Procedia*, vol. 78, pp. 483-488.
- "Masdar city". (2019). [Accessed 19 January 2019]. Available at: <https://masdar.ae/en/masdar-city/the-city>
- McNeil, A., & Burrell, G. (2016). Applicability of DGP and DGI for evaluating glare in a brightly daylight space. *ASHRAE and IBPSA-USA SimBuild 2016: Building Performance Modeling Conference*, vol. 1 (2016), pp. 57-64.
- Michael, A., Gregoriou, S. & Kalogirou, S. (2017). Environmental assessment of an integrated adaptive system for the improvement of indoor visual comfort of existing buildings. *Renewable Energy*, vol. 2017, pp. 1-32.
- Mohammed, Z., & Alibaba, B. (2015). Integration of Double Skin Facade with HVAC Systems: The State of the Art on Building Energy Efficiency. *International Journal of Recent Research in Civil and Mechanical Engineering (IJRCME)*, vol. 2, pp. 37-50.
- Monticelli, C., Lombardi, S., Wurfl, C., & Ibrahim, H. (2013). Ellipsoidal shape and daylighting control for the ETFE pneumatic envelope of a winter garden. *Conference: VI International Conference on Textile Composites and Inflatable Structures: Structural Membranes 2013 K.-U.Bletzinger, B. Kröplin and E. Oñate (Eds)*. Munich: Germany.
- Monticelli, C. & Zanellia, A. (2014). Mechanical properties of ETFE foils: testing and modelling. *Construction and Building Materials*, vol. 60, pp. 63-72.
- Mwasha, A. (2018). [Accessed 15 January 2019]. Available at: https://www.researchgate.net/figure/Environmental-loads-on-building-envelope_fig3_260757236
- Nagraj. (2015). *Abu Dhabi's Masdar City Launches Solar-Powered Eco-Villa*. [online]. [Accessed 30 July 2018]. Available at: <https://gulfbusiness.com/abu-dhabis-masdar-city-launches-solar-powered-eco-villas/>
- Nagy, Z., Svetozarevic, B., Jayathissa, P., Begle, M., Hofer, J., Lydon, G., Willmann, A. & Schlueter, A. (2016). The Adaptive Solar Façade: From concept to prototypes. *Frontiers of Architectural Research*, vol. 5 (2016), pp. 143-156.
- "Novum Structure". (2018). [online]. [Accessed 3 July 2018]. Available at: https://novumstructures.com/wp-content/uploads/2017/08/novum_product-data-sheet_afp.pdf
- O'Donnell, A. (2015). *Method and Design Tool For Improved Thermal Comfort in Glazed Spaces* [online]. Msc. Thesis. University of Lund. [Accessed 22 October 2018]. Available at: http://www.ebd.lth.se/fileadmin/energi_byggnadsdesign/publications/exjobb/15-12.pdf
- Peng, J., Curcija, D., Lu, L., Silkowitz, S., Yang, H., & Zhang, W. (2016). Numerical investigation of the energy saving potential of a semi-transparent photovoltaic double-skin facade in a cool-summer Mediterranean climate. *Applied Energy*, vol. 165, pp. 345-356.
- Peng, Z., Herfatmanesh, M. & Liu, Y. (2017). Cooled solar PV panels for output energy efficiency optimisation. *Energy Conversion and Management*, vol. 150 (2017), pp. 949-955.

- Pinhasi, R. & Tabadel, N. (2012). A Craniometric Perspective on the Transition to Agriculture in Europe. *Human Biology*, vol. 1 (2012), pp. 45-66.
- Przybyłek, R. (2018). Facade in Architecture: Definition & Design [online]. [Accessed 5 January 2018]. Available at: <https://study.com/academy/lesson/facade-in-architecture-definition-design.html>
- Radhi, S. (2012). Trade-off between environmental and economic implications of PV systems integrated into the UAE residential sector. *Renewable and Sustainable Energy Reviews*, vol. 16 (2012), pp. 2468-2474.
- Ramzy, N. & Fayed, H. (2017). Kinetic systems in architecture: New approach for environmental control systems and context-sensitive buildings. *Sustainable Cities and Society*, vol. 1 (2011), pp. 170-177.
- ReCREMA (2013). *The UAE Solar Atlas*. Abu Dhabi: Masdar Institute
- Reeves, T., Olbina, S. & Issa, R. (2012). Validation of Building Energy Modelling Tools: Ecotect, Green Building Studio and IES-VE. *Proceedings of the 2012 Winter Simulation Conference*, vol. 1, pp. 582-593.
- Reid, R. (2013). A Shade of Distinction. *Civil Engineering*, vol. 12 (2013), pp. 52-57.
- Rodriguez-Ubinas, E., Montero, C., Porteros, M., Vega, S., Navarro, I., Castillo-Cagigal, M., Matallanas, E. & Gutiérrez, A. (2014). Passive design strategies and performance of Net Energy Plus Houses. *Energy and Buildings*, vol. 83, pp. 10-22.
- Rossi, M., Pandharipande, A., Caicedo, D., Schenato, L. & Cenedese, A. (2015). Personal lighting control with occupancy and daylight adaptation. *Energy and Buildings*, vol. 105 (2015), pp. 263-272.
- Sakellaris, J. (2007). Office building facades and energy performance in urban environment in Greece. *2nd PALNEC Conference and 28th AIVC Conference on Building Low Energy Cooling and Advanced Ventilation Technologies in the 21st Century*, vol. 1 (2007), pp. 541-546
- Seenexus (2017). *Achieving Zero Net Energy in Dubai: Challenges and Opportunities*. Dubai: The Sustainable City.
- Schittich, C. (2012). *In Detail : Building Skin*. Basel: De Gruyter.
- Shameri, M., Alghoul, M., Sopian, K., Zain, M., & Elayeb, O. (2011). Perspectives of double skin facade systems in buildings and energy saving. *Renewable and Sustainable Energy reviews*, vol. 15, pp. 1468-1475.
- Sharaidin, S. & Salim, F. (2012). Design Considerations for Adopting Kinetic Facades in Building Practice. *Digital Physicality*, vol. 01, pp. 619-628.
- Suo, H., Angelotti, A. & Zanelli, A. (2015). Thermal-physical behavior and energy performance of air-supported membranes for sports halls: a comparison among traditional and advanced building envelopes. *Energy and Buildings*, vol. 109, pp. 35-46.
- Taleghani, M., Tenpierik, M., Kurvers, A., & Dobbelsteen, A. (2013). A review into thermal comfort in buildings. *Renewable and Sustainable Energy Reviews*, vol. 26, pp. 201-215.
- Thermal environmental conditions for human occupancy*. (2013). Atlanta:ASHRAE.
- "The Sustainable City". (2019). [Accessed 19 January 2019]. Available at: <https://www.thesustainablecity.ae/>

UAE Ministry of Energy. (2015). *UAE State of Energy Report*. Abu Dhabi: UAE Ministry of Energy. [Accessed 23 June 2018]. Available at: http://dcce.ae/wp-content/uploads/2015/06/SOER_2015_BOOK_draft7_171114_pp_V2_LOW1.pdf

"U.S Energy Information Administration". (2018). [Accessed 7 June 2018]. Available at: <https://www.eia.gov/tools/faqs/faq.php?id=86&t=1>

"U.N. Department of Economic and Social Affairs". (2018). [Accessed 21 June 2018]. Available at: <https://www.un.org/development/desa/en/news/population/2018-revision-of-world-urbanization-prospects.html>

Wen, Y., Guo, Q., Xiao, P. & Ming, T. (2017). The Impact of Opening Sizing on the Airflow Distribution of Double-skin Façade. *Procedia Engineering*, vol. 205, pp. 4111-4116.

"White Void". (2008). [Accessed 29 July 2018]. Available at: https://www.whitevoid.com/#/main/architecture_spaces/flare_facade/flare_4

Wilson, H., & Elstner, M. (2018). Spot Landing: Determining the Light and Solar Properties of Fritted and Coated Glass. *Challenging Glass 6 - Conference on Architectural and Structural Applications of Glass Louver, Bos, Belis, Veer, Nijse (Eds.)*. Delft University of Technology

Wong, I. (2017). A review of daylighting design and implementation in buildings. *Renewable and Sustainable Energy Reviews*, vol. 74 (2017), pp. 959-968.

Yang, H., Zhou, Y., Jin, F., & Zhan, X. (2016). Thermal Environment Dynamic Simulation of Double Skin Façade with Middle Shading Device in Summer. *Procedia Engineering*, vol. 146, pp. 251-256.

"Yas Mall | Home". (2019). [Accessed 2 March 2019]. Available at: <https://www.yasmall.ae/en/home>

Young, N. (2017). *Apple Dubai Mall/ Foster+ Partners*. [Accessed 23 June 2018]. Available at: <https://www.archdaily.com/870357/apple-dubai-mall-foster-plus-partners>

Zaihibee, F., Mekhilef, S., Seyedmahmoudian, M. & Horan, B. (2016). Dust as an unalterable deteriorative factor affecting PV panel's efficiency: Why and how. *Renewable and Sustainable Energy Reviews*, vol. 65 (2016), pp. 1267-1278.

Zhao, B., Chen, W., Hu, J., Qiu, Z., Qu, Y. & Ge, B. (2015). A thermal model for amorphous silicon photovoltaic integrated in ETFE cushion roofs. *Energy Conversion and Management*, vol. 100, pp. 440-448.